UC Berkeley
UC Berkeley Electronic Theses and Dissertations

Title

Iridium-Catalyzed Reactions of C-H, N-H, and O-H Bonds with Alkenes: Methodologies and Mechanisms

Permalink

https://escholarship.org/uc/item/1fk067s7

Author

Sevov, Christo

Publication Date

2014

Peer reviewed|Thesis/dissertation

Iridium-Catalyzed Reactions of C–H, N–H, and O–H Bonds with Alkenes: Methodologies and Mechanisms

by

Christo Sevov

A dissertation submitted in partial satisfaction of the
requirements for the degree of
Doctor of Philosophy
in
Chemistry
in the
Graduate Division
of the
University of California, Berkeley

Committee in charge:

Professor John F. Hartwig, Chair
Professor F. Dean Toste
Professor T. Don Tilley
Professor Alexis Bell

Spring 2014

Iridium-Catalyzed Reactions of C–H, N–H, and O–H Bonds with Alkenes:
Methodologies and Mechanisms

Christo Sevov

ABSTRACT

Iridium-Catalyzed Reactions of C–H, N–H, and O–H Bonds with Alkenes:
Methodologies and Mechanisms

by

Christo Sevov

Doctor of Philosophy in Chemistry

University of California, Berkeley

Professor John F. Hartwig, Chair

The following dissertation discusses methods for the addition of NH bonds of amides and indoles to alkenes, CH bonds of heteroarenes to bicycloalkenes, and OH bonds to unactivated alkenes. The final section describes a method for the oxidative coupling of unactivated alkenes with furans to generate vinylfurans. All of the processes, discussed herein, are catalyzed by iridium bisphosphine complexes. Mechanistic investigations of the catalytic processes provide information on elementary organometallic reactions such as oxidative addition of XH bonds, and the subsequent reactivity of the organometallic products with alkenes.

Chapter 1 is an introduction to reactions of CH, NH, and OH bonds of organic molecules with iridium complexes. Many of these stoichiometric reactions of iridium complexes have been incorporated into catalytic processes that involve alkenes. These reactions and other seminal contributions to the field of alkene hydrofuctionalization will be summarized.

Chapter 2 describes a method for the iridium-catalyzed intermolecular hydroamination of unactivated α-olefins with arylamides and sulfonamides to generate synthetically useful protected amine products in high yield. Reactions of bicycloalkenes form products in high enantiomeric excess. Mechanistic studies on this rare catalytic reaction revealed a resting state that is the product of N–H bond oxidative addition and coordination of the amide. Rapid, reversible dissociation of the amide precedes reaction with the alkene, but an intramolecular, kinetically significant rearrangement of the species occurs before this reaction with alkene. These data are summarized in a proposed catalytic cycle.

Chapter 3 describes a method for intermolecular, iridium-catalyzed addition of phenols to unactivated α-olefins. Mechanistic studies on this rare catalytic reaction reveal a dynamic mixture of resting states that undergo O–H bond oxidative addition and subsequent olefin insertion to form ether products. Studies on the resting state complexes of these OH addition reactions reveal fundamental differences between reactivities of iridium complexes with NH and OH bonds and the stabilities of the resulting Ir(phenoxide) or Ir(amidate) complexes.

Chapter 4 describes a method for intermolecular asymmetric addition of the C-H bonds of indoles, thiophenes, pyrroles and furans to bicycloalkenes in high yield and high enantiomeric excess (ee). These heteroarene alkylations occur *ortho* to the heteroatom. This selectivity is observed, even with unprotected indoles, which typically undergo alkylation at the C3 position. Initial mechanistic studies revealed that oxidative addition of a heteroarene C-H bond to a neutral Ir^I species occurs within minutes at room temperature and occurs in the catalytic cycle prior to the turnover-limiting step. Products from a *syn* addition of the C-H bond across the olefin were observed, which indicate that migratory insertion of an iridium-bound alkene occurs into an Ir–C bond.

Chapter 5 describes a method intermolecular hydroamination reactions of indoles with unactivated olefins. The reactions occur with as few as 1.5 equivalents of olefin to form *N*–alkylindoles exclusively and in good yield. Characterizations of the catalyst resting-state, kinetic data, labeling studies, and computational data imply that the addition occurs by olefin insertion into the Ir–N bond of an *N*-indolyl complex and that this insertion reaction is faster than insertion of olefin into the Ir–C bond of the isomeric C-2-indolyl complex.

Chapter 6 describes an Ir-catalyzed process for oxidative coupling of furans with unactivated olefins to generate branched vinylfuran products in high yields and selectivities with a second alkene as the hydrogen acceptor. Detailed mechanistic experiments revealed catalyst decomposition pathways that were alleviated by the judicious selection of reaction conditions and application of new ligands. The temperature dependence of the decomposition pathway and the product-forming pathway cause the reactions to occur faster at lower temperatures.

TABLE OF CONTENTS

ACKNOWLEDGEMENTS

I can't recall what my expectations were of graduate school. I know for a fact that they did not include spending my last days as a graduate student in Berkeley, California. I did not know what I would work on as a graduate student, and I had not run a single metal-catalyzed reaction before joining John's group. Thus, it is a testament to the kindness, patience, and mentorship of my coworkers, friends, and family that I survived to reach this point. For these reasons, I will always cherish my time as a graduate student.

First, I must thank Professor John Hartwig for allowing me to join his group. John has been the ultimate model of a mentor, scientist, and scholar. The environment that he has constructed is unlike any that I've ever experienced, which allowed me to grow and learn as a scientist. He has provided me with countless suggestions while allowing me to pursue my own research interests, and I will always be grateful to him.

I quickly discovered how much mental, physical, and emotional energy was required of me on an everyday basis. The first months of graduate school were a blur of chaos. Lisa Julian was extraordinarily kind and helpful during that time. This kindness was not an exception. I worked with an incredibly talented group of chemists, and I would like to thank Cass Richers, Seth Marquard, Dan Robbins, Allie Strom, Juana Du, Carl Liskey, and Patrick Hanley for their friendship and advice. I would also like to thank the mysterious Steve Zhou, who I never had the opportunity to meet. Steve planted the seed that would ultimately lead to the projects that I studied as a graduate student. I must also thank my classmates at Illinois for their friendship and the wonderful times that we had as first year students: Scott Sisco, Erin Davis, Matt Endo, and my then-roommate Tommy Osberger. I will be forever grateful to the friends and coworkers with whom I've had a tremendous number adventures, laughs, and who have kept my spirits up: Eric Simmons, Nichole Litvinas, Patrick Fier, Rebecca Green, Tyler Wilson, Mark Bartlett, and Matt Larsen.

After my second year at Illinois, John announced that we would be moving to Berkeley. I chose to attend Illinois, and I loved my time there; however, the move was a wonderful and beneficial experience. I had the opportunity to interact with the faculty and students at two excellent research universities. I would like to thank my previous committee at Illinois for their advice: Profs. Scott Denmark, Greg Girolami, and Christina White. The faculty at Berkeley has been equally kind and helpful and I must thank Profs. Don Tilley, Dean Toste, Richmond Sarpong, Alex Bell, and Bob Bergman.

I would like to thank my family for their endless support and love. My parents have been pillars of stability in times of turbulence. I've seen glimpses of what our lives could have been had we stayed in Bulgaria, and their sacrifices to provide us with this life and these opportunities are unimaginable. I have to thank my older sister Elli. Since the times that we were little and by ourselves in Bulgaria she has always been someone that I could freely speak with. I want to thank the brother that I've always wanted, Travis and my nephew Dylan who makes me smile every time I hear his voice. I would like to thank my Aunt Penka and Uncle Lubcho who have always been a second family, and my cousins

CHAPTER 1

Overview of Iridium-Catalyzed Additions of
N–H, O–H, and C–H Bonds to Alkenes

1.1 Introduction

The addition of an H–X bond across an olefin, when X is a carbon, nitrogen, or oxygen atom, represents the most direct strategy for the alkylation of arenes, amines, or alcohols. Reactions could be conducted with commodity chemicals, such as simple alkenes, to generate value-added products in a single step and with complete atom economy (Scheme 1). However, activation parameters for additions of H–X bonds to alkenes are generally large, and these reactions do not occur without catalyst. Extensive efforts have been dedicated to the development of catalysts that effect these processes.

Scheme 1. Alkylation of substrates by H–X bond additions to alkenes.
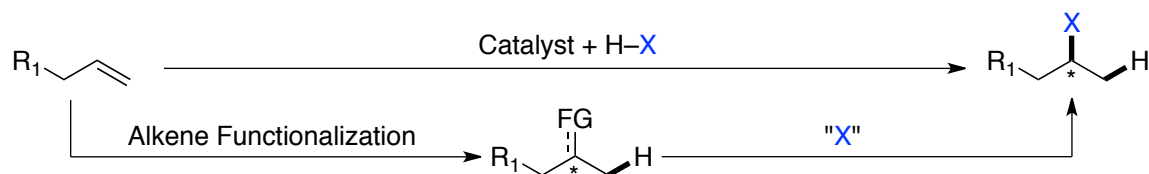
Hartwig and coworkers have demonstrated that the thermodynamics for additions of H–X bonds to alkenes must be considered when targeting hydrofunctionalization reactions. Additions of aniline derivatives to unsubstituted styrenyl compounds are thermodynamically favorable (Figure 1a).[1] The exergonic nature of this reaction was attributed to formation of a strong, primary C–H bond in the product. However, reactions conducted with internal olefins, such as indene or 1,2-dihydronaphthalene, are endergonic, and the conversion of starting materials is subject to the reaction equilibrium.
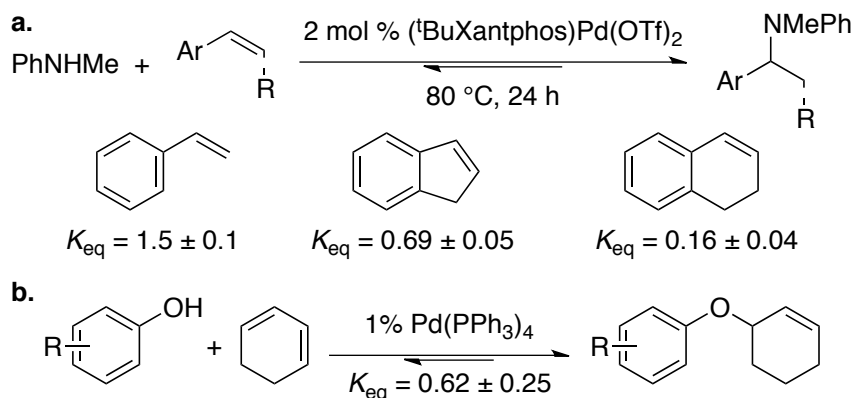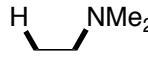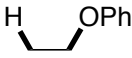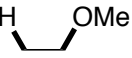
Figure 1. (a) Equilibrium constants for Pd-catalyzed additions of aniline derivatives to vinylarenes. (b) Pd-catalyzed additions of phenols to dienes are endergonic.

Reports on the palladium-catalyzed additions of phenols[2] and anilines[3-4] to 1,3-dienes allow for the direct comparison of the thermodynamics between diene hydrophenoxylation and hydroamination. Additions of phenols to 1,3-cyclohexadiene were found to be endergonic and reversible (Figure 1b), while reactions of anilines were irreversible. Because N–H addition is irreversible, the hydroamination process as amenable to asymmetric catalysis. Catalytic reactions conducted with chiral, non-racemic complexes of palladium formed allylamine products with excellent enantiomeric excess (ee).[4]

Table 1. Enthalpies of H–X Bond Addition to Ethylene and Selected Bond Dissociation Energies.[5]

$$H\!-\!X \;+\; = \;\xrightleftharpoons{\text{Catalyst}}\; \overset{H}{\diagdown}\underset{\diagup}{}\overset{X}{}$$

Nucleophile:	H–Ph	H–NMe$_2$	H–OPh	H–OMe	H–OH
H–X BDE:	113	95	88	104	119
Product:	H⌣Ph	H⌣NMe$_2$	H⌣OPh	H⌣OMe	H⌣OH
C–X BDE:	100	72	65	85	94
Rxn. ΔH:	-35 kcal/mol	-17 kcal/mol	-12 kcal/mol	-8 kcal/mol	-14 kcal/mol

The enthalpy of formation of products from C–H, N–H, and O–H to ethylene can be correlated to the difference between the bond dissociation energy (BDE) of the H–X bond and the resulting C–X bond (Table 1). Hydroarylation reactions are very enthalpically favorable because the BDE of the C–C bond that is formed is only slightly weaker than the C–H bond that was broken in the starting material (ΔBDE = 13 kcal/mol). Additions of O–H bonds to alkenes, however, form products with C–O bonds that are much weaker than the O–H bonds that were broken in the starting materials (ΔBDE = >20 kcal/mol). These processes are expected to be thermoneutral when the entropic penalty of combining two compounds is included into the calculation. Thermodynamics for hydroamination reactions fall between those for C–H and O–H addition reactions.

Despite the challenges that have been described above, many C–H, N–H, and O–H additions to alkenes catalyzed by metals, Brønsted acids, and Lewis acids have been reported. The following sections will serve to summarize major contributions to the field of metal-catalyze hydrofunctionalization of alkenes with a focus on iridium-catalyzed processes.

1.2 Reactions of Iridium Complexes with N–H Bonds, and Iridium-Catalyzed Hydroamination of Alkenes.

The alkylation of amines is a fundamental organic transformation. Products of these reactions are important chemical building blocks, pharmaceuticals, agrochemicals, solvents, polymers, and surfactants. Nucleophilic substitution of alkyl halides or pseudohalides and reductive amination of ketones are common procedures for amine alkylation.[6] However, the electrophiles employed for these classic methodologies are most commonly generated from functionalization of an alkene. Thus, a more direct route to alkylamines would be the addition of an N–H bond of an amine to an alkene, which is a reaction formally known as hydroamination.
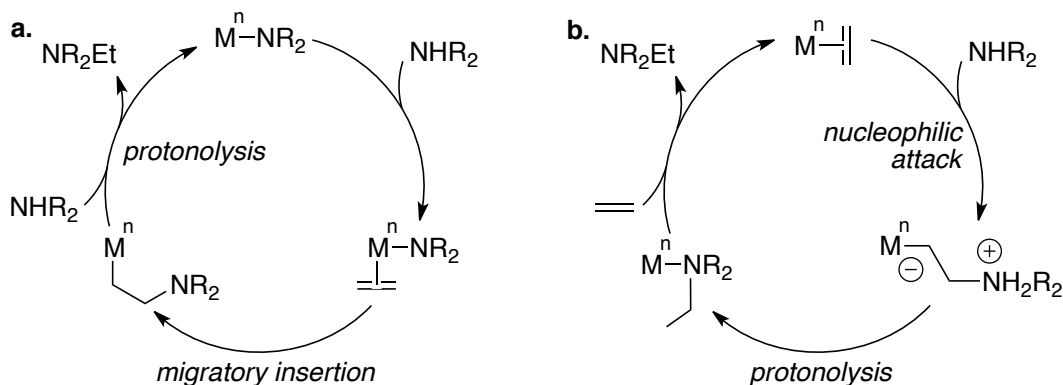
Figure 2. Common mechanisms for metal-catalyzed hydroamination.

The potential to generate valuable amine products in a single step from abundant chemicals with perfect atom economy is the incentive behind the tremendous efforts that have been dedicated toward the design of metal complexes that catalyze hydroamination. A vast number of metal complexes have been reported to catalyze hydroamination, and their mechanisms have been studied in detail.[7-14] Hydroamination reactions generally proceed through two different mechanistic pathways. One pathway involves insertion of an unsaturated C–C bond into a M–N bond, followed by protonolysis of the alkylmetal complex (Figure 2a). The alternative pathway involves nucleophilic attack of the amine reagent onto an olefin that is bound to a metal center (Figure 2b). The aim of this introduction is to summarize the typical trends in reactivities of iridium complexes with amines, rather than to summarize the scope and mechanisms of all previously reported studies on hydroamination. A discussion of intermolecular and intramolecular additions of N–H bonds to alkenes, dienes, allenes, and alkynes catalyzed by late and early transition metal complexes, as well as lanthanide complexes, is provided in the introductions to Chapters 2 and 6.

$$\text{(1.1)}$$
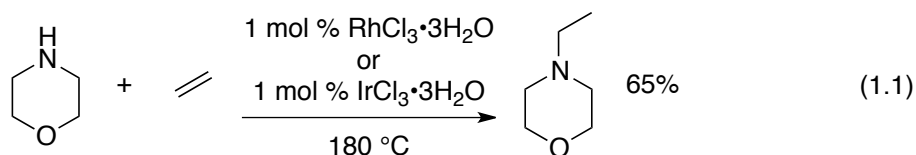
The first example of homogeneous metal-catalyzed hydroamination was reported

by Coulson at DuPont.[15] A solution of $RhCl_3 \cdot 3H_2O$ or $IrCl_3 \cdot 3H_2O$ in THF catalyzed the addition of morpholine to ethylene (eq 1.1). The mechanism and active catalyst for this process remains unclear because the reaction can be conducted iridium and rhodium precursors in the +3 or +1 oxidation state. Since this time, hydroamination reactions catalyzed by complexes of iridium have remained of great interest.

$$M + H-NR_2 \longrightarrow \underset{M-NR_2}{\overset{H}{|}} \xrightarrow{\parallel} \underset{M}{\overset{H}{|}} \diagup NR_2 \qquad (1.2)$$
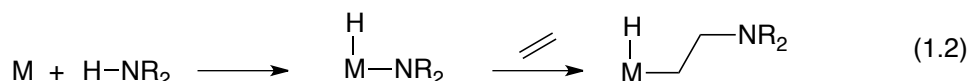
Unlike most other complexes that catalyze hydroamination, iridium complexes have been demonstrated to react with N–H bonds of amines to generate stable amidoiridium hydride complexes (eq 1.2). Many amido complexes of early transition metals have been reported; however, amido complexes of late transition metals are of particular interest to chemists. Metal-nitrogen bonds are much weaker for late transition metals such as iridium than for early transition metals, and late metal amido complexes should be more reactive than early metal amido complexes.[16] Consequently, organometallic reactions that break weak M–N bonds, such as migratory insertion of an alkene into an Ir–N bond, could be exergonic. Migratory insertion reactions of alkenes into amido complexes of late transition metals have been documented recently.[17-24] These elementary organometallic reactions are proposed to be responsible for the C–N bond-forming step during a number of catalytic amination reactions of alkenes.

Scheme 2. Synthesis and stability of Ir(PCP)(NH$_2$)(H) complexes.
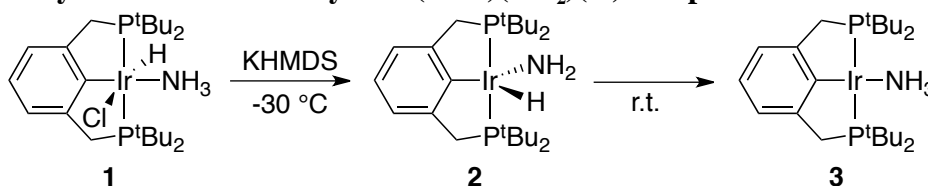
Extensive efforts have been dedicated to the identification of complexes that insert into N–H bonds. Goldman and Hartwig isolated the first mononuclear amido hydride complex **2** that would be the product from oxidative addition of ammonia. Amidoiridium complex **2** was generated at low temperatures upon deprotonation of the hydridochloride iridium precursor **1** with KHMDS (Scheme 2).[25] The iridium(III) complex **2** underwent rapid N–H bond-forming reductive elimination to generate the ammonia complex **3** upon warming to room temperature. However, this resulting ammonia complex **3** was not observed to insert into the N–H bond.
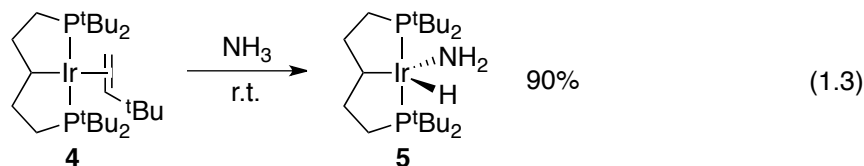
In a later study, Hartwig and Goldman targeted iridium complexes with more electron-donating ligands that would favor oxidative addition of the NH bond of ammo-

nia, in preference to dative ligation of ammonia.[26] To this end, an iridium complex of an alkyl pincer ligand (**4**) was synthesized, which is more electron-rich than the analogues complex of an aryl pincer ligand (**1**). Complex **4** was allowed to react with ammonia at room temperature and formed the product of N–H bond oxidative addition in 90% yield (eq 1.3). In addition to complexes that react with ammonia,[27] iridium pincer complexes have been developed for the oxidative addition of N–H bonds of hydrazine[28] and anilines.[29] These results demonstrated the propensity for iridium complexes to insert into strong N–H bonds and generate stable, mononuclear amido(hydride) complexes.

$$(PEt_3)_2Ir(CH_2CH_2)Cl \ + \ NH_3 \quad \xrightarrow{\text{r.t., 24 h}} \quad \text{[complex 7]} \qquad (1.4)$$

6   **7**

$$NH_2Ph \ + \ \text{[norbornene]} \quad \xrightarrow[70\ ^\circ C,\ 72\ h]{\substack{10\ \text{mol \% Ir(PEt_3)_3Cl} \\ 2\ \text{mol \% ZnCl_2}}} \quad \text{[NHPh-norbornane]} \quad 43\% \qquad (1.5)$$
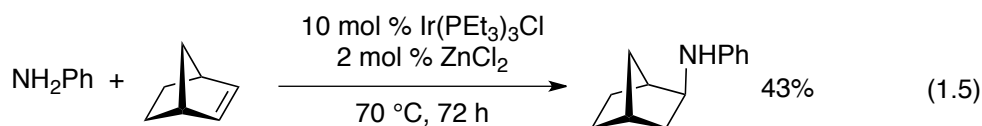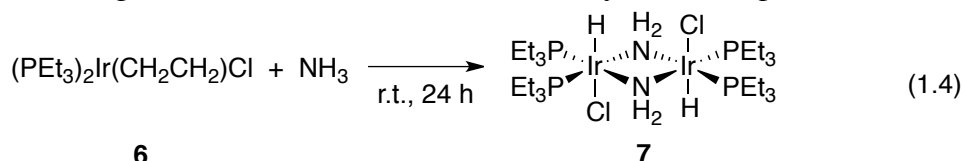
Insertion of iridium metal centers into N–H bonds was known prior to the studies on mononuclear complexes. The first example of N–H bond oxidative addition to an iridium complex was reported by Casalnuovo, Calbrese, and Milstein (eq 1.4).[16] The combination of ammonia and the electron-rich iridium complex **6** formed the dinuclear complex **7** with bridging amido ligands. These amidoiridium complexes do not catalyze hydroamination and do not insert alkenes. Building on these results, Casalnuovo and coworkers demonstrated that electron-rich iridium complexes with cocatalytic amounts of ZnCl$_2$ catalyzed the intermolecular hydroamination of norbornene with aniline (eq 1.4).[30] These results constituted the first examples of intermolecular hydroamination catalyzed by complexes of iridium.

Scheme 3. Reactions of iridium complexes with aniline and norbornene.
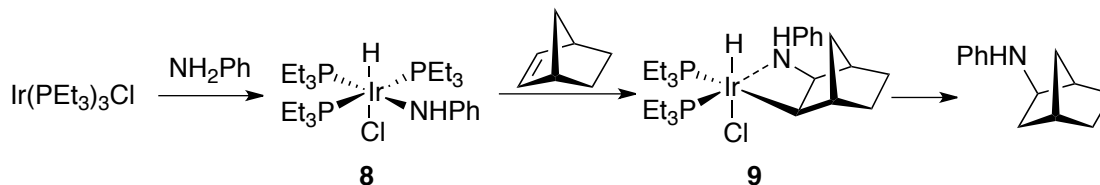
Insight into the mechanism of the iridium-catalyzed hydroamination reaction was provided from a series of stoichiometric transformations (Scheme 3). The combination of tris(triethylphosphine)IrCl in neat aniline afforded a stable anilidoiridium hydride **8**. Subjecting this product of N–H bond oxidative addition to an excess of norbornene formed alkyl complex **9**, which was characterized by single crystal x-ray diffraction. The relative stereochemistry of iridium and nitrogen at the norbornyl fragment was found to be syn. The syn facial selectivity of addition across the alkene is consistent with migratory insertion of norbornene into the Ir–N bond of complex **8**. Bond-forming reductive elimination of the norbornylaniline was observed only after heating the alkyl complex **9** in the presence of norbornene and ZnCl$_2$. These studies suggested a mechanism for catalytic hydroamination that had not been proposed previously for reactions catalyzed by complexes of early transition metals.

6

Scheme 4. The effect of additives on the iridium-catalyzed addition of aniline to norbornene.

no additive:	12%, 57% ee
8 mol % $[P(N(P(NMe_3)_2)_4]^+[F]^-$:	22%, 95% ee
2 mol % LiNHPh:	0%, n/a
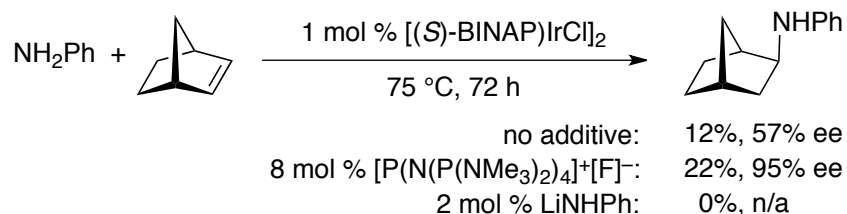
The studies reported by Casalnuovo and coworkers provided the foundation for future iridium-catalyzed addition reactions. Togni and coworkers reported the first examples of asymmetric intermolecular hydroamination with chiral, nonracemic iridium complexes. Enantioselective additions of aniline to norbornene catalyzed by (BINAP)IrCl formed norbornylanilines with 57% ee but in low chemical yield (Scheme 4).[31] Additives such as phosphazenium fluoride improved the yield (up to 51%, not shown) and enantioselectivity of the reaction over those conducted without the fluoride. Togni and coworkers postulated that under the reaction conditions, fluoride could be basic enough to deprotonate the aniline substrate. Prior to this work, Brunet and coworkers demonstrated that (phosphino)rhodium complexes in combination with lithium anilide formed active catalysts for the hydroamination of bicycloalkenes with arylamines.[32-33] However, cocatalytic amounts of lithium anilide inhibited the hydroamination reaction catalyzed by complexes of iridium, and the role of fluoride remained unclear.

In addition to complexes that catalyze additions of anilines, Togni reported similar iridium complexes for the catalytic hydroamination of bicycloalkenes with arylamides.[34] However, the norbornylamide products were formed in low yield (5-30%) as a result of competitive hydroarylation of norbornene. Under similar conditions, aminoalkenes were demonstrated to cyclize with 57% ee.[35]

Table 2. Catalyst systems for the addition of aniline to norbornene.

entry	[Ir] complex and additive	% yield, % ee
1	$[(R)$-DM-Segphos)IrCl]$_2$	6%, 37% ee
2	$[(R)$-DM-Segphos)IrCl]$_2$ + KHMDS	63%, 96% ee
3	$[(R)$-DM-Segphos)IrCl]$_2$ + KNHAr	61%, 96% ee
4	$K^+[(R)$-DM-Segphos)Ir(NHAr)$_2]^-$ + $[ArNH_3]^+[OTf]^-$	70%, 97% ee

Hartwig and Zhou studied the role of the fluoride additive in iridium-catalyzed hydroamination reactions. Reactions of norbornene and aniline with (DM-Segphos)IrCl as catalyst formed products in low yield and ee (Table 2, entry 1). However, reactions conducted with cocatalytic amounts of KHMDS or potassium anilide formed products in a high 96% ee and good chemical yield (entries 2 and 3). In a separate study, the combination of a preformed potassium (bisanilide)iridate complex and ammonium triflate formed products in similar yields and selectivities to those with the iridium chloride pre-

cursor and a base (entry 4 vs. entries 2 and 3). These data suggest that the iridium complexes with anilide ligands form more active and enantioselective catalysts than do complexes with chloride ligands.
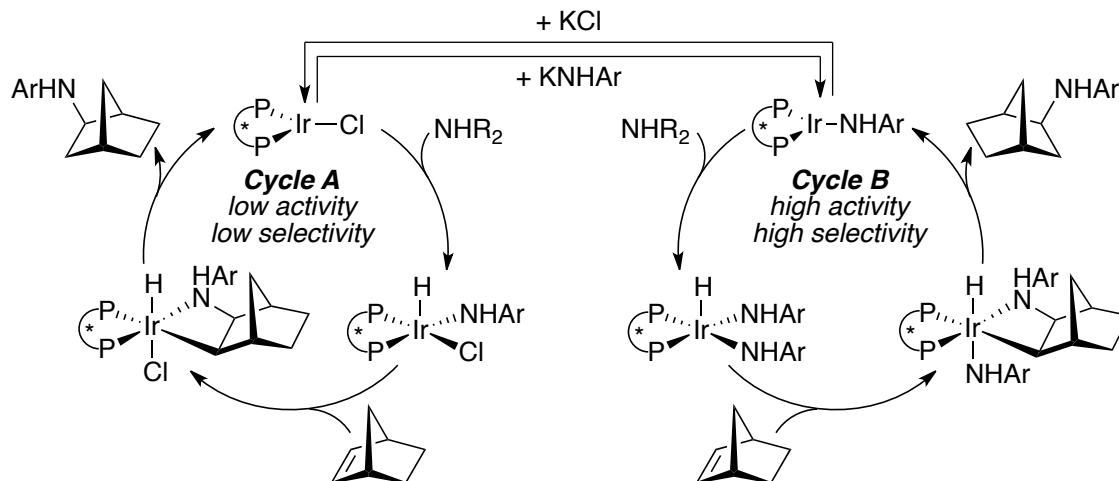
Figure 3. Proposed catalytic cycle for the iridium-catalyzed hydroamination of norbornene with anilines.

The results of these experimental studies are consistent with the proposed catalytic cycle that is illustrated in Figure 3. Reactions catalyzed by iridium chloride complexes form products in low yield and ee (Figure 3, Cycle A). Alternatively, reactions conducted with cocatalytic amounts of base could generate an iridium anilide complex that forms addition products in high yield and with high selectivity (Figure 3, Cycle B). Both processes are believed to occur by N–H oxidative addition of aniline and migratory insertion of norbornene into the Ir–N bond. Norbornylaniline products are formed following C–H reductive elimination, which regenerates the iridium(I) species.
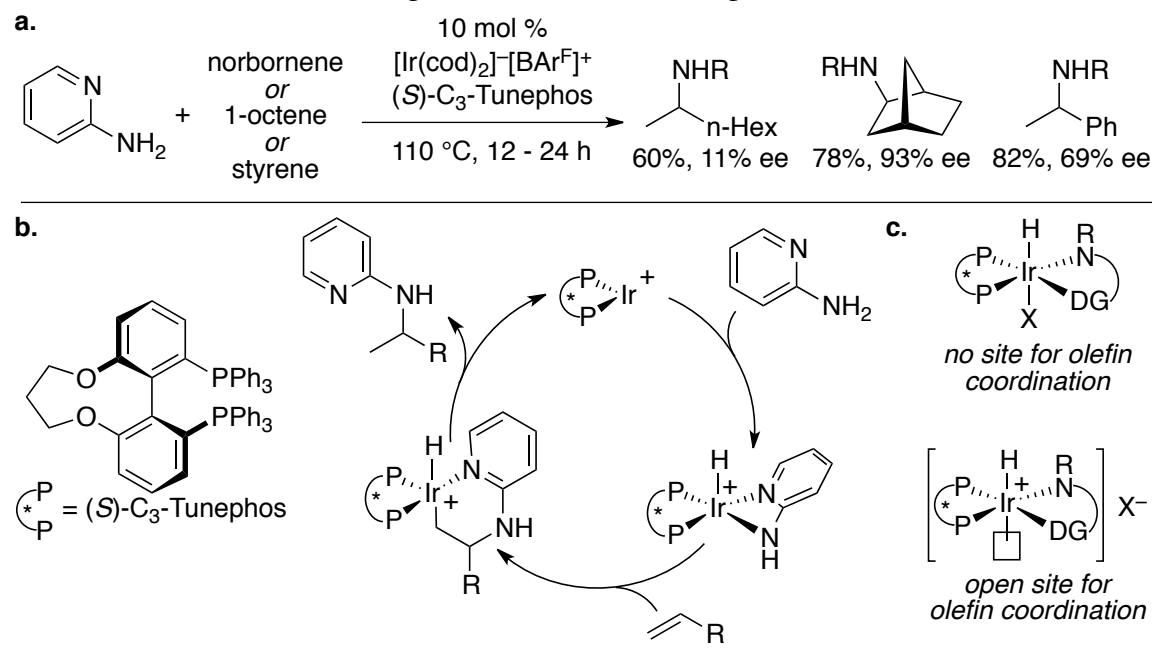
Figure 4. (a) Intermolecular hydroamination catalyzed by a cationic iridium complex (b) Proposed mechanism for the catalytic reaction. (c) Comparison of neutral and cationic iridium complexes.

Recently, Shibata and coworkers reported a cationic iridium complex as catalyst for the intermolecular addition of pyridylamines to vinylarenes (Figure 4a).[36] Unlike neutral iridium complexes, cationic iridium bisphosphine complexes do not readily insert into the N–H bonds of amines. For this reason, directing groups are incorporated into the amine substrate to facilitate formation of an amidoiridium intermediate, which can insertion olefin as illustrated in Figure 4b.

These cationic iridium complexes complement neutral iridium complexes as catalysts for hydroamination. Directed hydroamination catalyzed by *neutral* iridium complexes is unknown because the directing group occupies the site at the metal for coordination of the alkene. Alternatively, cationic iridium complexes lack X-type ligands bound to the metal and contain an open site for olefin coordination as illustrated in Figure 4c.
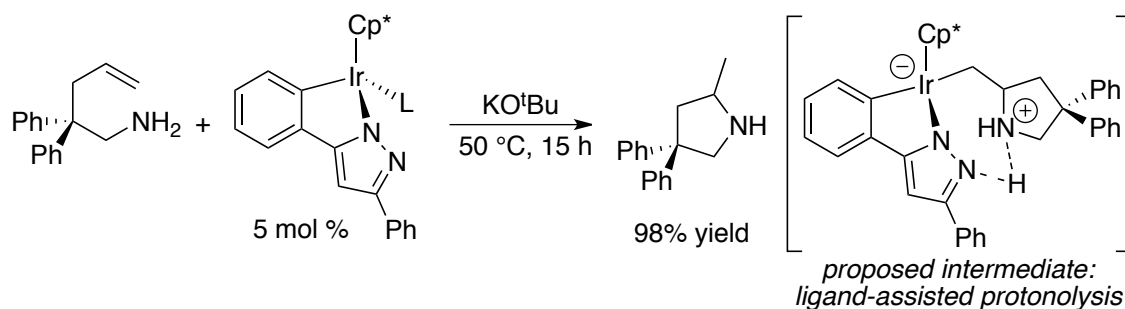
Figure 5. Iridium-catalyzed intramolecular hydroamination with ligand-assisted protonolysis.

Hydroamination reactions catalyzed by iridium complexes do not occur exclusively by insertion of an alkene into an Ir–N bond. Recently, many iridium-catalyzed reactions have been developed that are proposed to occur by nucleophilic attack of an amine onto an alkene bound to iridium.[37-39] Formation of the C–N bond is often reversible, and protonolysis of the Ir–C bond is turnover-limiting. Ikariaya and coworkers developed iridium complexes with pyrrazolide-based ligands that were designed to assist in the protonolysis of the Ir–C bond as illustrated in Figure 5.[40-41] The mechanism of this reaction remains debated;[42] however, structure-relationship studies have demonstrated that the nitrogen of the pyrrazolide group is a key component of the catalyst system.
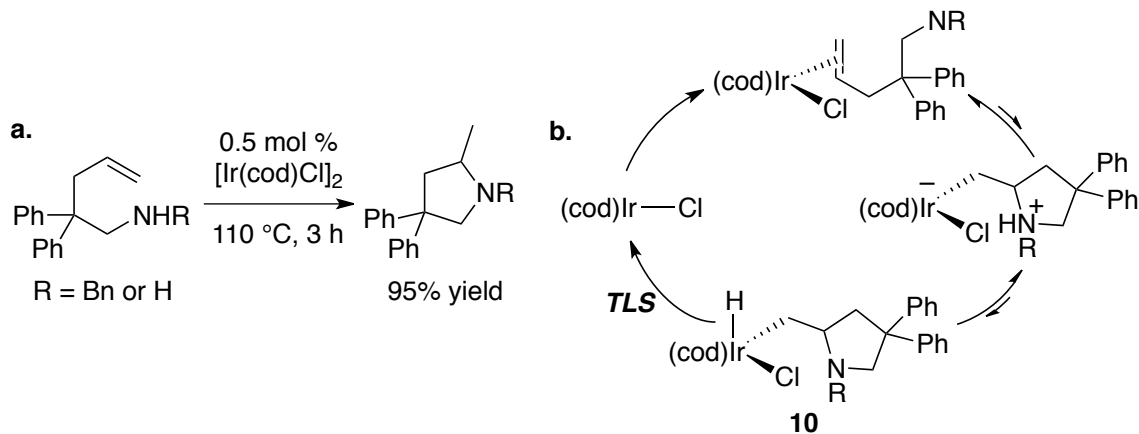
Figure 6. (a) Intramolecular hydroamination of primary aminoalkenes. (b) Proposed mechanism for the hydroamination reaction.

Complex ligand systems are not required for iridium-catalyzed hydroamination. Stradiotto and coworkers reported that iridium complexes of 1,5-cyclooctadiene could catalyze the intramolecular cyclization of secondary[43] and primary[44] aminoalkenes. Experimental and computational mechanistic studies were performed to gain insight into the mechanism of this reaction. A kinetic isotope effect of 3.4 was measured; however, this result and other kinetic data could not be employed to distinguish between a mechanism that involves turnover-limiting N–H bond oxidative addition and turnover-limiting Ir–C protonolysis. Studies by density functional theory predicted that oxidative addition of the N–H bond to a (cod)IrCl complex would occur with an energy barrier of 38 kcal/mol at 278 K, whereas a mechanism that occurs by attack of an amine onto an olefin that is bound to iridium was computed to occur with a highest transition state energy of 24 kcal/mol. The identity of the turnover-limiting step was predicted by calculations to be C–H reductive elimination from complex **10** (Figure 6). The energy barriers calculated for this mechanism were consistent with the activation parameters that were measured experimentally (E_a = 22 kcal/mol).

1.3 Summary

Reactions of amines with transition metal complexes have been limited to substitution reactions of X- or L-type ligands. Consequently, complexes that catalyze hydroamination by activation of an olefin for nucleophilic attack are inhibited by dative ligation of the amine to the metal. Alternatively, complexes of iridium have been demonstrated to undergo reactions that are distinct from those observed for complexes of early transition metals. Electron-rich iridium complexes can undergo N–H bond oxidative addition to form stable amidoiridium hydride complexes. Consequently, coordination of the amine to the iridium center is an elementary reaction that is on the catalytic cycle rather than a deactivation process. Under the appropriate conditions, these complexes can serve as intermediates that insert alkenes into the Ir–N bond to generate hydroamination products.

Despite the progress that has been made on intermolecular hydroamination, few complexes catalyze of N–H bonds across unactivated alkenes. Chapters 2 and 6 summarize the discovery and study of catalysts for the intermolecular hydroamination of unactivated alkenes with amides and heteroarenes. These studies provide insight into the mechanisms for C–N bond formation and barriers of migratory insertion of unactivated alkenes into Ir–N bonds.

1.4 Reactions of Iridium Complexes with O–H Bonds, and Iridium-Catalyzed Hydroalkoxylation of Alkenes.

Reactions of alcohols with alkenes constitute some of the most widely used processes catalyzed by homogeneous transition-metal complexes. The palladium-catalyzed oxidation of ethylene in water is used to synthesize of 10^6 tons of acetaldehyde annually.[45] Under standard reactions conditions, C–O bond formation occurs by insertion of ethylene into a Pd–OH bond (Figure 7).[46] Elimination of the proton beta- to palladium from the alkyl intermediate generates an enol, which tautomerizes to acetaldehyde. In the years following the discovery of ethylene oxidation, known as the Wacker process, chemists have isolated metal-alkoxide complexes that react with alkenes.[22] Stereochemical studies have revealed that the mechanisms for oxidative alkoxylation catalyzed by palladium[47-48] or mediated by rhodium[49] complexes occur by insertion of an alkene into a metal alkoxide bond.
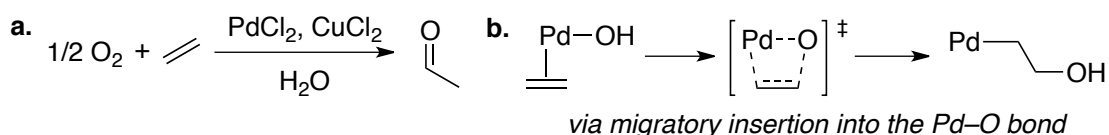
Figure 7. (a) Ethylene oxidation to acetaldehyde by the Wacker process. (b) Proposed mechanism of C–O bond formation.

The redox-neutral variant of this reaction to generate alcohols or ethers by additions of O–H bonds to alkenes remains challenging. Brønsted acids, or Lewis acids that generate Brønsted acids *in situ*, are traditional catalysts for additions of O–H bonds to alkenes.[50] However, acid-catalyzed processes occur under harsh conditions, form intermediates with carbocations that often undergo rearrangements, and occur without stereochemical control. To address these issues, metal complexes have been studied extensively as catalysts for hydroalkoxylation of alkenes.
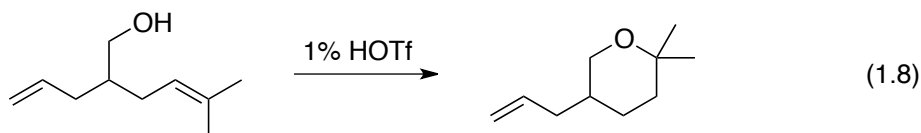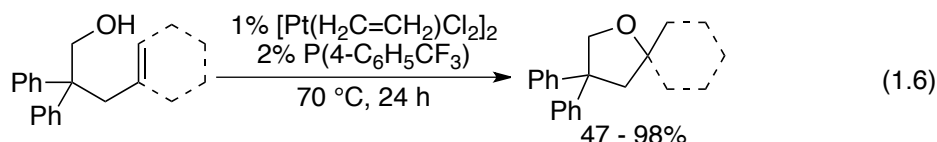
A variety of metal catalysts have been reported for the synthesis of alkylethers directly from alcohols and alkenes (eqs 1.6[51] and 1.7[52]). The mechanisms of these reactions are often unclear, and catalysis by trace amounts of acid cannot be excluded (eq 1.8).[53] Reactions catalyzed by triflates of coinage metals have been effective for intermolecular additions of alcohols to alkenes; however, these processes occur with selectivities and

product distributions that are similar to those of reactions catalyzed by triflic acid.[53-55] However, studies by ^{1}H NMR spectroscopy and control experiments have suggested that cationic silver and gold complexes are indeed the catalytic intermediates rather than acid.[56] The mechanism of these processes involves attack of alcohol onto an olefin, which is bound to the metal center. Protonolysis of the alkylmetal bond releases the ether product as illustrated in Scheme 5.

Scheme 5. Proposed mechanism for the gold-catalyzed hydroalkoxylation of alkenes.
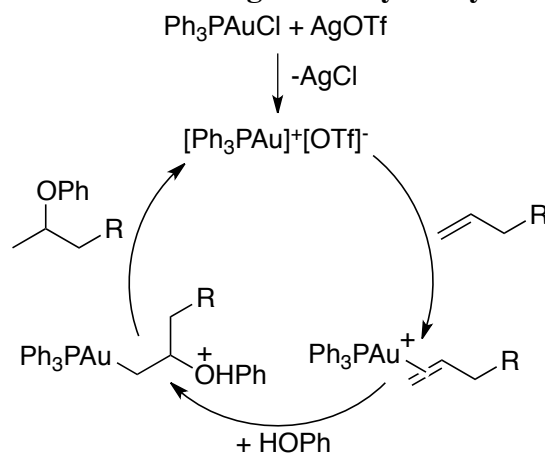
Additions of alcohols to alkenes that occur by migratory insertion of an olefin into a metal alkoxide bond are rare. Marks reported the cyclization of alkoxo-olefin complexes of rare earth metals.[57-60] However, until recently, there had been no examples of hydroalkoxylation catalyzed by late transition metal complexes that proceed by olefin insertion into a metal-alkoxo bond. The mismatch of soft-acid/hard-base pairing between late transition metals and alkoxides was thought to preclude formation of these intermediates under catalytic conditions.
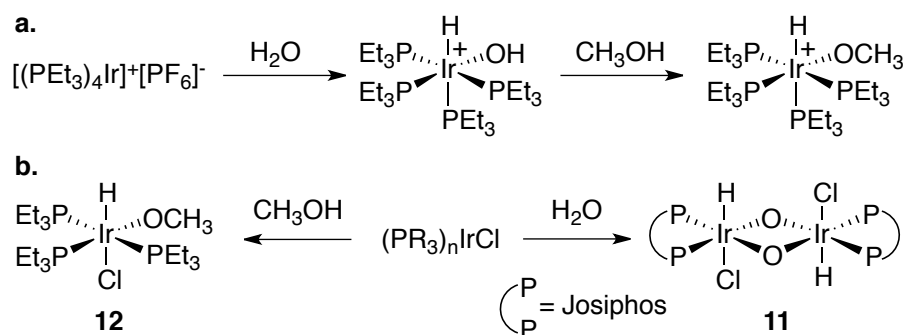
Figure 8. (a) Reactions of O–H bonds with cationic iridium complexes. (b) Reactions of O–H bonds with neutral iridium complexes.

Studies on activation of O–H bonds to electron-rich iridium complexes have indicated that stable alkoxoiridium complexes can be generated (Figure 8a). In analogy to their work with ammonia,[16] Milstein and coworkers demonstrated that stable hydroxoiridium (**11**) and alkoxoiridium (**12**) complexes could be prepared by insertion of cationic iridium centers into O–H bonds (Figure 8b).[61-62] Alternatively, reactions of *neutral* iridi-

12

um complexes with water formed dinuclear complexes.[63-64] Mononuclear products of O–H bond oxidative addition to iridium were isolated from reactions of alcohols.[65]

Scheme 6. Stoichiometric dehydroaryloxylation of ethylene.
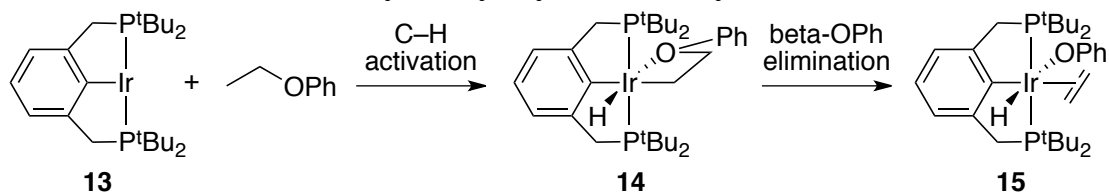
Although isolable, these iridium hydroxide and alkoxide complexes do not react with alkenes. Furthermore, prior to the work summarized in Chapter 3, there were no examples of well defined complexes that catalyze the intermolecular addition of an O–H bond of simple alkenes. Recently, Goldman and Krogh-Jespersen reported the dehydroaryloxylation of ethylene, mediated by (PCP)Ir complex **13** (Scheme 6).[66-67] Aryloxy elimination from the beta position of the alkyliridium complex **14** forms the phenoxoiridium olefin complex **15**. These reactions constitute the reverse of O–H addition of phenol to ethylene.
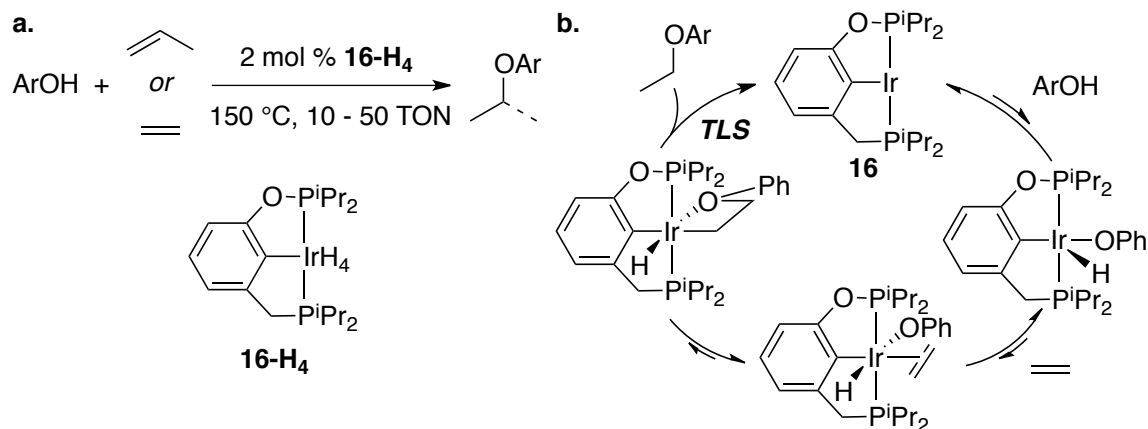
Figure 9. (a) Iridium-catalyzed hydroaryloxylation of alkenes. (b) Proposed mechanism of hydroaryloxylation.

Building upon these results, Goldman and Krogh-Jespersen discovered that (POCP)Ir complexes could catalyze the addition of aryl alcohols to ethylene, propene and butene (Figure 9a).[68] Computational studies by DFT suggested that the reaction occurs by reversible migratory insertion of the olefin into the Ir–O bond, and the product is released following turnover-limiting C–H reductive elimination from an alkyliridium intermediate (Figure 9b).

1.5 Summary

Hydroalkoxylation is a desirable process for the atom-economical synthesis of alcohols or ethers. Electrophilic complexes of late transition metals catalyze intermolecular additions of alcohols to alkenes; however, the mechanisms of these processes are unclear. Prior to the work summarized by Chapter 3, well-defined complexes that catalyze

intermolecular additions of alcohols to simple alkenes were unknown. Although migratory insertions into Ir–N bonds were documented, there were no examples of the analogous reactions with iridium alkoxide complexes. Thus, fundamental data on the elementary reactions of alkene insertions into Ir–O bonds was lacking.

Chapter 3 is a summary of our research efforts toward the development of an iridium-catalyzed, intermolecular O–H addition reaction to simple alkenes. The studies provide data regarding the stability of phenoxoiridium intermediates and their propensity to undergo alkene insertion from complexes that catalyze intermolecular hydroamination reactions.

1.6 Iridium-catalyzed additions of C–H bonds to alkenes.

The alkylation of arenes and heteroarenes by metal-catalyzed additions of C–H bonds to alkanes is a desirable complement to traditional alkylation procedures. In contrast to Friedel-Crafts alkylation reactions,[69-70] metal-catalyzed processes could generate products with regioselectivities that are determined by the metal, could form products under milder conditions, and could allow for stereochemical control.

$$ (1.9) $$
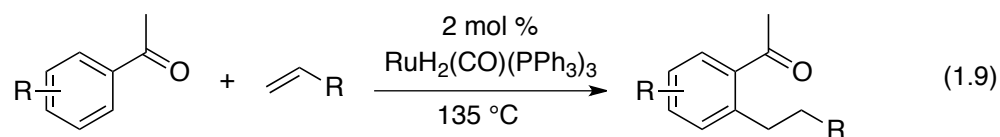
The addition of a C–H bond of an arene to an alkene, formally known as hydroarylation, was first reported by Murai and coworkers (eq 1.9).[71] Aryl and heteroaryl ketones were amenable to ruthenium-catalyzed alkylation, and the acyl group served to direct hydroarylation to the ortho position of the arene. Unlike acid-catalyzed reactions of arenes with alkenes, the linear alkylarene was formed selectively over the branched alkylarene.

Scheme 7. Rh-catalyzed hydroarylation en route to (+)-lithospermic acid.

NR* = (R)-aminoindane

88%, 73% ee

(+)-lithospermic acid
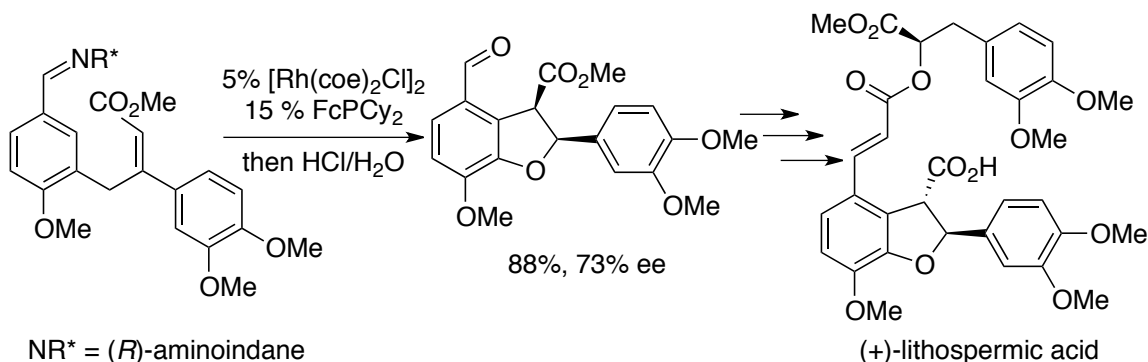
Following the report by Murai and coworkers, a variety of directing groups have been developed for metal-catalyzed inter- and intramolecular hydroarylation of alkenes.[72-76] Metal-catalyzed hydroarylation reactions have been incorporated into total syntheses of natural products and pharmaceutical compounds.[77] Bergman and Ellman installed a chi-

ral, non-racemic aldimine group to direct a rhodium-catalyzed intramolecular hydroaryla-tion reaction as a key step toward the synthesis of (+)-lithosperimic acid (Scheme 7).[78] The resulting dihydrobenzofuran was formed with good diastereoselectivity and was elaborated to the enantiopure natural product.

Scheme 8. Iridium-mediated C–H addition of an arene to an alkene.
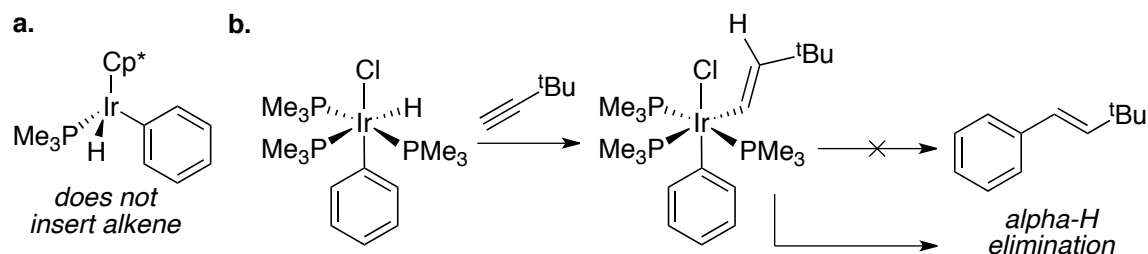
The activation of C–H bonds by iridium complexes was documented prior to the discovery of hydroarylation chemistry.[79-82] However, the prepared alkyl- and aryliridium hydrides did not undergo migratory insertion reactions with alkenes or alkynes to gener-ate addition products (Scheme 8). Rather, complexes underwent C–H reductive elimina-tion to generate complexes that reacted with the vinyl C–H bonds of alkenes.[83-85] Merola prepared aryliridium hydride complexes and observed insertion of a terminal alkyne into the Ir–H bond but not the Ir–C bond.[86-88] These vinyl(aryl)iridium complexes did not un-dergo C–C bond-forming reductive elimination to release addition products.
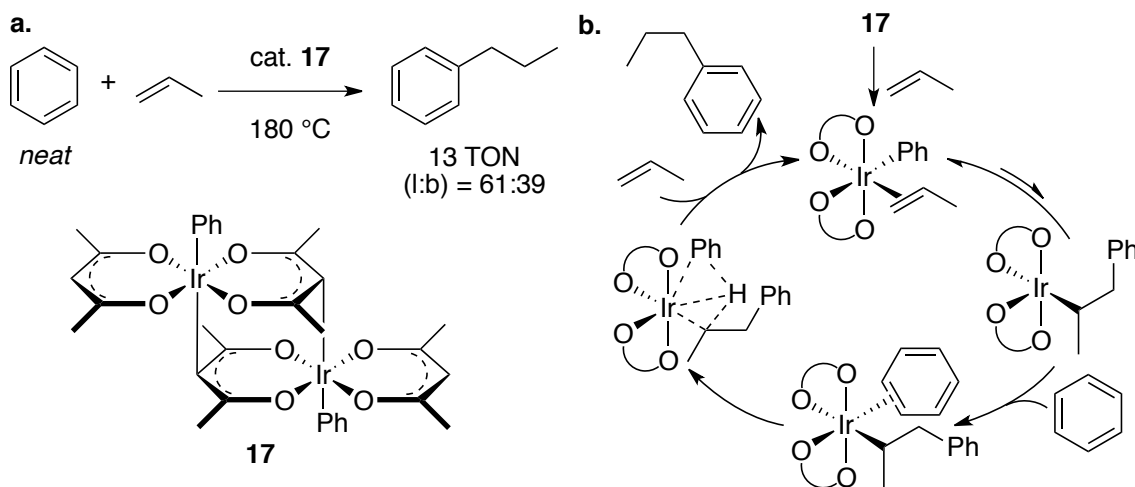
Figure 10. (a) Ir(III)-catalyzed anti-Markovnikov hydroarylation of propene with benzene. (b) Proposed mechanism of the Ir-catalyzed hydroarylation reaction.

In 2000, Periana[89] and Togni[34] reported the first examples of iridium-catalyzed additions of aryl C–H bonds to alkenes only months apart. However, the two reports de-scribed complexes that were vastly different from one another, and the researchers would later discover that the complexes catalyzed C–H additions of arenes to alkenes by very different mechanisms. Reactions conducted with acetylacetonato iridium(III) complex **17**, developed by Periana, formed linear alkylbenzene products (Figure 10a). The selectivity of Periana's metal-catalyzed process complements that of acid-catalyzed alkylation,

which generates branched alkylarenes exclusively. (Note: Gunnoe and coworkers report-ed a tri(pyrrazolyl)ruthenium complex that catalyzes anti-Markovnikov hydroarylation of propene with similar selectivities to that of Periana's iridium complex.)[90-91] The mecha-nism of the iridium-catalyzed reaction was studied by experimental and computational methods and is summarized in Figure 10b.[92-94] The active catalyst is generated upon dis-sociation of the dinuclear complex **17**. The mononuclear aryliridium(III) intermediate undergoes turnover-limiting migratory insertion of an alkene into the aryliridium bond to form the C–C bond of the product. Benzene coordinates in an η^2-fashion to the alkyliridi-um complex. Release of the alkylarene product is concomitant with cleavage of the ben-zene C–H bond. This process is believe to occur through an oxidative hydrogen migration mechanism as illustrated in Figure 10b. These complexes were later demonstrated to catalyze the hydrovinylation of ethylene to form butene isomers by a mechanism similar to the one reported for hydroarylation with benzene.[95-96]
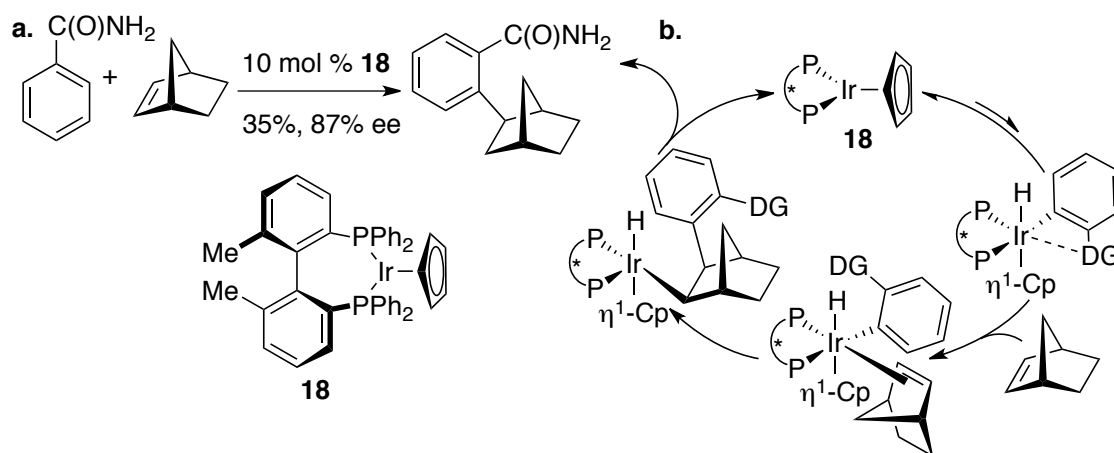
Figure 11. (a) Ir(I)-catalyzed hydroarylation. (b) Proposed mechanism for the directed hydroarylation reac-tion.

In contrast to the system discovered by Periana and coworkers, the system devel-oped by Togni employed chiral, non-racemic iridium(I) complexes for the asymmetric addition of benzamide C–H bonds to strained alkenes (Figure 11a). The cyclopentadienyl ligand of complex **18** was required to obtain C–H additions products. Reactions catalyzed by analogous complexes with chloride ligands formed primarily hydroamination products but in only 5-30% yield.[34-35] The reaction is proposed to occur following a ring slip of the cyclopentadienyl ligand from η^5 to η^3 (or lower hapticity). Coordination of the amide and subsequent C–H activation at the position ortho- to the amide forms an aryliridium inter-mediate. Olefin insertion into the Ir–C bond forms an alkyliridium complex that releases product by C–H bond-forming reductive elimination (Figure 11b). Togni and Dorta later described bisphosphine iridium chloride complexes that catalyze C–H additions of phe-nols to strained alkenes.[97]

Scheme 9. Directed hydroarylation reactions catalyzed cationic iridium complexes.

DG = Py, Ac
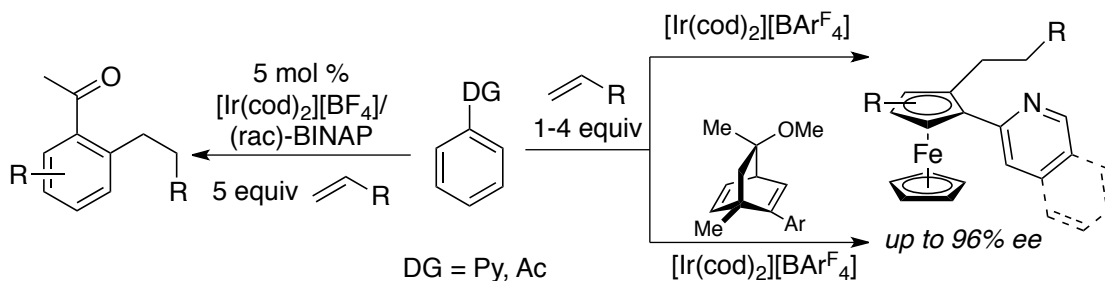
Cationic iridium complexes have been employed as catalyst for directed hydroarylation reactions.[98] Shibata first reported the hydroarylation of vinylarenes and alkynes with arylketones and catalytic amounts of [(BINAP)Ir(cod)][BF$_4$] (Scheme 9, left).[99] Later, Shibata and coworkers discovered that phosphine ligands were not required for the catalyst system, and [Ir(cod)$_2$][BAr$^F_4$] catalyzes additions of pyridylferrocene C–H bonds to a range of alkenes including: acrylates, vinylarenes, bicycloalkenes, and simple alpha-olefins.[100] Under these conditions, cyclooctadiene is believed to remain ligated to the cationic iridium complex (Scheme 9, right). Thus, Shibata and coworkers tested cationic iridium complexes of chiral, non-racemic dienes for asymmetric hydroarylation.[101] Under these conditions, alkylferrocenes were formed with high enantioenrichment.

Scheme 10. Selective alkylation of indoles with alkenes catalyzed by complexes of Ir.
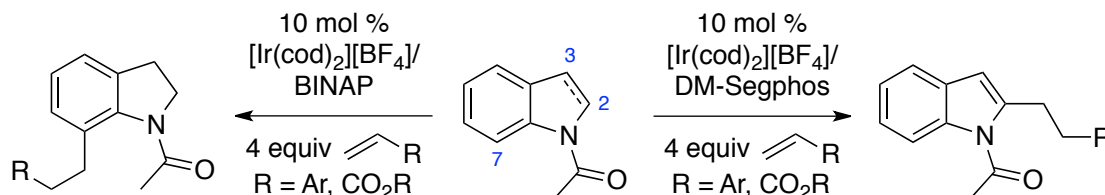
Directed hydroarylation reactions were applied to the alkylation of indoles. Substitution reactions generally occur at the nucleophilic C3 position of indole, and with few exceptions,[102-103] catalytic alkylation selectively at the C2 position of indole is challenging. Shibata and coworkers demonstrated the first catalytic alkylation of indole at the C2 position by C–H addition to an alkene (Scheme 10, left).[104] The acyl group not only protected the nitrogen atom, but served to direct C–H activation to the C2 position. A similar strategy can be applied for the alkylation of indol*ines* at the C7 position.[105] Oxidation of the alkylated indoline products yields C7-substituted-indoles, which are difficult to prepare by other methods (Scheme 10, right).[106]

1.7 Summary

Additions of C–H bonds of arenes to alkenes provides a direct route to alkylarenes and heteroarenes. Metal-catalyzed arene alkylations have been demonstrated to occur with regioselectivities that are complementary to those observed for acid-catalyzed reactions. Specifically, linear alkylarenes can be generated in preference to branched products, and asymmetric hydroarylations have been performed for intramolecular systems. Furthermore, the site of alkylation of an arene is not limited to the intrinsic electronic properties of the substrate under metal-catalyzed conditions.

Despite the progress that has been made in this field, *intermolecular* asymmetric hydroarylation reactions are limited. Furthermore, mechanistic data on hydroarylation reactions that occur by iridium I/III cycles are scarce. Detailed mechanistic studies have been conducted on the Periana complexes that catalyze anti-Markovnikov hydroarylation; however, these complexes are unlike most complexes that catalyze hydroarylation. Specifically, these complexes are in the +3 oxidation state throughout the catalytic cycle and mediate C–H activation through an oxidative hydrogen migration mechanism. Thus, it is unclear how barriers to elementary steps such as C–H oxidative addition, migratory insertion, and reductive elimination will be affected by complexes that can access +1/+3 oxidation states. Chapters 4 and 6 described our efforts toward the development of methods for iridium-catalyzed reactions of heteroarene C–H bonds with alkenes.

1.8 References

(1)   Johns, A. M.; Sakai, N.; Ridder, A.; Hartwig, J. F. *J. Am. Chem. Soc.*, **2006**, *128*, 9306.
(2)   Utsunomiya, M.; Kawatsura, M.; Hartwig, J. F. *Angew. Chem. Int. Ed.*, **2003**, *42*, 5865.
(3)   Sakai, N.; Ridder, A.; Hartwig, J. F. *J. Am. Chem. Soc.*, **2006**, *128*, 8134.
(4)   Löber, O.; Kawatsura, M.; Hartwig, J. F. *J. Am. Chem. Soc.*, **2001**, *123*, 4366.
(5)   Luo, Y. R. *Handbook of Bond Dissociation Energies in Organic Compounds*; Taylor & Francis, 2002.
(6)   Trost, B. M.; Fleming, I. *Comprehensive Organic Synthesis: Reduction*; Elsevier Science & Technology Books, 1991.
(7)   Schafer, L. L.; Yim, J. C. H.; Yonson, N. In *Metal-Catalyzed Cross-Coupling Reactions and More*; Wiley-VCH Verlag GmbH & Co. KGaA: 2014, p 1135.
(8)   Hannedouche, J.; Schulz, E. *Chem. Eur. J.*, **2013**, *19*, 4972.
(9)   Hesp, K. D.; Stradiotto, M. *Chemcatchem*, **2010**, *2*, 1192.
(10)   Müller, T. E.; Hultzsch, K. C.; Yus, M.; Foubelo, F.; Tada, M. *Chem. Rev.*, **2008**, *108*, 3795.
(11)   Müller, T. E.; Beller, M. *Chem. Rev.*, **1998**, *98*, 675.
(12)   Brunett, J. J.; Neibecker, D. In *Catalytic Heterofunctionalization. From Hydroamination to Hydrozirconation*; Togni, A., Grützmacher, H., Eds.; Wiley: New York, 2001, p 91.
(13)   Hartwig, J. F. In *Organotransition Metal Chemistry: From Bonding to Catalysis*; University Science Books: Sausalito, CA, 2010; Vol. 1, p 700.
(14)   Hong, S.; Marks, T. J. *Acc. Chem. Res.*, **2004**, *37*, 673.
(15)   Coulson, D. R. *Tetrahedron Lett.*, **1971**, *12*, 429.
(16)   Casalnuovo, A. L.; Calabrese, J. C.; Milstein, D. *Inorg. Chem.*, **1987**, *26*, 971.
(17)   Liu, G.; Stahl, S. S. *J. Am. Chem. Soc.*, **2007**, *129*, 6328.
(18)   Weinstein, A. B.; Stahl, S. S. *Angew. Chem. Int. Ed.*, **2012**, *51*, 11505.
(19)   White, P. B.; Stahl, S. S. *J. Am. Chem. Soc.*, **2011**, *133*, 18594.
(20)   Zhao, P.; Krug, C.; Hartwig, J. F. *J. Am. Chem. Soc.*, **2005**, *127*, 12066.
(21)   Neukom, J. D.; Perch, N. S.; Wolfe, J. P. *J. Am. Chem. Soc.*, **2010**, *132*, 6276.
(22)   Hanley, P. S.; Hartwig, J. F. *Angew. Chem. Int. Ed.*, **2013**, *52*, 8510.
(23)   Hanley, P. S.; Marković, D.; Hartwig, J. F. *J. Am. Chem. Soc.*, **2010**, *132*, 6302.
(24)   Hanley, P. S.; Hartwig, J. F. *J. Am. Chem. Soc.*, **2011**, *133*, 15661.

(25) Kanzelberger, M.; Zhang, X.; Emge, T. J.; Goldman, A. S.; Zhao, J.; Incarvito, C.; Hartwig, J. F. *J. Am. Chem. Soc.*, **2003**, *125*, 13644.

(26) Zhao, J.; Goldman, A. S.; Hartwig, J. F. *Science*, **2005**, *307*, 1080.

(27) Morgan, E.; MacLean, D. F.; McDonald, R.; Turculet, L. *J. Am. Chem. Soc.*, **2009**, *131*, 14234.

(28) Huang, Z.; Zhou, J.; Hartwig, J. F. *J. Am. Chem. Soc.*, **2010**, *132*, 11458.

(29) Sykes, A. C.; White, P.; Brookhart, M. *Organometallics*, **2006**, *25*, 1664.

(30) Casalnuovo, A. L.; Calabrese, J. C.; Milstein, D. *J. Am. Chem. Soc.*, **1988**, *110*, 6738.

(31) Dorta, R.; Egli, P.; Zürcher, F.; Togni, A. *J. Am. Chem. Soc.*, **1997**, *119*, 10857.

(32) Brunet, J.-J.; Commenges, G.; Neibecker, D.; Philippot, K. *J. Organomet. Chem.*, **1994**, *469*, 221.

(33) Brunet, J.-J.; Neibecker, D.; Philippot, K. *Journal of the Chemical Society, Chemical Communications*, **1992**, 1215.

(34) Aufdenblatten, R.; Diezi, S.; Togni, A. *Monat. für Chem.*, **2000**, *131*, 1345.

(35) Togni, A.; Dorta, R.; Kollner, C.; Pioda, G. *Pure Appl. Chem.*, **1998**, *70*, 1477.

(36) Pan, S. G.; Endo, K.; Shibata, T. *Org. Lett.*, **2012**, *14*, 780.

(37) Specht, Z. G.; Grotjahn, D. B.; Moore, C. E.; Rheingold, A. L. *Organometallics*, **2013**, *32*, 6400.

(38) Bauer, E. B.; Andavan, G. T. S.; Hollis, T. K.; Rubio, R. J.; Cho, J.; Kuchenbeiser, G. R.; Helgert, T. R.; Letko, C. S.; Tham, F. S. *Org. Lett.*, **2008**, *10*, 1175.

(39) Hesp, K. D.; McDonald, R.; Stradiotto, M. *Canadian Journal of Chemistry*, **2010**, *88*, 700.

(40) Kashiwame, Y.; Kuwata, S.; Ikariya, T. *Organometallics*, **2012**, *31*, 8444.

(41) Kashiwame, Y.; Kuwata, S.; Ikariya, T. *Chem. Eur. J.*, **2010**, *16*, 766.

(42) Tobisch, S. *Chem. Eur. J.*, **2012**, *18*, 7248.

(43) Hesp, K. D.; Stradiotto, M. *Org. Lett.*, **2009**, *11*, 1449.

(44) Hesp, K. D.; Tobisch, S.; Stradiotto, M. *J. Am. Chem. Soc.*, **2009**, *132*, 413.

(45) Eckert, M.; Fleischmann, G.; Jira, R.; Bolt, H. M.; Golka, K. In *Ullmann's Encyclopedia of Industrial Chemistry*; Wiley-VCH Verlag GmbH & Co. KGaA: 2000.

(46) Keith, J. A.; Henry, P. M. *Angew. Chem. Int. Ed.*, **2009**, *48*, 9038.

(47) Hayashi, T.; Yamasaki, K.; Mimura, M.; Uozumi, Y. *J. Am. Chem. Soc.*, **2004**, *126*, 3036.

(48) Trend, R. M.; Ramtohul, Y. K.; Stoltz, B. M. *J. Am. Chem. Soc.*, **2005**, *127*, 17778.

(49) Zhao, P.; Incarvito, C. D.; Hartwig, J. F. *J. Am. Chem. Soc.*, **2006**, *128*, 9642.

(50) Smith, M. B.; March, J. In *March's Advanced Organic Chemistry*; 5 ed.; John Wiley and Sons: New York, NY, 2001, p 996.

(51) Qian, H.; Han, X.; Widenhoefer, R. A. *J. Am. Chem. Soc.*, **2004**, *126*, 9536.

(52) Yang, C.-G.; He, C. *J. Am. Chem. Soc.*, **2005**, *127*, 6966.

(53) Rosenfeld, D. C.; Shekhar, S.; Takemiya, A.; Utsunomiya, M.; Hartwig, J. F. *Org. Lett.*, **2006**, *8*, 4179.

(54) Li, Z.; Zhang, J.; Brouwer, C.; Yang, C.-G.; Reich, N. W.; He, C. *Org. Lett.*, **2006**, *8*, 4175.

(55)   McKinney Brooner, R. E.; Widenhoefer, R. A. *Chem. Eur. J.*, **2011**, *17*, 6170.

(56)   Yang, C.-G.; Reich, N. W.; Shi, Z.; He, C. *Org. Lett.*, **2005**, *7*, 4553.

(57)   Weiss, C. J.; Marks, T. J. *Dalton Trans.*, **2010**, *39*, 6576.

(58)   Seo, S. Y.; Yu, X. H.; Marks, T. J. *J. Am. Chem. Soc.*, **2009**, *131*, 263.

(59)   Yu, X.; Seo, S.; Marks, T. J. *J. Am. Chem. Soc.*, **2007**, *129*, 7244.

(60)   Atesin, A. C.; Ray, N. A.; Stair, P. C.; Marks, T. J. *J. Am. Chem. Soc.*, **2012**, *134*, 14682.

(61)   Milstein, D.; Calabrese, J. C.; Williams, I. D. *J. Am. Chem. Soc.*, **1986**, *108*, 6387.

(62)   Blum, O.; Milstein, D. *Angewandte Chemie*, **1995**, *107*, 210.

(63)   Dorta, R.; Togni, A. *Organometallics*, **1998**, *17*, 3423.

(64)   Dorta, R.; Rozenberg, H.; Shimon, L. J. W.; Milstein, D. *J. Am. Chem. Soc.*, **2001**, *124*, 188.

(65)   Schaub, T.; Diskin-Posner, Y.; Radius, U.; Milstein, D. *Inorg. Chem.*, **2008**, *47*, 6502.

(66)   Kundu, S.; Choi, J.; Wang, D. Y.; Choliy, Y.; Emge, T. J.; Krogh-Jespersen, K.; Goldman, A. S. *J. Am. Chem. Soc.*, **2013**, *135*, 5127.

(67)   Choi, J.; Choliy, Y.; Zhang, X.; Emge, T. J.; Krogh-Jespersen, K.; Goldman, A. S. *J. Am. Chem. Soc.*, **2009**, *131*, 15627.

(68)   Haibach, M. C.; Guan, C.; Wang, D. Y.; Li, B.; Lease, N.; Steffens, A. M.; Krogh-Jespersen, K.; Goldman, A. S. *J. Am. Chem. Soc.*, **2013**, *135*, 15062.

(69)   Price, C. C. *Organic Reactions*, **1946**, *3*, 1.

(70)   Olah, G. A. *Friedel–Crafts Chemistry*; Wiley-Interscience: New York, NY, 1973.

(71)   Murai, S.; Kakiuchi, F.; Sekine, S.; Tanaka, Y.; Kamatani, A.; Sonoda, M.; Chatani, N. *Nature*, **1993**, *366*, 529.

(72)   Colby, D. A.; Bergman, R. G.; Ellman, J. A. *Chem. Rev.*, **2009**, *110*, 624.

(73)   Liu, G.; Wu, Y. In *C-H Activation*; Yu, J.-Q., Shi, Z., Eds.; Springer Berlin Heidelberg: 2010; Vol. 292, p 195.

(74)   Sonoda, M.; Kakiuchi, F.; Chatani, N.; Murai, S. *B. Chem. Soc. Jpn.*, **1997**, *70*, 3117.

(75)   Murai, S.; Chatani, N.; Kakiuchi, F. *Pure Appl. Chem.*, **1997**, *69*, 589.

(76)   Jia, C.; Piao, D.; Oyamada, J.; Lu, W.; Kitamura, T.; Fujiwara, Y. *Science*, **2000**, *287*, 1992.

(77)   Wilson, R. M.; Thalji, R. K.; Bergman, R. G.; Ellman, J. A. *Org. Lett.*, **2006**, *8*, 1745.

(78)   O'Malley, S. J.; Tan, K. L.; Watzke, A.; Bergman, R. G.; Ellman, J. A. *J. Am. Chem. Soc.*, **2005**, *127*, 13496.

(79)   Bergman, R. G. *Science*, **1984**, *223*, 902.

(80)   Crabtree, R. H. In *Iridium Catalysis*; Andersson, P. G., Ed.; Springer-Verlag Berlin: Berlin, 2011; Vol. 34, p 1.

(81)   Janowicz, A. H.; Bergman, R. G. *J. Am. Chem. Soc.*, **1982**, *104*, 352.

(82)   Janowicz, A. H.; Bergman, R. G. *J. Am. Chem. Soc.*, **1983**, *105*, 3929.

(83)   Krogh-Jespersen, K.; Czerw, M.; Summa, N.; Renkema, K. B.; Achord, P. D.; Goldman, A. S. *J. Am. Chem. Soc.*, **2002**, *124*, 11404.

(84)   Renkema, K. B.; Kissin, Y. V.; Goldman, A. S. *J. Am. Chem. Soc.*, **2003**, *125*, 7770.

(85)   Klei Steven, R.; Tan Kian, L.; Golden Jeffrey, T.; Yung Cathleen, M.; Thalji Reema, K.; Ahrendt Kateri, A.; Ellman Jonathan, A.; Tilley, T. D.; Bergman Robert, G. In *Activation and Functionalization of C?H Bonds*; American Chemical Society: 2004; Vol. 885, p 46.

(86)   Selnau, H. E.; Merola, J. S. *Organometallics*, **1993**, *12*, 3800.

(87)   Selnau, H. E.; Merola, J. S. *J. Am. Chem. Soc.*, **1991**, *113*, 4008.

(88)   Merola, J. S. *Organometallics*, **1989**, *8*, 2975.

(89)   Matsumoto, T.; Taube, D. J.; Periana, R. A.; Taube, H.; Yoshida, H. *J. Am. Chem. Soc.*, **2000**, *122*, 7414.

(90)   Foley, N. A.; Lee, J. P.; Ke, Z.; Gunnoe, T. B.; Cundari, T. R. *Acc. Chem. Res.*, **2009**, *42*, 585.

(91)   Andreatta, J. R.; McKeown, B. A.; Gunnoe, T. B. *J. Organomet. Chem.*, **2011**, *696*, 305.

(92)   Bischof, S. M.; Ess, D. H.; Meier, S. K.; Oxgaard, J.; Nielsen, R. J.; Bhalla, G.; Goddard, W. A.; Periana, R. A. *Organometallics*, **2010**, *29*, 742.

(93)   Bhalla, G.; Oxgaard, J.; Goddard, W. A.; Periana, R. A. *Organometallics*, **2005**, *24*, 3229.

(94)   Bhalla, G.; Bischof, S. M.; Ganesh, S. K.; Liu, X. Y.; Jones, C. J.; Borzenko, A.; Tenn, I. I. I. W. J.; Ess, D. H.; Hashiguchi, B. G.; Lokare, K. S.; Leung, C. H.; Oxgaard, J.; Goddard, I. I. I. W. A.; Periana, R. A. *Green Chem.*, **2011**, *13*, 69.

(95)   Oxgaard, J.; Bhalla, G.; Periana, R. A.; Goddard, W. A. *Organometallics*, **2006**, *25*, 1618.

(96)   Bhalla, G.; Oxgaard, J.; Goddard, W. A.; Periana, R. A. *Organometallics*, **2005**, *24*, 5499.

(97)   Dorta, R.; Togni, A. *Chem. Commun.*, **2003**, 760.

(98)   Pan, S.; Shibata, T. *ACS Catalysis*, **2013**, 704.

(99)   Tsuchikama, K.; Kasagawa, M.; Hashimoto, Y.-K.; Endo, K.; Shibata, T. *J. Organomet. Chem.*, **2008**, *693*, 3939.

(100)   Takebayashi, S.; Shibata, T. *Organometallics*, **2012**, *31*, 4114.

(101)   Shibata, T.; Shizuno, T. *Angew. Chem. Int. Ed.*, **2014**, n/a.

(102)   Jiao, L.; Herdtweck, E.; Bach, T. *J. Am. Chem. Soc.*, **2012**, *134*, 14563.

(103)   Jiao, L.; Bach, T. *J. Am. Chem. Soc.*, **2011**, *133*, 12990.

(104)   Pan, S.; Ryu, N.; Shibata, T. *J. Am. Chem. Soc.*, **2012**, *134*, 17474.

(105)   Pan, S.; Ryu, N.; Shibata, T. *Adv. Synth. Catal.*, **2014**, *356*, 929.

(106)   Robbins, D. W.; Boebel, T. A.; Hartwig, J. F. *J. Am. Chem. Soc.*, **2010**, *132*, 4068.

CHAPTER 2

Iridium-Catalyzed Intermolecular Hydroamination of
Unactivated Aliphatic Alkenes with Amides and Sulfonamides[1]

2.1 Introduction

Amine functionality is ubiquitous in biologically active and industrially useful molecules. Many strategies to form C–N bonds provide access to this functional group in fine chemical building blocks, pharmaceuticals, agrochemicals, solvents and surfactants. Classical methodologies for C–N bond formation involve reductive aminations of carbonyl compounds or substitution reactions of prefunctionalized aliphatic starting materials. An alternative, more synthetically efficient route to construct C–N bonds is the addition of an N–H bond across an unsaturated C–C bond, a transformation formally known as hydroamination. A majority of metal-catalyzed hydroamination are *intra*molecular, cyclizations of aminoalkenes to form amine heterocycles. Few complexes catalyze *inter*-molecular hydroamination of alkenes.[2-4]

With few exceptions,[5-9] intermolecular hydroaminations are limited to reactions of activated alkenes, such as bicycloalkenes,[10-12] 1,3-dienes,[13-14] allenes,[15-17] and vinylarenes,[18,5,19-20] or the unsubstituted ethylene.[21-22] Examples of intermolecular additions of N–H bonds across unactivated alkenes are rare, and additions of amides and sulfonamides to higher α-olefins are particularly unusual.[23-24] Here, we report a well-defined transition-metal complex that catalyzes the intermolecular hydroamination of unactivated alkenes with amides and sulfonamides to form *N*-alkyl amides and sulfonamides. The same system catalyzes additions of amides to norbornene and norbornadiene that are highly enantioselective. Mechanistic studies on these additions to unstrained and strained alkenes reveal the resting state of the catalyst and the turnover-limiting steps of the hydroamination processes.

2.2 Results and Discussions

Recent work in our laboratory has demonstrated the high activity and selectivity of bisphosphine-ligated iridium complexes for the intermolecular hydroamination of bicycloalkenes with arylamines.[11] On the basis of this observation, we sought to develop the catalytic addition of N–H bonds to unactivated alkenes with more versatile nitrogen donors, such as amides and sulfonamides, than had been added to unstrained alkenes previously.[5,8-9]

The combination of $[Ir(coe)_2Cl]_2$ and a series of bisphosphine ligands were tested as catalyst for the addition of 4-*tert*-butylbenzamide to 1-octene. The results are summarized in Table 2.1. Ir-complexes of aryl bisphosphines containing ethyl, propyl, and ferrocenyl backbones did not form active catalysts for the desired transformation (see the experimental section for the full ligand set). A small amount of product was observed for reactions catalyzed by complexes of methylene-bridged bisphosphines (entry 1), suggesting that a small bite angle in the ligand was important for generating an active catalyst.

A similar effect of the ligand bite angle on the yield of the catalytic reaction was observed for reactions catalyzed by iridium complexes of bisphosphine ligands containing biaryl backbones, and a survey of commercially available bisphosphines containing biaryl backbones led to a system that formed *N*-alkylamide and enamine products in high combined yield. Studies of ligands with varied dihedral angles of the ligand backbone showed that the yields were higher for reactions conducted with ligands having smaller dihedral angles (entries 2-4). An increase in the steric bulk from the parent Segphos ligand to the DTBM-Segphos (DTBM=3,5-di-*tert*-butyl-4-methoxy) derivative led to an increase in yield of addition products. Furthermore, the lipophilicity of the *tert*-butyl

23

groups imparted greater solubility of the catalyst in the alkene. An excess of the a-olefin was required to affect the transformation in high yield. Low conversion to the alkylamide and alkyl enamide products was observed with one equivalent of 1-octene to the amide catalyzed by the iridium catalyst ligated by DTBM-Segphos. Ultimately, reaction of the benzamide with 20 equiv of the alkene formed the hydroamination product in 56% yield and the corresponding enamide in 40% yield. The alkene is the terminal reductant for the enamide side product; the corresponding alkane was also formed in 40% yield.

Table 2.1. Reaction development for the Ir-catalyzed intermolecular addition of 4-*tert*-butylbenzamide to 1-octene[a]

entry	ligand	1-octene equiv	temp (°C)	% yield[b] 7+7a	ratio[b] (7/7a)
1	dcpm[c]	5	120	8	(12)
2	(R)-DM-BINAP	5	120	2	(4.1)
3	(R)-DM-MeOBIPHEP	5	120	12	(1.8)
4	(S)-DM-SEGPHOS[d]	5	120	18	(2.0)
5	(R)-DTBM-MeOBIPHEP	5	120	28	(1.9)
6	(S)-DTBM-SEGPHOS[e]	5	120	44	(1.9)
7	(S)-DTBM-SEGPHOS	1	120	13	(3.3)
8	(S)-DTBM-SEGPHOS	20	120	74	(1.3)
9	(S)-DTBM-SEGPHOS	20	100	47	(1.8)
10	(S)-DTBM-SEGPHOS	20	140	96	(1.4)

[a]Reactions were performed neat in 1-octene with 0.1 mmol 4-tert-butylbenzamide. [b]Yields and conversions were determined by GC analysis with dodecane as an internal standard. [c]dcpm = bis(dicyclohexylphosphino)methane. [d]DM = 3,5-dimethylphenyl. [e]DTBM = 3,5-di-tert-butyl-4-methoxyphenyl.

To generate a single amination product, the enamide was reduced to the alkyla-mide by subjecting the crude reaction mixture to 1 atm of H_2 or an excess of isopropanol after the amination process. Thus, a one-pot reaction workup with isopropanol formed the saturated product exclusively and in high yield. The alkylamide products were formed with low 10-19% ee, but these measurable values do rule out hydroamination of the alkene by a proton-catalyzed process alone.[23-24] Moreover, the enamide product was found to be stable to the catalytic conditions indicating that the stereogenic center of the N-alkyl-amide is set by the C–N bond-forming step rather than an asymmetric hydrogenation an enamide intermediate.

The scope of the Ir-catalyzed addition of amides to unactivated α-olefins by this procedure is summarized in Table 2.2. Following a one-pot reductive workup, high yields were obtained from reactions of the arylamides possessing electron-donating and elec-

tron-withdrawing aryl substituents. Products of more hindered alkenes were formed in slightly lower yields than those of less hindered alkenes, but in substantial yields. Finally, additions of sulfonamides occurred without alkene isomerization to form the Markovnikov product in high yield.

Table 2.2. Ir-catalyzed intermolecular addition of amides and sulfonamides to unactivated α-olefins[a]
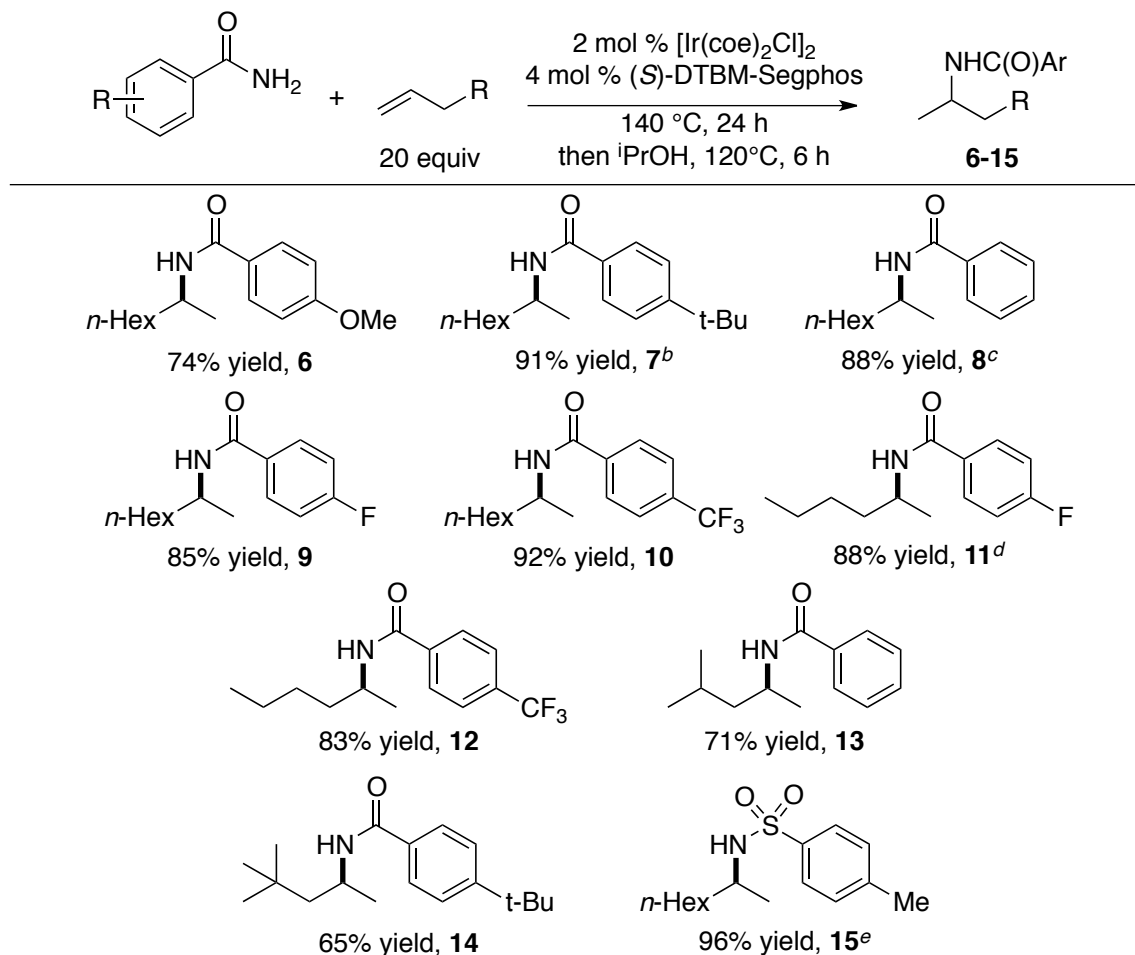
[a]Reactions were performed neat in 20 equiv of alkene with 0.3 mmol amide or sulfonamide. Reported yields are isolated yields following a reductive workup with isopropanol. ee was determined by chiral HPLC analysis prior to reductive workup. [b]12% ee. [c]13% ee. [d]19% ee. [e]12% ee.

Table 2.3. Ir-catalyzed enantioselective intermolecular addition of amides and sulfonamides to norbornene[a]

entry	product	% yield	% ee
16		85	91
17		88	92
18		91	92
19		93	92
22		93	92

[a]Reactions were performed with 0.3 mmol amide or sulfonamide and 4.0 equivalents of **nbe**. Reported yields are isolated yields. ee was determined by chiral HPLC analysis.

The scope of this methodology also encompasses the addition of N–H bonds of amides and sulfonamides to bicycloalkenes. As shown in Tables 2.3 and 2.4, products of the reactions of norbornadiene (**nbd**) and norbornene (**nbe**) with arylamides and tosylamide were formed in high yield and ee. These types of amides added to **nbd** in slightly lower yields than to **nbe**, but with ee's that were similar to those for the reactions with **nbe**. The catalytic process proceeds with excellent diastereoselectivity to form the mono-alkylated *exo* product.

26

Table 2.4. Ir-catalyzed enantioselective intermolecular addition of amides nor-bornadiene[a]

entry	product	% yield	% ee
20		76	91
21		79	93

[a]Reactions were performed with 0.3 mmol amide and 1.2 equivalents **nbd**. Reported yields are isolated yields. ee was determined by chiral HPLC analysis.

These enantioenriched amide products were elaborated through single-step synthetic transformations to important enantioenriched building blocks. Ring opening metathesis of **20** with ethylene forms the highly functionalized cyclopentylamide as a single diastereomer with no erosion of ee (eq 2.1). Alternatively, hydrolysis of amide **16** led to the 2-norbornylamine building block with no erosion of the ee (eq 2.2). Much effort has been spent to form norbornylamine by a catalytic process in enantioenriched form,[25] and this hydroamination provides the most direct route. The absolute stereochemistry of the amide was determined by optical rotation of the 2-aminonorbornane to be the 2*R* enantiomer. These results constitute the first intermolecular asymmetric hydroamination of an alkene with amides and sulfonamides in high yield and ee.

(2.1)

20, 93% ee   93% ee

(2.2)

16, 91% ee   91% ee
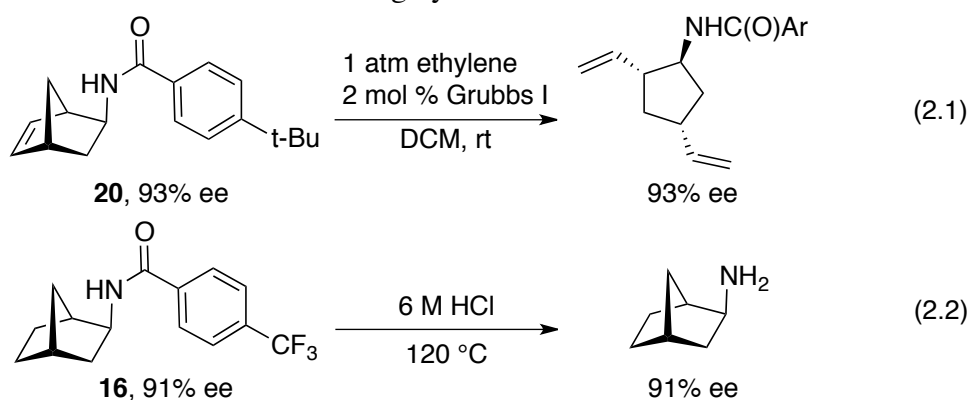
This catalytic process proved amenable to mechanistic studies. The combination of [Ir(coe)$_2$Cl]$_2$, 4-CF$_3$-benzamide and DTBM-Segphos formed a clear solution (from the initial orange solution) within 15 min at room temperature (Figure 2.1a). A similar color change was observed at the start of the catalytic reaction. This finding suggested that the catalyst resting state did not contain an alkene.

27

The structure of the complex formed from the amide, ligand and iridium was determined by X-ray diffraction (Figure 2.1b) and solution NMR spectroscopy. This complex results from oxidative addition of the N–H bond of the amide and coordination of a second amide to iridium through an unusual M–N dative bond. The assignment of the amide and amidate ligands of **1** was based on the difference between the two Ir–N bond lengths (2.076 Å for the amidate and 2.117 Å for the amide) and the Ir-N-C-O dihedral angle. The group assigned as a bound amide has a larger Ir–N–C–O dihedral angle (22°) than that of the nearly planar amidate (5°) because of the absence of a free lone pair to interact with the carbonyl group. The ^{31}P and ^{19}F NMR resonances of **1** matched the respective resonances of the complex that was formed in the catalytic reaction at room temperature and 50 °C. Thus, **1** is the resting state of the catalyst in these additions of amides to alkenes.
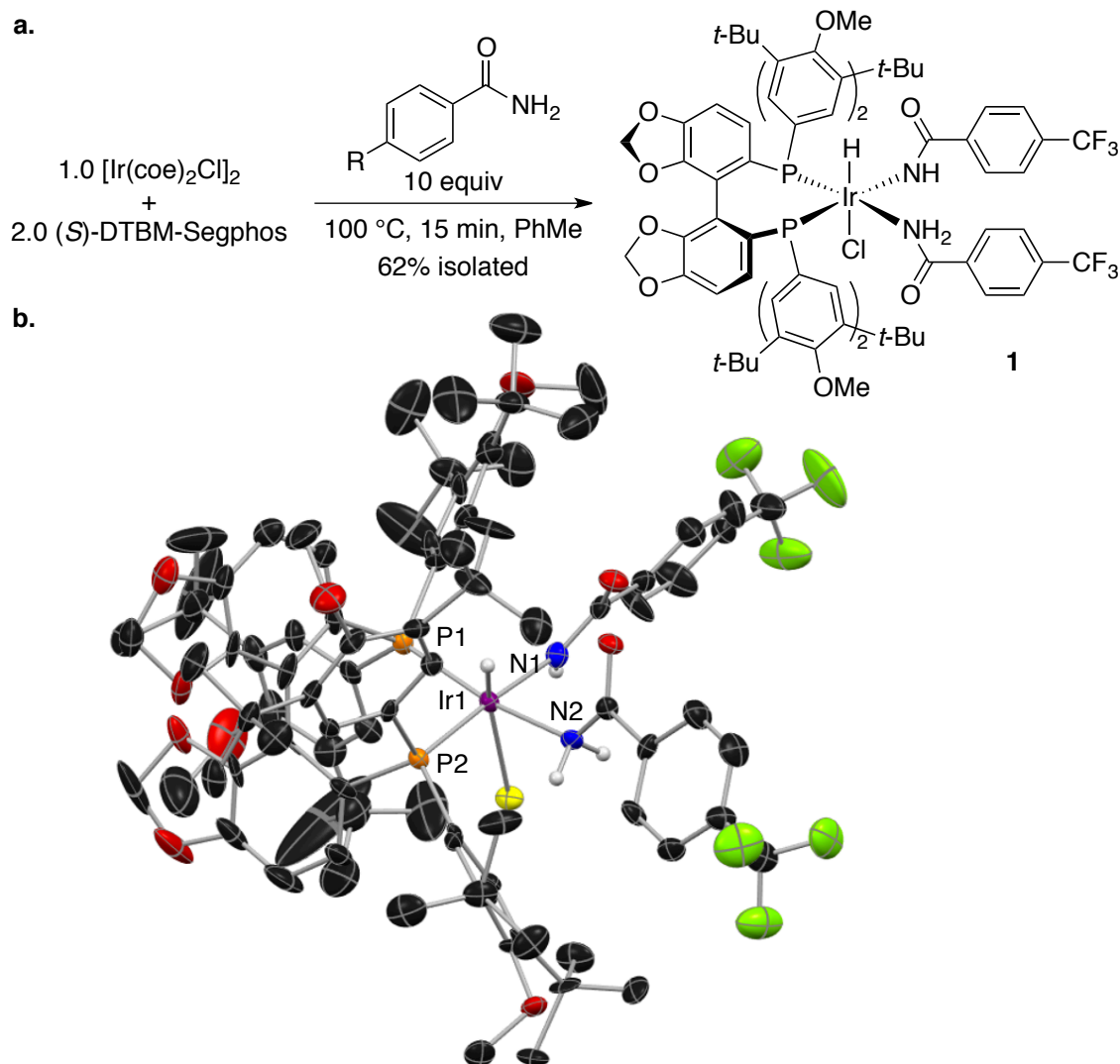
Figure 2.1. a. Synthesis of complex **1**. b. X-ray structure of **1**.

Scheme 2.1. Stoichiometric reaction of complex 1 with norbornene.

1
0.015 M

0.10 M

PhMe, 93 °C
1 h

0.028 M (both amides react)

Stoichiometric (93 °C): $k_{obs}=7\times10^{-6}$ M/s
96% yield, 94% ee
Catalytic (120 °C): $k_{obs}=6\times10^{-7}$ M/s
85% yield, 93% ee
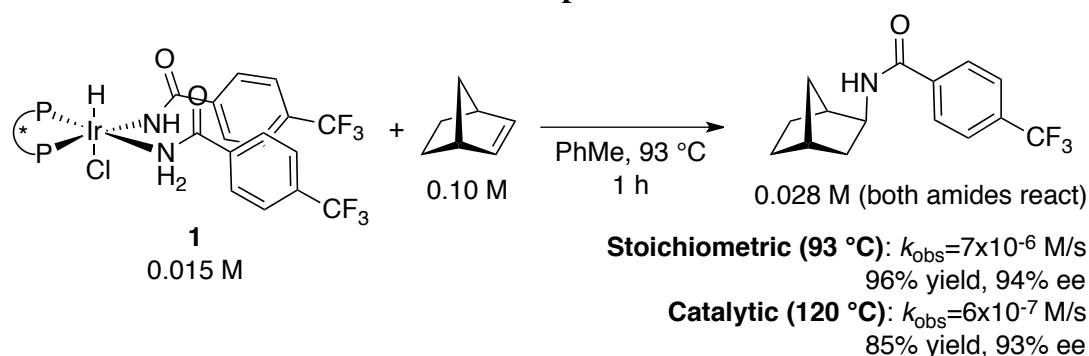
To determine if the observed complex is competent to be an intermediate in the catalytic reaction, a stoichiometric amount of **1** was subjected to a tenfold excess of **nbe** (Scheme 2.1). After 1 h at 93 °C – a time that is much shorter and a temperature that is lower than those of the catalytic process – complete consumption of the complex was observed. *N*-Norbornyl amide **16** was formed in 94% yield, based on consumption of both amides in the complex. The ee of **16** was similar to those of the catalytic process. Therefore, complex **1** is kinetically competent to be an intermediate in the catalytic cycle.

a.

b.
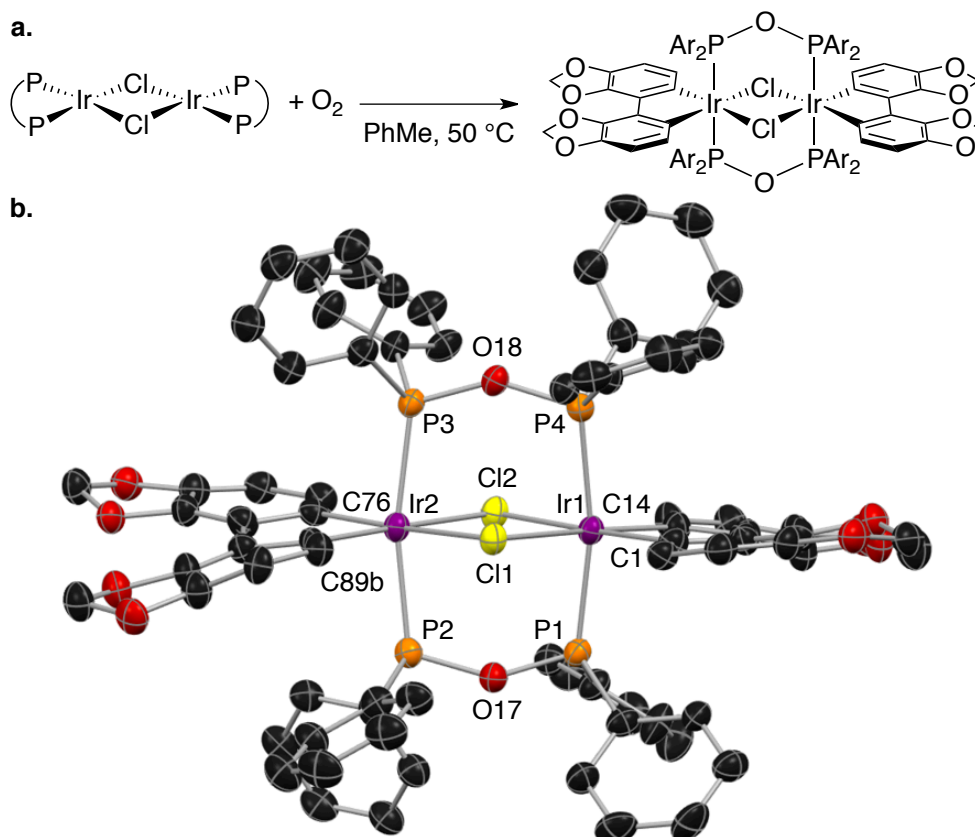
Figure 2.2. a. Synthesis of decomposition product **23**. b. X-ray structure of **23**.

Amidate complex **1** is stable to moisture but reacts rapidly with oxygen over the course of 2 h at room temperature to form complex **23** (Figure 2.2). This dimeric iridium

complex is the result of a formal oxidation of two Ir(I) centers to two Ir(III) centers by oxidative addition of the P–C bond of the ligand and subsequent P–O–P bond formation. This complex was prepared in the absence of amide with the simple bisphosphine iridium chloride precursor in the presence of air (Figure 2.2a). Complex **23** was tested catalyst for the addition of benzamide to 1-octene but no products were observed.

Kinetic measurements of the catalytic reaction as a function of the concentration of substrates were performed. The reactions were conducted with 2 mol % of isolated **1** at 100 °C, and initial rates (to 15% conversion) were measured by GC (see the experimental section). An inverse first-order dependence of the rate on the concentration of amide was observed. This order implies that the amide ligand dissociates reversibly prior to the turn-over-limiting step (TLS). These data are consistent with the observed differences in rate of stoichiometric reaction of complex **1** with octene and in rate of hydroamination with **1** as catalyst (Scheme 2.1). Under catalytic conditions, the concentration of amide is much greater than under stoichiometric reaction conditions, resulting in slower reaction rates for catalytic reactions. This system is, therefore, an unusual example of a catalytic process that is inverse-order in a reactant.[26-29] A first-order dependence of the rate on the concentration of 1-octene was observed, indicating that olefin coordination occurs before the TLS.
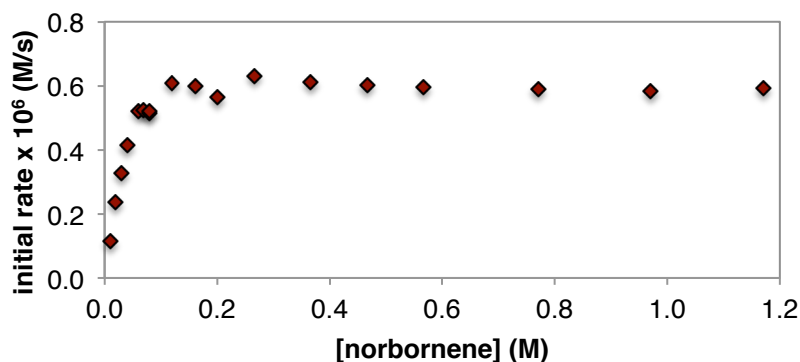
Figure 2.3. Plot of initial rate vs [**nbe**] for the addition of 4-trifluoromethylbenzamide to **nbe** catalyzed by **1**. Data for reactions with varied [trifluoromethylbenzamide] are included in the experimental section.

In contrast, the rate of the reaction was independent of the concentration of **nbe** under the standard catalytic conditions. A plot of the initial rate vs the concentration of **nbe** shows that the value of the rate saturates at high [**nbe**] (Figure 2.3). The reaction is first-order in **nbe** at low concentrations and zero order at high concentrations of the alkene. No intermediate that might contain the alkene was observed during these reactions. At high [**nbe**] (0.5 M), under which conditions the reaction is zero-order in alkene, the reaction is inverse first-order in amide. These data indicate that the amide amidate complex **1** undergoes reversible dissociation of the amide, followed by a turnover-limiting intramolecular rearrangement prior to reacting with the alkene.
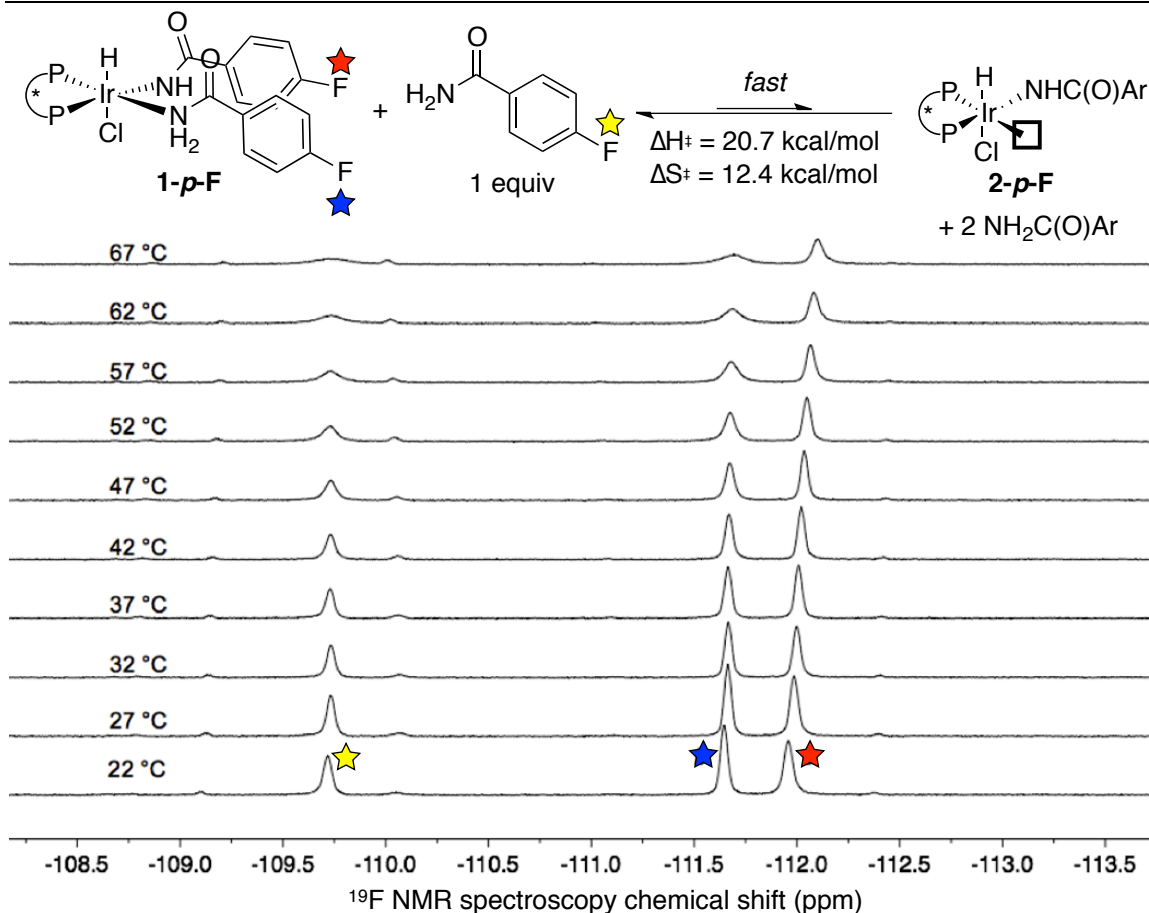
Figure 2.4. Variable temperature ^{19}F NMR spectra of 1-*p*-F with added 4-fluorobenzamide.

To gain information on the dynamics of complex **1**, we conducted variable-temperature (VT) NMR spectroscopy on a *p*-fluorobenzamide analogue of **1** (**1-*p*-F**). Spectra with added 4-fluorobenzamide were most informative (Figure 2.4). The ^{19}F NMR spectrum of the combination of **1-*p*-F** and one equiv of added amide contained three distinct ^{19}F NMR resonances for the amide and amidate ligands and for the free amide. Exchange between the free amide (yellow-labeled signal) and the datively bound amide (blue-labeled signal) was observed between room temperature and 60 °C; the for amidate ligand (red-labeled signal) remained unchanged in this regime. NMR exchange spectroscopy (EXSY) of the exchanging ligands was conducted by monitoring the ^{19}F resonances of the fluorine-labeled ligands. As confirmed by Figure 2.5, exchange only occurs between the dative ligand and the free amide in solution. Additional analysis of these ^{19}F-^{19}F NMR EXSY data reveals that the amidate ligand does not isomerize to the open coordination site of **2-*p*-F.** This is confirmed because the phosphine is chiral and the two coordination sites are diastereotopic. Consequently, exchange of the amidate ligand would be observed if the covalent amidate was interchanging between the two open coordination sites. Because no exchange crosspeaks are observed, the five-coordinate intermediate **2-*p*-F** formed by amide dissociation is stereochemically rigid on the NMR timescale below 60 °C.
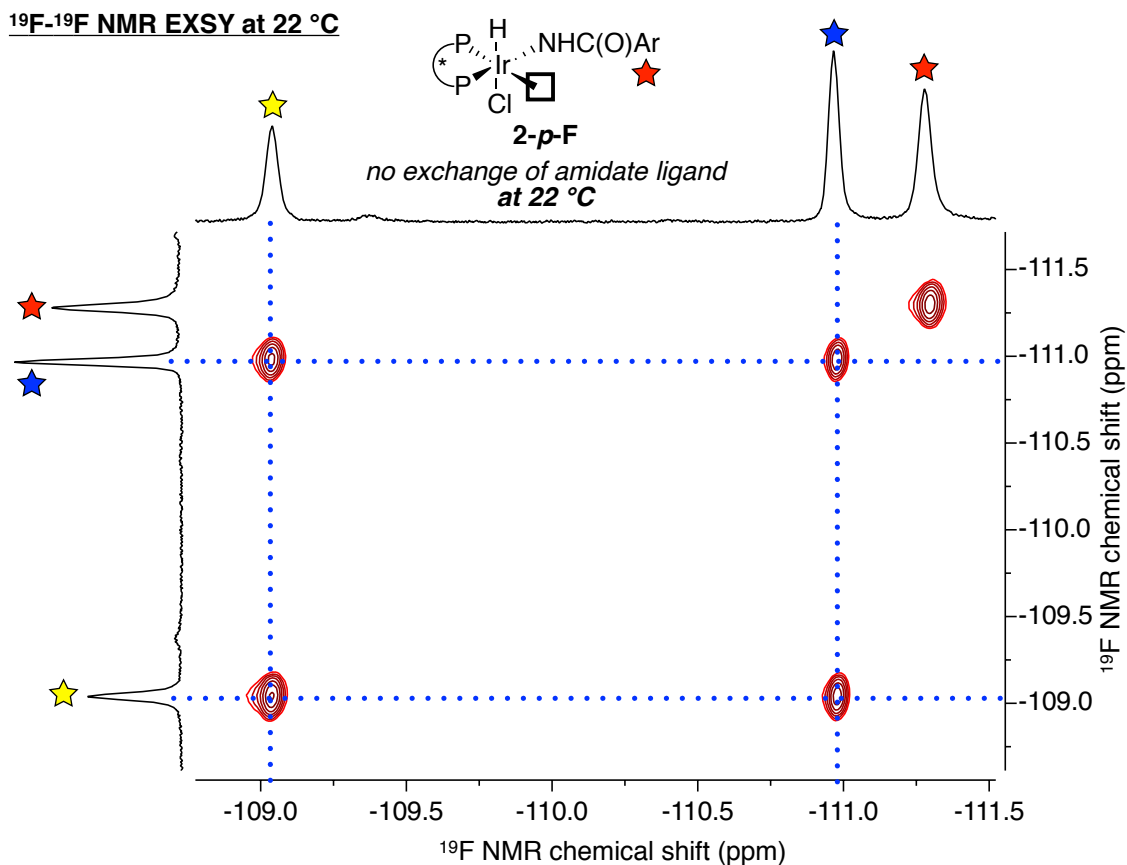
Figure 2.5. ^{19}F-^{19}F NMR EXSY of **1-p-F** at 22 °C.

Above 60 °C, the resonance for the amidate ligand (yellow-labeled signal) broadened, and VT NMR EXSY experiments confirmed that exchange occurred between the amide and amidate ligands as illustrated in Figure 2.6. The reversible dissociation of the amide is consistent with the inverse first-order dependence of the rate on the amide. Lineshape analysis on resonance *a* showed that the activation parameters for ligand dissociation from **2-p-F** are $\Delta H^{\ddagger} = 20.7$ kcal/mol and $\Delta S^{\ddagger} = 12.4$ eu. This positive entropy is consistent with a dissociative process.

¹⁹F-¹⁹F NMR EXSY at 72 °C
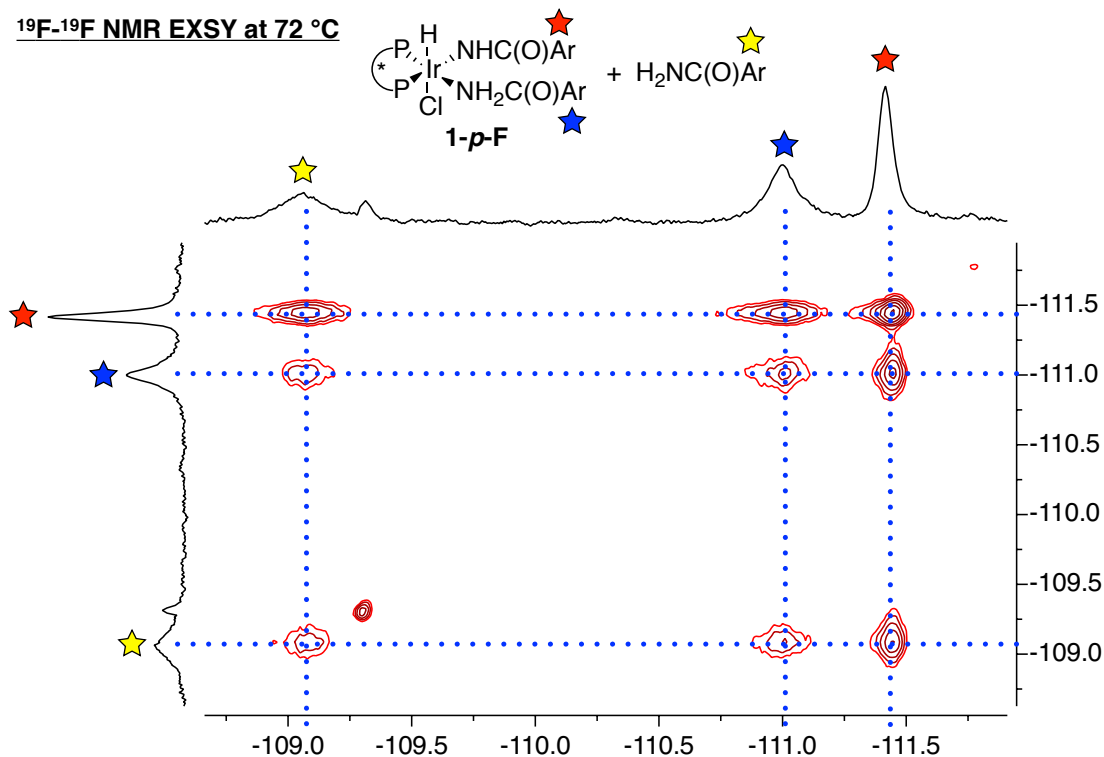
Figure 2.6. ¹⁹F-¹⁹F NMR EXSY of **1-*p*-F** at 72 °C.

The mechanism of exchange between the dative amide and covalent amidate ligands in the two diastereotopic binding sites was studied by variable temperature ¹H NMR spectroscopy. One common mechanism for ligand exchange is reversible reductive elimination/oxidative addition to the inequivalent coordination sites (eq 2.3). Under this mechanism, the hydride resonance would coalesce with the free amide N–H resonance (Δppm = 26 ppm). The mechanism illustrated in equation 2.3 was ruled out because the chemical shift of the hydride remains unchanged at temperatures that support rapid ligand exchange (Figure 2.7). These data indicate that the hydride does not exchange with free amide. A mechanism that does not contradict these data is proton transfer either directly between the amide and amidate ligands or mediated by free amide in solution (eq 2.4).

$$(2.3)$$

$$(2.4)$$

33

¹H NMR: 72 °C

¹H NMR: 22 °C Ir–H resonance of

H
|
P,,, | ,,\NHC(O)Ar
(* ␣Ir␣
P␣ | ␣NH₂C(O)Ar
Cl

1-*p*-F

| -17.5 | -18.0 | -18.5 | -19.0 | -19.5 | -20.0 | -20.5 |
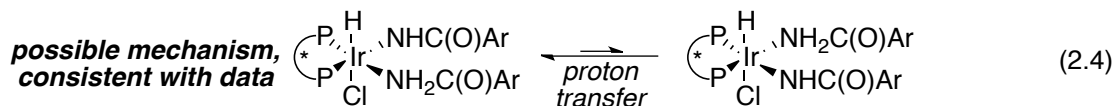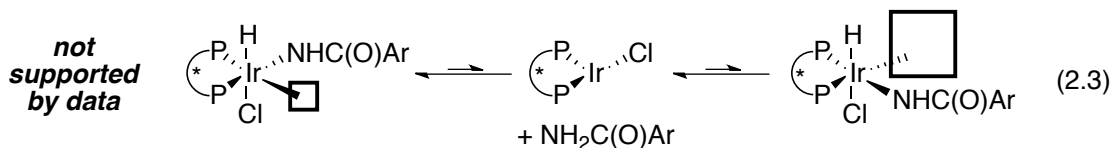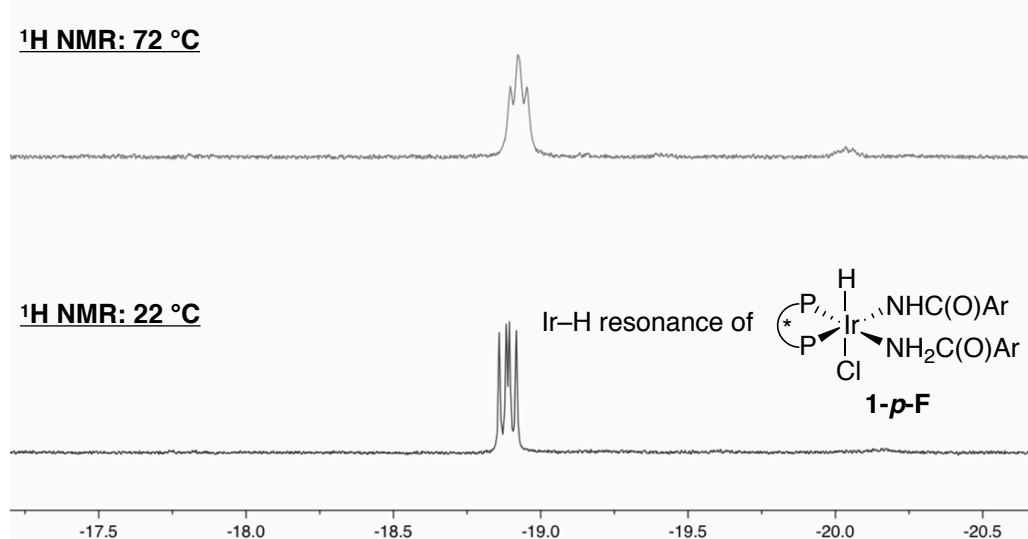
Figure 2.7. ¹H NMR spectroscopy chemical shift of the Ir-hydride resonance under conditions in which the amidate ligand undergoes exchange (72 °C, top) and no exchange (22 °C, bottom)

A consideration of the steric effects of the DTBM-Segphos ligand on the sites of amide and amidate ligands helps rationalize the preference for ligation of the amidate to one of the two diastereotopic coordination sites. The bulky aryl groups on the phosphorus atom in the chiral, C_2-symmetric ligand that is cis to the dative amide ligand (P2) both project toward the coordination site (Figure 2.8b). This steric demand of one phosphino group contrasts the antipodal orientation of the aryl groups on the other phosphorus atom, which is located cis to the covalent amidate ligand (P1). One aryl substituent of this group projects toward the coordination site of the amidate ligand, whereas the other aryl group occupies space away from the amide and amidate ligands. The C_1-symmetric quadrant diagram for **1** (Figure 2.8a) deviates from the classical C_2-symmetric quadrant diagram for BINAP-ligated complexes.[30] This difference in ligand coordination can be attributed to the different steric properties of the axial ligands (H vs. Cl).
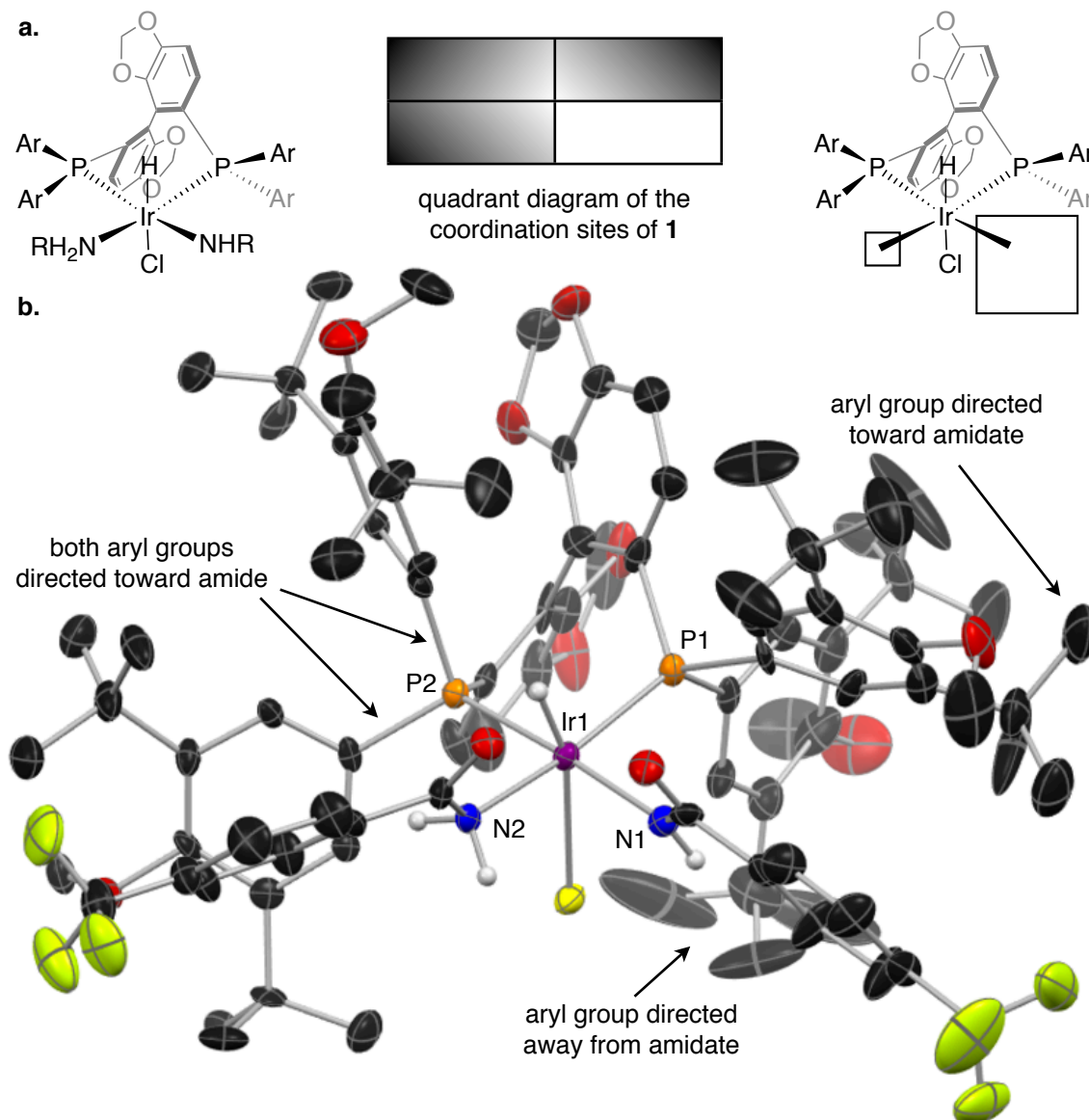
Figure 2.8. (a) Illustration of the steric interactions of the amide/amidate with the ligand and a quadrant diagram of the two coordination sites to which substates bind. (b) X-ray structure of **1** that highlights steric interactions of the ligand and bound substrates.

These conclusions are summarized as a proposed catalytic cycle in Scheme 2.2. Oxidative addition of the N–H bond of an arylamide to a bisphosphine iridium(I) complex forms the catalyst resting state. Reversible dissociation of the dative amide ligand occurs to generate a complex in which the amidate ligand occupies the most open coordination site. An intramolecular reorganization then precedes coordination of the alkene. This reorganization likely involves either migration of the amidate ligand to form the less stable isomer **4** containing a more open coordination site or a shift of the amidate from a κ^2 binding mode in an 18-electron intermediate to a κ^1 binding mode in a 16-electron intermediate. Coordination and insertion of the alkene into the Ir–N bond would then occur to form the alkyl iridium hydride **5**. This complex undergoes competitive C–H bond-

35

forming reductive elimination to form the *N*-alkyl amide and *β*-hydride elimination to form the enamide.

Scheme 2.2. Proposed catalytic cycle for the Ir-catalyzed N–H bond addition of arylamides to *α*-olefins.
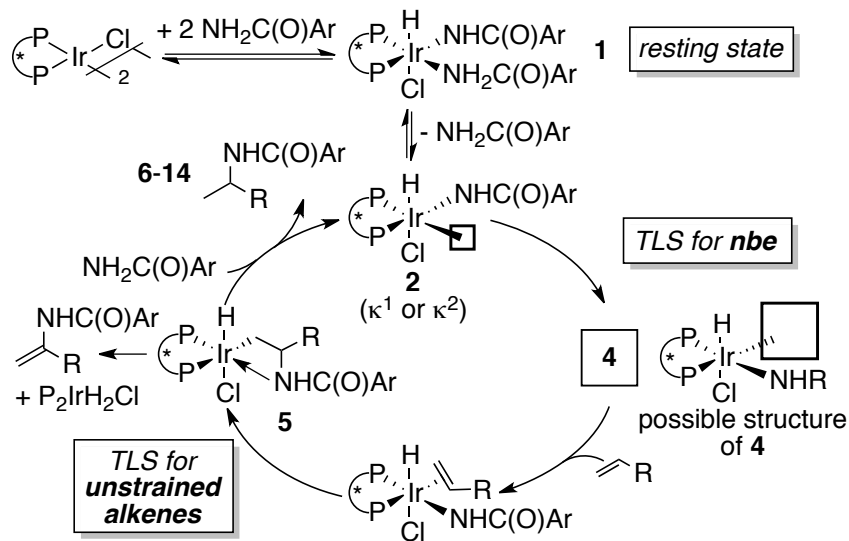
2.3 Conclusions and Future Directions

In conclusion, we have discovered a rare example of a catalytic process for the addition of amides and sulfonamides to unactivated alkenes and have identified the resting state of the catalyst and the components in the intermediate that adds the alkene. This methodology includes iridium-catalyzed reactions of bicycloalkenes with amides and sulfonamides to form products in high yield and ee. The resting state of the Ir-catalyzed hydroamination reaction was determined to result from oxidative addition of an N–H bond and coordination of an amide. Finally, kinetic data indicate that a kinetically detectable reorganization of the species formed by amide dissociation precedes alkene binding and insertion. Studies to further increase the reaction scope and to develop enantioselective additions to unstrained alkenes are in progress.

2.4 Experimental: General Remarks.

Unless noted otherwise, all manipulations were performed in a nitrogen-filled glovebox. Glassware was dried at 130 °C for at least 4 hours before use. Pentane, Et$_2$O, THF, and toluene were collected from a solvent purification system containing a 0.33 m column of activated alumina under nitrogen. Benzene-d_6 was degassed and subjected to 4 Å molecular sieves for at least 4 hours prior to use. All reagents were purchased from commercial suppliers, stored in the glove box and used as received. [Ir(coe)$_2$Cl]$_2$ was prepared following a published procedure.[31] Bisphosphine ligands were purchased from Strem Chemical Co. and used as received.

^{1}H NMR spectra were obtained at 500 MHz or 600 MHz, and chemical shifts were recorded relative to protiated solvents (CHCl$_3$ in CDCl$_3$: δ7.27 ppm; C$_6$H$_n$D$_{6-n}$ in C$_6$D$_6$: δ7.15 ppm) with a 45° pulse and a 10 s delay time.^{13}C NMR spectra were obtained at 126 MHz or 151 MHz on a 500 MHz or 600 MHz instrument, respectively. ^{31}P NMR spectra

were obtained at 202.2 MHz on a 500 MHz instrument and chemical shifts were reported in parts per million downfield of 85% H_3PO_4. ^{19}F NMR spectra were referenced to an external standard of $CFCl_3$. Probe temperatures for variable temperature NMR experiments were measured by ^1H shifts of neat ethylene glycol. Proof of purity is demonstrated by elemental analysis and by copies of NMR spectra. Chiral HPLC analysis was conducted on a Waters chromatography system with a dual wavelength detector at 220 and 254 nm. GC analysis was performed on an Agilent 7890 GC equipped with an HP-5 column (25 m x 0.20 mm x 0.33 µm film) and an FID detector. Quantitative GC analysis was performed by adding dodecane as an internal standard to the reaction mixture upon completion of the reaction. Response factors for the products relative to the internal standard were measured for kinetic studies and reaction development studies. GC-MS data were obtained on an Agilent 6890-N GC system containing an Alltech EC-1 capillary column and an Agilent 5973 mass selective detector.

Table 2.5. Full set of ligands evaluated with [Ir(coe)$_2$Cl]$_2$ as catalyst for the ligand set for the addition of 4-*tert*-butylbenzamide to 1-octene.

entry	ligand	equiv octene	temp (°C)	% yield 7a+7b	ratio 7a/7b	% ee
1	dppm	5	120	3	--	--
2	dcpm	5	120	8	12	--
3	dppe	5	120	0	--	--
4	dppp	5	120	0	--	--
5	dppf	5	120	0	--	--
6	tol-DPEphos	5	120	0	--	--
7	tBu-Xantphos	5	120	0	--	--
8	(R)-JOSIPHOS	5	120	0	--	--
9	(R)-DM-BINAP	5	120	2	4.1	--
10	(R)-DM-MeOBIPHEP	5	120	12	1.8	--
11	(S)-DM-SEGPHOS	5	120	18	2.0	--
12	(R)-DTBM-MeOBIPHEP	5	120	28	1.9	10
13	(S)-DTBM-SEGPHOS	5	120	44	1.9	--
14	(S)-DTBM-SEGPHOS	1	120	13	3.3	--
15	(S)-DTBM-SEGPHOS	20	120	74	1.3	15
16	(S)-DTBM-SEGPHOS	20	100	47	1.8	19
17	(S)-DTBM-SEGPHOS	20	140	96	1.4	12

[a]Yields were determined by GC analysis with dodecane as an internal standard. [b]ee's were measured by HPLC analysis with a chiral column stationary phase.

General Procedure A: Ir-catalyzed addition of arylamides and sulfonamides to α-olefins.

In a nitrogen-filled dry-box, an oven dried 4 ml screw-capped vial was charged with [Ir(coe)$_2$Cl]$_2$ (5.4 mg, 0.0060 mmol), (S)-DTBM-SEGPHOS (14 mg, 0.012 mmol), and the corresponding arylamide or sulfonamide (0.30 mmol). THF (0.50 ml) was added to these solids, and the mixture was stirred vigorously for 30 min. An orange homogenous solution immediately formed, and the color of this solution gradually became a pale yellow. The magnetic stirbar was removed from the solution, and THF was evaported under vacuum over 30 min. To the pale yellow solid was added the corresponding alkene (6.0 mmol), and the magnetic stirbar was returned to the vial. The vial was sealed tightly with a Teflon cap and removed from the dry-box. The reaction mixture was stirred in an aluminum heating block at 140 °C for 24 h and then cooled to room temperature. The reaction vial was taken into the dry-box where the excess alkene was evaporated under vacuum. The vial with the resulting residue was removed from the dry-box, and to the vial was added 2.0 ml of isopropanol under a cone of nitrogen gas. The vial was closed with a screw cap and placed in a 120 °C heating block for 6 h. The solution was cooled, and the isopropanol was removed by rotary evaporation. The residue was dry loaded onto Silacycle Siala-P60 silica gel (1.0 g). The product was purified by flash chromatography on a column (height = 20. cm, diameter = 3.0 cm) of Silacycle Siala-P60 silica gel (55 g). The conditions for chromatography and other data that are specific to each compound are given below.

4-Methoxy-*N*-(octan-2-yl)benzamide
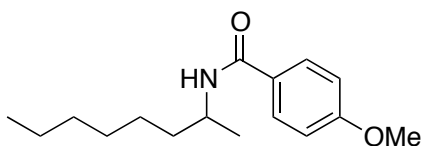
Following the general procedure **A** described above, 4-methoxybenzamide (45 mg, 0.30 mmol) was allowed to react with 1-octene (0.94 ml, 6.0 mmol). The crude material was purified by chromatography with 14% EtOAc in hexanes. The solvent was evaporated to yield the title compound as a white solid (58 mg, 74% yield).

^{1}H NMR (600 MHz, CDCl$_3$): δ 7.72 (d, *J* = 8.8 Hz, 2H), 6.99-6.83 (m, 2H), 5.91 (d, *J* = 8.0 Hz, 1H), 4.27-4.08 (m, 1H), 3.83 (s, 3H), 1.58-1.45 (m, 2H), 1.38-1.22 (m, 8H), 1.20 (d, *J* = 6.6 Hz, 3H), 0.86 (t, *J* = 6.9 Hz, 3H).

^{13}C NMR (151 MHz, CDCl$_3$): δ 166.3, 161.9, 128.6, 127.3, 113.6, 55.3, 45.6, 37.1, 31.7, 29.2, 26.1, 22.6, 21.1, 14.0.

Anal. Calcd for C$_{16}$H$_{25}$NO$_2$: C 72.96%, H 9.57%, N 5.32%; Found: C 73.04%, H 9.51%, N 5.67%.

4-(*tert*-Butyl)-*N*-(octan-2-yl)benzamide

Following the general procedure **A** described above, 4-*tert*-butylbenzamide (53 mg, 0.30 mmol) was allowed to react with 1-octene (0.94 ml, 6.0 mmol). The crude material was purified by chromatography with 12% EtOAc in hexanes. The solvent was evaporated to yield the title compound as a white solid (78 mg, 91% yield).

¹H NMR (600 MHz, CDCl₃): δ 7.70 (d, *J* = 8.2 Hz, 2H), 7.42 (d, *J* = 8.3 Hz, 2H), 6.03 (d, *J* = 8.0 Hz, 1H), 4.17 (m, 1H), 1.60-1.44 (m, 2H), 1.40-1.23 (m, 17H), 1.21 (d, *J* = 6.5 Hz, 3H), 0.86 (t, *J* = 6.7 Hz, 3H).

¹³C NMR (151 MHz, CDCl₃): δ 166.7, 154.6, 132.2, 126.7, 125.4, 45.6, 37.1, 34.8, 31.8, 31.1, 29.2, 26.1, 22.6, 21.1, 14.1.

HPLC analysis: 12% ee, Chiralcel OD-H column, 1% isopropanol in hexane, 0.5 mL/min flow rate 220 nm UV lamp, t[major] = 54.1 min, t[minor] = 59.0 min.

Anal. Calcd for $C_{19}H_{31}NO$: C 78.84%, H 10.79%, N 4.84%; Found: C 78.82%, H 10.72%, N 4.75%.

N-(Octan-2-yl)benzamide
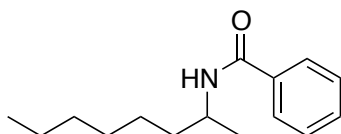
Following the general procedure **A** described above, ben-zamide (36 mg, 0.30 mmol) was allowed to react with 1-octene (0.94 ml, 6.0 mmol). The crude material was purified by chromatography with 14% EtOAc in hexanes. The sol-vent was evaporated to yield the title compound as a white solid (61.5 mg, 88% yield).

¹H NMR (600 MHz, CDCl₃): δ 7.75 (d, *J* = 7.3 Hz, 2H), 7.47 (t, *J* = 7.4 Hz, 1H), 7.40 (t, *J* = 7.6 Hz, 2H), 6.00 (d, *J* = 7.4 Hz, 1H), 4.23-4.08 (m, 1H), 1.59-1.45 (m, 2H), 1.41-1.24 (m, 8H), 1.22 (d, *J* = 6.6 Hz, 3H), 0.87 (t, *J* = 6.9 Hz, 3H).

¹³C NMR (151 MHz, CDCl₃): δ 166.8, 135.1, 131.2, 128.5, 126.8, 45.8, 37.0, 31.7, 29.2, 26.1, 22.6, 21.0, 14.0.

HPLC analysis: 13% ee, Chiralcel OD-H column, 1% isopropanol in hexane, 1.0 mL/min flow rate 220 nm UV lamp, t[major] = 49.3 min, t[minor] = 51.6 min.

Anal. Calcd for $C_{15}H_{23}NO$: C 77.21%, H 9.93%, N 6.00%; Found: C 76.97%, H 10.01%, N 5.88%.

4-Fluoro-*N*-(octan-2-yl)benzamide
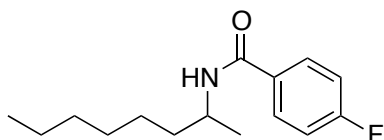
Following the general procedure **A** described above, 4-fluorobenzamide (42 mg, 0.30 mmol) was allowed to react with 1-octene (0.94 ml, 6.0 mmol). The crude mate-rial was purified by chromatography with 13% EtOAc in hexanes. The solvent was evaporated to yield the title compound as a white solid (64 mg, 85% yield).

¹H NMR (600 MHz, CDCl₃): δ 7.76 (dd, *J* = 7.6, 5.6 Hz, 2H), 7.07 (dd, *J* = 8.3 Hz, 2H), 5.98 (d, *J* = 6.8 Hz, 1H), 4.15 (m, 1H), 1.59-1.44 (m, 2H), 1.39-1.16 (m, 11H), 0.86 (t, *J* = 6.5 Hz, 3H).

¹³C NMR (151 MHz, CDCl₃): δ 165.7, 164.5 (d, *J* = 251.4 Hz), 131.2, 129.1 (d, *J* = 8.9 Hz), 115.4 (d, *J* = 21.9 Hz), 45.9, 37.0, 31.7, 29.2, 26.1, 22.6, 21.0, 14.0.

¹⁹F NMR (565 MHz, CDCl₃): δ -109.7.

Anal. Calcd for $C_{15}H_{22}FNO$: C 71.68%, H 8.82%, N 5.57%; Found: C 71.39%, H 8.77%, N 5.38%.

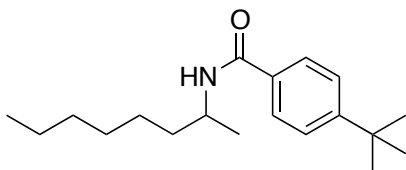## 4-Fluoro-*N*-(hex-2-en-2-yl)benzamide
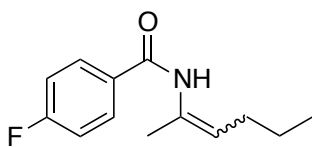
Following the general procedure **A** described above, 4-fluorobenzamide (70 mg, 0.50 mmol) was allowed to react with 1-octene (1.5 ml, 10. mmol). After heating for 12 h at 140 °C, the crude material was purified by chromatography with 8% EtOAc in hexanes without a reductive workup in iso-propanol. A mixture of E and Z isomers of the title compound were obtained as a white solid upon evaporation of the solvent (60 mg, 46% yield).

¹H NMR (600 MHz, CDCl₃): δ 7.77 (dd, *J* = 8.4, 5.4 Hz, 2H), 7.10 (dd, *J* = 8.5 Hz, 2H), 7.06 (br s, 1H), 5.78 (t, *J* = 7.3 Hz, 1H), 2.11-2.04 (m, 2H), 1.99 (s, 3H), 1.47-1.38 (m, 2H), 0.93 (t, *J* = 7.3 Hz, 3H).
¹⁹F NMR (565 MHz, CDCl₃): δ -109.1.

N-(Octan-2-yl)-4-(trifluoromethyl)benzamide
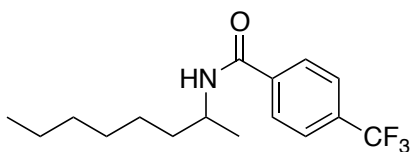
Following the general procedure **A** described above, 4-trifluoromethylbenzamide (57 mg, 0.30 mmol) was allowed to react with 1-octene (0.94 ml, 6.0 mmol). The crude material was purified by chromatography with 13% EtOAc in hexanes. The solvent was evaporated to yield the title compound as a white solid (83 mg, 92% yield).

¹H NMR (600 MHz, CDCl₃): δ 7.85 (d, *J* = 7.8 Hz, 2H), 7.66 (d, *J* = 7.8 Hz, 2H), 6.09 (d, *J* = 6.0 Hz, 1H), 4.33-4.05 (m, 1H), 1.63-1.46 (m, 2H), 1.40-1.18 (m, 11H), 0.87 (t, *J* = 6.3 Hz, 3H).
¹³C NMR (151 MHz, CDCl₃): δ 165.5, 138.3, 133.0 (q, *J* = 32.8 Hz), 127.3, 125.5 (q, *J* = 3.7 Hz), 123.7 (q, *J* = 272.4 Hz), 46.1, 36.9, 31.7, 29.1, 26.1, 22.6, 20.9, 14.0.
¹⁹F NMR (565 MHz, CDCl₃): δ -63.9.
Anal. Calcd for C₁₆H₂₂F₃NO: C 63.77%, H 7.36%, N 4.65%; Found: C 63.54%, H 7.54%, N 4.55%.

4-Fluoro-*N*-(hexan-2-yl)benzamide

Following the general procedure **A** described above, 4-fluorobenzamide (42 mg, 0.30 mmol) was allowed to react with 1-hexene (0.70 ml, 6.0 mmol). The crude material was purified by chromatography with 10% EtOAc in hexanes. The solvent was evaporated to yield the title compound as a white solid (59 mg, 88% yield).

¹H NMR (600 MHz, CDCl₃): δ 7.76 (dd, *J* = 8.6, 5.4 Hz, 2H), 7.05 (dd, *J* = 8.6 Hz, 2H), 6.15 (d, *J* = 7.6 Hz, 1H), 4.19-4.06 (m, 1H), 1.57-1.44 (m, 2H), 1.36-1.26 (m, 4H), 1.19 (d, *J* = 6.6 Hz, 3H), 0.87 (t, *J* = 6.9 Hz, 3H).
¹³C NMR (151 MHz, CDCl₃): δ 165.8, 164.5 (d, *J* = 251.3 Hz), 131.2, 129.1 (d, *J* = 8.8 Hz), 115.4 (d, *J* = 21.8 Hz), 45.9, 36.6, 28.3, 22.5, 20.9, 14.0.
¹⁹F NMR (565 MHz, CDCl₃): δ -109.8.
HPLC analysis: 19% ee, Chiralcel OD-H column, 2% isopropanol in hexane, 1.0 mL/min flow rate 220 nm UV lamp, t[minor] = 14.0 min, t[major] = 15.9 min.
Anal. Calcd for C₁₃H₁₈FNO: C 69.93%, H 8.13%, N 6.27%; Found: C 69.91%, H 8.22%, N 6.37%.

N-(Hexan-2-yl)-4-(trifluoromethyl)benzamide
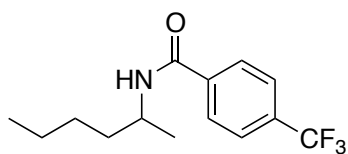
Following the general procedure **A** described above, 4-trifluoromethylbenzamide (57 mg, 0.30 mmol) was allowed to react with 1-hexene (0.70 ml, 6.0 mmol). The crude material was purified by chromatography with 13% EtOAc in hexanes. The solvent was evaporated to yield the title compound as a white solid (68 mg, 83% yield).

^{1}H NMR (600 MHz, CDCl$_3$): δ 7.85 (d, *J* = 7.9 Hz, 2H), 7.66 (d, *J* = 8.0 Hz, 2H), 6.07 (d, *J* = 6.5 Hz, 1H), 4.18 (dd, *J* = 13.9, 6.8 Hz, 1H), 1.62-1.47 (m, 2H), 1.38-1.17 (m, 7H), 0.89 (t, *J* = 6.7 Hz, 3H).

^{13}C NMR (151 MHz, CDCl$_3$): δ 165.6, 138.3, 133.0 (q, *J* = 33.0 Hz), 127.3, 125.5 (q, *J* = 3.7 Hz), 123.7 (q, *J* = 272.6 Hz), 46,1, 36.6, 28.2, 22.5, 20.9, 14.0.

^{19}F NMR (565 MHz, CDCl$_3$): δ -63.9.

Anal. Calcd for C$_{14}$H$_{18}$F$_3$NO: C 61.53%, H 6.64%, N 5.13%; Found: C 61.38%, H 6.53%, N 5.44%.

N-(4-Methylpentan-2-yl)benzamide
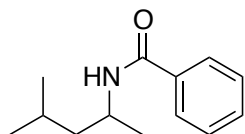
Following the general procedure **A** described above, benzamide (36 mg, 0.30 mmol) was allowed to reacted with 4-methylpent-1-ene (0.69 ml, 6.0 mmol). The crude material was purified by chromatography with 13% EtOAc in hexanes. The solvent was evaporated to yield the title compound as a white solid (47 mg, 71% yield).

^{1}H NMR (600 MHz, CDCl$_3$): δ 7.75 (d, *J* = 7.1 Hz, 1H), 7.49 (t, *J* = 7.4 Hz, 1H), 7.42 (t, *J* = 7.5 Hz, 1H), 5.85 (d, *J* = 6.1 Hz, 1H), 4.37-4.21 (m, 1H), 1.74-1.64 (m, 1H), 1.47 (ddd, *J* = 14.6, 8.4, 6.4 Hz, 1H), 1.34 (ddd, *J* = 13.8, 7.9, 6.1 Hz, 1H), 1.23 (d, *J* = 6.5 Hz, 3H), 0.95 (d, *J* = 6.7 Hz, 3H), 0.94 (d, *J* = 6.8 Hz, 3H).

^{13}C NMR (151 MHz, CDCl$_3$): δ 166.7, 135.0, 131.2, 128.5, 126.8, 46.5, 44.0, 25.2, 22.8, 22.5, 21.6.

Anal. Calcd for C$_{13}$H$_{19}$NO: C 76.06%, H 9.33%, N 6.82%; Found: C 76.39%, H 9.47%, N 6.71%.

4-(*tert*-Butyl)-*N*-(4,4-dimethylpentan-2-yl)benzamide
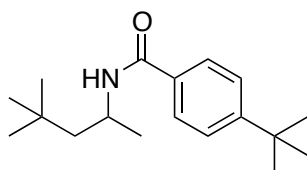
Following the general procedure **A** described above, 4-*tert*-butylbenzamide (53 mg, 0.30 mmol) was allowed to react with 4,4-dimethylpent-1-ene (0.82 ml, 6.0 mmol). The crude material was purified by chromatography with 13% EtOAc in hexanes. The solvent was evaporated to yield the title compound as a white solid (53 mg, 65% yield).

^{1}H NMR (600 MHz, CDCl$_3$): δ 7.68 (d, *J* = 8.1 Hz, 2H), 7.43 (d, *J* = 8.1 Hz, 2H), 5.92 (d, *J* = 7.4 Hz, 1H), 4.35 (s, 1H), 1.51-1.41 (m, 2H), 1.32 (s, 9H), 1.22 (d, *J* = 6.4 Hz, 3H), 0.96 (s, 9H).

^{13}C NMR (151 MHz, CDCl$_3$): δ 166.1, 154.6, 132.2, 126.5, 125.4, 51.2, 43.1, 34.8, 31.1, 30.6, 30.0, 23.9.

Anal. Calcd for C$_{18}$H$_{29}$NO: C 78.49%, H 10.61%, N 5.09%; Found: C 78.44%, H 10.73%, N 5.17%.

4-Methyl-*N*-(octan-2-yl)benzenesulfonamide
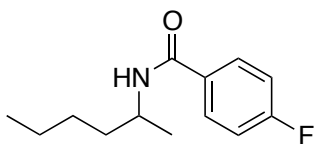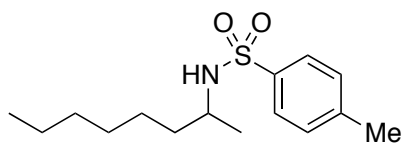
Following the general procedure **A** described above, *p*-toluenesulfonamide (51 mg, 0.30 mmol) was allowed to react with 1-octene (0.94 ml, 6.0 mmol). The crude material was purified by chromatography with 13% EtOAc in hexanes. The solvent was evaporated to yield the title compound as a white solid (81 mg, 96% yield).

^{1}H NMR (600 MHz, CDCl$_3$): δ 7.77 (d, *J* = 8.2 Hz, 2H), 7.28 (d, *J* = 8.0 Hz, 2H), 4.76 (d, *J* = 8.0 Hz, 1H), 3.34-3.19 (m, 1H), 2.41 (s, 3H), 1.37-1.27 (m, 2H), 1.23-1.16 (m, 3H), 1.15-1.06 (m, 5H), 1.01 (d, *J* = 6.6 Hz, 3H), 0.83 (t, *J* = 7.3 Hz, 3H).

^{13}C NMR (151 MHz, CDCl$_3$): δ 143.0, 138.3, 129.5, 127.0, 49.9, 37.4, 31.6, 28.9, 25.4, 22.5, 21.7, 21.4, 14.0.

HPLC analysis: 12% ee, Chiralcel OD-H column, 2% isopropanol in hexane, 1.0 mL/min flow rate 220 nm UV lamp, t$_{[major]}$ = 16.4 min, t$_{[minor]}$ = 18.6 min.

Anal. Calcd for C$_{15}$H$_{25}$NO$_2$S: C 63.56%, H 8.89%, N 4.94%; Found: C 63.59%, H 8.80%, N 5.06%.

General Procedure B: Ir-catalyzed addition of arylamides and sulfonamides to norbornene.

In a nitrogen-filled dry-box, an oven dried 4 ml screw-capped vial was charged with [Ir(coe)$_2$Cl]$_2$ (5.4 mg, 0.0060 mmol), (*S*)-DTBM-SEGPHOS (14 mg, 0.012 mmol), and the corresponding arylamide or sulfonamide (0.30 mmol). 0.30 ml toluene was added to these solids and the mixture was stirred vigorously at 50 °C for 30 minutes. Four equivalents of norbornene (113 mg, 1.20 mmol) were added to the resulting pale yellow solution. The vial was sealed with a Teflon cap and removed from the dry-box. The reaction mixture was stirred in an aluminum heating block at 120 °C for 24 h and then cooled to room temperature. The solvent was removed by rotary evaporation, and the residue was dry loaded onto Silacycle Siala-P60 silica gel (1.0 g). The product was purified by flash chromatography (column dimension: height = 20. cm, diameter = 3.0 cm) on Silacycle Siala-P60 silica gel (55 g). The conditions for chromatography and other data that are specific to each compound are given below.

N-((1*R*,2*R*,4*S*)-Bicyclo[2.2.1]heptan-2-yl)-4-(trifluoromethyl)benzamide
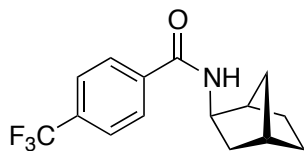
4-Trifluoromethylbenzamide (57 mg, 0.30 mmol) was allowed to react with norbornene following the general procedure **B**. The crude material was purified by chromatography with 15% EtOAc in hexanes. The solvent was evaporated to yield the title compound as a white solid (72 mg, 85% yield).

^{1}H NMR (500 MHz, CDCl$_3$): δ 7.81 (d, *J* = 8.1 Hz, 2H), 7.62 (d, *J* = 8.2 Hz, 2H), 6.26 (d, *J* = 5.8 Hz, 1H), 3.88 (dd, *J* = 7.4, 3.7 Hz, 1H), 2.30 (overlapping singlets, 2H), 1.86 (ddd, *J* = 13.1, 8.0, 2.1 Hz, 1H), 1.59-1.44 (m, 1H), 1.39 (d, *J* = 10.2 Hz, 1H), 1.36-1.20 (m, 2H), 1.16 (ddd, *J* = 10.8, 4.1, 1.8 Hz, 1H).

^{13}C NMR (126 MHz, CDCl$_3$): δ 165.8, 138.5, 133.1 (q, *J* = 32.7 Hz), 127.6, 125.6 (q, *J* = 3.7 Hz), 123.9 (q, *J* = 272.5 Hz), 53.8, 42.6, 40.5, 36.0, 35.9, 28.3, 26.7.

^{19}F NMR (470 MHz, CDCl$_3$): δ -63.9.

HPLC analysis: 93% ee, Chiralcel OD-H column, 2% isopropanol in hexane, 1.0 mL/min flow rate 220 nm UV lamp, $t_{[minor]}$ = 18.7 min, $t_{[major]}$ = 19.8 min.

Anal. Calcd for $C_{15}H_{14}F_3NO$: C 64.05%, H 5.02%, N 4.98%; Found: C 63.69%, H 5.33 %, N 5.27%.

N-((1*R*,2*R*,4*S*)-Bicyclo[2.2.1]heptan-2-yl)-4-fluorobenzamide
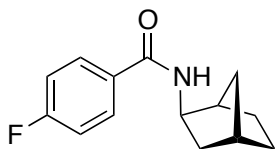
4-Fluorobenzamide (42 mg, 0.30 mmol) was allowed to react with norbornene following the general procedure **B**. The crude material was purified by chromatography with 15% EtOAc in hexanes. The solvent was evaporated to yield the title compound as a white solid (61 mg, 88% yield).

¹H NMR (600 MHz, CDCl₃): δ 7.73 (dd, *J* = 8.6, 5.4 Hz, 2H), 7.03 (dd, *J* = 8.6 Hz, 2H), 6.15 (s, 1H), 3.85 (br s, 1H), 2.28 (overlapping singlets, 2H), 1.84 (ddd, *J* = 12.9, 8.0, 1.9 Hz, 1H), 1.58-1.41 (m, 2H), 1.38 (d, *J* = 10.1 Hz, 1H), 1.34-1.10 (m, 4H).

¹³C NMR (151 MHz, CDCl₃): δ 165.8, 164.5 (d, *J* = 251.3 Hz), 131.1, 129.2 (d, *J* = 8.9 Hz), 115.4 (d, *J* = 21.8 Hz), 53.4, 42.4, 40.3, 35.7, 35.6, 28.1, 26.5.

¹⁹F NMR (565 MHz, CDCl₃): δ -109.7.

HPLC analysis: 92% ee, Chiralcel OD-H column, 2% isopropanol in hexane, 1.0 mL/min flow rate 220 nm UV lamp, $t_{[major]}$ = 24.7 min, $t_{[minor]}$ = 27.3 min.

Anal. Calcd for $C_{14}H_{16}FNO$: C 72.08%, H 9.28%, N 6.00%; Found: C 72.04%, H 9.22%, N 6.02%.

N-((1*R*,2*R*,4*S*)-Bicyclo[2.2.1]heptan-2-yl)benzamide
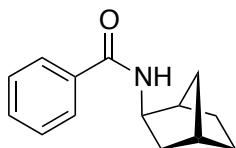
Benzamide (36 mg, 0.30 mmol) was allowed to react with norbornene following the general procedure **B**. The crude material was purified by chromatography with 15% EtOAc in hexanes. The solvent was evaporated to yield the title compound as a white solid (58 mg, 92% yield).

¹H NMR (600 MHz, CDCl₃): δ 7.73 (d, *J* = 7.4 Hz, 2H), 7.45 (t, *J* = 7.4 Hz, 1H), 7.38 (t, *J* = 7.6 Hz, 2H), 6.25-5.99 (m, 1H), 3.89 (ddd, *J* = 7.5, 3.7 Hz, 1H), 2.31 (d, *J* = 4.0 Hz, 2H), 1.86 (ddd, *J* = 13.1, 8.0, 2.1 Hz, 1H), 1.58-1.43 (overlapping singlets, 2H), 1.39 (d, *J* = 10.2 Hz, 1H), 1.34-1.26 (m, 2H), 1.22 (d, *J* = 10.1 Hz, 1H), 1.18-1.12 (m, 1H);

¹³C NMR (151 MHz, CDCl₃): δ 166.8, 134.9, 131.2, 128.4, 126.8, 53.3, 42.4, 40.4, 35.7, 35.6, 28.1, 26.5. For a sample with 91% *ee*, $[\alpha]^{23}_D$ = -15.2 (*c* = 2.0, CHCl₃).

HPLC analysis: 91% ee, Chiralcel OD-H column, 0.75% ethanol in hexane, 0.6 mL/min flow rate 220 nm UV lamp, $t_{[minor]}$ = 76.1 min, $t_{[major]}$ = 84.2 min.

Anal. Calcd for $C_{14}H_{17}NO$: C 78.10%, H 7.96%, N 6.51%; Found: C 77.63%, H 8.08%, N 6.49%.

N-((1*R*,2*R*,4*S*)-Bicyclo[2.2.1]heptan-2-yl)-4-(*tert*-butyl)benzamide
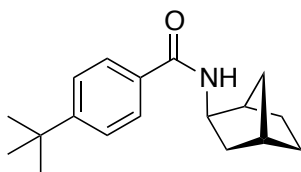
4-*tert*-Butylbenzamide (53 mg, 0.30 mmol) was allowed to react with norbornene following the general procedure **B**. The crude material was purified by chromatography with 15% EtOAc in hexanes. The solvent was evaporated to yield the title compound as a white solid (76 mg, 93% yield).

¹H NMR (600 MHz, CDCl₃): δ 7.67 (d, *J* = 8.3 Hz, 2H), 7.42

(d, *J* = 8.3 Hz, 2H), 6.01 (d, *J* = 5.5 Hz, 1H), 3.91 (d, *J* = 2.5 Hz, 1H), 2.31 (overlapping singlets, 2H), 1.95-1.82 (m, 1H), 1.59-1.44 (m, 2H), 1.37 (d, *J* = 10.0 Hz, 1H), 1.35-1.20 (m, 12H), 1.16 (t, *J* = 9.5 Hz, 1H).

13C NMR (151 MHz, CDCl$_3$): δ 166.7, 154.6, 132.1, 126.6, 125.4, 53.2, 42.4, 40.5, 35.7, 35.7, 34.8, 31.1, 28.1, 26.5.

HPLC analysis: 92% ee, Chiralcel OD-H column, 2% isopropanol in hexane, 1.0 mL/min flow rate 220 nm UV lamp, t$_{[major]}$ = 22.1 min, t$_{[minor]}$ = 25.7 min.

Anal. Calcd for C$_{18}$H$_{25}$NO: C 79.66%, H 9.28%, N 5.16%; Found: C 79.38%, H 9.35%, N 5.02%.

N-((1*R*,2*R*,4*S*)-bicyclo[2.2.1]heptan-2-yl)-4-methylbenzenesulfonamide
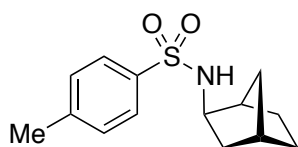
p-Toluenesulfonamide (51 mg, 0.30 mmol) was allowed to react with norbornene following the general procedure **B**. The crude material was purified by chromatography with 15% EtOAc in hexanes. The solvent was evaporated to yield the title compound as a white solid (74 mg, 93% yield).

1H NMR (600 MHz, CDCl$_3$): δ 7.75 (d, *J* = 8.3 Hz, 2H), 7.30 (d, *J* = 8.0 Hz, 2H), 4.63 (d, *J* = 7.1 Hz, 1H), 3.12 (dd, *J* = 7.5, 3.3 Hz, 1H), 2.43 (s, 3H), 2.21-2.15 (m, 1H), 2.09 (d, *J* = 3.9 Hz, 1H), 1.59 (ddd, *J* = 13.3, 8.0, 2.3 Hz, 1H), 1.46-1.34 (m, 2H), 1.32 (d, *J* = 10.2 Hz, 1H), 1.16 (ddd, *J* = 13.2, 7.0, 3.5 Hz, 1H), 1.10 (dd, *J* = 10.2, 0.8 Hz, 1H), 1.06-0.95 (m, 2H).

13C NMR (151 MHz, CDCl$_3$): δ 143.2, 137.9, 129.6, 127.1, 56.7, 42.5, 40.8, 35.6, 35.2, 28.0, 26.3, 21.6.

HPLC analysis: 92% ee, Chiralcel OD-H column, 2% isopropanol in hexane, 1.0 mL/min flow rate 220 nm UV lamp, t$_{[major]}$ = 19.7 min, t$_{[minor]}$ = 21.5 min.

Anal. Calcd for C$_{14}$H$_{19}$NO$_2$S: C 63.36%, H 7.22%, N 5.28%; Found: C 63.34%, H 7.31 %, N 5.22%.

(1*R*, 2*R*, 4*S*) 2-Aminonorbornane
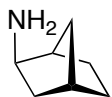
Under ambient conditions, a 20 ml vial was charged with **15** (187 mg, 0.66 mmol, 93% ee) and HCl (10 ml, 6.0 M solution). The vial was tightly capped and placed in a 120 °C heating block for 72 h. The reaction was cooled to room temperature and washed with diethylether 3 times. The mixture was basified with NaHCO$_3$ and the amine product was extracted with diethylether 3 times. The organic solution was washed with brine and dried over anhydrous MgSO$_4$. The organic solvent was removed by rotary evaporation to yield the title compound as a clear, colorless oil (64 mg, 87% yield). For a sample with 93% *ee*, [*α*]$^{23}_D$= -7.5° (*c* = 2.0, CHCl$_3$).

GC/MS: *m/z* 111 (43%, [M$^+$]), 94 (35%, [M-NH$_3$]$^+$), 82 (100%, [M-H$_2$N=CH$_2$]$^+$). ^{1}H NMR spectroscopy matched that of the literature reports.[32,25]

General Procedure C: Ir-catalyzed addition of arylamides to norbornadiene.

In a nitrogen-filled dry-box, an oven dried 4 ml screw-capped vial was charged with [Ir(coe)$_2$Cl]$_2$ (5.4 mg, 0.0060 mmol), (*S*)-DTBM-SEGPHOS (14 mg, 0.012 mmol), and the corresponding arylamide (0.30 mmol). Toluene (0.60 ml) was added to these solids, and the mixture was stirred vigorously at 50 °C for 30 min. Norbornadiene (1.3 equiv, 40 μl, 0.39 mmol) were added to the resulting pale yellow solution. The vial was sealed with

a Teflon cap and removed from the dry-box. The reaction mixture was stirred in an aluminum heating block at 120 °C for 24 h and then cooled to room temperature. The solvent was removed by rotary evaporation, and the residue was dry loaded onto Silacycle Siala-P60 silica gel (1.0 g). The product was purified by flash chromatography (column dimensions: height = 20. cm, diameter = 3.0 cm) with Silacycle Siala-P60 silica gel (55 g). The conditions for chromatography and other data that are specific to each compound are given below.

N-((1*S*,2*R*,4*S*)-Bicyclo[2.2.1]hept-5-en-2-yl)-4-(trifluoromethyl)benzamide
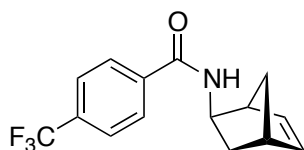
4-Trifluoromethylbenzamide (57 mg, 0.30 mmol) was allowed to react with norbornadiene following the general procedure **C**. The crude material was purified by chromatography with 15% EtOAc in hexanes. The solvent was evaporated to yield the title compound as a white solid (66 mg, 79% yield).

^{1}**H NMR** (600 MHz, CDCl$_3$): δ 7.83 (d, J = 8.1 Hz, 2H), 7.63 (d, J = 8.1 Hz, 2H), 6.48 (d, J = 5.9 Hz, 1H), 6.19 (dd, J = 5.4, 2.6 Hz, 1H), 6.13-6.04 (m, 1H), 3.92 (dd, J = 6.7, 4.9 Hz, 1H), 2.90 (overlapping singlets, 2H), 1.83-1.76 (m, 1H), 1.60 (d, J = 8.8 Hz, 1H), 1.48 (d, J = 8.9 Hz, 1H), 1.36 (dt, J = 12.4, 3.2 Hz, 1H).

^{13}**C NMR** (151 MHz, CDCl$_3$): δ 166.1, 138.9, 138.2, 134.5, 133.0 (q, J = 32.9 Hz), 127.3, 125.5 (q, J = 3.7 Hz), 123.6 (q, J = 272.5 Hz), 50.8, 47.9, 46.1, 41.0, 35.2.

^{19}**F NMR** (565 MHz, CDCl$_3$): δ -63.9.

HPLC analysis: 93% ee, Chiralcel OD-H column, 2% isopropanol in hexane, 1.0 mL/min flow rate 220 nm UV lamp, t$_{[minor]}$ = 20.2 min, t$_{[major]}$ = 21.9 min.

Anal. Calcd for C$_{15}$H$_{14}$F$_3$NO: C 64.05%, H 5.02%, N 4.98%; Found: C 63.77%, H 5.40%, N 4.74%.

N-((1*S*,2*R*,4*S*)-Bicyclo[2.2.1]hept-5-en-2-yl)-4-(*tert*-butyl)benzamide
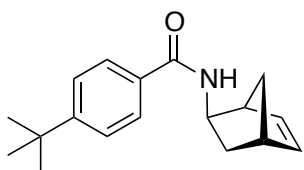
4-*tert*-Butylbenzamide (53 mg, 0.30 mmol) was allowed to react with norbornadiene following the general procedure **C**. The crude material was purified by chromatography with 15% EtOAc in hexanes. The solvent was evaporated to yield the title compound as a white solid (61 mg, 76% yield).

^{1}**H NMR** (600 MHz, CDCl$_3$): δ 7.70 (d, J = 8.2 Hz, 2H), 7.42 (d, J = 8.2 Hz, 2H), 6.26 (d, J = 5.9 Hz, 1H), 6.17 (d, J = 2.8 Hz, 1H), 6.11 (s, 1H), 4.03-3.88 (m, 1H), 2.89 (overlapping singlets, 2H), 1.80 (dd, J = 14.4, 5.7 Hz, 1H), 1.58 (d, J = 8.6 Hz, 1H), 1.47 (d, J = 8.8 Hz, 1H), 1.35-1.29 (m, 10H).

^{13}**C NMR** (151 MHz, CDCl$_3$): δ 167.3, 154.7, 138.7, 134.8, 132.0, 126.7, 125.4, 50.4, 48.0, 46.1, 41.0, 35.3, 34.9, 31.2.

HPLC analysis: 91% ee, Chiralcel OD-H column, 2% isopropanol in hexane, 1.0 mL/min flow rate 220 nm UV lamp, t$_{[major]}$ = 23.9 min, t$_{[minor]}$ = 27.1 min.

Anal. Calcd for C$_{18}$H$_{23}$NO: C 80.26%, H 8.61%, N 5.20%; Found: C 80.20%, H 8.69%, N 5.11%.

[((*S*)-DTBM-Segphos)Ir(H)(Cl)(4-CF₃-benzamide)(4-CF₃-benzamidate)], (1)
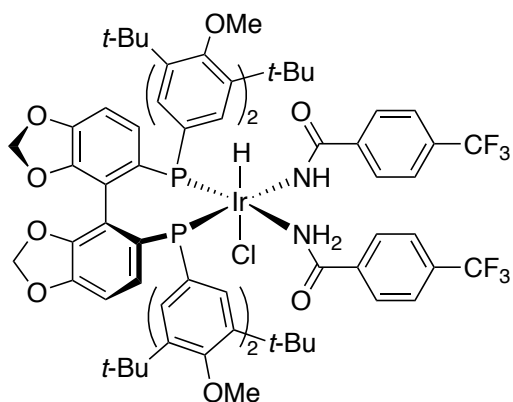
In a nitrogen-filled dry-box, an oven dried 4 ml screw-capped vial was charged with [Ir(coe)₂Cl]₂ (20. mg, 0.022 mmol), (*S*)-DTBM-SEGPHOS (53 mg, 0.045 mmol), and 4-trifluoromethyl benzamide (95 mg, 0.50 mmol). MTBE (0.60 ml) was added to these solids, and the vial was sealed with a Teflon cap and removed from the dry-box. The reaction mixture was stirred in an aluminum heating block at 100 °C for 1 h and then cooled to room temperature. The sealed vial was returned to the nitrogen-filled dry-box. Once inside the inert environment, pentane (2.5 ml) was added to precipitate the unreacted 4-trifluoromethylbenzamide. The white solid was filtered, and the liquor was collected and concentrated under vacuum. The residue was dissolved in 1.0 ml of pentane and cooled to -35 °C for 36 h. Over this time, complex **1** precipitated as a white solid. The solid was separated by filtration and was washed with cold (-35 °C) pentanes two times (49 mg, 62% yield).

¹H NMR (500 MHz, C₆D₆): δ 17.64 (br s, 1H), 10.15 (br s, 1H), 10.00 (d, *J* = 13.6 Hz, 1H), 8.99 (d, *J* = 14.7 Hz, 1H), 8.68 (d, *J* = 9.6 Hz, 1H), 7.84 (dd, *J* = 11.0, 8.3 Hz, 1H), 7.75 (s, 1H), 7.50-7.42 (m, 1H), 7.32-7.17 (m, 7H), 6.97 (d, *J* = 8.1 Hz, 2H), 6.91 (d, *J* = 10.4 Hz, 1H), 6.84-6.66 (m, 2H), 6.62 (d, *J* = 8.1 Hz, 1H), 6.29 (d, *J* = 8.2 Hz, 1H), 6.25 (br s, 1H), 5.50 (s, 1H), 5.19 (s, 1H), 5.17 (s, 1H), 5.04 (s, 1H), 3.64 (s, 3H), 3.54 (s, 3H), 3.29 (s, 3H), 2.78 (s, 3H), 2.06-0.94 (m, 72H), -18.79 (dd, *J* = 20.6, 14.2 Hz, 1H).

³¹P NMR (202 MHz, C₆D₆): δ 0.5 (d, J_{PP} = 19.2 Hz), -8.5 (d, J_{PP} = 19.1 Hz).

¹⁹F NMR (470 MHz, C₆D₆): δ -63.1, -63.3.

IR (neat on attenuated total reflectance tower): 2957 (s), 2871 (m), 2174 (w), 1685 (w), 1622 (m), 1597 (w), 1574 (m), 1455 (m), 1436 (m), 1412 (s), 1392 (m), 1361 (s), 1323 (s).

Anal. Calcd for $C_{90}H_{112}ClF_6IrN_2O_{10}P_2$: C 60.54%, H 6.32%, N 1.57%; Found: C 60.34%, H 6.17%, N 1.44%.

X-ray structure determination of complex 1:

Single crystals for x-ray analysis were obtained by dissolving 20 mg of complex **1** in 1.0 ml of pentane in a 4 ml vial. The vial was tightly sealed and the solution was allowed to sit undisturbed at room temperature. Clear colorless crystals formed over the course of 24 hours. A colorless plate 0.12 x 0.09 x 0.08 mm in size was mounted on a Cryoloop with Paratone oil. Data were collected in a nitrogen gas stream at 100(2) K using phi and omega scans. Crystal-to-detector distance was 60 mm and exposure time was 20 seconds per frame using a scan width of 0.5°. Data collection was 99.6% complete to 25.00° in q. A total of 43286 reflections were collected covering the indices, -16<=*h*<=13, -26<=*k*<=23, -38<=*l*<=38. 17059 reflections were found to be symmetry independent, with an R_{int} of 0.0689. Indexing and unit cell refinement indicated a primitive, orthorhombic lattice. The space group was found to be P2(1)2(1)2(1) (No. 19). The data were integrated using the Bruker SAINT software program and scaled using the SADABS software program. Solution by direct methods (SIR-2011) produced a complete heavy-

atom phasing model consistent with the proposed structure. All non-hydrogen atoms were refined anisotropically by full-matrix least-squares (SHELXL-97). All hydrogen atoms were placed using a riding model. Their positions were constrained relative to their parent atom using the appropriate HFIX command in SHELXL-97. Large atom displacement parameters were measured as a result of the rotation of the *tert*-butyl groups and the various conformations of 2 pentane molecules that were cocrystallized in the sample (not shown in Figure 2.9).
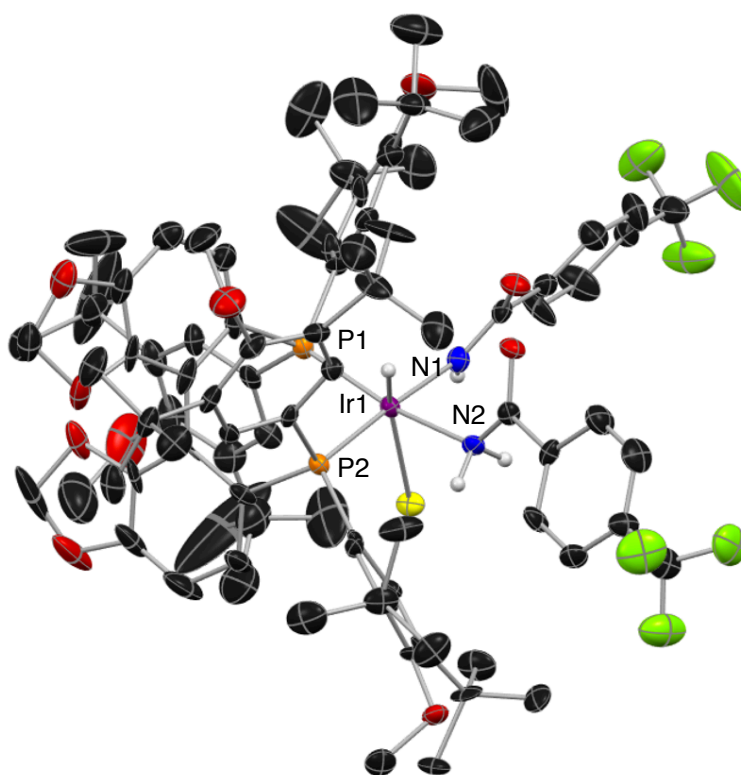
Figure 2.9. ORTEP representation of complex **1**. All hydrogens were omitted for clarity except hydrogens on atoms Ir1, N1, and N2. Thermal ellipsoids are drawn at the 50% probability level.

Table 2.6. Selected bond lengths (Å), bond angles (°), and dihedral angles(°)

Amide Ligand		Amidate Ligand	
Ir1–N2	2.117 Å	Ir1–N1	2.076 Å
N2–C9	1.306 Å	N1–C1	1.290 Å
C9–O2	1.280 Å	C1–O1	1.272 Å
Ir1–N2–C9	127.12 °	Ir1–N1–C1	131.62 °
Ir1–N2–C9–O2	22.44 °	Ir1–N1–C1–O1	5.49 °

Table 2.7. Crystal data and structure refinement for complex 1.

Empirical formula	C100 H136 Cl F6 Ir N2 O10 P2
Formula weight	1929.70
Temperature	100(2) K
Wavelength	0.71073 Å
Crystal system	Orthorhombic
Space group	P2(1)2(1)2(1)
Unit cell dimensions	a = 13.9419(8) Å a= 90°.
	b = 22.1802(12) Å b= 90°.
	c = 31.5865(13) Å g = 90°.
Volume	9767.6(9) Å^3
Z	4
Density (calculated)	1.312 Mg/m^3
Absorption coefficient	1.495 mm^{-1}
F(000)	4032
Crystal size	0.12 x 0.09 x 0.08 mm^3
Crystal color/habit	colorless plate
Theta range for data collection	1.58 to 25.40°.
Index ranges	-16<=h<=13, -26<=k<=23, -38<=l<=38
Reflections collected	43286
Independent reflections	17059 [R(int) = 0.0689]
Completeness to theta = 25.00°	99.6 %
Absorption correction	Analytical
Max. and min. transmission	0.8898 and 0.8410
Refinement method	Full-matrix least-squares on F^2
Data / restraints / parameters	17059 / 4 / 1133
Goodness-of-fit on F^2	1.063
Final R indices [I>2sigma(I)]	R1 = 0.0570, wR2 = 0.1076
R indices (all data)	R1 = 0.0736, wR2 = 0.1141
Absolute structure parameter	0.004(6)
Largest diff. peak and hole	1.708 and -1.370 e.Å^{-3}

Table 2.8. Atomic Coordinates of 1[a]

Atom	x	y	z	U(eq)
C(1)	2217(6)	2205(3)	2528(2)	23(2)
C(2)	2405(6)	2720(4)	2836(2)	28(2)
C(3)	1869(8)	2821(4)	3193(3)	49(3)
C(4)	2061(8)	3292(5)	3460(3)	54(3)
C(5)	2809(7)	3672(4)	3384(3)	36(2)
C(6)	3353(8)	3582(4)	3021(3)	46(3)
C(7)	3177(7)	3098(4)	2757(4)	42(2)
C(8)	2994(8)	4189(5)	3665(4)	51(3)
C(9)	1391(6)	1866(3)	1439(2)	20(2)
C(10)	1073(7)	2085(3)	1012(2)	23(2)
C(11)	1698(8)	2417(4)	757(3)	39(2)
C(12)	1414(8)	2608(5)	362(3)	42(3)
C(13)	498(7)	2468(4)	214(2)	29(2)
C(14)	-101(7)	2131(4)	453(2)	32(2)
C(15)	200(7)	1929(4)	849(2)	29(2)
C(16)	191(8)	2681(5)	-211(3)	42(3)
C(17)	2599(6)	860(3)	3016(2)	20(2)
C(18)	2564(7)	995(3)	3453(2)	28(2)
C(19)	3308(8)	1298(4)	3651(3)	33(2)
C(20)	4101(8)	1450(4)	3411(3)	35(2)
C(21)	4212(6)	1274(4)	2985(3)	34(2)
C(22)	3408(6)	1016(3)	2795(2)	27(2)
C(23)	3252(8)	1400(5)	4132(3)	44(3)
C(24)	2303(10)	1147(8)	4315(3)	110(6)
C(25)	4080(11)	1074(6)	4356(3)	86(4)
C(26)	3293(10)	2063(5)	4247(3)	69(4)
C(27)	4852(12)	2400(5)	3493(4)	89(5)
C(28)	5130(6)	1338(4)	2715(3)	40(2)
C(29)	6068(9)	1429(6)	2963(3)	79(4)
C(30)	5308(10)	711(6)	2494(5)	91(5)
C(31)	5034(8)	1822(6)	2384(4)	78(4)
C(32)	876(7)	218(3)	3208(2)	23(2)
C(33)	-22(6)	459(4)	3305(2)	26(2)
C(34)	-543(8)	266(5)	3653(3)	38(3)
C(35)	-133(9)	-190(4)	3901(3)	48(3)
C(36)	788(8)	-418(4)	3827(2)	36(3)
C(37)	1265(7)	-208(3)	3473(2)	28(2)
C(38)	-1500(10)	560(6)	3745(4)	62(4)
C(39)	-1897(18)	466(13)	4166(6)	290(20)
C(40)	-1456(11)	1212(6)	3670(5)	116(6)
C(41)	-2243(13)	324(7)	3397(8)	189(12)
C(42)	-1386(11)	-931(6)	4066(5)	102(5)
C(43)	1317(8)	-867(4)	4130(3)	42(3)

C(44)	1224(19)	-658(6)	4579(3)	178(12)
C(45)	2355(9)	-951(9)	4013(5)	146(9)
C(46)	840(9)	-1489(5)	4122(4)	76(4)
C(47)	2051(7)	-240(3)	2572(2)	25(2)
C(48)	3003(7)	-371(4)	2580(2)	31(2)
C(49)	3379(7)	-938(4)	2481(3)	36(2)
C(50)	2720(8)	-1381(4)	2373(2)	33(2)
C(51)	1965(8)	-2236(4)	2295(3)	45(3)
C(52)	1743(8)	-1253(3)	2361(2)	31(2)
C(53)	1356(8)	-695(4)	2450(2)	32(2)
C(54)	340(7)	-645(4)	2450(2)	26(2)
C(55)	-239(7)	-1007(3)	2697(2)	30(2)
C(56)	-725(11)	-1778(6)	3085(3)	84(6)
C(57)	-1199(7)	-991(4)	2723(3)	42(3)
C(58)	-1721(8)	-581(5)	2490(3)	57(3)
C(59)	-1209(6)	-202(4)	2222(3)	33(2)
C(60)	-214(6)	-214(3)	2191(2)	21(2)
C(61)	1301(6)	-99(3)	1564(2)	18(2)
C(62)	1122(7)	-699(3)	1437(2)	20(2)
C(63)	1785(6)	-999(3)	1188(2)	23(2)
C(64)	2620(7)	-693(4)	1076(2)	26(2)
C(65)	2759(6)	-83(4)	1145(2)	23(2)
C(66)	2081(6)	195(4)	1401(2)	20(2)
C(67)	1561(7)	-1636(4)	1011(2)	29(2)
C(68)	576(7)	-1861(4)	1153(3)	40(3)
C(69)	2300(8)	-2123(4)	1136(3)	46(3)
C(70)	1546(8)	-1589(4)	524(2)	42(3)
C(71)	4116(7)	-1162(5)	1206(3)	54(3)
C(72)	3552(7)	339(5)	961(3)	39(2)
C(73)	4120(8)	615(5)	1329(3)	64(3)
C(74)	3039(8)	847(5)	718(3)	50(3)
C(75)	4227(8)	38(5)	646(3)	55(3)
C(76)	-438(6)	534(3)	1445(2)	18(2)
C(77)	-1204(5)	930(3)	1519(2)	18(2)
C(78)	-1839(5)	1099(4)	1206(2)	21(2)
C(79)	-1714(6)	840(3)	803(2)	20(2)
C(80)	-918(7)	507(4)	697(2)	23(2)
C(81)	-300(6)	349(3)	1029(2)	19(2)
C(82)	-2602(6)	1590(4)	1300(3)	29(2)
C(83)	-2459(8)	1857(5)	1741(3)	45(3)
C(84)	-3637(6)	1325(4)	1272(2)	30(2)
C(85)	-2489(7)	2114(4)	988(3)	36(2)
C(86)	-3071(7)	468(4)	430(3)	36(2)
C(87)	-604(7)	294(4)	248(2)	33(2)
C(88)	-1102(9)	638(4)	-122(2)	46(3)
C(89)	-819(8)	-394(5)	207(3)	51(3)

C(90)	476(7)	410(5)	190(2)	44(3)
C(91)	-1904(18)	-1827(9)	-147(8)	209(14)
C(92)	-1133(14)	-2153(8)	70(6)	123(7)
C(93)	-800(14)	-2696(8)	-126(5)	110(7)
C(94)	5(14)	-3034(9)	70(6)	129(7)
C(95)	280(20)	-3600(12)	-104(9)	300(20)
C(96)	4720(20)	2919(15)	1539(7)	300(20)
C(97)	3862(13)	3166(9)	1367(6)	230(18)
C(98)	4116(15)	3789(9)	1455(9)	288(19)
C(99)	4943(17)	4180(8)	1489(8)	250(18)
C(100)	5175(11)	4800(6)	1418(5)	99(5)
N(1)	1487(5)	1855(3)	2580(2)	24(2)
N(2)	762(5)	1679(3)	1715(2)	21(2)
O(1)	2794(4)	2180(2)	2217(2)	28(1)
O(2)	2293(4)	1889(2)	1512(2)	24(1)
O(3)	4840(5)	1763(3)	3616(2)	49(2)
O(4)	-679(7)	-452(4)	4228(2)	90(3)
O(5)	2893(5)	-1969(2)	2265(2)	42(2)
O(6)	1269(5)	-1756(2)	2236(2)	40(2)
O(7)	117(5)	-1432(3)	2977(2)	41(2)
O(8)	-1538(6)	-1406(4)	3003(2)	66(3)
O(9)	3367(5)	-1026(3)	895(2)	46(2)
O(10)	-2425(4)	975(2)	503(2)	26(1)
F(1)	3509(6)	4623(3)	3495(3)	106(3)
F(2)	2213(5)	4443(3)	3811(2)	83(2)
F(3)	3507(5)	4035(3)	4009(2)	87(3)
F(4)	-755(5)	2687(3)	-260(2)	69(2)
F(5)	548(5)	2336(3)	-521(2)	72(2)
F(6)	505(5)	3236(3)	-302(2)	65(2)
P(1)	1577(2)	492(1)	2758(1)	21(1)
P(2)	413(2)	327(1)	1861(1)	18(1)
Cl(1)	-569(2)	1473(1)	2507(1)	25(1)
Ir(1)	1014(1)	1110(1)	2242(1)	18(1)

[a] Values represent atomic coordinates x 10^4 and equivalent isotropic displacement parameters (Å^2 x 10^3) for **1**. U(eq) is defined as one third of the trace of the orthogonalized U tensor.

Synthesis of 1-*p*-F
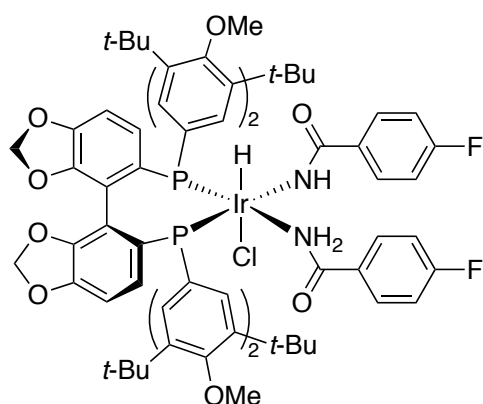
In a nitrogen-filled dry-box, an oven-dried 4 ml screw-capped vial was charged with [Ir(coe)$_2$Cl]$_2$ (20. mg, 0.022 mmol), (*S*)-DTBM-SEGPHOS (53 mg, 0.045 mmol), and 4-fluorobenzamide (70 mg, 0.50 mmol). MTBE (0.60 ml) was added to these solids, and the vial was sealed with a Teflon cap and removed from the dry-box. The reaction mixture was stirred in an aluminum heating block at 100 °C for 1 h and then cooled to room temperature. The sealed vial was returned to the nitrogen-filled dry-box. Once inside the inert environment, pentane (2.5 ml) was added to precipitate the unreacted 4-fluorobenzamide. The white solid was filtered and the liquor was collected and concentrated under vacuum. The residue was dissolved in 0.5 ml pentane and cooled to -35 °C for 36 h. Over this time, complex **1-*p*-F** precipiated as a white solid, which was subsequently washed with cold (-35 °C) pentanes once (21 mg, 28% yield). NMR spectroscopic analysis of this compound is complicated by a significant amount of dissociation of the dative amide ligand.

^{1}H NMR (600 MHz, C$_6$D$_6$): δ 17.46 (br s, 1H), 9.96 (br s, 1H), 9.89 (d, *J* = 13.5 Hz, 1H), 8.93 (d, *J* = 14.3 Hz, 1H), 8.70-8.50 (m, 1H), 7.78-7.71 (m, 1H), 7.45 (s, 1H), 7.42-7.30 (m, 2H), 7.06-7.01 (m, 2H), 6.83 (d, *J* = 10.2 Hz, 2H), 6.73-6.33 (m, 7H), 6.28 (dd, *J* = 8.3 Hz, 2H), 6.20 (d, *J* = 8.2 Hz, 1H), 5.41 (s, 1H), 5.12-5.05 (m, 2H), 4.95 (s, 1H), 3.54 (s, 3H), 3.44 (s, 3H), 3.21 (s, 3H), 2.73 (s, 3H), 1.80-1.50 (m, 36H), 1.34-1.09 (m, 36H), -18.87 (dd, *J* = 20.4, 14.4 Hz, 1H).

^{31}P NMR (243 MHz, C$_6$D$_6$): δ -0.43, -9.28.

^{19}F NMR (565 MHz, C$_6$D$_6$): δ -111.7, -112.0.

IR (neat on attenuated total reflectance tower): 3010 (s), 2888 (m), 2175 (w), 1621 (m), 1573 (m), 1483 (m), 1436 (m), 1411 (m), 1323 (s), 1129 (s).

Anal. Calcd for C$_{88}$H$_{112}$ClF$_2$IrN$_2$O$_{10}$P$_2$: C 62.71%, H 6.70%, N 1.66%; Found: C 62.61%, H 6.88%, N 1.89%.

Decomposition complex 23
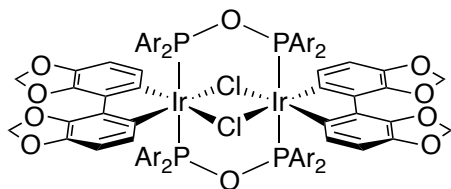
In a nitrogen-filled dry-box, an oven-dried 4 ml screw-capped vial was charged with [Ir(coe)$_2$Cl]$_2$ (15 mg, 0.017 mmol), (*S*)-DTBM-SEGPHOS (40 mg, 0.033 mmol), and toluene (0.5 ml). The vial was sealed with a Teflon cap and removed from the dry-box. The vial was unsealed and exposed to atmospheric conditions for 30 s. The vial was resealed and allowed to sit at room temperature for 2 h. The resulting dark black solution was taken into the dry-box and the solvent was removed under vacuum. The resulting residue was redissolved in toluene and placed in the freezer to overnight (-35 °C). White crystalline material suitable for single crystal x-ray diffraction had formed overnight.

Table 2.9. Crystal data and structure refinement for 23

Identification code	bc64oasq
Empirical formula	C155.50 H218 Cl2 Ir2 O18 P4
Formula weight	2954.48
Temperature	173(2) K
Wavelength	1.54178 Å
Crystal system	Monoclinic
Space group	P2(1)/n
Unit cell dimensions	a = 19.4769(16) Å a= 90°.
	b = 26.836(2) Å b= 91.779(5)°.
	c = 28.584(2) Å g = 90°.
Volume	14933(2) Å^3
Z	4
Density (calculated)	1.314 Mg/m^3
Absorption coefficient	4.618 mm^{-1}
F(000)	6172
Crystal size	0.276 x 0.179 x 0.065 mm^3
Theta range for data collection	2.26 to 68.56°.
Index ranges	-23<=h<=23, -26<=k<=32, -33<=l<=34
Reflections collected	76542
Independent reflections	25404 [R(int) = 0.0639]
Completeness to theta = 68.56°	92.2 %
Absorption correction	Integration
Max. and min. transmission	0.7878 and 0.5471
Refinement method	Full-matrix least-squares on F^2
Data / restraints / parameters	25404 / 13762 / 2496
Goodness-of-fit on F^2	1.109
Final R indices [I>2sigma(I)]	R1 = 0.0490, wR2 = 0.1294
R indices (all data)	R1 = 0.0737, wR2 = 0.1427
Largest diff. peak and hole	1.245 and -1.143 e.Å^{-3}

Table 2.10. Atomic Coordinates of 23[a]

Atom	x	y	z	U(eq)
Ir(1)	1250(1)	7973(1)	2517(1)	26(1)
Ir(2)	-20(1)	7964(1)	1586(1)	27(1)
Cl(1)	533(1)	7338(1)	2108(1)	29(1)
Cl(2)	658(1)	8604(1)	2019(1)	30(1)
P(1)	2024(1)	7922(1)	1924(1)	29(1)
P(2)	917(1)	7811(1)	1119(1)	30(1)
P(3)	-782(1)	8091(1)	2180(1)	28(1)
P(4)	312(1)	8005(1)	2998(1)	28(1)
O(1)	2656(7)	6628(5)	3994(5)	43(3)
O(2)	2873(8)	7472(5)	4018(5)	42(2)
O(3)	3290(7)	8435(5)	3791(5)	47(3)
O(4)	3346(7)	9268(4)	3612(5)	55(3)
C(1)	1743(6)	7473(4)	2951(5)	31(2)
C(2)	1647(14)	6962(4)	2923(8)	33(2)
C(3)	1901(10)	6653(5)	3287(6)	39(3)
C(4)	2342(11)	6863(5)	3606(7)	39(2)
C(5)	3112(8)	7001(6)	4181(6)	44(3)
C(6)	2482(16)	7371(5)	3613(9)	37(2)
C(7)	2230(20)	7681(6)	3270(13)	34(2)
C(8)	2344(16)	8225(6)	3211(13)	35(2)
C(9)	2893(8)	8525(5)	3360(7)	42(2)
C(10)	3673(8)	8876(6)	3856(6)	54(3)
C(11)	2850(9)	9037(5)	3319(7)	44(2)
C(12)	2408(9)	9269(5)	3011(7)	41(3)
C(13)	1916(10)	8957(5)	2778(7)	37(2)
C(14)	1890(20)	8454(5)	2870(16)	31(2)
O(1B)	2829(6)	6634(4)	3926(4)	42(2)
O(2B)	3018(7)	7484(5)	3945(4)	42(2)
O(3B)	3429(6)	8401(4)	3678(5)	48(2)
O(4B)	3516(6)	9230(4)	3473(4)	51(2)
C(1B)	1744(6)	7473(3)	2950(4)	31(2)
C(2B)	1599(12)	6968(4)	2966(7)	33(2)
C(3B)	2016(8)	6647(4)	3244(6)	37(2)
C(4B)	2438(10)	6867(4)	3569(6)	39(2)
C(5B)	3289(7)	7016(5)	4088(5)	44(3)
C(6B)	2534(14)	7380(4)	3589(7)	37(2)
C(7B)	2219(19)	7691(5)	3273(11)	34(2)
C(8B)	2360(14)	8227(5)	3189(11)	35(2)
C(9B)	2814(8)	8551(4)	3419(6)	42(2)
C(10B)	3843(7)	8828(5)	3701(6)	52(3)
C(11B)	2934(8)	9022(4)	3248(6)	42(2)
C(12B)	2492(8)	9255(4)	2942(6)	41(2)
C(13B)	1948(8)	8958(4)	2752(6)	37(2)

C(14B)	1890(18)	8460(4)	2862(13)	31(2)
C(15)	2700(2)	7452(1)	1919(1)	34(1)
C(16)	3111(2)	7372(1)	2318(1)	37(1)
C(17)	3592(2)	6989(2)	2327(1)	44(2)
C(18)	3662(2)	6686(1)	1937(2)	57(2)
C(19)	3251(2)	6766(1)	1537(1)	53(2)
C(20)	2770(2)	7149(1)	1528(1)	41(1)
C(21)	4158(3)	6962(3)	2733(2)	49(2)
C(22)	4151(5)	7437(4)	3030(3)	56(2)
C(23)	4066(6)	6518(4)	3063(4)	69(3)
C(24)	4869(5)	6923(4)	2522(4)	65(3)
C(21B)	4185(12)	7095(13)	2704(9)	51(4)
C(22B)	4130(20)	7538(15)	3042(11)	58(7)
C(23B)	4150(30)	6617(14)	2998(17)	57(6)
C(24B)	4905(18)	7121(17)	2500(17)	50(6)
O(5)	3980(2)	6226(2)	2009(2)	66(1)
C(25)	3522(5)	5835(3)	2170(3)	75(3)
C(25B)	3515(9)	5823(8)	2121(10)	84(10)
C(26)	3452(4)	6523(3)	1058(2)	60(2)
C(27)	3539(6)	5952(3)	1055(3)	84(3)
C(28)	4145(4)	6745(5)	928(4)	85(3)
C(29)	2920(5)	6638(4)	665(3)	70(3)
C(26B)	3580(14)	6662(10)	1047(5)	67(4)
C(27B)	3860(20)	6127(11)	1037(6)	71(6)
C(28B)	4184(17)	7008(15)	932(15)	76(8)
C(29B)	3062(15)	6708(8)	631(7)	72(6)
C(30)	2495(2)	8485(1)	1772(1)	35(1)
C(31)	3188(2)	8532(1)	1895(2)	48(2)
C(32)	3516(1)	8988(2)	1845(2)	60(2)
C(33)	3152(2)	9397(1)	1671(2)	50(2)
C(34)	2459(2)	9350(1)	1547(1)	42(1)
C(35)	2131(1)	8894(1)	1598(1)	36(1)
C(36)	4324(3)	8936(5)	1909(4)	74(3)
C(37)	4613(7)	8461(5)	1686(6)	71(4)
C(38)	4492(9)	8904(6)	2435(4)	91(5)
C(39)	4718(7)	9380(5)	1710(7)	85(5)
C(36B)	4328(3)	9008(4)	1876(4)	74(3)
C(38B)	4567(7)	9325(5)	2294(5)	87(4)
C(37B)	4623(6)	8485(4)	1964(6)	72(4)
C(39B)	4644(7)	9218(5)	1431(4)	72(4)
O(6)	3452(2)	9869(2)	1710(2)	67(1)
C(40)	3518(9)	10069(6)	2181(4)	65(5)
C(40B)	3265(7)	10173(6)	2108(4)	69(5)
C(41)	2058(6)	9799(4)	1311(4)	54(3)
C(42)	2485(9)	10051(7)	937(6)	64(4)
C(43)	1379(7)	9624(5)	1079(6)	59(4)

C(44)	1877(8)	10185(6)	1684(5)	72(4)
C(41B)	1986(5)	9771(3)	1323(4)	53(3)
C(42B)	2393(8)	10190(5)	1092(6)	66(4)
C(43B)	1485(7)	9572(5)	939(4)	49(3)
C(44B)	1553(7)	10006(5)	1707(4)	67(4)
C(46)	1193(2)	8200(1)	637(1)	34(1)
C(47)	1892(1)	8236(1)	558(1)	38(1)
C(48)	2119(1)	8501(1)	175(1)	42(1)
C(49)	1647(2)	8730(1)	-130(1)	43(2)
C(50)	948(2)	8694(1)	-51(1)	38(1)
C(51)	721(1)	8429(1)	332(1)	35(1)
C(52)	2922(3)	8479(3)	103(3)	56(2)
C(53)	3325(5)	8190(4)	489(4)	70(3)
C(54)	3297(5)	8980(3)	60(4)	78(3)
C(55)	3024(6)	8200(4)	-361(3)	77(3)
C(52B)	2904(4)	8456(5)	60(5)	60(3)
C(53B)	3160(7)	8629(7)	-416(5)	64(4)
C(54B)	3264(9)	8775(7)	440(6)	69(4)
C(55B)	3142(9)	7913(5)	123(7)	74(4)
O(7)	1884(2)	9039(2)	-472(2)	53(1)
C(56)	1951(3)	9553(2)	-355(3)	67(2)
C(57)	381(4)	8892(3)	-410(3)	48(2)
C(58)	606(5)	8996(4)	-910(3)	57(3)
C(59)	86(5)	9372(3)	-201(3)	57(3)
C(60)	-210(5)	8512(4)	-458(4)	58(3)
C(57B)	373(6)	8873(6)	-421(4)	51(3)
C(58B)	570(9)	8682(7)	-909(6)	59(4)
C(59B)	211(9)	9434(5)	-485(8)	78(5)
C(60B)	-344(7)	8645(7)	-334(7)	58(5)
C(61)	925(5)	7200(2)	850(2)	34(2)
C(62)	756(4)	7155(2)	375(2)	42(2)
C(63)	698(4)	6686(2)	172(2)	53(2)
C(64)	810(5)	6262(2)	442(3)	58(2)
C(65)	980(5)	6306(2)	916(3)	54(2)
C(66)	1037(5)	6775(2)	1120(2)	44(2)
C(67)	690(5)	6689(4)	-378(3)	78(3)
C(68)	-21(5)	6900(5)	-518(5)	105(4)
C(69)	798(7)	6201(4)	-642(5)	110(4)
C(70)	1222(6)	7060(4)	-560(4)	112(4)
O(8)	602(4)	5792(2)	251(3)	74(2)
C(71)	-119(6)	5705(4)	172(4)	89(4)
C(72)	1142(5)	5847(3)	1246(3)	69(2)
C(73)	460(5)	5598(5)	1378(5)	90(4)
C(74)	1597(6)	5461(4)	1009(4)	94(4)
C(75)	1506(6)	5995(3)	1714(3)	75(3)
C(61B)	1031(11)	7187(3)	873(5)	40(3)

C(62B)	896(11)	7101(4)	399(5)	41(3)
C(63B)	872(11)	6616(5)	228(4)	52(3)
C(64B)	982(12)	6217(3)	531(6)	60(3)
C(65B)	1116(11)	6302(4)	1005(5)	55(2)
C(66B)	1140(11)	6787(5)	1176(4)	45(3)
C(67B)	717(9)	6588(6)	-319(4)	67(3)
C(68B)	260(11)	6136(7)	-443(9)	78(6)
C(69B)	1393(9)	6523(8)	-582(8)	83(5)
C(70B)	369(12)	7042(7)	-561(8)	90(5)
O(8B)	1031(8)	5755(4)	326(5)	60(3)
C(71B)	1659(11)	5500(9)	219(7)	90(7)
C(72B)	1117(9)	5864(6)	1379(6)	74(3)
C(73B)	628(11)	5444(9)	1207(7)	89(6)
C(74B)	1815(9)	5611(10)	1492(7)	100(5)
C(75B)	854(13)	6016(8)	1864(7)	99(6)
O(9)	-1747(7)	9286(4)	242(4)	39(2)
O(10)	-1813(7)	8430(5)	161(4)	35(2)
O(11)	-1494(7)	7443(5)	37(4)	42(2)
O(12)	-1408(7)	6592(4)	136(4)	43(2)
C(76)	-540(20)	8462(3)	1164(13)	28(2)
C(77)	-469(9)	8975(4)	1176(6)	34(2)
C(78)	-860(8)	9291(4)	876(5)	36(3)
C(79)	-1321(10)	9059(4)	582(7)	36(2)
C(80)	-2143(7)	8886(5)	53(5)	40(3)
C(81)	-1357(10)	8544(4)	535(7)	34(2)
C(82)	-965(17)	8232(4)	810(11)	31(2)
C(83)	-922(12)	7676(4)	793(6)	32(2)
C(84)	-1196(11)	7349(4)	473(5)	37(2)
C(85)	-1762(8)	6980(5)	-123(5)	46(3)
C(86)	-1121(9)	6840(4)	524(5)	40(2)
C(87)	-952(8)	6630(4)	969(5)	36(2)
C(88)	-602(8)	6960(4)	1276(5)	34(2)
C(89)	-573(6)	7466(3)	1195(4)	29(2)
O(9B)	-1915(6)	9270(4)	340(4)	41(2)
O(10B)	-1963(6)	8413(4)	245(4)	35(2)
O(11B)	-1678(7)	7427(4)	113(4)	43(2)
O(12B)	-1621(6)	6575(4)	225(4)	46(2)
C(76B)	-540(20)	8450(3)	1155(13)	28(2)
C(77B)	-553(8)	8962(4)	1216(5)	33(2)
C(78B)	-997(7)	9275(4)	952(5)	34(2)
C(79B)	-1414(9)	9044(4)	629(6)	35(2)
C(80B)	-2321(6)	8865(5)	172(5)	40(2)
C(81B)	-1441(9)	8529(4)	577(6)	34(2)
C(82B)	-1003(16)	8219(4)	820(10)	32(2)
C(83B)	-989(11)	7662(4)	823(6)	32(2)
C(84B)	-1287(11)	7333(4)	514(5)	38(2)

C(85B)	-1976(8)	6967(5)	-25(5)	46(3)
C(86B)	-1267(8)	6824(4)	585(5)	39(2)
C(87B)	-796(8)	6608(4)	915(5)	37(2)
C(88B)	-516(8)	6947(4)	1244(5)	33(2)
C(89B)	-571(6)	7458(3)	1198(4)	28(2)
C(90)	-1144(2)	8714(1)	2244(1)	33(1)
C(91)	-742(1)	9103(1)	2421(1)	41(1)
C(92)	-1001(2)	9585(1)	2422(1)	43(2)
C(93)	-1662(2)	9679(1)	2247(2)	48(2)
C(94)	-2064(1)	9291(1)	2070(2)	54(2)
C(95)	-1805(2)	8808(1)	2069(1)	45(2)
C(96)	-603(5)	10001(3)	2710(4)	41(3)
C(97)	44(5)	9800(4)	2961(5)	40(3)
C(98)	-1051(7)	10243(6)	3081(5)	50(3)
C(99)	-382(7)	10409(6)	2371(5)	58(4)
C(96B)	-477(7)	9994(5)	2605(6)	51(3)
C(97B)	204(7)	9791(5)	2813(6)	50(4)
C(98B)	-843(10)	10276(8)	2992(7)	62(5)
C(99B)	-271(10)	10365(8)	2225(6)	72(5)
O(13)	-1863(2)	10171(2)	2179(2)	59(1)
C(100)	-1895(11)	10368(10)	1709(4)	74(5)
C(200)	-1792(11)	10322(13)	1693(5)	71(7)
C(101)	-2874(3)	9345(4)	2059(5)	64(3)
C(102)	-3195(7)	9819(4)	2261(6)	76(4)
C(103)	-3222(6)	8906(5)	2304(6)	66(4)
C(104)	-3085(9)	9316(6)	1537(5)	91(5)
C(201)	-2845(4)	9294(5)	1893(5)	59(3)
C(202)	-3238(8)	9768(5)	2027(7)	72(4)
C(203)	-3275(7)	8861(5)	2086(7)	58(4)
C(204)	-2899(8)	9247(6)	1355(5)	64(4)
C(105)	-1554(1)	7721(1)	2230(1)	34(1)
C(106)	-1930(2)	7606(2)	1823(1)	44(2)
C(107)	-2568(2)	7376(2)	1851(1)	51(2)
C(108)	-2828(1)	7263(2)	2286(1)	46(2)
C(109)	-2452(2)	7378(2)	2692(1)	45(2)
C(110)	-1814(2)	7607(1)	2664(1)	38(1)
C(111)	-2990(7)	7290(6)	1372(3)	57(3)
C(112)	-2858(9)	7723(7)	1033(6)	65(4)
C(113)	-3774(7)	7271(8)	1426(5)	66(4)
C(114)	-2768(10)	6815(6)	1114(6)	77(5)
C(211)	-3064(6)	7423(5)	1402(4)	57(3)
C(212)	-2860(9)	7845(6)	1070(5)	72(5)
C(213)	-3828(7)	7507(7)	1497(6)	70(4)
C(214)	-3001(10)	6929(5)	1138(6)	84(5)
O(14)	-3411(2)	6984(2)	2327(2)	62(1)
C(115)	-3241(11)	6456(3)	2291(6)	72(6)

C(215)	-3419(9)	6467(3)	2180(6)	62(5)
C(116)	-2724(8)	7256(6)	3197(3)	53(3)
C(117)	-3370(10)	7585(7)	3187(7)	77(5)
C(118)	-2944(10)	6741(5)	3381(6)	76(5)
C(119)	-2226(8)	7455(7)	3583(6)	66(5)
C(216)	-2847(6)	7385(5)	3164(3)	51(3)
C(217)	-3501(8)	7705(6)	3147(7)	66(4)
C(218)	-3035(8)	6846(5)	3276(5)	58(4)
C(219)	-2382(8)	7578(6)	3567(5)	59(4)
C(121)	160(2)	7456(1)	3354(1)	32(1)
C(122)	-154(2)	7034(1)	3164(1)	33(1)
C(123)	-174(2)	6596(1)	3422(1)	41(1)
C(124)	120(2)	6580(1)	3872(1)	44(2)
C(125)	435(2)	7002(1)	4062(1)	41(1)
C(126)	454(2)	7440(1)	3803(1)	35(1)
C(127)	-610(3)	6152(2)	3218(2)	55(2)
C(128)	-1000(4)	6288(3)	2761(2)	63(2)
C(129)	-1142(4)	6000(3)	3573(3)	73(2)
C(130)	-153(4)	5704(3)	3109(3)	72(2)
C(227)	-641(9)	6153(6)	3230(10)	61(4)
C(228)	-253(16)	5905(15)	2829(10)	66(7)
C(229)	-1310(9)	6367(9)	3009(14)	61(6)
C(230)	-869(12)	5728(9)	3553(10)	65(7)
O(15)	209(2)	6122(2)	4088(2)	54(1)
C(131)	886(4)	5908(3)	4059(3)	64(2)
C(231)	746(14)	5800(20)	3912(16)	56(10)
C(132)	648(3)	7071(2)	4597(2)	56(2)
C(133)	474(5)	6638(3)	4926(3)	72(2)
C(134)	1425(3)	7164(3)	4634(3)	67(2)
C(135)	279(4)	7530(3)	4794(3)	69(2)
C(232)	692(12)	7025(10)	4592(4)	61(4)
C(233)	81(16)	6874(18)	4889(16)	68(7)
C(234)	1292(16)	6679(14)	4736(11)	64(6)
C(235)	900(20)	7553(10)	4749(11)	65(6)
C(136)	181(2)	8483(1)	3438(1)	36(1)
C(137)	-483(1)	8601(1)	3564(1)	43(2)
C(138)	-588(1)	8926(2)	3933(2)	55(2)
C(139)	-29(2)	9134(1)	4177(1)	50(2)
C(140)	636(2)	9015(1)	4051(1)	45(2)
C(141)	740(1)	8690(1)	3682(1)	37(1)
C(142)	-1372(4)	8956(5)	4069(4)	66(3)
C(143)	-1900(6)	8957(7)	3656(5)	69(4)
C(144)	-1485(13)	8473(5)	4350(7)	75(4)
C(145)	-1585(7)	9380(5)	4400(5)	92(5)
C(242)	-1309(5)	8890(6)	4174(5)	65(3)
C(243)	-1816(9)	9040(9)	3777(6)	67(5)

C(244)	-1467(18)	8352(6)	4321(9)	71(5)
C(245)	-1467(7)	9220(6)	4597(5)	61(4)
O(16)	-129(2)	9507(2)	4496(2)	63(1)
C(146)	-195(7)	9986(4)	4255(7)	72(5)
C(246)	-116(12)	10024(5)	4350(11)	71(6)
C(147)	1247(4)	9129(4)	4412(3)	60(3)
C(148)	1422(6)	9685(3)	4426(5)	66(3)
C(149)	1099(6)	8964(4)	4913(3)	68(4)
C(150)	1909(6)	8862(5)	4270(5)	61(4)
C(247)	1305(5)	9183(5)	4336(4)	59(3)
C(248)	1661(9)	9588(6)	4051(6)	72(5)
C(249)	1187(7)	9396(6)	4825(5)	74(4)
C(250)	1810(9)	8746(5)	4410(6)	58(4)
O(17)	1633(2)	7794(1)	1427(1)	33(1)
O(18)	-421(2)	8022(1)	2697(1)	30(1)

[a]Values represent atomic coordinates x 10^4 and equivalent isotropic displacement parameters ($\mathring{A}^2$ x 10^3) for **23**. U(eq) is defined as one third of the trace of the orthogonalized U tensor.

Kinetic studies on the addition of 4-CF₃-benzamide to norbornene
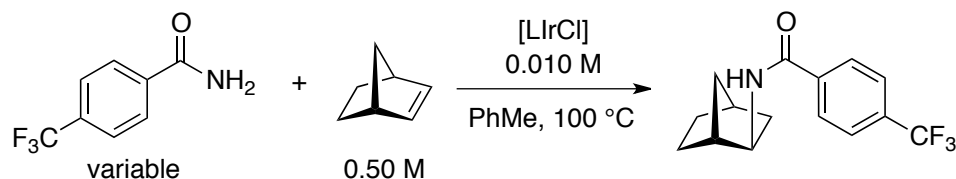
In a nitrogen-filled dry-box, stock solutions of complex **1** (0.015 M), 4-CF₃-benzamide (0.25 M), and norbornene (0.25 M) in THF were prepared. The appropriate volumes of the stocks solutions were dispensed into an oven dried 4 ml screw-capped vial. The THF was evaporated from the solution under vacuum over 2 hours. Toluene (0.29 ml), dodecane (10 μl) as internal standard and a magnetic stirbar were added to the residue, which was then sealed with a Teflon cap. The reaction mixture was stirred in an aluminum heating block at 100 °C outside of the dry-box. The reaction was removed every hour and rapidly cooled in a water bath. The vial was taken into the dry-box, and a 10 μl aliquot was removed from the reaction mixture. The vial was resealed and returned to the metal heating block. The aliquots were analyzed by gas chromatography with dodecane as the internal standard. Reaction rates were determined by measuring product formation at low conversion because the GC peak for the product was more accurate than that for the primary amide reactant. The peak for the primary amide was not symmetric due to a long tail. An example of the raw data acquired by gas chromatography analysis is provided in Figure 2.10. NMR analysis for a single sample at multiple time-points demonstrated that product formation equaled conversion of starting material. (Note: reactions conducted for kinetic measurements were run at lower temperatures and with lower catalyst loadings than those for evaluating the reaction scope and obtaining isolated porduct. The lower temperatures and catalyst loading allowed data to be collected at low conversions.)
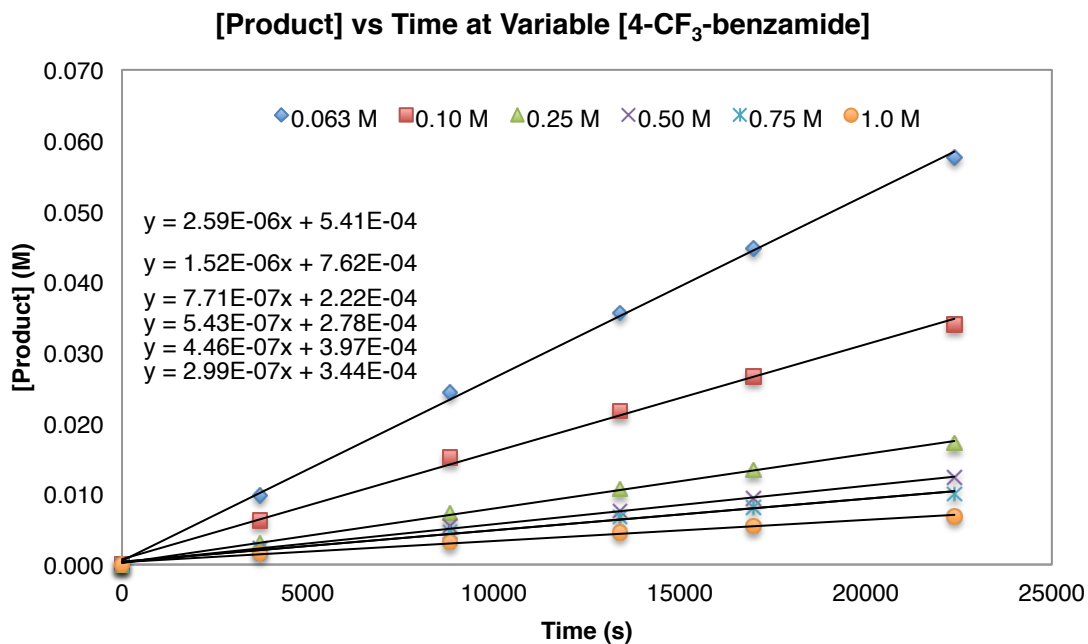
[Product] vs Time at Variable [4-CF₃-benzamide]

$y = 2.59E\text{-}06x + 5.41E\text{-}04$

$y = 1.52E\text{-}06x + 7.62E\text{-}04$

$y = 7.71E\text{-}07x + 2.22E\text{-}04$
$y = 5.43E\text{-}07x + 2.78E\text{-}04$
$y = 4.46E\text{-}07x + 3.97E\text{-}04$
$y = 2.99E\text{-}07x + 3.44E\text{-}04$

Figure 2.10. Product formation as a function of time at low conversion.

Rate vs [4-CF₃-benzamide]

$y = 0.3272x^{-0.699}$
$R^2 = 0.97514$

Rate vs 1/[4-CF₃-benzamide]
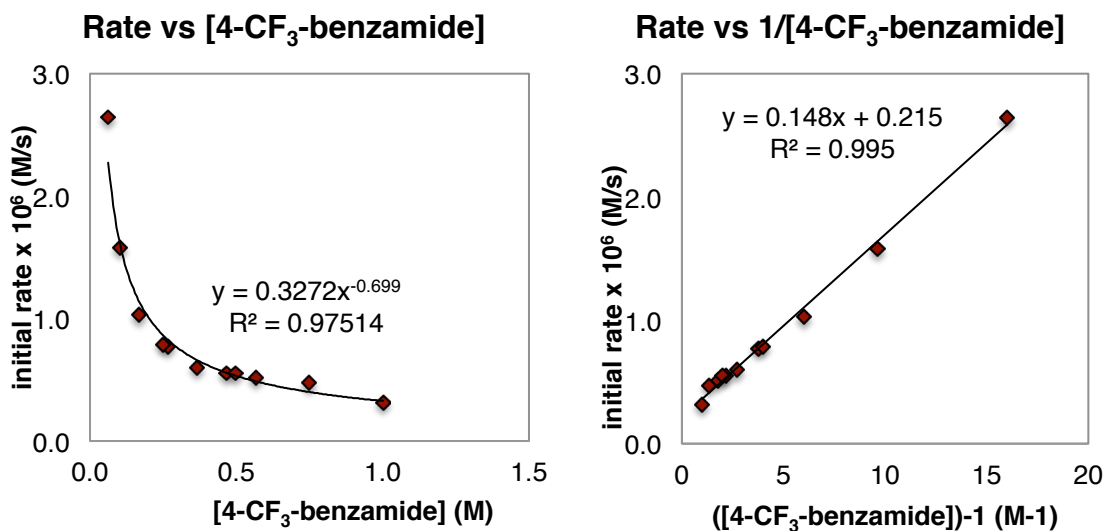

$y = 0.148x + 0.215$
$R^2 = 0.995$

Figure 2.11. Effect of 4-CF₃-benzamide concentration on the rate of Ir-catalyzed addition of 4-CF₃-benzamide to norbornene.

Kinetic studies on the addition of 4-CF$_3$-benzamide to norbornene: variable [norbornene]
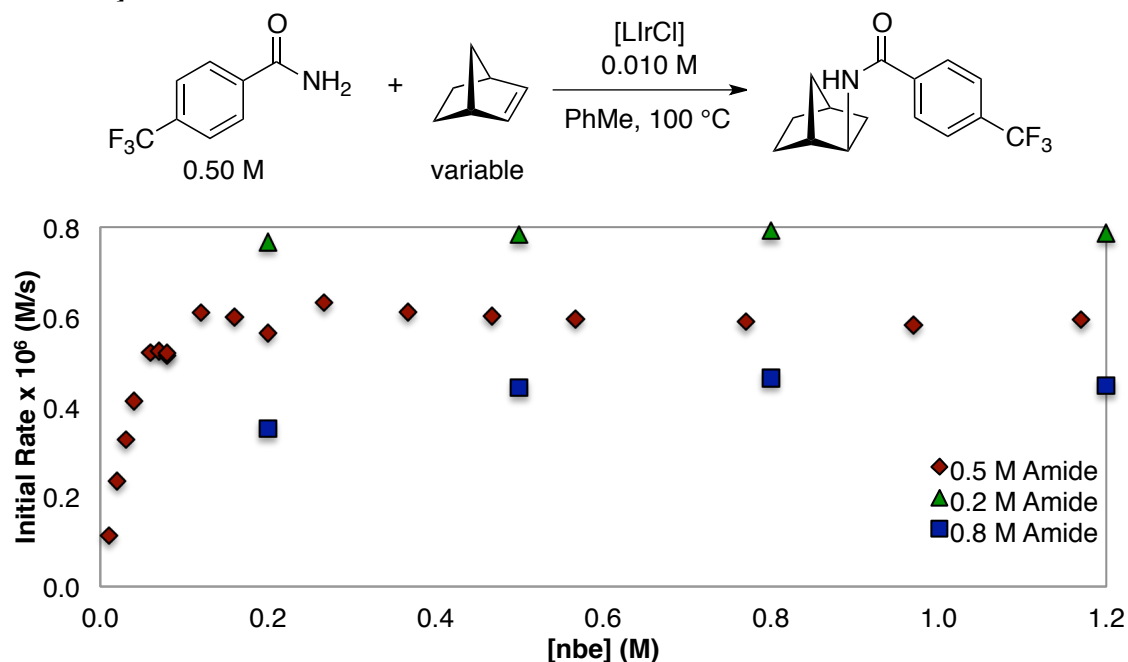

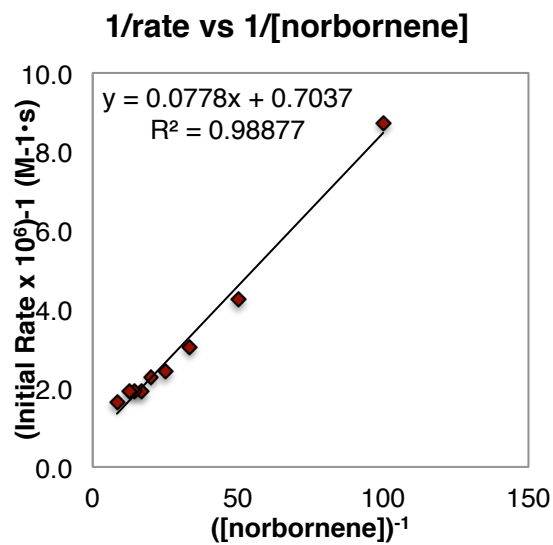**Figure 2.12.** Effect of norbornene concentration on the initial rate of Ir-catalyzed NH addition to norbornene.

Figure 2.13. Effect of norbornene concentration on the rate of Ir-catalyzed addition of 4-CF$_3$-benzamide to norbornene.
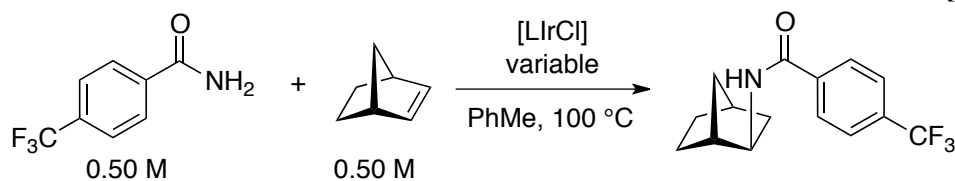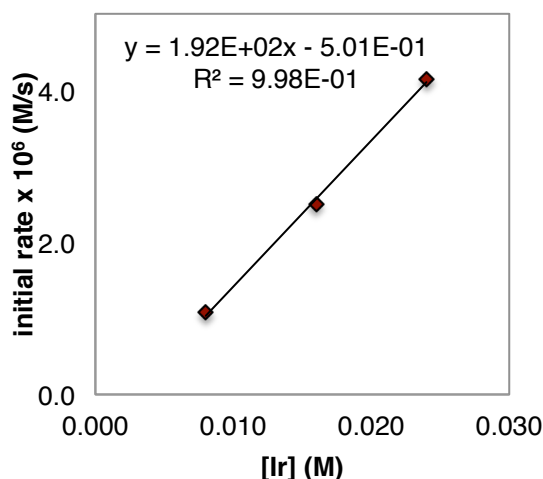
Kinetic studies on the addition of 4-CF₃-benzamide to norbornene: variable [Ir]

Figure 2.14. Effect of concentration of Ir catalyst on the rate of Ir-catalyzed addition of 4-CF₃-benzamide to norbornene.

Kinetic studies on the addition of 4-CF₃-benzamide to 1-octene

In a nitrogen-filled dry-box, stock solutions of complex **1** (0.015 M) and 4-CF₃-benzamide (0.25 M) in THF were prepared. The appropriate volumes of the stocks solutions were dispensed into an oven-dried 4 ml screw-capped vial. The THF was removed from the solution under vacuum over 2 h, and 10 µl of dodecane and a magnetic stirbar were added. Variable amounts of 1-octene were then added to the reaction vessels, and the volumes were brought to 0.50 ml by adding the appropriate amount of toluene. The reaction mixture was stirred in an aluminum heating block at 100 °C outside of the dry-box. The reaction was removed every hour and rapidly cooled in a water bath. The vial was taken into the dry-box, and a 10 µl aliquot was removed from the reaction mixture. The vial was resealed and returned to the metal heating block. Aliquots were analyzed by gas chromatography with dodecane as the internal standard. Reaction rates were determined by measuring product formation at low conversion because the GC peak for the product was more accurate than that for the primary amide reactant. The peak for the primary amide was not symmetric due to a long tail. An example of the raw data acquired by gas chromatography analysis is provided in Figure 2.15. NMR analysis for a single sample at multiple time-points demonstrated that product formation equaled conversion of starting material.

Note: reactions conducted for kinetic measurements were run at lower temperatures and with lower catalyst loadings than those for evaluating the reaction scope and obtaining isolated porduct. The lower temperatures and catalyst loading allowed data to be collected at low conversions.

[Products] vs Time at Variable [1-octene]

y = 6.13E-07x + 2.26E-04
y = 5.51E-07x + 1.54E-04
y = 4.49E-07x + 1.12E-04
y = 3.80E-07x + 1.73E-04
y = 2.80E-07x + 5.72E-05
y = 1.91E-07x + 5.98E-05
y = 1.22E-07x + 7.79E-05
y = 6.59E-08x + 6.12E-06

Figure 2.15. Formation of products as a function of time at low conversion.

Rate vs [1-octene]

y = 8.44E-01x - 4.83E-02
R^2 = 9.98E-01
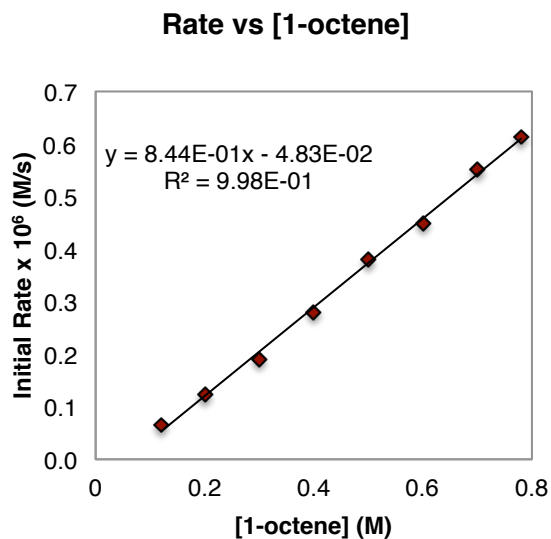
Figure 2.16. Effect of 1-octene concentration on the rate of Ir-catalyzed addition of 4-CF$_3$-benzamide to 1-octene.

Kinetic studies on the addition of 4-CF$_3$-benzamide to 1-octene: variable [4-CF$_3$-benzamide]

Rate vs [4-CF$_3$-benzamide]

$y = 0.0475x^{-0.75}$
$R^2 = 0.97978$

Figure 2.17. Effect of 4-CF$_3$-benzamide concentration on the rate of Ir-catalyzed addition of 4-CF$_3$-benzamide to 1-octene.

Rate vs 1/[4-CF$_3$-benzamide]

$y = 0.0233x + 0.0319$
$R^2 = 0.99824$

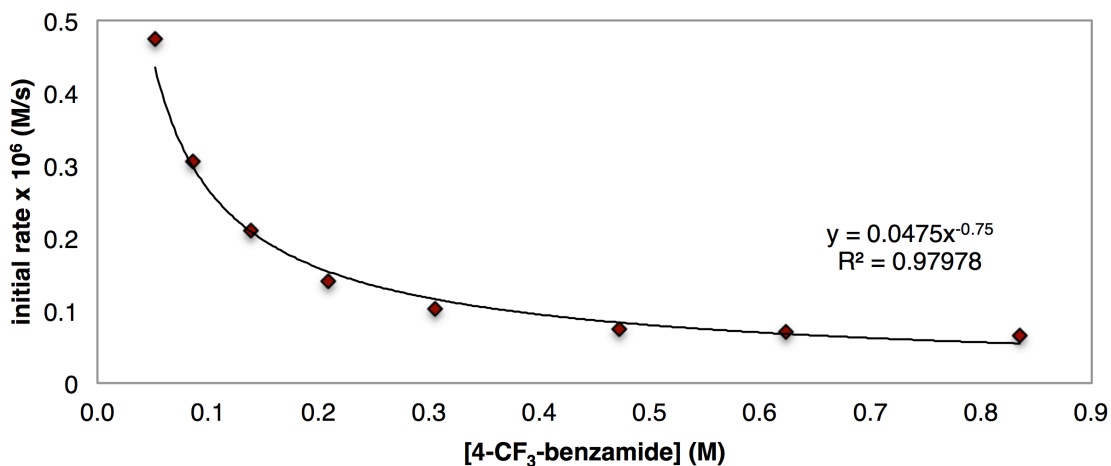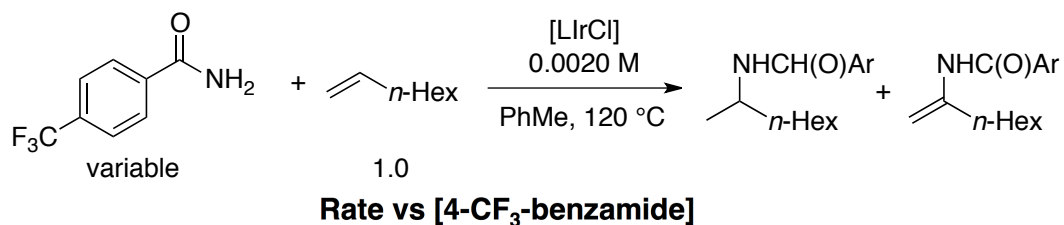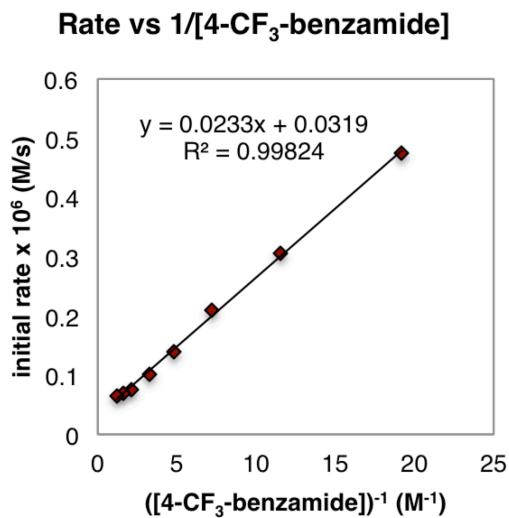**Figure 2.18.** Effect of 4-CF$_3$-benzamide concentration on the rate of Ir-catalyzed addition of 4-CF$_3$-benzamide to 1-octene.

Eyring analysis of the exchange of free and bound amide by the line shape of the resonance for the free amide (yellow-labeled signal Figure 2.4).

$\Delta H^{\ddagger} = 20.7$ kcal mol^{-1}
$\Delta S^{\ddagger} = 12.4$ cal K^{-1} mol^{-1}

1-p-F   **2-p-F**
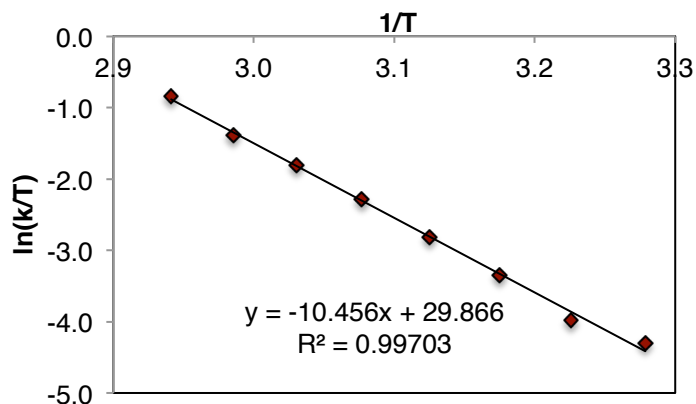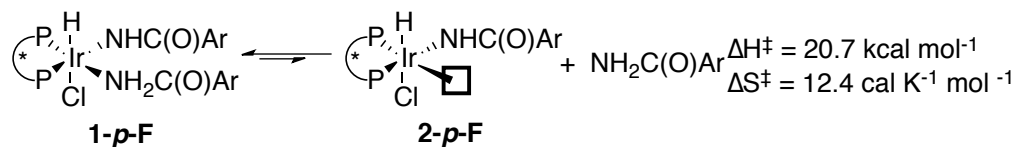
Figure 2.19. Eyring analysis of the exchange of free amide and bound amide in **1-p-F** by the line shape of the resonance for the free amide (yellow-labeled signal Figure 2.4).

$$k = \pi(\omega_{\frac{1}{2}} - \omega_0)$$

(ω_0 was measured as 11.5 Hz for a solution of 4-fluorobenzamide in toluene at room temperature)

$$\ln\left(\frac{k}{T}\right) = -\left(\frac{\Delta H^{\ddagger}}{R}\right)\frac{1}{T} + \left(23.76 + \frac{\Delta S^{\ddagger}}{R}\right)$$

$\Delta H^{\ddagger} = 20.7$ kcal/mol; $\Delta S^{\ddagger} = 12.4$ kcal/mol

2.5 References

(1)   Part of this chapter was reprinted with permission from Sevov, C. S.; Zhou, J.; Hartwig, J. F. *J. Am. Chem. Soc.*, **2012**, *134*, 11960. Copyright © 2012, American Chemical Society. Permission to include this co-authored material was obtained from Steve Zhou and John F. Hartwig. Professor Steve Zhou is gratefully acknowledged for preliminary results on the Ir-catalyzed NH bond addition of benzamide to 1-octene and norbornene.

(2)   Müller, T. E.; Hultzsch, K. C.; Yus, M.; Foubelo, F.; Tada, M. *Chem. Rev.*, **2008**, *108*, 3795.

(3)   Hartwig, J. F. In *Organotransition Metal Chemistry: From Bonding to Catalysis*; University Science Books: Sausalito, CA, 2010; Vol. 1, p 700.

(4)   Hesp, K. D.; Stradiotto, M. *Chemcatchem*, **2010**, *2*, 1192.

(5)   Ryu, J.-S.; Li, G. Y.; Marks, T. J. *J. Am. Chem. Soc.*, **2003**, *125*, 12584.

(6)   Wang, X.; Widenhoefer, R. A. *Organometallics*, **2004**, *23*, 1649.

(7)   Brunet, J. J.; Chu, N. C.; Diallo, O. *Organometallics*, **2005**, *24*, 3104.

(8)   Zhang, Z.; Lee, S. D.; Widenhoefer, R. A. *J. Am. Chem. Soc.*, **2009**, *131*, 5372.

(9)   Reznichenko, A. L.; Nguyen, H. N.; Hultzsch, K. C. *Angew. Chem. Int. Ed.*, **2010**, *49*, 8984.

(10)   Dorta, R.; Egli, P.; Zürcher, F.; Togni, A. *J. Am. Chem. Soc.*, **1997**, *119*, 10857.

(11)   Zhou, J.; Hartwig, J. F. *J. Am. Chem. Soc.*, **2008**, *130*, 12220.

(12)   Pan, S. G.; Endo, K.; Shibata, T. *Org. Lett.*, **2012**, *14*, 780.

(13)   Löber, O.; Kawatsura, M.; Hartwig, J. F. *J. Am. Chem. Soc.*, **2001**, *123*, 4366.

(14)   Sakai, N.; Ridder, A.; Hartwig, J. F. *J. Am. Chem. Soc.*, **2006**, *128*, 8134.

(15)   Nishina, N.; Yamamoto, Y. *Synlett*, **2007**, 1767.

(16)   Hesp, K. D.; Stradiotto, M. *J. Am. Chem. Soc.*, **2010**, *132*, 18026.

(17)   Butler, K. L.; Tragni, M.; Widenhoefer, R. A. *Angew. Chem. Int. Ed.*, **2012**, n/a.

(18)   Kawatsura, M.; Hartwig, J. F. *J. Am. Chem. Soc.*, **2000**, *122*, 9546.

(19)   Utsunomiya, M.; Hartwig, J. F. *J. Am. Chem. Soc.*, **2003**, *125*, 14286.

(20)   Qian, H.; Widenhoefer, R. A. *Org. Lett.*, **2005**, *7*, 2635.

(21)   Brunet, J.-J.; Cadena, M.; Chu, N. C.; Diallo, O.; Jacob, K.; Mothes, E. *Organometallics*, **2004**, *23*, 1264.

(22)   Cao, P.; Cabrera, J.; Padilla, R.; Serra, D.; Rominger, F.; Limbach, M. *Organometallics*, **2012**, *31*, 921.

(23)   Karshtedt, D.; Bell, A. T.; Tilley, T. D. *J. Am. Chem. Soc.*, **2005**, *127*, 12640.

(24)   Zhang, J.; Yang, C.-G.; He, C. *J. Am. Chem. Soc.*, **2006**, *128*, 1798.

(25)   Caille, S.; Boni, J.; Cox, G. B.; Faul, M. M.; Franco, P.; Khattabi, S.; Klingensmith, L. M.; Larrow, J. F.; Lee, J. K.; Martinelli, M. J.; Miller, L. M.; Moniz, G. A.; Sakai, K.; Tedrow, J. S.; Hansen, K. B. *Org. Process Res. Dev.*, **2009**, *14*, 133.

(26)   Beller, M.; Cornils, B.; Frohning, C. D.; Kohlpaintner, C. W. *J. Mol. Catal. A-Chem.*, **1995**, *104*, 17.

(27)   Lenges, C. P.; Brookhart, M.; White, P. S. *Angew. Chem. Int. Ed.*, **1999**, *38*, 552.

(28)   Muhoro, C. N.; He, X.; Hartwig, J. F. *J. Am. Chem. Soc.*, **1999**, *121*, 5033.

(29)   Lazzaroni, R.; Settambolo, R.; Alagona, G.; Ghio, C. *Coord. Chem. Rev.*, **2010**, *254*, 696.

(30)   Walsh, P. J.; Kozlowski, M. C. In *Fundamentals of Asymmetric Catalysis*; University Science Books: Sausalito, CA, 2009; Vol. 1, p 131.

(31)   Herde, J. L.; Lambert, J. C.; Senoff, C. V.; Cushing, M. A. In *Inorganic Syntheses*; John Wiley & Sons, Inc.: 2007, p 18.

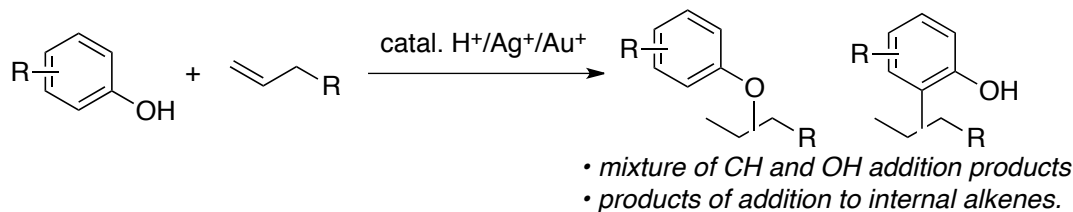(32)   Kirmse, W.; Siegfried, R. *J. Am. Chem. Soc.*, **1983**, *105*, 950.

CHAPTER 3

Iridium-Catalyzed, Intermolecular Hydroetherification
of Unactivated Aliphatic Alkenes with Phenols[1]

3.1 Introduction

Metal-catalyzed hydrofunctionalization of alkenes offers the potential to control regioselectivity, diastereoselectivity and enantioselectivity of the addition process and to form products from readily accessible starting materials without formation of waste. Metal-catalyzed hydrofunctionalizations also could be more tolerant of auxiliary functionality than acid-catalyzed additions and could occur without the rearrangements that are characteristic of acid-catalyzed additions to alkenes. Hydroamination, the addition of an N–H bond across an unsaturated C–C bond, remains one of the most studied transformations in hydrofunctionalization chemistry,[2-3] but hydroetherification, the addition of an O–H bond across an unsaturated C–C bond, is much less developed.

The ether products of hydroetherification are more often formed by substitution reactions than addition reactions.[4-8] The electrophiles in substitution reactions are typically prepared by a multistep sequence that often includes oxidation or reduction and functional group interconversion or activation of an alcohol. Moreover, these substitution reactions generate salt byproducts. Alternatively, ethers are formed by acid-catalyzed additions of alcohols to alkenes.[9] However, these additions often require strong acids and high temperatures, form side products from isomerization of carbocationic intermediates, and occur without control of the stereochemistry of the product. Moreover, acid-catalyzed additions of phenols to alkenes occur with competitive reaction of the alkene at the O–H bond and at an *ortho* or *para* C–H bond (Figure 3.1).[10-11] Thus, metal-catalyzed hydroetherification would exploit the abundance and stability of alkene starting materials, and could overcome many of the limitations of the classical syntheses of ethers.

Brønstead and Lewis acid-catalyzed reactions of phenols with alkenes:

• mixture of CH and OH addition products
• products of addition to internal alkenes.

This work:

• exclusive O-H addition
• no carbocation rearrangements
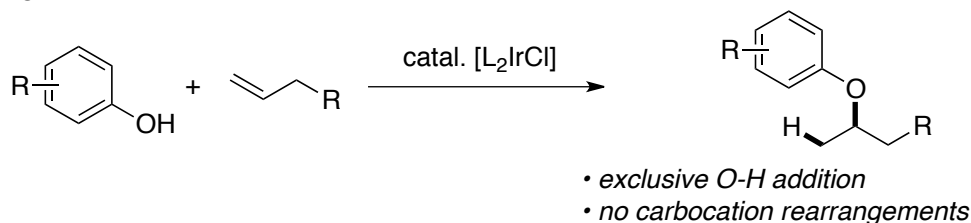
Figure 3.1. Common challenges to reactions of phenols with alkenes.

However, current hydroetherification reactions are limited in scope. Most reported metal-catalyzed hydroetherifications of unsaturated C–C bonds are intramolecular and occur with carbon-carbon multiple bonds that are more reactive than those of unactivated alkenes.[12] Cationic gold complexes catalyze the cyclization of allenyl-alcohols in high yield and excellent ee, but the reactions do not occur intermolecularly or with monoenes.[13-17] Likewise, Ir, Pd, Pt, and lanthanide complexes catalyze intramolecular additions of alcohols to alkenes and alkynes, but the intermolecular additions to alkenes catalyzed

by such complexes are unknown.[18-25] Intermolecular hydroetherification of allenes with both carboxylic acids and phenols to form allylic ethers has been reported to occur in high yield and ee in the presence of a Rh catalyst, but the reactions do not occur with mono-enes.[26-28] Finally, the intermolecular additions of alcohols to unstrained, isolated alkenes have been reported to occur in the presence of triflates of coinage metals.[29-31] In these cases, the reactions form side products that are characteristic of carbocation intermediates.[32]

Here, we report intermolecular, metal-catalyzed additions of phenols to unactivated a-olefins in good yields. The measurable enantioselectivity and lack of reaction in the presence of acid, but absence of the metal, show that the iridium complex, not a proton, catalyzes the addition reaction. Mechanistic studies imply that the reaction proceeds by reversible oxidative addition of the O–H bond of the phenol, followed by turnover-limiting insertion of the alkene. Shortly after publication of this research, the Goldman group reported a pincer-iridium complex that catalyzes the addition of phenol OH bonds to ethylene, propene and butene with 10-50 turnover numbers.[33]

3.2 Results and Discussions

We previously showed that the combination of iridium and DTBM-Segphos catalyzes the additions of amides to alkenes.[34] On the basis of these studies we tested the combination of $[Ir(coe)_2Cl]_2$ and a series of phosphine, bisphosphine, and chelating nitrogen ligands as catalyst for the addition of 3-OMe-phenol to 1-octene (see the experimental section for studies with various ligands). Only Ir complexes of (*S*)-DTBM-Segphos (DTBM = 3,5-di-*tert*-butyl-4-methoxy) led to substantial amounts of ether and enol-ether products. Further experiments conducted with (*S*)-DTBM-Segphos as ligand are summarized in Table 3.1. Isomerization of the terminal alkene to unreactive internal olefin isomers was observed over the course of the reaction; because internal alkenes are less reactive than terminal alkenes, this isomerization limited conversion of the alkene to the ether. Reactions conducted with $[Ir(cod)Cl]_2$ as a precursor with a slight excess of bisphosphine, relative to Ir, occurred with less alkene isomerization and concomitantly greater yield of products, compared to reactions conducted with $[Ir(coe)_2Cl]_2$ as the iridium precursor (entry 2 vs. 1).

Table 3.1. Reaction Development for the Ir-Catalyzed Addition of 3-OMe-Phenol to 1-Octene[a]

| entry	metal precursor	additive (mol %)	n equiv 1-octene	% 1-octene[b] remaining	% 1[b]	% 1-ox[b]
1	[Ir(coe)$_2$Cl]$_2$	--	10	11	30	4
2	[Ir(cod)Cl]$_2$	--	10	26	46[c]	10
3	--	HOTf (4%)	10	88	0	0
4	[Ir(cod)Cl]$_2$	Et$_3$N (17%)	10	48	35	6
5	[Ir(cod)Cl]$_2$	AgBF$_4$ (4%)	10	2	68[d]	0
6	[Ir(cod)$_2$][BF$_4$]	--	10	2	0	0
7	[Ir(cod)$_2$][BF$_4$]	KHMDS (4%)	10	5	18	2
8	[Ir(cod)Cl]$_2$	--	5	3	24	5
9	[Ir(cod)Cl]$_2$	--	20	48	60[e]	16
10	[Ir(cod)Cl]$_2$	--	40	64	51[f]	17
11	[Ir(cod)Cl]$_2$	--	80	70	38	20

[a]Reactions were performed with 0.2 mmol phenol. [b]Determined by GC analysis. [c]19% ee. [d]1:1:1 racemic mixture of 2-, 3-, 4-aryloxy octane. [e]25% ee. [f]36% ee.

Several experiments provide strong evidence that the reaction is catalyzed by iridium, not a proton. Measurable, albeit modest, ee values for this reaction (19-40%) rule out alkene hydroetherification catalyzed by a proton alone. Products were not detected from reactions conducted in the presence of ligand HOTf (entry 3), excluding an addition catalyzed by a phosphonium salt. Reactions conducted with excess tributylamine relative to iridium, which would quench trace acid, occurred with comparable yields (entry 4) to the reaction in the absence of this additive. Reactions conducted by initial halide abstraction from iridium with AgBF$_4$ led to the formation of a mixture of racemic ether products, consistent with an acid-catalyzed process. Reactions conducted with a cationic Ir precursor and ligand did not yield product (entry 6), but those conducted with a cationic Ir precursor, ligand, and base formed product (entry 7), presumably after generating a neutral Ir complex. A greater fraction of 1-octene vs. other isomers was observed for reactions conducted with 20 equivalents of olefin than reactions conducted with 5 or 10 equivalents of alkene and resulted in a 60% yield of **1** (entry 9).

The scope of the Ir-catalyzed addition of phenols to α-olefins by the procedure we developed is summarized in Chart 3.1. Products containing the phenoxy group at the 2-position of the alkyl chain were formed exclusively with ee's ranging from 8% to 60%, the highest value being observed for reaction of an alkene containing steric bulk proximal to the alkene (**13**). Upon completion of the reaction, the enol-ether products that result from oxidative etherification of the alkene were hydrolyzed with acid to facilitate isolation of the alkyl aryl ether products. A broad range of functional groups located *meta* and *para* to the OH-group were compatible with the addition process; the reaction between olefins and phenols containing halides, ethers, and tertiary amines occurred in good yields. Although reactions of 1-naphthol formed product **19** in good yield, other phenols

containing substituents *ortho* to the OH-group did not add to the a-olefins under similar conditions.

Chart 3.1. Ir-Catalyzed Additions of Phenols to α-Olefins[a]
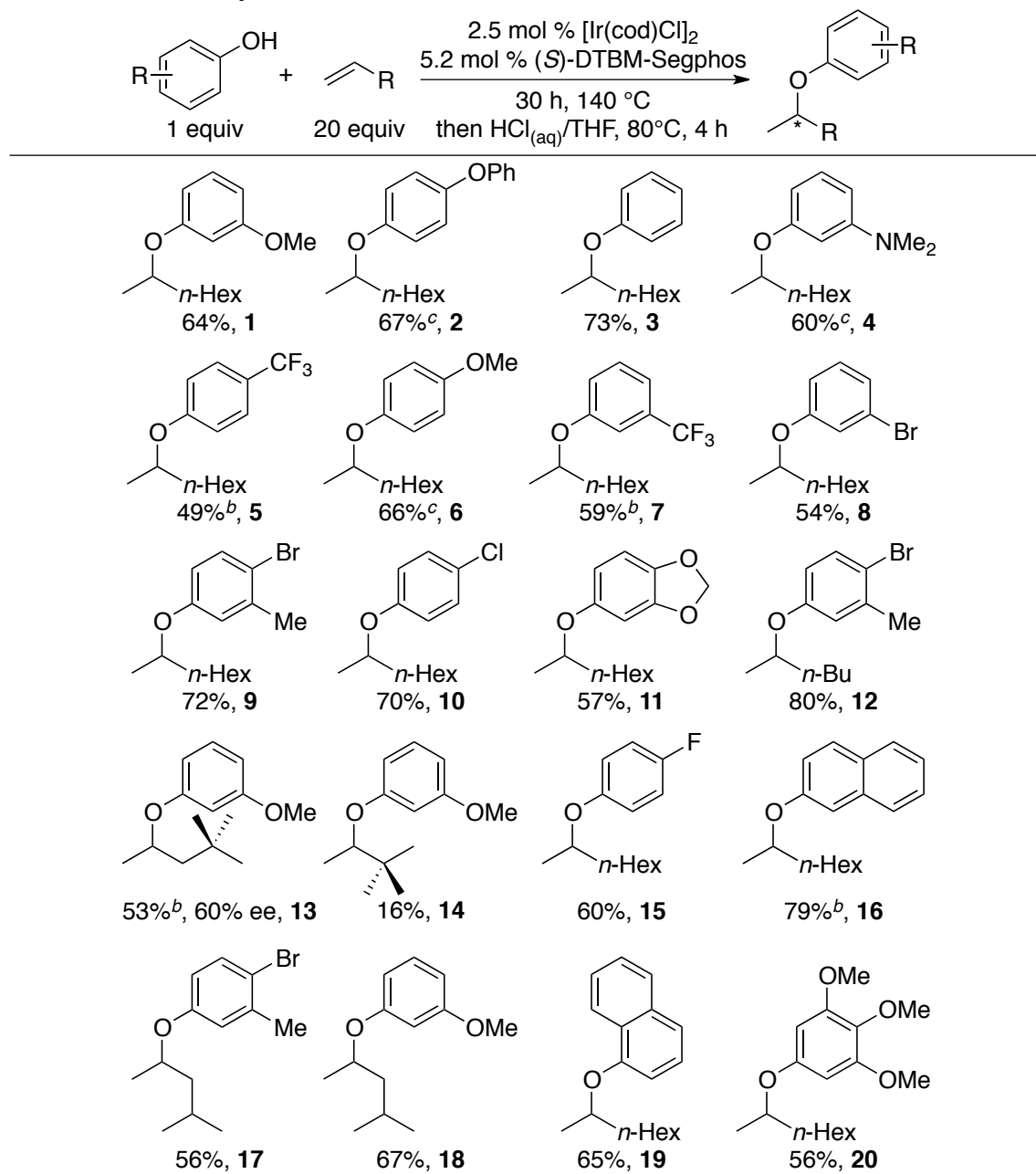
[a]Isolated yields. Reaction was performed with: [b]40 equivalents or [c]10 equivalents of alkene relative to ArOH. [d]Reactions were conducted in mesitylene solvent.

The electronic properties of the substituents on the phenol influenced the reaction conversion and yield. Reactions of electron-poor phenols typically occurred in lower yields than reactions of electron-rich phenols because there was a greater amount of al-kene isomerization during the reaction of the electron-poor phenol. Complete isomeriza-

tion of the terminal alkene was observed after 24 h for reactions of 4-CF$_3$-phenol while only half of the terminal alkene isomerized during reactions of 4-OMe-phenol. Consequently, reactions of electron-rich phenols conducted with 10 equivalents of olefin, rather than the 20 equivalents used for a majority of the reactions, formed the addition products in good yield.

The scope of the reaction in alkene also was examined. Addition products were not detected from reactions of phenols with olefins containing activated allylic C–H bonds, such as allylbenzene, under the conditions we developed. Rapid isomerization of these terminal alkenes occurred. Alkenes with steric bulk in close proximity to the reactive alkene reacted more slowly than alkenes lacking this property. For example, the reaction of *tert*-butyl ethylene formed addition product **14** in low yield. However, reaction of 4,4-dimethyl-1-pentene and 4-methyl-1-pentene did form products **13**, **17**, and **18** in substantial yields.

Chart 3.2. Ir-Catalyzed Additions of Phenols to Ethylene and Propene
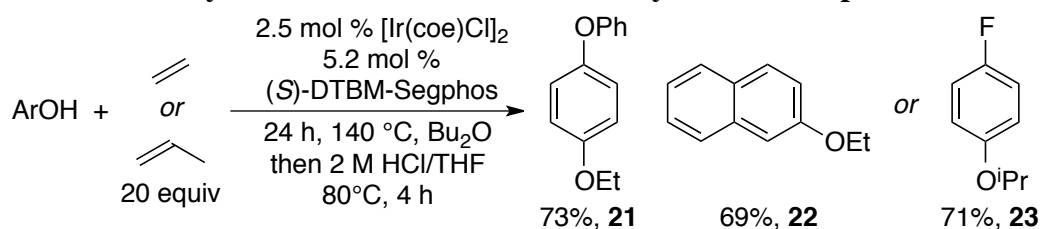
Reactions of phenols with ethylene and propene occurred with only 2.5 atm of alkene to form ether and enol ether products (Chart 3.2). Catalyst decomposition was observed upon accumulation of the enol ether during the reactions with ethylene. Nonetheless, the yields of reactions with these alkenes were higher than those with longer chain olefins because alkene isomers cannot form during reactions of these two alkenes.

The product of catalyst decomposition during reactions of ethylene was characterized by single crystal x-ray diffraction as the Ir(I) carbonyl complex **28** (Figure 3.2b). A similar decomposition was observed when heating the combination of [Ir(coe)$_2$Cl]$_2$ and ligand in dibutyl ether. A possible mechanism of formation of carbonyl complex **28** is illustrated in Figure 3.2a. CH bond activation alpha- to oxygen, followed by beta-alkyl elimination would release butane and generate pentanal. Decarbonylation of the resulting aldehyde would form complex 28 and another equivalent of butane. This proposed mechanism for catalyst decomposition is supported by evidence from a recent report on Ir-mediated CH activation of methyl phenylethers followed by phenoxy migration.[35] This pathway for catalyst decomposition likely occurs only during reactions of ethylene, which form linear alkyl ethers, because CH activation alpha- to oxygen of these compounds is more favorable than the analogues process of branched alkyl phenylethers.
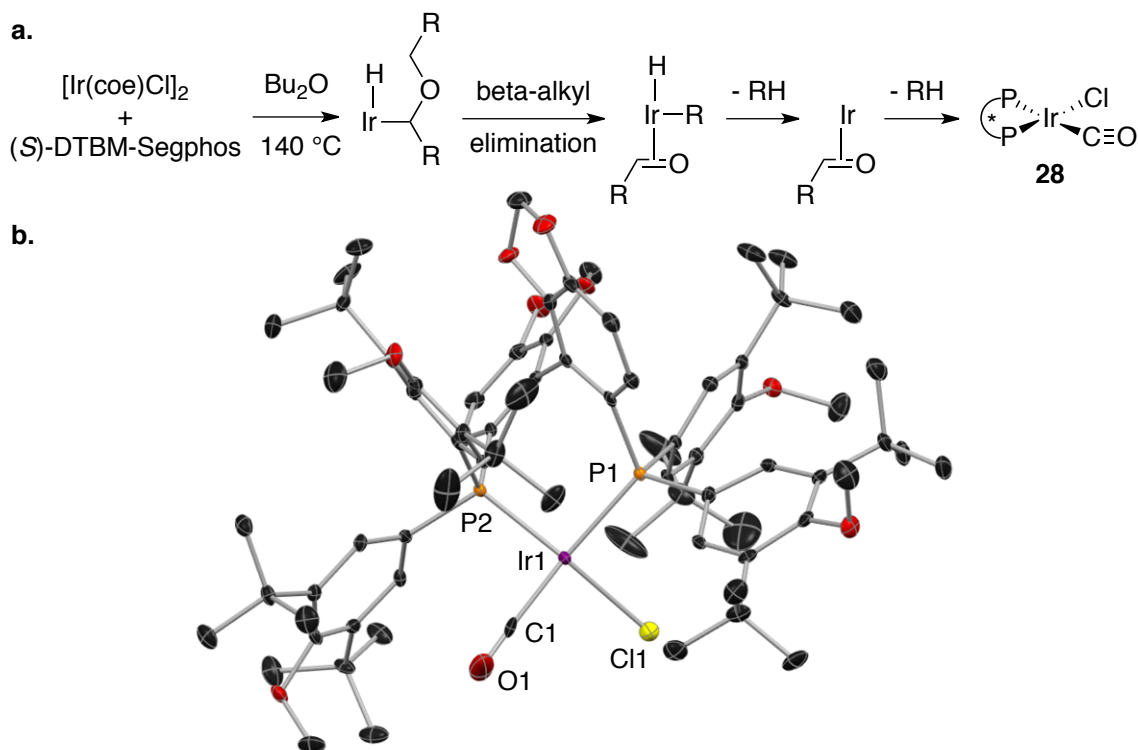
Figure 3.2. (a) Proposed mechanism for the formation of decomposition product **28**. Solid-state structure of complex **28**.

Mechanistic studies were conducted to gain insight into the elementary steps of this unusual process. Kinetic analysis of the additions of 4-F-phenol to propene was conducted. Initial rates (to 15% conversion) were measured by ^{19}F NMR spectroscopy (see the experimental section). The reaction was found to be first-order in catalyst, zero-order in the concentration of alkene and partial positive order (0.6) in the concentration of 4-F-phenol.

Figure 3.3. ^{31}P (left) and ^{1}H (right, Ir–H region only) NMR spectra *i.-v.* of **24** in the presence of varying concentrations of 4-F-phenol at 294 K.

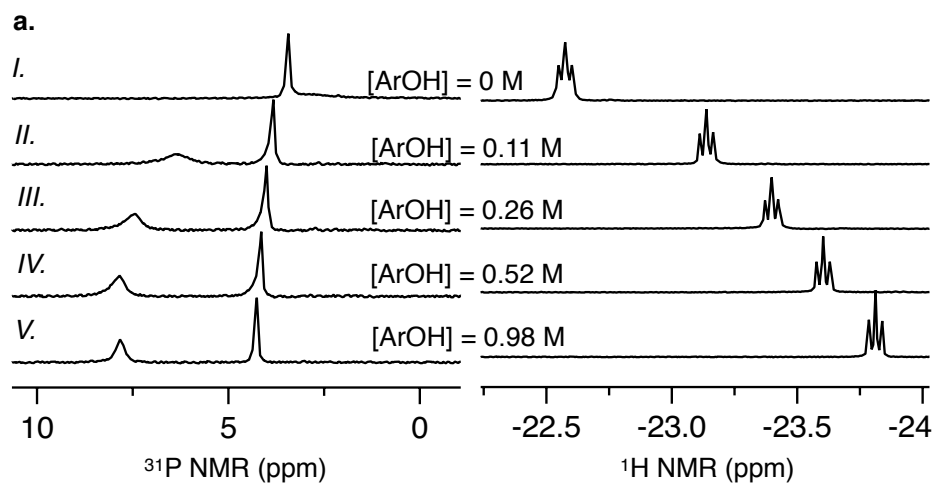Monitoring the reactions by ^{31}P NMR spectroscopy indicated that an unsymmetrical bisphosphine complex persisted throughout the course of the reaction (Figure 3.3, spectrum *V*). This observed species was characterized to allow interpretation of the kinetic data. The oxidative addition of O–H bonds to Ir(I) is well established.[36-40] However, addition of 4-F-phenol to a solution of [Ir(cod)Cl]$_2$ and DTBM-Segphos in benzene did not form any new species. In contrast, the combination of Ir, ligand, and olefin in the absence of alcohol did react; the original orange solution turned light yellow in 1 h at 294 K. A similar color change was observed at the start of the catalytic reaction. The product of this reaction was shown by NMR spectroscopy to be the Ir(allyl)hydride complex **24** illustrated in Figure 3.4.
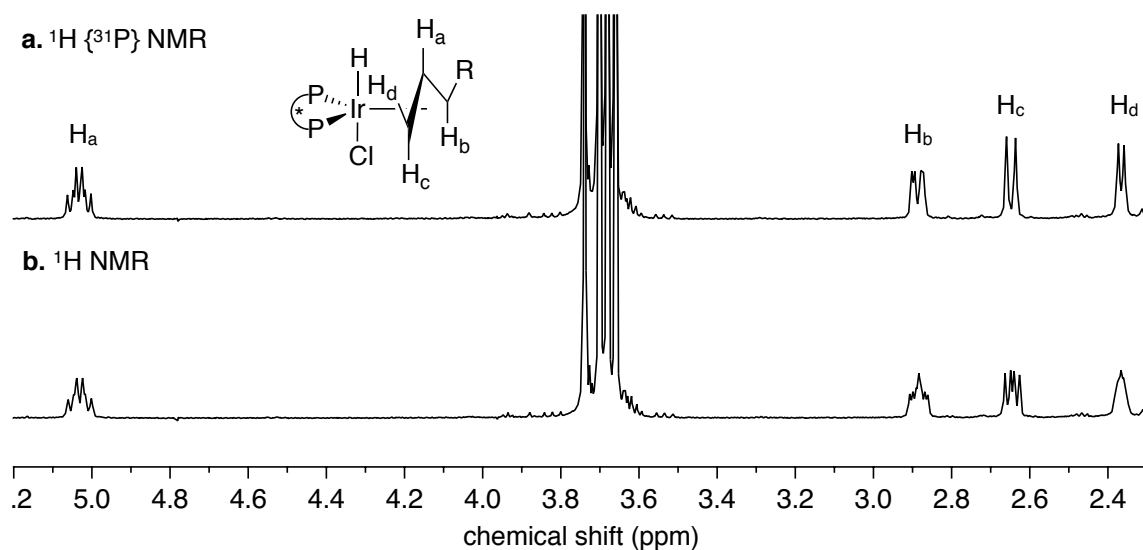
Figure 3.4. Assignment of protons of Ir(allyl)H complex **24** by the comparison of the (a) ^{31}P-decoupled ^{1}H NMR spectrum and (b) ^{1}H NMR spectrum.

The hydride resonance and phosphorus resonances observed by NMR spectroscopy of isolated **24** in C$_6$D$_6$ (Figure 3.3, spectrum *I*) did not match those of the species in the catalytic reaction (Figure 3.3, spectrum *V*). However, the hydride chemical shift in the ^{1}H NMR spectrum of solutions of **24** containing varying concentrations of 4-F-phenol depended on the concentration of the phenol, and the ^{1}H and ^{31}P NMR spectra of the solution containing a 1 M concentration of alcohol matched those of the complex observed in the catalytic reactions (Figure 3.3, spectra *I-V*).
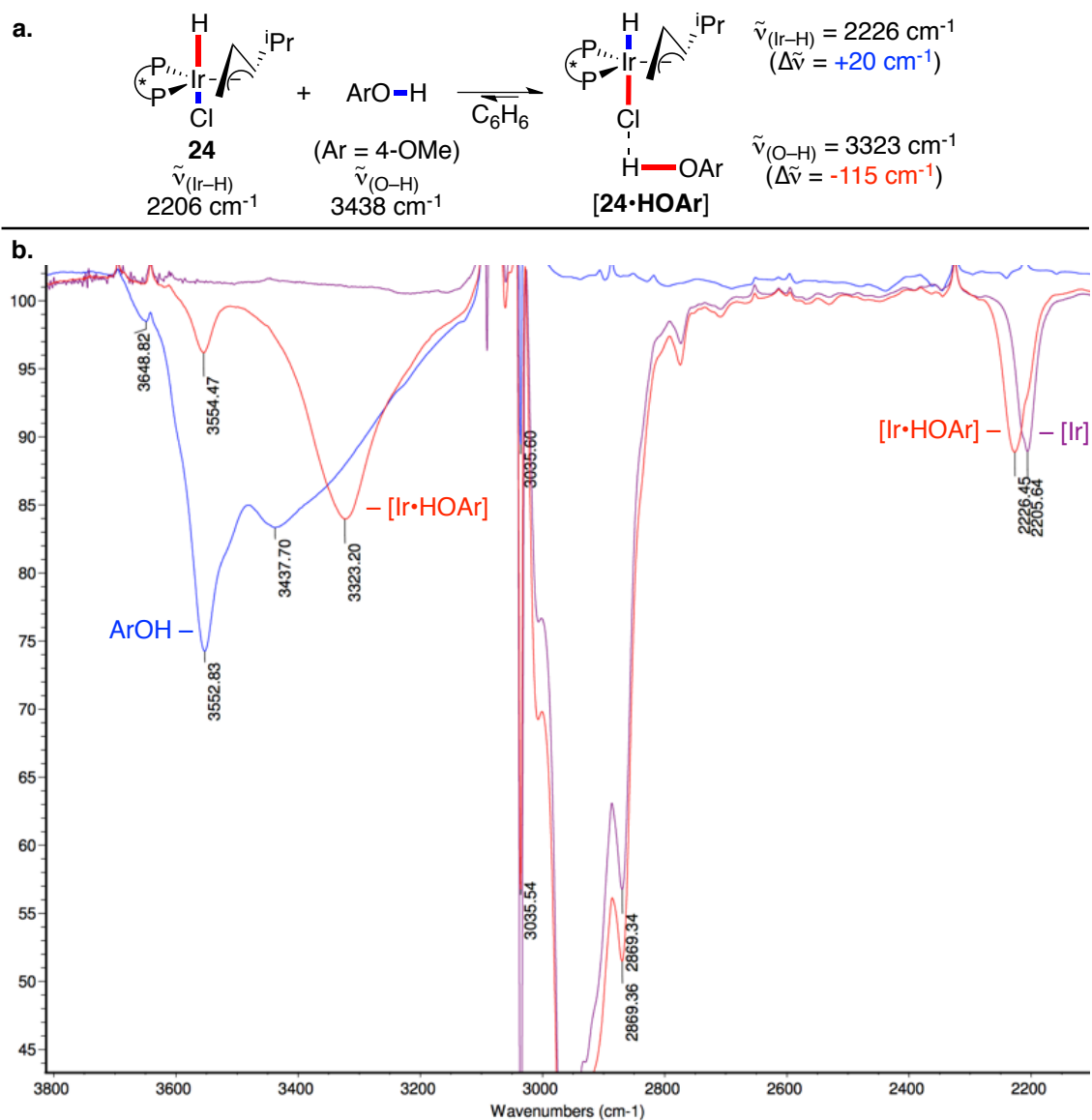
Figure 3.5. (a) Proposed noncovalent interaction between **24** and 4-fluorophenol and the effect of the inter-action on the observed IR stretching frequencies. (b) Overlaid IR spectra of **24**, 4-fluorophenol, and **[24•HOAr]**.

The interaction of the phenol with **24** was investigated by NOESY (Scheme 3.1) and IR spectroscopy (Figure 3.5). Metal-hydride complexes are known to be hydrogen-bond acceptors. NOE correlations between metal-hydrides and alcoholic protons, as well as a reduced metal-hydride IR stretching frequency in the presence of an alcohol, are commonly observed for systems containing these hydrogen-bonding interactions.[41-43] In contrast to these characteristics of a M-H•HX interaction, no NOE was observed between the Ir–H resonance of **24** and the OH resonance of 4-F-phenol (Scheme 3.1).

Scheme 3.1. Observed NOE correlations to the Ir(hydride) proton.
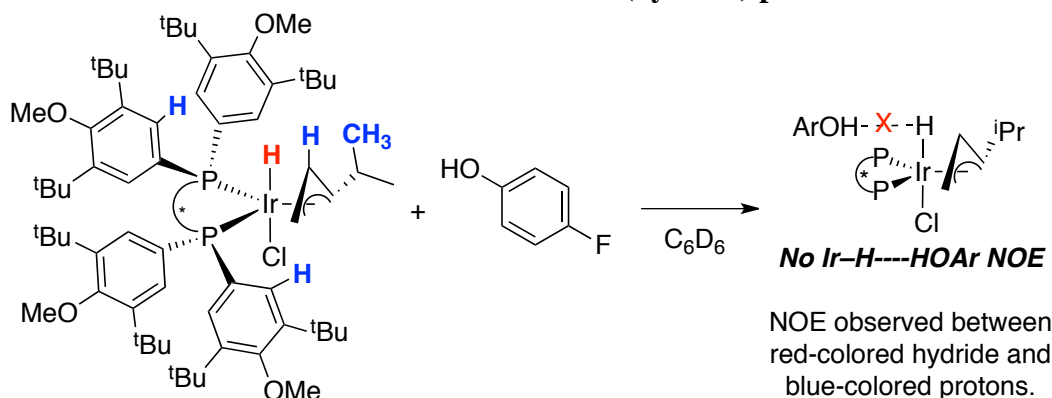
In addition, the IR stretching frequency of the Ir–H bond of **24** *increased* by 20 cm^{-1} to 2226 cm^{-1} in the presence of 1 M 4-F-phenol (vs. **24** in the absence of alcohol), while the O-H stretching frequency of the phenol decreased by 115 cm^{-1} to 3323 cm^{-1} (vs. 1 M 4-F-phenol in the absence of **24**). These data suggest that the hydrogen-bond acceptor in complex [**24•HOAr**] is a ligand other than the hydride. The remaining likely hydrogen-bond acceptor in the coordination sphere of **1** is the chloride ligand (Figure 3.5a). We suggest that the reduced electron donation by a hydrogen-bound Ir–Cl ligand strengthens the Ir–H bond *trans* to the chloride and accounts for the increased Ir–H stretching frequency observed by IR spectroscopy.

$$\delta_{obs} = \delta_{24}\mu_{24} + \delta_{[24•HOAr]}\mu_{[24•HOAr]} \qquad (1)$$

$$\delta_{obs} = \frac{\delta_{24} + \delta_{[24•HOAr]}K_{eq}[ArOH_o]}{1 + K_{eq}[ArOH_o]} \qquad (2)$$

$K_{eq} = 4.35 \pm 0.07$ M^{-1}
$\delta_{[24•HOAr]} = -24.09 \pm 0.06$ ppm
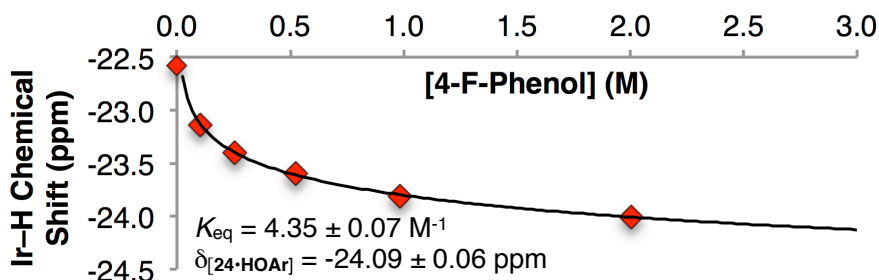
Figure 3.6. Plot of the Ir–H chemical shift as a function of 4-F-phenol concentration in C$_6$D$_6$ at 294 K, fit to Eq 2.

The fraction of **24** and **24•HOAr** was determined by ^{1}H NMR spectroscopy, and this ratio was consistent with the order of the reaction in phenol. The resonance in the Ir–H region of the ^{1}H NMR spectrum results from the average of the fractional contributions of the absolute Ir–H chemical shifts of **24** and [**24•HOAr**] (Eq 1). The equilibrium concentrations of the two complexes were determined by measuring the observed chemical shift of the Ir–H resonance as a function of the concentration of 4-F-phenol (Figure 3.6). The value of K_{eq} from fitting the data to eq 2 is 4.4 M^{-1}, and the chemical shift of the Ir–H

of [**24•HOAr**] is -24.1 ppm at 294 K. Van't Hoff analysis of the equilibrium constants determined by conducting this experiment at temperatures from 294 to 335 K (see the experimental section) revealed the following thermodynamic parameters for the equilibrium: ΔH_{eq} = -1.9 kcal/mol and ΔS_{eq} = -3.5 eu.[44] From these thermodynamic parameters, an equilibrium constant of 1.6 M^{-1} at the 140 °C temperature of the reaction was calculated; this equilibrium constant corresponds to a 40:60 ratio of **24**:[**24•HOAr**]. A significant concentration of both complexes is consistent with the measured partial-order (0.6) of the catalytic addition reaction in [4-F-phenol].

Table 3.2. Measured and extrapolated K_{eq} values at variable temperatures.

temp (°C)	K_{eq} (M^{-1})	% μ_{24}
21	4.35 ± 0.04	19
32	4.00 ± 0.04	20
42	3.64 ± 0.03	22
52	3.28 ± 0.03	24
62	2.92 ± 0.03	26
140^a	1.6^a	39^a

^{a}Equilibrium constant at 140 °C was determined by extrapolation of the thermodynamic parameters measured for equilibria between 21-62 °C: ΔH_{eq} = -1.9 kcal/mol, ΔS_{eq} = -3.5 eu.

A comparison of the initial rates for the addition of *O*-deuterated 4-F-phenol and proteo 4-F-phenol to propene in separate vessels revealed a kinetic isotope effect (KIE) of 1.6 (Scheme 3.2). Although greater than unity, this KIE is likely too small to be consistent with a turnover-limiting protonolysis or oxidative addition of the O–H bond,[16] but it would be consistent with reversible oxidative addition of the alcohol O–H bond to the Ir center prior to a turnover-limiting step. In this case, the product of oxidative addition would be less stable than the catalyst resting state. This conclusion is consistent with the lack of O-H addition product from the reaction of DTBM-Segphos, [Ir(coe)$_2$Cl]$_2$ and 4-F-phenol.

Scheme 3.2. Kinetic isotope effect on the rate of reaction
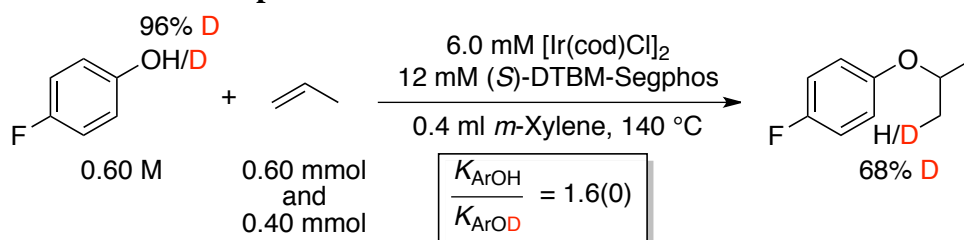
These mechanistic data are consistent with the proposed catalytic cycle in Scheme 3.3. In this mechanism, the (allyl)iridium hydride resting state **24**, which equilibrates with hydrogen bonded **24•HAr**, undergoes C–H bond-forming reductive elimination to release olefin and form an Ir(I) complex that can undergo reversible, endergonic oxidative addition of the O–H bond of the phenol to form **25**. Subsequent olefin coordination and turnover-limiting insertion into the Ir–O bond forms an alkyl-Ir complex **26**. C–H bond-forming reductive elimination would then release the ether product, whereas b-H elimination from the same intermediate would form the enol-ether side product. This mechanism is consistent with the observed zero-order dependence of the rate on the concentration of alkene because the alkene is released and added prior to the turnover-limiting transition state. This mechanism is also consistent with the partial positive order dependence of the rate on the concentration of alcohol because a significant fraction of the resting state exists as the alcohol adduct [**24•HOAr**]. The alcohol dissociates and adds prior to the turnover-limiting step of a reaction initiated from [**24•HOAr**].

Scheme 3.3. Proposed Catalytic Cycle for the Ir-Catalyzed Hydroetherification of α-Olefins
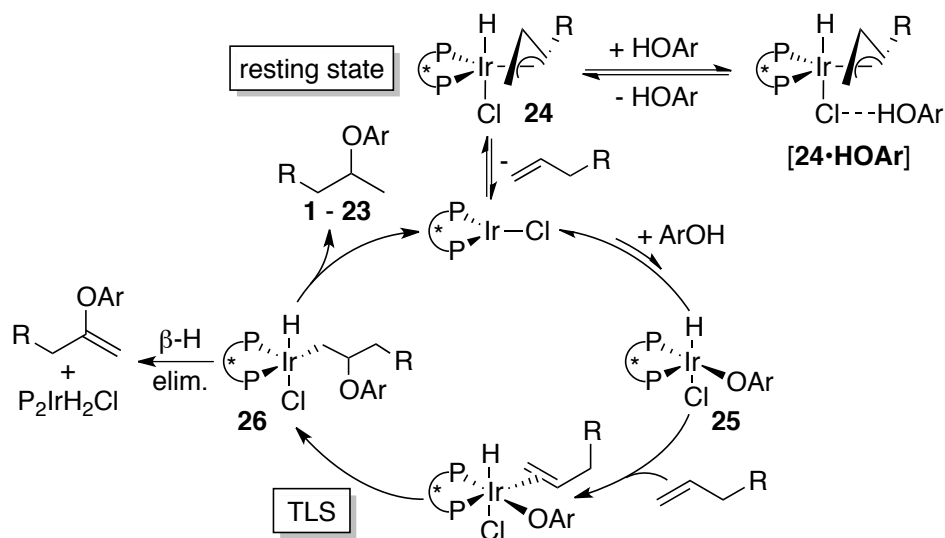
Several aspects of this mechanism are distinct from those for addition of the N-H bonds of amides to alkenes catalyzed by the combination of [Ir(coe)$_2$Cl]$_2$ and Segphos.[34] The product from oxidative addition of the amide was the resting state of the catalyst in the hydroamidations of alkenes; the open coordination site of the L$_2$IrCl(H)(amide) complex formed by oxidative addition was occupied by a second amide. The system for the catalytic additions of phenols lacks a basic component, making the stable 18-electrin Ir(III) complex in the system the allyl hydride complex **24** and its phenol adduct **24•HOAr**. Consequently, isomerization of the alkene occurs faster during the Ir-catalyzed additions of phenols to alkenes than during the additions of amides to alkenes.

The possibility of a transient intermediate that results from OH bond oxidative addition to Ir complexes of DTBM-Segphos as proposed in Scheme 3.3 was explored further. As discussed above, 5-coordinate Ir(phenoxy)(hydride) complexes are unstable are unstable in the absence of good L-type donors. Thus, we prepared an alcohol substrate

with a tethered pyridyl group that is capable of forming a stable chelate after OH bond oxidative addition. The red Ir(I) solution of [Ir(coe)₂Cl]₂ and DM-Segphos quickly changed colors to clear a clear solution upon heating in the presence of 2-pyridyl-isopropanol (Figure 3.7a). The resulting complex was characterized by NMR spectroscopy and single crystal x-ray diffraction as the product of OH oxidative addition **27** (Figure 3.7b). The analogous complex of DTBM-Segphos could be prepared *in situ* with 1 equivalent of alcohol relative to metal. Heating this complex in the presence of 1-octene formed a mixture of addition product and oxidative etherification product. These results indicate OH bond oxidative addition to Ir complexes of Segphos and olefin insertion into the resulting complexes are consistent with the elementary steps in the proposed catalytic cycle illustrated in Scheme 3.3.
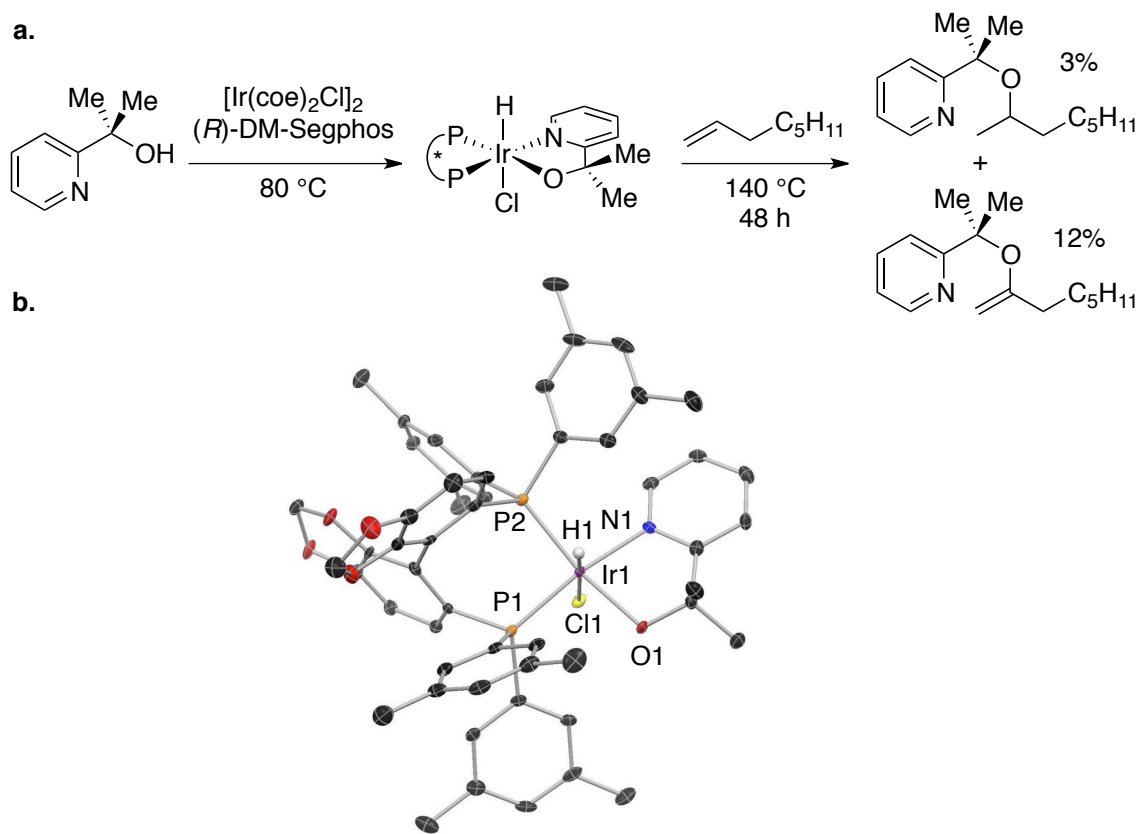
Figure 3.7. (a) Synthesis of Ir(alkoxy)(hydride) **27** and the stoichiometric reaction of **27** with octene. Solid-state structure of **27**.

3.3 Conclusions and Future Directions

In summary, we report a rare example of a metal-catalyzed intermolecular addition of an alcohol to an unactivated alkene. The lack of products from rearrangements and addition of the *ortho* C–H bond, the measurable enantiomeric excess, the absence of product from phosphonium salts, the lack of an effect of added tertiary alkylamine, and kinetic data that are consistent with the observed species show that the reaction is not purely acid-catalyzed. Instead, it likely occurs by generation of an Ir(I) intermediate by reductive elimination of the observed allyliridium hydride species, followed by reversible O–H bond oxidative addition, turnover-limiting olefin insertion, and product-releasing reductive elimination. Efforts to mitigate olefin isomerization are in progress.

3.4 Experimental

General Remarks.

Unless noted otherwise, all manipulations were performed in a nitrogen-filled glove-box. Glassware was dried at 130 °C for at least 4 hours before use. Pentane, Et_2O, THF, benzene and toluene were collected from a solvent purification system containing a 0.33 m column of activated alumina under nitrogen. Benzene-d_6 was degassed and subjected to 4 Å molecular sieves for at least 4 hours prior to use. All reagents were purchased from commercial suppliers, stored in the glove box and used as received. $[Ir(coe)_2Cl]_2$ was prepared following a published procedure.[45] Bisphosphine ligands were purchased from Strem Chemical Co. and used as received.

^{1}H NMR spectra were obtained at 500 MHz or 600 MHz with a 45° pulse and a 10 s delay time, and chemical shifts were recorded relative to protiated solvents ($CHCl_3$ in $CDCl_3$: δ7.27 ppm; $C_6H_nD_{6-n}$ in C_6D_6: δ7.15 ppm). ^{13}C NMR spectra were obtained at 126 MHz or 151 MHz on a 500 MHz or 600 MHz instrument, respectively. ^{31}P NMR spectra were obtained at 202.2 MHz on a 500 MHz instrument, and chemical shifts were reported in parts per million downfield of 85% H_3PO_4. ^{19}F NMR spectra were referenced to an external standard of $CFCl_3$. Probe temperatures for variable temperature NMR experiments were measured by ^{1}H shifts of neat ethylene glycol. Proof of purity is demonstrated by elemental analysis and by copies of NMR spectra. Chiral HPLC analysis was conducted on a Waters chromatography system with a dual wavelength detector at 220 and 254 nm.

GC analysis was performed on an Agilent 7890 GC equipped with an HP-5 column (25 m x 0.20 mm x 0.33 μm film) and an FID detector. Quantitative GC analysis was performed by adding dodecane as an internal standard to the reaction mixture upon completion of the reaction. Response factors for the products relative to the internal standard were measured for kinetic studies and reaction development studies. GC-MS data were obtained on an Agilent 6890-N GC system containing an Alltech EC-1 capillary column and an Agilent 5973 mass selective detector.

Table 3.3. Full set of ligands evaluated with [Ir(coe)₂Cl]₂ as catalyst for the addition of 3-OMe-phenol to 1-octene.<superscript>a</superscript>
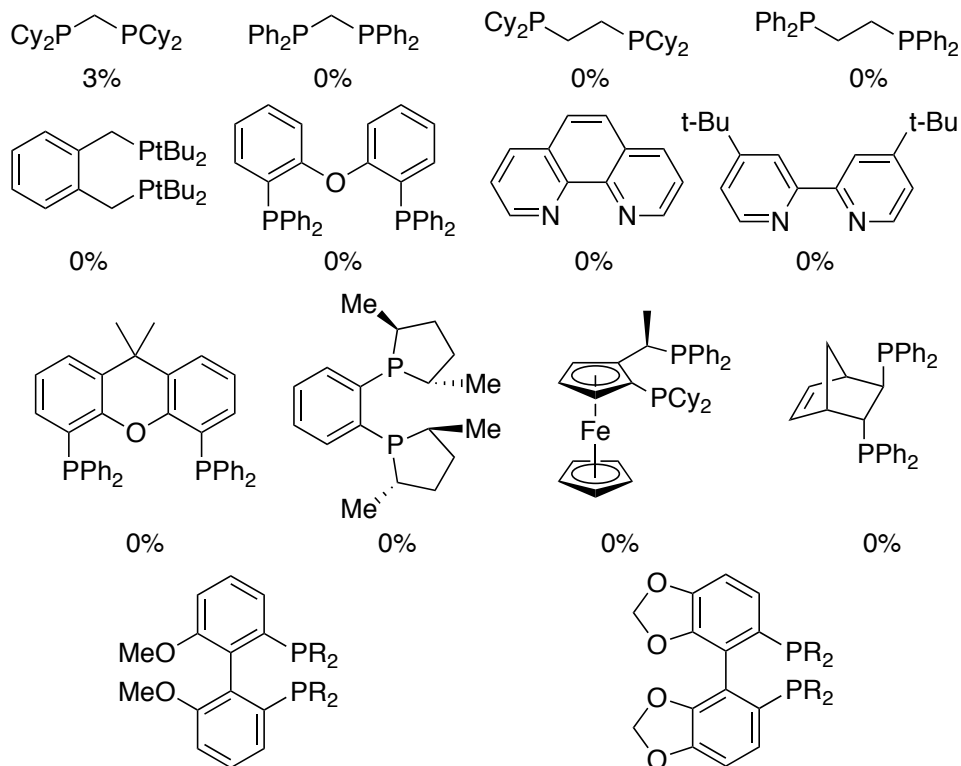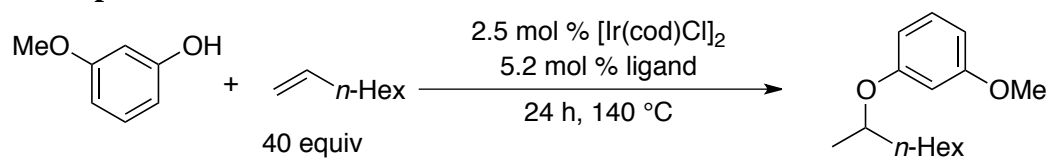
R Group:	GC Yield
Ph	0%
3,5-diMe	4%
3,5-ditBu-4-methoxy	26%
iPr	2%
3,5-diiPr-4-dimethylamino	4%

R Group:	GC Yield
Ph	6%
3,5-diMe	11%
3,5-ditBu-4-methoxy	48%
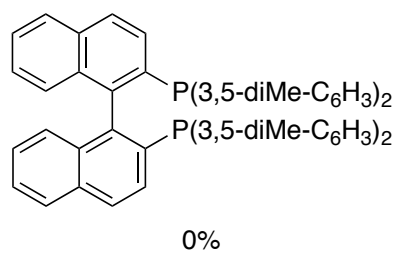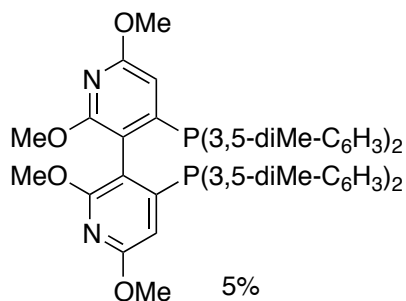
aReported yields are GC yields that were corrected against dodecane as an internal standard.

General Procedure A: Ir-catalyzed addition of phenols to α-olefins.
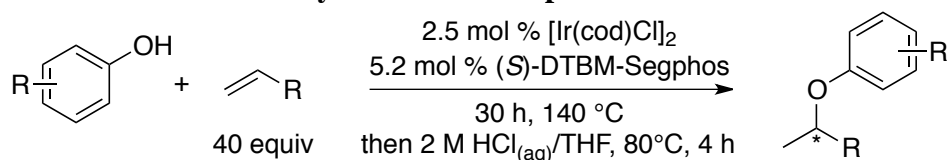
In a nitrogen-filled dry-box, an oven-dried 4 ml screw-capped vial was charged with [Ir(cod)Cl]₂ (4.2 mg, 0.0063 mmol), (S)-DTBM-SEGPHOS (15.3 mg, 0.0130 mmol), the corresponding aryl alcohol (0.25 mmol), and a magnetic stirbar. THF (0.40 ml) was added to these solids, and the mixture was stirred vigorously until an orange homogeneous solution was obtained (5 min). The magnetic stirbar was removed from the solution, and THF was evaporated under vacuum over 30 min. To the orange residue was added the corresponding alkene, and the magnetic stirbar was returned to the vial. The vial was sealed tightly with a Telfon cap and removed from the dry-box. The reaction mixture was stirred in an aluminum heating block at 140 °C for 30 h and then cooled to room temperature. The olefin solvent was removed by rotary evaporation. A 1:1 (v/v) solution of THF/2 M HCl₍aq₎ (1.0 ml) was added to the resulting residue. The vial was closed with a Teflon cap and placed in an 80 °C aluminum heating block for 4 h. The solution was allowed to cool to room temperature at which point the organic material was extracted from the solution with EtOAc (2 ml, three times). The products were purified by flash chromatography on a column (height = 20. cm, diameter = 3.0 cm) of Silacycle Silia-P60 silica gel (55 g). The conditions for chromatography and other data that are specific to each compound are given below.

1-Methoxy-3-(octan-2-yloxy)benzene

Following the general procedure **A** described above, 3-methoxyphenol (32 mg, 0.25 mmol) was allowed to react with 1-octene (0.75 ml, 5.0 mmol). The crude material was purified by flash chromatography with 1% EtOAc in hexanes as eluent. The solvent was evaporated to yield the title compound as a clear oil (38 mg, 64% yield).
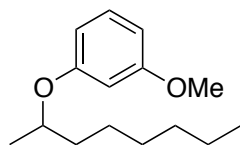
¹H NMR (600 MHz, CDCl₃): δ 7.17 (t, J = 8.2 Hz, 1H), 6.52-6.47 (m, 2H), 6.46 (t, J = 2.1 Hz, 1H), 4.34 (h, J = 6.1 Hz, 1H), 3.79 (s, 3H), 1.79-1.69 (m, 1H), 1.61-1.52 (m, 1H), 1.50-1.41 (m, 1H), 1.40-1.23 (m, 10H), 0.89 (t, J = 6.4 Hz, 3H).
¹³C NMR (151 MHz, CDCl₃): δ 160.8, 159.5, 129.8, 107.9, 105.9, 102.2, 73.8, 55.2, 36.5, 31.8, 29.3, 25.5, 22.6, 19.7, 14.0.
HPLC analysis: 25% ee, Chiralcel OD-H column, 100% hexane, 1.0 mL/min flow rate, 220 nm UV lamp, $t_{[major]}$ = 21.2 min, $t_{[minor]}$ = 23.4 min.
Anal. Calcd for $C_{15}H_{24}O_2$: C 76.23%, H 10.24%; Found: C 76.13%, H 10.24%.

1-(Octan-2-yloxy)-4-phenoxybenzene
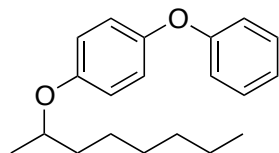
Following the general procedure **A** described above, 4-phenoxyphenol (56 mg, 0.3 mmol) was allowed to react with 1-octene (0.45 ml, 3.0 mmol). The crude material was purified by flash chromatography with 1% EtOAc in hexanes as eluent. The solvent was evaporated to yield the title compound as a clear oil (60 mg, 67% yield).

¹H NMR (600 MHz, CDCl₃): δ 7.31 (dd, *J* = 7.6 Hz, 2H), 7.05 (t, *J* = 7.3 Hz, 1H), 7.01-6.93 (m, 4H), 6.88 (d, *J* = 8.4 Hz, 2H), 4.36-4.24 (m, 1H), 1.81-1.70 (m, 1H), 1.62-1.54 (m, 1H), 1.51-1.43 (m, 1H), 1.42-1.27 (m, 10H), 0.90 (t, *J* = 6.5 Hz, 3H).

¹³C NMR (151 MHz, CDCl₃): δ 166.9, 164.1, 158.5, 154.5, 150.0, 129.5, 122.4, 120.7, 117.6, 117.1, 74.7, 36.5, 31.8, 29.3, 25.5, 22.6, 19.7, 14.1.

HPLC analysis: 8% ee, Chiralcel AD-H column, 100% hexane, 1.0 mL/min flow rate, 220 nm UV lamp, $t_{[major]}$ = 8.2 min, $t_{[minor]}$ = 10.2 min.

Anal. Calcd for $C_{20}H_{26}O_2$: C 80.50%, H 8.78%; Found: C 80.71%, H 9.12%.

(Octan-2-yloxy)benzene
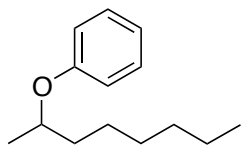
Following the general procedure **A** described above, phenol (24 mg, 0.25 mmol) was allowed to react with 1-octene (0.80 ml, 5.0 mmol). The crude material was purified by flash chromatography with 1.5% EtOAc in hexanes as eluent. The solvent was evaporated to yield the title compound as a clear oil (38 mg, 73% yield).

¹H NMR (600 MHz, CDCl₃): δ 7.28 (dd, *J* = 8.6, 7.4 Hz, 2H), 6.93 (t, *J* = 11.5, 4.0 Hz, 1H), 6.90 (d, *J* = 7.8 Hz, 2H), 4.42-4.32 (m, 1H), 1.80-1.71 (m, 1H), 1.62-1.54 (m, 1H), 1.53-1.43 (m, 1H), 1.42-1.28 (m, 10H), 0.90 (t, *J* = 7.0 Hz, 3H).

¹³C NMR (151 MHz, CDCl₃): δ 158.2, 129.4, 120.4, 115.9, 73.8, 36.5, 31.8, 29.3, 25.5, 22.6, 19.7, 14.0.

HPLC analysis: 13% ee, Chiralcel AD-H column, 100% hexane, 0.7 mL/min flow rate, 220 nm UV lamp, $t_{[major]}$ = 7.4 min, $t_{[minor]}$ = 8.5 min.

Anal. Calcd for $C_{14}H_{22}O$: C 81.50%, H 10.75%; Found: C 79.92%, H 10.36%.

N,N-dimethyl-3-(octan-2-yloxy)aniline
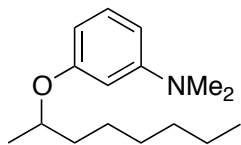
Following the general procedure **A** described above, 3-dimethylaminophenol (42 mg, 0.3 mmol) was allowed to react with 1-octene (0.45 ml, 3.0 mmol). After the acid-catalyzed hydrolytic workup, the mixture was basified with a solution of NaOH (4 ml, 2 M). The organic material was extracted with EtOAc (2 ml, 3 times). The crude material was purified by flash chromatography with 1% EtOAc in hexanes as eluent. The title compound was found to be unstable under atmospheric conditions at high concentrations. The solvent was evaporated in a nitrogen-filled dry-box to yield the title compound as a clear oil (45 mg, 60% yield).

¹H NMR (600 MHz, C₆D₆): δ 7.16 (t, *J* = 8.2 Hz, 1H), 6.47 (s, 1H), 6.42 (d, *J* = 8.0 Hz, 1H), 6.30 (d, *J* = 8.2 Hz, 1H), 4.31-4.21 (m, 1H), 2.51 (s, 6H), 1.79-1.68 (m, 1H), 1.52-1.39 (m, 2H), 1.37-1.27 (m, 1H), 1.25-1.16 (m, 9H), 0.84 (t, *J* = 6.7 Hz, 3H).

¹³C NMR (151 MHz, C₆D₆): δ 159.6, 152.2, 129.6, 105.7, 103.3, 101.6, 72.9, 39.9, 36.7, 31.8, 29.4, 25.6, 22.6, 19.7, 13.9.

HPLC analysis: 26% ee, Chiralcel OD-H column, 100% hexane, 1.0 mL/min flow rate, 220 nm UV lamp, $t_{[minor]}$ = 85.9 min, $t_{[major]}$ = 102.4 min.

Anal. Calcd for $C_{16}H_{27}NO$: C 77.06%, H 10.91%, N 5.62%; Found: C 76.73%, H 11.03%, N 5.32%.

1-(Octan-2-yloxy)-4-(trifluoromethyl)benzene

Following the general procedure **A** described above, 4-trifluoromethylphenol (49 mg, 0.3 mmol) was allowed to react with 1-octene (1.8 ml, 12 mmol). The crude material was purified by flash chromatography with hexanes as eluent. The solvent was evaporated to yield the title compound as a clear oil (41 mg, 49% yield).
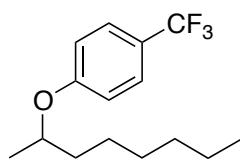
¹H NMR (600 MHz, CDCl₃): δ 7.53 (d, J = 8.4 Hz, 2H), 6.93 (d, J = 8.4 Hz, 2H), 4.48-4.35 (m, 1H), 1.81-1.70 (m, 1H), 1.65-1.54 (m, 1H), 1.49-1.42 (m, 1H), 1.39-1.24 (m, 10H), 0.89 (t, J = 6.5 Hz, 3H).

¹³C NMR (151 MHz, CDCl₃): δ 160.8, 126.8 (q, J = 3.7 Hz), 124.5 (q, J = 270.9 Hz), 122.3 (q, J = 32.6 Hz), 115.4, 74.1, 36.3, 31.7, 29.2, 25.4, 22.5, 19.5, 14.0.

¹⁹F NMR (565 MHz, CDCl₃): δ -62.4.

HPLC analysis: 25% ee, Chiralcel AS-H column, 100% hexane, 0.5 mL/min flow rate, 254 nm UV lamp, $t_{[major]}$ = 7.5 min, $t_{[major]}$ = 9.0 min.

Anal. Calcd for $C_{15}H_{21}F_3O$: C 65.67%, H 7.72%; Found: C 66.05%, H 7.68%.

1-Methoxy-4-(octan-2-yloxy)benzene

Following the general procedure **A** described above, 4-methoxyphenol (38 mg, 0.3 mmol) was allowed to react with 1-octene (0.45 ml, 3.0 mmol). The crude material was purified by flash chromatography with 2% EtOAc in hexanes as eluent. The solvent was evaporated to yield the title compound as a clear oil (46 mg, 66% yield).
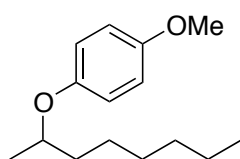
¹H NMR (600 MHz, CDCl₃): δ 6.91-6.76 (m, 4H), 4.27-4.16 (m, 1H), 3.77 (s, 3H), 1.76-1.67 (m, 1H), 1.58-1.49 (m, 1H), 1.49-1.41 (m, 1H), 1.40-1.35 (m, 1H), 1.35-1.28 (m, 6H), 1.26 (d, J = 6.1 Hz, 3H), 0.89 (t, J = 6.8 Hz, 3H).

¹³C NMR (151 MHz, CDCl₃): δ 153.7, 152.2, 117.4, 114.6, 99.9, 75.0, 55.7, 36.5, 31.8, 29.3, 25.5, 22.6, 19.8, 14.1.

HPLC analysis: 14% ee, Chiralcel OD-H column, 100% hexane, 1.0 mL/min flow rate, 220 nm UV lamp, $t_{[major]}$ = 17.6 min, $t_{[minor]}$ = 19.5 min.

Anal. Calcd for $C_{15}H_{24}O_2$: C 76.23%, H 10.24%; Found: C 76.52%, H 10.60%.

1-(Octan-2-yloxy)-3-(trifluoromethyl)benzene
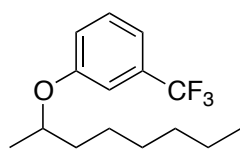
Following the general procedure **A** described above, 3-trifluoromethylphenol (49 mg, 0.3 mmol) was allowed to react with 1-octene (1.8 ml, 12 mmol). The crude material was purified by flash chromatography with 1.5% EtOAc in hexanes as eluent. The solvent was evaporated to yield the title compound as a clear oil (48 mg, 59% yield).

¹H NMR (600 MHz, CDCl₃): δ 7.37 (dd, J = 7.9 Hz, 1H), 7.17 (d, J = 7.6 Hz, 1H), 7.11 (s, 1H), 7.04 (d, J = 8.2 Hz, 1H), 4.45-4.35 (m, 1H), 1.80-1.70 (m, 1H), 1.64-1.54 (m, 1H), 1.49-1.43 (m, 1H), 1.40-1.25 (m, 10H), 0.89 (t, J = 6.5 Hz, 3H).

¹³C NMR (151 MHz, CDCl₃): δ 158.4, 131.8 (q, J = 32.2 Hz), 129.9, 124.0 (q, J = 272.4 Hz), 119.0, 116.9 (q, J = 3.9 Hz), 112.6 (q, J = 4.0 Hz), 74.3, 36.3, 31.7, 29.2, 25.4, 22.5, 19.5, 14.0.

¹⁹F NMR (565 MHz, CDCl₃): δ -63.7.
HPLC analysis: 43% ee, Chiralcel OD-H column, 100% hexame, 0.1 mL/min flow rate, 220 nm UV lamp, $t_{[minor]}$ = 22.4 min, $t_{[major]}$ = 23.9 min.
Anal. Calcd for C₁₅H₂₁F₃O: C 65.67%, H 7.72%; Found: C 65.70%, H 7.42%.
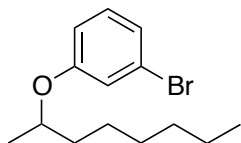
1-Bromo-3-(octan-2-yloxy)benzene

Following the general procedure **A** described above, 3-bromophenol (44 mg, 0.25 mmol) was allowed to react with 1-octene (0.80 ml, 5.0 mmol). The crude material was purified by flash chromatography with 1% EtOAc in hexanes as eluent. The solvent was evaporated to yield the title compound as a clear oil (38 mg, 54% yield).
¹H NMR (600 MHz, CDCl₃): δ 7.12 (dd, J = 8.3 Hz, 1H), 7.08-7.00 (m, 2H), 6.85-6.77 (m, 1H), 4.41-4.27 (m, 1H), 1.78-1.67 (m, 1H), 1.59-1.51 (m, 1H), 1.50-1.40 (m, 1H), 1.38-1.25 (m, 10H), 0.89 (t, J = 6.9 Hz, 3H).
¹³C NMR (151 MHz, CDCl₃): δ 159.1, 130.5, 123.4, 122.7, 119.1, 114.7, 74.3, 36.4, 31.7, 29.2, 25.4, 22.5, 19.6, 14.0.
HPLC analysis: 20% ee, Chiralcel OD-H column, 100% hexane, 0.5 mL/min flow rate, 220 nm UV lamp, $t_{[minor]}$ = 11.4 min, $t_{[major]}$ = 12.1 min.
Anal. Calcd for C₁₄H₂₁BrO: C 58.95%, H 7.42%; Found: C 59.98%, H 60.03%.

1-Bromo-2-methyl-4-(octan-2-yloxy)benzene

Following the general procedure **A** described above, 4-bromo-3-methylphenol (47 mg, 0.25 mmol) was allowed to react with 1-octene (0.80 ml, 5.0 mmol). The crude material was purified by flash chromatography with 1% EtOAc in hexanes as eluent. The solvent was evaporated to yield the title compound as a clear oil (53 mg, 72% yield).
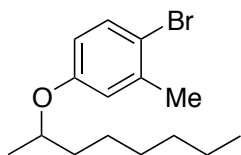**¹H NMR** (600 MHz, CDCl₃): δ 7.39 (d, J = 8.7 Hz, 1H), 6.79 (d, J = 2.9 Hz, 1H), 6.61 (dd, J = 8.7, 2.9 Hz, 1H), 4.30 (dd, J = 12.2, 6.1 Hz, 1H), 2.36 (s, 3H), 1.78-1.67 (m, 1H), 1.60-1.51 (m, 1H), 1.48-1.40 (m, 1H), 1.39-1.26 (m, 10H), 0.90 (t, J = 6.9 Hz, 3H).
¹³C NMR (151 MHz, CDCl₃): δ 157.4, 138.8, 132.8, 118.6, 115.0, 114.7, 74.2, 36.4, 31.8, 29.2, 25.5, 23.1, 22.6, 19.6, 14.0.
HPLC analysis: 34% ee, Chiralcel OD-H column, 100% hexane, 0.5 mL/min flow rate, 220 nm UV lamp, $t_{[minor]}$ = 12.5 min, $t_{[major]}$ = 14.3 min.
Anal. Calcd for C₁₅H₂₃BrO: C 60.20%, H 7.75%; Found: C 60.56%, H 7.99%.

1-Chloro-4-(octan-2-yloxy)benzene
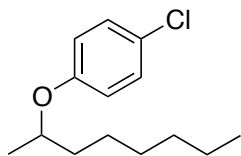
Following the general procedure **A** described above, 4-chlorophenol (32 mg, 0.25 mmol) was allowed to react with 1-octene (0.80 ml, 5.0 mmol). The crude material was purified by flash chromatography with 0.7% EtOAc in hexanes as eluent. The solvent was evaporated to yield the title compound as a clear oil (42 mg, 70% yield).
¹H NMR (600 MHz, CDCl₃): δ 7.22 (d, J = 8.9 Hz, 2H), 6.81 (d, J = 8.9 Hz, 2H), 4.36-4.22 (m, 1H), 1.77-1.68 (m, 1H), 1.60-1.51 (m, 1H), 1.49-1.40 (m, 1H), 1.39-1.26 (m, 10H), 0.89 (t, J = 6.9 Hz, 3H).

^{13}**C NMR** (151 MHz, CDCl$_3$): δ 156.8, 129.3, 125.1, 117.2, 74.4, 36.4, 31.8, 29.2, 25.4, 22.6, 19.6, 14.0.

HPLC analysis: 23% ee, Chiralcel OD-H column, 100% hexane, 0.7 mL/min flow rate, 220 nm UV lamp, t$_{[minor]}$ = 7.6 min, t$_{[major]}$ = 8.1 min.

Anal. Calcd for C$_{14}$H$_{21}$ClO: C 69.84%, H 8.79%; Found: C 70.21%, H 9.16%.

5-(Octan-2-yloxy)benzo[*d*][1,3]dioxole
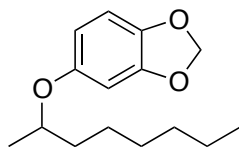
Following the general procedure **A** described above, sesamol (35 mg, 0.25 mmol) was allowed to react with 1-octene (0.80 ml, 5.0 mmol). The crude material was purified by flash chromatography with 1.5% EtOAc in hexanes as eluent. The solvent was evaporated to yield the title compound as a clear oil (36 mg, 57% yield).

^{1}**H NMR** (600 MHz, CDCl$_3$): δ 6.69 (d, J = 8.4 Hz, 1H), 6.48 (d, J = 2.4 Hz, 1H), 6.33 (dd, J = 8.4, 2.4 Hz, 1H), 5.91 (s, 2H), 4.21-4.14 (m, 1H), 1.75-1.65 (m, 1H), 1.56-1.48 (m, 1H), 1.47-1.40 (m, 1H), 1.39-1.22 (m, 10H), 0.89 (t, J = 6.9 Hz, 3H).

^{13}**C NMR** (151 MHz, CDCl$_3$): δ 153.6, 148.1, 141.5, 108.1, 108.0, 101.0, 99.6, 75.5, 36.5, 31.8, 29.3, 25.5, 22.6, 19.7, 14.0.

HPLC analysis: 14% ee, Chiralcel OD-H column, 100% hexane, 0.7 mL/min flow rate, 220 nm UV lamp, t$_{[major]}$ = 23.1 min, t$_{[minor]}$ = 27.0 min.

Anal. Calcd for C$_{15}$H$_{22}$O$_3$: C 71.97%, H 8.86%; Found: C 71.67%, H 8.53%.

2-Bromo-4-(hexan-2-yloxy)-1-methylbenzene
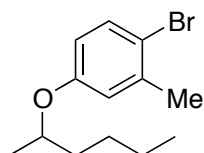
Following the general procedure **A** described above, 4-bromo-3-methylphenol (47 mg, 0.25 mmol) was allowed to react with 1-hexene (0.63 ml, 5.0 mmol). The crude material was purified by flash chromatography with 1% EtOAc in hexanes as eluent. The solvent was evaporated to yield the title compound as a clear oil (54 mg, 80% yield).

^{1}**H NMR** (600 MHz, CDCl$_3$): δ 7.39 (d, J = 8.7 Hz, 1H), 6.79 (d, J = 2.9 Hz, 1H), 6.61 (dd, J = 8.7, 3.0 Hz, 1H), 4.30 (dd, J = 12.2, 6.1 Hz, 1H), 2.36 (s, 3H), 1.79-1.65 (m, 1H), 1.62-1.52 (m, 1H), 1.48-1.39 (m, 1H), 1.39-1.32 (m, 3H), 1.28 (d, J = 6.1 Hz, 3H), 0.92 (t, J = 7.1 Hz, 3H).

^{13}**C NMR** (151 MHz, CDCl$_3$): δ 157.4, 138.8, 132.8, 118.6, 115.0, 114.7, 74.1, 36.1, 27.7, 23.1, 22.6, 19.6, 14.0.

HPLC analysis: 31% ee, Chiralcel OD-H column, 100% hexane, 0.5 mL/min flow rate, 220 nm UV lamp, t$_{[minor]}$ = 12.5 min, t$_{[major]}$ = 14.3 min.

Anal. Calcd for C$_{13}$H$_{19}$BrO: C 57.57%, H 7.06%; Found: C 57.88%, H 6.82%.

2-Bromo-4-(hexan-2-yloxy)-1-methylbenzene
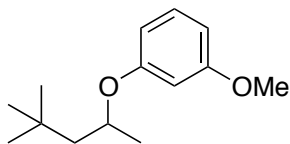
Following the general procedure **A** described above, 3-methoxyphenol (38 mg, 0.3 mmol) was allowed to react with 4,4-dimethylpent-1-ene (1.6 ml, 12 mmol). The crude material was purified by flash chromatography with 2% EtOAc in hexanes as eluent. The solvent was evaporated to yield the title compound as a clear oil (36 mg, 53% yield).

^{1}**H NMR** (600 MHz, CDCl$_3$): δ 7.17 (t, J = 8.2 Hz, 1H), 6.53-6.47 (m, 2H), 6.45 (s, 1H), 4.55-4.43 (m, 1H), 3.79 (s, 3H), 1.79 (dd, J = 14.6, 8.4 Hz, 1H), 1.40 (dd, J = 14.6, 2.2 Hz, 1H), 1.29 (d, J = 6.0 Hz, 3H), 0.96 (s, 9H).

^{13}**C NMR** (151 MHz, CDCl$_3$): δ 160.9, 159.1, 129.8, 107.7, 105.6, 101.9, 71.2, 55.2, 50.4, 30.2, 30.1, 21.3.

HPLC analysis: 60% ee, Chiralcel OD-H column, 100% hexane, 1.0 mL/min flow rate, 220 nm UV lamp, t$_{[major]}$ = 9.8 min, t$_{[minor]}$ = 11.7 min.

Anal. Calcd for C$_{14}$H$_{22}$O$_2$: C 75.63%, H 9.97%; Found: C 75.53%, H 9.98%.

1-((3,3-Dimethylbutan-2-yl)oxy)-3-methoxybenzene
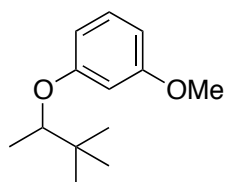
Following the general procedure **A** described above, 3-methoxyphenol (38 mg, 0.3 mmol) was allowed to react with *tert*-butylethylene (1.3 ml, 12 mmol). The crude material was purified by flash chromatography with 1% EtOAc in hexanes as eluent. The solvent was evaporated to yield the title compound as a clear oil (9 mg, 16% yield).

^{1}**H NMR** (600 MHz, CDCl$_3$): δ 7.16 (t, J = 8.1 Hz, 1H), 6.53-6.43 (m, 3H), 4.00 (q, J = 6.2 Hz, 1H), 3.79 (s, 3H), 1.20 (d, J = 6.3 Hz, 3H), 0.98 (s, 9H).

^{13}**C NMR** (151 MHz, CDCl$_3$): δ 160.8, 160.2, 129.7, 107.9, 105.7, 102.2, 81.2, 55.2, 35.1, 25.8, 14.1.

HPLC analysis: 44% ee, Chiralcel OD-H column, 100% hexane, 1.0 mL/min flow rate, 220 nm UV lamp, t$_{[major]}$ = 13.2 min, t$_{[minor]}$ = 15.1 min.

GC-MS: m/z 208 (30%, [M$^+$]), 151 (18%, [M–^{t}Bu]$^+$), 124 (100%, [M-CH$_2$=CH$_2$–^{t}Bu]$^+$).

1-Fluoro-4-(octan-2-yloxy)benzene
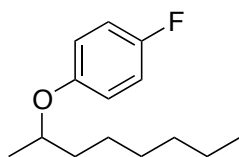
Following the general procedure **A** described above, 4-fluorophenol (34 mg, 0.3 mmol) was allowed to react with 1-octene (0.90 ml, 6.0 mmol). The crude material was purified by flash chromatography with 2% EtOAc in hexanes as eluent. The solvent was evaporated to yield the title compound as a clear oil (40 mg, 60% yield).

^{1}**H NMR** (600 MHz, CDCl$_3$): δ 6.95 (t, J = 8.5 Hz, 2H), 6.82 (dd, J = 8.6, 4.3 Hz, 2H), 4.30-4.19 (m, 1H), 1.76-1.68 (m, 1H), 1.59-1.50 (m, 1H), 1.48-1.40 (m, 1H), 1.39-1.24 (m, 10H), 0.89 (t, J = 6.5 Hz, 3H).

^{13}**C NMR** (151 MHz, CDCl$_3$): δ 157.1 (d, J = 238.1 Hz), 154.3, 117.2 (d, J = 7.9 Hz), 115.7 (d, J = 22.9 Hz), 74.9, 36.4, 31.8, 29.2, 25.5, 22.6, 19.7, 14.0.

^{19}**F NMR** (565 MHz, CDCl$_3$): δ -125.1.

HPLC analysis: 13% ee, Chiralcel AD-H column, 100% hexane, 0.5 mL/min flow rate, 220 nm UV lamp, t$_{[major]}$ = 8.2 min, t$_{[minor]}$ = 9.0 min.

Anal. Calcd for C$_{14}$H$_{21}$FO: C 74.96%, H 9.44%; Found: C 75.23%, H 9.14%.

2-(Octan-2-yloxy)naphthalene
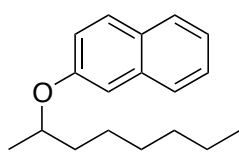
Following the general procedure **A** described above, 2-napthol (44 mg, 0.3 mmol) was allowed to react with 1-octene (0.90 ml, 6.0 mmol). The crude material was purified by flash chromatography with 1% EtOAc in hexanes as eluent. The solvent was evaporated to yield the title compound as a clear oil (61 mg, 79% yield).

¹H NMR (600 MHz, CDCl₃): δ 7.77 (t, J = 9.7 Hz, 2H), 7.73 (d, J = 8.2 Hz, 1H), 7.45 (t, J = 7.5 Hz, 1H), 7.34 (t, J = 7.5 Hz, 1H), 7.21-7.12 (m, 2H), 4.61-4.47 (m, 1H), 1.88-1.79 (m, 1H), 1.70-1.60 (m, 1H), 1.56-1.48 (m, 1H), 1.46-1.29 (m, 10H), 0.92 (t, J = 6.5 Hz, 3H).

¹³C NMR (151 MHz, CDCl₃): δ 156.1, 134.6, 129.4, 128.8, 127.6, 126.6, 126.2, 123.4, 119.8, 108.3, 73.8, 36.5, 31.8, 29.3, 25.5, 22.6, 19.7, 14.1.

HPLC analysis: 30% ee, Chiralcel OD-H column, 100% hexane, 1.0 mL/min flow rate, 220 nm UV lamp, $t_{[minor]}$ = 35.2 min, $t_{[major]}$ = 39.4 min.

Anal. Calcd for C₁₈H₂₄O: C 84.32%, H 9.44%; Found: C 84.51%, H 9.16%.

1-Bromo-2-methyl-4-((4-methylpentan-2-yl)oxy)benzene

Following the general procedure **A** described above, 4-bromo-3-methylphenol (47 mg, 0.25 mmol) was allowed to react with 4-methylpent-1-ene (0.65 ml, 5.0 mmol). The crude material was purified by flash chromatography with hexanes as eluent. The solvent was evaporated to yield the title compound as a clear oil (38 mg, 56% yield).

¹H NMR (600 MHz, CDCl₃): δ 7.38 (d, J = 8.7 Hz, 1H), 6.78 (d, J = 2.9 Hz, 1H), 6.60 (dd, J = 8.7, 2.9 Hz, 1H), 4.47-4.30 (m, 1H), 2.35 (s, 3H), 1.85-1.74 (m, 1H), 1.69 (ddd, J = 14.0, 7.7, 6.5 Hz, 1H), 1.39-1.32 (m, 1H), 1.27 (d, J = 6.0 Hz, 3H), 0.95 (d, J = 6.7 Hz, 3H), 0.91 (d, J = 6.6 Hz, 3H).

¹³C NMR (151 MHz, CDCl₃): δ 157.4, 138.8, 132.8, 118.5, 115.0, 114.6, 72.4, 45.8, 24.7, 23.1, 22.9, 22.5, 19.9.

HPLC analysis: 26% ee, Chiralcel OD-H column, 100% hexane, 0.7 mL/min flow rate, 220 nm UV lamp, $t_{[minor]}$ = 7.5 min, $t_{[major]}$ = 8.4 min.

Anal. Calcd for C₁₃H₁₉BrO: C 57.57%, H 7.06%; Found: C 57.84%, H 6.97%.

1-Methoxy-3-((4-methylpentan-2-yl)oxy)benzene
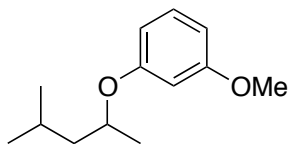
Following the general procedure **A** described above, 3-methoxyphenol (32 mg, 0.25 mmol) was allowed to react with 4-methylpent-1-ene (0.65 ml, 5.0 mmol). The crude material was purified by flash chromatography with 1% EtOAc in hexanes as eluent. The solvent was evaporated to yield the title compound as a clear oil (35 mg, 67% yield).

¹H NMR (600 MHz, CDCl₃): δ 7.17 (t, J = 8.2 Hz, 1H), 6.49 (td, J = 8.3, 2.0 Hz, 2H), 6.46 (t, J = 2.3 Hz, 1H), 4.48-4.37 (m, 1H), 3.79 (s, 3H), 1.86-1.77 (m, 1H), 1.71 (ddd, J = 14.0, 7.6, 6.6 Hz, 1H), 1.40-1.33 (m, 1H), 1.29 (d, J = 6.0 Hz, 3H), 0.95 (d, J = 6.7 Hz, 3H), 0.92 (d, J = 6.6 Hz, 3H).

¹³C NMR (151 MHz, CDCl₃): δ 160.9, 159.5, 129.8, 107.9, 105.9, 102.2, 72.0, 55.2, 45.8, 24.7, 22.9, 22.6, 20.0.

HPLC analysis: 37% ee, Chiralcel OD-H column, 100% hexane, 0.3 mL/min flow rate, 220 nm UV lamp, $t_{[major]}$ = 36.8 min, $t_{[minor]}$ = 38.5 min.

Anal. Calcd for C₁₃H₂₀O₂: C 74.96%, H 9.68%; Found: C 74.97%, H 9.83%.

1-(Octan-2-yloxy)naphthalene
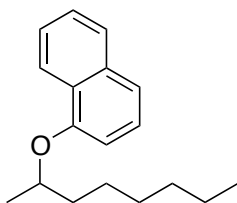
Following the general procedure **A** described above, 1-napthol (44 mg, 0.3 mmol) was allowed to react with 1-octene (0.90 ml, 6.0 mmol). The crude material was purified by flash chromatography with 1% EtOAc in hexanes as the eluent. The solvent was evaporated to yield the title compound as a clear oil (50 mg, 65% yield).
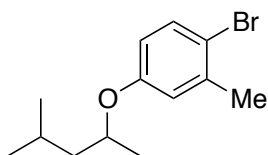
^{1}H NMR (600 MHz, CDCl$_3$): δ 8.30 (d, $J = 7.9$ Hz, 1H), 7.80 (d, $J = 7.7$ Hz, 1H), 7.52-7.43 (m, 2H), 7.43-7.35 (m, 2H), 6.83 (d, $J = 7.3$ Hz, 1H), 4.65-4.54 (m, 1H), 1.96-1.86 (m, 1H), 1.75-1.67 (m, 1H), 1.59-1.51 (m, 1H), 1.50-1.44 (m, 1H), 1.42 (d, $J = 5.9$ Hz, 3H), 1.39-1.29 (m, 6H), 0.90 (t, $J = 6.5$ Hz, 3H).
^{13}C NMR (151 MHz, CDCl$_3$): δ 153.9, 134.7, 127.4, 126.5, 126.2, 125.9, 124.9, 122.3, 119.7, 105.9, 74.1, 36.6, 31.8, 29.3, 25.6, 22.6, 19.7, 14.0.
HPLC analysis: 26% ee, Chiralcel OD-H column, 100% hexane, 1.0 mL/min flow rate, 220 nm UV lamp, t$_{[minor]}$ = 30.6 min, t$_{[major]}$ = 36.2 min.
Anal. Calcd for C$_{18}$H$_{24}$O: C 84.32%, H 9.44%; Found: C 84.24%, H 9.12%.
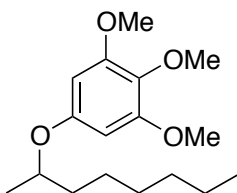
1,2,3-Trimethoxy-5-(octan-2-yloxy)benzene

Following the general procedure **A** described above, 3,4,5-trimethoxyphenol (55 mg, 0.3 mmol) was allowed to react with 1-octene (0.90 ml, 6.0 mmol). The crude material was purified by flash chromatography with 8% EtOAc in hexanes as eluent. The solvent was evaporated to yield the title compound as a clear oil (50 mg, 56% yield).

^{1}H NMR (600 MHz, CDCl$_3$): δ 6.13 (s, 2H), 4.33-4.21 (m, 1H), 3.82 (s, 6H), 3.78 (s, 3H), 1.78-1.67 (m, 1H), 1.60-1.51 (m, 1H), 1.48-1.41 (m, 1H), 1.39-1.25 (m, 10H), 0.87 (t, $J = 6.5$ Hz, 3H).
^{13}C NMR (151 MHz, CDCl$_3$): δ 154.7, 153.7, 132.2, 93.8, 74.4, 61.0, 56.0, 36.5, 31.8, 29.3, 25.5, 22.6, 19.8, 14.0.
HPLC analysis: 36% ee, Chiralcel OD-H column, 1% isopropanol in hexane, 0.7 mL/min flow rate, 254 nm UV lamp, t$_{[minor]}$ = 12.7 min, t$_{[major]}$ = 14.5 min.
Anal. Calcd for C$_{17}$H$_{28}$O$_4$: C 68.89%, H 9.52%; Found: C 68.84%, H 9.27%.

General Procedure B: Ir-catalyzed addition of phenols to ethylene and propylene.
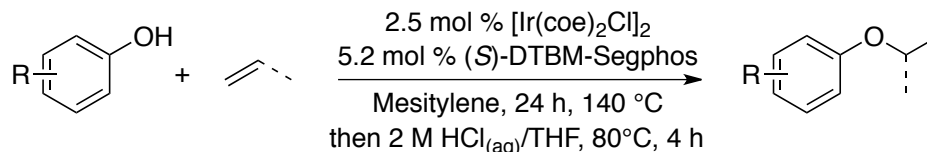
In a nitrogen-filled dry-box, an oven-dried round bottom Schlenk flask (58 ml volume) was charged with [Ir(coe)$_2$Cl]$_2$ (6.7 mg, 0.0075 mmol), (S)-DTBM-SEGPHOS (18.4 mg, 0.0156 mmol), the corresponding aryl alcohol (0.30 mmol), and a magnetic stirbar. Mesitylene (0.3 ml) was added to these solids to form a dark red solution. The flask was sealed with a Kontes valve and removed from the dry-box. Olefin gas (20 equiv, 6.0 mmol) was introduced to the flask according to the following procedure. The solution was frozen in liquid nitrogen and degassed under vacuum. Once the solvent was degassed, the flask was resealed and a manifold bulb adapter (61 ml) was filled with the alkene gas (605 Torr at 23 °C). The gas in the adapter was condensed into the Schlenk

91

flask at 77 K. The adapter was refilled with the alkene gas (605 Torr at 23 °C) and condensed into the Schlenk flask two additional times. The Schlenk flask was resealed and allowed to warm to room temperature. Upon warming, the red solution gradually became a pale yellow solution. The flask was placed in a 140 °C oil bath with vigorous stirring. After 24 h, the solution was allowed to cool to room temperature, and the solvent was removed under vacuum. A solution of THF/2M HCl (1:1 ratio, 1.5 ml) was added to the resulting residue in a 4 ml vial outside of the dry-box. The vial was sealed with a Teflon-lined cap and placed in an 80 °C heating block for 4 h to hydrolize enol ether products. The organic material was extracted with EtOAc (2 ml, 3 times). The product was purified by flash chromatography on a column (height = 20. cm, diameter = 3.0 cm) of Silacycle Siala-P60 silica gel (55 g). The conditions for hydrolysis, chromatography, and other data that are specific to each compound are given below.

1-Ethoxy-4-phenoxybenzene
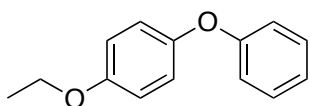
Following the general procedure **B** described above, 4-phenoxyphenol (56 mg, 0.30 mmol) was allowed to react with ethylene (6.0 mmol). The crude material was purified by flash chromatography with 2% EtOAc in hexanes as the eluent. The solvent was evaporated to yield the title compound as a clear oil (46 mg, 73% yield).

^{1}H NMR (600 MHz, CDCl$_3$): δ 7.31 (t, J = 7.2 Hz, 2H), 7.05 (t, J = 7.4 Hz, 1H), 7.02-6.93 (m, 4H), 6.89 (d, J = 7.3 Hz, 2H), 4.03 (q, J = 6.9 Hz, 2H), 1.43 (t, J = 6.9 Hz, 3H).
^{13}C NMR (151 MHz, CDCl$_3$): δ 158.5, 155.2, 150.0, 129.6, 122.4, 120.8, 117.6, 115.5, 63.9, 14.9.
Anal. Calcd for C$_{14}$H$_{14}$O$_2$: C 78.48%, H 6.59%; Found: C 78.18%, H 6.65%.

2-Ethoxynaphthalene
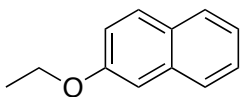
Following the general procedure **B** described above, 2-naphthol (44 mg, 0.30 mmol) was allowed to react with ethylene (6.0 mmol). The crude material was purified by flash chromatography with 2% EtOAc in hexanes as the eluent. The solvent was evaporated to yield the title compound as a pale white solid (36 mg, 69% yield).

^{1}H NMR (600 MHz, CDCl$_3$): δ 7.79 (d, J = 8.1 Hz, 1H), 7.75 (t, J = 8.7 Hz, 2H), 7.46 (t, J = 7.5 Hz, 1H), 7.35 (t, J = 7.4 Hz, 1H), 7.18 (d, J = 8.9 Hz, 1H), 7.15 (s, 1H), 4.17 (q, J = 6.8 Hz, 2H), 1.51 (t, J = 6.9 Hz, 3H).
^{13}C NMR (151 MHz, CDCl$_3$): δ 156.9, 134.6, 129.3, 128.9, 127.6, 126.7, 126.3, 123.5, 119.0, 106.5, 63.4, 14.8.
Anal. Calcd for C$_{12}$H$_{12}$O: C 83.69%, H 7.02%; Found: C 82.92%, H 7.30%.

1-fluoro-4-isopropoxybenzene
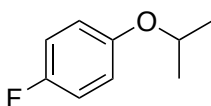
Following the general procedure **B** described above, 4-fluorophenol (34 mg, 0.30 mmol) was allowed to react with propene (6.0 mmol). The crude material was purified by flash chromatography with 2% EtOAc in hexanes as the eluent. The solvent was evaporated to yield the title compound as a clear oil (33 mg, 71% yield).

^{1}H NMR (600 MHz, CDCl$_3$): δ 6.96 (t, J = 8.6 Hz, 2H), 6.87-6.80 (m, 2H), 4.54-4.38 (h, J = 6.0 Hz, 1H), 1.32 (d, J = 6.1 Hz, 6H).

^{13}**C NMR** (151 MHz, CDCl$_3$): δ 157.1 (d, J = 238.4 Hz), 153.9, 117.2 (d, J = 8.0 Hz), 115.7 (d, J = 22.9 Hz), 70.8, 22.0.

^{19}**F NMR** (565 MHz, CDCl$_3$): δ -125.0 (m).

Anal. Calcd for C$_9$H$_{11}$FO: C 70.11%, H 7.19%; Found: C 70.33%, H 6.94%.

[((*S*)-DTBM-Segphos)Ir(Cl)(H)(η^3-allyl-^{i}Pr)], (24)
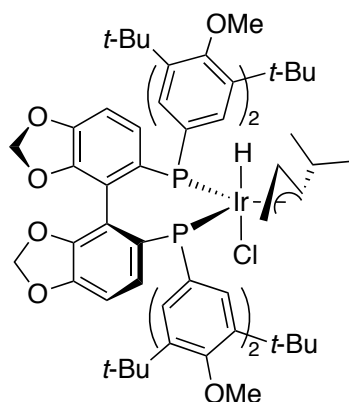
In a nitrogen-filled dry-box, an oven-dried 4 ml screw-capped vial was charged with [Ir(coe)$_2$Cl]$_2$ (25 mg, 0.028 mmol), (*S*)-DTBM-SEGPHOS (66 mg, 0.056 mmol), and a magnetic stirbar. The solids were dissolved in 4-methylpent-1-ene (1.5 ml, 13 mmol) to form a dark red solution. The vial was sealed with a Teflon-lined cap and placed in a 120 °C heating block. After 24 h, the light brown solution was allowed to cooled to room temperature and concentrated by rotary evaporation under atmospheric conditions. The crude material was purified by flash chromatography. UV active TLC plates were employed to analyze the contents of the collected fractions. Upon elution of the first UV active compound with 4% EtOAc in hexanes, the solvent polarity was increased to 12% EtOAc in hexanes. The last spot to elute (R$_f$ = 0.5 with 15% EtOAc in hexanes) was collected. The fractions were concentrated in a nitrogen filled dry-box to yield the title compound as a white solid (51 mg, 61% yield).
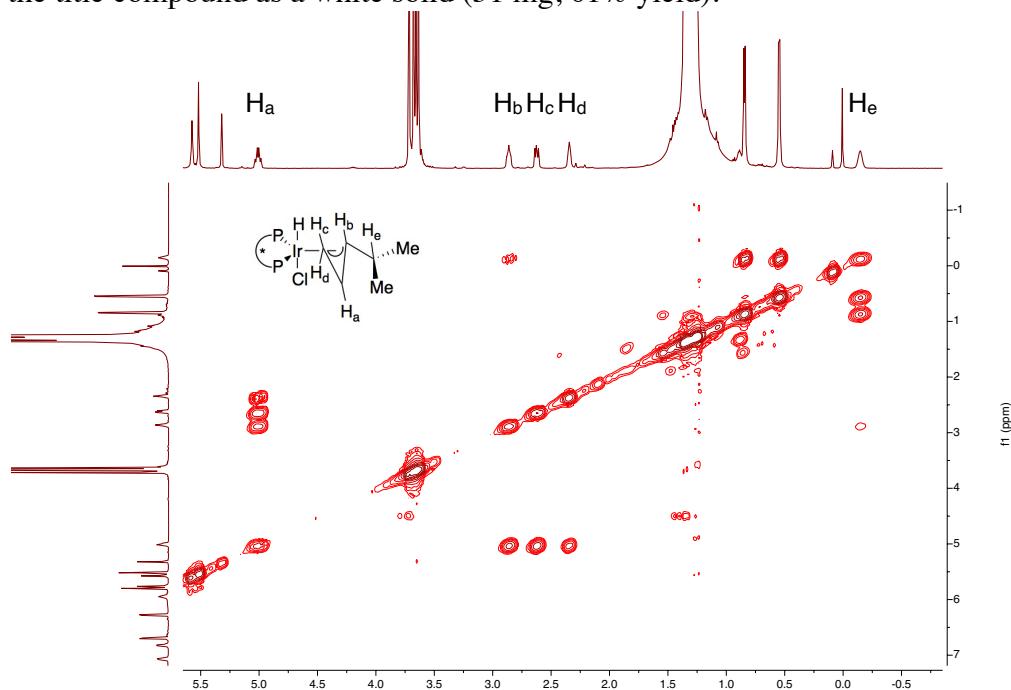
^{1}**H NMR** (600 MHz, CD$_2$Cl$_2$): δ 8.32-5.88 (br s, 2H), 8.04 (d, J = 13.0 Hz, 1H), 7.78 (d, J = 13.9 Hz, 1H), 7.92-7.50 (m, 1H), 7.45 (dd, J = 10.1, 8.4 Hz, 1H), 7.07 (d, J = 8.8 Hz, 1H), 6.82 (d, J = 8.8 Hz, 1H), 6.70 (d, J = 8.0 Hz, 1H), 6.28 (d, J = 8.1 Hz, 1H), 6.04 (br s, 1H), 6.01-5.90 (m, 1H), 5.80 (s, 1H), 5.76 (s, 1H), 5.57 (s, 1H), 5.52 (s, 1H), 5.01 (ddd, J = 18.6, 11.0 Hz, 1H), 3.72 (s, 3H), 3.68 (s, 3H), 3.66 (s, 3H), 3.64 (s, 3H), 2.92-2.81

(m, 1H), 2.62 (dd, J = 11.1, 7.1 Hz, 1H), 2.39-2.30 (m, 1H), 1.49-1.16 (m, 72H), 0.84 (d, J = 6.6 Hz, 3H), 0.55 (d, J = 6.8 Hz, 3H), -0.15 (br m, 1H), -23.66 (t, J = 13.0 Hz, 1H).

^{31}P NMR (243 MHz, C_6D_6): δ 4.3, 2.8.

ESI-MS: *m/z* 1455.8 (100%, [M–Cl]$^+$).

IR (0.44 M solution in C_6H_6 on KBr salt plates): 3035 (w), 2960 (s), 2869 (m), 2206 (m), 1473 (s), 1451 (m), 678 (s).

Anal. Calcd for $C_{80}H_{112}ClIrO_8P_2$: C 64.43%, H 7.57%; Found: C 64.17%, H 7.54%.

2-(Pyridin-2-yl)propan-2-ol
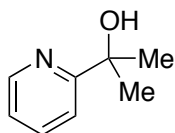
An oven dried 2-neck round-bottom flask (250 ml volume) with a magnetic stirbar was flushed with nitrogen and placed in a -78 °C bath. The flask was charged with a 2.5 M solution of [n]BuLi (14.2 ml, 35.7 mmol). Neat 2-bromopyridine (2.9 ml, 30. mmol) was added dropwise via syringe over 5 minutes to the solution at -78 °C. The red solution was allowed to stir at -78 °C for 20 minutes, after which time a 1.3 M solution of dried acetone in THF (40 ml, 52 mmol) was added. During the addition, the red solution underwent a color change to form a dark green solution. The green solution was allowed to warm to room temperature overnight. The reaction mixture was acidified with 2.5 M H_2SO_4 and washed with ether. The aqueous layer was basified with 2 M NaOH and the organic material was extracted with EtOAc (25 ml x 3). The crude material was purified by flash chromatography with 25% EtOAc in hexanes as eluent. The yellow oil was subjected to vacuum distillation at 60 °C and 150 mTorr to yield the title compound as a white solid (1.59 g, 39% yield). ^{1}H and ^{13}C NMR spectroscopic data matched those of previous reports.[40]

[((*S*)-DM-Segphos)Ir(Cl)(H)(alkoxide)], (27)

27   95 : 5 Ratio   **27-diastereo**
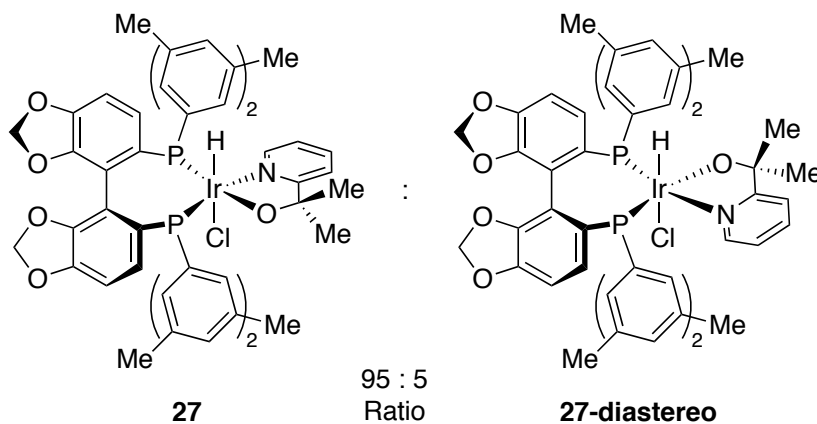
In a nitrogen-filled dry-box, an oven-dried 4 ml screw-capped vial was charged with [Ir(cod)Cl]$_2$ (50.4 mg, 0.0750 mmol), (*S*)-DM-SEGPHOS (177 mg, 0.150 mmol), 2-(pyridin-2-yl)propan-2-ol (82 mg, 0.60 mmol), and a magnetic stirbar. THF (1.5 ml) was added to these solids, and the suspension was stirred vigorously at room temperature until an orange solution formed (5 min). The vial was sealed with a Teflon-lined cap and placed in an 80 °C heating block. After 2 h, the orange solution was allowed to cool to room temperature in a nitrogen-filled dry-box. Pentane (15 ml) was added to the orange solution while stirring to induce an immediate formation of a white precipitate. The vial was sealed and placed in a -35 °C freezer for 1 hour. The solid was filtered and washed with pentane. Diethyl ether (5 ml) was added to the isolated precipitate, and the liquor was collected by filtra-

tion through Celite. The yellow solution was placed in a -35 °C freezer overnight to yield a white crystalline material. Diethyl ether was found to co-crystallize with the title compound. The crystals were dissolved in benzene, and the solvents were evaporated under vacuum to yield the title compound as a white powder (91 mg, 56% yield).

¹H NMR (500 MHz, C₆D₆): δ 8.75 (s, 1H), 8.74-8.68 (m, 1H), 8.01 (s, 3H), 7.81-7.72 (m, 1H), 7.21 (dd, J = 12.2, 8.2 Hz, 1H), 7.09-6.99 (m, 1H), 6.96 (dd, J = 10.7, 8.2 Hz, 1H), 6.78-6.69 (m, 3H), 6.62 (d, J = 7.9 Hz, 1H), 6.56 (s, 1H), 6.46 (s, 1H), 6.27 (d, J = 8.0 Hz, 1H), 6.15 (d, J = 8.0 Hz, 1H), 5.74 (dd, J = 6.5 Hz, 1H), 5.48 (s, 1H), 5.39 (s, 1H), 5.33 (s, 1H), 5.02 (s, 1H), 2.21 (s, 6H), 2.09 (s, 6H), 2.03 (s, 3H), 2.00 (s, 6H), 1.95 (s, 3H), 1.89 (s, 3H), 1.72-1.62 (m, 3H), -18.77 (dd, J = 20.4, 14.6 Hz, 1H). Note: two aryl proton resonances were not located, likely as a result of the fluctional nature of the aryl groups.

³¹P NMR (162 MHz, C₆D₆): δ -7.39 (d, J = 16.5 Hz), -10.41 (d, J = 16.6 Hz).

IR (0.5 M solution in C₆H₆ on KBr salt plates): 3070 (m), 3030 (s), 2964 (s), 2916 (s), 2207 (m), 1739 (m), 1598 (m), 1457 (s), 1439 (s), 1261 (s).

Anal. Calcd for C₅₄H₅₅ClIrNO₅P₂: C 59.63%, H 5.10%, N 1.29%; Found: C 59.34%, H 4.97%, N 1.24%.
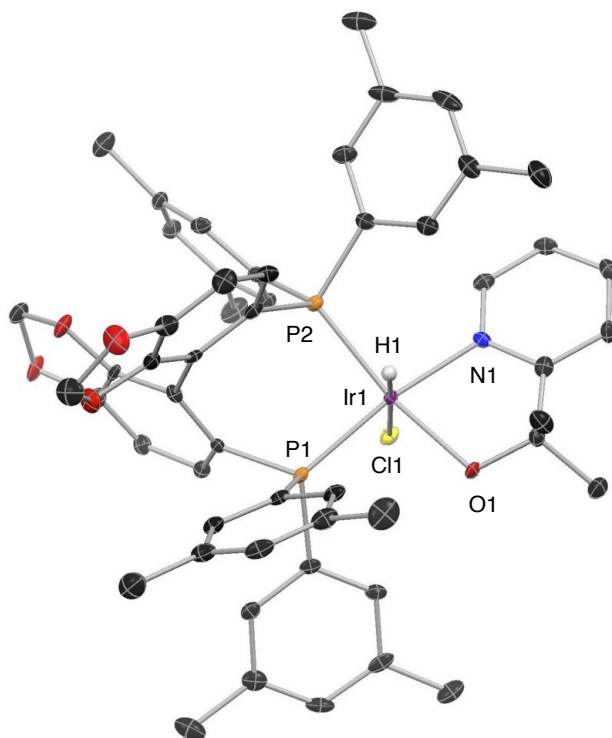
Figure 3.8. ORTEP representation of complex **27**. All hydrogens except the hydrogen atom bound to iridium were omitted for clarity. Thermal ellipsoids are drawn at the 50% probability level.

X-ray structure determination: Single crystals for x-ray analysis were obtained by dissolving **27** (90. mg, 0.083 mmol) in refluxing diethyl ether (0.2 ml) in an NMR tube. The vessel was allowed to cool to room temperature overnight. Over this period, clear colorless prisms formed on the inner walls of the NMR tube. A colorless prism 0.080 x 0.060 x 0.040 mm in size was mounted on a Cryoloop with Paratone oil. Data were collected in a nitrogen gas stream at 100(2) K using phi and omega scans. The crystal-to-detector distance was 40 mm, and the exposure time was 5 seconds per frame using a scan width of

0.5°. Data collection was 99.9% complete to 25.000° in q. A total of 55452 reflections were collected covering the indices, -18<=h<=18, -19<=k<=19, -23<=l<=25. 9664 reflections were found to be symmetry independent, with an R_{int} of 0.0366. Indexing and unit cell refinement indicated a primitive, orthorhombic lattice. The space group was found to be P 21 21 21 (No. 19). The data were integrated using the Bruker SAINT software program and scaled using the SADABS software program. Solution by iterative methods (SHELXT) produced a complete heavy-atom phasing model consistent with the proposed structure. All non-hydrogen atoms were refined anisotropically by full-matrix least-squares (SHELXL-2013). All hydrogen atoms were placed using a riding model. Their positions were constrained relative to their parent atom using the appropriate HFIX command in SHELXL-2013.

Table 3.4. Crystal data and structure refinement for complex 27

Empirical formula	C58 H65 Cl Ir N O6 P2
Formula weight	1161.70
Temperature	100(2) K
Wavelength	0.71073 Å
Crystal system	Orthorhombic
Space group	P 21 21 21
Unit cell dimensions	a = 15.5895(8) Å a= 90°.
	b = 16.1747(10) Å b= 90°.
	c = 21.0664(13) Å g = 90°.
Volume	5312.0(5) Å^3
Z	4
Density (calculated)	1.453 Mg/m^3
Absorption coefficient	2.675 mm^{-1}
F(000)	2368
Crystal size	0.080 x 0.060 x 0.040 mm^3
Crystal color/habit	colorless prism
Theta range for data collection	1.587 to 25.330°.
Index ranges	-18<=h<=18, -19<=k<=19, -23<=l<=25
Reflections collected	55452
Independent reflections	9664 [R(int) = 0.0366]
Completeness to theta = 25.000°	99.9 %
Absorption correction	Semi-empirical from equivalents
Max. and min. transmission	0.745 and 0.619
Refinement method	Full-matrix least-squares on F^2
Data / restraints / parameters	9664 / 0 / 634
Goodness-of-fit on F^2	1.040
Final R indices [I>2sigma(I)]	R1 = 0.0209, wR2 = 0.0460
R indices (all data)	R1 = 0.0244, wR2 = 0.0475
Absolute structure parameter	-0.019(2)
Extinction coefficient	n/a
Largest diff. peak and hole	0.838 and -0.438 e.Å^{-3}
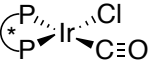
Table 3.5. Atomic Coordinates of 27[a]

Atom	x	y	z	U(eq)
C(1)	4089(3)	1545(3)	-183(2)	13(1)
C(2)	3300(2)	1843(2)	-1(3)	14(1)
C(3)	3034(3)	1707(3)	626(2)	18(1)
C(4)	3586(3)	1312(3)	1042(2)	15(1)
C(5)	4389(3)	1046(3)	831(2)	13(1)
C(6)	5073(3)	657(3)	1256(2)	13(1)
C(7)	5119(3)	1126(4)	1894(2)	23(1)
C(8)	4833(3)	-256(3)	1377(2)	20(1)
C(9)	8022(3)	775(3)	335(2)	11(1)
C(10)	8887(3)	669(3)	181(2)	12(1)
C(11)	9535(3)	1034(3)	534(2)	15(1)
C(12)	9299(3)	1528(3)	1052(2)	17(1)
C(13)	8446(3)	1628(3)	1231(2)	17(1)
C(14)	7798(3)	1249(3)	864(2)	12(1)
C(15)	10468(3)	877(3)	377(3)	24(1)
C(16)	8220(4)	2152(3)	1796(2)	25(1)
C(17)	7503(3)	-845(2)	33(2)	11(1)
C(18)	8239(3)	-1210(3)	-211(2)	14(1)
C(19)	8521(3)	-1980(3)	21(3)	18(1)
C(20)	8032(3)	-2375(3)	480(2)	18(1)
C(21)	7277(3)	-2041(3)	713(2)	19(1)
C(22)	7018(3)	-1259(3)	486(2)	14(1)
C(23)	9346(4)	-2371(3)	-227(3)	28(1)
C(24)	6744(4)	-2501(3)	1199(3)	30(2)
C(25)	7578(3)	444(3)	-956(2)	9(1)
C(26)	7969(3)	1204(3)	-1083(2)	12(1)
C(27)	8211(3)	1443(3)	-1699(2)	14(1)
C(28)	8065(3)	874(3)	-2173(2)	12(1)
C(29)	7841(3)	242(3)	-3108(2)	17(1)
C(30)	7663(3)	125(3)	-2058(2)	10(1)
C(31)	7382(3)	-110(3)	-1458(2)	10(1)
C(32)	6837(3)	-859(3)	-1386(2)	10(1)
C(33)	7149(3)	-1642(3)	-1510(2)	13(1)
C(34)	7979(4)	-2735(3)	-1710(3)	26(1)
C(35)	6651(3)	-2340(3)	-1470(2)	16(1)
C(36)	5796(4)	-2311(3)	-1311(2)	20(1)
C(37)	5456(3)	-1517(3)	-1194(2)	14(1)
C(38)	5953(3)	-802(3)	-1226(2)	12(1)
C(39)	5702(3)	837(3)	-1730(2)	10(1)
C(40)	5649(3)	506(3)	-2345(2)	13(1)
C(41)	5765(3)	1000(3)	-2879(2)	14(1)
C(42)	5994(3)	1827(3)	-2791(2)	14(1)
C(43)	6078(3)	2170(3)	-2189(2)	13(1)

C(44)	5921(3)	1667(3)	-1657(2)	12(1)
C(45)	5641(3)	651(3)	-3537(2)	21(1)
C(46)	6362(4)	3063(3)	-2117(2)	23(1)
C(47)	4318(3)	14(3)	-1089(2)	13(1)
C(48)	3863(3)	166(3)	-1647(2)	16(1)
C(49)	2985(3)	29(3)	-1683(3)	22(1)
C(50)	2550(3)	-236(3)	-1138(3)	22(1)
C(51)	2984(3)	-386(3)	-575(2)	16(1)
C(52)	3866(3)	-283(3)	-558(2)	14(1)
C(53)	2505(4)	157(4)	-2304(3)	32(1)
C(54)	2503(3)	-627(3)	24(3)	25(1)
C(55)	87(4)	-906(4)	-1446(3)	43(2)
C(56)	-118(4)	1(4)	-1562(3)	36(2)
C(57)	479(5)	1349(4)	-1417(4)	50(2)
C(58)	1301(4)	1781(4)	-1331(3)	42(2)
N(1)	4614(2)	1125(2)	214(2)	10(1)
O(1)	5882(2)	745(2)	966(1)	13(1)
O(2)	8281(2)	926(2)	-2804(2)	18(1)
O(3)	7587(2)	-322(2)	-2606(1)	16(1)
O(4)	7969(2)	-1851(2)	-1685(2)	18(1)
O(5)	7122(2)	-3032(2)	-1617(2)	24(1)
O(6)	608(3)	477(3)	-1385(2)	44(1)
P(1)	7205(1)	234(1)	-147(1)	9(1)
P(2)	5486(1)	213(1)	-1022(1)	9(1)
Cl(1)	6285(1)	2083(1)	-90(1)	12(1)
Ir(1)	5818(1)	619(1)	-16(1)	8(1)

[a]Values represent atomic coordinates x 10^4 and equivalent isotropic displacement parameters (Å^2 x 10^3) for **28**. U(eq) is defined as one third of the trace of the orthogonalized U tensor.

[(*S*)-DTBM-Segphos]Ir(CO)(Cl), 28

$\overset{*}{\underset{P}{\overset{P}{\big(}}}$ = (*S*)-DTBM-Segphos

In a nitrogen-filled dry-box, an oven-dried 4 ml screw-capped vial was charged with [Ir(cod)Cl]$_2$ (20. mg, 0.030 mmol), (*S*)-DTBM-SEGPHOS (70. mg, 0.60 mmol), and a magnetic stirbar. Dibutylether (0.5 ml) was added to these solids, and the suspension was stirred vigorously at room temperature until an orange solution formed (5 min). The vial was sealed with a Teflon-lined cap and placed in a 100 °C heating block. After 12 h, orange crystalline solids had formed. In the dry-box, the solids were washed with pentane and residual solvents were removed under vacuum to yield the title compound as orange crystals (48 mg, 56% yield).

¹H NMR (500 MHz, C$_6$D$_6$): δ 8.90 (br m, 2H), 8.29 (s, 2H), 8.14 (d, *J* = 11.7 Hz, 2H), 7.38 (s, 1H), 7.12-7.07 (m, 2H), 6.59 (dd, *J* = 11.0, 8.2 Hz, 1H), 6.10 (d, *J* = 8.1 Hz, 1H), 5.99 (d, *J* = 8.1 Hz, 1H), 5.40 (s, 1H), 5.30 (s, 1H), 5.01 (s, 1H), 4.99 (s, 1H), 3.44 (s, 3H), 3.43 (s, 3H), 3.31 (s, 3H), 3.26 (s, 3H), 1.51 (s, 18H), 1.46 (s, 36H), 1.43 (s, 18H).

³¹P NMR (243 MHz, C$_6$D$_6$): δ 22.26 (d, *J* = 29 Hz), 14.34 (d, *J* = 29 Hz).

IR (0.5 M solution in C$_6$H$_6$ on KBr salt plates): 1973 (s) (carbonyl C–O stretch).

Anal. Calcd for C$_{75}$H$_{100}$ClIrO$_9$P$_2$: C 62.76%, H 7.02%; Found: C 63.18%, H 6.80%.

98

X-ray Structure Determination: An orange prism 0.060 x 0.040 x 0.020 mm in size was mounted on a Cryoloop with Paratone oil. Data were collected in a nitrogen gas stream at 100(2) K using phi and omega scans. Crystal-to-detector distance was 60 mm and exposure time was 10 seconds per frame using a scan width of 0.5°. Data collection was 99.8% complete to 25.000° in θ. A total of 110334 reflections were collected covering the indices, -22<=h<=23, -20<=k<=20, -24<=l<=25. 25645 reflections were found to be symmetry independent, with an R_{int} of 0.0348. Indexing and unit cell refinement indicated a primitive, monoclinic lattice. The space group was found to be P 21 (No. 4). The data were integrated using the Bruker SAINT software program and scaled using the SADABS software program. Solution by iterative methods (SHELXT) produced a complete heavy-atom phasing model consistent with the proposed structure. All non-hydrogen atoms were refined anisotropically by full-matrix least-squares (SHELXL-2013). All hydrogen atoms were placed using a riding model. Their positions were constrained relative to their parent atom using the appropriate HFIX command in SHELXL-2013.
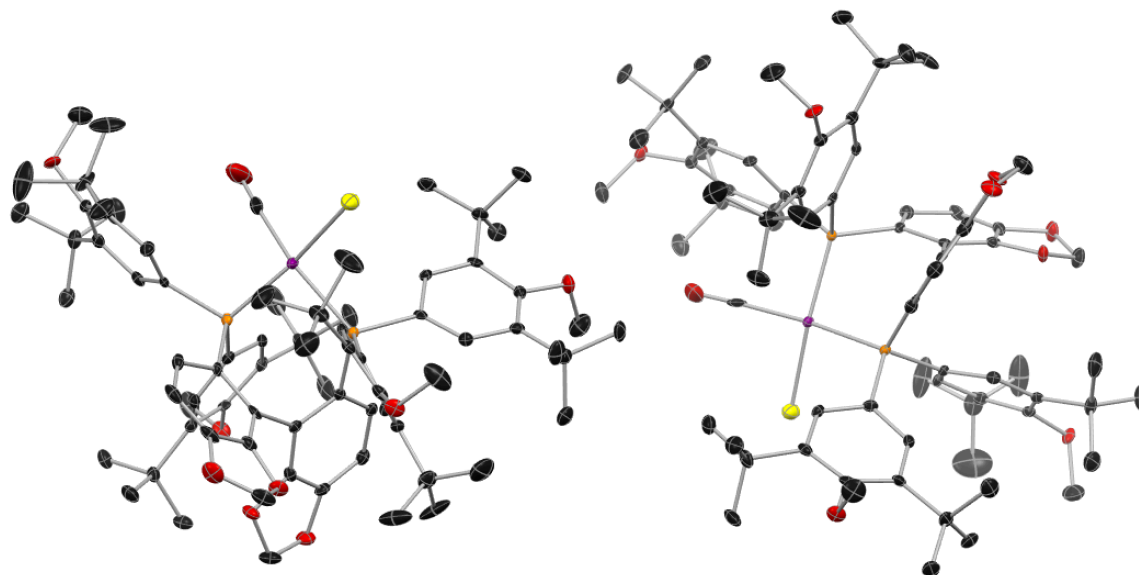
Figure 3.9. ORTEP representation of complex **28**. All hydrogens were omitted for clarity. Thermal ellipsoids are drawn at the 50% probability level.

Table 3.6. Crystal data and structure refinement for 28.

Empirical formula	C75 H100 Cl Ir O9 P2
Formula weight	1435.13
Temperature	100(2) K
Wavelength	0.71073 Å
Crystal system	Monoclinic
Space group	P 21
Unit cell dimensions	a = 19.1512(9) Å $\quad$ a= 90°.
	b = 17.4973(9) Å $\quad$ b= 93.578(2)°.
	c = 21.3048(10) Å $\quad$ g = 90°.
Volume	7125.2(6) Å^3
Z	4
Density (calculated)	1.338 Mg/m^3
Absorption coefficient	2.011 mm^{-1}
F(000)	2984
Crystal size	0.060 x 0.040 x 0.020 mm^3
Crystal color/habit	yellow prism
Theta range for data collection	1.387 to 25.357°.
Index ranges	-22<=h<=23, -20<=k<=20, -24<=l<=25
Reflections collected	110334
Independent reflections	25645 [R(int) = 0.0348]
Completeness to theta = 25.000°	99.8 %
Absorption correction	Analytical
Max. and min. transmission	1.000 and 0.910
Refinement method	Full-matrix least-squares on F^2
Data / restraints / parameters	25645 / 1 / 1641
Goodness-of-fit on F^2	1.034
Final R indices [I>2sigma(I)]	R1 = 0.0270, wR2 = 0.0530
R indices (all data)	R1 = 0.0335, wR2 = 0.0553
Absolute structure parameter	-0.0135(12)
Extinction coefficient	n/a
Largest diff. peak and hole	0.868 and -0.784 e.Å^{-3}

Table 3.7. Atomic Coordinates of 28[a]

Atom	x	y	z	U(eq)
C(1)	1853(2)	8227(3)	5636(2)	10(1)
C(1A)	1499(3)	11017(3)	5310(3)	31(2)
C(2)	1877(2)	8652(3)	6188(2)	10(1)
C(2A)	3529(3)	5948(3)	9780(3)	26(1)
C(3)	1883(2)	8301(3)	6775(2)	11(1)
C(4)	1887(2)	7494(3)	6787(2)	13(1)
C(5)	1786(3)	7050(3)	6240(2)	14(1)
C(6)	1787(2)	7444(3)	5669(2)	12(1)
C(7)	1836(2)	8797(3)	7371(2)	14(1)
C(8)	2501(3)	8734(3)	7813(2)	20(1)
C(9)	1731(3)	9637(3)	7204(2)	19(1)
C(10)	1203(3)	8537(3)	7725(2)	20(1)
C(11)	2680(3)	6873(3)	7503(3)	31(1)
C(12)	1663(3)	6175(3)	6203(2)	18(1)
C(13)	2329(3)	5786(3)	5986(3)	28(1)
C(14)	1054(3)	6006(3)	5712(3)	29(1)
C(15)	1444(3)	5801(3)	6813(2)	23(1)
C(16)	1481(3)	8125(3)	4300(2)	10(1)
C(17)	1760(3)	7426(3)	4123(2)	14(1)
C(18)	1400(3)	6932(3)	3713(2)	14(1)
C(19)	729(3)	7182(3)	3460(2)	15(1)
C(20)	483(2)	7920(3)	3562(2)	13(1)
C(21)	853(2)	8365(3)	4010(2)	11(1)
C(22)	1719(3)	6150(3)	3555(2)	22(1)
C(23)	1758(3)	6042(4)	2841(3)	42(2)
C(24)	2470(3)	6081(3)	3827(3)	40(2)
C(25)	1287(4)	5499(3)	3804(3)	57(2)
C(26)	-219(3)	6321(4)	3406(3)	42(2)
C(27)	-164(3)	8302(3)	3217(2)	20(1)
C(28)	-379(3)	7963(3)	2575(2)	34(2)
C(29)	14(3)	9153(3)	3084(3)	34(2)
C(30)	-772(3)	8323(4)	3653(3)	47(2)
C(31)	2835(2)	8589(3)	4724(2)	10(1)
C(32)	3319(2)	8317(3)	5185(2)	12(1)
C(33)	4023(3)	8186(3)	5068(2)	14(1)
C(34)	4200(3)	8301(3)	4462(2)	15(1)
C(35)	4688(3)	8265(3)	3551(2)	22(1)
C(36)	3724(3)	8580(3)	4005(2)	12(1)
C(37)	3041(2)	8758(3)	4110(2)	10(1)
C(38)	2591(2)	9125(3)	3593(2)	12(1)
C(39)	2437(3)	8742(3)	3038(2)	16(1)
C(40)	2204(3)	7847(3)	2314(2)	24(1)
C(41)	2064(3)	9072(3)	2528(2)	18(1)

C(42)	1834(2)	9803(3)	2536(2)	21(1)
C(43)	1993(2)	10212(3)	3094(2)	16(1)
C(44)	2350(2)	9894(3)	3618(2)	10(1)
C(45)	2276(2)	11433(3)	4182(2)	12(1)
C(46)	1621(3)	11680(3)	3942(2)	16(1)
C(47)	1449(3)	12450(3)	3906(2)	14(1)
C(48)	1935(3)	12972(3)	4191(2)	12(1)
C(49)	2613(3)	12756(3)	4393(2)	12(1)
C(50)	2770(3)	11974(3)	4382(2)	12(1)
C(51)	743(3)	12685(3)	3562(3)	22(2)
C(52)	448(3)	12048(3)	3132(3)	31(2)
C(53)	859(4)	13379(4)	3127(3)	55(2)
C(54)	200(3)	12864(4)	4029(3)	45(2)
C(55)	1441(3)	13849(3)	4876(2)	31(1)
C(56)	3199(3)	13296(3)	4662(2)	14(1)
C(57)	3117(3)	14132(3)	4466(2)	23(1)
C(58)	3920(3)	13036(3)	4433(2)	21(1)
C(59)	3240(3)	13233(3)	5390(2)	28(1)
C(60)	3346(2)	10400(3)	4621(2)	10(1)
C(61)	3870(2)	10494(3)	4207(2)	12(1)
C(62)	4572(2)	10569(3)	4413(2)	11(1)
C(63)	4731(2)	10550(3)	5075(2)	11(1)
C(64)	4216(2)	10406(3)	5504(2)	11(1)
C(65)	3526(2)	10345(3)	5263(2)	12(1)
C(66)	5137(2)	10656(3)	3931(2)	14(1)
C(67)	4829(3)	10514(3)	3256(2)	22(1)
C(68)	5434(3)	11475(3)	3940(2)	24(1)
C(69)	5734(2)	10077(4)	4056(2)	20(1)
C(70)	5662(3)	11360(3)	5501(3)	30(1)
C(71)	4371(3)	10323(3)	6225(2)	21(1)
C(72)	4389(4)	11113(4)	6536(3)	42(2)
C(73)	5046(3)	9865(4)	6396(2)	38(2)
C(74)	3780(3)	9870(4)	6516(2)	24(1)
C(75)	3157(3)	3191(3)	9356(2)	11(1)
C(76)	3122(2)	3643(3)	8815(2)	11(1)
C(77)	3104(2)	3314(3)	8220(2)	12(1)
C(78)	3090(2)	2506(3)	8181(2)	12(1)
C(79)	3204(3)	2039(3)	8713(2)	13(1)
C(80)	3220(2)	2410(3)	9298(2)	12(1)
C(81)	3148(3)	3828(3)	7638(2)	18(1)
C(82)	2483(3)	3788(3)	7190(2)	23(1)
C(83)	3257(3)	4667(3)	7824(2)	22(1)
C(84)	3778(3)	3576(3)	7280(2)	24(1)
C(85)	2259(3)	1930(3)	7469(3)	30(1)
C(86)	3322(3)	1160(3)	8730(2)	18(1)
C(87)	3474(3)	799(3)	8100(2)	27(1)

C(88)	3974(3)	983(3)	9170(2)	24(1)
C(89)	2676(3)	775(3)	8987(2)	25(1)
C(90)	3523(2)	3031(3)	10697(2)	9(1)
C(91)	3257(3)	2313(3)	10832(2)	10(1)
C(92)	3616(2)	1801(3)	11235(2)	11(1)
C(93)	4272(3)	2042(3)	11501(2)	11(1)
C(94)	4508(3)	2801(3)	11439(2)	12(1)
C(95)	4138(2)	3276(3)	11013(2)	12(1)
C(96)	3284(3)	1003(3)	11335(2)	16(1)
C(97)	2481(3)	1049(3)	11252(3)	28(1)
C(98)	3517(3)	442(3)	10837(3)	30(1)
C(99)	3450(3)	664(3)	11992(2)	26(1)
C(100)	5111(3)	1032(3)	11527(3)	31(1)
C(101)	5157(3)	3124(3)	11813(2)	23(1)
C(102)	5114(4)	2971(4)	12513(3)	55(2)
C(103)	5211(4)	3985(3)	11743(3)	50(2)
C(104)	5824(3)	2757(5)	11586(4)	65(2)
C(105)	2165(2)	3503(2)	10269(2)	11(1)
C(106)	1693(2)	3240(3)	9799(2)	12(1)
C(107)	990(3)	3091(3)	9908(2)	14(1)
C(108)	805(3)	3185(3)	10513(2)	15(1)
C(109)	305(3)	3093(3)	11421(2)	23(1)
C(110)	1274(2)	3446(3)	10982(2)	12(1)
C(111)	1955(2)	3642(3)	10886(2)	10(1)
C(112)	2406(2)	3982(3)	11419(2)	9(1)
C(113)	2551(2)	3571(3)	11959(2)	12(1)
C(114)	2760(3)	2624(3)	12650(2)	20(1)
C(115)	2940(2)	3859(3)	12475(2)	13(1)
C(116)	3177(2)	4592(3)	12498(2)	14(1)
C(117)	3026(2)	5036(3)	11957(2)	14(1)
C(118)	2654(2)	4750(3)	11422(2)	9(1)
C(119)	2727(2)	6330(3)	10890(2)	11(1)
C(120)	3375(2)	6598(3)	11143(2)	11(1)
C(121)	3554(3)	7365(3)	11129(2)	12(1)
C(122)	3084(3)	7860(3)	10789(2)	12(1)
C(123)	2403(2)	7641(3)	10592(2)	10(1)
C(124)	2242(2)	6864(3)	10647(2)	10(1)
C(125)	4244(3)	7643(3)	11470(2)	15(1)
C(126)	4113(3)	8361(3)	11863(3)	27(1)
C(127)	4800(3)	7817(3)	10997(2)	25(1)
C(128)	4556(3)	7029(3)	11927(2)	22(1)
C(129)	3576(3)	8648(3)	10029(2)	24(1)
C(130)	1818(3)	8164(3)	10297(2)	14(1)
C(131)	1929(3)	9022(3)	10410(2)	21(1)
C(132)	1736(3)	8011(3)	9579(2)	24(1)
C(133)	1112(3)	7963(3)	10577(2)	19(1)

C(134)	1667(2)	5299(3)	10433(2)	10(1)
C(135)	1145(2)	5394(3)	10851(2)	11(1)
C(136)	436(2)	5460(3)	10649(2)	12(1)
C(137)	284(2)	5446(3)	9990(2)	12(1)
C(138)	798(2)	5308(3)	9557(2)	12(1)
C(139)	1486(2)	5243(2)	9796(2)	12(1)
C(140)	-118(2)	5541(3)	11146(2)	15(1)
C(141)	168(3)	5238(3)	11791(2)	26(1)
C(142)	-294(3)	6388(3)	11242(3)	37(2)
C(143)	-780(2)	5072(4)	10970(2)	23(1)
C(144)	-676(3)	6269(3)	9673(3)	33(2)
C(145)	623(3)	5205(3)	8839(2)	21(1)
C(146)	1264(3)	4923(4)	8510(2)	25(1)
C(147)	394(4)	5953(4)	8534(3)	49(2)
C(148)	55(3)	4592(4)	8720(3)	43(2)
O(1)	1981(2)	7143(2)	7373(1)	18(1)
O(1A)	1487(3)	11561(3)	5546(2)	57(2)
O(2)	337(2)	6663(2)	3090(2)	18(1)
O(2A)	3559(3)	6513(3)	9561(2)	55(1)
O(3)	4841(2)	8206(2)	4214(2)	21(1)
O(4)	4050(2)	8684(2)	3452(1)	17(1)
O(5)	2628(2)	8007(2)	2883(2)	19(1)
O(6)	2005(2)	8558(2)	2036(2)	27(1)
O(7)	1711(2)	13716(2)	4269(2)	18(1)
O(8)	5427(2)	10624(2)	5283(2)	17(1)
O(9)	2973(2)	2177(2)	7590(1)	18(1)
O(10)	4694(2)	1550(2)	11866(1)	14(1)
O(11)	162(2)	3070(2)	10752(2)	22(1)
O(12)	942(2)	3512(2)	11536(2)	18(1)
O(13)	2349(2)	2832(2)	12082(1)	15(1)
O(14)	3002(2)	3315(2)	12940(1)	20(1)
O(15)	3328(2)	8589(2)	10653(2)	16(1)
O(16)	-408(2)	5519(2)	9751(2)	17(1)
P(1)	1920(1)	8735(1)	4891(1)	9(1)
P(2)	2419(1)	10418(1)	4365(1)	10(1)
P(3)	3087(1)	3662(1)	10118(1)	9(1)
P(4)	2592(1)	5319(1)	10694(1)	8(1)
Cl(1)	523(1)	9636(1)	5402(1)	26(1)
Cl(2)	4486(1)	4573(1)	9637(1)	24(1)
Ir(1)	1590(1)	10013(1)	4978(1)	12(1)
Ir(2)	3423(1)	4942(1)	10072(1)	10(1)

[a]Values represent atomic coordinates x 10^4 and equivalent isotropic displacement parameters (Å^2 x 10^3) for **28**. U(eq) is defined as one third of the trace of the orthogonalized U tensor.

Analysis of the Hydrogen-Bonding Interaction between 24 and 4-F-Phenol by ^{1}H NMR NOESY techniques.

    A solution of **24** (78 mg, 0.052 mmol) and 4-F-phenol (6.0 mg, 0.052 mmol) in C_6D_6 (0.4 ml) was analyzed by NOESY spectroscopy. NOE correlations of the Ir–H proton were observed, but no NOE correlation with the aryl alcohol was detected.
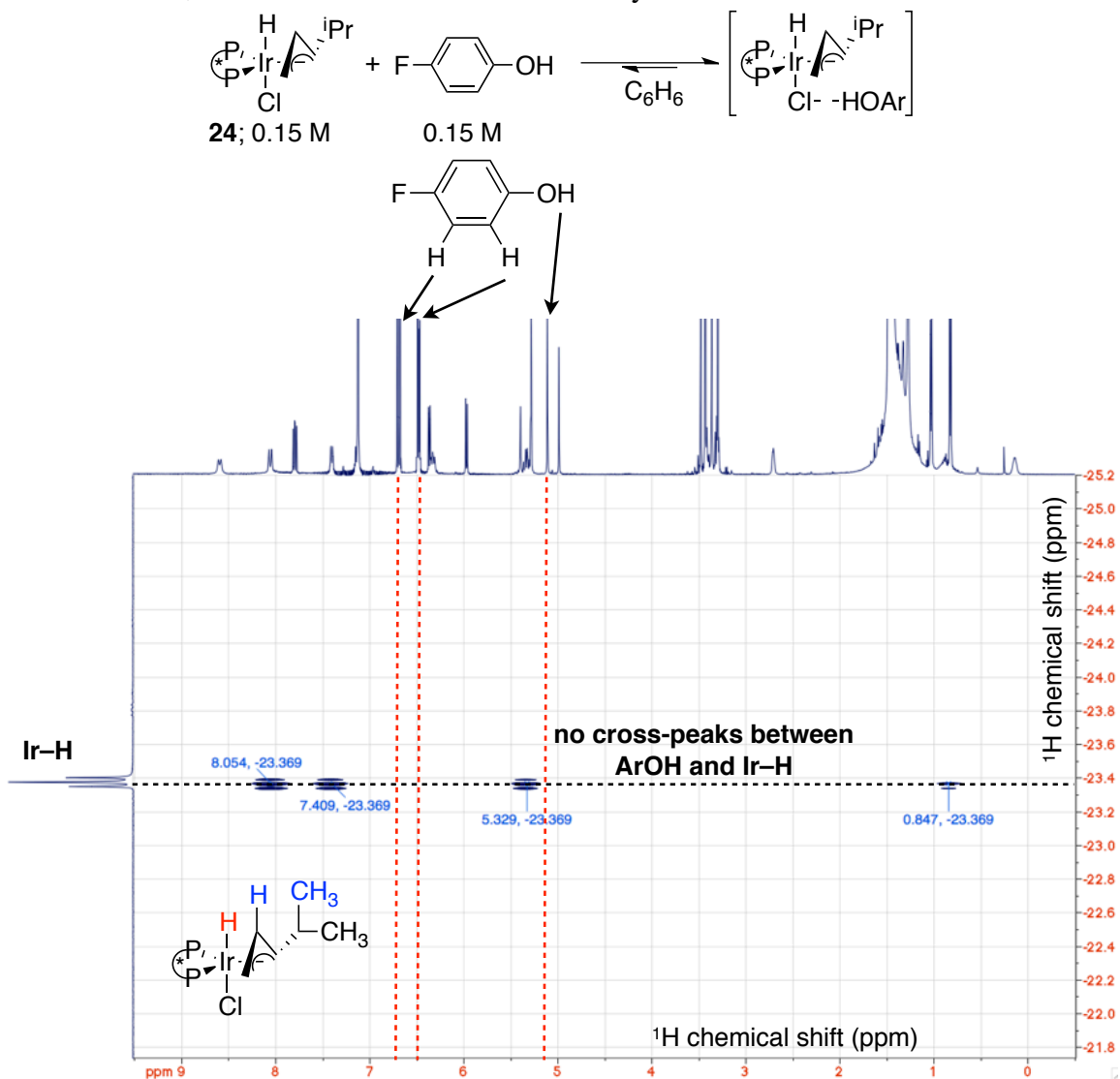

Figure 3.10. Top: Illustration of the equilibrium that was studied by NOESY. Bottom: NOE correlations with the Ir–H proton.

Analysis of the Hydrogen-Bonding Interaction between 24 and ArOH by IR spectroscopy.

Solutions of of **24** (78 mg, 0.052 mmol, purple trace) and 4-OMe-phenol (6.0 mg, 0.050 mmol, blue trace) in C_6H_6 (0.1 ml each) were analyzed by IR spectroscopy independently. A solution of **24** and 4-OMe-phenol (red trace) is overlayed to demonstrate changes in IR stretching frequencies: most notably those of the Ir–H and O–H bonds. See results and discussion section for further discussion.
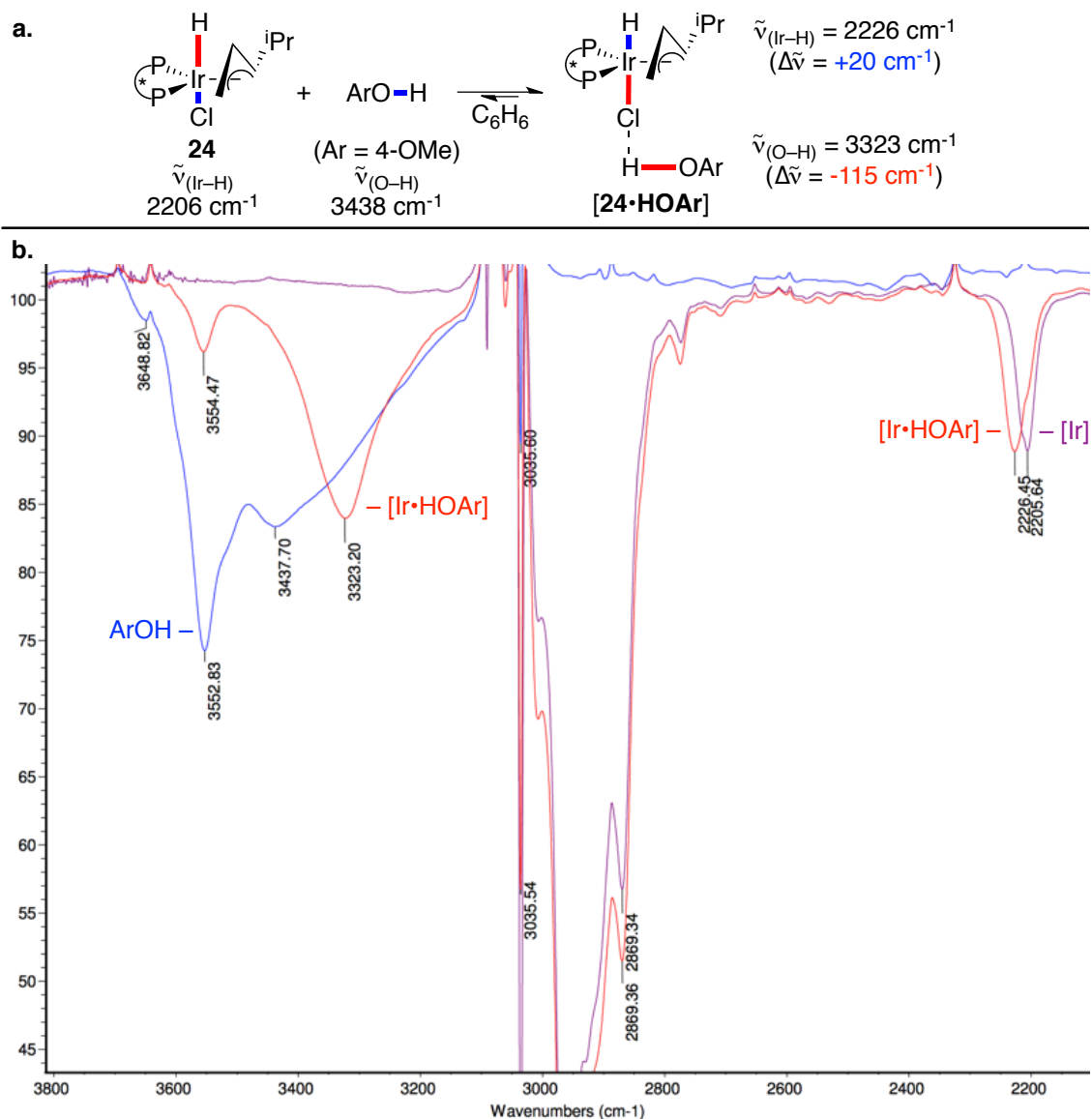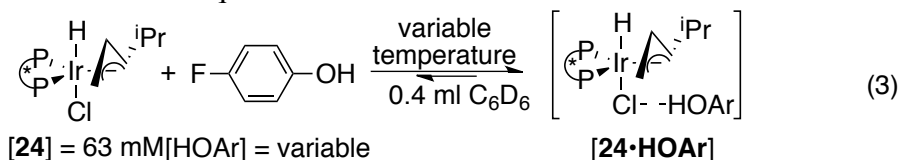

Figure 3.11. Equilibrium between **24** and phenol studied by IR spectroscopy.

106

Determination of the thermodynamic parameters for hydrogen bonding of an aryl alcohol with 24

The observed chemical shift in the Ir–H region of the ^{1}H NMR of the reaction mixture summarized in Eq 3 was related to the equilibrium mixtures of **24** and [**24•HOAr**] by the Eq 8, which was derived from equations 4-6.

$$[\mathbf{24}] = 63 \text{ mM} \quad [\text{HOAr}] = \text{variable} \qquad [\mathbf{24 \cdot HOAr}]$$

$$\delta_{obs} = \delta_{\mathbf{24}}\chi_{\mathbf{24}} + \delta_{[\mathbf{24 \cdot HOAr}]}\chi_{[\mathbf{24 \cdot HOAr}]} \tag{4}$$

$$\chi_{\mathbf{x}} = \frac{[\mathbf{x}]}{[\text{Ir}]_0} \tag{5}$$

$$K_{eq} = \frac{[\mathbf{24 \cdot HOAr}]}{[\mathbf{24}][\text{ArOH}]} \tag{6}$$

$$[\text{ArOH}] \approx [\text{ArOH}]_0 \tag{7}$$

$$\delta_{obs} = \frac{\delta_{\mathbf{24}} + \delta_{[\mathbf{24 \cdot HOAr}]}K_{eq}[\text{ArOH}]_0}{1 + K_{eq}[\text{ArOH}]_0} \tag{8}$$
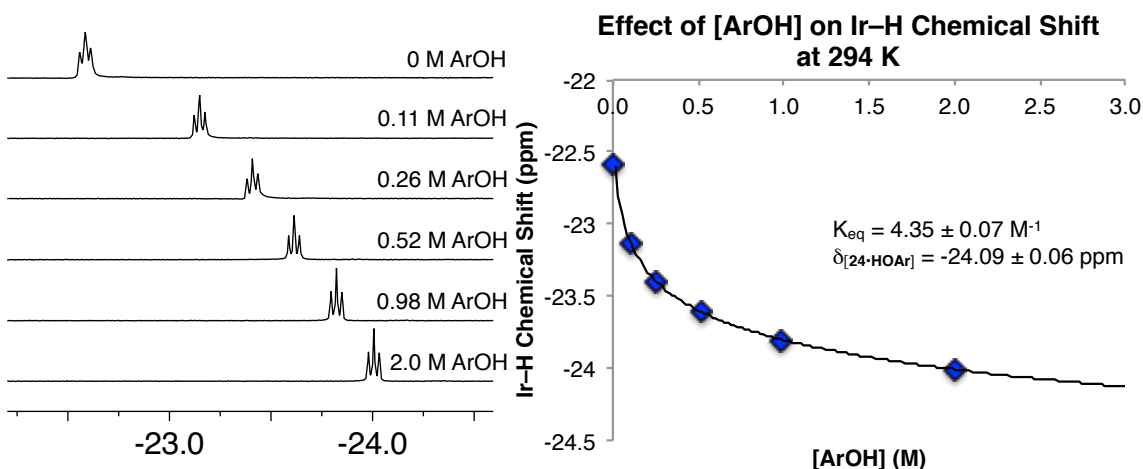

Figure 3.12. Left: ^{1}H NMR spectra of Ir–H region of **24** in the presence of varying concentrations of 4-F-phenol. Right: Plot of the observed Ir–H chemical shift as a function of ArOH concentration with a data fitting to Eq 8.

The equilibrium constant was determined to be 4.4 M^{-1} at 294 K after fitting the data of Figure 3.12 to eq 8. Variable temperature analysis by ^{1}H NMR spectroscopy was conducted to determine the equilibrium mixtures of **24** and [**24•HOAr**] at 140 °C: the temperature of the catalytic reaction. The temperature-dependent Ir–H chemical shift was measured by ^{1}H NMR spectroscopy from 294 K to 335 K for solutions with identical concentrations of **24** (63 mM) and varying concentrations of 4-F-phenol (0 M, 0.11 M, 0.26 M, 0.98 M, 2.0 M). These data are plotted in Figure 3.13.

An analysis similar to that described for the data in Figure 3.13 was conducted for the data in Figure 3.12 at each measured temperature to reveal the temperature-dependent equilibrium constants that are summarized in Figure 3.14a. A Van't Hoff analysis of the equilibrium constants as a function of temperature revealed the thermodynamic parameters of the equilibrium (Figure 3.14b). From the measured thermodynamic parameters, the equilibrium constant was calculated to be 1.6 M^{-1} at 140 °C, which corresponds to a 0.39 mole-fraction of **24** in the resting state mixture.
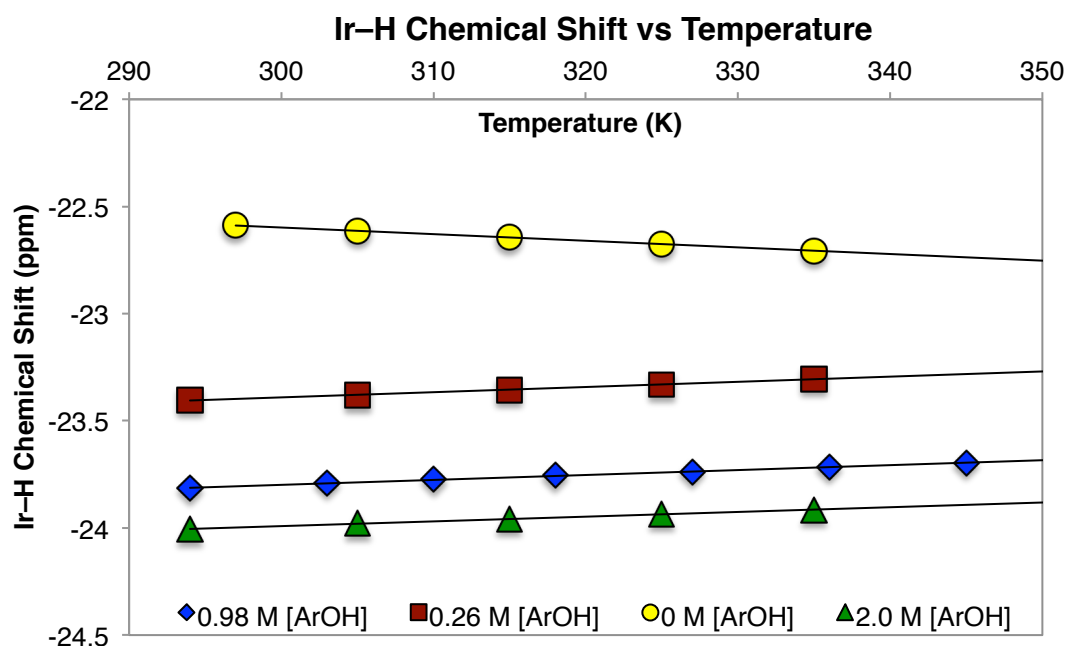

Figure 3.13. Chemcial shift of the Ir–H proton in the reaction described by Eq 1 by ^{1}H NMR spectroscopy as a function of temperature at various aryl alcohol concentrations.
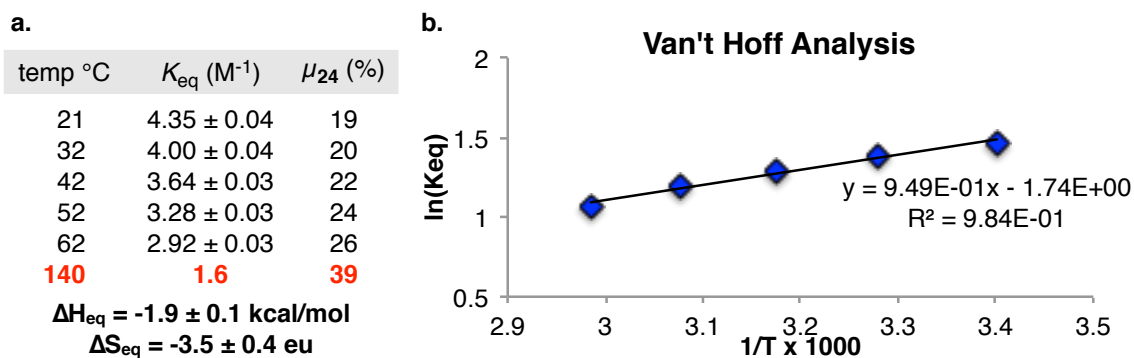
a.

temp °C	K_{eq} (M^{-1})	μ_{24} (%)
21	4.35 ± 0.04	19
32	4.00 ± 0.04	20
42	3.64 ± 0.03	22
52	3.28 ± 0.03	24
62	2.92 ± 0.03	26
140	**1.6**	**39**

ΔH_{eq} = -1.9 ± 0.1 kcal/mol
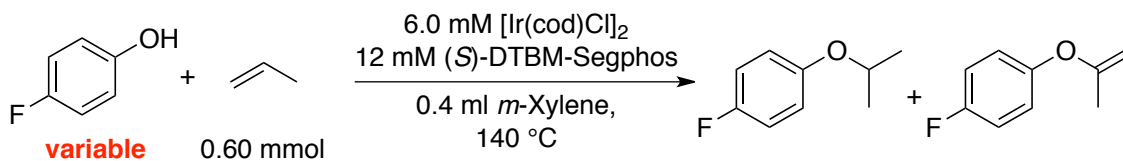ΔS_{eq} = -3.5 ± 0.4 eu

b.

Figure 3.14. a. Measured equilibrium constants at various temperatures. b. Van't Hoff analysis of the data in Figure S6a.

Kinetic studies on the addition of 4-F-phenol to propene: variable [4-F-phenol]

In a nitrogen-filled glove box, a volumetric flask (5.0 ml) was charged with [Ir(cod)Cl]$_2$ (20. mg, 0.030 mmol) and (S)-DTBM-Segphos (71 mg, 0.060 mmol). The solids were dissolved in *meta*-xylene (5.0 ml) over the course of 1 h at room temperature. The appropriate amount of 4-F-phenol was dissolved with the prepared stock solution (0.4 ml) along with a known amount of internal standard C$_6$F$_6$. The solution of aryl alcohol, ligand, metal, and standard was transferred into a 9 inch NMR tube. The NMR tube was connected to a Schlenk-line adapter, sealed, and removed from the dry-box. The sample was frozen in liquid nitrogen and degassed under vacuum. The appropriate amount of propene was charged into the NMR tube by filling a gas adapter (1.55 ml volume) with the appropriate pressure (calculated according to the ideal gas law) and condensing the propene into the NMR tube at 77 K. The NMR tube was flame-sealed under vacuum and subsequently allowed to warm to room temperature. The NMR tube was submerged in a 140 °C oil bath. Periodically, the NMR tube was removed from the oil bath and rapidly cooled in a room-temperature water bath. Reaction progress was monitored with ^{19}F NMR spectroscopy by measuring the decay of the 4-F-phenol resonance at -125.0 ppm against the internal standard of C$_6$F$_6$.
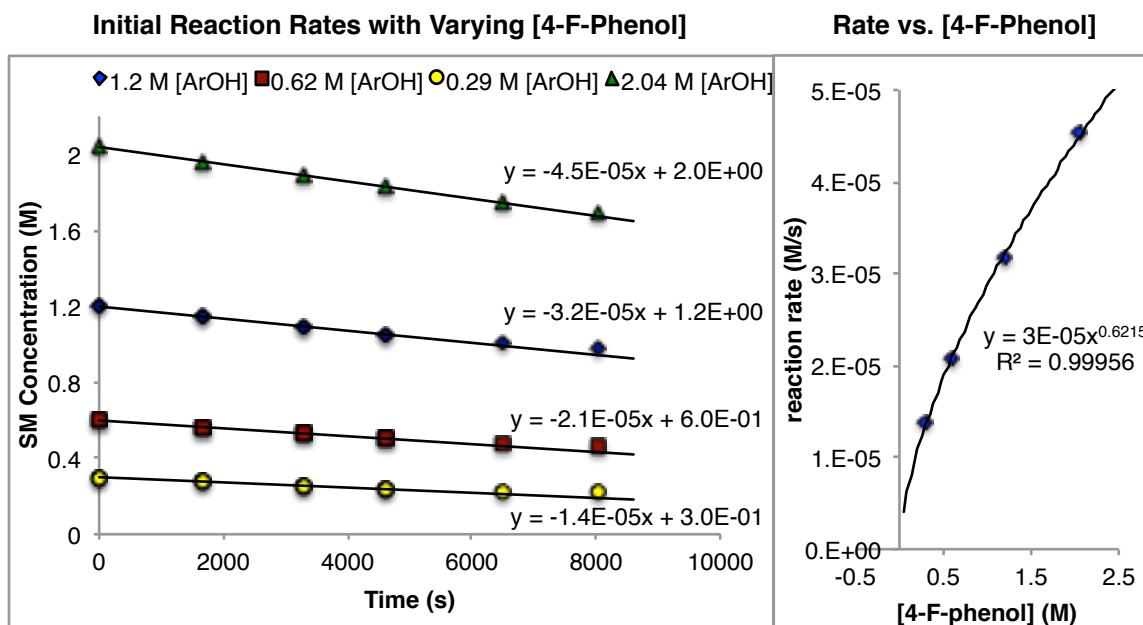

Figure 3.15. Effect of 4-F-phenol concentration on the rate of Ir-catalyzed addition of 4-F-phenol to propene.

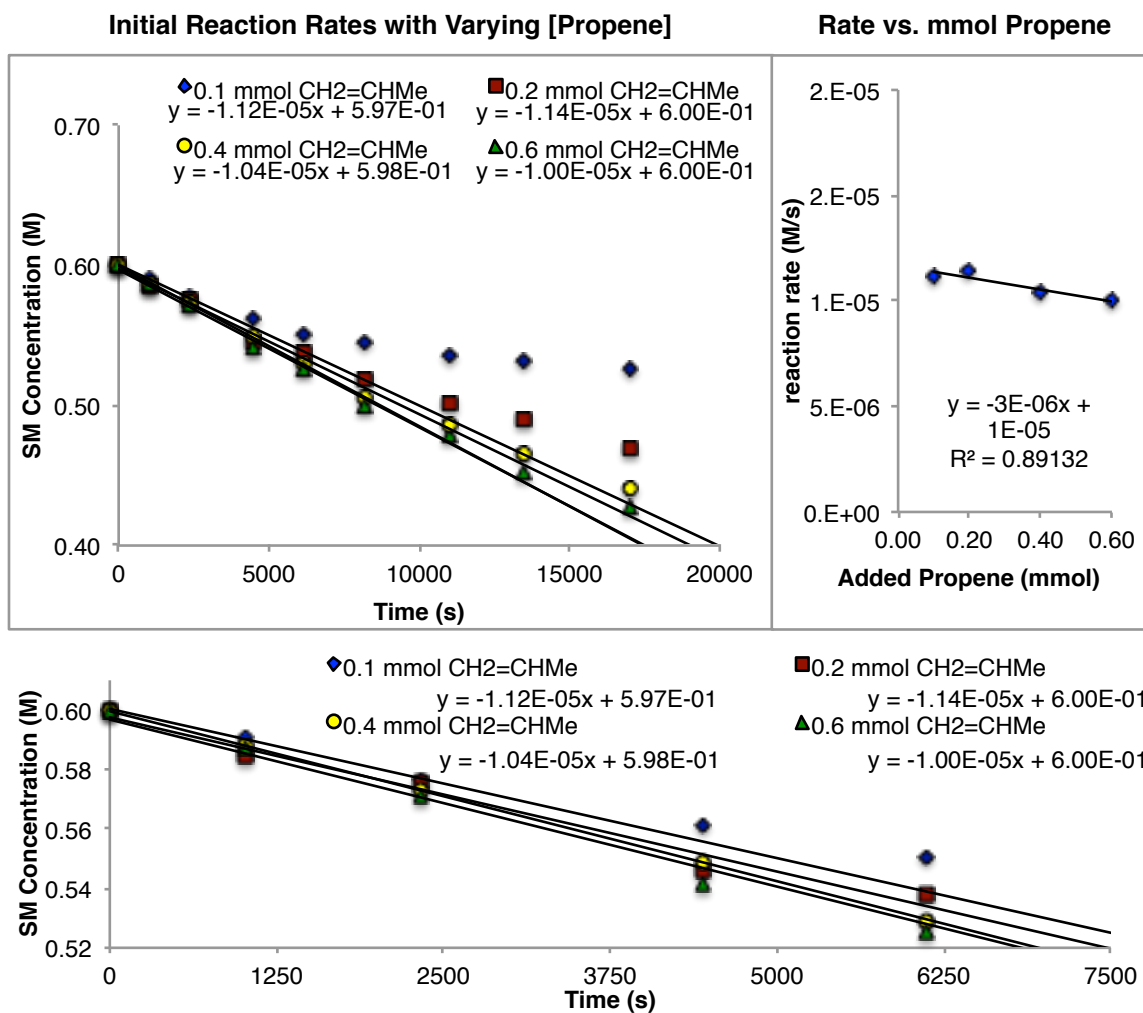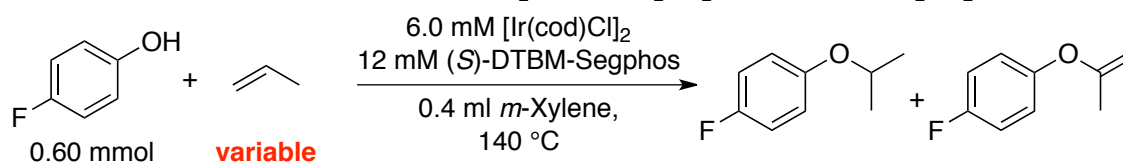## Kinetic studies on the addition of 4-F-phenol to propene: variable [propene]

Figure 3.16. Effect of added propene on the rate of Ir-catalyzed addition of 4-F-phenol to propene. Bottom: Expansion of the region between 0 and 7500 seconds.

Measurement of the Ir-catalyzed addition of 4-F-phenol-H/D to propene kinetic isotope effect

Kinetic studies on the addition of 4-F-phenol and 4-F-phenol-D to propene were conducted in separate vessels. Measurements were conducted with 0.6 mmol propene and repeated under identical conditions, but with 0.4 mmol propene. Measured rates for reactions conducted with 0.40 and 0.60 mmol propene were identical. A KIE of 1.6 ± 0.1 was calculated from the average of the two measured rates of addition of 4-F-phenol and 4-F-phenol-D.
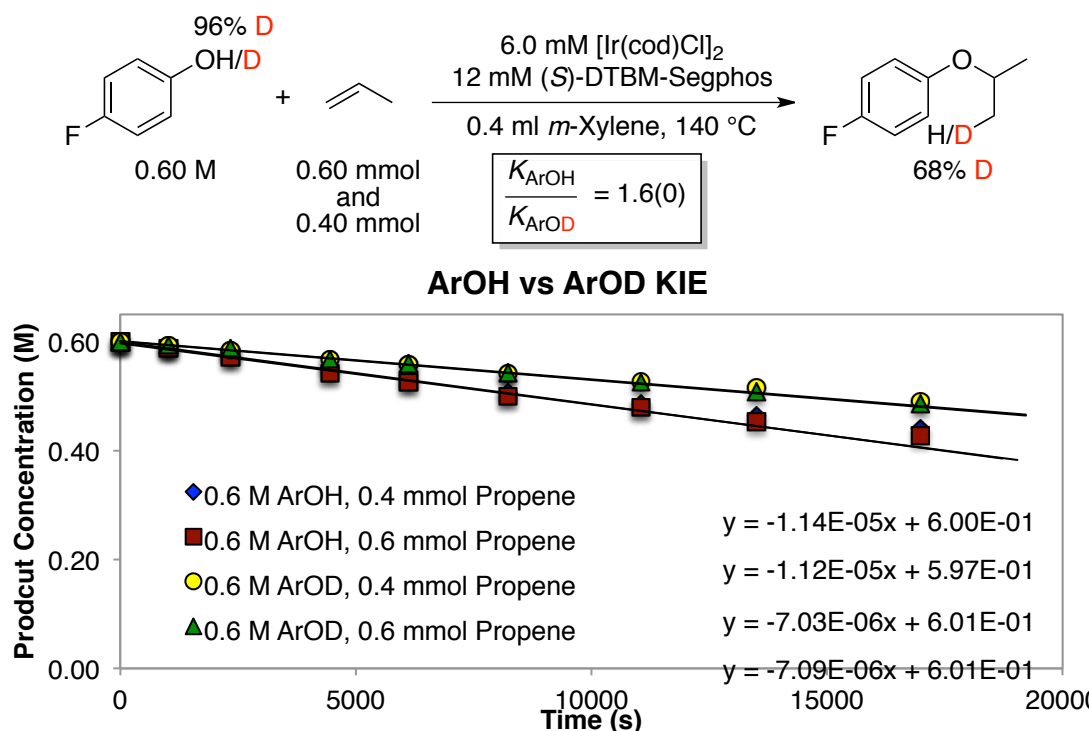

Figure 3.17. Consumption of 4-F-phenol and 4-F-phenol-D as a function of time in the Ir-catalyzed reaction with propene.

111

Kinetic studies on the addition of 4-F-phenol to propene: variable [Ir]
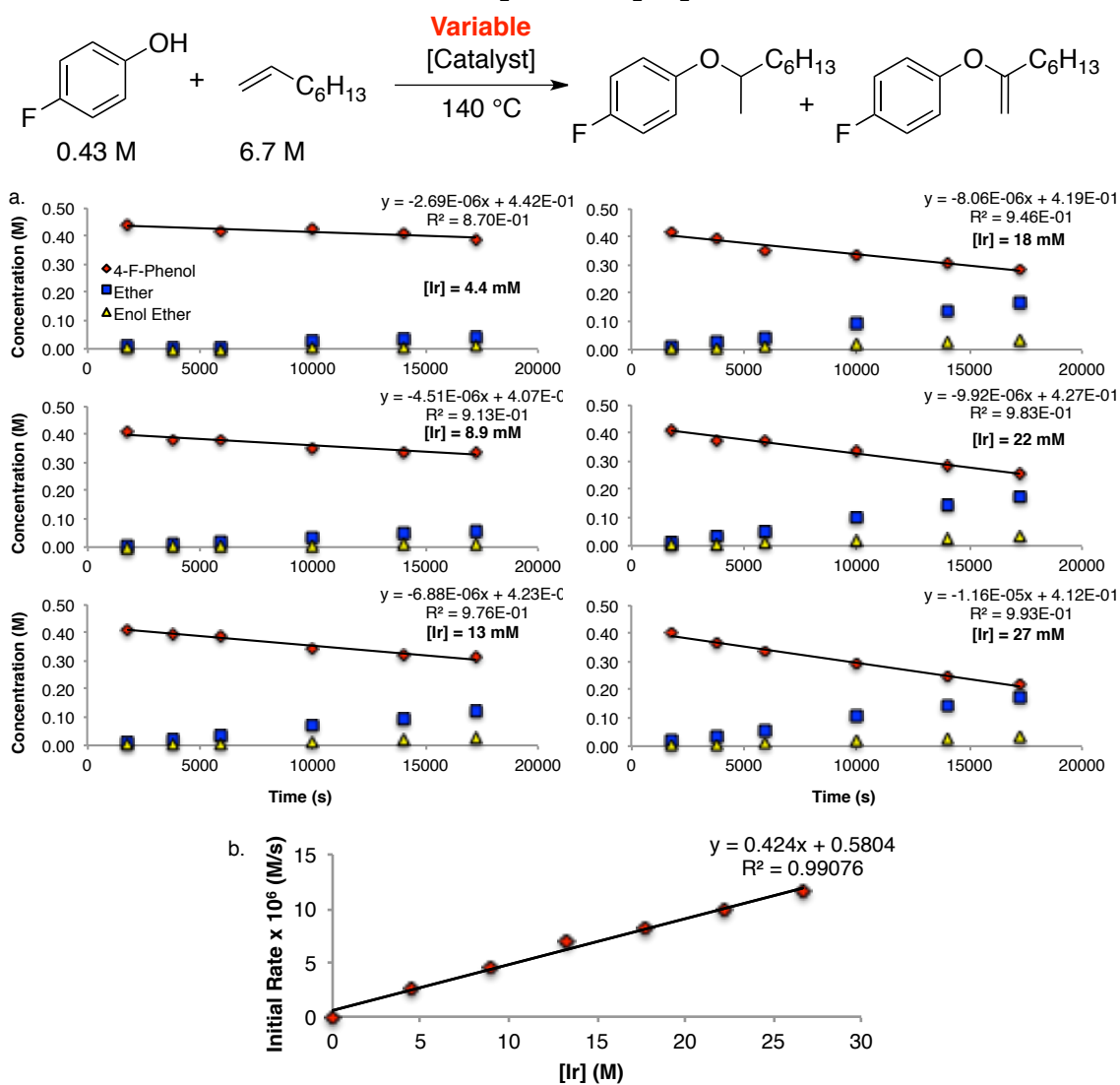

Figure 3.18. Effect of iridium concentration on the initial rate of Ir-catalyzed addition of 4-F-phenol to 1-octene.

3.5 References

(1)   Part of this chapter was reprinted with permission from Sevov, C. S.; Hartwig, J. F. *J. Am. Chem. Soc.*, **2013**, *135*, 9303. Copyright © 2013, American Chemical Society. Permission to include this co-authored material was obtained from John F. Hartwig.

(2)   Müller, T. E.; Hultzsch, K. C.; Yus, M.; Foubelo, F.; Tada, M. *Chem. Rev.*, **2008**, *108*, 3795.

(3)   Hannedouche, J.; Schulz, E. *Chem. Eur. J.*, **2013**, *19*, 4972.

(4)   Trost, B. M.; Toste, F. D. *J. Am. Chem. Soc.*, **1999**, *121*, 4545.

(5)   Muci, A. R.; Buchwald, S. L. *Cross-Coupling Reactions*, **2002**, *219*, 131.

(6)   López, F.; Ohmura, T.; Hartwig, J. F. *J. Am. Chem. Soc.*, **2003**, *125*, 3426.

(7)   Beletskaya, I. P.; Cheprakov, A. V. *Coord. Chem. Rev.*, **2004**, *248*, 2337.

(8)   Onitsuka, K.; Okuda, H.; Sasai, H. *Angew. Chem. Int. Ed.*, **2008**, *47*, 1454.

(9)   Smith, M. B.; March, J. In *March's Advanced Organic Chemistry*; 5 ed.; John Wiley and Sons: New York, NY, 2001, p 996.

(10)   Ronchin, L.; Quartarone, G.; Vavasori, A. *J. Mol. Catal. A-Chem.*, **2012**, *353*, 192.

(11)   Ronchin, L.; Vavasori, A.; Toniolo, L. *J. Mol. Catal. A-Chem.*, **2012**, *355*, 134.

(12)   Hintermann, L.; Vigalok, A., Ed.; Springer Berlin / Heidelberg: 2010; Vol. 31, p 123.

(13)   Hamilton, G. L.; Kang, E. J.; Mba, M.; Toste, F. D. *Science*, **2007**, *317*, 496.

(14)   Zhang, Z. B.; Widenhoefer, R. A. *Angew. Chem. Int. Ed.*, **2007**, *46*, 283.

(15)   Wang, Z. J.; Brown, C. J.; Bergman, R. G.; Raymond, K. N.; Toste, F. D. *J. Am. Chem. Soc.*, **2011**, *133*, 7358.

(16)   Brown, T. J.; Weber, D.; Gagné, M. R.; Widenhoefer, R. A. *J. Am. Chem. Soc.*, **2012**, *134*, 9134.

(17)   Butler, K. L.; Tragni, M.; Widenhoefer, R. A. *Angew. Chem. Int. Ed.*, **2012**, *51*, 5175.

(18)   Qian, H.; Han, X.; Widenhoefer, R. A. *J. Am. Chem. Soc.*, **2004**, *126*, 9536.

(19)   Li, X.; Chianese, A. R.; Vogel, T.; Crabtree, R. H. *Org. Lett.*, **2005**, *7*, 5437.

(20)   Patil, N. T.; Lutete, L. M.; Wu, H.; Pahadi, N. K.; Gridnev, I. D.; Yamamoto, Y. *J. Org. Chem.*, **2006**, *71*, 4270.

(21)   Messerle, B. A.; Vuong, K. Q. *Organometallics*, **2007**, *26*, 3031.

(22)   Yu, X.; Seo, S.; Marks, T. J. *J. Am. Chem. Soc.*, **2007**, *129*, 7244.

(23)   Seo, S. Y.; Yu, X. H.; Marks, T. J. *J. Am. Chem. Soc.*, **2009**, *131*, 263.

(24)   Weiss, C. J.; Marks, T. J. *Dalton Trans.*, **2010**, *39*, 6576.

(25)   Atesin, A. C.; Ray, N. A.; Stair, P. C.; Marks, T. J. *J. Am. Chem. Soc.*, **2012**, *134*, 14682.

(26)   Kim, I. S.; Krische, M. J. *Org. Lett.*, **2008**, *10*, 513.

(27)   Kawamoto, T.; Hirabayashi, S.; Guo, X.-X.; Nishimura, T.; Hayashi, T. *Chem. Commun.*, **2009**, 3528.

(28)   Koschker, P.; Lumbroso, A.; Breit, B. *J. Am. Chem. Soc.*, **2011**, *133*, 20746.

(29)   Yang, C.-G.; He, C. *J. Am. Chem. Soc.*, **2005**, *127*, 6966.

(30)   Yang, C.-G.; Reich, N. W.; Shi, Z.; He, C. *Org. Lett.*, **2005**, *7*, 4553.

(31)   Hirai, T.; Hamasaki, A.; Nakamura, A.; Tokunaga, M. *Org. Lett.*, **2009**, *11*, 5510.

(32) For a discussion of the parallels between intermolecular O–H bond additions to unactivated alkenes catalyzed by metal triflates and Brønsted acids see: (a) Li, Z.; Zhang, J.; Brouwer, C.; Yang, C.-G.; Reich, N. W.; He, C. Org. Lett. 2006, 8, 4175. (b) Rosenfeld, D. C.; Shekhar, S.; Takemiya, A.; Utsunomiya, M.; Hartwig, J. F. Org. Lett. 2006, 8, 4179.

(33) Haibach, M. C.; Guan, C.; Wang, D. Y.; Li, B.; Lease, N.; Steffens, A. M.; Krogh-Jespersen, K.; Goldman, A. S. *J. Am. Chem. Soc.*, **2013**.

(34) Sevov, C. S.; Zhou, J.; Hartwig, J. F. *J. Am. Chem. Soc.*, **2012**, *134*, 11960.

(35) Kundu, S.; Choi, J.; Wang, D. Y.; Choliy, Y.; Emge, T. J.; Krogh-Jespersen, K.; Goldman, A. S. *J. Am. Chem. Soc.*, **2013**, *135*, 5127.

(36) Ladipo, F. T.; Kooti, M.; Merola, J. S. *Inorg. Chem.*, **1993**, *32*, 1681.

(37) Blum, O.; Milstein, D. *J. Organomet. Chem.*, **2000**, *593–594*, 479.

(38) Dorta, R.; Rozenberg, H.; Shimon, L. J. W.; Milstein, D. *J. Am. Chem. Soc.*, **2001**, *124*, 188.

(39) Blum, O.; Milstein, D. *J. Am. Chem. Soc.*, **2002**, *124*, 11456.

(40) Schaub, T.; Diskin-Posner, Y.; Radius, U.; Milstein, D. *Inorg. Chem.*, **2008**, *47*, 6502.

(41) Stevens, R. C.; Bau, R.; Milstein, D.; Blum, O.; Koetzle, T. F. *J. Chem. Soc., Dalton Trans.*, **1990**, *0*, 1429.

(42) Lee, J. C.; Peris, E.; Rheingold, A. L.; Crabtree, R. H. *J. Am. Chem. Soc.*, **1994**, *116*, 11014.

(43) Siegbahn, P. E. M.; Eisenstein, O.; Rheingold, A. L.; Koetzle, T. F. *Acc. Chem. Res.*, **1996**, *29*, 348.

(44) The small negative value of ΔS_{eq} is consistent with an equilibrium between a self associated phenol and [24•HOAr], as would be expected in the nonpolar organic solvent benzene.

(45) Herde, J. L.; Lambert, J. C.; Senoff, C. V.; Cushing, M. A. In *Inorganic Syntheses*; John Wiley & Sons, Inc.: 2007, p 18.

CHAPTER 4

Iridium-Catalyzed Intermolecular Asymmetric Hydroheteroarylation
of Bicycloalkenes[1]

4.1 Introduction

Arene and heteroarene alkylation is one of the most fundamental transformations in synthetic chemistry. The Friedel-Crafts reaction is the most common method used for arene alkylation, but this reaction often generates stoichiometric quantities of waste, forms byproducts from isomerization of intermediate carbocations, and occurs without control of the stereochemistry of the product.[2-3] Metal-catalyzed additions of aromatic C–H bonds across alkenes to form alkylarenes could occur under conditions that are milder than those of classical methods,[4-19] could occur with site-selectivity that complements that of acid-catalyzed reactions, and could occur enantioselectively.[20-32] Thus, many groups have sought catalysts for regioselective and enantioselective alkylations of arenes.

Scheme 4.1. Regioselectivity of indole CH bond additions to alkenes.

Friedel-Crafts-type selectivity: many examples
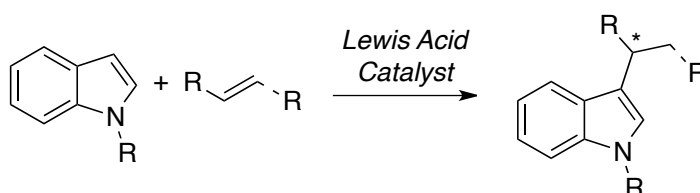
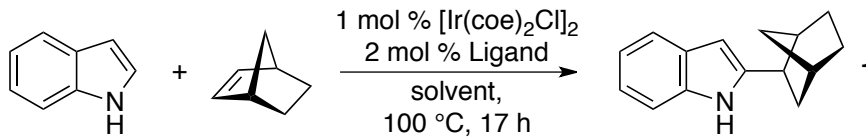**Undirected C2 alkylation:** *this work*
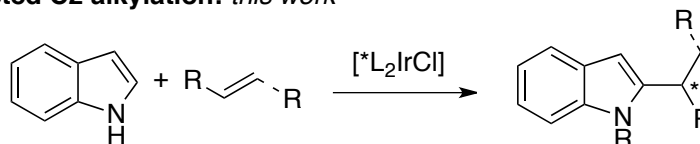
Additions of heteroaryl C-H bonds are particularly valuable because of the importance of heteroarenes in biologically active structures[33-35] and materials applications.[36-38] Recently, the Shibata group reported the hydroarylation of *N*-acyl indoles, which is one of the few cases of intermolecular alkene hydroheteroarylation with selectivity that is complementary to that of Friedel-Crafts alkylation.[39] However, the reactions reported by Shibata required a directing group on the nitrogen of the indole and occurred with low enantioselectivities. No systems have been reported for asymmetric intermolecular hydroheteroarylation of unconjugated alkenes with high enantioselectivity (Scheme 4.1).[40-44]

Here, we report enantioselective, iridium-catalyzed additions of the C-H bonds of indoles, thiophenes, pyrroles and furans across bicycloalkenes. These reactions form a single constitutional isomer in both high yield and high enantioselectivity. Mechanistic studies show that the addition of the heteroaryl C-H bond to iridium is rapid and is followed by a turnover-limiting insertion of the alkene.

4.2 Results and Discussions

Our observation of asymmetric hydroheteroarylation of bicycloalkenes stemmed from our recent work on iridium catalyzed additions of N-H bonds of amides and sulfonamides to alkenes.[45] While investigating potential hydroaminations involving alkenes and heteroaryl N-H bonds, we observed the additions of heteroaryl C-H bonds across alkenes. We then evaluated a range of iridium catalysts for potential asymmetric hydroheteroarylations.

Table 4.1. Reaction development for the Ir-catalyzed enantioselective addition of indole to norbornene[a]

entry	ligand	[indole] (M), solvent	equiv NBE	% conv[b]	% yield[b]	% ee[b]
1	(R)-Binap	0.75, PhMe	1.2	23	22	43
2	(R)-MeOBiphep	0.75, PhMe	1.2	33	30	56
3	(S)-Segphos	0.75, PhMe	1.2	53	48	60
4	(S)-DTBM-MeOBiphep	0.75, PhMe	1.2	65	63	90
5	(S)-DTBM-Segphos[c]	0.75, PhMe	1.2	80	70	96
6	dcpm[d]	0.75, PhMe	1.2	64	60	--
7	(S)-DTBM-Segphos	0.75, Heptane	1.2	100	85	97
8	(S)-DTBM-Segphos	0.75, MTBE	1.2	100	87	96
9	(S)-DTBM-Segphos	0.75, THF	1.2	100	94	96
10	(S)-DTBM-Segphos	0.75, m-Xylene	1.2	87	79	96
11	(S)-DTBM-Segphos	1.50, THF	1.2	62	44	93
12	(S)-DTBM-Segphos	0.50, THF	1.2	100	97	96
13	(S)-DTBM-Segphos	0.75, THF	2.2	61	58	94
14	(S)-DTBM-Segphos	0.75, THF	4	38	33	90

[a]Reactions were performed with 0.2 mmol indole. [b]Determined by GC analysis. [c]DTBM = 3,5-di-tert-butyl-4-methoxyphenyl. [d]dcpm = bisdicyclohexylphosphino methane. [e]Determined by HPLC analysis equipped with a chiral stationary phase.

The results of the reactions of indole with norbornene (nbe) catalyzed by the combination of [Ir(coe)₂Cl]₂ and a series of bisphosphine ligands under a range of conditions are summarized in Table 4.1. Iridium complexes of Segphos were more reactive than complexes of MeOBiphep and Binap (entries 1-3), suggesting that a small dihedral angle in the ligand was important for generating a more active and selective catalyst. In a similar vein, substantial yields were obtained from reactions catalyzed by iridium complexes of a one-carbon methylene-bridged bisphosphines (entry 6), whereas no addition product was observed from reactions catalyzed by complexes containing analogous two-carbon or three-carbon bridged phosphines. An increase in the steric bulk from the parent Segphos ligand to the DTBM-Segphos (DTBM=3,5-di-*tert*-butyl-4-methoxy) derivative led to an increase in yield and ee of **1** (entry 5). These reactions constitute the first enantioselective intermolecular additions of indoles across alkenes at the non-nucleophilic C2 position in high ee.

The solvent had a pronounced effect on the yields of the reaction of indole with norbornene catalyzed by [Ir(coe)₂Cl]₂ and (S)-DTBM-Segphos The reactions conducted in relatively non-polar, aliphatic solvents proceeded with complete consumption of the starting material (entries 7-8). However, the reaction yields were lower than the conver-

sions by 10-15% in these solvents, due to the formation of a side product from oxidative dimerization of the heteroarene starting material.[46] The reactions conducted in coordinating solvents, such as acetonitrile, DMF, and DMSO, did not occur, presumably because of competitive binding of these solvents to the iridium catalyst. However, the reaction did occur to full conversion with high product yields when conducted in the moderately polar THF (entry 12).

The amount of nbe and indole affected the rate and enantioselectivity of the reaction. Reactions conducted with an excess amount of nbe were significantly slower than those conducted with 1.2 equivalents of nbe (entries 14 vs. 12), and the ee of the product of the reaction with 4 equiv of nbe was lower (90% ee) than that of the reaction conducted with 1.2 equiv of nbe. Reactions with a lower 0.6 M concentration of indole formed the hydroarylation product **1** in 97% yield with no detectable amount of product from indole homocoupling (entry 12).

Chart 4.1. Ir-catalyzed enantioselective addition of indoles to norbornene[a]
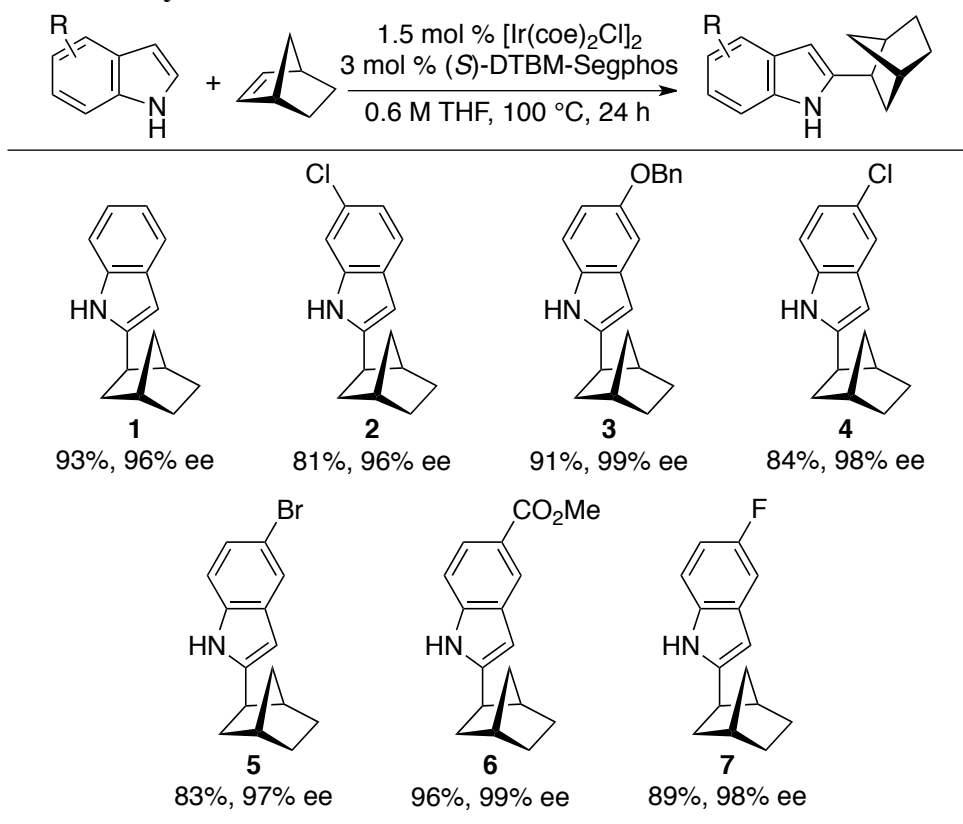
[a]Reactions were performed with 0.5 mmol indole and 1.2 equivalents of nbe. Reported yields are isolated yields. ee was determined by HPLC analysis equipped with a chiral stationary phase.

The scope of the Ir-catalyzed addition of indoles to nbe by this procedure is summarized in Chart 4.1. High yields and ee's were obtained from reactions of the indoles possessing electron-donating or electron-withdrawing substituents. Halides, protected alcohols, and esters were tolerated by the reaction conditions. The 2-substituted indole located in the *exo* position of the bicycloalkane was the exclusive isomer formed. Indoles bearing chloride and bromide substituents underwent oxidative homocoupling to a greater extent than did the other indoles studied, but the yields of the addition products remained high.
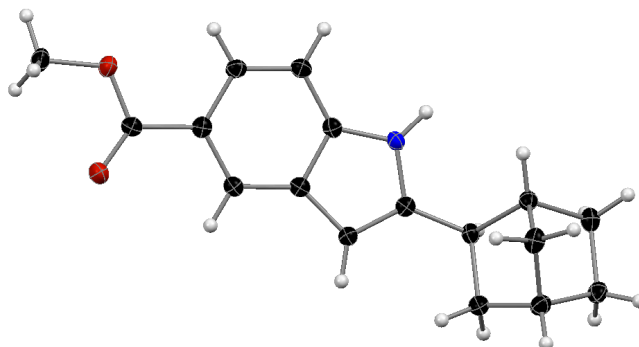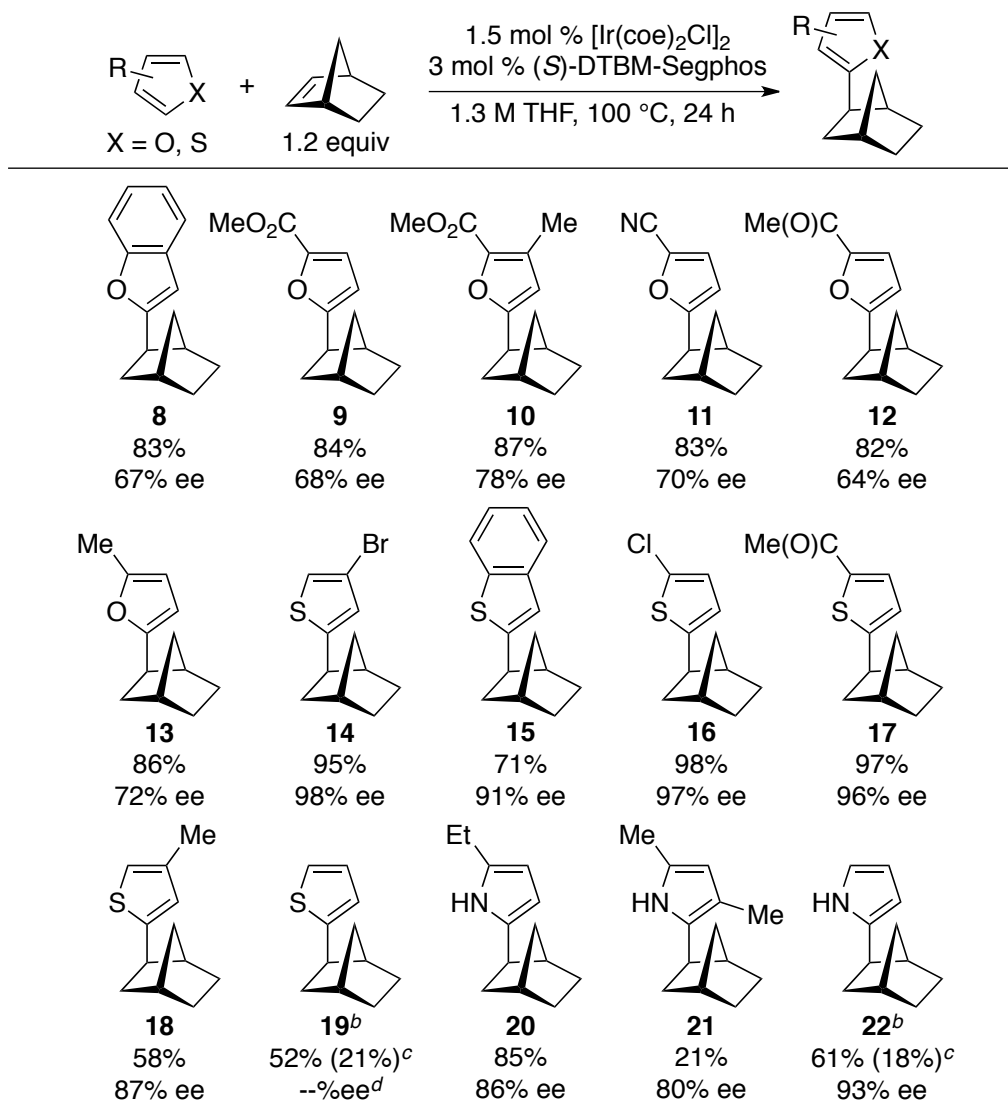

Figure 4.1. ORTEP representation of **6** with unambiguous determination of the stereochemistry at C2 to be (*R*). Thermal ellipsoids are drawn at the 50% probability level.

The absolute stereochemistry of ester-substituted **6** was determined by single crystal x-ray analysis with a copper radiation source to be 2*R* (Figure 4.1). The solid-state analysis also confirmed that the indole is connected at the C2 carbon. Thus, these reactions occur at the C2 position of the indole without a protecting or directing group on nitrogen.

The scope of the hydroheteroarylation process extends to furans, thiophenes and pyrroles, as summarized in Chart 4.2. These heteroarenes did not undergo oxidative homocoupling reactions under the catalytic conditions. Therefore, the rates could be increased without a reduction in yield by running the reactions at concentrations higher than those of the reactions of indoles (see experimental for reaction development).

119

Chart 4.2. Ir-catalyzed enantioselective addition of furans, thiophenes and pyrroles to norbornene[a]

8
83%
67% ee

9
84%
68% ee

10
87%
78% ee

11
83%
70% ee

12
82%
64% ee

13
86%
72% ee

14
95%
98% ee

15
71%
91% ee

16
98%
97% ee

17
97%
96% ee

18
58%
87% ee

19[b]
52% (21%)[c]
--%ee[d]

20
85%
86% ee

21
21%
80% ee

22[b]
61% (18%)[c]
93% ee

[a]Reactions were performed with 0.4 mmol heteroarene and 1.2 equiv of nbe. Reported yields are isolated yields. ee was determined by HPLC analysis equipped with a chiral stationary phase. [b]Reactions were performed with 0.9 equiv of nbe to heteroarene. [c]yield of 2,5-dialkylated product. [d]ee could not be determined because the mono and dialkylated product signals overlapped.

Reactions of substituted thiophenes and pyrroles formed products from alkylation at the 2-position in high yield and excellent ee. Thiophenes substituted at the 2- or 3-position with alkyl groups or ketone and halogen functionality occurred in high yield and ee. Reactions of pyrrole and a 2-alkyl pyrrole occurred in high yield and enantioselectivity. However, the reactions of 2-acetylpyrrole or methyl-2-pyrrole carboxylate did not form detectable amounts of product, most likely because the substrate or product chelates to the Ir center through the nitrogen and oxygen atoms. The reactions of N-methyl and N-phenyl pyrrole also formed the product in only trace amounts, in this case because the

substituent leads to steric hindrance at the 2-position. This steric influence also leads to a lower yield for the reaction of 2,4-dimethyl pyrrole (**21**) than for 2-ethyl pyrrole.
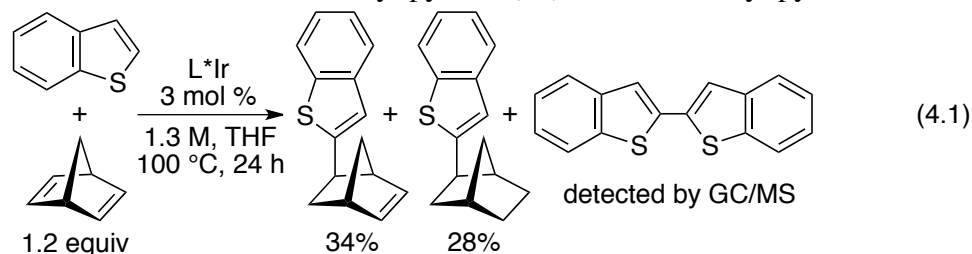
Reactions of furans also formed products in good yield. Although the enantiose-lectivity was lower than it was for the reactions of thiophenes and pyrroles, a broad range of functional groups that can undergo further transformations, such as esters, ketones, and nitriles, were tolerated by the hydroheteroarylation reaction.[47-50,39]
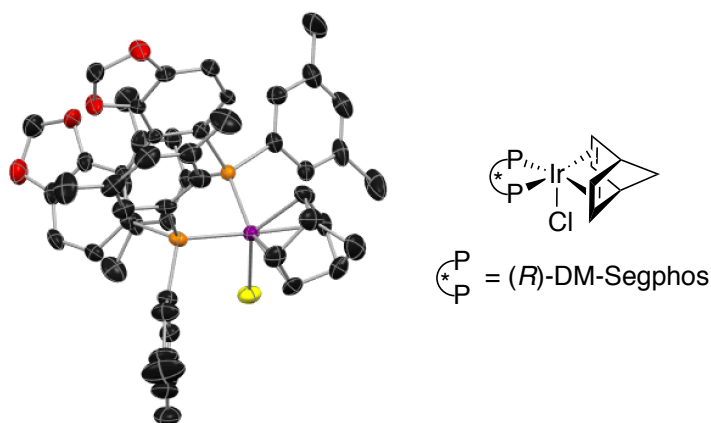

Figure 4.2. Solid-state structure of resting state complex for reactions of nbe.

The scope of the hydroheteroarylation also encompasses the addition of the C-H bonds of heteroarenes to norbornadiene (nbd). However, some modification of the reaction conditions was needed to obtain good yields of the product from addition to the diene. The reactions of nbd conducted under the same conditions as the reactions of nbe with thiophenes and furans gave a significant amount of product from heteroarene oxidative homocoupling. Moreover, the equivalent of hydrogen formed by oxidative coupling led to the formation of substituted norbornanes from reduction of the substituted norbornenes and the two classes of products could not be separated (eq 4.1). In addition, rates of reaction with nbd were slower than those of reactions with nbe. Analysis of the catalyst resting state revealed an off-cycle intermediate as the major species, illustrated in Figure 4.2. This compound that results from nbd chelation to Ir(I) is inconsistent with the observed resting state for reactions of nbe (*vide infra*).

Chart 4.3. Ir-catalyzed enantioselective addition of heteroarenes to norbornadiene[a]

23
77%
38% ee

24
62%
85% ee

25
90%
96% ee
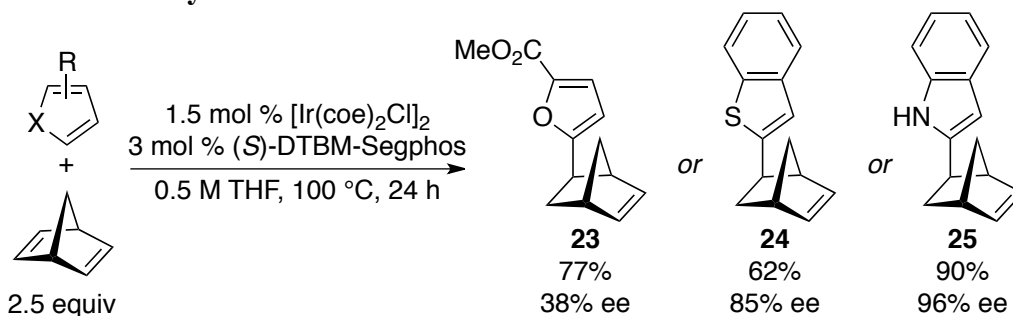
[a]Reactions were performed with 1.0 mmol heteroarene and 2.5 equivalents of norbornadiene. Reported yields are isolated yields. ee was determined by HPLC analysis equipped with a chiral stationary phase.

Thus, the reaction conditions were modified to reduce the amount of product formed by homocoupling of the heteroarene. The reactions were conducted at 0.5 M instead of 1.3 M concentrations of the heteroarene and 2.5 equiv instead of 1.2 equiv of the alkene (Chart 4.3). Under these modified conditions, the products of the addition of indoles and thiophenes to nbd occurred in high yield and with excellent ee. Like the reactions of furans with nbe, the reaction of 2-methylfuroate with nbd occurred in high yield but in low ee. The origin of the low enantioselectivity of the reactions of furans is unknown at this time. No products from additions of the heteroarenes to alpha-olefins such as 1-octene or styrene were obtained under the conditions for the additions to nbe and nbd.

26
94%, 96% ee

(4.2)

27
82%, 68% ee

(4.3)
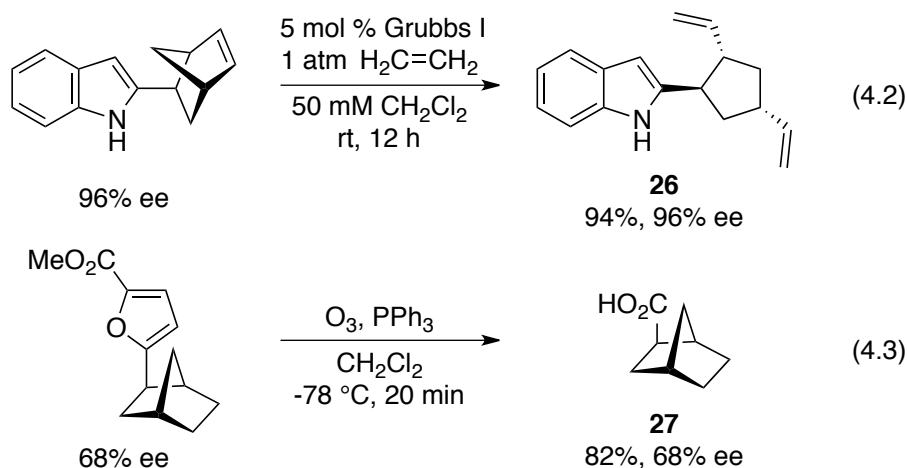
The products of the asymmetric hydroheteroarylation of bicycloalkenes can be elaborated to chiral, enantioenriched building blocks. Ring opening metathesis of **26** with ethylene formed the highly functionalized cyclopentane **27** as a single diastereomer with no erosion of ee (eq 4.2). Oxidation of the furan led to the alkyl carboxylic acid, also with no erosion of ee (eq 4.3). Finally, the compatibility of the catalyst with a broad range of halides, ketones, esters, and nitriles allows further transformations to be conducted on the addition products.
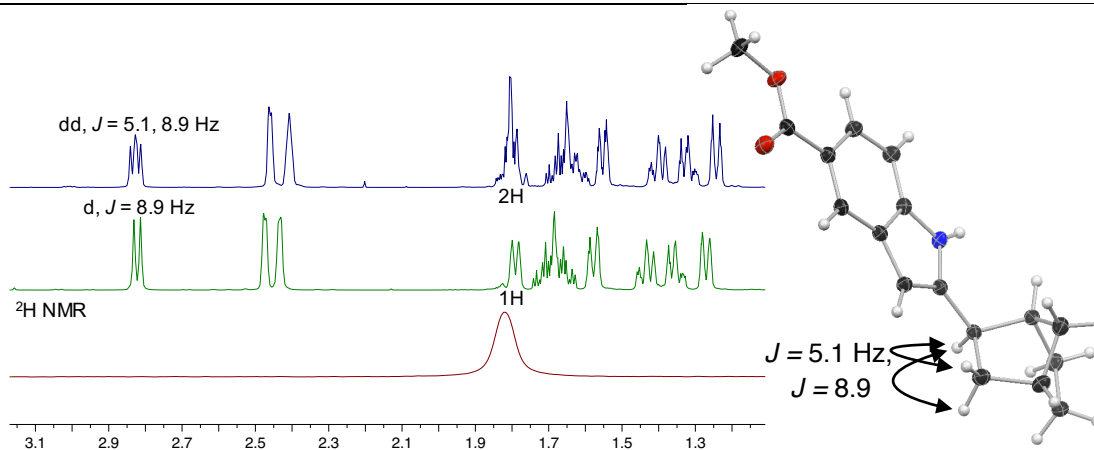

(4.4)

KIE = 1.4 ± 0.1

85%, >95% D
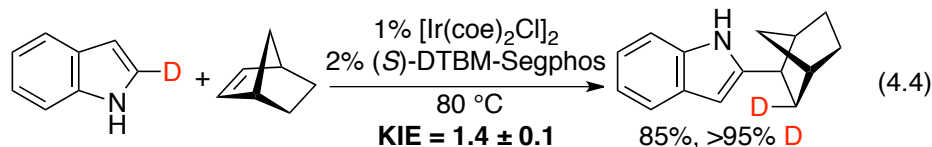
Figure 4.3. Determination of the geometry of C–D bond addition to nbe by analysis of coupling constants.

Initial mechanistic studies on addition reactions of heteroarenes across bicycloalkenes were conducted by deuterium labeling and by studying the individual steps of the process. The reaction of nbe with 2-D-indole formed the *syn*-deutero(indolyl)norbornane in eq 4.4 as determined by analysis of the coupling constants of the protons alpha- and beta- to the heteroarene (Figure 4.3). This relative stereochemistry implies that the hydroheteroarylation occurs by a mechanism involving olefin insertion into an Ir-C or Ir-H bond. A comparison of the initial rates for the addition of 2-H-indole and 2-D-indole to nbe in separate vessels revealed a kinetic isotope effect (KIE) of 1.4. This small, but greater than unity, KIE could result from reversible addition of the indole C-H bond to the iridium center prior to the turnover-limiting step.
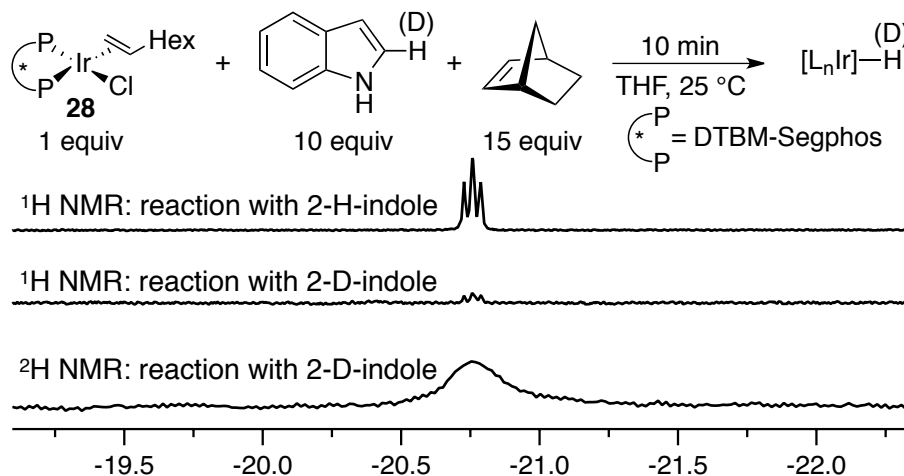
Figure 4.4. Comparison of the hydride region of the ^{1}H and ^{2}H NMR spectra of the resting state iridium complex under catalytic conditions with 2-H-indole and 2-D-indole.

To probe whether cleavage of the 2-C-H bond occurs prior to the turnover-limiting step, reactions of 2-H- and 2-D-indole with nbe under catalytic conditions were followed by ^{1}H and ^{2}H NMR spectroscopy. Illustrative spectra are shown in Figure 4.4. The combination of indole, nbe and the iridium bisphosphine complex **28**, which was formed from 1-octene, DTBM-Segphos, and [Ir(coe)$_2$Cl]$_2$, formed a light yellow solution (from the initial red solution) within 10 min at room temperature. A doublet of doublets

123

hydride resonance at -20.8 ppm was observed by ^{1}H NMR spectroscopy. A similar experiment with 2-D-indole gave rise to an Ir-deuteride resonance at -20.8 ppm in the ^{2}H NMR spectrum and a much smaller hydride resonance in the ^{1}H NMR spectrum. No hydroheteroarylation products were detected after 24 h at room temperature. These data indicate that C-H activation occurs at the 2-position of indole at temperatures below those required for catalytic turnover.

Scheme 4.2. Proposed Catalytic Cycle for the Ir-Catalyzed Hydroheteroarylation of Norbornene
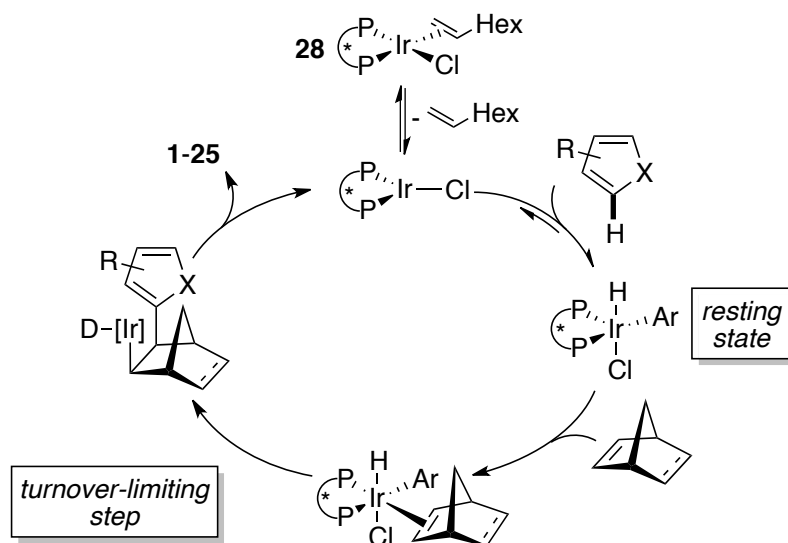
Because oxidative addition at the C2 position of indole occurs much faster than the overall catalytic cycle, the turnover-limiting step likely follows the C-H cleavage process. Because reductive eliminations to form carbon-carbon bonds from an iridium center are rare or unknown, we propose that the C-H bond addition reaction is followed by insertion of the alkene into the Ir-C bond and C-H bond-forming reductive elimination, as illustrated in Scheme 4.2. Product formation by insertion of the alkene into the Ir-H bond requires C-C bond-forming reductive elimination from an alkyl-aryl intermediate.

4.3 Conclusions and Future Directions

In summary, we report examples of intermolecular asymmetric additions of the 2-C-H bonds of indoles, thiophenes, pyrroles and furans to bicycloalkenes. The additions of indoles, thiophenes and pyrroles to bicycloalkenes occurred in high yields with high ee's. Alkylation of the heteroarene occurs at the C-H bond adjacent to the heteroatom by the transition-metal catalyst, even for indoles, which typically undergo alkylation at the C3 position. The neutral catalyst that we have developed for this reaction tolerates a broad range of functional groups, which can be elaborated to form additional enantioenriched products. Initial mechanistic studies on the identity of the catalyst resting state and the measured KIE demonstrated that heteroarene C-H bond oxidative addition to an Ir^I species occurs prior to the turnover-limiting step. Efforts to extend the scope of enantioselective reactions to encompass unstrained alkenes are in progress.

124

4.4 Experimental

General Remarks

Unless noted otherwise, all manipulations were performed in a nitrogen-filled glove-box. Glassware was dried at 130 °C for at least 4 hours before use. Pentane, Et_2O, THF, benzene and toluene were collected from a solvent purification system containing a 0.33 m column of activated alumina under nitrogen. Benzene-d_6 was degassed and subjected to 4 Å molecular sieves for at least 4 hours prior to use. All reagents were purchased from commercial suppliers, stored in the glove box and used as received. $[Ir(coe)_2Cl]_2$[51] and 2-D-indole[52] were prepared following published procedures. Bisphosphine ligands were purchased from Strem Chemical Co. and used as received.

^1H NMR spectra were obtained at 500 MHz or 600 MHz, and chemical shifts were recorded relative to protiated solvents ($CHCl_3$ in $CDCl_3$: $\delta 7.27$ ppm; $C_6H_nD_{6-n}$ in C_6D_6: $\delta 7.15$ ppm) with a 45° pulse and a 10 s delay time.^{13}C NMR spectra were obtained at 126 MHz or 151 MHz on a 500 MHz or 600 MHz instrument, respectively. ^{31}P NMR spectra were obtained at 202.2 MHz on a 500 MHz instrument and chemical shifts were reported in parts per million downfield of 85% H_3PO_4. ^{19}F NMR spectra were referenced to an external standard of $CFCl_3$. Probe temperatures for variable temperature NMR experiments were measured by ^1H shifts of neat ethylene glycol. Proof of purity is demonstrated by elemental analysis and by copies of NMR spectra. Racemic product mixtures were obtained following the general procedures described herein with the application of bis(dicyclohexylphosphino)methane as a ligand. Chiral HPLC analysis was conducted on a Waters chromatography system with a dual wavelength detector at 210 and 254 nm.
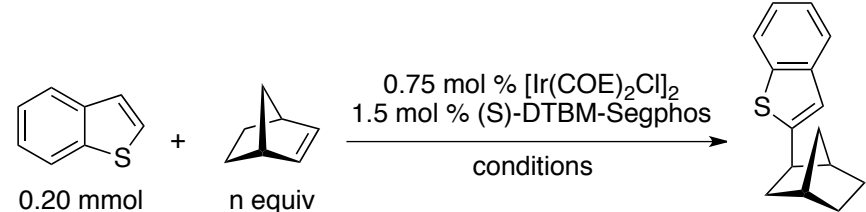
GC analysis was performed on an Agilent 7890 GC equipped with an HP-5 column (25 m x 0.20 mm x 0.33 μm film) and an FID detector. Quantitative GC analysis was performed by adding dodecane as an internal standard to the reaction mixture upon completion of the reaction. Response factors for the products relative to the internal standard were measured for kinetic studies and reaction development studies. GC-MS data were obtained on an Agilent 6890-N GC system containing an Alltech EC-1 capillary column and an Agilent 5973 mass selective detector.

Table 4.2. Development of Conditions for the Ir-Catalyzed Addition of 3-Br-Thiophene to Norbornene

entry	[HetAr] (M)	solvent	temp (°C)	equiv NBE	time (h)	% yield[a]	%ee[b]
1	0.75	PhMe	100	1.25	5	11	
					42	62	98
2	1.25	PhMe	100	1.25	5	14	
					42	82	96
3	0.75	PhMe	80	1.25	5	2	
					42	13	--
4	0.75	PhMe	100	2.25	5	8	
					42	45	--
5	0.75	PhMe	100	4.00	5	3	
					42	9	--
6	0.75	Heptane	100	1.25	5	12	
					42	94	98
7	0.75	MTBE	100	1.25	5	12	
					42	69	80
8	0.75	THF	100	1.25	5	14	
					42	80	96
9	0.75	m-Xyl	100	1.25	5	16	
					42	84	88

[a]Yields were determined by GC analysis with dodecane as an internal standard. [b]ee's were determined by chiral HPLC analysis.

Table 4.3. Development of Conditions for the Ir-Catalyzed Addition of Benzothiophene to Norbornene

| entry	[HetAr] (M)	solvent	temp (°C)	equiv NBE	time (h)	% yield	%ee
1	0.75	PhMe	100	1.25	5	4	
					42	26	96
2	1.25	PhMe	100	1.25	5	7	
					42	48	91
3	0.75	PhMe	80	1.25	5	1	
					42	5	--
4	0.75	PhMe	100	2.25	5	3	
					42	21	--
5	0.75	PhMe	100	4	5	1	
					42	4	--
6	0.75	Heptane	100	1.25	5	5	
					42	46	91
7	0.75	MTBE	100	1.25	5	5	
					42	40	94
8	0.75	THF	100	1.25	5	7	
					42	46	93
9	0.75	m-Xyl	100	1.25	5	6	
					42	43	90

[a]Yields were determined by GC analysis with dodecane as an internal standard. [b]ee's were determined by chiral HPLC analysis.

General Procedure A: Ir-catalyzed hydroheteroarylation of norbornene with indoles and thiophenes.

In a nitrogen-filled dry-box, an oven-dried 4 ml screw-capped vial was charged with [Ir(coe)$_2$Cl]$_2$ (6.7 mg, 0.0075 mmol), (S)-DTBM-SEGPHOS (17.7 mg, 0.0150 mmol), the corresponding indole (0.50 mmol), and a magnetic stirbar. THF (0.40 ml) was added to these solids, and the mixture was stirred vigorously until an orange homogeneous solution was obtained (5 min). A 1.5 M solution of norbornene in THF (0.40 ml, 0.60 mmol) was added to the reaction mixture. The vial was sealed tightly with a Teflon cap and removed from the dry-box. The reaction mixture was stirred in an aluminum heating block at 100 °C for 24 h and then cooled to room temperature. The solvent was removed by rotary evaporation. The product was purified by flash chromatography on a column (height

= 20. cm, diameter = 3.0 cm) of Silacycle Silia-P60 silica gel (55 g). The conditions for chromatography and other data that are specific to each compound are given below. All products were found to be prone to oxidation over a period of hours and stored under nitrogen.

2-((1*R*,2*R*,4*S*)-bicyclo[2.2.1]heptan-2-yl)-1*H*-indole
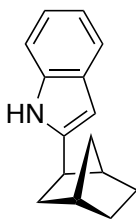
Following the general procedure **A** described above, indole (59 mg, 0.50 mmol) was allowed to react with norbornene (56 mg, 0.60 mmol) in THF (0.60 ml). The crude material was purified by chromatography with 5% EtOAc in hexanes. The collected fractions were concentrated by rotary evaporation, and the resulting solution was sparged with nitrogen gas. The solvent was removed under vacuum in a nitrogen-filled dry-box to yield the title compound as an air sensitive white solid (97 mg, 93% yield).

¹H NMR (500 MHz, CDCl₃): δ 7.83 (br s, 1H), 7.59 (d, *J* = 7.7 Hz, 1H), 7.32 (dd, *J* = 7.9, 0.8 Hz, 1H), 7.19-7.14 (m, 1H), 7.12 (ddd, *J* = 7.5, 7.5, 1.1 Hz, 1H), 6.31-6.21 (m, 1H), 2.90-2.80 (m, 1H), 2.48 (d, *J* = 3.5 Hz, 1H), 2.43 (s, 1H), 1.87-1.79 (m, 2H), 1.74-1.61 (m, 2H), 1.60-1.55 (m, 1H), 1.47-1.39 (m, 1H), 1.37-1.31 (m, 1H), 1.29-1.24 (m, 1H).

¹³C NMR (126 MHz, CDCl₃): δ 145.2, 136.1, 128.8, 121.2, 120.1, 119.8, 110.5, 98.3, 42.9, 41.6, 37.6, 36.6, 36.5, 30.0, 29.2.

HPLC analysis: 96% ee, Chiralcel AD-H column, 1.5% isopropanol in hexane, 1.0 mL/min flow rate, 254 nm UV lamp, t$_{[major]}$ = 18.6 min, t$_{[minor]}$ = 19.9 min.

Anal. Calcd for C₁₅H₁₇N: C 85.26%, H 8.11%, N 6.63%; Found: C 84.98%, H 8.20 %, N 6.30%.

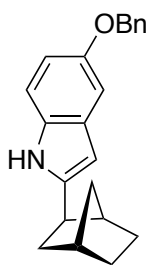### 2-((1*R*,2*R*,4*S*)-bicyclo[2.2.1]heptan-2-yl)-6-chloro-1*H*-indole
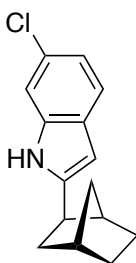
Following the general procedure **A** described above, 6-chloroindole (78 mg, 0.50 mmol) was allowed to react with norbornene (56 mg, 0.60 mmol) in THF (0.60 ml). The crude material was purified by chromatography with 6% EtOAc in hexanes. The collected fractions were concentrated by rotary evaporation, and the resulting solution was sparged with nitrogen gas. The solvent was removed under vacuum in a nitrogen-filled dry-box to yield the title compound as an air sensitive white solid (99 mg, 81% yield).

¹H NMR (600 MHz, C₆D₆): δ 7.27 (d, *J* = 8.3 Hz, 1H), 7.14 (d, *J* = 8.6 Hz, 1H), 7.07 (s, 1H), 6.47 (br s, 1H), 5.94 (s, 1H), 2.25 (dd, *J* = 8.3, 5.4 Hz, 1H), 2.13 (s, 1H), 2.02 (s, 1H), 1.53-1.46 (m, 1H), 1.42 (t, *J* = 10.2 Hz, 3H), 1.31 (d, *J* = 9.8 Hz, 1H), 1.16-1.05 (m, 2H), 0.96 (d, *J* = 9.8 Hz, 1H).

¹³C NMR (151 MHz, C₆D₆): δ 145.1, 136.4, 127.4, 126.6, 120.7, 120.1, 110.3, 98.1, 42.5, 40.9, 36.8, 36.2, 35.8, 29.5, 28.8.

HPLC analysis: 96% ee, Chiralcel AD-H column, 5% isopropanol in hexane, 0.7 mL/min flow rate, 254 nm UV lamp, t$_{[major]}$ = 16.2 min, t$_{[minor]}$ = 17.9 min.

Anal. Calcd for C₁₅H₁₆ClN: C 73.31%, H 6.56%, N 5.70%; Found: C 73.24%, H 6.72%, N 5.46%.

## 5-(benzyloxy)-2-((1*R*,2*R*,4*S*)-bicyclo[2.2.1]heptan-2-yl)-1*H*-indole

Following the general procedure **A** described above, 5-benzyloxyindole (114 mg, 0.50 mmol) was allowed to react with norbornene (56 mg, 0.60 mmol) in THF (0.60 ml). The crude material was purified by chromatography with 5% EtOAc in hexanes. The collected fractions were concentrated by rotary evaporation, and the resulting solution was sparged with nitrogen gas. The solvent was removed under vacuum in a nitrogen-filled drybox to yield the title compound as an air sensitive white solid (144 mg, 91% yield).

¹H NMR (600 MHz, C_6D_6): δ 7.35 (d, *J* = 7.6 Hz, 2H), 7.18 (s, 1H), 7.13 (d, *J* = 6.9 Hz, 2H), 7.11-7.04 (m, 2H), 6.95 (d, *J* = 8.6 Hz, 1H), 6.68 (br s, 1H), 6.07 (s, 1H), 4.91 (s, 2H), 2.35 (dd, *J* = 8.4, 5.3 Hz, 1H), 2.15 (s, 1H), 2.11 (s, 1H), 1.65-1.55 (m, 1H), 1.50-1.38 (m, 4H), 1.17-1.07 (m, 2H), 0.99 (d, *J* = 9.7 Hz, 1H).

¹³C NMR (151 MHz, C_6D_6): δ 153.6, 145.0, 138.2, 131.5, 129.4, 128.2, 127.4, 127.4, 111.6, 110.9, 103.9, 98.2, 70.6, 42.7, 41.2, 36.9, 36.2, 36.0, 29.6, 28.9.

HPLC analysis: 99% ee, Chiralcel AD-H column, 0.5% isopropanol in hexane, 0.5 mL/min flow rate, 254 nm UV lamp, $t_{[major]}$ = 12.1 min, $t_{[minor]}$ = 13.2 min.

Anal. Calcd for $C_{22}H_{23}NO$: C 83.24%, H 7.30%, N 4.41%; Found: C 83.06%, H 7.47%, N 4.26%.

2-((1*R*,2*R*,4*S*)-bicyclo[2.2.1]heptan-2-yl)-5-chloro-1*H*-indole
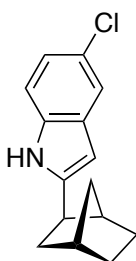
Following the general procedure **A** described above, 5-chloroindole (78 mg, 0.50 mmol) was allowed to react with norbornene (56 mg, 0.60 mmol) in THF (0.60 ml). The crude material was purified by chromatography with 6% EtOAc in hexanes. The solvent was removed by rotary evaporation to yield the title compound as a white solid (103 mg, 84% yield).

¹H NMR (600 MHz, C_6D_6): δ 7.57 (s, 1H), 7.18 (d, *J* = 8.5 Hz, 1H), 6.76 (d, *J* = 8.5 Hz, 1H), 6.52 (br s, 1H), 5.87 (s, 1H), 2.24 (dd, *J* = 8.2, 5.5 Hz, 1H), 2.12 (s, 1H), 2.00 (s, 1H), 1.50-1.36 (m, 4H), 1.28 (d, *J* = 9.8 Hz, 1H), 1.16-1.04 (m, 2H), 0.95 (d, *J* = 9.8 Hz, 1H).

¹³C NMR (151 MHz, C_6D_6): δ 145.7, 134.3, 130.0, 125.1, 121.0, 119.4, 111.2, 97.9, 42.5, 41.0, 36.7, 36.2, 35.8, 29.5, 28.8.

HPLC analysis: 98% ee, Chiralcel AD-H column, 5% isopropanol in hexane, 0.7 mL/min flow rate, 254 nm UV lamp, $t_{[minor]}$ = 15.2 min, $t_{[major]}$ = 17.5 min.

Anal. Calcd for $C_{15}H_{16}ClN$: C 73.31%, H 6.56%, N 5.70%; Found: C 73.20%, H 6.34%, N 5.45%.

2-(Bicyclo[2.2.1]heptan-2-yl)-5-bromo-1*H*-indole
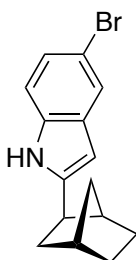
Following the general procedure **A** described above, 5-bromoindole (99 mg, 0.50 mmol) was allowed to react with norbornene (56 mg, 0.60 mmol) in THF (0.60 ml). The crude material was purified by chromatography with 6% EtOAc in hexanes. The collected fractions were concentrated by rotary evaporation, and the resulting solution was sparged with nitrogen gas. The solvent was removed under vacuum in a nitrogen-filled dry-box to yield the title compound as an air sensitive white solid (120 mg, 84% yield).

¹H NMR (600 MHz, C₆D₆): δ 7.72 (s, 1H), 7.32 (d, J = 8.5 Hz, 1H), 6.72 (d, J = 8.5 Hz, 1H), 6.53 (br s, 1H), 5.86 (s, 1H), 2.24 (dd, J = 8.4, 5.4 Hz, 1H), 2.12 (s, 1H), 2.00 (s, 1H), 1.49-1.37 (m, 4H), 1.28 (d, J = 9.8 Hz, 1H), 1.12-1.06 (m, 2H), 0.94 (d, J = 9.8 Hz, 1H).

¹³C NMR (151 MHz, C₆D₆): δ 145.5, 134.6, 130.7, 123.6, 122.5, 112.7, 111.6, 97.8, 42.5, 40.9, 36.8, 36.2, 35.8, 29.5, 28.8.

HPLC analysis: 97% ee, Chiralcel AD-H column, 5% isopropanol in hexane, 0.7 mL/min flow rate, 254 nm UV lamp, $t_{[minor]}$ = 14.9 min, $t_{[major]}$ = 19.1 min.

Anal. Calcd for C₁₅H₁₆BrN: C 62.08%, H 5.56%, N 4.83%; Found: C 62.07%, H 5.71%, N 4.80%.

Methyl 2-((1*R*,2*R*,4*S*)-bicyclo[2.2.1]heptan-2-yl)-1*H*-indole-5-carboxylate

Following the general procedure **A** described above, 5-chloroindole (89 mg, 0.50 mmol) was allowed to react with norbornene (56 mg, 0.60 ml). The crude material was purified by chromatography with 6% EtOAc in hexanes. The solvent was removed by rotary evaporation to yield the title compound as a white solid (129 mg, 96% yield).
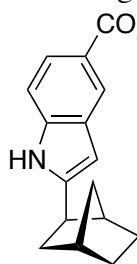
¹H NMR (600 MHz, THF): δ 10.29 (br s, 1H), 8.18 (s, 1H), 7.72 (d, J = 8.5 Hz, 1H), 7.23 (d, J = 8.5 Hz, 1H), 6.24 (s, 1H), 3.82 (s, 3H), 2.85 (dd, J = 8.5, 5.3 Hz, 1H), 2.44 (d, J = 3.2 Hz, 1H), 2.35 (s, 1H), 1.85 (ddd, J = 12.1, 7.6, 4.4 Hz, 1H), 1.80-1.74 (m, 1H), 1.68-1.56 (m, 2H), 1.54 (d, J = 9.6 Hz, 1H), 1.39 (dd, J = 10.2 Hz, 1H), 1.33-1.27 (m, 1H), 1.19 (d, J = 9.7 Hz, 1H).

¹³C NMR (151 MHz, THF): δ 167.1, 146.4, 139.3, 128.2, 122.0, 121.7, 121.0, 109.5, 98.4, 50.4, 42.8, 41.3, 36.7, 36.3, 35.6, 29.5, 28.7.

HPLC analysis: 99% ee, Chiralcel AD-H column, 6% isopropanol in hexane, 1.0 mL/min flow rate, 254 nm UV lamp, $t_{[minor]}$ = 31.8 min, $t_{[major]}$ = 35.4 min.

Anal. Calcd for C₁₇H₁₉NO₂: C 75.81%, H 7.11%, N 5.20%; Found: C 75.48%, H 7.22%, N 4.99%.

2-((1*R*,2*R*,4*S*)-bicyclo[2.2.1]heptan-2-yl)-5-fluoro-1*H*-indole
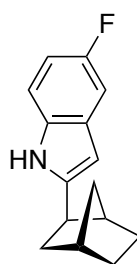
Following the general procedure **A** described above, 5-fluoroindole (69 mg, 0.50 mmol) was allowed to react with norbornene (56 mg, 0.60 mmol) in THF (0.60 ml). The crude material was purified by chromatography with 5% EtOAc in hexanes. The collected fractions were concentrated by rotary evaporation, and the resulting solution was sparged with nitrogen gas. The solvent was removed under vacuum in a nitrogen-filled dry-box to yield the title compound as an air sensitive white solid (102 mg, 89% yield).

¹H NMR (600 MHz, C₆D₆): δ 7.27 (d, J = 9.8 Hz, 1H), 6.95 (ddd, J = 9.0, 9.0, 2.0 Hz, 1H), 6.79 (dd, J = 8.6, 4.4 Hz, 1H), 6.55 (s, 1H), 5.92 (s, 1H), 2.27 (dd, J = 8.4, 5.4 Hz, 1H), 2.13 (s, 1H), 2.03 (s, 1H), 1.54-1.47 (m, 1H), 1.46-1.36 (m, 3H), 1.32 (d, J = 9.8 Hz, 1H), 1.14-1.06 (m, 2H), 0.96 (d, J = 9.8 Hz, 1H).

¹³C NMR (151 MHz, C₆D₆): δ 158.2 (d, J = 233.1 Hz), 146.1, 132.6, 129.29 (d, J = 10.3 Hz), 110.7 (d, J = 9.6 Hz), 108.8 (d, J = 26.0 Hz), 104.9 (d, J = 23.2 Hz), 98.4 (d, J = 4.4 Hz), 42.6, 41.1, 36.8, 36.2, 35.9, 29.5, 28.8.

^{19}F NMR (565 MHz, C_6D_6): δ -126.0 (ddd, J = 9.4, 9.4, 4.4 Hz).

HPLC analysis: 98% ee, Chiralcel OD-H column, 1.5% isopropanol in hexane, 1.0 mL/min flow rate, 254 nm UV lamp, $t_{[major]}$ = 21.1 min, $t_{[minor]}$ = 22.4 min.

Anal. Calcd for $C_{15}H_{16}FN$: C 78.57%, H 7.03%, N 6.11%; Found: C 78.28%, H 7.18%, N 5.82%.

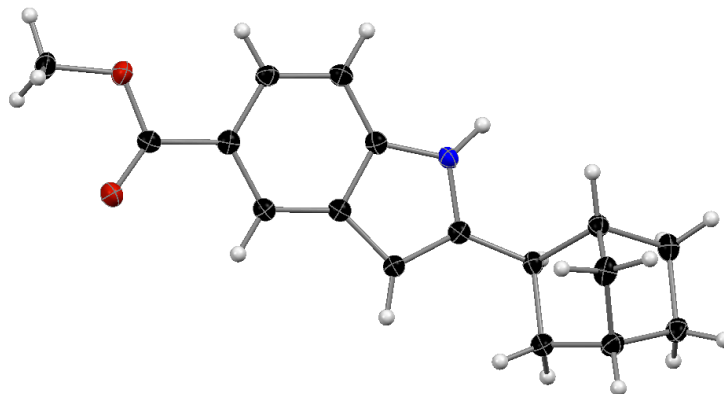**X-ray structure and absolute configuration determination of 6**

Figure 4.5. ORTEP representation of **6**. Thermal ellipsoids are drawn at the 50% probability level.

Single crystals for x-ray analysis were obtained by dissolving **6** (45 mg, 0.17 mmol) in toluene (0.6 ml) at 110 °C in an NMR tube under an atmosphere of nitrogen. The hot solution was allowed to cool to room temperature and sit undisturbed for 12 h. Over this period, clear colorless crystals formed on the sides of the NMR tube. A colorless prism 0.08 x 0.06 x 0.04 mm in size was mounted on a Cryoloop with Paratone oil. Data from a Cu radiation source were collected in a nitrogen gas stream at 100(2) K using phi and omega scans. Crystal-to-detector distance was 60 mm and exposure time was 5 seconds per frame using a scan width of 1.0°. Data collection was 99.8% complete to 67.00° in q. A total of 10826 reflections were collected covering the indices, -7<=h<=7, -21<=k<=21, -7<=l<=6. 2430 reflections were found to be symmetry independent, with an R_{int} of 0.0270. Indexing and unit cell refinement indicated a primitive, monoclinic lattice. The space group was found to be P2(1) (No. 4). The data were integrated using the Bruker SAINT software program and scaled using the SADABS software program. Solution by direct methods (SIR-2011) produced a complete heavy-atom phasing model consistent with the proposed structure. All non-hydrogen atoms were refined anisotropically by full-matrix least-squares (SHELXL-97). All hydrogen atoms were placed using a riding model. Their positions were constrained relative to their parent atom using the appropriate HFIX command in SHELXL-97. Absolute stereochemistry was unambiguously determined to be *R* at C1 and C2, and *S* at C5, respectively.

Table 4.4. Crystal data and structure refinement for 6

|	
Empirical formula	C17 H19 N O2
Formula weight	269.33
Temperature	100(2) K
Wavelength	1.54178 Å
Crystal system	Monoclinic
Space group	P2(1)
Unit cell dimensions	a = 6.0151(4) Å a= 90°.
	b = 18.2558(12) Å b= 95.614(2)°.
	c = 6.2350(4) Å g = 90°.
Volume	681.38(8) Å^3
Z	2
Density (calculated)	1.313 Mg/m^3
Absorption coefficient	0.681 mm^{-1}
F(000)	288
Crystal size	0.08 x 0.06 x 0.04 mm^3
Crystal color/habit	colorless prism
Theta range for data collection	4.84 to 68.23°.
Index ranges	-7<=h<=7, -21<=k<=21, -7<=l<=6
Reflections collected	10826
Independent reflections	2430 [R(int) = 0.0270]
Completeness to theta = 67.00°	99.8 %
Absorption correction	Semi-empirical from equivalents
Max. and min. transmission	0.9733 and 0.9475
Refinement method	Full-matrix least-squares on F^2
Data / restraints / parameters	2430 / 1 / 182
Goodness-of-fit on F^2	1.060
Final R indices [I>2sigma(I)]	R1 = 0.0300, wR2 = 0.0729
R indices (all data)	R1 = 0.0300, wR2 = 0.0729
Absolute structure parameter	-0.03(16)
Largest diff. peak and hole	0.125 and -0.237 e.Å^{-3}

Table 4.5. Atomic Coordinates of 6[a]

Atom	x	y	z	U(eq)
C(1)	8256(2)	4733(1)	13631(2)	16(1)
C(2)	10622(2)	5073(1)	14051(2)	18(1)
C(3)	11013(2)	5248(1)	16479(2)	22(1)
C(4)	9394(2)	5901(1)	16738(2)	21(1)
C(5)	8346(2)	6034(1)	14424(2)	21(1)
C(6)	6707(2)	5409(1)	13823(2)	23(1)
C(7)	10281(2)	5840(1)	13087(2)	22(1)
C(8)	7806(2)	4330(1)	11530(2)	16(1)
C(9)	5986(2)	4329(1)	10039(2)	17(1)
C(10)	6381(2)	3795(1)	8424(2)	16(1)
C(11)	5177(2)	3539(1)	6537(2)	17(1)
C(12)	6155(2)	3013(1)	5301(2)	17(1)
C(13)	8329(2)	2747(1)	5923(2)	19(1)
C(14)	9524(2)	2980(1)	7796(2)	19(1)
C(15)	8530(2)	3499(1)	9039(2)	17(1)
C(16)	4888(2)	2744(1)	3298(2)	17(1)
C(17)	4947(2)	1933(1)	346(2)	23(1)
N(1)	9340(2)	3828(1)	10924(2)	17(1)
O(1)	3075(2)	2960(1)	2569(2)	24(1)
O(2)	5992(2)	2210(1)	2366(2)	22(1)

[a]Values represent atomic coordinates x 10^4 and equivalent isotropic displacement parameters (Å^2 x 10^3) for **6**. U(eq) is defined as one third of the trace of the orthogonalized U tensor.

General Procedure B: Ir-catalyzed hydroheteroarylation of norbornene with furans.

In a nitrogen-filled dry-box, an oven dried 4 ml screw-capped vial was charged with [Ir(coe)$_2$Cl]$_2$ (5.4 mg, 0.0060 mmol), (*S*)-DTBM-SEGPHOS (14.2 mg, 0.0120 mmol), the corresponding furan (0.40 mmol), and a magnetic stirbar. THF (0.10 ml) was added to these solids, and the mixture was stirred vigorously until an orange homogeneous solution was obtained (5 min). A 2.5 M solution of norbornene in THF (0.20 ml, 0.50 mmol) was added to the reaction mixture. The vial was sealed tightly with a Teflon cap and removed from the dry-box. The reaction mixture was stirred in an aluminum heating block at 100 °C for 24 h and then cooled to room temperature. The solvent was removed by rotary evaporation. The product was purified by flash chromatography on a column (height = 20. cm, diameter = 3.0 cm) of Silacycle Silia-P60 silica gel (55 g). The conditions for chromatography and other data that are specific to each compound are given below.

2-((1*R*,2*R*,4*S*)-Bicyclo[2.2.1]heptan-2-yl)benzofuran
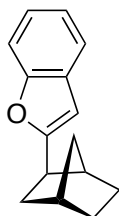
Following the general procedure **B** described above, methyl benzofuran (47 mg, 0.40 mmol) was allowed to react with norbornene (47 mg, 0.50 mmol) in THF (0.50 ml). The crude material was purified by flash chromatography on silica gel with hexanes. The solvent was removed by rotary evaporation to yield the title compound as a clear oil (70 mg, 83% yield).

¹H NMR (600 MHz, C$_6$D$_6$): δ 7.38 (d, *J* = 7.6 Hz, 1H), 7.35 (d, *J* = 8.0 Hz,

1H), 7.09 (t, J = 7.4 Hz, 1H), 7.04 (t, J = 7.6 Hz, 1H), 6.05 (s, 1H), 2.72-2.61 (m, 1H), 2.39 (s, 1H), 2.11 (s, 1H), 1.70-1.58 (m, 1H), 1.50-1.41 (m, 2H), 1.36 (p, J = 12.5 Hz, 2H), 1.10 (dd, J = 9.3 Hz, 1H), 1.05-0.93 (m, 2H).

13C NMR (151 MHz, C_6D_6): δ 163.3, 155.0, 129.0, 123.2, 122.4, 120.2, 110.7, 100.7, 41.8, 41.4, 36.2, 36.0, 35.9, 29.4, 28.7.

HPLC analysis: 67% ee, Chiralcel OD-H column, 100% hexane, 0.5 mL/min flow rate, 220 nm UV lamp, $t_{[major]}$ = 13.1 min, $t_{[minor]}$ = 15.4 min.

Anal. Calcd for $C_{15}H_{16}O$: C 84.87%, H 7.60%; Found: C 84.60%, H 7.77%.

Methyl 5-((1*R*,2*R*,4*S*)-bicyclo[2.2.1]heptan-2-yl)furan-2-carboxylate
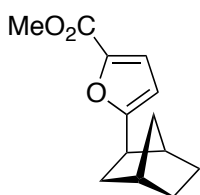
Following the general procedure **B** described above, methyl-2-furoate (51 mg, 0.40 mmol) was allowed to react with norbornene (47 mg, 0.50 mmol) in THF (0.50 ml). The crude material was purified by flash chromatography on silica gel with 3% ethyl acetate in hexanes. The solvent was removed by rotary evaporation to yield the title compound as a clear oil (74 mg, 84% yield).

1H NMR (600 MHz, C_6D_6): δ 6.99 (d, J = 2.8 Hz, 1H), 5.68 (s, 1H), 3.45 (s, 3H), 2.54-2.42 (m, 1H), 2.23 (s, 1H), 2.03 (s, 1H), 1.56-1.45 (m, 1H), 1.36-1.30 (m, 2H), 1.27 (d, J = 6.2 Hz, 2H), 0.99 (dd, J = 8.6 Hz, 1H), 0.92 (m, 2H).

13C NMR (151 MHz, C_6D_6): δ 164.8, 158.6, 143.3, 118.5, 106.1, 50.6, 42.0, 41.2, 36.1, 35.9, 35.8, 29.2, 28.5.

HPLC analysis: 68% ee, Chiralcel OB-H column, 0.5% isopropanol in hexane, 0.5 mL/min flow rate, 220 nm UV lamp, $t_{[major]}$ = 21.0 min, $t_{[minor]}$ = 23.5 min.

Anal. Calcd for $C_{13}H_{16}O_3$: C 70.89%, H 7.32%; Found: C 71.05%, H 7.40%.

Methyl 5-((1*R*,2*R*,4*S*)-bicyclo[2.2.1]heptan-2-yl)-3-methylfuran-2-carboxylate

Following the general procedure **B** described above, methyl 3-methyl-2-furoate (56 mg, 0.40 mmol) was allowed to react with norbornene (47 mg, 0.50 mmol) in THF (0.50 ml). The crude material was purified by flash chromatography on silica gel with 3% ethyl acetate in hexanes. The solvent was removed by rotary evaporation to yield the title compound as a clear oil (81 mg, 87% yield).
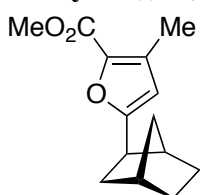
1H NMR (600 MHz, C_6D_6): δ 6.29 (s, 1H), 3.47 (s, 3H), 2.54-2.44 (m, 1H), 2.40 (s, 3H), 2.26 (s, 1H), 2.06 (s, 1H), 1.54-1.45 (m, 1H), 1.35 (m, 4H), 1.10-1.03 (m, 1H), 1.01-0.90 (m, 2H).

13C NMR (151 MHz, C_6D_6): δ 163.9, 158.2, 157.4, 113.8, 104.7, 50.3, 41.8, 40.7, 36.1, 35.7, 35.6, 29.2, 28.6, 13.2.

HPLC analysis: 78% ee, Chiralcel AS-H column, 100% hexane, 0.1 mL/min flow rate, 220 nm UV lamp, $t_{[major]}$ = 65.2 min, $t_{[minor]}$ = 70.2 min.

Anal. Calcd for $C_{14}H_{18}O_3$: C 71.77%, H 7.74%; Found: C 72.05% , H 7.71%.
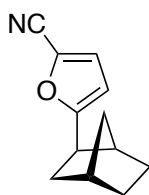
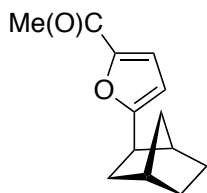## 5-((1*R*,2*R*,4*S*)-Bicyclo[2.2.1]heptan-2-yl)furan-2-carbonitrile

Following the general procedure **B** described above, 2-furonitrile (37 mg, 0.40 mmol) was allowed to react with norbornene (47 mg, 0.50 mmol) in THF (0.50 ml). The crude material was purified by flash chromatography on silica gel with 2% ethyl acetate in hexanes. The solvent was removed by rotary evaporation to yield the title compound as a clear oil (62 mg, 83% yield).

¹H NMR (600 MHz, C_6D_6): δ 6.24 (d, J = 2.7 Hz, 1H), 5.41 (s, 1H), 2.33-2.23 (m, 1H), 2.04 (s, 1H), 2.00 (s, 1H), 1.35-1.23 (m, 4H), 1.12 (d, J = 9.8 Hz, 1H), 1.01-0.90 (m, 2H), 0.87 (d, J = 9.9 Hz, 1H).

¹³C NMR (151 MHz, C_6D_6): δ 165.8, 124.4, 122.2, 111.9, 105.4, 41.8, 41.0, 36.0, 35.9, 35.8, 29.1, 28.4.

HPLC analysis: 70% ee, Chiralcel OJ-H column, 100% hexane, 0.3 mL/min flow rate, 220 nm UV lamp, $t_{[major]}$ = 29.3 min, $t_{[minor]}$ = 30.8 min.

Anal. Calcd for $C_{12}H_{13}NO$: C 76.98%, H 7.00%, N 7.48%; Found: C 76.65%, H 7.28%, N 7.17%.

## 1-(5-((1*R*,2*R*,4*S*)-Bicyclo[2.2.1]heptan-2-yl)furan-2-yl)ethanone, (12)

Following the general procedure **B** described above, 2-acetylfuran (44 mg, 0.40 mmol) was allowed to react with norbornene (47 mg, 0.50 mmol) in THF (0.50 ml). The crude material was purified by flash chromatography on silica gel with 3% ethyl acetate in hexanes. The solvent was removed by rotary evaporation to yield the title compound as a clear oil (67 mg, 82% yield).

¹H NMR (600 MHz, C_6D_6): δ 6.79 (s, 1H), 5.70 (d, J = 2.4 Hz, 1H), 2.51-2.42 (m, 1H), 2.22 (s, 1H), 2.07 (s, 3H), 2.06 (s, 1H), 1.55-1.45 (m, 1H), 1.40-1.25 (m, 4H), 1.02 (dd, J = 8.7 Hz, 1H), 0.99-0.91 (m, 2H).

¹³C NMR (151 MHz, C_6D_6): δ 184.5, 164.5, 151.9, 117.3, 106.5, 42.1, 41.2, 36.1, 36.0, 35.9, 29.2, 28.5, 25.2.

HPLC analysis: 64% ee, Chiralcel OD-H column, 0.5% isopropanol in hexane, 0.5 mL/min flow rate, 254 nm UV lamp, $t_{[major]}$ = 13.8 min, $t_{[minor]}$ = 14.7 min.

Anal. Calcd for $C_{13}H_{16}O_2$: C 76.44%, H 7.90%; Found: C 76.56%, H 8.02%.

2-((1*R*,2*R*,4*S*)-Bicyclo[2.2.1]heptan-2-yl)-5-methylfuran
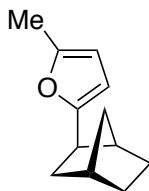
Following the general procedure **B** described above, 2-methylfuran (41 mg, 0.50 mmol) was allowed to react with norbornene (56 mg, 0.60 mmol) in THF (0.50 ml). The crude material was purified by flash chromatography on silica gel with 1% ethyl acetate in hexanes. The solvent was removed by rotary evaporation to yield the title compound as a clear oil (76 mg, 86% yield).

¹H NMR (600 MHz, CDCl₃): δ 5.88-5.85 (m, 1H), 5.83 (d, J = 2.6 Hz, 1H), 2.75-2.66 (m, 1H), 2.40 (s, 1H), 2.33 (s, 1H), 2.28 (s, 3H), 1.72-1.53 (m, 4H), 1.48 (d, J = 9.7 Hz, 1H), 1.35 (dd, J = 13.4, 5.9 Hz, 1H), 1.29-1.22 (m, 1H), 1.17 (d, J = 9.7 Hz, 1H).

**^{13}C NMR** (151 MHz, CDCl$_3$): δ 158.9, 150.1, 105.6, 104.0, 42.0, 41.2, 36.2, 36.1, 35.9, 29.5, 28.9, 13.5.

HPLC analysis: 72% ee, Chiralcel OJ-H column, 100 %hexane, 0.5 mL/min flow rate, 254 nm UV lamp, t$_{[major]}$ = 8.4 min, t$_{[minor]}$ = 9.4 min.

Anal. Calcd for C$_{13}$H$_{16}$O: C 81.77%, H 9.15%; Found: C 81.45%, H 8.98%.

General Procedure C: Ir-catalyzed hydroheteroarylation of norbornene with thiophenes and pyrroles.

In a nitrogen-filled dry-box, an oven dried 4 ml screw-capped vial was charged with [Ir(coe)$_2$Cl]$_2$ (6.7 mg, 0.0075 mmol), (S)-DTBM-SEGPHOS (17.7 mg, 0.0150 mmol), the corresponding thiophene or pyrrole (0.50 mmol), and a magnetic stirbar. THF (0.20 ml) was added to these solids, and the mixture was stirred vigorously until an orange homogeneous solution was obtained (5 min). A 3.0 M solution of norbornene in THF (0.20 ml, 0.60 mmol) was added to the reaction mixture. The vial was sealed tightly with a Teflon cap and removed from the dry-box. The reaction mixture was stirred in an aluminum heating block at 100 °C for 24 h and then cooled to room temperature. The solvent was removed by rotary evaporation. The product was purified by flash chromatography on a column (height = 20. cm, diameter = 3.0 cm) of Silacycle Silia-P60 silica gel (55 g). The conditions for chromatography and other data that are specific to each compound are given below.

2-((1R,2R,4S)-Bicyclo[2.2.1]heptan-2-yl)-4-bromothiophene
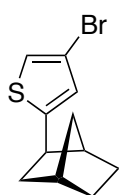
Following the general procedure **C** described above, 3-bromothiophene (82 mg, 0.50 mmol) was allowed to react with norbornene (56 mg, 0.60 mmol) in THF (0.60 ml). The crude material was purified by flash chromatography on silica gel with hexanes. The solvent was removed by rotary evaporation and unreacted 3-bromothiophene was removed under vacuum (15 mTorr) for 4 hours to yield the title compound as a white solid (125 mg, 97% yield).

^{1}H NMR (600 MHz, CDCl$_3$): δ 7.00 (d, J = 1.1 Hz, 1H), 6.70 (s, 1H), 2.93-2.82 (m, 1H), 2.35 (overlapping singlets, J = 5.6 Hz, 2H), 1.81 (dd, J = 15.9, 5.4 Hz, 1H), 1.70-1.48 (m, 4H), 1.34 (dd, J = 9.8 Hz, 1H), 1.23 (dd, J = 23.3, 9.7 Hz, 2H).

^{13}C NMR (151 MHz, CDCl$_3$): δ 153.6, 125.3, 119.7, 108.9, 44.7, 43.2, 40.1, 36.5, 36.1, 29.7, 28.6.

HPLC analysis: 98% ee, Chiralcel OD-H column, 100% hexane, 1.0 mL/min flow rate, 254 nm UV lamp, t$_{[minor]}$ = 5.2 min, t$_{[major]}$ = 6.2 min.

Anal. Calcd for C$_{11}$H$_{13}$BrS: C 51.37%, H 5.09%%; Found: C 51.75%, H 5.29%.

2-((1R,2R,4S)-bicyclo[2.2.1]heptan-2-yl)benzo[b]thiophene
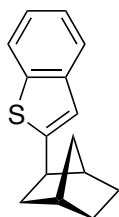
Following the general procedure **C** described above, benzothiophene (67 mg, 0.50 mmol) was allowed to react with norbornene (56 mg, 0.60 mmol) in THF (0.60 ml). The crude material was purified by flash chromatography on silica gel with hexanes. The solvent was removed by rotary evaporation and unreacted benzothiophene was removed under vacuum (15 mTorr) for 4 hours to yield the title compound as a white solid (81 mg, 71% yield).

^{1}H NMR (600 MHz, C$_6$D$_6$): δ 7.54 (d, J = 8.0 Hz, 1H), 7.51 (d, J = 7.8 Hz,

1H), 7.16 (t, J = 7.5 Hz, 1H), 7.03 (t, J = 7.4 Hz, 1H), 6.74 (s, 1H), 2.79-2.70 (m, 1H), 2.35 (s, 1H), 2.12 (s, 1H), 1.74-1.63 (m, 1H), 1.60-1.49 (m, 2H), 1.42-1.29 (m, 2H), 1.09 (t, J = 9.1 Hz, 1H), 1.05-0.97 (m, 2H).

^{13}C NMR (151 MHz, C$_6$D$_6$): δ 152.5, 140.3, 139.2, 124.0, 123.4, 122.8, 122.1, 118.8, 44.3, 43.6, 39.6, 36.5, 36.1, 29.7, 28.5.

HPLC analysis: 91% ee, Chiralcel OD-H column, 100% hexane, 1.0 mL/min flow rate, 220 nm UV lamp, $t_{[major]}$ = 11.3 min, $t_{[minor]}$ = 14.0 min.

Anal. Calcd for C$_{15}$H$_{16}$S: C 78.90%, H 7.06%%; Found: C 79.20 %, H 7.36%.

2-((1R,2R,4S)-Bicyclo[2.2.1]heptan-2-yl)-5-chlorothiophene
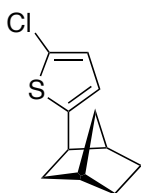
Following the general procedure **C** described above, 2-chlorothiophene (60. mg, 0.50 mmol) was allowed to react with norbornene (56 mg, 0.60 mmol) in THF (0.60 ml). The crude material was purified by flash chromatography on silica gel with hexanes. The solvent was removed by rotary evaporation and unreacted 2-chlorothiophene was removed under vacuum (15 mTorr) for 4 hours to yield the title compound as a white solid (104 mg, 98% yield).

^{1}H NMR (600 MHz, CDCl$_3$): δ 6.70 (d, J = 3.6 Hz, 1H), 6.53 (d, J = 3.5 Hz, 1H), 2.89-2.80 (m, 1H), 2.35 (s, 1H), 2.32 (s, 1H), 1.82-1.75 (m, 1H), 1.69-1.53 (m, 3H), 1.51 (d, J = 9.9 Hz, 1H), 1.33 (dd, J = 9.8 Hz, 1H), 1.27-1.19 (m, 2H).

^{13}C NMR (151 MHz, CDCl$_3$): δ 151.1, 126.3, 125.34, 121.5, 44.7, 43.5, 40.0, 36.5, 36.1, 29.7, 28.6.

HPLC analysis: 97% ee, Chiralcel OD-H column, 100% hexane, 1.o mL/min flow rate, 220 nm UV lamp, $t_{[minor]}$ = 4.5 min, $t_{[major]}$ = 4.9 min.

Anal. Calcd for C$_{11}$H$_{13}$ClS: C 62.10%, H 6.10%; Found: C 62.39%, H 6.49 %.

1-(5-((1R,2R,4S)-bicyclo[2.2.1]heptan-2-yl)thiophen-2-yl)ethanone
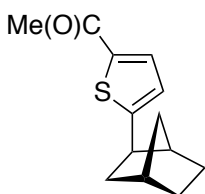
Following the general procedure **C** described above, 2-acetylthiophene (63 mg, 0.50 mmol) was allowed to react with norbornene (56 mg, 0.60 mmol) in THF (0.60 ml). The crude material was purified by flash chromatography on silica gel with 3% ethyl acetate in hexanes. The solvent was removed by rotary evaporation to yield the title compound as a clear oil (104 mg, 95% yield).

^{1}H NMR (600 MHz, C$_6$D$_6$): δ 7.05 (d, J = 3.4 Hz, 1H), 6.41 (d, J = 3.4 Hz, 1H), 2.57 (ddz, J = 7.0 Hz, 1H), 2.14 (s, 1H), 2.06 (s, 3H), 2.05 (s, 1H), 1.48 (d, J = 7.1 Hz, 2H), 1.40 (d, J = 10.0 Hz, 1H), 1.29 (overlapping br singlets, J = 6.3 Hz, 2H), 1.00 (dd, J = 8.6 Hz, 1H), 0.97-0.91 (m, 2H).

^{13}C NMR (151 MHz, C$_6$D$_6$): δ 188.6, 161.2, 142.0, 131.9, 123.5, 44.7, 43.6, 40.3, 36.5, 36.0, 29.6, 28.3, 25.7.

HPLC analysis: 96% ee, Chiralcel AD-H column, 0.5% isopropanol in hexane, 0.5 mL/min flow rate, 254 nm UV lamp, $t_{[minor]}$ = 9.9 min, $t_{[major]}$ = 10.9 min.

Anal. Calcd for C$_{13}$H$_{16}$OS: C 70.87%, H 7.32 %; Found: C 71.23%, H 7.60%.

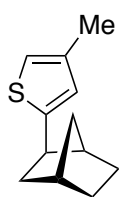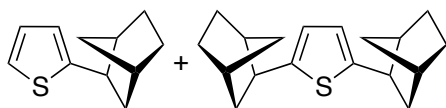## 2-((1R,2R,4S)-Bicyclo[2.2.1]heptan-2-yl)-4-methylthiophene

Following the general procedure **C** described above, 3-methylthiophene (49 mg, 0.50 mmol) was allowed to react with norbornene (56 mg, 0.60 mmol) in THF (0.60 ml). The crude material was purified by flash chromatography on silica gel with hexanes. The solvent was removed by rotary evaporation to yield the title compound as a clear oil (55 mg, 58% yield).

¹H NMR (600 MHz, CDCl₃): δ 6.69 (s, 1H), 6.61 (s, 1H), 2.91 (dd, J = 8.5, 5.4 Hz, 1H), 2.36 (overlapping s, 2H), 2.23 (s, 3H), 1.81 (ddd, J = 11.3, 8.9, 2.1 Hz, 1H), 1.72 (ddd, J = 9.3, 7.4, 4.8 Hz, 1H), 1.66-1.52 (m, 3H), 1.36 (dd, J = 13.5, 6.1 Hz, 1H), 1.30-1.24 (m, 1H), 1.21 (d, J = 9.9 Hz, 1H).

¹³C NMR (151 MHz, CDCl₃): δ 152.3, 137.1, 124.9, 117.6, 44.9, 43.2, 40.4, 36.5, 36.1, 29.8, 28.7, 15.8.

HPLC analysis: 87% ee, Chiralcel OJ-H column, 100% hexane, 0.5 mL/min flow rate, 254 nm UV lamp, $t_{[minor]}$ = 11.4 min, $t_{[major]}$ = 15.0 min.

Anal. Calcd for $C_{12}H_{16}S$: C 74.94%, H 8.39%; Found: C 74.58%, H 8.07%.

2-((1R,2R,4S)-Bicyclo[2.2.1]heptan-2-yl)thiophene

Following the general procedure **C** described above, thiophene (42 mg, 0.50 mmol) was allowed to react with norbornene (42 mg, 0.45 mmol) in THF (0.60 ml). The crude material was purified by flash chromatography on silica gel with hexanes. The solvent was removed by rotary evaporation to yield the title compound as a 3.5:1.0 mono:dialkylated mixture of products as a clear oil (55 mg total, 52% yield monoalkylation,). A copy of the ¹H NMR spectrum (600 MHz, CDCl₃) is included.

2-((1R,2R,4S)-Bicyclo[2.2.1]heptan-2-yl)-5-ethyl-1H-pyrrole
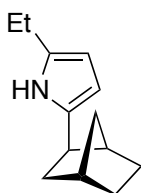
Following the general procedure **C** described above, 2-ethylpyrrole (48 mg, 0.50 mmol) was allowed to react with norbornene (56 mg, 0.60 mmol) in THF (0.60 ml). The crude material was purified by flash chromatography on silica gel with 5% ethyl acetate in hexanes. The solvent was removed by rotary evaporation to yield a yellow oil. The sample was taken into the dry-box and filtered through a 1 cm plug of silica gel with pentane to yield the title compound as a clear liquid (80 mg, 85% yield).

¹H NMR (600 MHz, C₆D₆): δ 6.72 (s, 1H), 5.93 (s, 1H), 5.88 (s, 1H), 2.38 (dd, J = 8.2, 5.2 Hz, 1H), 2.31 (q, J = 7.5 Hz, 2H), 2.15 (s, 1H), 2.09 (s, 1H), 1.64 (dd, J = 8.6, 3.5 Hz, 1H), 1.49 (dd, J = 9.5 Hz, 2H), 1.43 (d, J = 2.4 Hz, 2H), 1.14 (dd, J = 20.0, 5.4 Hz, 2H), 1.06 (t, J = 7.6 Hz, 3H), 0.99 (d, J = 9.6 Hz, 1H).

¹³C NMR (151 MHz, C₆D₆): δ 135.5, 131.9, 104.0, 103.8, 43.1, 40.9, 37.2, 36.1, 35.7, 29.5, 29.0, 20.8, 13.7.

HPLC analysis: 86% ee, Chiralcel AD-H column, 100% hexane, 1.0 mL/min flow rate, 254 nm UV lamp, $t_{[major]}$ = 9.8 min, $t_{[minor]}$ = 10.9 min.

Anal. Calcd for $C_{13}H_{19}N$: C 82.48%, H 10.12%, N 7.40%; Found: C 82.21 %, H 10.42%, N 7.16%.

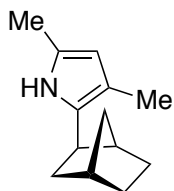## 2-((1*R*,2*R*,4*S*)-Bicyclo[2.2.1]heptan-2-yl)-3,5-dimethyl-1*H*-pyrrole

Following the general procedure **C** described above, 2,4-dimethypyrrole (46 mg, 0.50 mmol) was allowed to react with norbornene (56 mg, 0.60 mmol) in THF (0.60 ml). The crude material was purified by flash chromatography on silica gel with 3% ethyl acetate in hexanes. The solvent was removed by rotary evaporation to yield a yellow oil. The sample was taken into the dry-box and filtered through a 1 cm plug of silica gel with pentane. The solvent and residual starting material was removed under high vacuum overnight to yield the title compound as a clear liquid (20 mg, 21% yield).

^{1}H NMR (600 MHz, C_6D_6): δ 6.78 (br s, 1H), 5.84 (d, J = 1.7 Hz, 1H), 2.66 (dd, J = 8.6, 5.9 Hz, 1H), 2.12 (s, 3H), 2.10 (br s, 1H), 2.06 (br s, 1H), 1.96 (s, 3H), 1.54-1.47 (m, 1H), 1.41-1.35 (m, 2H), 1.31-1.27 (m, 1H), 1.16 (d, J = 10.2 Hz, 2H), 1.11-1.05 (m, 1H), 0.98 (d, J = 9.6 Hz, 1H).

^{13}C NMR (151 MHz, C_6D_6): δ 130.5, 123.3, 113.0, 108.6, 42.6, 38.8, 37.9, 36.8, 36.2, 30.1, 28.5, 12.8, 11.3.

HPLC analysis: 80% ee, Chiralcel OD-H column, 100% hexane, 0.8 mL/min flow rate, 254 nm UV lamp, $t_{[minor]}$ = 6.4 min, $t_{[major]}$ = 8.9 min.

GC/MS: *m/z* 189 (70%, [M]$^+$), 108 (100%, [M-C_6H_9]$^+$).

HRMS (ESI) calcd for [$C_{13}H_{19}N$]$^+$: *m/z* 189.2967, found 189.2971.

2-((1*R*,2*R*,4*S*)-Bicyclo[2.2.1]heptan-2-yl)-1*H*-pyrrole
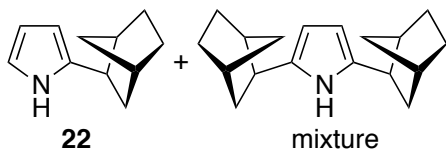
Following the general procedure **C** described above, pyrrole (34 mg, 0.50 mmol) was allowed to react with norbornene (56 mg, 0.60 ml). The crude material was purified by flash chromatography on silica gel with 3% ethyl acetate in hexanes. The solvent was removed by rotary evaporation to yield a yellow oil. The sample was taken into the dry-box and filtered through a 1 cm plug of silica gel with pentane. The solvent and residual starting material was removed under high vacuum overnight to yield the title compound as a 3.4:1.0 mono:dialkylated mixture of products as a clear oil (75 mg total, 61% yield monoalkylation). A copy of the ^{1}H NMR spectrum (600 MHz, C_6D_6) is included.

GC/MS: *m/z* 161 (10%, [M]$^+$), 93 (65%, [M-C_5H_8]$^+$), 67 (100%, [M-norbornene]$^+$).

General Procedure D: Ir-catalyzed hydroheteroarylation of norbornadiene with hetero-arenes.

In a nitrogen-filled dry-box, an oven dried 4 ml screw-capped vial was charged with [Ir(coe)$_2$Cl]$_2$ (13.4 mg, 0.0149 mmol), (*S*)-DTBM-SEGPHOS (35.4 mg, 0.0300 mmol), the corresponding heteroarene (1.0 mmol), and a magnetic stirbar. THF (1.0 ml) was added to these solids, and the mixture was stirred vigorously until an orange homogeneous solution was obtained (5 min). A 2.5 M solution of norbornadiene (1.0 ml, 2.5 mmol) was added to the reaction mixture. The vial was sealed tightly with a Teflon cap and removed from the dry-box. The reaction mixture was stirred in an aluminum heating block at 100 °C for 24 h and then cooled to room temperature. The solvent was removed by rotary evaporation. The product was purified by flash chromatography on a column (height = 20. cm, diameter = 3.0 cm) of Silacycle Silia-P60 silica gel (55 g). The conditions for

chromatography and other data that are specific to each compound are given below. Products were found to be prone to oxidation over a period of hours and stored under nitrogen.

Methyl 5-((1*S*,2*R*,4*S*)-bicyclo[2.2.1]hept-5-en-2-yl)furan-2-carboxylate

Following the general procedure **D** described above, methyl-2-furoate (126 mg, 1.0 mmol) was allowed to react with norbornadiene (230 mg, 2.5 mmol) in THF (2.0 ml). The crude material was purified by flash chromatography on silica gel with 5% ethyl acetate in hexanes. The solvent was removed by rotary evaporation to yield the title compound as a clear oil (167 mg, 77% yield).
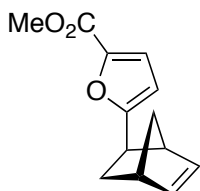
¹H NMR (600 MHz, C_6D_6): δ 6.99 (s, 1H), 5.88 (s, 2H), 5.78 (s, 1H), 3.48 (d, J = 1.0 Hz, 3H), 2.77 (s, 1H), 2.62 (s, 1H), 2.45 (dd, J = 8.2, 4.3 Hz, 1H), 1.61-1.53 (m, 1H), 1.33 (d, J = 8.3 Hz, 1H), 1.25 (dd, J = 10.3 Hz, 2H).

¹³C NMR (151 MHz, C_6D_6): δ 164.1, 158.5, 143.3, 137.1, 135.8, 118.6, 106.9, 50.7, 47.7, 46.0, 41.7, 37.8, 31.4.

HPLC analysis: 38% ee, Chiralcel OJ-H column, 1% isopropanol in hexane, 1.0 mL/min flow rate, 254 nm UV lamp, $t_{[major]}$ = 8.5 min, $t_{[minor]}$ = 9.1 min.

Anal. Calcd for $C_{13}H_{14}O_3$: C 71.54%, H 6.47%; Found: C 71.75%, H 6.62%.

2-((1*S*,2*R*,4*S*)-Bicyclo[2.2.1]hept-5-en-2-yl)benzo[*b*]thiophene

Following the general procedure **D** described above, benzothiophene (134 mg, 1.0 mmol) was allowed to react with norbornadiene (230 mg, 2.5 mmol) in THF (2.0 ml). The crude material was purified by flash chromatography on silica gel with hexanes. The solvent was removed by rotary evaporation to yield the title compound as a white solid (140 mg, 62% yield).
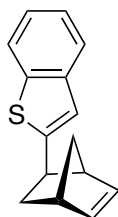
¹H NMR (600 MHz, CDCl₃): δ 7.79 (d, J = 7.9 Hz, 1H), 7.70 (d, J = 7.9 Hz, 1H), 7.36-7.31 (m, 1H), 7.31-7.25 (m, 1H), 7.10 (s, 1H), 6.28 (dd, J = 5.6, 3.1 Hz, 1H), 6.22 (dd, J = 5.6, 2.9 Hz, 1H), 3.07 (s, 1H), 3.04 (s, 1H), 2.98 (dd, J = 8.7, 4.4 Hz, 1H), 1.95-1.90 (m, 1H), 1.76 (ddd, J = 11.5, 8.7, 2.4 Hz, 1H), 1.69 (d, J = 8.7 Hz, 1H), 1.57-1.51 (m, 1H).

¹³C NMR (151 MHz, CDCl₃): δ 151.8, 140.1, 139.0, 137.4, 136.5, 124.1, 123.4, 122.7, 122.1, 119.5, 49.8, 46.4, 42.2, 40.3, 34.9.

HPLC analysis: 85% ee, Chiralcel OD-H column, 100% hexane, 1.0 mL/min flow rate, 254 nm UV lamp, $t_{[major]}$ = 13.4 min, $t_{[minor]}$ = 18.4 min.

Anal. Calcd for $C_{15}H_{14}S$: C 79.60%, H 6.23%; Found: C 79.37%, H 6.52%.

2-((1*S*,2*R*,4*S*)-Bicyclo[2.2.1]hept-5-en-2-yl)-1*H*-indole

Following the general procedure **D** described above, indole (117 mg, 1.0 mmol) was allowed to react with norbornadiene (230 mg, 2.5 mmol) in THF (2.0 ml). The crude material was purified by flash chromatography on silica gel with 5% ethyl acetate in hexanes. The solvent was removed by rotary evaporation to yield the title compound as a white solid (188 mg, 90% yield).
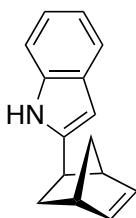
¹H NMR (600 MHz, C_6D_6): δ 7.62 (d, J = 7.4 Hz, 1H), 7.27-7.15 (m, 2H),

7.06 (d, J = 7.6 Hz, 1H), 6.69 (s, 1H), 6.14 (s, 1H), 6.07 (br s, 1H), 6.04 (br s, 1H), 2.70 (s, 1H), 2.65 (s, 1H), 2.33 (dd, J = 8.4, 3.9 Hz, 1H), 1.65-1.58 (m, 1H), 1.43-1.31 (m, 3H).

^{13}C NMR (151 MHz, C_6D_6): δ 143.2, 137.2, 136.2, 136.0, 129.0, 120.9, 120.0, 119.6, 110.4, 98.8, 48.1, 46.2, 41.8, 37.5, 32.2.

HPLC analysis: 96% ee, Chiralcel AD-H column, 1.5% isopropanol in hexane, 1.0 mL/min flow rate, 254 nm UV lamp, $t_{[major]}$ = 21.1 min, $t_{[minor]}$ = 22.5 min.

Anal. Calcd for $C_{15}H_{15}N$: C 86.08%, H 7.22%, N 6.69%; Found: C 85.78%, H 7.29%, N 6.38%.

1-(*Ortho*-D-phenylsulfonyl)-2-D-indole

An oven-dried round-bottom flask (100 ml) was charged with 1-phenylsulfonyl-indole (2.1 g, 8.0 mmol), a magnetic stirbar, and dry THF (40 ml). The flask was sealed with a septum and placed under a nitrogen gas atmosphere. The solution was cooled to -78 °C, and a 2.5 M solution of ^{n}BuLi in hexane (6.4 ml, 16 mmol) was slowly added to the solution via syringe. The -78 °C bath was removed, and the solution was allowed to warm to room temperature. The re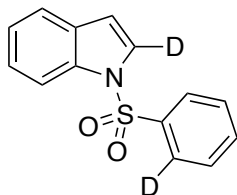sulting orange solution was allowed to stir at room temperature. After 1 h, the solution was cooled to -78 °C and CH$_3$OD (1.0 ml) was added to the solution. The solution was allowed to warm to room temperature. The brown solution was diluted with ether (50 ml), and K$_2$CO$_3$ (4 g) was added. The liquor was collected after filtering and washing the solids with ether on a fritted funnel. The liquor was concentrated by rotary evaporation to yield a dark brown residue. The crude material was purified by flash column chromatography with 10% ethyl acetate in hexanes. The solvent removed by rotary evaporation to yield the title compound as a white solid (1.97 g, 95%). NMR spectral data matched published data.[52]

2-D-indole
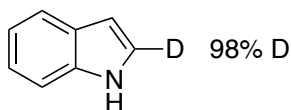
A round-bottom flask (100 ml) was charged with 1-(*ortho*-D-phenylsulfonyl)-2-D-indole (1.9 g, 7.5 mmol), methanol (18 ml), a 2.0 M solution of NaOH in water (25 ml, 50 mmol), and a magnetic stirbar. The flask was sealed with a septum, and the solution was sparged with nitrogen gas for 15 minutes. Once the solution was under a nitrogen atmosphere, the solution was heated to reflux at 90 °C. Complete consumption of the starting material was observed by gas chromatography after 21 h. The solvent was removed by gently blowing nitrogen gas over the solution. The products were extracted with ether (15 ml, x3), dried over MgSO$_4$, and run through a silica plug with diethyl ether as eluent. Hexanes (30 ml) were added to the solution, and the solvents were removed by rotary evaporation to yield a light brown solid. The light brown solid was washed with hexane (10 ml) to yield title compound as a white solid (602 mg, 68%). NMR spectral data match published data.[52]

2-((1R,2S,4S)-2,4-divinylcyclopentyl)-1H-indole
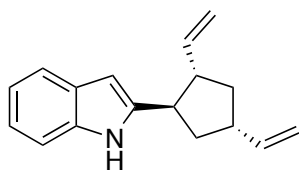
In a nitrogen-filled dry-box, a round-bottom flask (100 ml) was charged with 2-((1R,2S,4S)-2,4-divinylcyclopentyl)-1H-indole (188 mg, 0.899 mmol), a magnetic stirbar, and sealed with a septum. The solid was dissolved in dichloromethane (40 ml), and the resulting solution was sparged with ethylene gas for 10 minutes. A purple solution of Grubbs 1st generation catalyst (37 mg, 0.045 mmol) in dichloromethane (10 ml) was syringed into a round-bottom flask through the septum. A balloon of ethylene gas with a needle valve was connected to the flask through the septum. The solution was allowed to stir vigorously for 10 hours. The solvent was removed by rotary evaporation, and the crude material was purified by flash chromatography on silica gel with an eluent that consisted of 3% ethyl acetate in hexanes. The solvent was evaporated to yield the title compound as a clear oil (200. mg, 93%).

¹H NMR (600 MHz, C$_6$D$_6$): δ 7.64 (d, J = 7.2 Hz, 1H), 7.24-7.16 (m, 2H), 7.09 (d, J = 7.4 Hz, 1H), 7.03 (br s, 1H), 6.22 (s, 1H), 5.72 (ddd, J = 17.4, 10.0, 7.7 Hz, 1H), 5.69-5.60 (m, 1H), 4.99 (d, J = 17.1 Hz, 1H), 4.94 (d, J = 10.2 Hz, 1H), 4.91-4.82 (m, 2H), 2.64 (dd, J = 17.6, 9.1 Hz, 1H), 2.59-2.47 (m, 1H), 2.45-2.35 (m, 1H), 1.94-1.87 (m, 1H), 1.83 (ddd, J = 13.0, 8.4 Hz, 1H), 1.78-1.69 (m, 1H), 1.27 (dd, J = 22.3, 10.9 Hz, 1H).

¹³C NMR (151 MHz, C$_6$D$_6$): δ 142.5, 141.9, 141.2, 136.2, 128.9, 121.0, 120.1, 119.7, 114.4, 112.6, 110.4, 98.5, 51.0, 43.4, 42.1, 39.9, 38.4.

HPLC analysis: 96% ee, Chiralcel AD-H column, 1.5% isopropanol in hexane, 0.7 mL/min flow rate, 254 nm UV lamp, $t_{[major]}$ = 21.0 min, $t_{[major]}$ = 23.7 min.

Anal. Calcd for C$_{17}$H$_{19}$N: C 86.03%, H 8.07%, N 5.90%; Found: C 85.81%, H 8.11%, N 5.60%.

(1R,2R,4S)-bicyclo[2.2.1]heptane-2-carboxylic acid
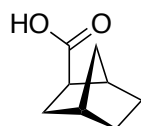
A round-bottom flask (50 ml) was charged with 1-(5-((1R,2R,4S)-bicyclo[2.2.1]heptan-2-yl)furan-2-yl)ethanone (176 mg, 0.80 mmol) and dichloromethane (20 ml). The resulting solution was cooled to -78 °C and ozone gas was bubbled through the solution. After 20 minutes, the clear solution turned dark blue. Following the color change, the solution was sparged with nitrogen gas, and a solution of triphenylphosphine (586 mg, 2.24 mmol) in dichloromethane (5 ml) was added to the reaction mixture at -78 °C. The reaction mixture was allowed to warm to room temperature slowly. The resulting yellow solution was basified with a 2 M solution of NaOH. The basic solution was washed with dichloromethane (25 ml) two times. The aqueous layer was acidified with a 2 M solution of HCl, and the organic material was extracted with dichloromethane (25 ml, x3). The dichloromethane solution was dried over MgSO$_4$. The solvent was removed by rotary evaporation, and the crude material was purified by flash chromatography on silica gel with 25% ethylacetate in hexanes. Upon elution of byproducts with 25% ethyl acetate in hexanes, pure ethylacetate was employed for elution of the title compound. The solvent was evaporated to yield the title compound as a white solid (91 mg, 82%).

¹H NMR (600 MHz, C$_6$D$_6$): δ 12.70 (s, 1H), 2.44 (s, 1H), 2.14 (dd, J = 8.5, 5.7 Hz, 1H), 2.01 (s, 1H), 1.84-1.76 (m, 1H), 1.44 (d, J = 9.7 Hz, 1H), 1.28-1.18 (m, 3H), 0.96-0.84 (m, 3H).

^{13}**C NMR** (151 MHz, C$_6$D$_6$): δ 183.0, 46.3, 40.8, 36.3, 35.9, 33.7, 29.1, 28.3. These data match data from previous reports.[53]

[((*S*)-DTBM-Segphos)Ir(Cl)(η^2-1-octene)], (28)
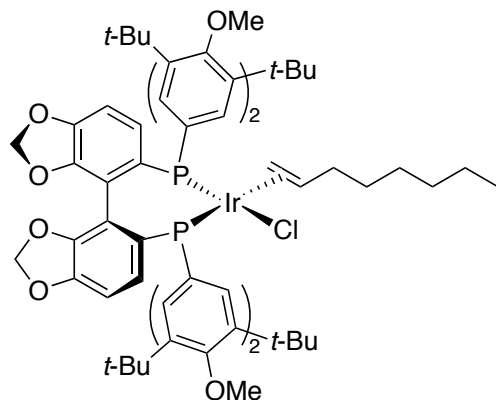
In a nitrogen-filled dry-box, an oven-dried 20 ml screw-capped vial was charged with [Ir(coe)$_2$Cl]$_2$ (60. mg, 0.067 mmol) and (*S*)-DTBM-SEGPHOS (158 mg, 0.13 mmol). Pentane (1.0 ml) was added to these solids and suspension was stirred vigorously for 10 min. 1-octene (3.0 ml, 20. mmol) was added to the slurry, which immediately formed a dark red solution. The solution was allowed to sit at room temperature for 30 min at which point red crystals began to form. The vial was cooled to -35 °C for 12 h. The red solid was filtered through a fritted funnel and washed with cold pentanes (-35 °C, 3 x 2 ml). The fluffy red solid was dissolved in benzene and lyophilized under vacuum to remove co-crystallized pentane and 1-octene. The title compound was isolated as an air sensitive red solid (180 mg, 88% yield).

^{1}**H NMR** (600 MHz, C$_6$D$_6$): δ 9.82-7.21 (m, 8H), 7.00 (br s, 1H), 6.92-6.79 (m, 1H), 6.24 (d, *J* = 7.5 Hz, 1H), 6.14 (d, *J* = 7.7 Hz, 1H), 5.44 (s, 1H), 5.14 (s, 1H), 5.02 (s, 1H), 4.95 (s, 1H), 4.48 (br s, 1H), 3.82 (br s, 1H), 3.50 (overlapping singlets, 6H), 3.33 (s, 3H), 3.28 (s, 3H), 2.91 (br s, 1H), 2.62 (br s, 1H), 2.08 (br s, 1H), 1.64-1.19 (m, 80H), 0.86 (t, *J* = 6.4 Hz, 3H).

^{31}**P NMR** (243 MHz, CDCl$_3$): δ 23.2 (d, *J* = 29.7 Hz), 12.4 (d, *J* = 28.2 Hz).

Anal. Calcd for C$_{82}$H$_{116}$ClIrO$_8$P$_2$: C 64.82%, H 7.70%; Found: C 65.10%, H 7.84%.

X-ray structure determination of 28: Single crystals for x-ray analysis were obtained by dissolving [Ir(coe)$_2$Cl]$_2$ (8 mg, 0.009 mmol) and (*S*)-DTBM-SEGPHOS (21 mg, 0.018 mmol) in 1-octene (50 mg, 0.45 mmol) and pentane (1.0 ml) in a 4 ml vial. The vial was sealed with a Teflon-lined cap and the red solution was allowed to sit undisturbed for 24 h. Over this period, red crystalline clusters formed at the bottom of the vial. A red rod 0.06 x 0.06 x 0.04 mm in size was mounted on a Cryoloop with Paratone oil. Data were collected in a nitrogen gas stream at 100(2) K using phi and omega scans. Crystal-to-detector distance was 40 mm and exposure time was 20 seconds per frame using a scan width of 0.5°. Data collection was 99.2% complete to 25.00° in q. A total of 67021 reflections were collected covering the indices, -17<=*h*<=17, -22<=*k*<=21, -38<=*l*<=30. 15437 reflections were found to be symmetry independent, with an R$_{int}$ of 0.0594. Indexing and unit cell refinement indicated a primitive, orthorhombic lattice. The space group was found to be P2(1)2(1)2(1) (No. 19). The data were integrated using the Bruker SAINT software program and scaled using the SADABS software program. Solution by direct methods (SIR-2011) produced a complete heavy-atom phasing model consistent with the proposed structure. All non-hydrogen atoms were refined anisotropically by full-matrix least-squares (SHELXL-97). All hydrogen atoms were placed using a riding model. Their positions were constrained relative to their parent atom using the appropriate

HFIX command in SHELXL-97. Short non-bonding inter H..H contacts were measured as a result of the rotational disorder of C56, C57, C58, and C59 of the *tert*-butyl group and C55 of the methoxy group.
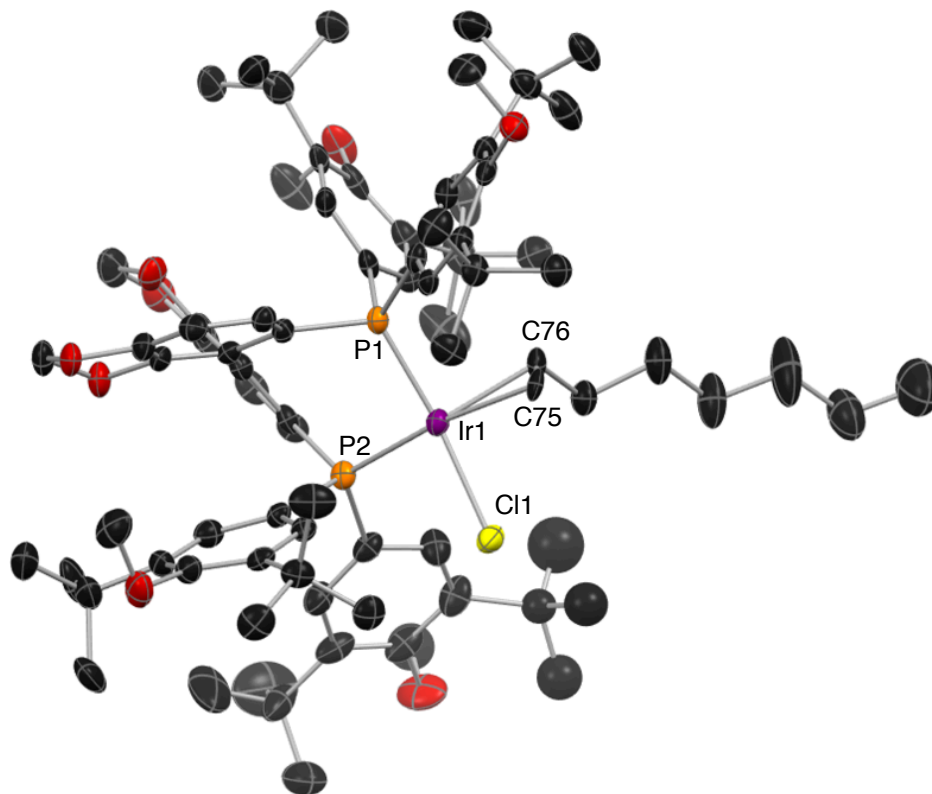
Figure 4.6. ORTEP representation of complex **28**. All hydrogens were omitted for clarity. Thermal ellipsoids are drawn at the 50% probability level.

Table 4.6. Selected bond lengths (Å) and bond angles (°).

Bond Lengths (Å)		Bond Angles (°)	
Ir1–C75	2.196	P2–Ir1–C75	177.8°
Ir1–C76	2.166	P2–Ir1–C76	143.0°
Ir1–Cl1	2.401		
Ir1–P1	2.211		
Ir1–P2	2.302		
C75–C76	1.379		

Table 4.7. Crystal data and structure refinement for 28.

Empirical formula	C82 H116 Cl Ir O8 P2
Formula weight	1519.34
Temperature	100(2) K
Wavelength	0.71073 Å
Crystal system	Orthorhombic
Space group	P2(1)2(1)2(1)
Unit cell dimensions	a = 14.6721(8) Å a= 90°.
	b = 18.2645(9) Å b= 90°.
	c = 32.1473(15) Å g = 90°.
Volume	8614.8(7) Å^3
Z	4
Density (calculated)	1.171 Mg/m^3
Absorption coefficient	1.666 mm^{-1}
F(000)	3184
Crystal size	0.06 x 0.06 x 0.04 mm^3
Crystal color/habit	red rod
Theta range for data collection	1.53 to 25.42°.
Index ranges	-17<=h<=17, -22<=k<=21, -38<=l<=30
Reflections collected	67021
Independent reflections	15437 [R(int) = 0.0594]
Completeness to theta = 25.00°	99.2 %
Absorption correction	Semi-empirical from equivalents
Max. and min. transmission	0.9364 and 0.9067
Refinement method	Full-matrix least-squares on F^2
Data / restraints / parameters	15437 / 0 / 869
Goodness-of-fit on F^2	1.020
Final R indices [I>2sigma(I)]	R1 = 0.0379, wR2 = 0.0780
R indices (all data)	R1 = 0.0465, wR2 = 0.0808
Absolute structure parameter	-0.013(4)
Largest diff. peak and hole	0.879 and -0.611 e.Å^{-3}

Table 4.8. Atomic Coordinates of 28[a]

Atom	x	y	z	U(eq)
C(1)	837(3)	3251(2)	3386(1)	23(1)
C(2)	1497(3)	3358(2)	3089(1)	26(1)
C(3)	1293(4)	3523(3)	2676(2)	34(1)
C(4)	368(4)	3518(2)	2568(2)	36(1)
C(5)	-333(4)	3498(2)	2871(2)	30(1)
C(6)	-80(3)	3346(2)	3279(2)	27(1)
C(7)	2094(4)	3719(3)	2386(2)	44(2)
C(8)	2625(4)	4337(3)	2601(2)	45(1)
C(9)	2732(5)	3057(3)	2330(2)	80(2)
C(10)	1837(5)	4021(3)	1952(2)	59(2)
C(11)	207(5)	2841(3)	1949(2)	65(2)
C(12)	-1329(4)	3678(3)	2767(2)	44(2)
C(13)	-1337(4)	4455(3)	2562(2)	50(2)
C(14)	-1921(4)	3720(3)	3159(2)	49(2)
C(15)	-1775(4)	3130(3)	2461(2)	57(2)
C(16)	749(3)	3870(2)	4199(1)	21(1)
C(17)	489(3)	4500(2)	3997(1)	24(1)
C(18)	284(3)	5157(2)	4203(1)	25(1)
C(19)	261(3)	5129(3)	4639(2)	30(1)
C(20)	594(3)	4515(3)	4865(1)	25(1)
C(21)	841(3)	3901(2)	4635(1)	24(1)
C(22)	148(4)	5853(3)	3931(2)	36(1)
C(23)	212(4)	6580(3)	4166(2)	48(2)
C(24)	926(5)	5869(3)	3606(2)	48(2)
C(25)	-750(4)	5806(3)	3697(2)	52(2)
C(26)	-1031(4)	5780(3)	4878(2)	43(1)
C(27)	738(4)	4524(3)	5336(2)	30(1)
C(28)	1387(4)	5159(3)	5453(2)	39(1)
C(29)	1199(4)	3808(3)	5492(2)	41(2)
C(30)	-155(4)	4606(3)	5574(2)	45(2)
C(31)	360(3)	2326(2)	4075(1)	21(1)
C(32)	-128(3)	2369(2)	4452(1)	24(1)
C(33)	-730(3)	1822(3)	4585(2)	28(1)
C(34)	-835(3)	1243(3)	4323(2)	27(1)
C(35)	-1401(4)	322(3)	3966(2)	35(1)
C(36)	-365(3)	1185(2)	3954(1)	26(1)
C(37)	249(3)	1701(2)	3818(1)	23(1)
C(38)	716(3)	1577(3)	3409(2)	24(1)
C(39)	173(4)	1454(3)	3059(2)	27(1)
C(40)	-945(5)	1126(3)	2646(2)	50(2)
C(41)	535(4)	1310(3)	2675(2)	35(1)
C(42)	1451(4)	1291(3)	2609(2)	36(1)
C(43)	2011(4)	1398(2)	2956(1)	30(1)

C(44)	1667(3)	1528(2)	3351(1)	23(1)
C(45)	3494(3)	1265(3)	3572(2)	29(1)
C(46)	3598(4)	516(3)	3514(2)	36(1)
C(47)	4338(4)	228(3)	3305(2)	39(1)
C(48)	4990(4)	723(3)	3154(2)	39(1)
C(49)	4928(4)	1467(3)	3219(2)	42(2)
C(50)	4164(4)	1725(3)	3428(2)	39(1)
C(51)	4421(4)	-601(3)	3239(2)	56(2)
C(52)	5297(5)	-911(4)	3394(2)	73(2)
C(53)	4440(7)	-742(5)	2744(3)	124(4)
C(54)	3606(6)	-979(4)	3382(3)	113(4)
C(55)	5464(12)	562(9)	2447(5)	83(6)
C(55A)	6563(10)	581(8)	3297(4)	73(5)
C(56)	5790(10)	1997(7)	3154(4)	45(4)
C(57)	5497(16)	2484(12)	2875(6)	117(7)
C(58)	5965(10)	2466(8)	3544(5)	71(5)
C(59)	6681(10)	1632(8)	3125(5)	76(5)
C(56A)	5501(14)	2016(11)	3012(7)	80(6)
C(57A)	4826(16)	2661(12)	2744(7)	134(8)
C(58A)	5780(9)	2649(7)	3262(4)	53(4)
C(59A)	6085(9)	1856(7)	2636(4)	60(4)
C(60)	2064(3)	1003(2)	4184(1)	22(1)
C(61)	2189(3)	1200(2)	4594(1)	24(1)
C(62)	1924(3)	760(3)	4925(1)	24(1)
C(63)	1456(3)	120(3)	4820(2)	30(1)
C(64)	1397(4)	-151(3)	4404(2)	32(1)
C(65)	1684(3)	327(2)	4095(2)	31(1)
C(66)	2139(4)	1051(3)	5371(2)	32(1)
C(67)	1512(4)	1701(3)	5463(2)	50(2)
C(68)	2056(4)	491(3)	5722(2)	44(2)
C(69)	3137(4)	1298(3)	5376(2)	38(1)
C(70)	168(4)	-22(4)	5250(2)	53(2)
C(71)	1102(4)	-935(3)	4297(2)	46(2)
C(72)	151(4)	-1136(3)	4454(2)	59(2)
C(73)	1799(4)	-1453(3)	4509(2)	56(2)
C(74)	1114(5)	-1080(3)	3833(2)	54(2)
C(75)	2937(3)	3882(2)	4343(1)	25(1)
C(76)	2976(4)	3929(2)	3915(2)	31(1)
C(77)	3857(4)	3966(3)	3680(2)	35(1)
C(78)	4168(4)	4769(3)	3628(2)	48(2)
C(79)	5125(5)	4834(4)	3454(2)	66(2)
C(80)	5479(6)	5595(4)	3470(3)	102(3)
C(81)	6500(5)	5692(4)	3324(3)	81(2)
C(82)	6823(6)	6438(5)	3391(3)	119(4)
O(1)	104(3)	3550(2)	2152(1)	46(1)
O(2)	-58(2)	5717(2)	4868(1)	33(1)

O(3)	-1378(2)	629(2)	4379(1)	34(1)
O(4)	-588(2)	529(2)	3762(1)	33(1)
O(5)	-755(2)	1483(2)	3032(1)	37(1)
O(6)	-151(3)	1209(2)	2390(1)	43(1)
O(7)	5732(3)	456(3)	2939(1)	67(1)
O(8)	1046(3)	-304(2)	5131(1)	43(1)
P(1)	1166(1)	3062(1)	3925(1)	22(1)
P(2)	2455(1)	1658(1)	3791(1)	24(1)
Cl(1)	4043(1)	2449(1)	4361(1)	32(1)
Ir(1)	2607(1)	2813(1)	4069(1)	23(1)

[a]Values represent atomic coordinates x 10^4 and equivalent isotropic displacement parameters (Å^2 x 10^3) for **28**. U(eq) is defined as one third of the trace of the orthogonalized U tensor.

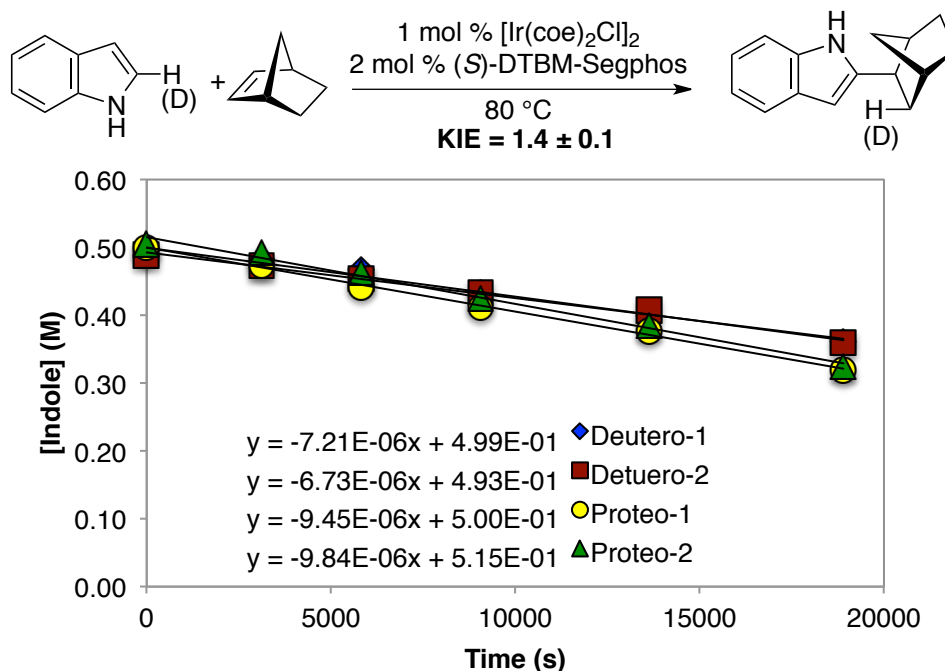**Studies on the kinetic isotope effect on the Ir-catalyzed addition of 2-H-indole and 2-D-indole to norbornene.**

Figure 4.7. Consumption of starting material as a function of time.

Solutions described in Table S4 were made following general procedure **A**. The reaction mixture was stirred in an aluminum heating block at 80 °C outside of the dry-box. The reaction was removed every hour, and rapidly cooled in a water bath. The vial was taken into the dry-box, and a 10 μl aliquot was removed from the reaction mixture. The vial was resealed and returned to the metal heating block. The aliquots were analyzed by gas chromatography with dodecane as the internal standard. Reaction rates were determined by measuring consumption of starting material at low conversion (up to 30%). An example of the raw data acquired by gas chromatography analysis is provided in Figure S2. (Note: reactions conducted for kinetic measurements were run at lower temperatures and with lower catalyst loadings than those for evaluating the reaction scope and obtaining isolated product. The lower temperatures and catalyst loading allowed a sufficient number of data points to be collected at low conversions to obtain reproducible rates.)

Table 4.9. Reactions conditions for rate measurements.

Entry	[Indole] M	[nbe] M	[catalyst] mM	Rate (M/s)
Deutero-1	0.5	1.5	10	$7.2\pm0.4 \times 10^{-6}$
Deutero-2	0.5	1.5	10	$6.7\pm0.4 \times 10^{-6}$
Proteo-1	0.5	1.5	10	$9.5\pm0.4 \times 10^{-6}$
Proteo-2	0.5	1.5	10	$9.8\pm0.4 \times 10^{-6}$

4.5 References

(1)   Part of this chapter was reprinted with permission from Sevov, C. S.; Hartwig, J. F. *J. Am. Chem. Soc.*, **2013**, *135*, 2116. Copyright © 2013, American Chemical Society. Permission to include this co-authored material was obtained from John F. Hartwig.

(2)   Price, C. C. *Organic Reactions*, **1946**, *3*, 1.

(3)   Olah, G. A. *Friedel–Crafts Chemistry*; Wiley-Interscience: New York, NY, 1973.

(4)   Periana, R. A.; Liu, X. Y.; Bhalla, G. *Chem. Commun.*, **2002**, 3000.

(5)   Lail, M.; Arrowood, B. N.; Gunnoe, T. B. *J. Am. Chem. Soc.*, **2003**, *125*, 7506.

(6)   Oxgaard, J.; Periana, R. A.; Goddard, W. A. *J. Am. Chem. Soc.*, **2004**, *126*, 11658.

(7)   Bhalla, G.; Oxgaard, J.; Goddard, W. A.; Periana, R. A. *Organometallics*, **2005**, *24*, 3229.

(8)   Foley, N. A.; Lail, M.; Lee, J. P.; Gunnoe, T. B.; Cundari, T. R.; Petersen, J. L. *J. Am. Chem. Soc.*, **2007**, *129*, 6765.

(9)   Chernyak, N.; Gevorgyan, V. *J. Am. Chem. Soc.*, **2008**, *130*, 5636.

(10)   McKeown, B. A.; Foley, N. A.; Lee, J. P.; Gunnoe, T. B. *Organometallics*, **2008**, *27*, 4031.

(11)   Nakao, Y.; Kanyiva, K. S.; Hiyama, T. *J. Am. Chem. Soc.*, **2008**, *130*, 2448.

(12)   Nakao, Y.; Kashihara, N.; Kanyiva, K. S.; Hiyama, T. *J. Am. Chem. Soc.*, **2008**, *130*, 16170.

(13)   Colby, D. A.; Bergman, R. G.; Ellman, J. A. *Chem. Rev.*, **2009**, *110*, 624.

(14)   Foley, N. A.; Lee, J. P.; Ke, Z.; Gunnoe, T. B.; Cundari, T. R. *Acc. Chem. Res.*, **2009**, *42*, 585.

(15)   Nakao, Y.; Idei, H.; Kanyiva, K. S.; Hiyama, T. *J. Am. Chem. Soc.*, **2009**, *131*, 15996.

(16)   Nakao, Y.; Yamada, Y.; Kashihara, N.; Hiyama, T. *J. Am. Chem. Soc.*, **2010**, *132*, 13666.

(17)   Andreatta, J. R.; McKeown, B. A.; Gunnoe, T. B. *J. Organomet. Chem.*, **2011**, *696*, 305.

(18)   Bhalla, G.; Bischof, S. M.; Ganesh, S. K.; Liu, X. Y.; Jones, C. J.; Borzenko, A.; Tenn, I. I. I. W. J.; Ess, D. H.; Hashiguchi, B. G.; Lokare, K. S.; Leung, C. H.; Oxgaard, J.; Goddard, I. I. I. W. A.; Periana, R. A. *Green Chem.*, **2011**, *13*, 69.

(19)   Tamura, R.; Yamada, Y.; Nakao, Y.; Hiyama, T. *Angew. Chem. Int. Ed.*, **2012**, *51*, 5679.

(20)   Murai, S.; Kakiuchi, F.; Sekine, S.; Tanaka, Y.; Kamatani, A.; Sonoda, M.; Chatani, N. *Nature*, **1993**, *366*, 529.

(21)   Fujii, N.; Kakiuchi, F.; Yamada, A.; Chatani, N.; Murai, S. *Chem. Lett.*, **1997**, *26*, 425.

(22)   Murai, S.; Chatani, N.; Kakiuchi, F. *Pure Appl. Chem.*, **1997**, *69*, 589.

(23)   Sonoda, M.; Kakiuchi, F.; Chatani, N.; Murai, S. *B. Chem. Soc. Jpn.*, **1997**, *70*, 3117.

(24)   Jia, C.; Piao, D.; Oyamada, J.; Lu, W.; Kitamura, T.; Fujiwara, Y. *Science*, **2000**, *287*, 1992.

(25)   Jun, C.-H.; Hong, J.-B.; Kim, Y.-H.; Chung, K.-Y. *Angew. Chem. Int. Ed.*, **2000**, *39*, 3440.

(26) Lim, S.-G.; Lee, J. H.; Moon, C. W.; Hong, J.-B.; Jun, C.-H. *Org. Lett.*, **2003**, *5*, 2759.

(27) Lim, S.-G.; Ahn, J.-A.; Jun, C.-H. *Org. Lett.*, **2004**, *6*, 4687.

(28) Thalji, R. K.; Ellman, J. A.; Bergman, R. G. *J. Am. Chem. Soc.*, **2004**, *126*, 7192.

(29) Kuninobu, Y.; Tokunaga, Y.; Kawata, A.; Takai, K. *J. Am. Chem. Soc.*, **2005**, *128*, 202.

(30) Tarselli, M. A.; Gagne, M. R. *J. Org. Chem.*, **2008**, *73*, 2439.

(31) Tarselli, M. A.; Liu, A.; Gagne, M. R. *Tetrahedron*, **2009**, *65*, 1785.

(32) Weber, D.; Tarselli, M. A.; Gagne, M. R. *Angew. Chem. Int. Ed.*, **2009**, *48*, 5733.

(33) Bagley, M. C.; Dale, J. W.; Merritt, E. A.; Xiong, X. *Chem. Rev.*, **2005**, *105*, 685.

(34) Kim, J.; Movassaghi, M. *Chem. Soc. Rev.*, **2009**, *38*, 3035.

(35) Cho, S. H.; Kim, J. Y.; Kwak, J.; Chang, S. *Chem. Soc. Rev.*, **2011**, *40*, 5068.

(36) Cheng, Y.-J.; Yang, S.-H.; Hsu, C.-S. *Chem. Rev.*, **2009**, *109*, 5868.

(37) Mishra, A.; Ma, C.-Q.; Ba uerle, P. *Chem. Rev.*, **2009**, *109*, 1141.

(38) Schipper, D. J.; Fagnou, K. *Chem. Mater.*, **2011**, *23*, 1594.

(39) Pan, S.; Ryu, N.; Shibata, T. *J. Am. Chem. Soc.*, **2012**, *134*, 17474.

(40) Bandini, M.; Melloni, A.; Umani-Ronchi, A. *Angew. Chem. Int. Ed.*, **2004**, *43*, 550.

(41) Bandini, M.; Melloni, A.; Tommasi, S.; Umani-Ronchi, A. *Synlett*, **2005**, 1199.

(42) Tsogoeva, S. B. *Eur. J. Org. Chem.*, **2007**, *2007*, 1701.

(43) Alexakis, A.; Ba ckvall, J. E.; Krause, N.; Pàmies, O.; Diéguez, M. *Chem. Rev.*, **2008**, *108*, 2796.

(44) You, S. L.; Cai, Q.; Zeng, M. *Chem. Soc. Rev.*, **2009**, *38*, 2190.

(45) Sevov, C. S.; Zhou, J.; Hartwig, J. F. *J. Am. Chem. Soc.*, **2012**, *134*, 11960.

(46) Norbornane was detected, and the presence of this material indicated that nbe was the terminal reductant for the oxidative consumption of the heteroarene.

(47) Baran, P. S.; Guerrero, C. A.; Corey, E. J. *J. Am. Chem. Soc.*, **2003**, *125*, 5628.

(48) Wilson, R. M.; Thalji, R. K.; Bergman, R. G.; Ellman, J. A. *Org. Lett.*, **2006**, *8*, 1745.

(49) Jiao, L.; Bach, T. *J. Am. Chem. Soc.*, **2011**, *133*, 12990.

(50) Jiao, L.; Herdtweck, E.; Bach, T. *J. Am. Chem. Soc.*, **2012**, *134*, 14563.

(51) Herde, J. L.; Lambert, J. C.; Senoff, C. V.; Cushing, M. A. In *Inorganic Syntheses*; John Wiley & Sons, Inc.: 2007, p 18.

(52) Maresh, J. J.; Giddings, L.-A.; Friedrich, A.; Loris, E. A.; Panjikar, S.; Trout, B. L.; Stöckigt, J.; Peters, B.; O'Connor, S. E. *J. Am. Chem. Soc.*, **2007**, *130*, 710.

(53) Roberts, J. D.; Grutzner, J. B.; Jautelat, M.; Dence, J. B.; Smith, R. A. *J. Am. Chem. Soc.*, **1970**, *92*, 7107.
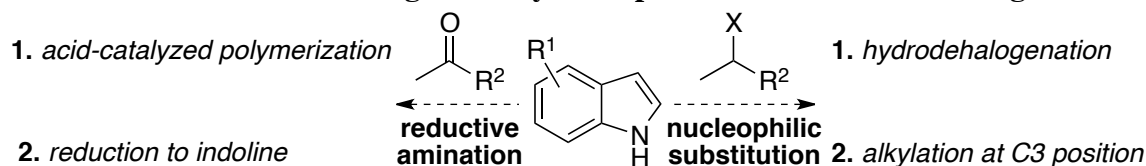
CHAPTER 5

Iridium-Catalyzed, Intermolecular Hydroamination of Unactivated Alkenes with Indoles[1]

5.1 Introduction

Nitrogen-containing heterocycles constitute many biologically active and medicinally important compounds.[2-4] The indole core is one of the most prevalent architectures found in these compounds.[5] As a result, extensive effort has been dedicated to developing new strategies for site-selective functionalization of the indole ring.[6-8] However, participation of the lone pair on nitrogen in the aromatic system renders indoles competent carbon nucleophiles as well as poor nitrogen nucleophiles. Thus, in the absence of deactivating groups,[9] intermolecular alkylation of indoles selectively at nitrogen remains challenging.[10]

Scheme 5.1. Common challenges to alkylation protocols of indoles at nitrogen

1. *acid-catalyzed polymerization*

2. *reduction to indoline*

reductive amination

nucleophilic substitution

1. *hydrodehalogenation*

2. *alkylation at C3 position*

Classical methodologies for the alkylation of amines involve substitution reactions of aliphatic electrophiles or reductive amination of carbonyl compounds.[11] However, the scope of these processes does not include reactions of indoles. Brønsted or Lewis acid-catalyzed formation of *N*-vinyl indoles that could undergo reduction is often slow and indole polymerization is common under these conditions. Furthermore, indoles are often competitively reduced to indolines under hydridic conditions.[12] Alternatively, nucleophilic substitution with secondary alkyl electrophiles leads to hydrodehalogenation or competitive alkylation at the C3 position of indole (Scheme 5.1).[13]

Alternatively, *N*-alkyl products can be synthesized by hydroamination: the formal addition of an N–H bond across an unsaturated C–C bond. Such addition reactions would exploit the abundance of alkene starting materials to form products with complete atom economy, but these reactions do not occur without a catalyst.[14] Metal-catalyzed hydroamination with indole nucleophiles provides the potential to form *N*-alkyl rather than *C*-alkyl indole products in a single step with chemo-, regio-, or stereochemical control, but there are no examples of additions of indole N–H bonds to alkenes.

Catalytic hydroamination has been studied by many researchers,[15-17] but hydroaminations of unactivated alkenes are limited in scope. Most reported hydroaminations are intramolecular cyclizations of aminoalkenes.[18-24] With few exceptions,[25-31] intermolecular hydroamination is limited to reactions of activated alkenes, such as bicycloalkenes,[32-35] vinylarenes,[36-39] allenes,[40-41] or dienes,[42-43] or to reactions of ethylene.[44-46] Hydroaminations of unactivated alkenes are conducted with solvent quantities or large excesses of the alkene and are limited to amides,[31] cyclic ureas,[29] sulfonamides,[27-28] or cyclopentyl and benzyl amines.[30] The prevalence of indole cores in biologically active molecules renders indoles an important, yet unexplored class of substrate for hydroamination.[5] Furthermore, synthesis of *N*-alkyl indoles by olefin hydroamination, instead of reaction with an alkyl electrophile, could occur selectively at the N–H bond over the nucleophilic C3 position. These reactions would provide valuable mechanistic data on reactions of N–H bonds of azoles with organometallic complexes and subsequent addition to olefins.

153

Scheme 5.2. Ir-Catalyzed C–H vs. N–H Bond Addition to Olefins
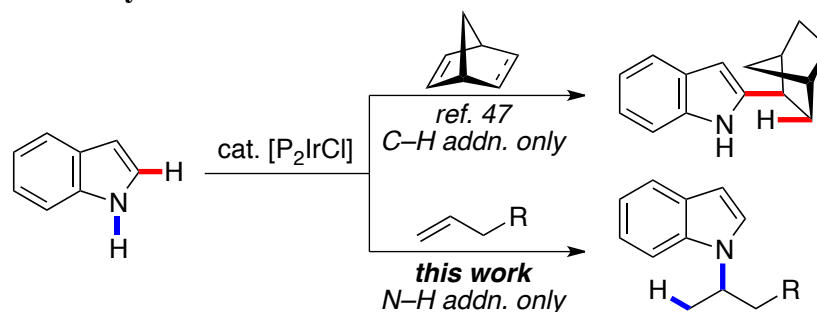
We report iridium-catalyzed additions of the N–H bond of indoles to unactivated α-olefins. In contrast to the reactions of strained alkenes, which form the products from C-H addition of indole (top of Scheme 5.2),[47] the reactions of indole with unstrained α-olefins formed exclusively the products of N-H addition (bottom of Scheme 5.2). These N-H addition reactions require as few as 1.5 equivalents of olefin and form *N*-alkylindole products in good yield. Experimental mechanistic studies reveal information about the effect of ligand on the structure of the catalyst resting-state. A combination of experimental and computational studies indicate that the barrier to insertion of alkenes into the Ir–N bond of an indolyl complex is lower than that for insertion into the Ir–C bond of the tautomer and imply that the turnover-limiting step is olefin insertion into an Ir–N bond.

5.2 Results and Discussions

Method Development. The reactions of the indole N–H bond with an α-olefin under a variety of conditions are shown in Table 5.1. Previously, we showed that Ir complexes of DTBM-Segphos (DTBM = 3,5-di-*tert*-butyl-4-methoxyphenyl) catalyze the hydrohet-eroarylation of bicycloalkenes with indoles.[47] In contrast, the combination of [Ir(cod)Cl]$_2$ (cod = 1,5-cyclooctadiene) and a series of bisphosphine ligands as catalyst led to the addition of the indole N-H bond to 1-octene in varying yields. In all cases, the reaction occurred exclusively at the N–H bond with Markovnikov selectivity to form **1**, along with smaller amounts of oxidative amination product **1-ene**. The reaction occurred with substantial enantiomeric excess (70% at 80 °C, *vide infra*), a result that rules out hydroamination of the alkene by a proton-catalyzed process alone. Trace amounts of octane were detected, suggesting that 1-octene is the terminal reductant for the oxidative process that forms **1-ene**.

Table 5.1. Development of Ir-catalyzed N–H bond addition of indole to 1-octene[a]

entry	ligand	x mol % $[Ir(cod)Cl]_2$	temp (°C)	equiv EtOAc	% 1	% 1-ene	ratio 1/1-ene
1	(*S*)-SEGPHOS	1	150	0	9	7	1.3
2	(*S*)-DM-SEGPHOS	1	150	0	15	5	3
3	(*S*)-DTBM-SEGPHOS	1	150	0	74[b]	23	3.2
4	(*S*)-DTBM-SEGPHOS	2	120	0	72	20	3.6
5	(*S*)-DTBM-SEGPHOS	2	100	0	45	11	4.1
6	(*S*)-DTBM-SEGPHOS	2	100	10	50	13	3.8
7	(*S*)-DTBM-SEGPHOS	2	100	5	52	13	4
8	**(*S*)-DTBM-SEGPHOS**	**2**	**100**	**1**	**76**[c]	**18**	**4.2**
9	(*S*)-DTBM-SEGPHOS	2	100	0.5	63	16	3.9
10[d]	(*S*)-DTBM-SEGPHOS	4	80	1	65[e]	12	5.4

[a]Yields were determined by GC analysis. [b]20% ee. [c]64% ee. [d]48 h reaction time. [e]70% ee.

Reactions conducted with Ir complexes of Segphos or DM-Segphos (DM = 3,5-dimethylphenyl) formed products in low yield at 150 °C (Table 5.1, entries 1 and 2). Much higher reactivity was observed when the bulky DTBM-analogue of Segphos was used as ligand (entry 3). The selectivity for **1** over **1-ene** was higher when the reaction was conducted at 100 °C instead of 150 °C, but **1** was formed in only 45% yield, due to slow rates and low conversion (entry 5 vs. 3). Various solvents were tested to increase the reaction rate at 100 °C, but reactions in most solvents occurred to lower conversion.
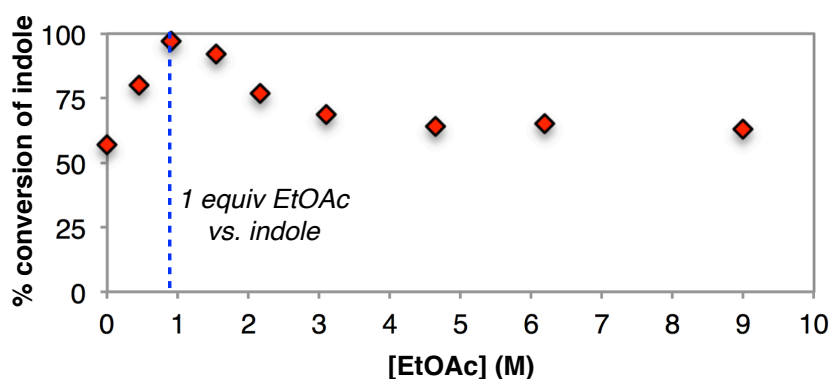

Figure 5.1. Effect of added EtOAc on reaction conversion after 18 h with 0.9 M initial indole concentration.

However, an increase in the reaction rate and yield was observed when the reactions were conducted with added EtOAc. A plot of the conversion vs. the amount of added EtOAc is given in Figure 5.1. These data show that this promoting effect of the ester is the largest with 1 equiv of EtOAc, relative to the indole (Table 5.1, entry 8) and was smaller at higher concentrations of EtOAc. This promoting effect of ester additives on the rate and conversion of the hydroamination reaction was observed for a range of other esters (Figure 5.2).
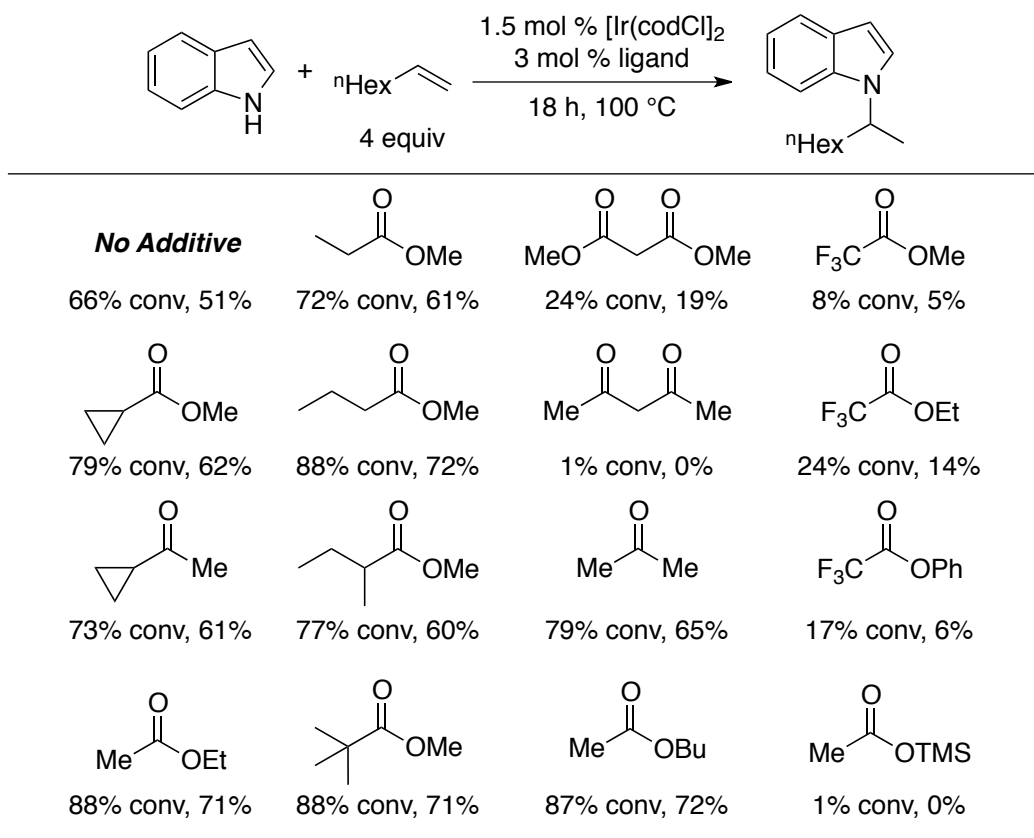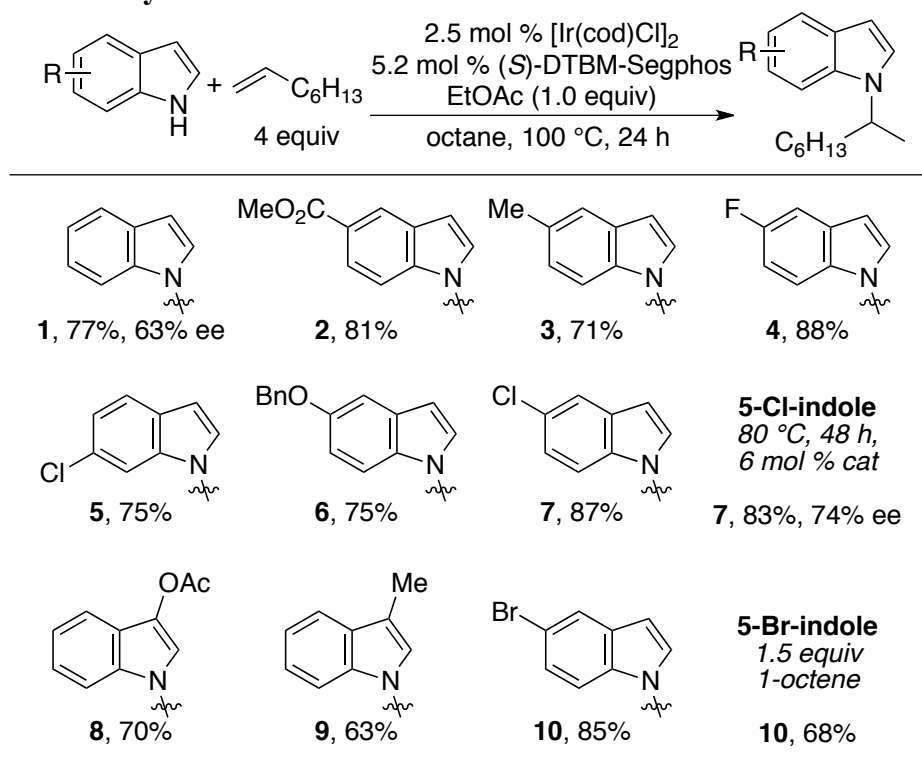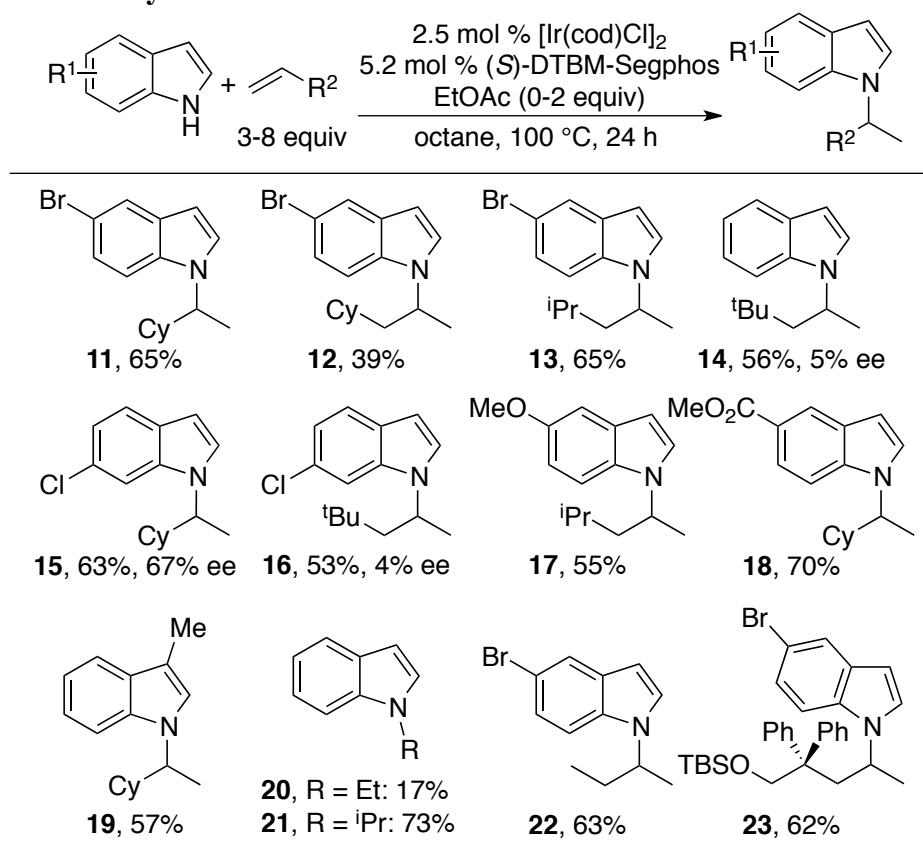

Figure 5.2. Effect of added esters or ketones on the conversion of the Ir-catalyzed hydroamination reaction.

The reaction conducted with 1 equivalent of added EtOAc proceeded with a 1.6-fold higher initial rate than the reaction conducted in the absence of EtOAc. The origin of its positive effect on reaction rate is unknown at this time; the added EtOAc was not consumed during the reaction. Nevertheless, with this protocol involving added EtOAc, the yields of reactions at 100 °C were comparable to those of reactions conducted at 150 °C without EtOAc, and smaller amounts of **1-ene** formed.

Chart 5.1. Ir-catalyzed additions of indoles to 1-octene[a]

1, 77%, 63% ee **2**, 81% **3**, 71% **4**, 88%

5, 75% **6**, 75% **7**, 87%

5-Cl-indole
80 °C, 48 h,
6 mol % cat

7, 83%, 74% ee

8, 70% **9**, 63% **10**, 85%

5-Br-indole
1.5 equiv
1-octene

10, 68%

[a]Reported yields are isolated yields.

Scope of Olefin Hydroamination with Indoles. The scope of addition of the N–H bond of a range of indoles to 1-octene by the procedure just described is illustrated in Chart 5.1. The products from addition of indoles containing benzyl or acetyl protected alcohols, esters, and halides were formed in good yield. No products were formed from reactions of indoles with substituents at the 2- or 7-positions, but electron-donating or -withdrawing substituents at the 3-position were tolerated (products **8** and **9**). The electron density of the indole ring had little influence on the final yield, but reactions of electron-poor indoles proceeded with higher rates than reactions of electron-rich indoles. The limits on the temperature at which the reaction can be performed and the amount of olefin that can be used were tested. The addition of 5-chloroindole to octene occurred at just 80 °C. Under these conditions, compound **7** was generated in a high 83% yield with 74% ee. The reaction conducted with just 1.5 equivalents of 1-octene at 100 °C formed **10** in 68% yield.

Chart 5.2. Ir-catalyzed addition of indoles to α-olefins[a]

11, 65%	**12**, 39%	**13**, 65%	**14**, 56%, 5% ee
15, 63%, 67% ee	**16**, 53%, 4% ee	**17**, 55%	**18**, 70%
19, 57%	**20**, R = Et: 17% **21**, R = iPr: 73%	**22**, 63%	**23**, 62%

[a]Reported yields are isolated yields.

The scope of alkene that undergoes the addition reaction is summarized in Chart 5.2. Products from additions to olefins containing bulky substituents near the alkene moiety were generally formed in lower yields than those from additions to 1-octene. In these reactions, significant amounts of vinyl-indole side products were formed (20% to 30%), and isomerization of the terminal alkene to unreactive internal olefin isomers was observed for reactions of allyl cyclohexane (entry **12**, 15% terminal alkene remains). Good yields of product were obtained with bulky alkenes by conducting the reaction with up to 8 equivalents of olefin. Reactions conducted with these higher concentrations of alkene required up to 2 equivalents of EtOAc to achieve an increase in the reaction rate that equals the increase observed for additions to the less hindered 1-octene (see the experimental section for conditions specific to each substrate).

Ir-catalyzed addition to gaseous alkenes was achieved with only 4 equivalents of ethene, propene, or butene (entries **20**-**22**). Reactions of indole and ethene proceed to complete conversion, but they formed **20** in poor yield as a result of competitive reaction at the C2 position of indole. In contrast, additions to propene and butene occurred exclusively at nitrogen.

Mechanistic Studies of Olefin Hydroamination with Indoles. Intermolecular hydroamination of unactivated alkenes remains challenging and reactions are generally conducted with large excesses of olefin. However, little mechanistic data are available that provides insight into that challenges associated with additions to this class of olefin. Our studies on the scope of α-olefin hydroamination with indoles has revealed that reactions can be conducted with as few as 1.5 equivalents of alkene and reactions occur at temperatures as low as 80 °C. Mechanistic study of this mild reaction, relative to other NH additions to unactivated alkenes, could provide information about the properties of the catalytic system that promote hydroamination. Thus, we conducted experimental mechanistic studies and computational studies on the reported reactions.

Isotope Labeling Experiments. We began our mechanistic investigation by measuring the enantiomeric excess (ee) with which the addition product is formed. The ee of the products from a range of Ir-catalyzed additions of indoles to α-olefins were not exceptional, but were substantial (45-74%, see the experimental section for details). In contrast to reactions of alkenes that are linear or have a tertiary branch point, the ee's of the product from the reaction of indoles with *tert*-butyl propene were only 4-5% ee (Chart 5.2: see **1** vs. **14** or **15** vs. **16**).
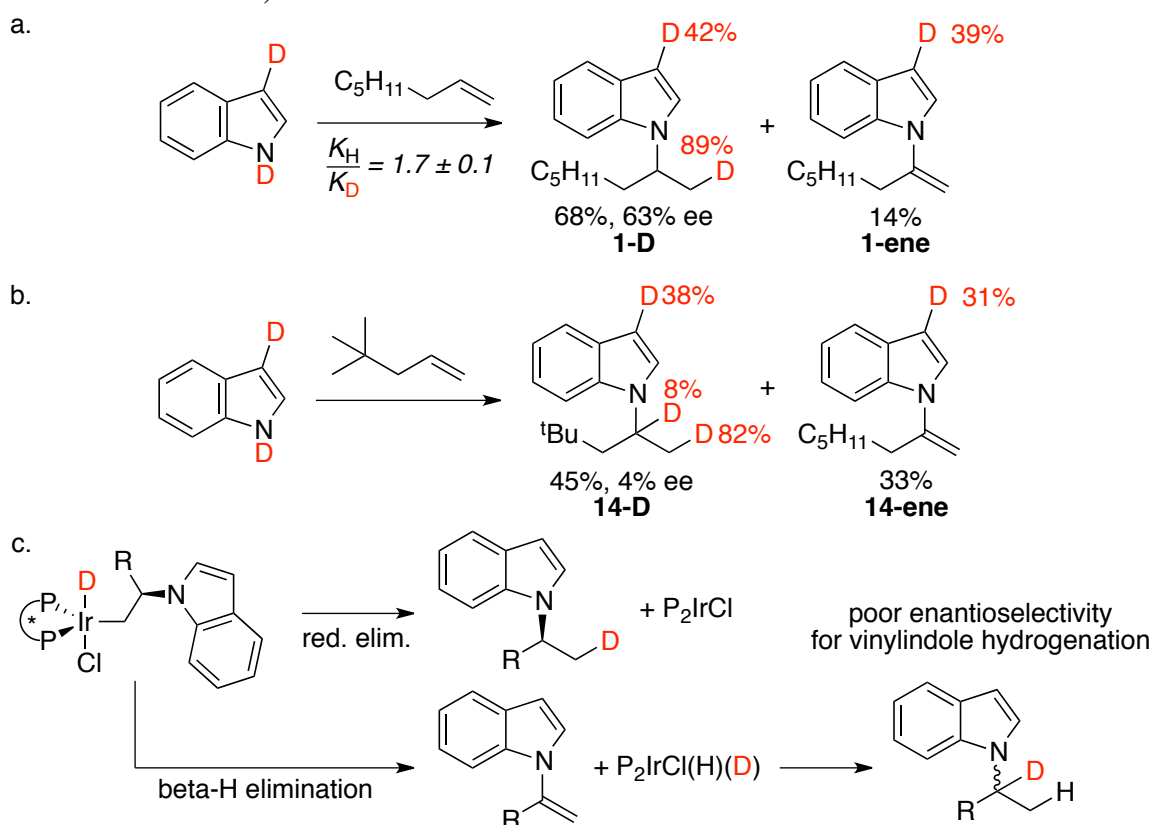

Figure 5.3. (a) Isotope distribution in the product of the reaction conducted with deutero-labeled indole and 1-octene (KIE for the relative rates in separate reaction vessels). (b) Isotope distribution in the product of the reaction conducted with deutero-labeled indole and 4,4-dimethylpent-1-ene. (c) Proposed mechanism for the incorporation of deuterium at the position alpha- to nitrogen and racemization of the product.

An isotope labeling experiment was conducted to gain insight into the mechanism of N–H bond addition across an alkene, potential side reactions, and the origin of the large differences in ee for the two classes of alkenes. The addition of 1,3-dideuterio-indole to 1-octene formed **1-D** with deuterium located exclusively β- to nitrogen (Figure 5.3a). However, addition to *tert*-butyl propene formed **14-D** with measurable amounts of deuterium α- to nitrogen (Figure 5.3b). Furthermore, a larger amount of oxidative amination product was generated from *tert*-butyl propene than from octene. Incorporation of deuterium α- to nitrogen in the product from *tert*-butyl propene likely occurs by hydrogenation of the vinyl-indole product by an Ir-D complex (Figure 5.3c).

To determine the effect of this reduction of the vinyl-indole on stereoselectivity, we determined the absolute configuration of the products from hydroamination and vinyl-indole reduction. The absolute stereochemistry of the major enantiomer of representative hydroamination product **22** was determined to be 2S by single crystal x-ray diffraction of the crystalline derivative **24** (eq 5.1). Reductive workup of vinyl-indole **1-ene** with ^{i}PrOH catalyzed by the Ir complex remaining in solution converted **1-ene** into **1**. Quantitative conversion of **1-ene** was observed, but this reduction of **1-ene** formed the opposite enantiomer of **1** than did the hydroamination reaction. These data suggest that a significant amount of **14** may be generated in low ee from unselective *in situ* reduction of **14-ene**. A similar correlation was observed during our study on the addition of amides to alpha-olefins.[31] The reactions of amides produced alkyl amide products with poor ee, along with equimolar amounts of eneamide products.

(1)
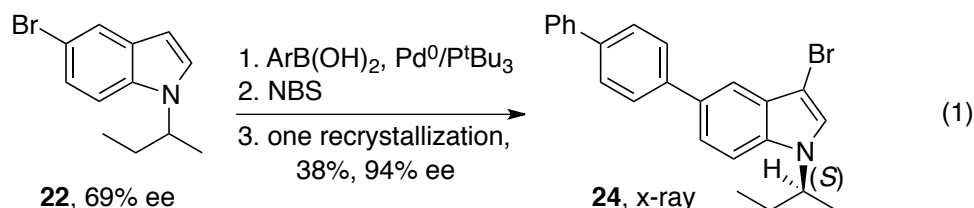
Mechanism of C–N Bond Formation. Iridium-catalyzed C–H and N–H additions to bicycloalkenes have been shown to occur by olefin insertion into an Ir–C[47] or Ir–N[48,35,31] bond, respectively. Alternatively, hydroaminations of α-olefins catalyzed by late transition metal complexes have been proposed to occur by nucleophilic attack on a coordinated olefin ligand.[45,27,29] Moreover, palladium-catalyzed oxidative amination of alkenes occurs by both syn- and anti-aminopalladation of the olefin.[49-54] Given the different chemoselectivity of Ir-catalyzed indole addition to bicycloalkenes (C-H addition) versus α-olefins (N-H addition) the mechanism of C–N bond formation in Ir-catalyzed additions to α-olefins was studied.
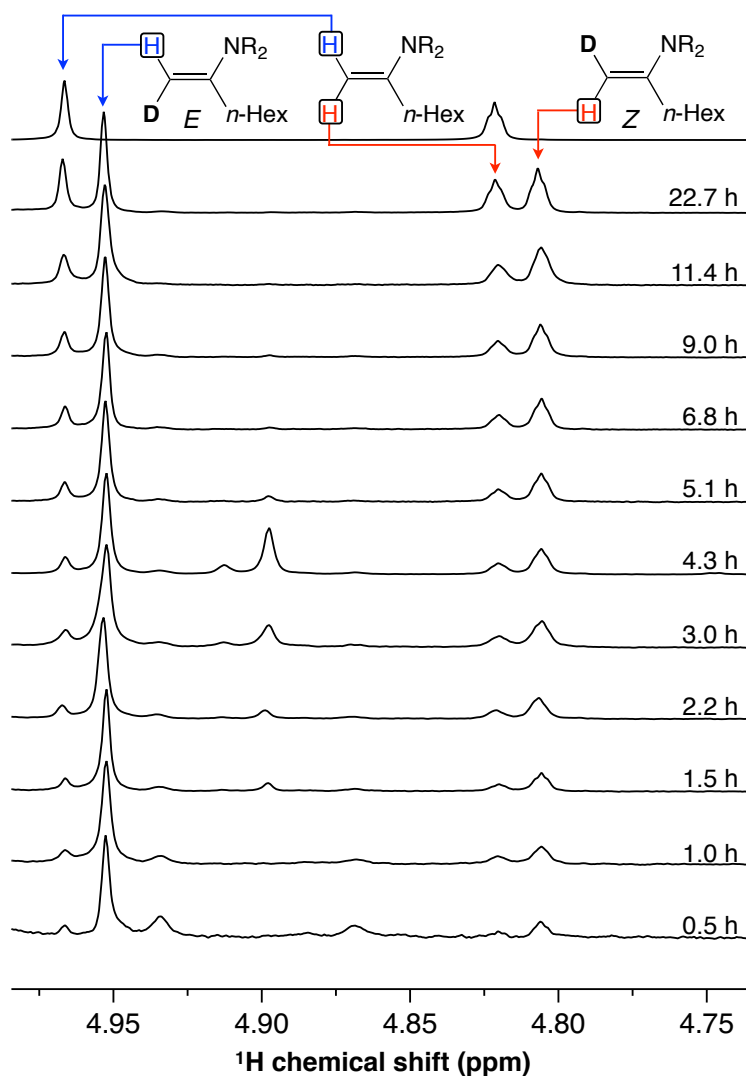
Figure 5.4. Observed products at multiple timepoints for the amination of (*E*)-octene-1-d$_1$ with indole.

To distinguish between the pathways described above, the geometry of the vinyl-indole products from reactions with geometrically defined alkenes was determined. The Ir-catalyzed reaction was performed with indole and (*E*)-D-octene (Figure 5.5a). The ^{1}H NMR chemical shift of the vinylic protons of **1-ene** were assigned by NOESY. After 23 h a 1:1 ratio of *E* and *Z* isomers of **1-ene** had formed (Figure 5.4, top). When the reaction was monitored at lower conversions, (***E***)-**1-ene** was observed as the major vinyl-indole isomer (Figure 5.4 and 5.5b). These results suggest that (***E***)-**1-ene** is the product of the Ir-catalyzed reaction, while the *Z* isomer is formed by isomerization of the *E* isomer. The formation of (***E***)-**1-ene** as the kinetic product is consistent with a mechanism involving migratory insertion of (*E*)-D-octene into an Ir–N bond, followed by stereospecific *β*-H elimination, as illustrated in Figure 5.5c.
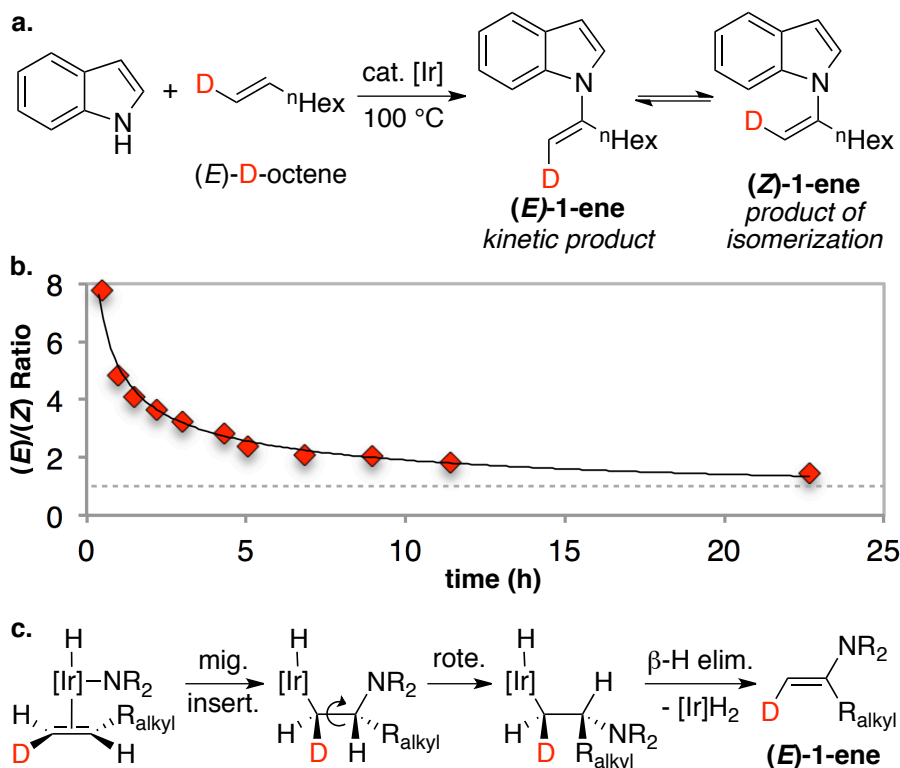
161

Figure 5.5. (a) Ir-catalyzed addition of indole to (*E*)-D-octene. (b) Ratio of (*E*)-**1-ene** to (*Z*)-**1-ene** vs. time. (c) Proposed mechanism for the stereospecific formation of (*E*)-**1-ene**.

Characterization of the Resting State Ir Complexes. The mode by which the indole binds to the catalyst was determined by synthesis of potential intermediates and was unexpected. The reaction of DTBM-Segphos, $[Ir(cod)Cl]_2$, with 1 equivalent of indole and 10 equivalents of 1-octene cleanly formed a complex with corresponding NMR signals matching those of the major species observed during catalytic reactions. This complex was characterized by NMR spectroscopy in solution and was shown to be complex **25**, the product of C–H activation at the C2 position of indole (eq 2).
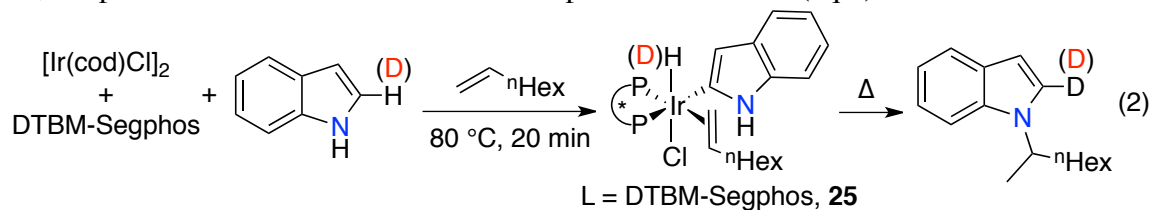
An Ir(deuteride) resonance was observed by ^2H NMR spectroscopy when a similar experiment was conducted with 2-D-indole, a result that further supports a carbon- rather than nitrogen-bound indolyl group in the catalyst resting-state. Correlations of ligand ^{31}P atoms with upfield-shifted vinylic protons at 3.1 and 2.6 ppm and with alkyl protons at 0.8 ppm were observed in the ^{31}P-^1H HMBC NMR spectrum, indicating that the sixth ligand of the octahedron is 1-octene (Figure 5.6). Although this complex contains a carbon-bound indolyl ligand, heating the solution of **25** to 100 °C for 2 h formed *N*-alkyl products **1** and **1-ene** in a combined yield of 94%. No product from reaction at the C2 position of indole was observed (eq 2, right).
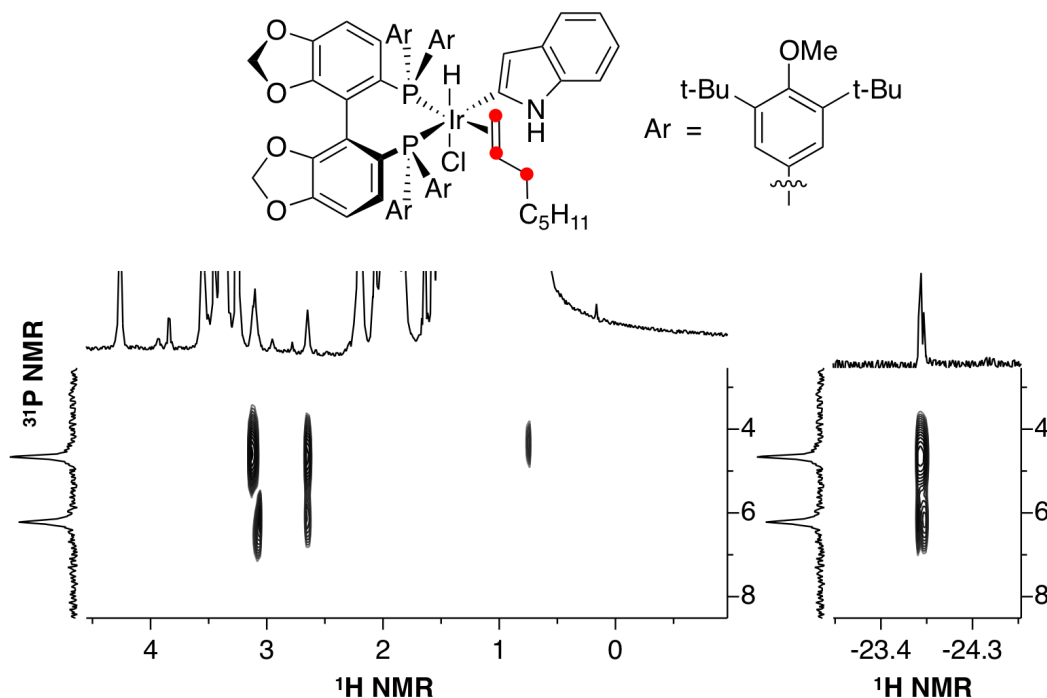
162

Figure 5.6. ^{1}H–^{31}P correlations by HMBC NMR spectroscopy. Spectral windows are limited to the regions of Ir(H) and Ir(olefin) chemical shifts.

The high solubility of **25** prevented isolation in pure form. Thus, we conducted similar stoichiometric reactions with more polar Segphos derivatives that also formed catalysts for the addition of the indole N–H bond to α-olefins, albeit less active catalysts than those containing DTBM-Segphos. In contrast to stoichiometric studies with Ir complexes of DTBM-Segphos, reaction of indole with Ir complexes of Segphos and DM-Segphos formed a product (Figure 5.7a) containing two Ir(hydride) ligands (as determined by ^{1}H NMR spectroscopy) and one indole-derived ligand per two iridium centers. In addition, the ^{31}P NMR spectrum of the new complex contained four chemically inequivalent resonances of equal intensity.

Single crystals of the Segphos-ligated version of this complex **26** were obtained, and the structure was determined by x-ray diffraction (Figure 5.7b). Complex **26** results from a rare combination of N–H and C–H oxidative addition of the same substrate to two different metal centers. Complexes **26** and **27** were prepared in the absence of 1-octene, and their spectra match those of the iridium species in the reactions of indole with 1-octene catalyzed by Ir complexes of DM-Segphos.
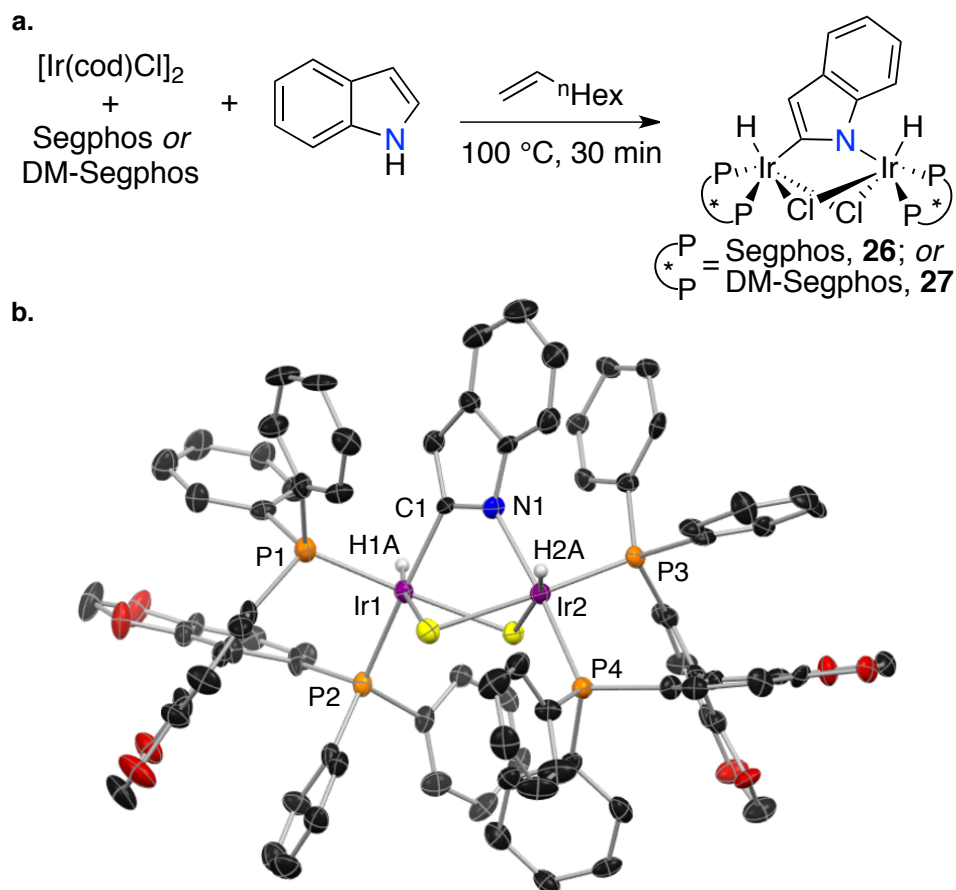
163

a.

b.

Figure 5.7. (a) Formation of the observed dinuclear catalyst resting state with Segphos or DM-Segphos as ligand. (b) Crystal structure of **26**.

One possible reaction pathway for C–N bond formation is olefin insertion into the Ir–N bond of dinuclear complexes **26** and **27**. These complexes could be generated with racemic ligand mixtures, however, diastereomers were formed that result from combinations of (*R*) and (*S*) ligand enantiomers. If the dinuclear complexes were complexes that lie on the catalytic cycle, the different diastereomers would have different rates of catalytic turnover and enantioselectivities. Thus, we tested for possible nonlinear effects on the asymmetric hydroamination of 1-octene with indole catalyzed by Ir complexes of scalemic ligand mixtures of DTBM-Segphos (Figure 5.8). The observed ee of the product matched the predicted ee, indicating that dimers **26** and **27** are likely off-cycle intermediates that form catalytically active monomers.
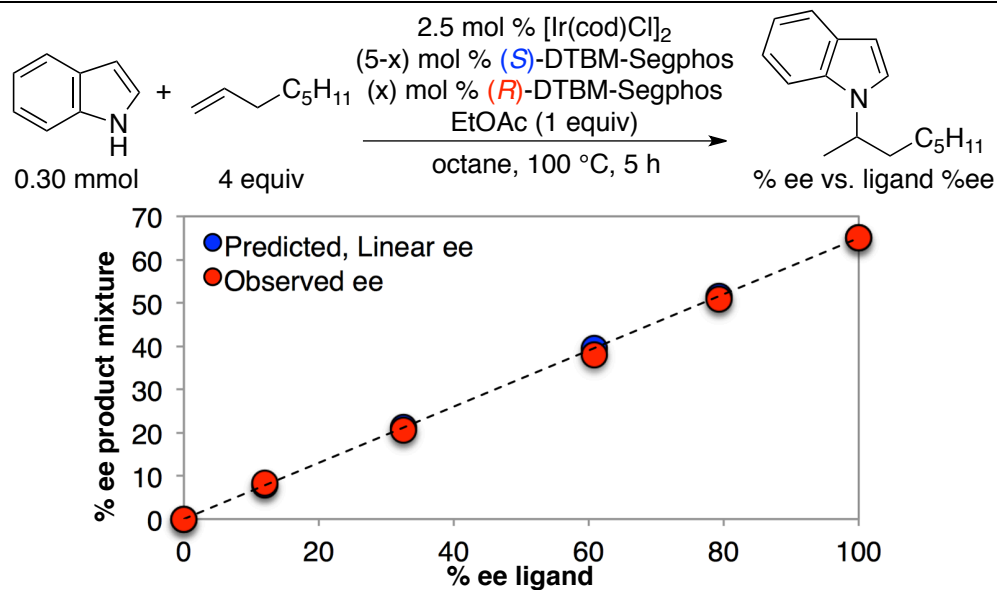
Figure 5.8. Examination of possible nonlinear effects on the asymmetric hydroamination of 1-octene with indole catalyzed by Ir complexes of scalemic ligand mixtures.

The nuclearity of **25-27** in solution was assessed by NMR DOSY techniques. The diffusion coefficients of complexes **25**-**27** were measured under the standard catalytic reaction conditions by monitoring the hydride resonances of the metal complexes. The measured values were compared to the diffusion coefficient of the known mononuclear complex **28** (Figure 5.9a). The diffusion coefficients for **26** and **27** were smaller than that for the model mononuclear complex **28**, while the diffusion coefficient of **25** was similar to that of **28**. Furthermore, DOSY NMR data for **25** were acquired with equimolar amounts of **27** (Figure 5.9b, left) and **28** (Figure 5.9b, right) present in solution as internal standards. These data are consistent with the structures for these three complexes in solution being those shown in eq 2 and Figure 5.7.
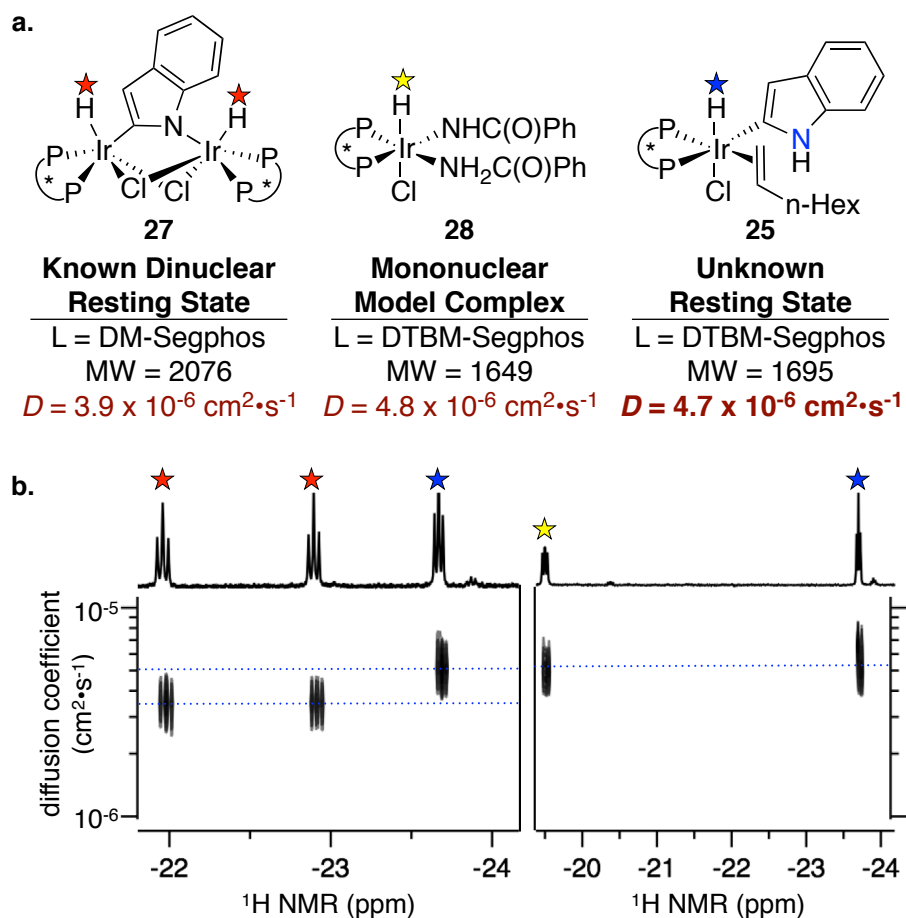
Figure 5.9. (a) Structures, molecular weights, and diffusion coefficients of **27**, **28**, and unknown resting state complex **25**. (b) NMR DOSY of the Ir-H region of complexes **25**, **27**, and **28**.

Kinetic Studies of a Representative Catalytic Reaction. Kinetic analysis of the addition of indole to 1-octene catalyzed by **25** was conducted by the method of initial rates (to 20% conversion). The reaction was found to be first order in catalyst and zeroth order in indole. The rate of the reaction was independent of the concentration of 1-octene under the standard catalytic conditions but depended positively on the concentration of alkene below 1.5 M. These measurements support a turnover-limiting step (TLS) that occurs from a resting-state containing a bound indolyl group and olefin.

The identity of the TLS was revealed by kinetic isotope effects (KIEs) and activation parameters. A comparison of the initial rates for the hydroamination of 1-octene with indole and 1,3-dideutero-indole in separate vessels revealed a KIE of 1.7 (Scheme 5.3a). Although greater than unity, this KIE is likely too small to result from a turnover-limiting N–H cleavage.[20,24] This isotope effect is more consistent with reversible oxidative addition of the indole N–H bond to the Ir center prior to the TLS.

Scheme 5.3. Proposed catalytic cycle
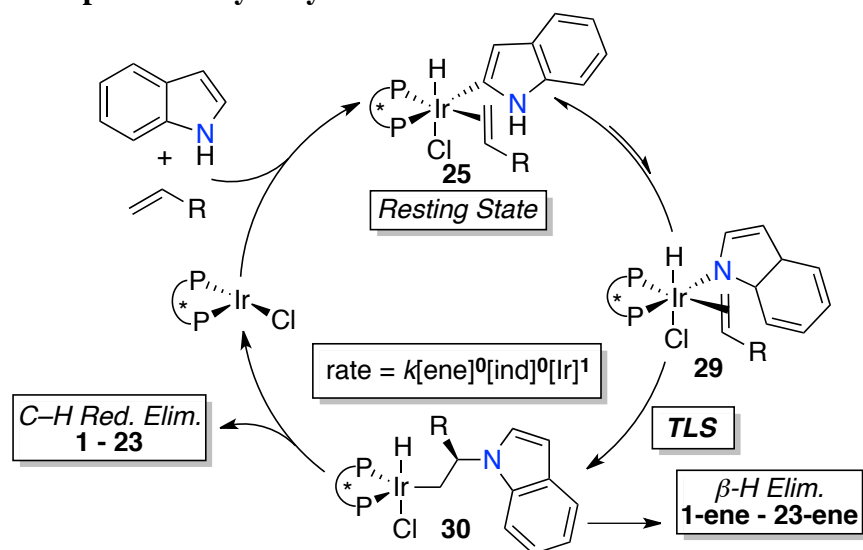
Scheme 5.3 shows a catalytic cycle that is consistent with our mechanistic data. The mononuclear resting state complex **25** is supported by the NMR DOSY experiments and a first order dependence of the rate on the conentration of iridium. The deuterium labeling experiments indicate that **25** contains a *C*-bound indolyl ligand, and ³¹P-¹H HMBC NMR spectroscopy reveals coupling correlations between resonances of the ligand phosphorus atoms and resonances of vinylic protons of a metal-bound olefin.

The isotope effect and stereochemical study revealed the events that occur from the resting state. The KIE of 1.7 suggests that reversible isomerization of *C*-bound **25** to a less stable *N*-bound intermediate **29** occurs prior to the TLS. The stereochemistry of the vinyl indole product from the reaction of (*E*)-D-octene (Figure 5.5) implied that insertion of the bound alkene into the transient *N*-bound indolyl iridium complex occurs from **29**. The alkylindole product then would be generated by C–H bond-forming reductive elimination from **30**; the vinyl-indole product would be formed by *β*-H elimination from the alkyl group of **30**.

Further data on the composition of the highest energy transition state was obtained by conducting an Eyring analysis of the observed rate constants for additions of 5-fluoroindole to 1-octene at temperatures from 353 to 396 K. These data revealed the following thermodynamic parameters for the catalytic process: $\Delta H^{\ddagger} = 30.0$ kcal/mol and $\Delta S^{\ddagger} = 6$ eu (Figure 5.10). The small $\Delta S^{\ddagger}$ is consistent with the same composition of the highest energy transition state as of the resting state. The highest energy transition state is likely the C–N bond formation, occurring by olefin insertion into the Ir–N bond of **29**.
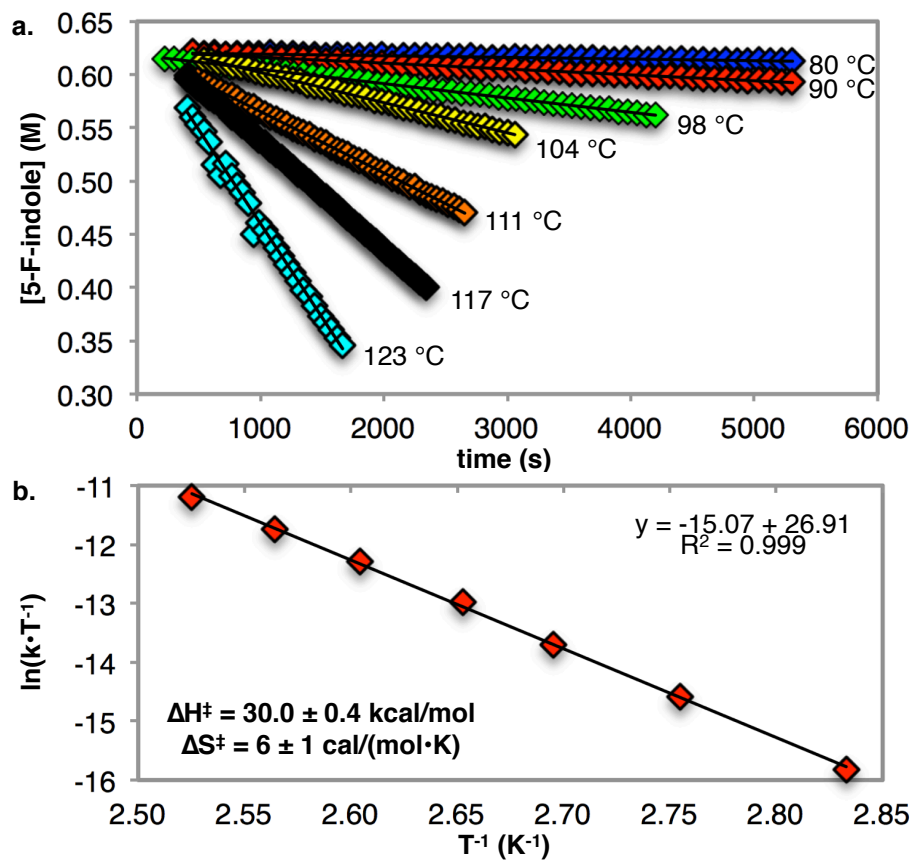
167

Figure 5.10. (a) Consumption of 5-F-indole vs. time at variable temperatures (b) Eyring analysis of the measured rate constants.

Computational Studies. This reaction system provides fundamental data on rates of alkene migratory insertion into Ir–C and Ir–N bonds. The proposed mechanism in Scheme 5.3 includes olefin insertion into the Ir–N bond of **29** to form the observed hydroamination product, even though C-bound **25** is more stable than N-bound **29**.
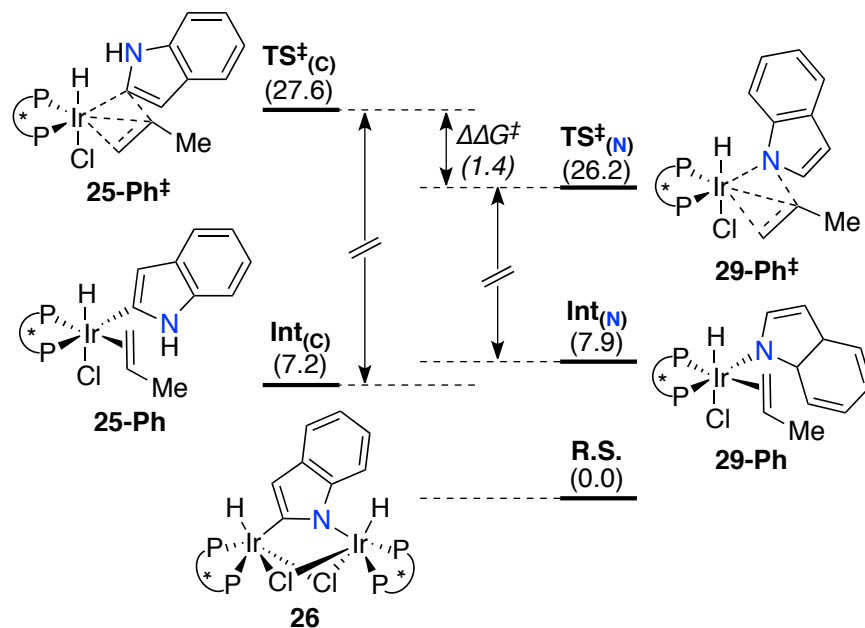

Figure 5.11. Depictions of the transition-state structures for olefin insertion into the Ir–C and Ir–N bond calculated by density functional theory. Free energies at 298 K are provided in parentheses.

To address this issue, we calculated by density functional theory (DFT) the barriers for migratory insertion reactions of propene analogues of **25** and **29**. To simplify calculations, transition states of mononuclear complexes **25-Ph‡** and **29-Ph‡** containing the parent Segphos ligand were modeled, rather than the systems containing the full DTBM-Segphos ligand. As previously discussed and illustrated in Figure 5.7, reactions catalyzed by iridium complexes of the parent Segphos ligand form a dinuclear resting state complex **26**. Thus, all calculated energies were normalized to **26** (Figure 5.11).

The calculations were conducted at the M06L level with the lanl2dz basis set for iridium and the 6-31g(d,p) basis set for all other atoms at 298 K. Solvation in mesitylene on optimized geometries was modeled at the M06L level with the lanl2tz(f) basis set for iridium and the 6-311++g** basis set for all other atoms.

Similar studies on the energy barriers for alkene insertions into late transition metal-nitrogen and metal-carbon bonds have been performed by DFT.[55] Calculations of a bisphosphine amidorhodium(I) and methylrhodium(I) complexes predicted that the barrier to ethylene insertion into the Rh–N bond of the amido complex will be lower than that for insertion into the Rh–C bond of the analogous methyl complex. These calculations suggested that a major contributing factor to the difference in rates of alkene insertion stems from the presence of a lone pair of electrons on the amido ligand. The ground state of the Rh-amido species is destabilized, relative to the analogous methyl complex, by repulsive interactions between the filled metal *d* orbital and the filled amido *p* orbital, whereas the product of insertion is stabilized by a dative Rh-N interaction. Thus, there is

less Rh-N bond cleavage than Rh-C bond cleavage in the two transition states.

Results from these prior calculations on olefin insertions of rhodium(amido) and rhodium(alkyl) are consistent with the lower energy for insertion of the alkene into the Ir-N indolide bond than for insertion into the Ir-C indolide bond required by the catalytic cycle in Scheme 5.3. However, the indolides are bound through $M-C_{sp}^2$ and $M-N_{sp}^2$ bonds, rather than $M-C_{sp}^3$ and $M-N_{sp}^3$ bonds of alkyl and amido complexes. Therefore, it is unclear whether this trend in relative rates would translate to our hydroamination of alkenes with indoles. Migratory insertion into metal aryl bonds is generally slower than insertion into metal alkyl bonds, due to the stronger metal-arene bond.[56-57] Thus, we sought to determine how the change in hybridization at nitrogen and the inclusion of the electron pair as part of an aromatic system would affect the barrier to insertion into the Ir-N bond.

All possible diastereomeric transition states of *C*-bound **25-Ph**[‡] and *N*-bound **29-Ph**[‡] were calculated. The barriers to propene insertion into the Ir–N bond by **29-Ph**[‡] fell within a range of 26-32 kcal/mol while barriers to insertion into the Ir–C bond by **25-Ph**[‡] ranged between 28-33 kcal/mol. The lowest computed barrier for propene insertion into the Ir–N bond by **29-Ph**[‡] is 1.4 kcal/mol lower than the lowest computed barrier for propene insertion into the Ir–C bond by **25-Ph**[‡]. Although the experimental difference in energies of the system with DTBM-Segphos as ligand must be higher than 1.4 kcal/mol, the results of calculations on the truncated system with Segphos as ligand follow the trend of faster insertion into the Ir–N bond of **29** than into the Ir–C bond of **25**. These computed results parallel the trend for previously studied olefin insertion into amido- and methyl-rhodium complexes and support the mechanism as required by the catalytic cycle in Scheme 4.
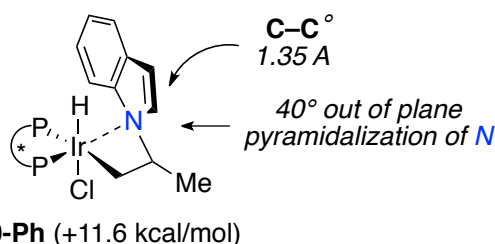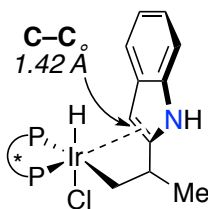

30-Ph (+11.6 kcal/mol)

Figure 5.12. Computed geometry of the product from propene migratory insertion into the Ir–N (**30-Ph**) by transition state **29-Ph**[‡].

Analysis of the optimized geometry of alkyliridium product **30-Ph** provides insight into factors that control the energy barrier for olefin insertion into *N*-indolide iridium bonds and the relationship between this insertion reaction and the insertion into an amido complex. Interaction between iridium and nitrogen through the lone pair of electrons on nitrogen is revealed by a pyramidalization of the nitrogen atom (Figure 5.12). The alkyl group on nitrogen projects 40° out of the trigonal plane. As would be expected from the hybridization at nitrogen approaching sp[3], and weak interaction of the lone pair with the π-system of the indole ring, the C2-C3 bond of the indolyl fragment in **30-Ph** has more double bond character than that of unbound indole. The alkyliridium product **30-Ph** of migratory insertion into the Ir–N bond is higher in energy than the olefin complex **29-Ph** (11.6 vs. 7.9 kcal/mol). In accordance with the Hammond postulate, this elementary reaction would have a late transition state. The nitrogen atom would be significantly pyramidalized in the transition state species. Thus, these calculations suggest that the lone pair

on nitrogen is available for stabilizing interaction with iridium in the transition state, even though the starting ligand is a planar indolide with an sp²-hybridized nitrogen.

Examination of the computed product of olefin insertion into the Ir–C bond **31-Ph** reveals that significant interaction between the C–C double bond of the indole ring with the Ir center (Figure 5.13). This alkyl intermediate is 3.8 kcal/mol more stable than the starting *C*-bound Ir(olefin)(indolyl) complex. Invoking the Hammond postulate, the transition state for olefin insertion into the Ir–C bond is early. Consequently, the observed stabilization of the metal center by the C–C double bond of indole, which is observed in the product, does not stabilize the transition state for olefin insertion into the Ir–C bond.

31-Ph (+3.4 kcal/mol)

Figure 5.13. Computed geometry of the product from propene migratory insertion into the Ir–N (**30-Ph**) by transition state **29-Ph**[‡].

5.3 Conclusions and Future Directions

In summary, we have reported a rare example of a catalytic process for the addition of the N-H bonds of indoles to simple α-olefins. This strategy for indole alkylation occurs exclusively at nitrogen. Good product yields were obtained from reactions conducted with as few as 1.5 equivalents of alkene. These data reveal properties of this catalytic system that promote hydroamination of α-olefins with indoles.

1. The bulky ligand facilitates turnover-limiting olefin insertion into the Ir–N bond.[52]

2. The bulky ligand promotes the persistence of an active mononuclear catalyst resting-state, rather than off-cycle dinuclear complexes, such as complexes of the less bulky Segphos- and DM-Segphos ligands that form dinuclear species **26** and **27**, respectively.

3. The Ir[III] complex **25** containing a hydride, a C-bound indolyl ligand and an alkene does not catalyze isomerization of the terminal alkene to less reactive internal isomers. However, bisphosphine Ir[I] complexes do catalyze isomerization; therefore reactions containing an Ir[I] resting-state tend to occur with a larger amount of alkene isomerization than the reaction described here.

4. The resting-state contains both substrate and olefin bound to the metal center. The presence of the alkene in the resting state mitigates the requirement for conducting the reaction under conditions with neat alkene because the rate of the reaction is not dependent on the concentration of alkene.

5. The reactions occurring with less formation of vinyl-indole side product occur in higher ee than those occurring with more formation of the vinyl-indole side product. The vinyl indole is reduced *in situ* to the opposite enantiomer of the product than the alkyl indole formed directly from hydroamination.

Efforts to mitigate oxidative amination processes and increase the enantioselectivity of the reaction are in progress.

5.4 Experimental

General Remarks

Unless noted otherwise, all manipulations were performed in a nitrogen-filled glovebox. Glassware was dried at 130 °C for at least 4 hours before use. Pentane, Et_2O, THF, benzene and toluene were collected from a solvent purification system containing a 0.33 m column of activated alumina under nitrogen. Benzene-d_6 was degassed and subjected to 4 Å molecular sieves for at least 4 hours prior to use. All reagents purchased from commercial suppliers were stored in the glove box and used as received. Bisphosphine ligands were purchased from Strem Chemical Co. and used as received.

^{1}H NMR spectra were obtained at 500 MHz or 600 MHz with a 45° pulse and a 10 s delay time, and chemical shifts were recorded relative to protiated solvents ($CHCl_3$ in $CDCl_3$: $\delta 7.27$ ppm; $C_6H_nD_{6-n}$ in C_6D_6: $\delta 7.15$ ppm). ^{13}C NMR spectra were obtained at 126 MHz or 151 MHz on a 500 MHz or 600 MHz instrument, respectively. ^{31}P NMR spectra were obtained at 202.2 MHz on a 500 MHz instrument, and chemical shifts were reported in parts per million downfield of 85% H_3PO_4. ^{19}F NMR spectra were referenced to an external standard of $CFCl_3$. Probe temperatures for variable temperature NMR experiments were measured by ^{1}H shifts of neat ethylene glycol. Proof of purity is demonstrated by elemental analysis and by copies of NMR spectra. Chiral HPLC analysis was conducted on a Waters chromatography system with a dual wavelength detector at 220 and 254 nm.

GC analysis was performed on an Agilent 7890 GC equipped with an HP-5 column (25 m x 0.20 mm x 0.33 μm film) and an FID detector. Quantitative GC analysis was performed by adding dodecane as an internal standard to the reaction mixture upon completion of the reaction. Response factors for the products relative to the internal standard were measured for kinetic studies and reaction development. GC-MS data were obtained on an Agilent 6890-N GC system containing an Alltech EC-1 capillary column and an Agilent 5973 mass selective detector.

General Procedure: Ir-catalyzed addition of indoles to α-olefins.
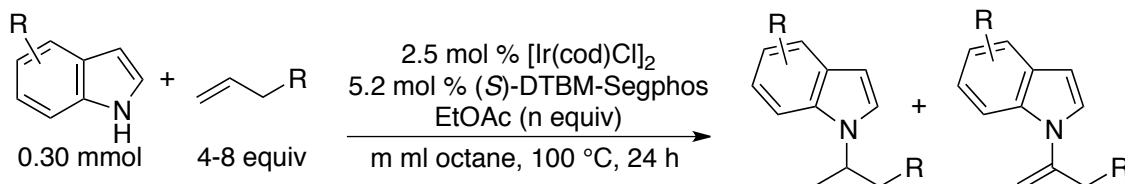
In a nitrogen-filled dry-box, an oven dried volumetric flask (5.0 ml) was charged with [Ir(cod)Cl]$_2$ (84.0 mg, 0.125 mmol) and (S)-DTBM-Segphos (306 mg, 0.260 mmol). Diethyl ether was added to the volumetric flask to the desired volume (5.0 ml). The resulting mixture was stirred at room temperature for 30 minutes until the solids dissolved. Separately, a 4 ml screw-capped vial was charged with the corresponding indole (0.30 mmol). The solution of [Ir(cod)Cl]$_2$ and (S)-DTBM-Segphos (0.30 ml, 0.015 mmol [Ir(cod)Cl]$_2$, 0.016 mmol (S)-DTBM-Segphos) was added by syringe to the vial containing the indole. The solvent was removed under vacuum in the dry-box. To the green residue was added the corresponding alkene, the appropriate amount of octane, and the appropriate amount of ethyl acetate that is specific to each reaction. The magnetic stirbar was returned to the vial, and the vial was sealed tightly with a Teflon cap. The vial was

removed from the dry-box, and the reaction mixture was stirred in an aluminum heating block at 100 °C. After 24 h the vial was allowed to cool to room temperature, and the solvents were removed by rotary evaporation. The product was purified by flash chromatography on a column (height = 20. cm, diameter = 3.0 cm) of Silacycle Siala-P60 silica gel (55 g). The conditions for chromatography and other data that are specific to each compound are given below.

1-(Octan-2-yl)-indole
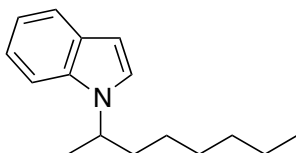
Following the general procedure **A** described above, indole (35 mg, 0.30 mmol) was allowed to react with 1-octene (180 μl, 1.2 mmol) in the presence of octane (180 μl) and ethyl acetate (30. μl, 0.30 mmol). The crude material was purified by flash chromatography with hexanes as eluent. The fractions were monitored by thin layer chromatography with a UV lamp. The material to elute first was determined to be the enamine product and was discarded. The second spot to elute was determined to be the title compound (R_f = 0.3, hexanes). The solvent was evaporated to yield the title compound as a clear oil (53 mg, 77% yield).

^{1}H NMR (600 MHz, C_6D_6): δ 7.72 (d, J = 7.6 Hz, 1H), 7.23 (s, 2H), 7.20-7.15 (m, 1H), 6.86 (s, 1H), 6.57 (s, 1H), 4.11-3.94 (m, 1H), 1.60-1.48 (m, 1H), 1.43-1.29 (m, 1H), 1.19-0.89 (m, 11H), 0.80 (t, J = 7.2 Hz, 3H).

^{13}C NMR (151 MHz, C_6D_6): δ 136.2, 128.9, 123.5, 121.2, 121.1, 119.3, 109.4, 101.6, 51.1, 36.9, 31.5, 29.0, 26.2, 22.5, 20.9, 13.9.

HPLC analysis: 63% ee, Chiralcel OD-H column, 100% hexane, 0.7 mL/min flow rate, 220 nm and 254 nm UV lamp, $t_{[minor]}$ = 53.5 min, $t_{[major]}$ = 56.2 min.

Anal. Calcd for $C_{16}H_{23}N$: C 83.79%, H 10.11%, N 6.11%; Found: C 83.84%, H 10.32%, N 6.14%.

1-(Oct-1-en-2-yl)-indole
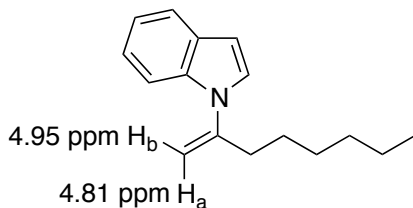
4.95 ppm H_b

4.81 ppm H_a

In a nitrogen-filled dry-box, an oven-dried 4 ml screw-capped vial was charged with [Ir(cod)Cl]$_2$ (3.4 mg, 0.010 mmol), (±)-3,5-bisTMS-Segphos (24 mg, 0.020 mmol), indole (59 mg, 0.50 mmol), and a magnetic stirbar. To these solids was added 1-octene (0.30 ml, 2.0 mmol), octane (0.30 ml), and ethyl acetate (60. μl, 0.6 mmol). The vial sealed with a Teflon-lined cap, was removed from the dry-box, and was allowed to stir in an aluminum heating block at 100 °C. After 24 h the vial was allowed to cool to room temperature, and the solvents were removed by rotary evaporation. The crude material was purified by flash chromatography with hexanes as eluent. The fractions were monitored by thin layer chromatography with a UV lamp. The material to elute first was determined to be the enamine product and was collected. The fractions containing the desired compound were concentrated by rotary evaporation. The remaining solvent was removed in the dry-box to yield the title compound as a clear oil (43 mg, 38% yield).
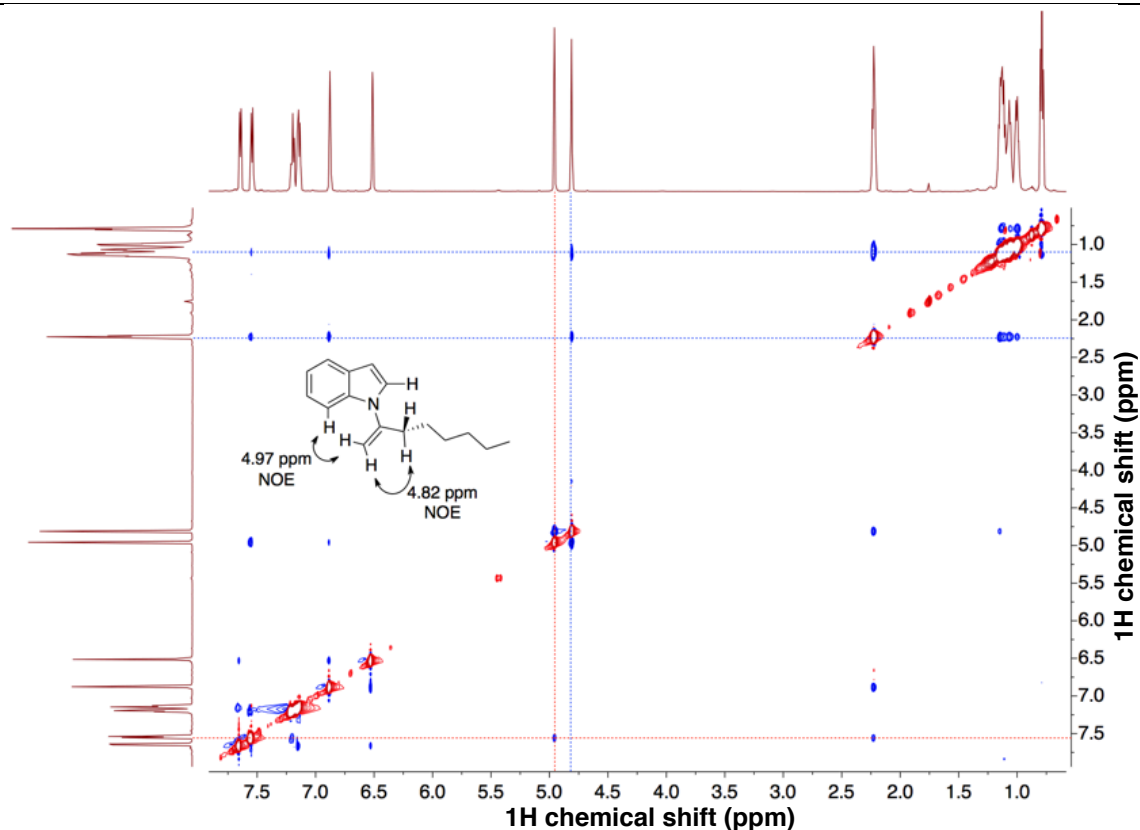
Figure 5.14. ^{1}H NRM spectroscopy NOE correlations of vinylindole **1-ene**.

^{1}**H NMR** (600 MHz, C$_6$D$_6$): δ 7.64 (d, J = 7.7 Hz, 1H), 7.54 (d, J = 8.2 Hz, 1H), 7.19 (t, J = 7.6 Hz, 1H), 7.16-7.12 (m, 1H), 6.87 (s, 1H), 6.51 (s, 1H), 4.95 (s, 1H, H$_b$), 4.81 (s, 1H, H$_a$), 2.22 (t, J = 7.3 Hz, 2H), 1.19-1.03 (m, 6H), 1.00 (dd, J = 13.3, 6.4 Hz, 2H), 0.78 (t, J = 7.3 Hz, 3H).

^{13}**C NMR** (151 MHz, C$_6$D$_6$): δ 145.1, 136.1, 129.5, 126.0, 122.2, 121.1, 120.2, 111.3, 106.1, 102.9, 35.2, 31.3, 28.5, 26.8, 22.5, 13.9.

Anal. Calcd for C$_{16}$H$_{21}$N: C 84.53%, H 9.31%, N 6.16%; Found: C 84.36 %, H 9.33%, N 6.45%.

Methyl-1-(octan-2-yl)-indole-5-carboxylate
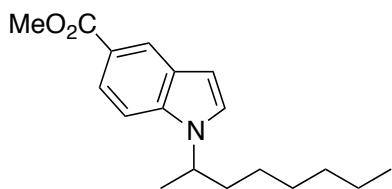
Following the general procedure **A** described above, methyl indole-5-carboxylate (67 mg, 0.30 mmol) was allowed to react with 1-octene (180 μl, 1.2 mmol) in the presence of octane (180 μl) and ethyl acetate (30. μl, 0.30 mmol). The crude material was purified by flash chromatography with 1.5% EtOAc in hexanes as eluent. The fractions were monitored by thin layer chromatography with a UV lamp. The material to elute first was determined to be the enamine product and was discarded. The second spot to elute was determined to be the title compound (R_f = 0.1, hexanes). The solvent was evaporated to yield the title compound as a clear oil (70 mg, 81% yield).

174

¹H NMR (600 MHz, C$_6$D$_6$): δ 8.72 (s, 1H), 8.26 (d, J = 8.7 Hz, 1H), 7.09 (d, J = 8.7 Hz, 1H), 6.79 (s, 1H), 6.51 (s, 1H), 4.03-3.82 (m, 1H), 3.61 (s, 3H), 1.49-1.38 (m, 1H), 1.31-1.24 (m, 1H), 1.16-1.08 (m, 2H), 1.05-0.93 (m, 7H), 0.92-0.81 (m, 2H), 0.79 (t, J = 7.3 Hz, 3H).

¹³C NMR (151 MHz, C$_6$D$_6$): δ 167.5, 138.5, 128.2, 125.0, 124.2, 122.8, 121.9, 109.1, 103.2, 51.4, 51.0, 36.8, 31.5, 28.9, 26.0, 22.5, 20.7, 13.8.

HPLC analysis: 62% ee, Chiralcel OD-H column, 1% isopropanol in hexane, 0.8 mL/min flow rate, 220 nm and 254 nm UV lamp, t$_{[minor]}$ = 33.8 min, t$_{[major]}$ = 44.8 min.

Anal. Calcd for C$_{18}$H$_{25}$NO$_2$: C 75.22%, H 8.77%, N 4.87%; Found: C 75.40%, H 8.65%, N 5.11%.

5-Methyl-1-(octan-2-yl)-indole
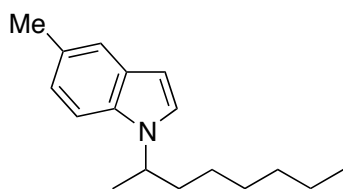
Following the general procedure **A** described above, 5-methylindole (39 mg, 0.30 mmol) was allowed to react with 1-octene (180 µl, 1.2 mmol) in the presence of octane (180 µl) and ethyl acetate (30. µl, 0.30 mmol). The crude material was purified by flash chromatography with hexanes as eluent. The fractions were monitored by thin layer chromatography with a UV lamp. The material to elute first was determined to be the enamine product and was discarded. The second spot to elute was determined to be the title compound (R$_f$ = 0.3, hexanes). The solvent was evaporated to yield the title compound as a clear oil (52 mg, 71% yield).

¹H NMR (600 MHz, C$_6$D$_6$): δ 7.49 (s, 1H), 7.16 (d, J = 8.3 Hz, 1H), 7.08 (d, J = 8.3 Hz, 1H), 6.86 (d, J = 1.5 Hz, 1H), 6.54 (s, 1H), 4.09-3.92 (m, 1H), 2.42 (s, 3H), 1.55 (d, J = 8.9 Hz, 1H), 1.36 (dd, J = 13.5, 10.1 Hz, 1H), 1.17-1.11 (m, 2H), 1.08 (d, J = 6.7 Hz, 3H), 1.06-0.87 (m, 6H), 0.80 (t, J = 7.3 Hz, 3H).

¹³C NMR (151 MHz, C$_6$D$_6$): δ 134.7, 129.2, 128.0, 123.6, 122.8, 120.9, 109.1, 101.1, 51.2, 36.9, 31.5, 29.0, 26.2, 22.6, 21.2, 20.9, 13.9.

HPLC analysis: 58% ee, Chiralcel OJ-H column, 100% hexane, 0.3 mL/min flow rate, 220 nm UV lamp, t$_{[major]}$ = 49.1 min, t$_{[minor]}$ = 53.0 min.

Anal. Calcd for C$_{17}$H$_{25}$N: C 83.89%, H 10.35%, N 5.75%; Found: C 83.94%, H 10.54%, N 5.63%.

5-Fluoro-1-(octan-2-yl)-indole
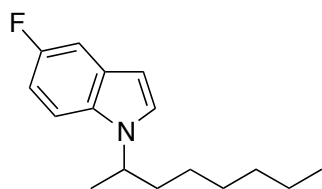
Following the general procedure **A** described above, 5-fluoroindole (41 mg, 0.30 mmol) was allowed to react with 1-octene (180 µl, 1.2 mmol) in the presence of octane (180 µl) and ethyl acetate (30. µl, 0.30 mmol). The crude material was purified by flash chromatography with hexanes as eluent. The fractions were monitored by thin layer chromatography with a UV lamp. The material to elute first was determined to be the enamine product and was discarded. The second spot to elute was determined to be the title compound (R$_f$ = 0.35, hexanes). The solvent was evaporated to yield the title compound as a clear oil (65 mg, 88% yield).

¹H NMR (600 MHz, C$_6$D$_6$): δ 7.34 (d, J = 9.4 Hz, 1H), 6.97 (t, J = 8.8 Hz, 1H), 6.94-6.89 (m, 1H), 6.81 (s, 1H), 6.38 (s, 1H), 4.01-3.72 (m, 1H), 1.52-1.42 (m, 1H), 1.37-1.26

(m, 1H), 1.17-1.09 (m, 2H), 1.07-0.97 (m, 7H), 0.95-0.83 (m, 2H), 0.80 (t, J = 7.2 Hz, 3H).

^{13}C NMR (151 MHz, C_6D_6): δ 158.0 (d, J = 233 Hz), 132.7, 128.9 (d, J = 10 Hz), 125.2, 109.9 (d, J = 10 Hz), 109.5 (d, J = 26 Hz), 105.7 (d, J = 23 Hz), 101.5 (d, J = 5 Hz), 51.4, 36.8, 31.5, 28.9, 26.1, 22.5, 20.7, 13.8.

^{19}F NMR (565 MHz, C_6D_6): δ -126.4.

HPLC analysis: 64% ee, Chiralcel OD-H column, 100% hexane, 0.8 mL/min flow rate, 220 nm and 254 nm UV lamp, $t_{[major]}$ = 25.6 min, $t_{[minor]}$ = 28.2 min.

Anal. Calcd for $C_{16}H_{22}FN$: C 77.69%, H 8.96%, N 5.66%; Found: C 77.69%, H 9.11%, N 5.50%.

6-Chloro-1-(octan-2-yl)-indole
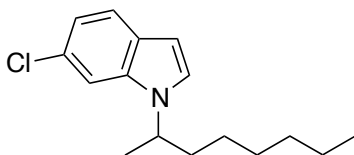
Following the general procedure **A** described above, 6-chloroindole (46 mg, 0.30 mmol) was allowed to react with 1-octene (180 μl, 1.2 mmol) in the presence of octane (180 μl) and ethyl acetate (30. μl, 0.30 mmol). The crude material was purified by flash chromatography with hexanes as eluent. The fractions were monitored by thin layer chromatography with a UV lamp. The material to elute first was determined to be the enamine product and was discarded. The second material to elute was determined to be the title compound (R_f = 0.3, hexanes). The fractions containing the desired compound were concentrated by rotary evaporation. The remaining solvent was removed in the dry-box under vacuum to yield the title compound as a clear oil (59 mg, 75% yield).

^{1}H NMR (600 MHz, C_6D_6): δ 7.38 (d, J = 8.4 Hz, 1H), 7.33 (s, 1H), 7.13 (s, 1H), 6.74 (d, J = 1.8 Hz, 1H), 6.41 (s, 1H), 3.84-3.65 (m, 1H), 1.44-1.37 (m, 1H), 1.27-1.20 (m, 1H), 1.15-1.09 (m, 2H), 1.02-0.92 (m, 7H), 0.89-0.77 (m, 5H).

^{13}C NMR (151 MHz, C_6D_6): δ 136.5, 127.4, 127.2, 124.3, 121.9, 120.0, 109.5, 101.8, 51.3, 36.7, 31.5, 28.9, 26.0, 22.5, 20.7, 13.9.

HPLC analysis: 58% ee, Chiralcel OB-H column, 100% hexane, 0.5 mL/min flow rate, 220 nm and 254 nm UV lamp, $t_{[minor]}$ = 12.8 min, $t_{[major]}$ = 15.3 min.

Anal. Calcd for $C_{16}H_{22}ClN$: C 72.85%, H 8.41%, N 5.31%; Found: C 72.45%, H 8.08%, N 5.18%.

5-(Benzyloxy)-1-(octan-2-yl)-indole

Following the general procedure **A** described above, 5-benzyloxylindole (67 mg, 0.30 mmol) was allowed to react with 1-octene (180 μl, 1.2 mmol) in the presence of octane (180 μl) and ethyl acetate (30. μl, 0.30 mmol). The solvent was removed under vacuum and a deoxygenated mixture of THF:2M $HCl_{(aq)}$ (1:1, 2 ml) was added to the residue. The vial was sealed with a Teflon cap and placed in an 80 °C heating block for 6 h. The solution was basified and the organic material was extracted with EtOAc (2 ml, three times). The crude material was purified by flash chromatography with 1.5% EtOAc in hexanes as eluent. The fractions containing the desired compound were concentrated by rotary evaporation. The remaining solvent was removed in the dry-box under vacuum to yield the title compound as a clear oil (75 mg, 75% yield).
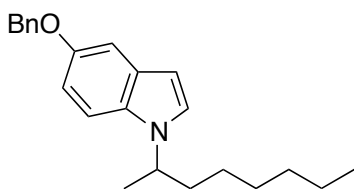
¹H NMR (600 MHz, C₆D₆): δ 7.35 (d, *J* = 7.5 Hz, 2H), 7.24 (s, 1H), 7.18-7.11 (m, 3H), 7.07 (dd, *J* = 16.6, 8.3 Hz, 2H), 6.88 (d, *J* = 2.1 Hz, 1H), 6.52 (d, *J* = 1.9 Hz, 1H), 4.90 (s, 2H), 4.09-3.83 (m, 1H), 1.58-1.48 (m, 1H), 1.39-1.30 (m, 1H), 1.18-1.10 (m, 2H), 1.07 (d, *J* = 6.7 Hz, 3H), 1.05-0.88 (m, 6H), 0.80 (t, *J* = 7.3 Hz, 3H).

¹³C NMR (151 MHz, C₆D₆): δ 153.5, 138.2, 131.7, 129.2, 128.2, 127.4, 127.3, 124.1, 112.5, 110.1, 104.2, 101.2, 70.4, 51.4, 36.9, 31.5, 29.0, 26.2, 22.6, 20.9, 13.9.

HPLC analysis: 60% ee, Chiralcel OD-H column, 1% isopropanol in hexane, 0.8 mL/min flow rate, 220 nm and 254 nm UV lamp, $t_{[minor]}$ = 13.0 min, $t_{[major]}$ = 14.0 min.

Anal. Calcd for $C_{23}H_{29}NO$: C 82.34%, H 8.71%, N 4.18%; Found: C 82.71%, H 8.76%, N 4.12%.

5-Chloro-1-(octan-2-yl)-indole
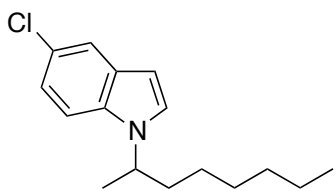
Following the general procedure **A** described above, 5-chloroindole (46 mg, 0.30 mmol) was allowed to react with 1-octene (180 μl, 1.2 mmol) in the presence of octane (180 μl) and ethyl acetate (30. μl, 0.30 mmol). The crude material was purified by flash chromatography with hexanes as eluent. The fractions were monitored by thin layer chromatography with a UV lamp. The material to elute first was determined to be the enamine product and was discarded. The second spot to elute was determined to be the title compound (R_f = 0.2, hexanes). The solvent was evaporated to yield the title compound as a clear oil (69 mg, 87% yield).

¹H NMR (600 MHz, C₆D₆): δ 7.64 (s, 1H), 7.19 (d, *J* = 8.7 Hz, 1H), 6.89 (d, *J* = 8.7 Hz, 1H), 6.76 (d, *J* = 1.9 Hz, 1H), 6.32 (s, 1H), 3.92-3.78 (m, 1H), 1.49-1.40 (m, 1H), 1.34-1.25 (m, 1H), 1.18-1.09 (m, 2H), 1.06-0.94 (m, 7H), 0.93-0.82 (m, 2H), 0.80 (t, *J* = 7.3 Hz, 3H).

¹³C NMR (151 MHz, C₆D₆): δ 134.4, 129.7, 125.0, 124.9, 121.5, 120.4, 110.4, 101.2, 51.4, 36.8, 31.5, 28.9, 26.1, 22.5, 20.7, 13.9.

HPLC analysis: 65% ee, Chiralcel OD-H column, 100% hexane, 0.8 mL/min flow rate, 220 nm UV lamp, $t_{[major]}$ = 42.7 min, $t_{[minor]}$ = 46.3 min.

Anal. Calcd for $C_{16}H_{22}ClN$: C 72.85%, H 8.41%, N 5.31%; Found: C 73.19%, H 8.28%, N 5.16%.

1-(Octan-2-yl)-indol-3-yl acetate
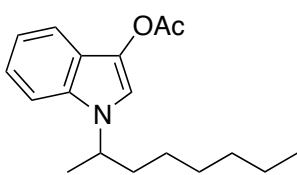
Following the general procedure **A** described above, 3-acetoxyindole (53 mg, 0.30 mmol) was allowed to react with 1-octene (180 μl, 1.2 mmol) in the presence of octane (180 μl) and ethyl acetate (30. μl, 0.30 mmol). The solvent was removed under vacuum and a deoxygenated mixture of THF:2M HCl₍aq₎ (1:1, 2 ml) was added to the residue. The vial was sealed with a Teflon cap and placed in an 80 °C heating block for 6 h. The solution was basified and the organic material was extracted with EtOAc (2 ml, three times). The crude material was purified by flash chromatography with 3% EtOAc in hexanes as eluent. The fractions containing the desired compound were concentrated by rotary evaporation. The remaining solvent was removed in the dry-box under vacuum to yield the title compound as a clear oil (60 mg, 70% yield).

¹H NMR (600 MHz, C₆D₆): δ 7.82 (d, *J* = 7.9 Hz, 1H), 7.59 (s, 1H), 7.23-7.18 (m, 1H), 7.16 (d, *J* = 7.7 Hz, 1H), 7.13 (s, 1H), 4.05-3.92 (m, 1H), 1.79 (s, 3H), 1.56-1.45 (m, 1H), 1.31-1.27 (m, 1H), 1.17-1.07 (m, 2H), 1.03 (d, *J* = 6.7 Hz, 3H), 1.00-0.85 (m, 6H), 0.79 (t, *J* = 7.3 Hz, 3H).

¹³C NMR (151 MHz, C₆D₆): δ 167.3, 133.0, 130.5, 122.1, 120.3, 119.3, 117.8, 112.9, 109.4, 51.3, 36.8, 31.5, 28.9, 26.2, 22.5, 20.7, 20.1, 13.8.

HPLC analysis: 45% ee, Chiralcel OD-H column, 1% isopropanol in hexane, 0.8 mL/min flow rate, 220 nm and 254 nm UV lamp, $t_{[minor]}$ = 13.7 min, $t_{[major]}$ = 25.5 min.

Anal. Calcd for $C_{18}H_{25}NO_2$: C 75.22%, H 8.77%, N 4.87%; Found: C 74.94%, H 8.93%, N 4.67%.

3-Methyl-1-(octan-2-yl)-indole
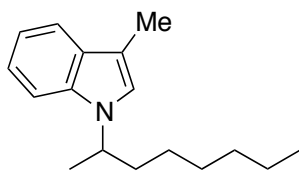
Following the general procedure **A** described above, 3-methylindole (39 mg, 0.30 mmol) was allowed to react with 1-octene (180 µl, 1.2 mmol) in the presence of octane (180 µl) and ethyl acetate (30. µl, 0.30 mmol). The crude material was purified by flash chromatography with hexanes as eluent. The fractions were monitored by thin layer chromatography with a UV lamp. The material to elute first was determined to be the enamine product and was discarded. The second spot to elute was determined to be the title compound (R_f = 0.3, hexanes). The solvent was evaporated to yield the title compound as a clear oil (46 mg, 63% yield).

¹H NMR (600 MHz, C₆D₆): δ 7.65 (d, *J* = 7.7 Hz, 1H), 7.26 (t, *J* = 7.5 Hz, 1H), 7.23-7.18 (m, 2H), 6.68 (s, 1H), 4.12-3.93 (m, 1H), 2.31 (s, 3H), 1.62-1.51 (m, 1H), 1.42-1.32 (m, 1H), 1.16-1.11 (m, 2H), 1.10 (d, *J* = 6.7 Hz, 3H), 1.07-0.88 (m, 6H), 0.80 (t, *J* = 7.3 Hz, 3H).

¹³C NMR (151 MHz, C₆D₆): δ 136.6, 129.0, 121.2, 121.2, 119.2, 118.6, 110.3, 109.2, 50.8, 37.0, 31.5, 29.1, 26.3, 22.6, 21.0, 13.9, 9.6.

HPLC analysis: 54% ee, Chiralcel OD-H column, 1% isopropanol in hexane, 0.5 mL/min flow rate, 220 nm and 254 nm UV lamp, $t_{[minor]}$ = 12.5 min, $t_{[major]}$ = 14.1 min.

Anal. Calcd for $C_{17}H_{25}N$: C 83.89%, H 10.35%, N 5.75%; Found: C 83.71%, H 10.37%, N 5.92%.

5-Bromo-1-(octan-2-yl)-indole
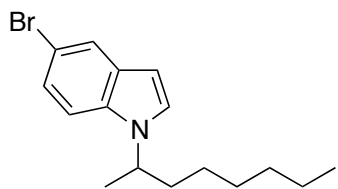
Following the general procedure **A** described above, 5-bromoindole (59 mg, 0.30 mmol) was allowed to react with 1-octene (180 µl, 1.2 mmol) in the presence of octane (180 µl) and ethyl acetate (30. µl, 0.30 mmol). The crude material was purified by flash chromatography with hexanes as eluent. The fractions were monitored by thin layer chromatography with a UV lamp. The material to elute first was determined to be the enamine product and was discarded. The second spot to elute was determined to be the title compound (R_f = 0.25, hexanes). The solvent was evaporated to yield the title compound as a clear oil (79 mg, 85% yield).

¹H NMR (600 MHz, C$_6$D$_6$): δ 7.78 (s, 1H), 7.31 (d, J = 8.6 Hz, 1H), 6.84 (d, J = 8.7 Hz, 1H), 6.73 (s, 1H), 6.30 (s, 1H), 3.90-3.77 (m, 1H), 1.50-1.36 (m, 1H), 1.34-1.21 (m, 1H), 1.17-1.08 (m, 2H), 0.98 (d, J = 6.7 Hz, 7H), 0.88 (s, 1H), 0.84-0.78 (m, 4H).

¹³C NMR (151 MHz, C$_6$D$_6$): δ 134.7, 130.4, 124.8, 124.0, 123.6, 112.6, 110.8, 101.2, 51.4, 36.8, 31.5, 28.9, 26.1, 22.5, 20.7, 13.9.

HPLC analysis: 61% ee, Chiralcel OD-H column, 100% hexane, 0.8 mL/min flow rate, 220 nm and 254 nm UV lamp, t$_{[major]}$ = 53.5 min, t$_{[minor]}$ = 57.8 min.

Anal. Calcd for C$_{16}$H$_{22}$BrN: C 62.34%, H 7.19%, N 4.54%; Found: C 62.55%, H 7.32%, N 4.58%.

5-Bromo-1-(1-cyclohexylethyl)-indole
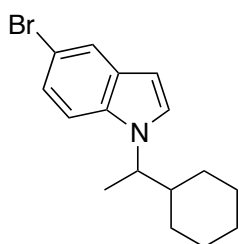
Following the general procedure **A** described above, 5-bromoindole (59 mg, 0.30 mmol) was allowed to react with vinyl cyclohexane (240 µl, 1.8 mmol) in the presence of octane (90 µl) and ethyl acetate (30. µl, 0.30 mmol). The crude material was purified by flash chromatography with hexanes as eluent. The fractions were monitored by thin layer chromatography with a UV lamp. The material to elute first was determined to be the enamine product and was discarded. The second spot to elute was determined to be the title compound (R$_f$ = 0.25, hexanes). The solvent was evaporated to yield the title compound as a clear oil (60. mg, 65% yield).

¹H NMR (600 MHz, C$_6$D$_6$): δ 7.80 (s, 1H), 7.32 (d, J = 8.7 Hz, 1H), 6.82 (d, J = 8.7 Hz, 1H), 6.70 (d, J = 2.1 Hz, 1H), 6.30 (d, J = 1.9 Hz, 1H), 3.67-3.49 (m, 1H), 1.54 (d, J = 13.3 Hz, 1H), 1.49-1.41 (m, 2H), 1.40-1.33 (m, 1H), 1.32-1.25 (m, 1H), 1.04-0.95 (m, 5H), 0.85 (td, J = 25.1, 12.1 Hz, 2H), 0.68-0.58 (m, 1H), 0.55-0.46 (m, 1H).

¹³C NMR (151 MHz, C$_6$D$_6$): δ 135.0, 130.1, 125.4, 124.0, 123.5, 112.5, 111.1, 101.1, 56.3, 43.9, 29.8, 29.5, 26.0, 25.8, 25.7, 17.8.

HPLC analysis: 55% ee, Chiralcel OD-H column, 100% hexane, 0.8 mL/min flow rate, 220 nm and 254 nm UV lamp, t$_{[minor]}$ = 29.9 min, t$_{[major]}$ = 54.0 min.

Anal. Calcd for C$_{16}$H$_{20}$BrN: C 62.75%, H 6.58%, N 4.57%; Found: C 63.05%, H 6.95%, N 4.31%.

5-Bromo-1-(1-cyclohexylpropan-2-yl)-indole
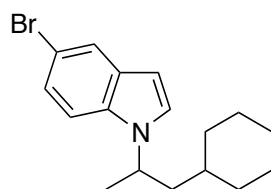
Following the general procedure **A** described above, 5-bromoindole (59 mg, 0.30 mmol) was allowed to react with allyl cyclohexane (180 µl, 1.2 mmol). The crude material was purified by flash chromatography with hexanes as eluent. The fractions were monitored by thin layer chromatography with a UV lamp. The material to elute first was determined to be the enamine product and was discarded. The second spot to elute was determined to be the title compound (R$_f$ = 0.25, hexanes). The solvent was evaporated to yield the title compound as a clear oil (37 mg, 39% yield).

¹H NMR (600 MHz, C$_6$D$_6$): δ 7.79 (s, 1H), 7.33 (d, J = 8.6 Hz, 1H), 6.86 (d, J = 8.7 Hz, 1H), 6.73 (d, J = 1.5 Hz, 1H), 6.30 (s, 1H), 4.16-3.93 (m, 1H), 1.54-1.40 (m, 5H), 1.32 (d, J = 11.8 Hz, 1H), 1.16 (ddd, J = 13.7, 6.7 Hz, 1H), 0.98-0.82 (m, 7H), 0.71-0.59 (m, 2H).

¹³**C NMR** (151 MHz, C₆D₆): δ 134.5, 130.4, 124.8, 124.1, 123.7, 112.6, 110.7, 101.3, 48.7, 44.4, 34.0, 33.1, 32.9, 26.3, 25.9, 25.8, 21.2.

HPLC analysis: 52% ee, Chiralcel OD-H column, 100% hexane, 0.8 mL/min flow rate, 220 nm and 254 nm UV lamp, $t_{[minor]}$ = 57.5 min, $t_{[major]}$ = 61.3 min.

Anal. Calcd for $C_{17}H_{22}BrN$: C 63.75%, H 6.92%, N 4.37%; Found: C 64.11%, H 7.04%, N 4.21%.

5-Bromo-1-(4-methylpentan-2-yl)-indole
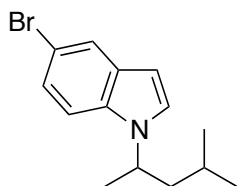
Following the general procedure **A** described above, 5-bromoindole (59 mg, 0.30 mmol) was allowed to react with 4-methyl-1-pentene (300 μl, 2.4 mmol) in the presence of ethyl acetate (60. μl, 0.60 mmol). The crude material was purified by flash chromatography with hexanes as eluent. The fractions were monitored by thin layer chromatography with a UV lamp. The material to elute first was determined to be the enamine product and was discarded. The second spot to elute was determined to be the title compound (R_f = 0.25, hexanes). The solvent was evaporated to yield the title compound as a clear oil (55 mg, 65% yield).

¹**H NMR** (600 MHz, C₆D₆): δ 7.79 (s, 1H), 7.31 (d, J = 8.7 Hz, 1H), 6.83 (d, J = 8.7 Hz, 1H), 6.69 (d, J = 1.7 Hz, 1H), 6.29 (s, 1H), 4.08-3.88 (m, 1H), 1.41 (dd, J = 8.9 Hz, 1H), 1.12-1.00 (m, 2H), 0.94 (d, J = 6.6 Hz, 3H), 0.60 (d, J = 5.8 Hz, 3H), 0.58 (d, J = 5.9 Hz, 3H).

¹³**C NMR** (151 MHz, C₆D₆): δ 134.5, 130.4, 124.8, 124.1, 123.6, 112.6, 110.7, 101.3, 49.3, 45.6, 24.6, 22.4, 21.9, 21.2.

HPLC analysis: 54% ee, Chiralcel OD-H column, 100% hexane, 0.8 mL/min flow rate, 220 nm and 254 nm UV lamp, $t_{[minor]}$ = 33.6 min, $t_{[major]}$ = 54.7 min.

Anal. Calcd for $C_{14}H_{18}BrN$: C 60.01%, H 6.47%, N 5.00%; Found: C 60.14%, H 6.45%, N 4.77%.

1-(4,4-dimethylpentan-2-yl)-indole
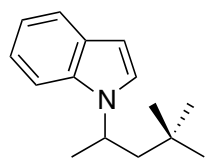
Following the general procedure **A** described above, indole (35 mg, 0.30 mmol) was allowed to react with 4,4-dimethyl-1-pentene (240 mg, 1.8 mmol) in the presence of octane (90 μl) and ethyl acetate (30. μl, 0.30 mmol). The crude material was purified by flash chromatography with hexanes as eluent. The fractions were monitored by thin layer chromatography with a UV lamp. The material to elute first was determined to be the enamine product and was discarded. The second spot to elute was determined to be the title compound (R_f = 0.25, hexanes). The solvent was evaporated to yield the title compound as a white solid (36 mg, 56% yield).

¹**H NMR** (600 MHz, C₆D₆): δ 7.71 (d, J = 7.8 Hz, 1H), 7.28-7.20 (m, 2H), 7.19-7.14 (m, 1H), 6.83 (d, J = 3.2 Hz, 1H), 6.55 (d, J = 3.1 Hz, 1H), 4.37-4.17 (m, 1H), 1.69 (dd, J = 14.5, 9.2 Hz, 1H), 1.23 (dd, J = 14.5, 3.7 Hz, 1H), 1.05 (d, J = 6.8 Hz, 3H), 0.60 (s, 9H).

¹³**C NMR** (151 MHz, C₆D₆): δ 135.6, 129.1, 124.1, 121.4, 121.3, 119.4, 109.6, 101.8, 49.9, 48.3, 30.1, 29.2, 23.8.

HPLC analysis: 5% ee, Chiralcel OD-H column, 100% hexane, 0.8 mL/min flow rate, 220 nm and 254 nm UV lamp, $t_{[minor]}$ = 15.4 min, $t_{[major]}$ = 21.8 min.

Anal. Calcd for $C_{15}H_{21}N$: C 83.67%, H 9.83%, N 6.50%; Found: C 83.91%, H 10.22%, N 6.10%.

6-Chloro-1-(1-cyclohexylethyl)-indole
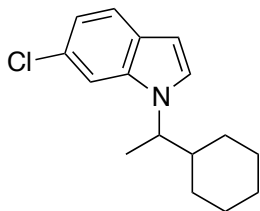
Following the general procedure **A** described above, 5-chloroindole (46 mg, 0.30 mmol) was allowed to react with vinyl cyclohexane (240 μl, 1.8 mmol) in the presence of octane (90 μl) and ethyl acetate (30. μl, 0.30 mmol). The crude material was purified by flash chromatography with hexanes as eluent. The fractions were monitored by thin layer chromatography with a UV lamp. The material to elute first was determined to be the enamine product and was discarded. The second spot to elute was determined to be the title compound (R_f = 0.25, hexanes). The solvent was evaporated to yield the title compound as a clear oil (49 mg, 63% yield).

^{1}H NMR (500 MHz, C_6D_6): δ 7.38 (d, J = 8.4 Hz, 1H), 7.34 (s, 1H), 7.14 (dd, J = 8.4, 1.8 Hz, 1H), 6.71 (d, J = 3.2 Hz, 1H), 6.40 (d, J = 3.1 Hz, 1H), 3.59-3.44 (m, 1H), 1.50 (dd, J = 8.9, 5.5 Hz, 1H), 1.45-1.36 (m, 2H), 1.35-1.21 (m, 2H), 0.96 (d, J = 6.9 Hz, 5H), 0.88-0.73 (m, 2H), 0.57 (ddd, J = 12.5, 3.6 Hz, 1H), 0.47 (ddd, J = 12.5, 3.6 Hz, 1H).

^{13}C NMR (126 MHz, $CDCl_3$): δ 136.9, 127.4, 126.9, 125.7, 121.9, 120.0, 110.0, 101.6, 57.1, 44.4, 30.3, 30.2, 26.4, 26.3, 26.2, 18.7.

HPLC analysis: 67% ee, Chiralcel OD-H column, 0.1% ethanol in hexane, 0.3 mL/min flow rate, 220 nm and 254 nm UV lamp, $t_{[minor]}$ = 21.6 min, $t_{[major]}$ = 24.3 min.

Anal. Calcd for $C_{16}H_{20}ClN$: C 73.41%, H 7.70%, N 5.35%; Found: C 73.19%, H 7.75%, N 5.17%.

6-Chloro-1-(4,4-dimethylpentan-2-yl)-indole
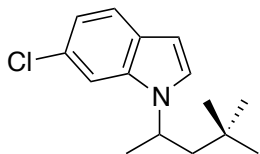
Following the general procedure **A** described above, 6-chloroindole (46 mg, 0.30 mmol) was allowed to react with 4,4-dimethyl-1-pentene (240 mg, 1.8 mmol) in the presence of octane (90 μl) and ethyl acetate (30. μl, 0.30 mmol). The crude material was purified by flash chromatography with hexanes as eluent. The fractions were monitored by thin layer chromatography with a UV lamp. The material to elute first was determined to be the enamine product and was discarded. The second spot to elute was determined to be the title compound (R_f = 0.25, hexanes). The solvent was evaporated to yield the title compound as a clear oil (40. mg, 53% yield).

^{1}H NMR (500 MHz, C_6D_6): δ 7.40 (d, J = 0.5 Hz, 1H), 7.35 (d, J = 8.4 Hz, 1H), 7.13 (d, J = 1.8 Hz, 1H), 6.70 (d, J = 3.2 Hz, 1H), 6.37 (d, J = 3.1 Hz, 1H), 4.09-3.94 (m, 1H), 1.56 (dd, J = 14.6, 9.2 Hz, 1H), 1.13 (dd, J = 14.5, 3.7 Hz, 1H), 0.93 (d, J = 6.8 Hz, 3H), 0.52 (s, 9H).

^{13}C NMR (126 MHz, C_6D_6): δ 136.1, 127.8, 127.6, 125.2, 122.3, 120.3, 109.8, 102.1, 49.8, 48.7, 30.1, 29.3, 23.8.

HPLC analysis: 4% ee, Chiralcel OJ-H column, 0.05% ethanol in hexane, 0.3 mL/min flow rate, 220 nm and 254 nm UV lamp, $t_{[minor]}$ = 17.5 min, $t_{[major]}$ = 19.1 min.

Anal. Calcd for $C_{15}H_{20}ClN$: C 72.13%, H 8.07%, N 5.61%; Found: C 72.33%, H 8.19%, N 5.66%.

5-Methoxy-1-(4-methylpentan-2-yl)-indole

Following the general procedure **A** described above, 5-methoxyindole (44 mg, 0.30 mmol) was allowed to react with 4-methyl-1-pentene (300 µl, 2.4 mmol) in the presence of ethyl acetate (60. µl, 0.60 mmol). The crude material was purified by flash chromatography with hexanes as eluent. The fractions were monitored by thin layer chromatography with a UV lamp. The material to elute first was determined to be the enamine product and was discarded. The second spot to elute was determined to be the title compound (R_f = 0.15, hexanes). The solvent was evaporated to yield the title compound as a clear oil (38 mg, 55% yield).

^{1}**H NMR** (500 MHz, C_6D_6): δ 7.13 (d, J = 1.3 Hz, 1H), 7.10-7.06 (m, 2H), 6.84 (d, J = 3.1 Hz, 1H), 6.53 (d, J = 3.1 Hz, 1H), 4.15-4.03 (m, 1H), 3.50 (s, 3H), 1.58-1.47 (m, 1H), 1.21-1.09 (m, 2H), 1.03 (d, J = 6.7 Hz, 3H), 0.64 (d, J = 6.3 Hz, 3H), 0.61 (d, J = 6.4 Hz, 3H).

^{13}**C NMR** (126 MHz, C_6D_6): δ 154.7, 131.6, 129.4, 124.2, 112.3, 110.3, 102.7, 101.6, 55.3, 49.5, 46.1, 24.9, 22.7, 22.2, 21.7.

HPLC analysis: 52% ee, Chiralcel OJ-H column, 0.05% ethanol in hexane, 0.3 mL/min flow rate, 220 nm and 254 nm UV lamp, $t_{[minor]}$ = 22.7 min, $t_{[major]}$ = 26.6 min.

Anal. Calcd for $C_{15}H_{21}NO$: C 77.88%, H 9.15%, N 6.05%; Found: C 77.91%, H 9.11%, N 6.98%.

Methyl 1-(1-cyclohexylethyl)-indole-5-carboxylate

Following the general procedure **A** described above, methyl 5-indolecarboxylate (53 mg, 0.30 mmol) was allowed to react with vinyl cyclohexane (240 µl, 1.8 mmol) in the presence of octane (90 µl) and ethyl acetate (30. µl, 0.30 mmol). The crude material was purified by flash chromatography with 1% ethyl acetate in hexanes as eluent. The fractions were monit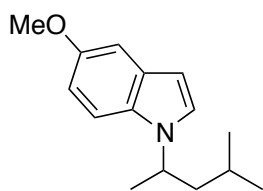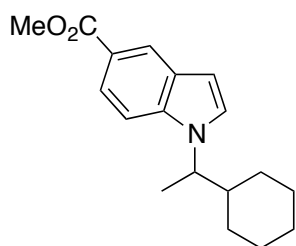ored by thin layer chromatography with a UV lamp. The material to elute first was determined to be the enamine product and was discarded. The second spot to elute was determined to be the title compound (R_f = 0.25, hexanes). The solvent was evaporated to yield the title compound as a clear oil (60 mg, 70% yield).

^{1}**H NMR** (500 MHz, CDCl$_3$): δ 8.42 (d, J = 1.0 Hz, 1H), 7.91 (dd, J = 8.7, 1.6 Hz, 1H), 7.38 (d, J = 8.7 Hz, 1H), 7.23 (d, J = 3.2 Hz, 1H), 6.65 (d, J = 3.2 Hz, 1H), 4.32-4.16 (m, 1H), 3.95 (s, 3H), 1.89 (d, J = 12.6 Hz, 1H), 1.84-1.71 (m, 2H), 1.66-1.59 (m, 2H), 1.54 (d, J = 6.9 Hz, 3H), 1.29-1.19 (m, 2H), 1.16-1.01 (m, 3H), 0.93-0.81 (m, 1H).

^{13}**C NMR** (126 MHz, CDCl$_3$): δ 168.5, 139.0, 127.9, 126.4, 124.2, 122.7, 121.3, 109.6, 103.2, 57.2, 52.0, 44.6, 30.3, 30.1, 26.4, 26.3, 26.1, 18.7.

HPLC analysis: 45% ee, Chiralcel OJ-H column, 0.05% ethanol in hexane, 0.3 mL/min flow rate, 220 nm and 254 nm UV lamp, $t_{[major]}$ = 21.3 min, $t_{[minor]}$ = 27.3 min.

Anal. Calcd for $C_{18}H_{23}NO_2$: C 75.76%, H 8.12%, N 4.91%; Found: C 75.50%, H 8.12%, N 4.73%.
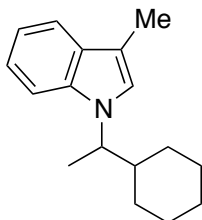
1-(1-Cyclohexylethyl)-3-methyl-indole

Following the general procedure **A** described above, 3-methylindole (39 mg, 0.30 mmol) was allowed to react with vinyl cyclohexane (240 μl, 1.8 mmol) in the presence of octane (90 μl) and ethyl acetate (30. μl, 0.30 mmol). The crude material was purified by flash chromatography with hexanes as eluent. The fractions were monitored by thin layer chromatography with a UV lamp. The material to elute first was determined to be the enamine product and was discarded. The second spot to elute was determined to be the title compound (R_f = 0.20, hexanes). The solvent was evaporated to yield the title compound as a clear oil (41 mg, 57% yield).

^{1}H NMR (499 MHz, C_6D_6): δ 7.69-7.63 (m, 1H), 7.29-7.24 (m, 1H), 7.23-7.18 (m, 2H), 6.66 (d, J = 0.8 Hz, 1H), 3.79 (dq, J = 13.9, 6.9 Hz, 1H), 2.32 (d, J = 1.0 Hz, 3H), 1.61-1.52 (m, 2H), 1.49-1.33 (m, 3H), 1.18 (dd, J = 8.1, 6.5 Hz, 1H), 1.11 (d, J = 6.9 Hz, 3H), 1.06-0.95 (m, 1H), 0.89 (dddd, J = 13.1, 9.7, 6.7 Hz, 2H), 0.71 (ddd, J = 25.6, 11.0, 5.3 Hz, 1H), 0.63 (ddd, J = 16.0, 12.8, 6.5 Hz, 1H).

^{13}C NMR (126 MHz, C_6D_6): δ 137.2, 128.9, 122.2, 121.5, 119.3, 118.8, 110.4, 109.7, 56.1, 44.4, 30.2, 29.9, 26.4, 26.2, 26.1, 18.4, 9.9.

HPLC analysis: 60% ee, Chiralcel OJ-H column, 0.05% ethanol in hexane, 0.3 mL/min flow rate, 220 nm and 254 nm UV lamp, $t_{[major]}$ = 20.0 min, $t_{[minor]}$ = 25.0 min.

Anal. Calcd for $C_{17}H_{23}N$: C 84.59%, H 9.60%, N 5.80%; Found: C 84.31%, H 9.43%, N 5.57%.

5-Bromo-1-(5-((*tert*-butyldimethylsilyl)oxy)-4,4-diphenylpentan-2-yl)-indole
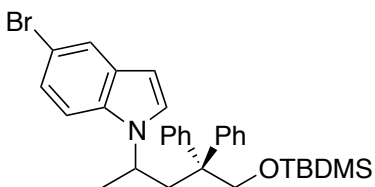
Following the general procedure **A** described above, 5-bromoindole (59 mg, 0.30 mmol) was allowed to react with *tert*-butyl((2,2-diphenylpent-4-en-1-yl)oxy)dimethylsilane (422 mg, 1.2 mmol). The solvent was removed under vacuum and a deoxygenated mixture of THF:2M $HCl_{(aq)}$ (1:1, 2 ml) was added to the residue. The vial was sealed with a Teflon cap and placed in an 80 °C heating block for 6 h. The solution was basified and the organic material was extracted with EtOAc (2 ml, three times). The crude material was purified by flash chromatography with 1% EtOAc in hexanes as eluent. The solvent was evaporated to yield the title compound as a clear oil (0.10 g, 62% yield).

^{1}H NMR (600 MHz, C_6D_6): δ 7.76 (d, J = 1.7 Hz, 1H), 7.24 (dd, J = 8.7, 1.8 Hz, 1H), 7.06-6.96 (m, 5H), 6.95 (d, J = 7.0 Hz, 1H), 6.92 (dd, J = 7.4, 1.9 Hz, 3H), 6.87-6.82 (m, 2H), 6.49 (d, J = 8.7 Hz, 1H), 6.30 (d, J = 3.1 Hz, 1H), 4.01-3.90 (m, 1H), 3.67 (d, J = 9.4 Hz, 1H), 3.46 (d, J = 9.4 Hz, 1H), 3.00 (dd, J = 14.2, 8.6 Hz, 1H), 2.26 (dd, J = 14.2, 3.3 Hz, 1H), 0.94 (d, J = 6.8 Hz, 3H), 0.73 (s, 9H), -0.39 (s, 3H), -0.42 (s, 3H).

^{13}C NMR (151 MHz, C_6D_6): δ 147.3, 145.6, 133.8, 130.5, 128.2, 128.1, 128.1, 126.2, 125.8, 125.6, 123.8, 123.4, 112.7, 111.3, 101.4, 67.1, 51.1, 48.6, 41.6, 25.6, 23.5, 18.0, -6.2, -6.5.

HPLC analysis: 30% ee, Chiralcel OD-H column, 100% hexane, 0.8 mL/min flow rate, 220 nm and 254 nm UV lamp, $t_{[minor]}$ = 13.5 min, $t_{[major]}$ = 33.9 min.

Anal. Calcd for $C_{31}H_{38}BrNOSi$: C 67.87%, H 6.98%, N 2.55%; Found: C 68.23%, H 7.21%, N 2.34%.

General Procedure B: Ir-catalyzed addition of indoles to ethylene and propylene.
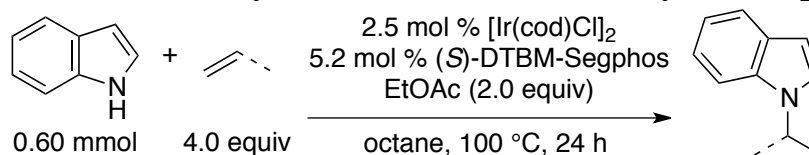
In a nitrogen-filled dry-box, an oven-dried, round-bottom Schlenk flask (58 ml volume) was charged with [Ir(cod)Cl]$_2$ (10. mg, 0.015 mmol), (S)-DTBM-Segphos (35 mg, 0.030 mmol), the corresponding indole (0.60 mmol), and a magnetic stirbar. Octane (1.0 ml) and ethyl acetate (120 μl, 1.2 mmol) was added to these solids. The flask was sealed with a Kontes valve and removed from the dry-box. Olefin gas (4 equiv, 2.4 mmol) was introduced into the flask according to the following procedure. The solution was frozen in liquid nitrogen and degassed under vacuum. Once the solvent was degassed, the flask was resealed and a manifold bulb adapter (62 ml) was filled with the alkene gas (720 Torr at 23 °C). The gas in the adapter was condensed into the Schlenk flask at 77 K. The Schlenk flask was resealed and allowed to warm to room temperature. The flask was placed in a 100 °C oil bath with vigorous stirring. After 24 h, the solution was allowed to cool to room temperature, and the solvent was removed under vacuum. The product was purified by flash chromatography on a column (height = 20. cm, diameter = 3.0 cm) of Silacycle Siala-P60 silica gel (55 g). The conditions for chromatography, and other data that are specific to each compound are given below.

1-Ethylindole

Following the general procedure **B** described above, indole (59 mg, 0.60 mmol) was allowed to react with ethylene (720 Torr in 62 ml, 2.4 mmol). The crude material was purified by flash chromatography with hexanes as eluent. The fractions were monitored by thin layer chromatography with a UV lamp. The material to elute first was determined to be the enamine product and was discarded. The second spot to elute was determined to be the title compound. The solvent was evaporated to yield the title compound as a clear oil (19 mg, 22% yield).
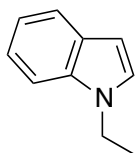
^{1}H NMR (600 MHz, C$_6$D$_6$): δ 7.72 (d, J = 7.7 Hz, 1H), 7.27-7.15 (m, 2H), 7.08 (d, J = 8.0 Hz, 1H), 6.65 (d, J = 1.9 Hz, 1H), 6.51 (s, 1H), 3.41 (q, J = 7.3 Hz, 2H), 0.84 (t, J = 7.3 Hz, 3H).

^{13}C NMR (151 MHz, C$_6$D$_6$): δ 135.9, 129.1, 126.4, 121.3, 121.1, 119.3, 109.2, 101.2, 40.2, 14.8. NMR data match those published previously.[58]
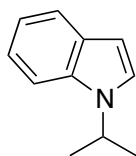
1-Isopropyl-indole

Following the general procedure **B** described above, indole (59 mg, 0.60 mmol) was allowed to react with propylene (720 Torr in 62 ml, 2.4 mmol). The crude material was purified by flash chromatography with hexanes as eluent. The fractions were monitored by thin layer chromatography with a UV lamp. The material to elute first was determined to be the enamine

product and was discarded. The second spot to elute was determined to be the title compound (R_f = 0.20, hexanes). The solvent was evaporated to yield the title compound as a clear oil (70. mg, 73% yield).

^{1}H NMR (600 MHz, C_6D_6): δ 7.73 (d, J = 7.7 Hz, 1H), 7.24 (t, J = 7.5 Hz, 1H), 7.19 (t, J = 7.3 Hz, 1H), 7.14 (d, J = 8.2 Hz, 1H), 6.84 (d, J = 1.9 Hz, 1H), 6.54 (s, 1H), 4.17-3.92 (m, 1H), 0.97 (d, J = 6.8 Hz, 6H).

^{13}C NMR (151 MHz, C_6D_6): δ 135.8, 129.1, 123.0, 121.2, 121.1, 119.4, 109.4, 101.4, 46.4, 22.0. NMR data match those published previously.[59]

5-Bromo-1-(*sec*-butyl)-indole
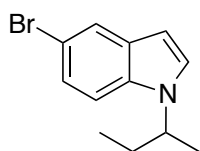
In a nitrogen-filled dry-box, an oven-dried, round-bottom Schlenk flask (58 ml volume) was charged with [Ir(cod)Cl]$_2$ (40. mg, 0.060 mmol), (*S*)-DTBM-Segphos (140 mg, 0.12 mmol), 5-bromoindole (360 mg, 1.8 mmol), and a magnetic stirbar. Octane (2.0 ml) and ethyl acetate (200 μl, 2 mmol) were added to these solids. Following the general procedure **B** described above, this mixture was allowed to react with 1-butene (1500 Torr in 223 ml, 18 mmol) in an 80 °C oil bath for 36 h. To the crude material was added degassed HCl (2M in H_2O, 3 ml), and the mixture was stirred for 2 hours at 100 °C. The organic material was extracted from the biphasic mixture with ethyl acetate (10 ml, 2 times). The combined organic material was concentrated to a residue by rotary evaporation. The residue was purified by flash chromatography with hexanes as eluent (R_f = 0.4). The fractions containing the desired product were collected and the solvent was evaporated to yield the title compound as a clear oil (313 mg, 68% yield).

^{1}H NMR (600 MHz, $CDCl_3$): δ 7.81 (s, 1H), 7.32 (d, J = 8.7 Hz, 1H), 7.27 (d, J = 8.7 Hz, 1H), 7.21 (d, J = 2.8 Hz, 1H), 6.51 (d, J = 2.8 Hz, 1H), 4.45-4.30 (m, 1H), 1.97-1.82 (m, 2H), 1.53 (d, J = 6.8 Hz, 3H), 0.84 (t, J = 7.4 Hz, 3H).

^{13}C NMR (151 MHz, $CDCl_3$): δ 134.7, 130.1, 125.3, 124.0, 123.3, 112.4, 111.0, 100.9, 53.4, 30.1, 20.9, 10.9.

HPLC analysis: 69% ee, Chiralcel OD-H column, 100% hexane, 0.8 mL/min flow rate, 220 nm and 254 nm UV lamp, $t_{[minor]}$ = 7.9 min, $t_{[major]}$ = 8.5 min.

Anal. Calcd for $C_{12}H_{24}BrN$: C 57.16%, H 5.60%, N 5.55%; Found: C 57.53%, H 5.78%, N 5.45%.

5-([1,1'-biphenyl]-4-yl)-1-(*sec*-butyl)- indole
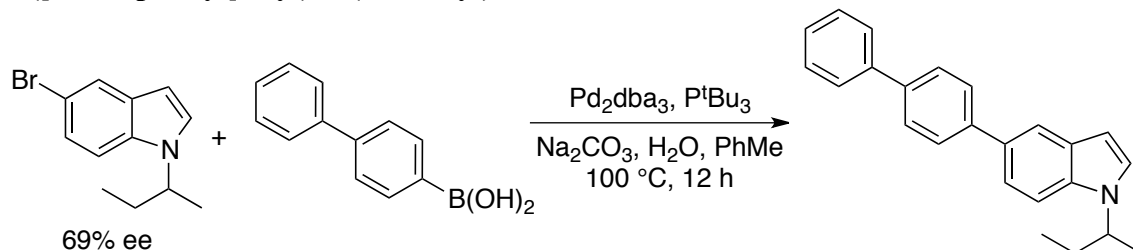
In a nitrogen-filled dry-box, a 20 ml screw-capped vial was charged with Pd$_2$dba$_3$ (9.6 mg, 0.011 mmol), tri-*tert*-butylphosphine (8.5 mg, 0.042 mmol), compound **22** (176 mg, 0.700 mmol), 4-biphenyl boronic acid (277 mg, 1.40 mmol), and a magnetic stirbar. Toluene (2.0 ml) was added to these solids, and the vial was sealed and removed from the

185

dry box. Under a stream of nitrogen, a degassed, aqueous solution of Na_2CO_3 (1.8 ml, 1 M) was added to the vial. The vial was placed in a 100 °C heating block. After 12 hours, the vial was allowed to cool to room temperature, and the organic material was extracted from the biphasic mixture with ethyl acetate (10 ml, 2 times). The combined organic material was concentrated to a residue by rotary evaporation. The residue was purified by flash chromatography with 1% ethyl acetate in hexanes as eluent (hexanes, $R_f = 0.2$). The fractions containing the desired product were collected and the solvent was evaporated to yield the title compound as a white solid (211 mg, 93% yield).

^{1}H NMR (600 MHz, CDCl₃): δ 7.92 (s, 1H), 7.76 (d, $J = 7.4$ Hz, 2H), 7.72-7.65 (m, 4H), 7.52 (d, $J = 8.5$ Hz, 1H), 7.50-7.45 (m, 3H), 7.37 (t, $J = 7.3$ Hz, 1H), 7.24 (s, 1H), 6.62 (s, 1H), 4.52-4.35 (m, 1H), 2.01-1.94 (m, 1H), 1.94-1.86 (m, 1H), 1.56 (d, $J = 6.7$ Hz, 3H), 0.89 (t, $J = 7.3$ Hz, 3H).

^{13}C NMR (151 MHz, CDCl₃): δ 141.6, 141.0, 139.0, 135.6, 132.2, 129.0, 128.7, 127.6, 127.4, 127.1, 127.0, 124.8, 120.9, 119.3, 109.8, 101.7, 53.3, 30.1, 20.9, 11.0.

Anal. Calcd for $C_{24}H_{23}N$: C 88.57%, H 7.12%, N 4.30%; Found: C 8.59%, H 7.09%, N 4.24%.

5-([1,1'-biphenyl]-4-yl)-3-bromo-1-(*sec*-butyl)-1*H*-indole, (24)
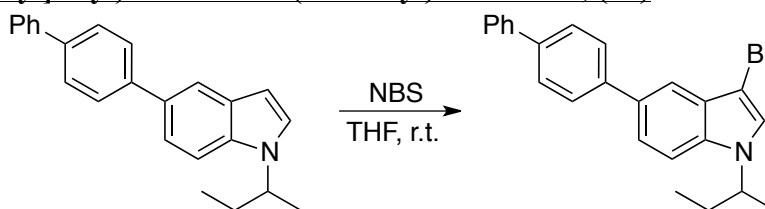
A 20 ml vial was charged with 5-([1,1'-biphenyl]-4-yl)-1-(*sec*-butyl)- indole (140 mg, 0.55 mmol) and a magnetic stirbar under ambient conditions. The solid was dissolved in THF (3.0 ml). While vigorously stirring the solution, *N*-bromosuccinamide (110 mg, 0.60 mmol) was added to the vial as a solid. A dark pink solution formed after 5 h stirring at room temperature. The reaction mixture was diluted with ethyl acetate (10 ml) and subsequently quenched with a saturated solution of sodium bisulfite. The organic layer was washed with brine (20 ml, 2 times). The crude material was adsorbed onto Celite and purified by column chromatography with 1% ethyl acetate in hexanes as eluent. The solvent was removed by rotary evaporation from the collected fractions to yield the title compound as a white solid (128 mg, 58% yield).

^{1}H NMR (400 MHz, CDCl₃): δ 7.88 (d, $J = 1.5$ Hz, 1H), 7.82 (d, $J = 8.4$ Hz, 2H), 7.75 (d, $J = 8.6$ Hz, 2H), 7.72 (d, $J = 7.2$ Hz, 2H), 7.61 (dd, $J = 8.6, 1.7$ Hz, 1H), 7.56-7.46 (m, 3H), 7.42 (t, $J = 7.4$ Hz, 1H), 7.29 (s, 1H), 4.56-4.37 (m, 1H), 1.95 (ddq, $J = 13.9, 7.0$ Hz, 2H), 1.58 (d, $J = 6.8$ Hz, 3H), 0.93 (t, $J = 7.4$ Hz, 3H).

^{13}C NMR (101 MHz, CDCl₃): δ 141.0, 140.9, 139.4, 135.2, 133.1, 128.8, 127.7, 127.7, 127.5, 127.2, 127.1, 124.0, 122.1, 117.7, 110.2, 90.4, 53.9, 30.2, 21.1, 11.0.

HPLC analysis: 69% ee, Chiralcel OJ-H column, 5% isopropanol in hexane, 1.0 mL/min flow rate, 220 nm and 254 nm UV lamp, $t_{[major]} = 21.3$ min, $t_{[minor]} = 28.1$ min.

Anal. Calcd for $C_{24}H_{22}BrN$: C 71.29%, H 5.48%, N 3.46%; Found: C 70.94%, H 5.24%, N 3.19%.

Determination of absolute stereochemistry of 24
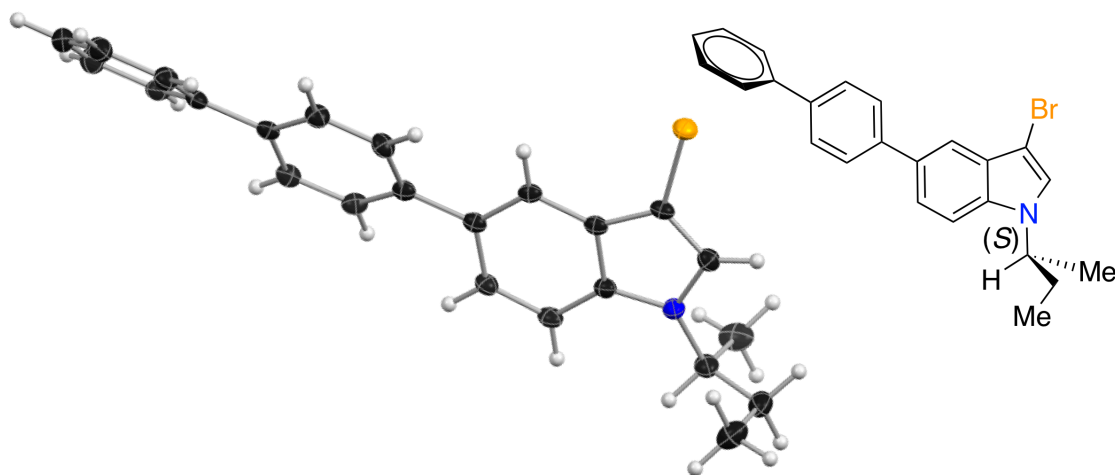
Single crystals suitable for x-ray diffraction of 24 were obtained by recrystallization from hexanes. A 20 ml vial was charged with the title compound (40 mg, 0.09 mmol) and hexanes (10 ml). The vial was sealed and the mixture was placed in an 80 °C oil bath until the solids dissolved. The warm solution was allowed to cool to room temperature overnight. After 10 h, colorless plates had formed. A colorless plate 0.150 x 0.100 x 0.020 mm in size was mounted on a Cryoloop with Paratone oil. Data were collected in a nitrogen gas stream at 100(2) K using phi and omega scans. Crystal-to-detector distance was 60 mm and exposure time was 10 seconds per frame using a scan width of 0.5°. Data collection was 100.0% complete to 25.000° in θ. A total of 60941 reflections were collected covering the indices, -9<=h<=9, -12<=k<=12, -29<=l<=29. 3541 reflections were found to be symmetry independent, with a R_{int} of 0.0491. Indexing and unit cell refinement indicated a primitive, orthorhombic lattice. The space group was found to be $P2_12_12_1$ (No. 19). The data were integrated using the Bruker SAINT software program and scaled using the SADABS software program. Solution by iterative methods (SHELXT) produced a complete heavy-atom phasing model consistent with the proposed structure. All non-hydrogen atoms were refined anisotropically by full-matrix least-squares (SHELXL-2013). All hydrogen atoms were placed using a riding model. Their positions were constrained relative to their parent atom using the appropriate HFIX command in SHELXL-2013. Absolute stereochemistry was unambiguously determined to be *S* at C1. The residual crystalline material was dissolved in hexane and isopropanol (5:1, 4 ml). HPLC analysis of the solution revealed an upgrade to 94% ee of the product mixture, which is consistent with the absolute stereochemistry of the single crystal being the same as the major product formed from the catalytic reaction.

Table 5.2. Crystal data and structure refinement for 24

Empirical formula	C24 H22 Br N
Formula weight	404.33
Temperature	100(2) K
Wavelength	0.71073 Å
Crystal system	Orthorhombic
Space group	$P2_12_12_1$
Unit cell dimensions	a = 7.7727(4) Å a= 90°.
	b = 10.1494(6) Å b= 90°.
	c = 24.4112(14) Å g = 90°.
Volume	1925.76(19) Å^3
Z	4
Density (calculated)	1.395 Mg/m^3
Absorption coefficient	2.141 mm^{-1}
F(000)	832
Crystal size	0.150 x 0.100 x 0.020 mm^3
Crystal color/habit	colorless plate
Theta range for data collection	1.668 to 25.382°.
Index ranges	-9<=h<=9, -12<=k<=12, -29<=l<=29
Reflections collected	60941
Independent reflections	3541 [R(int) = 0.0491]
Completeness to theta = 25.000°	100.0 %
Absorption correction	Semi-empirical from equivalents
Max. and min. transmission	0.929 and 0.733
Refinement method	Full-matrix least-squares on F^2
Data / restraints / parameters	3541 / 0 / 237
Goodness-of-fit on F^2	1.077
Final R indices [I>2sigma(I)]	R1 = 0.0194, wR2 = 0.0469
R indices (all data)	R1 = 0.0210, wR2 = 0.0477
Absolute structure parameter	-0.014(3)
Extinction coefficient	n/a
Largest diff. peak and hole	0.297 and -0.229 e$^-$Å^{-3}

Table 5.3. Atomic coordinates of 24

Atom	x	y	z	U(eq)
C(1)	184(3)	11409(3)	8213(1)	25(1)
C(2)	778(4)	12512(3)	8603(1)	36(1)
C(3)	47(4)	11867(3)	7624(1)	30(1)
C(4)	-582(4)	10814(3)	7232(1)	35(1)
C(5)	2947(3)	10140(2)	8031(1)	20(1)
C(6)	3723(3)	9046(3)	8238(1)	18(1)
C(7)	2609(3)	8448(3)	8627(1)	17(1)
C(8)	2716(3)	7337(2)	8967(1)	17(1)
C(9)	1365(3)	7045(3)	9320(1)	18(1)
C(10)	-87(3)	7892(3)	9327(1)	20(1)
C(11)	-231(3)	8983(3)	8995(1)	22(1)
C(12)	1123(4)	9252(2)	8637(1)	18(1)
C(13)	1418(3)	5869(2)	9683(1)	18(1)
C(14)	2477(3)	4788(3)	9571(1)	22(1)
C(15)	2520(3)	3694(3)	9908(1)	22(1)
C(16)	1483(3)	3602(3)	10373(1)	18(1)
C(17)	414(3)	4677(3)	10487(1)	21(1)
C(18)	401(3)	5779(3)	10154(1)	21(1)
C(19)	1510(3)	2418(3)	10730(1)	20(1)
C(20)	1979(4)	1183(3)	10531(1)	23(1)
C(21)	2018(4)	87(3)	10867(1)	28(1)
C(22)	1580(4)	194(3)	11414(1)	30(1)
C(23)	1101(4)	1411(3)	11623(1)	30(1)
C(24)	1069(4)	2505(3)	11286(1)	23(1)
N(1)	1338(3)	10261(2)	8264(1)	20(1)
Br(1)	5980(1)	8494(1)	8076(1)	23(1)

[a]Values represent atomic coordinates x 10^4 and equivalent isotropic displacement parameters (Å^2 x 10^3) for **24**. U(eq) is defined as one third of the trace of the orthogonalized U tensor.

4-(5-Bromo-indol-1-yl)-2,2-diphenylpentan-1-ol
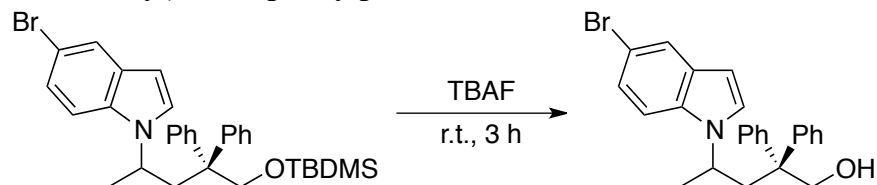
Compound **20** (75 mg, 0.14 mmol) was charged into an oven-dried flask (25 ml, round-bottom) under nitrogen. Dry, degassed THF was added to the flask through a septum (0.2 ml). The resulting solution was placed in an ice bath at 0 °C and a 0.5 M solution of TBAF in THF was added (0.56 ml, 0.28 mmol). The flask was removed from the ice bath and was allowed to stir at room temperature. Upon complete consumption of the starting material (3 h), a 1:1 mixture of brine and saturated $NaHCO_3$ (2 ml) was added to the solution. The organic material was extracted with ethyl acetate (3 ml, 4 times). The solvent

was removed under rotary evaporation to yield a waxy solid. The solid was dissolved in refluxing hexanes (1.5 ml). Toluene was added to the warm solution (0.1 ml), and the solution was allowed to cool. The title compound was isolated as a white crystalline material after washing with hexanes (56 mg, 92% yield).

¹H NMR (500 MHz, CDCl₃): δ 7.76 (d, J = 1.8 Hz, 1H), 7.25 (dd, J = 8.7, 1.9 Hz, 1H), 7.04-6.99 (m, 3H), 6.99-6.92 (m, 3H), 6.87 (dd, J = 8.0, 1.4 Hz, 2H), 6.84-6.78 (m, 3H), 6.48 (d, J = 8.8 Hz, 1H), 6.28 (d, J = 3.1 Hz, 1H), 4.01-3.88 (m, 1H), 3.54 (dd, J = 10.8, 6.2 Hz, 1H), 3.34 (dd, J = 10.8, 6.7 Hz, 1H), 2.83 (dd, J = 14.3, 8.2 Hz, 1H), 2.21 (dd, J = 14.3, 3.9 Hz, 1H), 0.90 (d, J = 6.8 Hz, 3H), 0.53 (t, J = 6.4 Hz, 1H).

¹³C NMR (151 MHz, C₆D₆): δ 146.2, 145.1, 133.9, 130.4, 128.2, 128.2, 128.0, 127.9, 126.4, 126.2, 125.5, 123.9, 123.4, 112.7, 111.3, 101.6, 66.9, 51.3, 48.5, 42.2, 23.3.

HPLC analysis: 30% ee, Chiralcel OD-H column, 5% isopropanol in hexane, 0.8 mL/min flow rate, 220 nm and 254 nm UV lamp, $t_{[major]}$ = 13.4 min, $t_{[minor]}$ = 32.4 min.

Anal. Calcd for $C_{25}H_{24}BrNO$: C 69.13%, H 5.57%, N 3.22%; Found: C 69.40%, H 5.54%, N 3.14%.

tert-Butyl((2,2-diphenylpent-4-en-1-yl)oxy)dimethylsilane
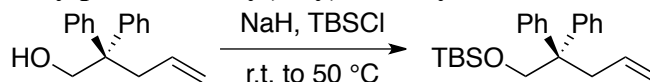
In a nitrogen-filled dry-box, an oven dried flask (100 ml, round bottom) was charged with sodium hydride (440 mg, 60 weight %, 11 mmol) and dry THF (5 ml). A syringe was charged with 2,2-diphenylpent-4-en-1-ol[60] in THF (2.0 g, 8.4 mmol in 20 ml THF). A septum was placed on the round bottom flask, and the flask was removed from the dry-box. The flask was placed in an ice bath and the syringe containing the alcohol was added over 2 minutes. The flask was brought to room temperature and stirred for 15 minutes. A second syringe was charged with TBSCl in dry THF (1.95 g, 12.6 mmol in 10 ml THF) in the dry-box. The solution of TBSCl was added to the flask through the syringe and the flask was placed in a 50 °C oil bath. The reaction was complete after 3 h at 50 °C as monitored by TLC. The reaction was slowly quenched with water at 0 °C and brine was added to the flask. The organic material was extracted with ethyl acetate (30 ml, 3 times) and dried over MgSO₄. The solvent was removed by rotary evaporation and the residue was purified by silica-gel chromatography with hexanes as eluent to yield the title compound as a clear oil (2.95 g, 99% yield).

¹H NMR (600 MHz, C₆D₆): δ 7.16-7.07 (m, 8H), 7.01 (t, J = 7.0 Hz, 2H), 5.50 (td, J = 17.1, 7.4 Hz, 1H), 5.09 (d, J = 17.1 Hz, 1H), 4.93 (d, J = 10.1 Hz, 1H), 4.10 (s, 2H), 2.96 (d, J = 7.0 Hz, 2H), 0.83 (s, 9H), -0.21 (s, 6H).

¹³C NMR (151 MHz, C₆D₆): δ 146.4, 134.9, 128.3, 127.6, 125.8, 117.4, 67.9, 51.1, 40.6, 25.6, 18.0, -6.1.

Anal. Calcd for $C_{23}H_{32}OSi$: C 78.35%, H 9.15%; Found: C 78.64%, H 9.50%.

(*E*)-1-D-Oct-1-ene

DIBAL, -78 to r.t.; MeOD, -78 to r.t. → D-substituted oct-1-ene, >98% D incorporation
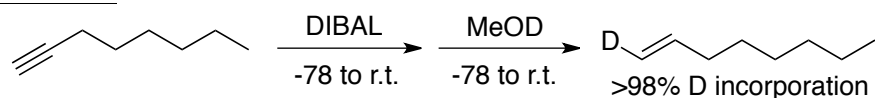
In a nitrogen-filled dry-box, an oven-dried flask (100 ml, round bottom) was charged with 1-octyne (5.5 ml, 38 mmol). The flask was sealed with a septum and removed from the dry-box. Under nitrogen, the flask was placed in a -78 °C bath and a 1.0 M solution of DIBAL in hexane was added by syringe to the flask (30. ml, 30. mmol). The reaction mixture was allowed to warm to room temperature and was stirred vigorously. After 6 h, the residual 1-octyne was removed under vacuum without exposing the solution to atmospheric conditions. The clear viscous oil was diluted with dry pentane (40 ml) and the resulting solution was placed in a -78 °C bath. Methanol-D (4.0 ml) was added to the flask and the mixture was vigorously stirred. The flask was removed from the cold bath and was allowed to warm to room temperature. Deuteronolysis of the vinyl aluminum intermediate occurred over a 10 h period and was noted by formation of a white, waxy solid. The solid was washed with pentane and discarded. The liquor was washed with brine, dried over $MgSO_4$, and was further purified by elution through a plug of silica gel. The pentane solvent was removed by rotary evaporation to yield the title compound as a clear liquid (3.1 g, 93% yield, >98% D incorporation).

Synthesis of Segphos-ligated Ir complex 26
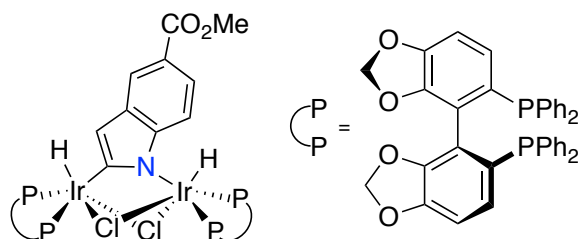
In a nitrogen-filled dry-box, a screw-capped vial (4 ml) was charged with $[Ir(cod)Cl]_2$ (17 mg, 0.025 mmol), (*S*)-Segphos (31 mg, 0.050 mmol), 5-methyl-indolecarboxylate (18 mg, 0.10 mmol), and a magnetic stirbar. The solids were dissolved in THF (1.5 ml), and the vial was sealed with a Teflon-lined cap. The vial was placed in a 100 °C heating block. After 1 hour, complete conversion to the dinuclear structure was observed by ^{31}P NMR spectroscopy. The vial was returned to the dry-box, and a solution of diethyl ether and pentane (3 ml, 2:1 Et$_2$O:pentane) was added to the solution while stirring, which induced the precipitation of a tan solid. The solid was washed with a solution of diethyl ether and benzene (1:1 Et$_2$O:C$_6$H$_6$) on a fritted funnel and subsequently discarded. The liquor was collected and the solvent was removed under high vacuum. The residue was dissolved in benzene (2 ml) and filtered through Celite to remove solids. A solution of diethyl ether and pentane (5 ml, 1:2 Et$_2$O:pentane) was added to the solution, causing the precipitation of the desired complex. The solid was washed with diethyl ether on a fritted funnel to yield the title compound as an orange solid (34 mg, 74% yield).

^{1}H NMR (600 MHz, C$_6$D$_6$): δ 8.32 (br m, 3H), 8.10 (br m, 2H), 8.05 (br m, 4H), 7.86 (s, 1H), 7.71 (d, *J* = 8.4 Hz, 1H), 7.67 (br s, 2H), 7.60 (br s, 2H), 7.48 (d, *J* = 8.5 Hz, 1H), 7.27-7.21 (m, 2H), 7.19-7.15 (m, 3H), 7.04-6.94 (m, 9H), 6.93-6.88 (m, 2H), 6.87-6.82 (m, 3H), 6.73 (br s, 2H), 6.65-6.51 (m, 8H), 6.49 (s, 1H), 6.43 (dd, *J* = 7.0 Hz, 1H), 6.34-6.26 (m, 1H), 6.11 (d, *J* = 8.1 Hz, 1H), 5.96 (d, *J* = 8.0 Hz, 1H), 5.87 (d, *J* = 8.0 Hz, 1H),

5.69 (d, J = 8.1 Hz, 1H), 5.29 (s, 1H), 5.24 (s, 2H), 5.21 (s, 2H), 5.00 (s, 1H), 4.83 (s, 2H), 3.54 (s, 3H), -20.57 (dd, J = 17.0 Hz, 1H), -22.26 (dd, J = 18.0, 14.5 Hz, 1H).

^{31}P NMR (162 MHz, CDCl$_3$): δ 5.4 (d, J = 7 Hz), 3.8 (d, J = 7 Hz), 1.1 (d, J = 17 Hz), -4.6 (d, J = 17 Hz).

Anal. Calcd for C$_{86}$H$_{65}$Cl$_2$Ir$_2$NO$_{10}$P$_4$: C 55.78%, H 3.54%, N 0.76%; Found: C 56.08%, H 3.64%, N 0.80%.

Structure determination of complex 26 by x-ray diffraction
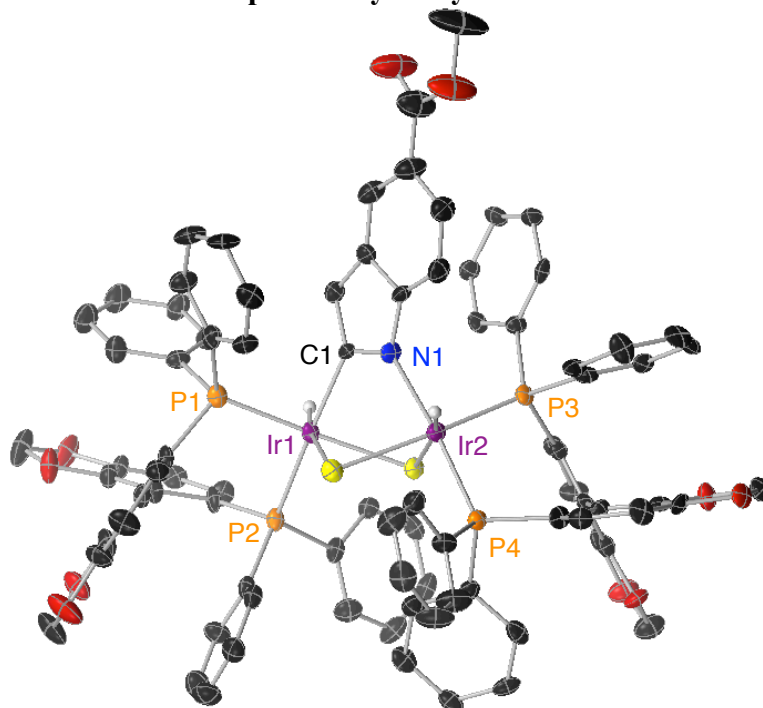
Single crystals suitable for x-ray diffraction of **26** were obtained by vapor diffusion of diethyl ether into a solution of toluene and benzene. The title compound (30 mg, 0.016 mmol) was dissolved in a 4 ml vial by a mixture of toluene and benzene (0.6 ml, 1:1 PhMe:PhH). The vial was placed within a 20 ml vial containing diethyl ether. The 20 ml vial was sealed with a Teflon-lined cap and was allowed to sit undisturbed at 2 °C for 4 days at which time orange prisms had formed. An orange prism 0.120 x 0.100 x 0.100 mm in size was mounted on a Cryoloop with Paratone oil. Data were collected in a nitrogen gas stream at 100(2) K using phi and omega scans. Crystal-to-detector distance was 60 mm and exposure time was 10 seconds per frame using a scan width of 0.5°. Data collection was 99.9% complete to 25.000° in θ. A total of 69388 reflections were collected covering the indices, -22<=h<=21, -22<=k<=22, -32<=l<=31. 17211 reflections were found to be symmetry independent, with an R$_{int}$ of 0.0637. Indexing and unit cell refinement indicated a primitive, orthorhombic lattice. The space group was found to be P2$_1$2$_1$2$_1$ (No. 19). The data were integrated using the Bruker SAINT software program and scaled using the SADABS software program. Solution by iterative methods (SHELXT) produced a complete heavy-atom phasing model consistent with the proposed structure. All non-hydrogen atoms were refined anisotropically by full-matrix least-squares (SHELXL-2013). All hydrogen atoms were placed using a riding model. Their positions were constrained relative to their parent atom using the appropriate HFIX

command in SHELXL-2013. SQUEEZE was used to treat the electronic contribution of disordered and diffuse benzene that was unable to be modeled satisfactorily. Its use has been noted in the CIF file.

Table 5.4. Crystal data and structure refinement for 26

Empirical formula	C96 H81 Cl2 Ir2 N O11 P4
Formula weight	2003.79
Temperature	100(2) K
Wavelength	0.71073 Å
Crystal system	Orthorhombic
Space group	$P2_12_12_1$
Unit cell dimensions	a = 18.4583(15) Å a= 90°.
	b = 18.8093(15) Å b= 90°.
	c = 26.944(2) Å g = 90°.
Volume	9354.7(13) Å^3
Z	4
Density (calculated)	1.423 Mg/m^3
Absorption coefficient	3.024 mm^{-1}
F(000)	4000
Crystal size	0.120 x 0.100 x 0.100 mm^3
Crystal color/habit	orange prism
Theta range for data collection	1.320 to 25.518°.
Index ranges	-22<=h<=21, -22<=k<=22, -32<=l<=31
Reflections collected	69388
Independent reflections	17211 [R(int) = 0.0637]
Completeness to theta = 25.000°	99.9 %
Absorption correction	Semi-empirical from equivalents
Max. and min. transmission	0.745 and 0.608
Refinement method	Full-matrix least-squares on F^2
Data / restraints / parameters	17211 / 0 / 1048
Goodness-of-fit on F^2	1.064
Final R indices [I>2sigma(I)]	R1 = 0.0391, wR2 = 0.0770
R indices (all data)	R1 = 0.0485, wR2 = 0.0803
Absolute structure parameter	-0.012(3)
Largest diff. peak and hole	2.101 and -1.156 e$^-$Å^{-3}

Table 5.5. Atomic Coordinates of 26

Atom	x	y	z	U(eq)
C(1)	8245(5)	3491(5)	6757(3)	23(2)
C(2)	7808(5)	3586(5)	7163(3)	26(2)
C(3)	7519(5)	2935(5)	7308(3)	25(2)
C(4)	7060(5)	2709(5)	7681(3)	33(2)
C(5)	6885(5)	1970(6)	7725(4)	39(3)
C(6)	7191(5)	1480(5)	7382(3)	32(2)
C(7)	7659(5)	1695(5)	7018(3)	29(2)
C(8)	7831(5)	2408(5)	6976(3)	23(2)
C(9)	6427(7)	1755(6)	8125(4)	56(3)
C(10)	5794(9)	794(7)	8502(5)	102(6)
C(11)	6891(4)	4284(4)	6289(3)	24(2)
C(12)	6349(5)	4500(5)	6617(3)	33(2)
C(13)	5805(5)	4029(5)	6742(3)	34(2)
C(14)	5777(5)	3352(5)	6558(3)	36(3)
C(15)	6299(5)	3144(5)	6229(3)	34(2)
C(16)	6865(5)	3591(5)	6097(3)	27(2)
C(17)	7561(5)	5570(4)	6618(3)	22(2)
C(18)	7012(5)	6044(5)	6496(3)	29(2)
C(19)	6846(6)	6599(5)	6818(4)	39(3)
C(20)	7236(6)	6681(5)	7258(4)	38(3)
C(21)	7759(5)	6207(5)	7378(3)	33(2)
C(22)	7930(5)	5649(5)	7063(3)	29(2)
C(23)	7678(5)	5210(4)	5581(3)	22(2)
C(24)	7349(5)	4847(5)	5203(3)	29(2)
C(25)	7366(5)	5078(5)	4703(3)	35(2)
C(26)	7708(5)	5708(5)	4627(3)	35(2)
C(27)	8230(6)	6683(6)	4291(4)	46(3)
C(28)	8029(5)	6081(5)	4999(3)	30(2)
C(29)	8062(5)	5844(5)	5482(3)	23(2)
C(30)	8512(5)	6243(4)	5846(3)	26(2)
C(31)	8329(5)	6923(5)	6000(3)	25(2)
C(32)	7748(5)	7941(5)	6142(5)	48(3)
C(33)	8720(5)	7278(4)	6354(3)	25(2)
C(34)	9332(5)	7017(5)	6552(3)	27(2)
C(35)	9563(5)	6337(4)	6400(3)	23(2)
C(36)	9170(4)	5953(4)	6061(3)	23(2)
C(37)	9526(5)	5161(4)	5197(3)	24(2)
C(38)	9845(5)	5764(5)	4984(3)	30(2)
C(39)	9917(5)	5830(5)	4488(3)	35(2)
C(40)	9679(6)	5294(5)	4175(4)	39(3)
C(41)	9343(5)	4712(5)	4372(3)	29(2)
C(42)	9261(5)	4643(5)	4876(3)	25(2)

C(43)	10423(5)	5006(4)	6062(3)	23(2)
C(44)	10990(5)	5058(5)	5741(3)	32(2)
C(45)	11696(5)	5005(5)	5909(4)	37(3)
C(46)	11831(5)	4900(5)	6408(4)	36(3)
C(47)	11258(5)	4838(4)	6732(3)	25(2)
C(48)	10560(5)	4892(4)	6567(3)	22(2)
C(49)	9323(4)	2037(4)	7401(3)	20(2)
C(50)	9338(5)	2760(4)	7545(3)	22(2)
C(51)	9084(5)	2966(4)	7995(3)	25(2)
C(52)	8764(5)	2475(4)	8316(3)	28(2)
C(53)	8717(5)	1770(5)	8173(3)	26(2)
C(54)	9002(5)	1556(4)	7725(3)	24(2)
C(55)	9615(5)	797(5)	6840(3)	23(2)
C(56)	9109(5)	409(4)	6579(3)	25(2)
C(57)	9076(6)	-334(5)	6653(3)	34(2)
C(58)	9535(5)	-666(5)	6977(3)	32(2)
C(59)	10057(5)	-276(4)	7232(3)	28(2)
C(60)	10082(5)	455(4)	7166(3)	23(2)
C(61)	10603(5)	1989(4)	6759(3)	22(2)
C(62)	10917(5)	2510(4)	7056(3)	24(2)
C(63)	11637(5)	2730(5)	7000(3)	26(2)
C(64)	12027(5)	2419(4)	6643(3)	25(2)
C(65)	12907(5)	2005(5)	6143(4)	39(2)
C(66)	11741(5)	1885(4)	6345(3)	25(2)
C(67)	11030(5)	1659(4)	6379(3)	21(2)
C(68)	10776(4)	1046(4)	6089(3)	19(2)
C(69)	11079(4)	394(4)	6205(3)	20(2)
C(70)	11701(5)	-489(4)	6563(3)	27(2)
C(71)	10858(5)	-240(4)	5987(3)	25(2)
C(72)	10350(5)	-259(5)	5627(3)	31(2)
C(73)	10053(5)	386(5)	5490(3)	26(2)
C(74)	10258(5)	1040(4)	5713(3)	24(2)
C(75)	9264(5)	1634(5)	4990(3)	23(2)
C(76)	9621(6)	1494(6)	4552(4)	42(3)
C(77)	9264(6)	1256(6)	4143(4)	44(3)
C(78)	8510(6)	1171(5)	4158(4)	38(3)
C(79)	8165(6)	1329(5)	4580(4)	40(3)
C(80)	8535(5)	1546(5)	5007(3)	33(2)
C(81)	10503(5)	2422(5)	5283(3)	23(2)
C(82)	10356(5)	3114(5)	5147(3)	29(2)
C(83)	10853(5)	3523(5)	4907(3)	31(2)
C(84)	11531(5)	3243(5)	4793(3)	27(2)
C(85)	11692(5)	2568(5)	4936(3)	26(2)
C(86)	11200(5)	2144(4)	5175(3)	28(2)
C(87)	9799(7)	7750(6)	5091(5)	58(3)
C(88)	9864(7)	7898(7)	4591(5)	66(4)

C(89)	10540(8)	8093(8)	4414(5)	84(5)
C(90)	11131(7)	8122(7)	4740(4)	66(4)
C(91)	11004(7)	7979(6)	5232(4)	52(3)
C(92)	10343(6)	7776(5)	5406(4)	43(3)
C(93)	8505(7)	4992(8)	3008(4)	76(4)
C(94)	9159(8)	4628(9)	2819(4)	84(5)
C(95)	10151(7)	3935(7)	3045(4)	69(4)
C(96)	10532(9)	3592(9)	3465(6)	113(6)
N(1)	8294(4)	2760(3)	6659(2)	22(2)
O(1)	6188(5)	2127(4)	8453(3)	74(3)
O(2)	6269(5)	1034(4)	8104(3)	70(3)
O(3)	7814(4)	6062(4)	4176(2)	53(2)
O(4)	8343(4)	6698(3)	4812(2)	37(2)
O(5)	7739(3)	7306(3)	5850(2)	37(2)
O(6)	8398(4)	7932(3)	6445(3)	43(2)
O(7)	12744(3)	2522(3)	6514(2)	35(2)
O(8)	12258(3)	1623(3)	6030(2)	27(2)
O(9)	11605(3)	277(3)	6551(2)	28(2)
O(10)	11243(3)	-794(3)	6199(2)	27(1)
O(11)	9499(5)	4241(4)	3189(2)	63(2)
P(1)	7727(1)	4809(1)	6200(1)	23(1)
P(2)	9452(1)	5060(1)	5864(1)	21(1)
P(3)	9640(1)	1774(1)	6788(1)	20(1)
P(4)	9783(1)	1880(1)	5555(1)	20(1)
Cl(1)	8519(1)	3219(1)	5595(1)	25(1)
Cl(2)	9813(1)	3425(1)	6356(1)	22(1)
Ir(1)	8754(1)	4186(1)	6278(1)	19(1)
Ir(2)	9069(1)	2348(1)	6172(1)	20(1)

[a]Values represent atomic coordinates x 10^4 and equivalent isotropic displacement parameters (Å^2 x 10^3) for **26**. U(eq) is defined as one third of the trace of the orthogonalized U tensor.

Synthesis of DM-Segphos-ligated Ir complex 27
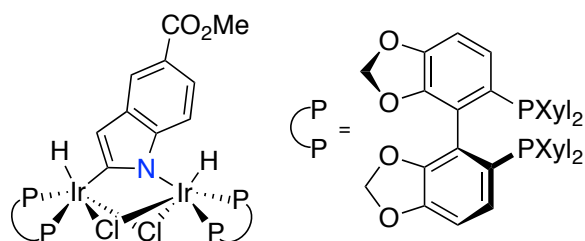
In a nitrogen-filled dry-box, a screw-capped vial (4 ml) was charged with [Ir(cod)Cl]$_2$ (34 mg, 0.050 mmol), (*S*)-DM-Segphos (72 mg, 0.10 mmol), 5-methyl-indolecarboxylate (35 mg, 0.20 mmol), and a magnetic stirbar. The solids were dissolved in toluene (3.5 ml), and the vial was sealed with a Teflon-lined cap. The vial was placed in a 100 °C heating block. After 1 hour, complete conversion to the dinuclear structure was observed by ^{31}P NMR spectroscopy. The vial was returned to the dry-box and heptane (20 ml) was added to the solution while stirring, which induced the precipitation of a tan solid. The solid was washed with a solution of benzene and heptane (1:4 C$_6$H$_6$:heptane) on a fritted funnel and subsequently discarded. The liquor was collected and the solution was concentrated under vacuum (ca. 5 ml final volume). The

residual suspension was allowed to warm to 70 °C, and undissolved solids were filtered from the solution. The yellow solution was allowed to sit undisturbed for 24 h at -35 °C. The title compound was isolated as a yellow solid with 5-methyl-indolecarboxylate as a residual impurity (38 mg, ca. 37% yield).

^{1}H NMR (500 MHz, C$_6$D$_6$): δ 8.71 (s, 1H), 8.26 (dd, J = 8.6, 1.6 Hz, 1H), 7.95 (br m, 6H), 7.75 (dd, J = 8.5, 1.7 Hz, 1H), 7.67-7.54 (m, 5H), 7.49 (br s, 2H), 7.04 (br s, 1H), 7.00-6.96 (m, 1H), 6.79 (s, 1H), 6.76 (s, 2H), 6.72 (s, 1H), 6.69-6.58 (m, 4H), 6.56 (s, 1H), 6.52-6.49 (m, 1H), 6.48 (s, 1H), 6.42-6.38 (m, 1H), 6.36 (s, 1H), 6.27-6.19 (m, 2H), 6.14 (s, 1H), 6.12 (s, 1H), 5.47 (dd, J = 8.2, 1.1 Hz, 1H), 5.32 (d, J = 1.1 Hz, 1H), 5.26 (d, J = 1.1 Hz, 1H), 5.25 (d, J = 1.7 Hz, 1H), 5.17 (d, J = 1.6 Hz, 1H), 5.13 (d, J = 1.4 Hz, 1H), 4.95 (d, J = 1.4 Hz, 1H), 4.94 (d, J = 1.7 Hz, 1H), 4.68 (d, J = 1.6 Hz, 1H), 3.60 (s, 3H), 2.34 (s, 6H), 2.25 (br s, 6H), 2.15 (s, 6H), 2.06 (br s, 6H), 1.92 (s, 12H), 1.88 (s, 6H), 1.63 (s, 6H), -21.02 (dd, J = 17.6 Hz, 1H), -22.90 (dd, J = 18.7, 15.3 Hz, 1H).

^{31}P NMR (162 MHz, C$_6$D$_6$): δ 7.8 (d, J = 7 Hz), 4.6 (d, J = 7 Hz), -1.2 (d, J = 17 Hz), -4.8 (d, J = 17 Hz).

ESI-MS: m/z 2076 (100%, [M]$^{\bullet+}$), 1637 (30%, [L$_2$Ir]$^+$).

Measurement of the diffusion coefficients of resting state complexes by NMR DOSY
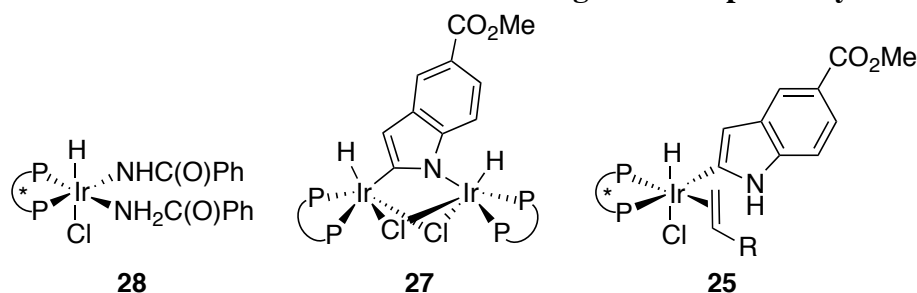

Figure 5.15 Structures of mononuclear and dinuclear model complexes employed for comparison of diffusion coefficients to complex **25**.

The complex observed under catalytic reaction conditions was prepared in a nitrogen-filled dry-box by charging a vial with [Ir(cod)Cl]$_2$ (10. mg, 0.015 mmol), (*S*)-DTBM-Segphos (35 mg, 0.030 mmol), 5-Me-indole-carboxylate (90. mg, 0.50 mmol), and 1-octene (0.2 ml). The mixture was dissolved in toluene-d_8 (0.45 ml) and sealed with a Teflon-lined cap. The solution was placed in a 100 °C heating block for 45 min at which point a light brown solution had formed. The vial was returned to the dry-box and complex **27** (39 mg, 0.019 mmol) was added to the solution. NMR DOSY experiments were conducted on the solution with complex **27** as an internal model of the dinuclear iridium complex by monitoring the iridium-hydride resonances. Diffusion coefficients were determined for the resting-state complex and the dinuclear model complex to be 4.7 x 10^{-6} cm^2/s and 3.9 x 10^{-6} cm^2/s, respectively. Independently, mononuclear model complex **28** was prepared following a previously reported procedure.[31] The model mononuclear complex (49 mg, 0.050 mmol) was dissolved in toluene-d_8 (0.45 ml). To this solution was added 1-octene (0.10 ml) and 5-Me-indolecarboxylate (90. mg, 0.50 mmol). The diffusion coefficient was measured by NMR DOSY to be 4.8 x 10^{-6} cm^2/s.

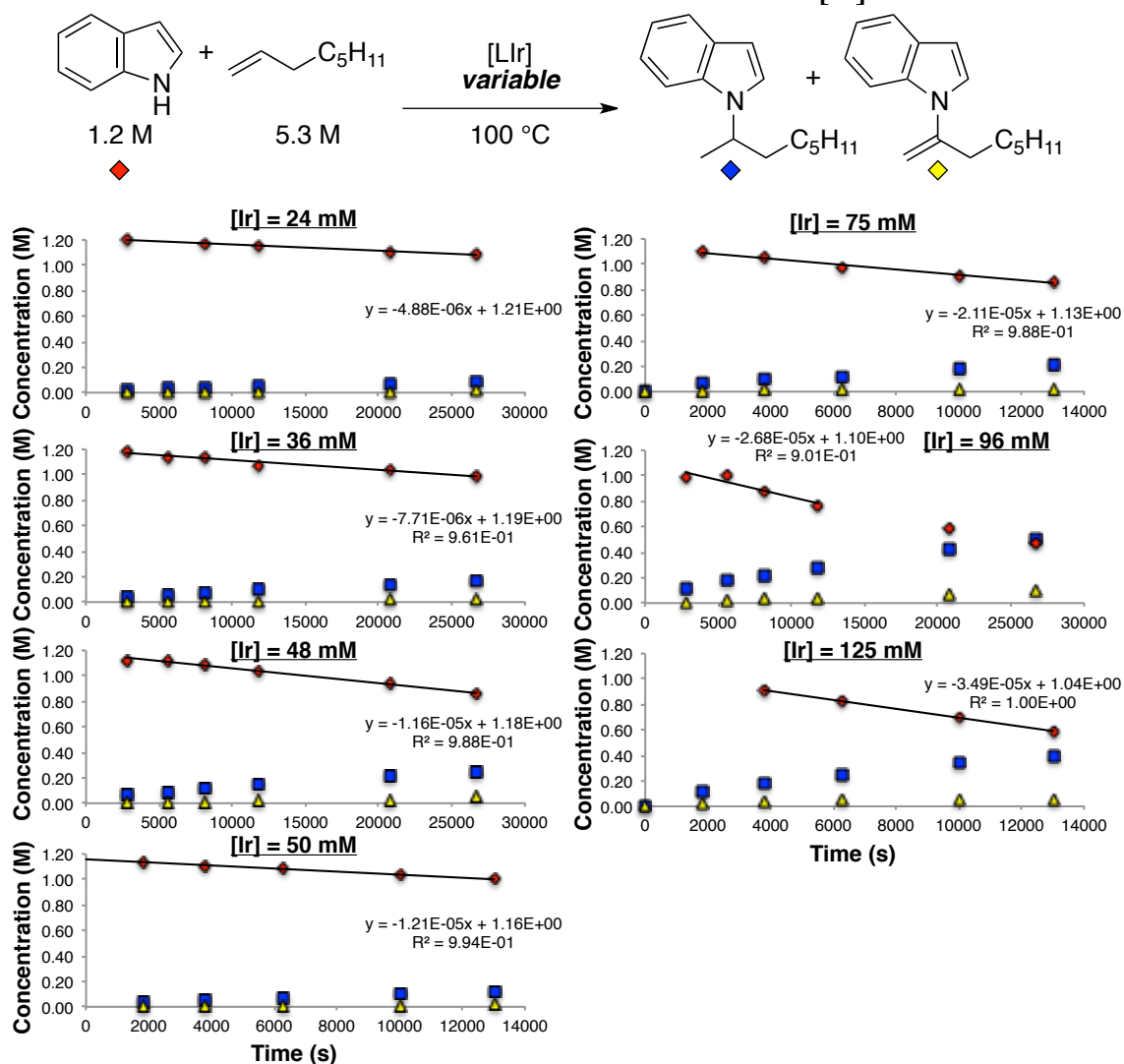**Kinetic studies on the addition of indole to 1-octene: variable [Ir]**

Figure 5.16. Initial rates of Ir-catalyzed hydroamination with varying Ir concentrations.

In a nitrogen-filled glove box, a volumetric flask (5.0 ml) was charged with [Ir(cod)Cl]$_2$ (101 mg, 0.150 mmol) and (*S*)-DTBM-Segphos (357 mg, 0.303 mmol). The solids were dissolved in THF (5.0 ml, 0.060 M solution). An oven-dried 4 ml vial was charged with the appropriate amount of the described catalyst solution and the THF was removed under vacuum in the dry-box. Indole (35 mg, 0.30 mmol) was added to each vial, which contained the metal-ligand residue. To these solids was added 1-octene (200. μl, 1.33 mmol) and octane (50. μl). Each vial was charged with a magnetic stirbar, sealed with a Teflon-lined cap, and removed from the dry-box. The reaction mixture was stirred in an aluminum heating block at 100 °C outside of the dry-box. The reaction was removed every 45-60 min and rapidly cooled in a water bath. The vial was taken into the dry-box, and a 10 μl aliquot was removed from the reaction mixture. The vial was resealed and returned to the metal heating block. The aliquots were analyzed by gas chromatography with dodecane as the internal standard. Reaction rates were determined by

measuring consumption of the indole substrate. The plot of initial rate as a function of iridium concentration reveals a first order dependence of the rate of reaction on the concentration of catalyst (Figure 5.17).
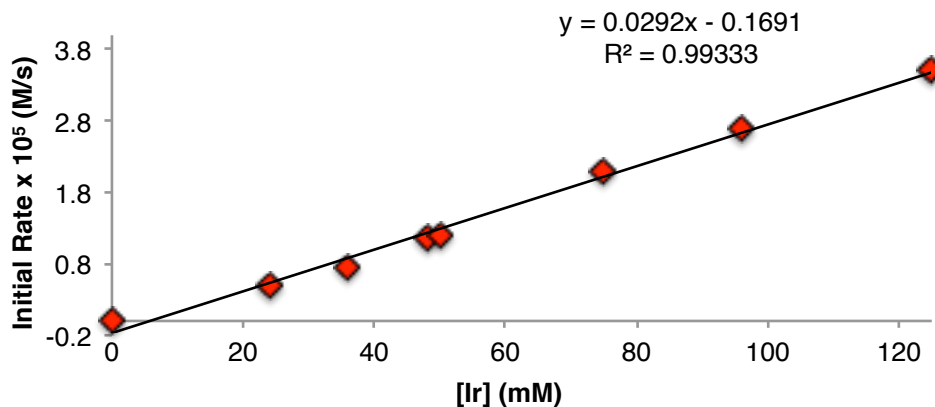

Figure 5.17. Effect of iridium concentration on the initial rate of Ir-catalyzed addition of indole to 1-octene.

Kinetic studies on the addition of indole to 1-octene: variable [1-octene]

Figure 5.18. Rates of indole consumption in Ir-catalyzed additions to 1-octene for reactions conducted with various concentrations of 1-octene.

In a nitrogen-filled glove box, a volumetric flask (5.0 ml) was charged with [Ir(cod)Cl]$_2$ (101 mg, 0.150 mmol) and (S)-DTBM-Segphos (357 mg, 0.303 mmol). The solids were dissolved in THF (5.0 ml, 0.060 M solution). An oven-dried 4 ml vial was charged with the described catalyst solution (190 μl, 0.011 mmol Ir) and the THF was removed under vacuum in the dry-box. Indole (35 mg, 0.30 mmol) was added to each vial, which contained the metal-ligand residue. To these solids were added appropriate amounts of 1-octene. Octane was added to bring the total volume of the reaction mixture to 0.25 ml. Each vial was charged with a magnetic stirbar, sealed with a Teflon-lined cap, and removed from the dry-box. The reaction mixture was stirred in an aluminum heating block at 100 °C outside of the dry-box. The reaction was removed every 45-60 min and rapidly cooled in a water bath. The vial was taken into the dry-box, and a 10 µl aliquot was removed from the reaction mixture. The vial was resealed and returned to the metal heating block. The aliquots were analyzed by gas chromatography with dodecane as the internal standard. Reaction rates were determined by measuring consumption of the indole substrate. The plot of initial rate as a function of 1-octene concentration reveals a zeroth order dependence of the rate of reaction on the concentration of olefin under the catalytically relevant conditions at 3.5 M [1-octene] (Figure 5.19).

Figure 5.19. Effect of 1-octene concentration on the initial rate of Ir-catalyzed addition of indole to 1-octene.

Kinetic studies on the addition of indole to 1-octene: variable [indole]
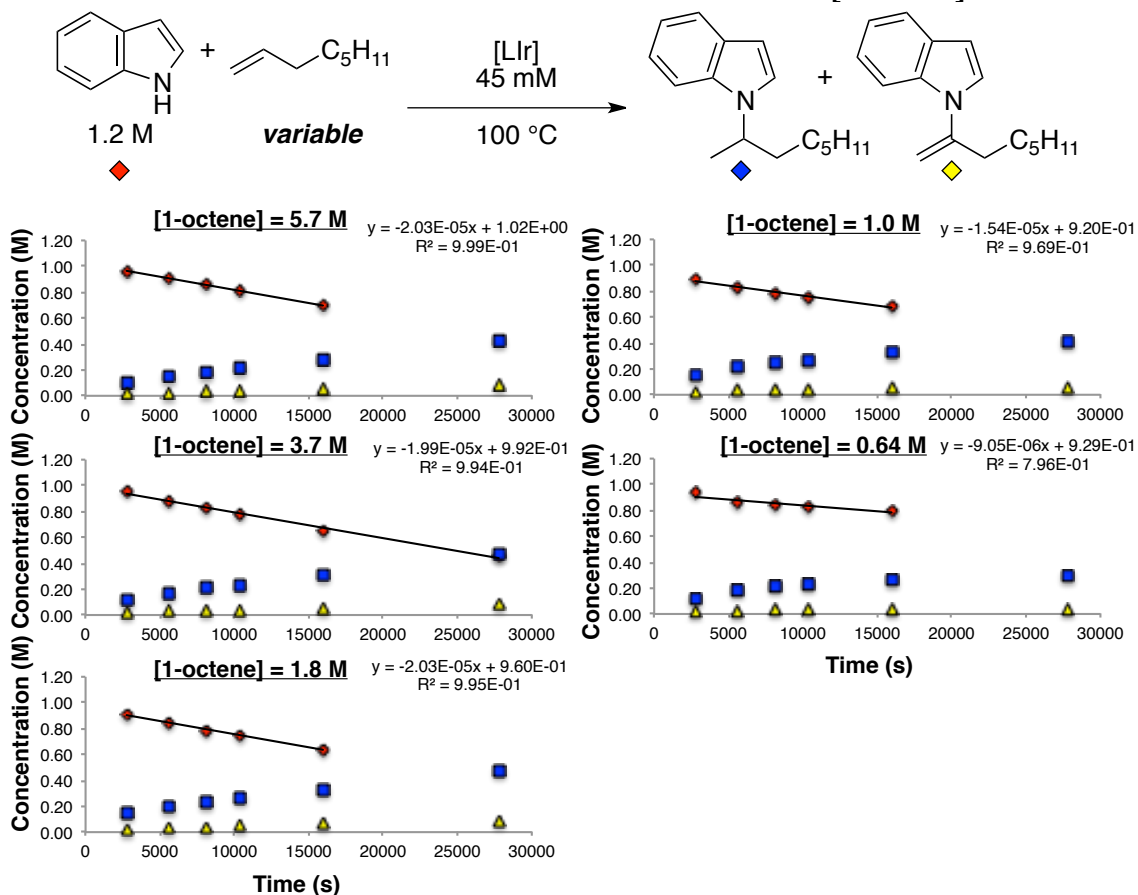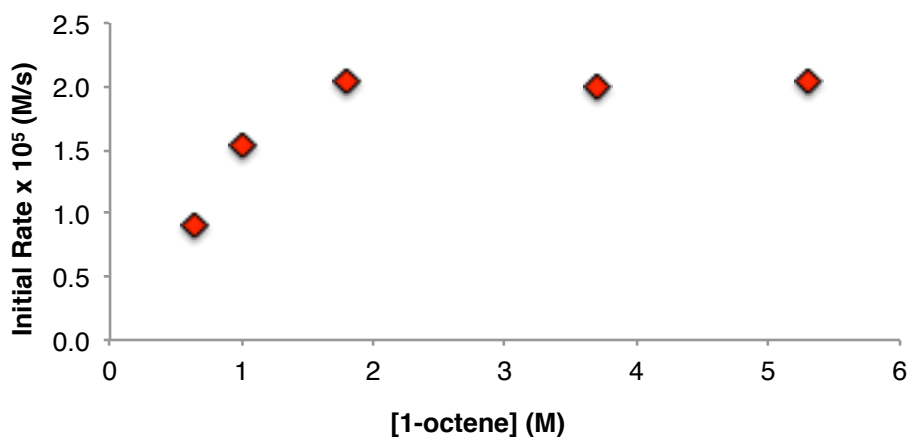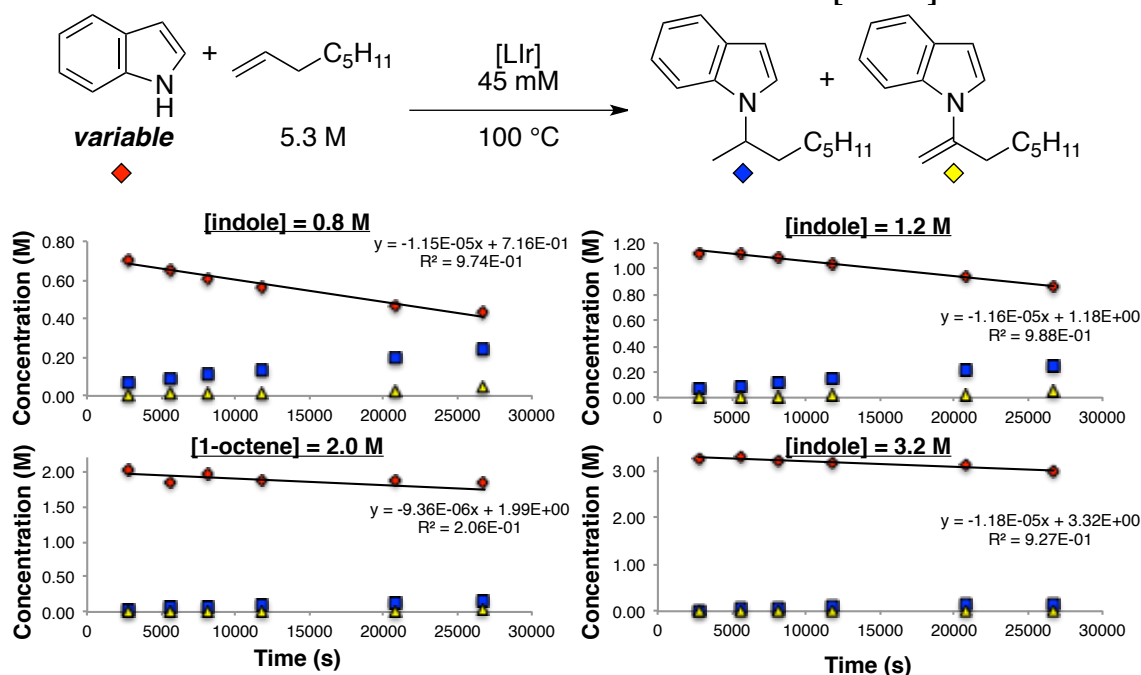

Figure 5.20. Rates of indole consumption in Ir-catalyzed additions to 1-octene for reactions conducted with various concentrations of indole.

In a nitrogen-filled glove box, a volumetric flask (5.0 ml) was charged with [Ir(cod)Cl]$_2$ (101 mg, 0.150 mmol) and (S)-DTBM-Segphos (357 mg, 0.303 mmol). The solids were dissolved in THF (5.0 ml, 0.060 M solution). An oven-dried 4 ml vial was charged with the described catalyst solution (0.20 ml, 0.012 mmol Ir), and the THF was removed under vacuum in the dry-box. The appropriate mass of indole was added to each vial, which contained the metal-ligand residue. To these solids was added 1-octene (200. μl, 1.33 mmol) and octane (50. μl). Each vial was charged with a magnetic stirbar, sealed with a Teflon-lined cap, and removed from the dry-box. The reaction mixture was stirred in an aluminum heating block at 100 °C outside of the dry-box. The reaction was removed every 45-60 min and rapidly cooled in a water bath. The vial was taken into the dry-box, and a 10 μl aliquot was removed from the reaction mixture. The vial was resealed and returned to the metal heating block. The aliquots were analyzed by gas chromatography with dodecane as the internal standard. Reaction rates were determined by measuring consumption of the indole substrate. The plot of initial rate as a function of indole concentration reveals a zeroth order dependence of the rate of reaction on the concentration of indole (Figure 5.21).
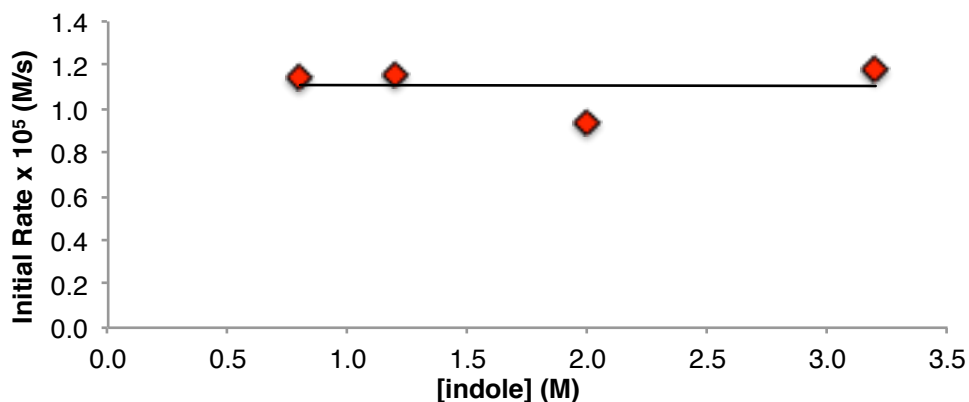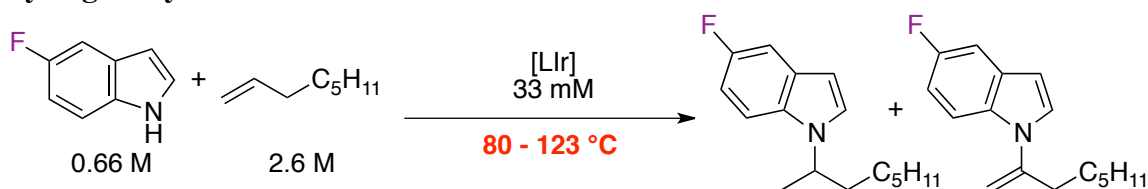
Figure 5.21. Effect of indole concentration on the initial rate of Ir-catalyzed addition of indole to 1-octene

Eyring analysis on the addition of indole to 1-octene.

In a nitrogen-filled glove box, an oven-dried 20 ml capped vial was charged with [Ir(cod)Cl]$_2$ (61 mg, 0.091 mmol, 33 mM final [iridium]), (*S*)-DTBM-Segphos (214 mg, 0.182 mmol, 33 mM final [ligand]), 5-fluoroindole (491 mg, 3.63 mmol, 0.66 M final [5-F-indole]), 1-octene (2.16 ml, 14.4 mmol, 2.6 M final [1-octene]), butyl acetate (0.48 ml), octane (2.16 ml), and 4-fluoro-bromobenzene (341 mg, 1.95 mmol, 0.35 M final concentration) as internal standard. The vial was sealed with a Teflon-lined cap and removed from the box. The vial was placed in a 110 °C heating block for 25 min to generate a yellow-green solution (5.5 ml total volume). The vial was removed from the heating block and returned to the glove-box. The solution was transferred into NMR tubes (0.6 ml per tube), which were sealed and removed from the box. Reaction rates were measured at temperatures ranging 80-123 °C by monitoring the consumption of 5-F-indole by ^{19}F NMR spectroscopy. Rate constants (s^{-1}) were calculated according to the empirical rate law in Figure 5.22.

$$\frac{\partial[\text{indole}]}{\partial t} = -k[\text{Ir}]^1[\text{indole}]^0[\,\diagup\!\!\!R\,]^0$$

$$k = \frac{k_{obs}}{[\text{Ir}]} \; , \; [\text{Ir}] = 0.033 \text{ M}$$

$$\ln\left(\frac{k}{T}\right) = -\left(\frac{\Delta H^{\ddagger}}{R}\right)\frac{1}{T} + \left(\frac{\Delta S^{\ddagger}}{R} - \ln\left(\frac{h}{k_b}\right)\right)$$

202
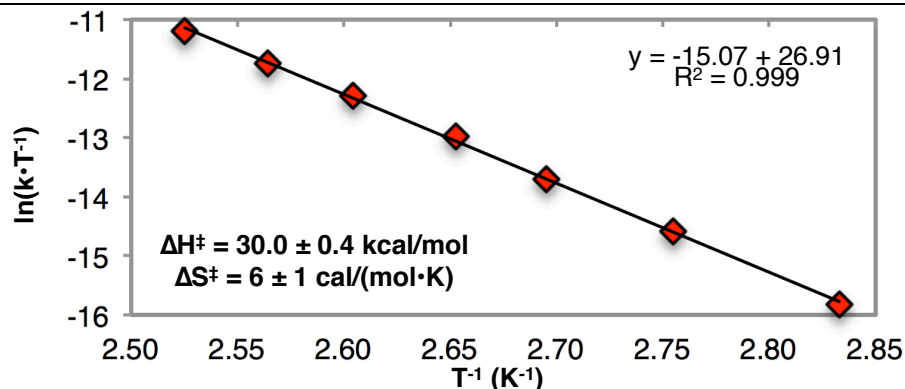
Figure 5.22. Eyring analysis for the iridium-catalyzed addition of 5-F-indole to 1-octene.

Measurement of the kinetic isotope effect of deutero-substituted indoles
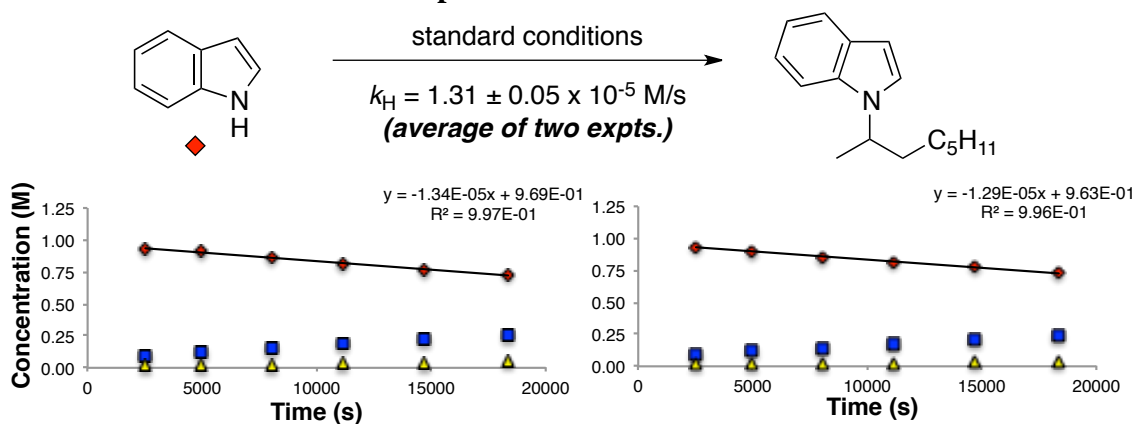
Figure 5.23. Initial rate of Ir-catalyzed addition of indole to 1-octene.

In a nitrogen-filled glove box, a volumetric flask (5.0 ml) was charged with [Ir(cod)Cl]$_2$ (101 mg, 0.150 mmol) and (S)-DTBM-Segphos (357 mg, 0.303 mmol). The solids were dissolved in THF (5.0 ml, 0.060 M solution). An oven-dried 4 ml vial was charged with the described catalyst solution (0.20 ml, 0.012 mmol Ir) and the THF was removed under vacuum in the dry-box. The appropriate detuero-indole (33 mg, 0.28 mmol) was added to each vial, which contained the metal-ligand residue. To these solids was added 1-octene (200. μl, 1.33 mmol) and octane (50. μl). Each vial was charged with a magnetic stirbar, sealed with a Teflon-lined cap, and removed from the dry-box. The reaction mixture was stirred in an aluminum heating block at 100 °C outside of the dry-box. The reaction was removed every 45-60 min and rapidly cooled in a water bath. The vial was taken into the dry-box, and a 10 μl aliquot was removed from the reaction mixture. The vial was resealed and returned to the metal heating block. The aliquots were analyzed by gas chromatography with dodecane as the internal standard. Reaction rates were determined by measuring consumption of the indole substrate.

Figure 5.24 Initial rate of Ir-catalyzed addition of 2-D-indole to 1-octene.
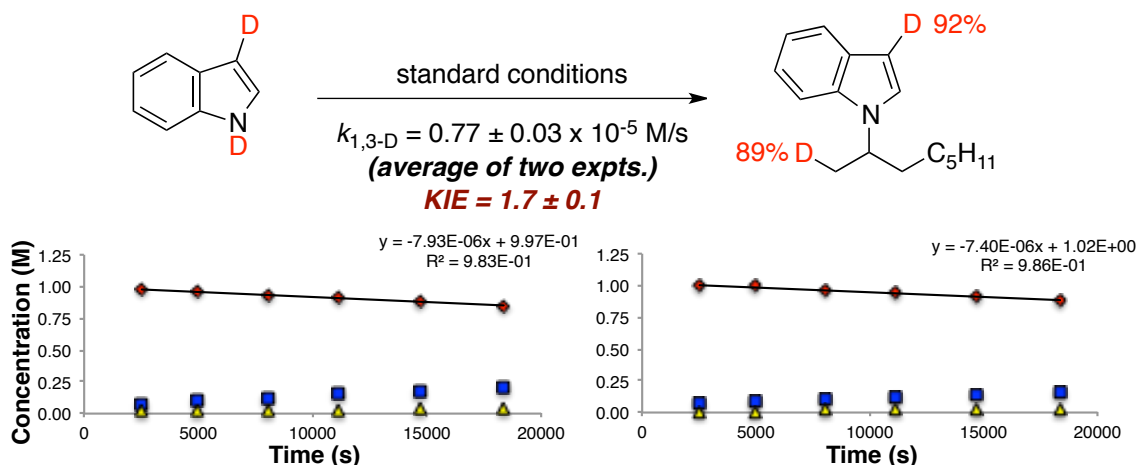
Figure 5.25 Initial rate of Ir-catalyzed addition of 1,3-D-indole to 1-octene.

Computational Details

All DFT calculations were performed with the Gaussian 09 software package. Geometry optimization of all the minima and transition states involved was carried out at the M06 level of theory at 298 K. The LANL2DZ basis set and pseudo potential were used for the iridium atom, and the 6-31G(d,p) basis set was used for other atoms. Five d-type orbitals were used as basis sets in all elements of the calculations. Vibrational frequencies were computed at the same level for each structure to determine if it is an energy minimum or a transition state and to evaluate its zero-point vibrational energy (ZPVE). Single point energy solvent effects were computed based on the gas-phase optimized structures using the LANL2DZ basis set and pseudo potential for the iridium atom and the 6-31+G(d,p) basis set was used for other atoms. The lowest energy transition state structures were reevaluated with single point energy solvent effects that employ higher order basis sets: the expanded basis set and pseudo potential for the iridium atom[61] and the 6-311++G** basis set was used for other atoms. Solvation energies in mesitylene were evaluated by a self-consistent reaction field (SCRF) using the CPCM model in which a

universal force field model (UFF) was used to define the atomic radii. In this paper, all energies discussed are Gibbs free energies in mesitylene ($\Delta G_{\text{mes 298 K}}$ and $\Delta G_{\text{mes 298 K}}$) unless specified; the entropy contributions were estimated by using the gas phase entropy values. The Gibbs free energy ($\Delta G_{\text{gas 298 K}}$) and the enthalpies ($\Delta H_{\text{gas 298 K}}$) in the gas phase are also given for reference.

Computational Results

Computational analysis was conducted on the Segphos-ligated analogues of **27** and **28**, rather than the DTBM-Segphos ligated complexes. All eight possible diastereomeric transition states that result from olefin or indole rotation were found for propene insertion into the Ir–C bond of **27**. Similarly, all eight possible diastereomeric transition states were found for propene insertion into the Ir–N bond of **28**. Gibbs free energies are related to the energy of the experimentally identified resting-state complex **25**.

Table 5.6. Relative energies of computed ground state.[a]

Ground State	G_{gas}	H_{gas}	G_{corr}	H_{corr}	ΔG_{gas}	ΔH_{gas}	ΔG_{sol}
Dimer	-6386.6767	-6386.4691	1.1325	1.3401	---	---	---
Indole	-363.4414	-363.4038	0.0991	0.1368	---	---	---
Propene	-117.7495	-117.7194	0.0543	0.0843	---	---	---
Dimer System	-3492.8085	-3492.6558	---	---	**0.0**	**0.0**	**0.0**

[a]Values for H and G are in Hartree. Values for ΔH and ΔG are in kcal/mol. Solvation modeling was conducted in a mesitylene medium.

Table 5.7. Relative energies of computed intermediate complexes.[a]

Ir–C Intermediate	G_{gas}	H_{gas}	G_{corr}	H_{corr}	ΔG_{gas}	ΔH_{gas}	ΔG_{sol}
Ir–C1	-3492.7965	-3492.6649	0.6951	0.8267	**7.5**	**-5.7**	**7.8**
Ir–C2	-3492.7969	-3492.6626	0.6914	0.8257	**7.3**	**-4.3**	**7.4**
Ir–C3	-3492.7969	-3492.6649	0.6947	0.8268	7.3	-5.7	7.9
Ir–C4	-3492.7978	-3492.6632	0.6912	0.8258	**6.7**	**-4.6**	**7.2**
Ir–N Intermediate	G_{gas}	H_{gas}	G_{corr}	H_{corr}	ΔG_{gas}	ΔH_{gas}	ΔG_{sol}
Ir–N1	-3492.7935	-3492.6617	0.6941	0.8259	**9.4**	**-3.7**	**8.2**
Ir–N2	-3492.7942	-3492.6598	0.6910	0.8254	**9.0**	**-2.5**	**9.5**
Ir–N3	-3492.7899	-3492.6562	0.6922	0.8259	**11.7**	**-0.2**	**11.0**
Ir–N4	-3492.7964	-3492.6635	0.6921	0.8250	**7.6**	**-4.8**	**7.9**

[a]Values for H and G are in Hartree. Values for ΔH and ΔG are in kcal/mol. Solvation modeling was conducted in a mesitylene medium.

Table 5.8. Relative energies of computed transition states.[a]

Mig. Ins. Ir–C TS	G_{gas}	H_{gas}	G_{corr}	H_{corr}	ΔG_{gas}	ΔH_{gas}	ΔG_{sol}
C1	-3492.7725	-3492.6414	0.6940	0.8251	22.6	9.1	30.6
C2	-3492.7741	-3492.6417	0.6923	0.8247	21.6	8.9	27.6
C1_rote	-3492.7676	-3492.6353	0.6919	0.8242	25.7	12.9	31.4
C2_rote	-3492.7716	-3492.6381	0.6903	0.8239	23.2	11.2	28.8
C1_flip	-3492.7710	-3492.6401	0.6937	0.8246	23.5	9.9	29.2
C2_flip	-3492.7726	-3492.6431	0.6957	0.8252	22.5	8.0	28.4
C1_rote_flip	-3492.7673	-3492.6351	0.6922	0.8244	25.9	13.0	31.2
C2_rote_flip	-3492.7647	-3492.6338	0.6944	0.8253	27.5	13.8	33.0
Mig. Ins. Ir–N TS	G_{gas}	H_{gas}	G_{corr}	H_{corr}	ΔG_{gas}	ΔH_{gas}	ΔG_{sol}
N1	-3492.7712	-3492.6391	0.6923	0.8244	23.4	10.5	27.8
N2	-3492.7733	-3492.6412	0.6920	0.8241	22.1	9.2	26.2
N1_rote	-3492.7633	-3492.6317	0.6919	0.8235	28.4	15.2	31.9
N2_rote	-3492.7665	-3492.6356	0.6936	0.8246	26.3	12.7	30.8
N1_flip	-3492.7738	-3492.6427	0.6928	0.8239	21.8	8.2	26.5
N2_flip	-3492.7724	-3492.6423	0.6944	0.8246	22.7	8.5	30.8
N1_rote_flip	-3492.7697	-3492.6380	0.6918	0.8234	24.4	11.2	29.2
N2_rote_flip	-3492.7680	-3492.6366	0.6924	0.8238	25.4	12.1	29.9

[a]Values for H and G are in Hartree. Values for ΔH and ΔG are in kcal/mol. Solvation modeling was conducted in a mesitylene medium.

Table 5.9. Relative energies of computed products of migratory insertion.[a]

Alkyl Product	G_{gas}	H_{gas}	G_{corr}	H_{corr}	ΔG_{gas}	ΔH_{gas}	ΔG_{sol}
C_MI_prod	-3492.8111	-3492.6785	0.6943	0.8269	-1.6	-14.2	3.4
N_MI_prod	-3492.7972	-3492.6645	0.6938	0.8264	7.1	-5.4	11.6

[a]Values for H and G are in Hartree. Values for ΔH and ΔG are in kcal/mol. Solvation modeling was conducted in a mesitylene medium.

5.5 References

(1)   Part of this chapter was reprinted with permission from Sevov, C. S.; Zhou, J.; Hartwig, J. F. *J. Am. Chem. Soc.*, **2014**, *136*, 3200. Copyright © 2014, American Chemical Society. Professor Steve Zhou is gratefully acknowledged for preliminary results on the Ir-catalyzed NH bond addition of indole to 1-octene. Permission to include this co-authored material was obtained from Steve Zhou and John F. Hartwig.

(2)   Bagley, M. C.; Dale, J. W.; Merritt, E. A.; Xiong, X. *Chem. Rev.*, **2005**, *105*, 685.

(3)   Kim, J.; Movassaghi, M. *Chem. Soc. Rev.*, **2009**, *38*, 3035.

(4)   Joule, J. A.; Mills, K. *Heterocyclic Chemistry*; John Wiley & Sons, 2010.

(5)   Sundberg, R. J.; Katritzky, A. R.; Meth-Cohn, O.; Rees, C. S. *Indoles*; Elsevier Science, 1996.

(6)   Bandini, M.; Melloni, A.; Umani-Ronchi, A. *Angew. Chem. Int. Ed.*, **2004**, *43*, 550.

(7)   Bandini, M.; Melloni, A.; Tommasi, S.; Umani-Ronchi, A. *Synlett*, **2005**, 1199.

(8)   Bandini, M.; Eichholzer, A. *Angew. Chem. Int. Ed.*, **2009**, *48*, 9608.

(9)   Stanley, L. M.; Hartwig, J. F. *Angewandte Chemie*, **2009**, *121*, 7981.

(10)   Cui, H.-L.; Feng, X.; Peng, J.; Lei, J.; Jiang, K.; Chen, Y.-C. *Angew. Chem. Int. Ed.*, **2009**, *48*, 5737.

(11)   Trost, B. M.; Fleming, I. *Comprehensive Organic Synthesis: Reduction*; Elsevier Science & Technology Books, 1991.

(12)   Robinson, B. *Chem. Rev.*, **1969**, *69*, 785.

(13)   Heaney, H.; Ley, S. V. *Journal of the Chemical Society, Perkin Transactions 1*, **1973**, 499.

(14)   Hartwig, J. F. In *Organotransition Metal Chemistry: From Bonding to Catalysis*; University Science Books: Sausalito, CA, 2010; Vol. 1, p 700.

(15)   Müller, T. E.; Hultzsch, K. C.; Yus, M.; Foubelo, F.; Tada, M. *Chem. Rev.*, **2008**, *108*, 3795.

(16)   Hesp, K. D.; Stradiotto, M. *Chemcatchem*, **2010**, *2*, 1192.

(17)   Hannedouche, J.; Schulz, E. *Chem. Eur. J.*, **2013**, *19*, 4972.

(18)   Hong, S.; Marks, T. J. *Acc. Chem. Res.*, **2004**, *37*, 673.

(19)   Dunne, J. F.; Fulton, D. B.; Ellern, A.; Sadow, A. D. *J. Am. Chem. Soc.*, **2010**, *132*, 17680.

(20)   Hesp, K. D.; Tobisch, S.; Stradiotto, M. *J. Am. Chem. Soc.*, **2010**, *132*, 413.

(21)   Julian, L. D.; Hartwig, J. F. *J. Am. Chem. Soc.*, **2010**, *132*, 13813.

(22)   Shen, X.; Buchwald, S. L. *Angew. Chem. Int. Ed.*, **2010**, *49*, 564.

(23)   Leitch, D. C.; Platel, R. H.; Schafer, L. L. *J. Am. Chem. Soc.*, **2011**, *133*, 15453.

(24)   Liu, Z.; Yamamichi, H.; Madrahimov, S. T.; Hartwig, J. F. *J. Am. Chem. Soc.*, **2011**, *133*, 2772.

(25)   Ryu, J.-S.; Li, G. Y.; Marks, T. J. *J. Am. Chem. Soc.*, **2003**, *125*, 12584.

(26)   Brunet, J. J.; Chu, N. C.; Diallo, O. *Organometallics*, **2005**, *24*, 3104.

(27)   Karshtedt, D.; Bell, A. T.; Tilley, T. D. *J. Am. Chem. Soc.*, **2005**, *127*, 12640.

(28)   Zhang, J.; Yang, C.-G.; He, C. *J. Am. Chem. Soc.*, **2006**, *128*, 1798.

(29)   Zhang, Z.; Lee, S. D.; Widenhoefer, R. A. *J. Am. Chem. Soc.*, **2009**, *131*, 5372.

(30)   Reznichenko, A. L.; Nguyen, H. N.; Hultzsch, K. C. *Angew. Chem. Int. Ed.*, **2010**, *49*, 8984.

(31)   Sevov, C. S.; Zhou, J.; Hartwig, J. F. *J. Am. Chem. Soc.*, **2012**, *134*, 11960.

(32)   Brunet, J.-J.; Commenges, G.; Neibecker, D.; Philippot, K. *J. Organomet. Chem.*, **1994**, *469*, 221.

(33)   Dorta, R.; Egli, P.; Zürcher, F.; Togni, A. *J. Am. Chem. Soc.*, **1997**, *119*, 10857.

(34)   McBee, J. L.; Bell, A. T.; Tilley, T. D. *J. Am. Chem. Soc.*, **2008**, *130*, 16562.

(35)   Zhou, J.; Hartwig, J. F. *J. Am. Chem. Soc.*, **2008**, *130*, 12220.

(36)   Kawatsura, M.; Hartwig, J. F. *J. Am. Chem. Soc.*, **2000**, *122*, 9546.

(37)   Utsunomiya, M.; Hartwig, J. F. *J. Am. Chem. Soc.*, **2003**, *125*, 14286.

(38)   Qian, H.; Widenhoefer, R. A. *Org. Lett.*, **2005**, *7*, 2635.

(39)   Pan, S. G.; Endo, K.; Shibata, T. *Org. Lett.*, **2012**, *14*, 780.

(40)   Nishina, N.; Yamamoto, Y. *Synlett*, **2007**, 1767.

(41)   Butler, K. L.; Tragni, M.; Widenhoefer, R. A. *Angew. Chem. Int. Ed.*, **2012**, *51*, 5175.

(42)   Löber, O.; Kawatsura, M.; Hartwig, J. F. *J. Am. Chem. Soc.*, **2001**, *123*, 4366.

(43)   Johns, A. M.; Sakai, N.; Ridder, A.; Hartwig, J. F. *J. Am. Chem. Soc.*, **2006**, *128*, 9306.

(44)   Brunet, J.-J.; Cadena, M.; Chu, N. C.; Diallo, O.; Jacob, K.; Mothes, E. *Organometallics*, **2004**, *23*, 1264.

(45)   Wang, X.; Widenhoefer, R. A. *Organometallics*, **2004**, *23*, 1649.

(46)   Cao, P.; Cabrera, J.; Padilla, R.; Serra, D.; Rominger, F.; Limbach, M. *Organometallics*, **2012**, *31*, 921.

(47)   Sevov, C. S.; Hartwig, J. F. *J. Am. Chem. Soc.*, **2013**, *135*, 2116.

(48)   Casalnuovo, A. L.; Calabrese, J. C.; Milstein, D. *J. Am. Chem. Soc.*, **1988**, *110*, 6738.

(49)   Liu, G.; Stahl, S. S. *J. Am. Chem. Soc.*, **2007**, *129*, 6328.

(50)   Hanley, P. S.; Marković, D.; Hartwig, J. F. *J. Am. Chem. Soc.*, **2010**, *132*, 6302.

(51)   Neukom, J. D.; Perch, N. S.; Wolfe, J. P. *J. Am. Chem. Soc.*, **2010**, *132*, 6276.

(52)   Hanley, P. S.; Hartwig, J. F. *J. Am. Chem. Soc.*, **2011**, *133*, 15661.

(53)   Weinstein, A. B.; Stahl, S. S. *Angew. Chem. Int. Ed.*, **2012**, *51*, 11505.

(54)   Hanley, P. S.; Hartwig, J. F. *Angew. Chem. Int. Ed.*, **2013**, *52*, 8510.

(55)   Tye, J. W.; Hartwig, J. F. *J. Am. Chem. Soc.*, **2009**, *131*, 14703.

(56)   Garrou, P. E.; Heck, R. F. *J. Am. Chem. Soc.*, **1976**, *98*, 4115.

(57)   Hartwig, J. F. In *Organotransition Metal Chemistry: From Bonding to Catalysis*; University Science Books: Sausalito, CA, 2010; Vol. 1, p 349.

(58)   Bähn, S.; Imm, S.; Mevius, K.; Neubert, L.; Tillack, A.; Williams, J. M. J.; Beller, M. *Chem. Eur. J.*, **2010**, *16*, 3590.

(59)   Zeng, F.; Alper, H. *Org. Lett.*, **2013**, *15*, 2034.

(60)   Qian, H.; Han, X.; Widenhoefer, R. A. *J. Am. Chem. Soc.*, **2004**, *126*, 9536.

CHAPTER 6

Iridium-Catalyzed Oxidative Olefination of Furans
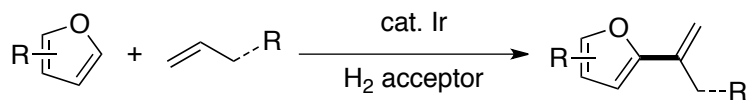with Unactivated Alkenes

6.1 Introduction

The oxidative coupling of arenes with alkenes to generate vinylarenes is an attractive alternative to the Mizoroki-Heck reaction because the oxidative functionalization reaction does not require a functionalized coupling partner.[1-3] First discovered by Fujiwara and Moritani as a Pd-mediated process[4-5] and later developed into a Pd-catalyzed[6] coupling of benzene with styrene, the oxidative-Heck reaction has been reported with a range of arenes,[7-20] heteroarenes,[11,21-27] and alkenes.[28-29] These oxidative olefinations of aryl C-H bonds have the potential to provide, in a single step, access to vinyl monomers for polymerization chemistry, as well as vinylarenes for further functionalization during the synthesis of complex structures.

Previous work on Oxidative-Heck reactions:

R limited to: CO₂R', CN, Aryl, SO₂R', P(O)R'₂

R limited to: CO_2R', CN, Aryl, SO_2R', $P(O)R'_2$
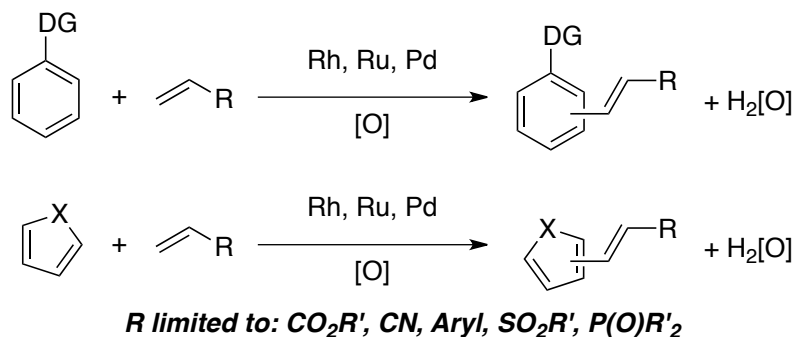
This work:

First examples of olefination with unactived alkenes

Figure 6.1. Previous oxidative coupling methods were limited to reactions of arenes or heteroarenes with conjugated alkenes (top). Rare examples of olefination with unactivated alkenes are presented in this chapter.

However, current methods for the coupling of alkenes and arenes are limited to reactions of conjugated olefins such as acrylates,[1,8-9,15,19-20,27-28,30-31] acrylonitriles,[32-35] or styrenes[25,36] (Figure 6.1). In contrast, olefinations with unconjugated alkenes are rare. Oxidative couplings of arenes with allyl esters[24,37] have been reported, but these reactions form mixtures of branched and linear isomers. Directed olefination of benzamides with isobutylene or cyclopentene occur in low yield and generate large amounts of alkylarene side-products.[38] Only single examples of the olefination of benzothiazole[27] and thiophene[24] with 1-octene have been reported, and these reactions formed complex mixtures of products in low yield.

Vinylarenes that would be generated by coupling reactions of arenes with simple α-olefins are desirable building blocks for materials that cannot be prepared from furyl-substituted acrylates. Specifically, polymers of vinylfuran monomers have the potential to serve as biorenewable surrogates for polystyrene,[39-42] but polymerization of furyl-substituted acrylates is challenging. Alkylfurylacrylates are not amenable to cationic polymerization reaction conditions, and most furan monomers decompose by opening of

the ring under conditions of anionic polymerization. Radical polymerization of these substrates forms only di- or trimers because of slow chain propagation of the stable radical intermediates.[41] In contrast, cationic polymerizations of isopropenylfurans, which are currently prepared by stoichiometric transformations,[40] occur readily.[39,41]

We report the first examples of olefination of furans with unactivated alkenes, including unstrained internal alkenes and propene, to generate branched vinylfurans in excellent yields and selectivities with a second inexpensive alkene as the terminal oxidant. Mechanistic studies indicate that olefination occurs by turnover-limiting migratory insertion of an alkene into an Ir–C bond and studies on catalyst speciation explains an unusual observation: these catalytic reactions are faster at lower temperatures.

6.2 Results and Discussion

The observation of furan olefination stemmed from our recent studies on enantioselective additions of heteroarene C-H bonds to strained bicycloalkenes catalyzed by iridium complexes of DTBM-SEGPHOS (DTBM = 3,5-di-tBu-4-OMe-phenyl).[43] Selected results gained during the development of the olefination of furans are summarized in Table 6.11. These results reveal a counterintuitive effect of temperature on the rate and yield.

Table 6.1. Reaction Development for the Iridium-Catalyzed Olefination of Furans[a]

entry	temp (°C)	n equiv 1-octene	H$_2$ acceptor (m equiv)	% conv	% 1	% 1-H$_2$	ratio 1/1-H$_2$
1	100	1.5	inherent 1-octene	<5	2	0	--
2	140	6	inherent 1-octene	68	61	7	9
3	140	6	(vinyl-Me$_2$Si)$_2$O, (2)	41	33	2	17
4	50	6	inherent 1-octene	70	64	5	13
5	50	2.5	inherent 1-octene	86	69	17	6
6[b]	50	2.5	$tert$-butylethylene, (5)	84	78	6	13

[a]Yields determined by GC analysis. [b]Reaction was conducted with [Ir(coe)$_2$Cl]$_2$, rather than [Ir(cod)Cl]$_2$.

Reactions of 2-methyl-3-methylfuroate conducted with 1-octene under conditions analogous to those reported for reactions with strained alkenes formed only trace amounts of products from the reaction of the alkene with the heteroarene at 100 °C (entry 1). These low yields resulted from isomerization of the terminal alkene to the less reactive internal alkenes. Conducting the reaction neat with an excess of 1-octene at elevated temperatures led to substantial conversion of the starting material to form the vinylfuran **1**, rather than alkylfuran **1-H$_2$** (entry 2). A variety of olefins that could serve as hydrogen acceptors for the oxidative coupling of octene with furan were tested. Reactions with vinylsiloxanes

as a hydrogen acceptor formed product mixtures with greater ratios of **1** over **1-H$_2$** than reactions conducted in the absence of the additive, but these additives decreased the over-all rates and yields of the reactions (entry 3). Reactions conducted with the combination of [Ir(COE)$_2$Cl]$_2$ and ligand formed higher yields of products than did those conducted with [Ir(COD)Cl]$_2$ metal precursor. Cyclooctadiene inhibited the reaction by forming a stable and off-cycle complex as the resting state of the catalytic reaction (*vide infra*).

Ultimately, we discovered that reactions conducted at 50 °C occurred with con-versions comparable to reactions conducted at 140 °C (entry 4). In addition, isomeriza-tion of 1-octene to unreactive isomers was not observed under these conditions; this lack of isomerization eliminated the requirement for reactions to be conducted with a large excess of olefin. Reactions performed with only 2.5 equivalents of 1-octene and *tert*-butylethylene as a sacrificial hydrogen acceptor generated **1** in good yield and selectivity.

The effect of temperature on the rate of the reaction was more counterintuitive than was its effect on the yield. Initial rates of reactions conducted at 50 °C *were an or-der of magnitude greater* than those conducted at 100 °C. This unexpected result merited additional mechanistic study and aided in the improvement of the catalytic reaction.
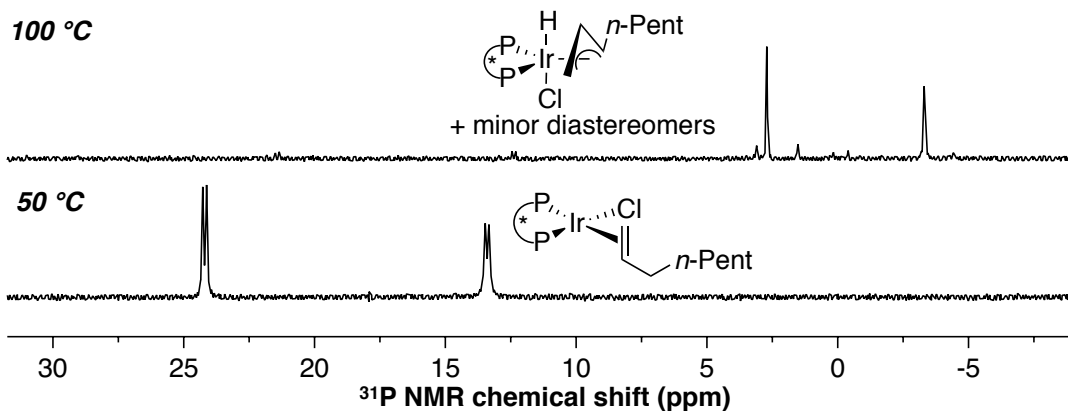

Figure 6.2. Resting state complex under catalytic conditions observed at 100 °C (top) and 50 °C (bottom) by ^{31}P NMR spectroscopy.

We monitored catalytic reactions at 50 °C and 130 °C by ^{31}P NMR spectroscopy. These experiments revealed different resting-states of the catalytic intermediates at the two temperatures. At 50 °C, a red colored resting state was observed and was shown by NMR spectroscopy and x-ray diffraction to be the Ir(olefin) complex **21** (Figure 6.2, top). At 130 °C, a colorless resting state was observed, and this complex was shown by NMR spectroscopy to be the Ir(allyl)(H) complex **22** (Figure 6.2, top).[44] Complex **22** formed from olefin complex **21** within seconds at 130 °C with a rate constant greater than 10^{-1} s^{-1}. This rate constant is much greater than that of the catalytic reaction ($k \approx 10^{-4}$ s^{-1}). Thus, we were surprised to observe that the olefination of furan occurred to 84% conversion after 16 h at 50 °C with only 28% of **21** having decomposed to **22**. These data indicate that at 50 °C the olefination is faster than formation of **22**, whereas at 130 ° the formation of **22** is faster than olefination.

The origin of the observation of different rates at different temperatures was re-vealed by performing separate Eyring analyses on the rate constants for formation of **22** from isolated **21** and the olefination of furan catalyzed by **21** (Figure 6.3a). Analysis of

the rate of formation of **22** in the temperature range 72-106 °C revealed the following activation parameters: $\Delta H^{\ddagger} = 22.5$ kcal/mol and $\Delta S^{\ddagger} = -8$ eu. The small $\Delta S^{\ddagger}$ is consistent with the same composition of the starting complex **21** and product **22**. The dependence of the rate of formation of complex **22** on temperature is large because of the large enthalpic difference between the ground and transition states.
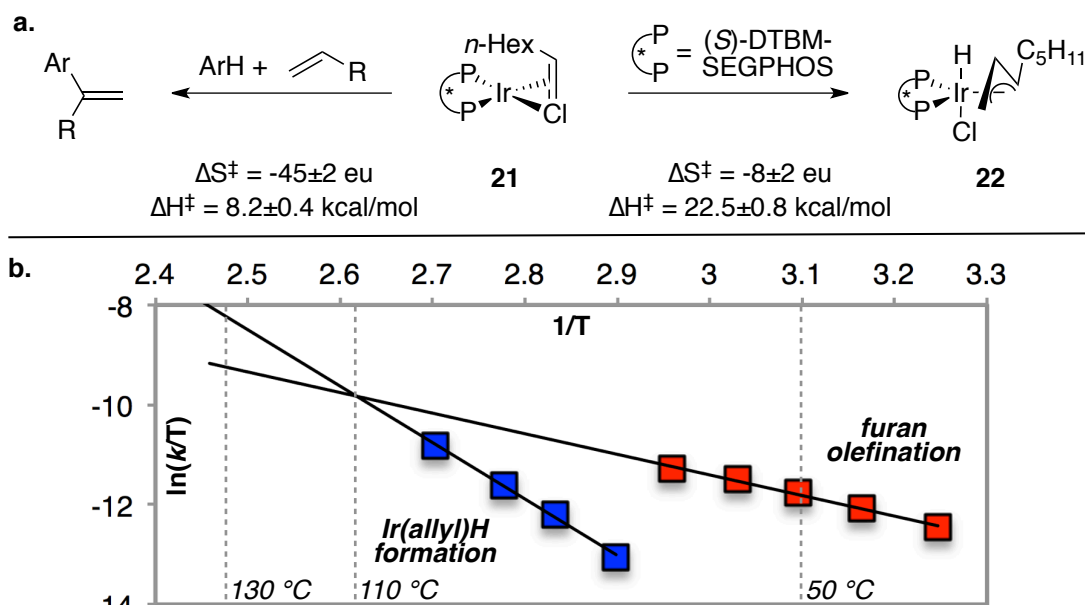
a.

$\Delta S^{\ddagger} = -45\pm2$ eu
$\Delta H^{\ddagger} = 8.2\pm0.4$ kcal/mol

21

$\Delta S^{\ddagger} = -8\pm2$ eu
$\Delta H^{\ddagger} = 22.5\pm0.8$ kcal/mol

22

b.

Figure 6.3. (a) Competing processes: olefination catalyzed by complex **21** (left) and decomposition of **21** to form complex **22** (right). (b) Eyring plot of the competing processes.

The activation parameters for the olefination of furan in the temperature range 35-65 °C were $\Delta H^{\ddagger} = 8.2$ kcal/mol and $\Delta S^{\ddagger} = -45$ eu. The large, negative entropy suggests that the transition state forms by a combination of the furan and resting state. The small dependence of the rate of olefination on temperature is due to the small enthalpy of activation. Consistent with our observations, the overlay of the Eyring plots for the competing processes reveals that the furan olefination is faster than the catalyst decomposition at temperatures below 110 °C, while formation of complex **22** is faster than olefination at temperatures greater than 110 °C (Figure 6.3b).

Scheme 6.1. General route for the synthesis of Segphos derivatives.
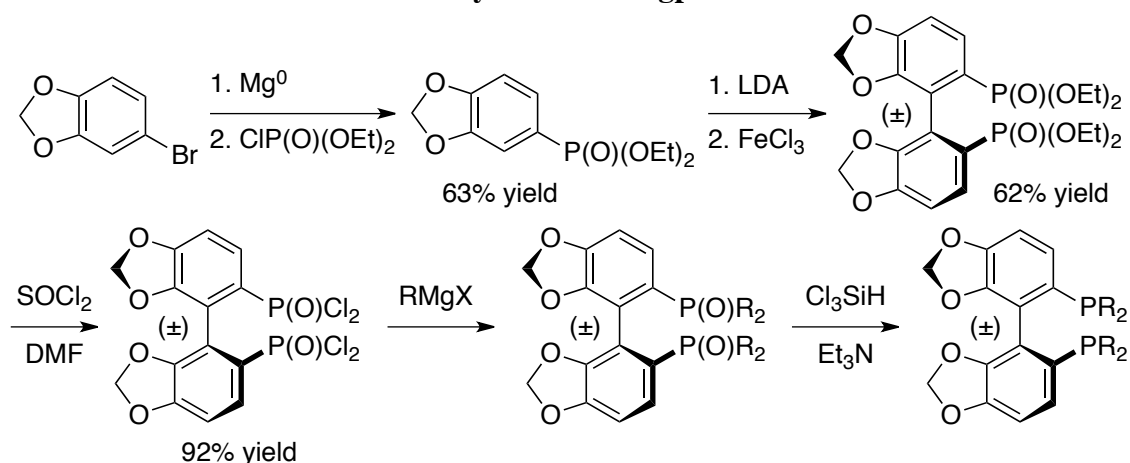
These mechanistic insights directed the development of new complexes that would disfavor formation of Ir(allyl)(H) intermediates, improve rates of olefination, and increase the selectivity for **1** over **1-H$_2$**. We prepared ligands that were less electron donating than DTBM-SEGPHOS to reduce the rate of allylic C-H activation, more sterically bulky than DTBM-SEGPHOS to prevent formation of Ir dimers, and soluble in the nonpolar reaction media. The ligands illustrated in Figure 6.4 were prepared according to the synthetic sequence illustrated in Scheme 6.1. A variety of arylgrignard reagents were added to the dichlorophosphine oxide species, which was accessed on gram scales in three steps with an overall yield of 36%. Subsequent reduction of the products with trichlorosilane afforded the target ligands illustrated in Figure 6.4.
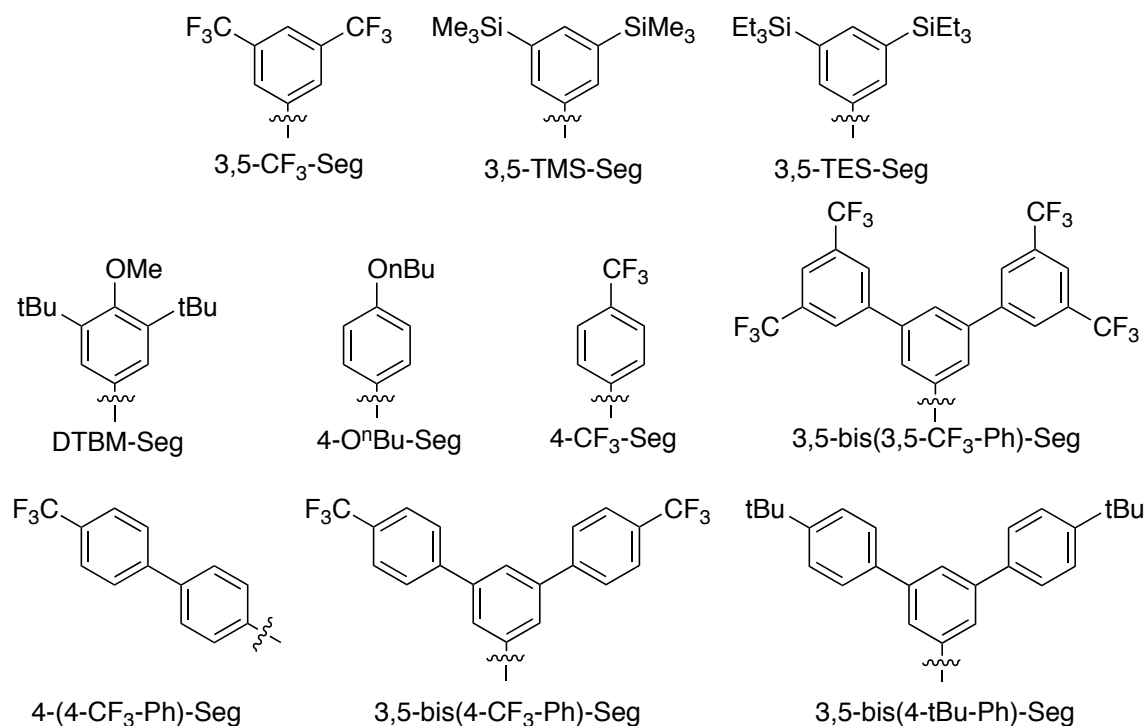

Figure 6.4. Aryl groups of SEGPHOS ligands.

As summarized in Table 6.2, complexes of SEGPHOS-based ligands formed more active catalysts than those of analogous biaryl bisphosphine ligands (entries 1-3; see the supporting information for the full set of ligands tested). Complexes of ligands containing electron-withdrawing substituents were more reactive than those containing-donating substituents (entry 5 vs. 4); however, additional electron-withdrawing groups decreased reactivity, as was observed for reactions of 3,5-bis-CF_3-substituted ligands (entry 6). SEGPHOS derivatives with bi- and terphenylarenes formed complexes that generated vinylfuran **1** with high selectivity over alkyl product **1-H$_2$**, but in low yield (entries 7-10). High yield, as well as high selectivity for olefination products, was observed for reactions catalyzed by Ir complexes of SEGPHOS derivatives containing 3,5-bis(trialkylsilyl) arenes (entry 11-12). This air-stable TMS-SEGPHOS ligand was prepared as a racemate on gram scales, forms Ir complexes that are soluble in pentane, and does not readily decompose to analogues of **22** under catalytic conditions. Thus, we studied olefination reactions under the conditions of entry 11.

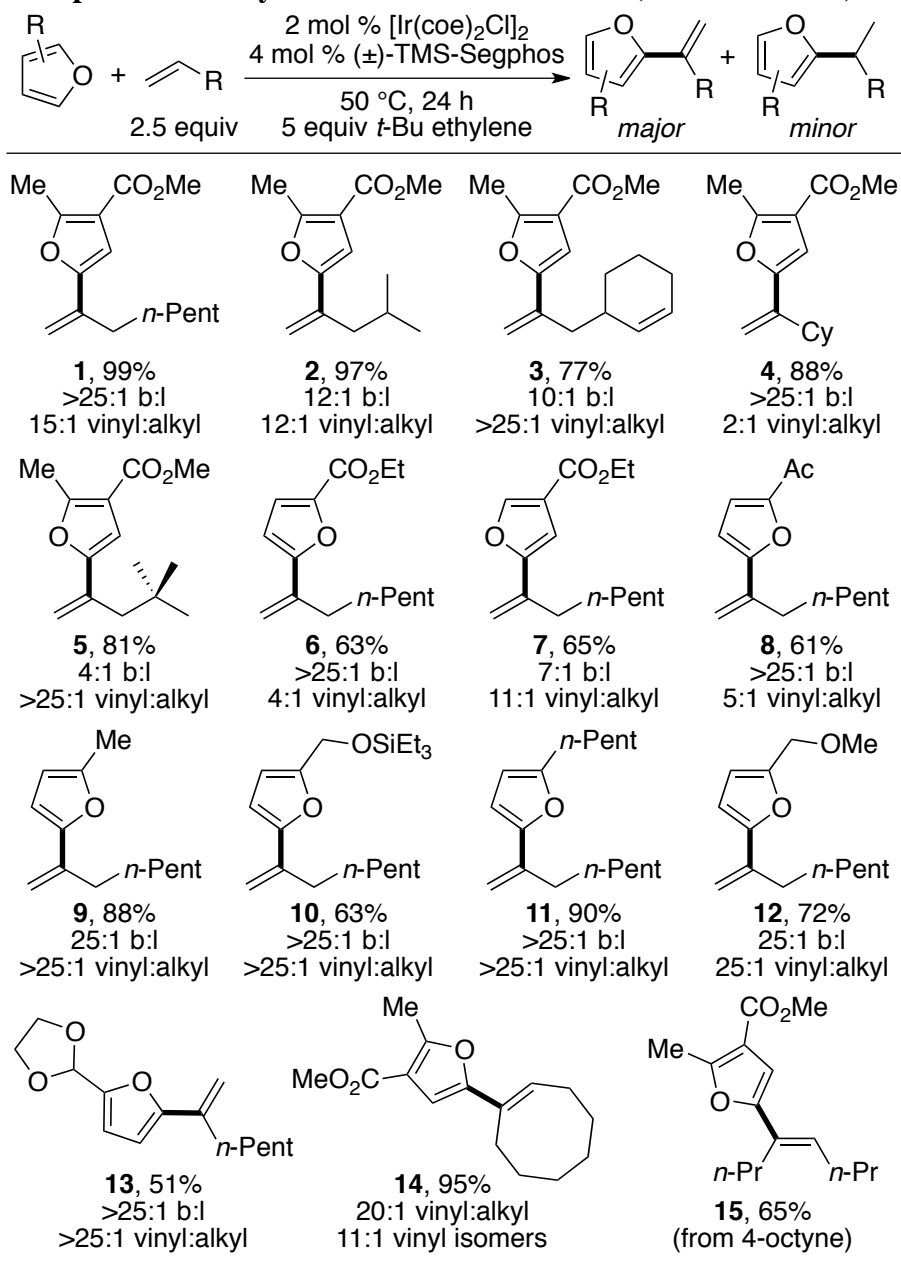**Table 6.2. Effect of Ligand on the Reaction^a**

entry	ligand	substituents on aryl group	% conv	% 1	% 1-H$_2$	ratio 1/1-H$_2$
1	(S)-Ar-SEGPHOS	3,5-^{t}Bu-4-OMe-	84	78	6	11
2	(R)-Ar-MeOBIPHEP	3,5-^{t}Bu-4-OMe-	54	47	3	14
3	(S)-Ar-Garphos	3,5-^{t}Bu-4-OMe-	37	30	3	13
4	(±)-Ar-SEGPHOS	4-O^{n}Bu-	16	4	0	12
5	(±)-Ar-SEGPHOS	4-CF$_3$-	25	19	1	18
6	(±)-Ar-SEGPHOS	3,5-CF$_3$-	7	3	0	>40
7	(±)-Ar-SEGPHOS	4-(4-CF$_3$-Ph-)-	37	37	0	>40
8	(±)-Ar-SEGPHOS	3,5-(4-CF$_3$-Ph-)-	28	28	1	>40
9	(±)-Ar-SEGPHOS	3,5-(4-^{t}Bu-Ph-)-	18	9	1	15
10	(±)-Ar-SEGPHOS	3,5-(3,5-CF$_3$-Ph-)-	39	38	1	>40
11	(±)-Ar-SEGPHOS	3,5-TMS-	100	96	4	24
12	(±)-Ar-SEGPHOS	3,5-TES-	100	96	4	27

^{a}Reactions were conducted following the conditions of entry 6, Table 1. Yields determined by GC analysis.

The olefination of a range of furans with a variety of alkenes by the procedure just described is illustrated in Chart 6.1. Branched vinylfurans formed in high yields with reaction exclusively α to oxygen and good to excellent selectivity over formation of alkyl-furans or linear vinylfurans. The resulting 1,1-disubstituted alkenes are kinetic products

and do not undergo isomerization to other olefins under these mild conditions. Reactions of furans possessing electron-donating substituents formed products in higher yields and selectivities than did reactions of furans containing electron-withdrawing groups (**6** vs. **9**). The reactivity of furan **1** bearing the combination of electron-donating and electron-withdrawing groups at the C2 and C3 positions, respectively, was more comparable to that of 2-methylfuran **9** than to that of 3-ethylfuroate **7**. These data indicate that reactions occurring at the C5-position are more strongly influenced by substitution at the C2-position than at the C3-position of the furan. The effects of substitutions of furan on the reactivity of the heteroarene are analogous to the effects of substituents on the reactivity of non-aromatic dienes.[45]

Chart 6.1. Scope of Ir-Catalyzed Olefination of Furans (Isolated Yields)

1, 99%
>25:1 b:l
15:1 vinyl:alkyl

2, 97%
12:1 b:l
12:1 vinyl:alkyl

3, 77%
10:1 b:l
>25:1 vinyl:alkyl

4, 88%
>25:1 b:l
2:1 vinyl:alkyl

5, 81%
4:1 b:l
>25:1 vinyl:alkyl

6, 63%
>25:1 b:l
4:1 vinyl:alkyl

7, 65%
7:1 b:l
11:1 vinyl:alkyl

8, 61%
>25:1 b:l
5:1 vinyl:alkyl

9, 88%
25:1 b:l
>25:1 vinyl:alkyl

10, 63%
>25:1 b:l
>25:1 vinyl:alkyl

11, 90%
>25:1 b:l
>25:1 vinyl:alkyl

12, 72%
25:1 b:l
25:1 vinyl:alkyl

13, 51%
>25:1 b:l
>25:1 vinyl:alkyl

14, 95%
20:1 vinyl:alkyl
11:1 vinyl isomers

15, 65%
(from 4-octyne)

No coupling products were observed from reactions of the commodity chemical furfural, but derivatives of furfural generated from aldehyde reduction (**9**), hydrosilylation (**10**), or protection (**13**) underwent the Ir-catalyzed olefination to form products in good yields and selectivities. These results highlight the compatibility of this process with substrates bearing ester, dioxolane, protected alcohol, and ketone functionality. In addition, reactions of substrates possessing multiple alkenes occurred selectivity at the terminal alkene without isomerization of the internal alkene (**3**). In the absence of reactants containing terminal olefins, cyclooctene reacted to form the conjugated vinylfuran product in high yield (**14**).
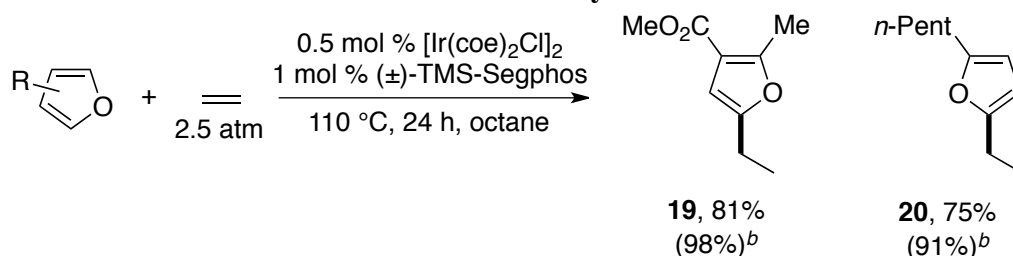
Reactions of furans with acyclic internal alkenes did not form coupled products. However, these products were accessed by Ir-catalyzed CH addition of a furan to an alkyne catalyzed by same complex that catalyzes olefination reactions with alkenes. Hydroheteroarylation of 4-octyne occurred at 100 °C to form the addition product as a single isomer (**15**). The geometry of this isomer was determined by ^{1}H NMR NOESY and is consistent with a syn addition of the C–H bond across the alkyne.

Chart 6.2. Olefination of Furans with Propene[a]

16, 94% (98%)[b]
20:1 vinyl:alkyl

17, (87%)[b]
>25:1 vinyl:alkyl

18, 47% (55%)[b]
22:1 vinyl:alkyl
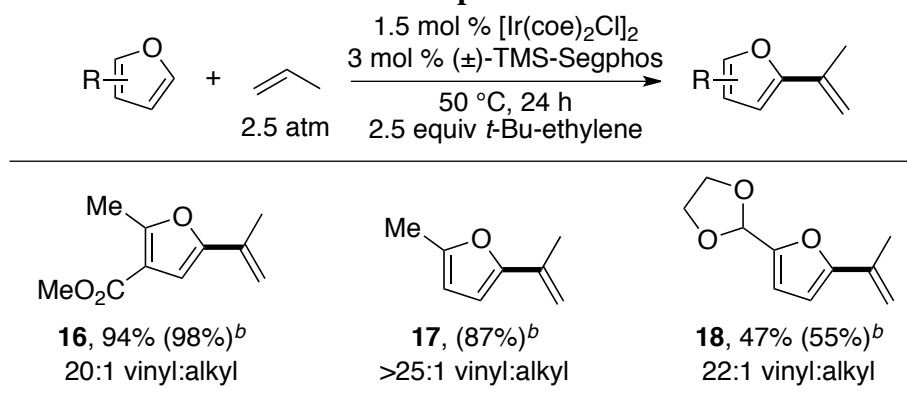
[a]Reported yields are isolated yields. [b]NMR yield.

Finally, we assessed whether vinylfurans would form from the most abundant alkenes, propene and ethene. At high pressures of propene (>5 atm), the Ir(propene) analogue of **21** rapidly forms the (allyl)Ir(H) analogue of **22**, even at 50 °C. No olefination products were formed under these conditions after 24 h. Monitoring reactions containing a lower 2.5 atm pressure of propene indicated that the catalyst resting state was an Ir(*t*Bu-ethylene) complex, rather than an Ir(propene) complex. Thus, the rate of catalyst decomposition at these lower pressures has a first order dependence on the concentration of propene, rather than a zeroth order dependence. At this lower pressure of propene, catalyst decomposition did not occur at 50 °C, and furan olefination occurred to form the isopropenylfurans in high yield and selectivity, as summarized in Chart 6.2.

Chart 6.3. CH Bond Additions of Furans to Ethylene[a]

R (furan) + ethylene (2.5 atm)
$\xrightarrow{\text{0.5 mol % [Ir(coe)}_2\text{Cl]}_2 \quad 1 \text{ mol % (±)-TMS-Segphos}}{\text{110 °C, 24 h, octane}}$

19, 81% (98%)[b]

20, 75% (91%)[b]

[a]Reported yields are isolated yields. [b]NMR yield.

Reactions of ethylene formed products of hydroarylation exclusively. The absence of allylic protons on the alkene substrate allowed the reaction to be conducted at elevated temperatures without catalyst deactivation. Consequently, higher catalyst turnover numbers (up to 144) were achieved for reactions of ethylene than for those of α-olefins. The reactions illustrated in Chart 6.3 were conducted with only 1% catalyst under 2.5 atm of ethylene to form ethylfuran products in high yield.
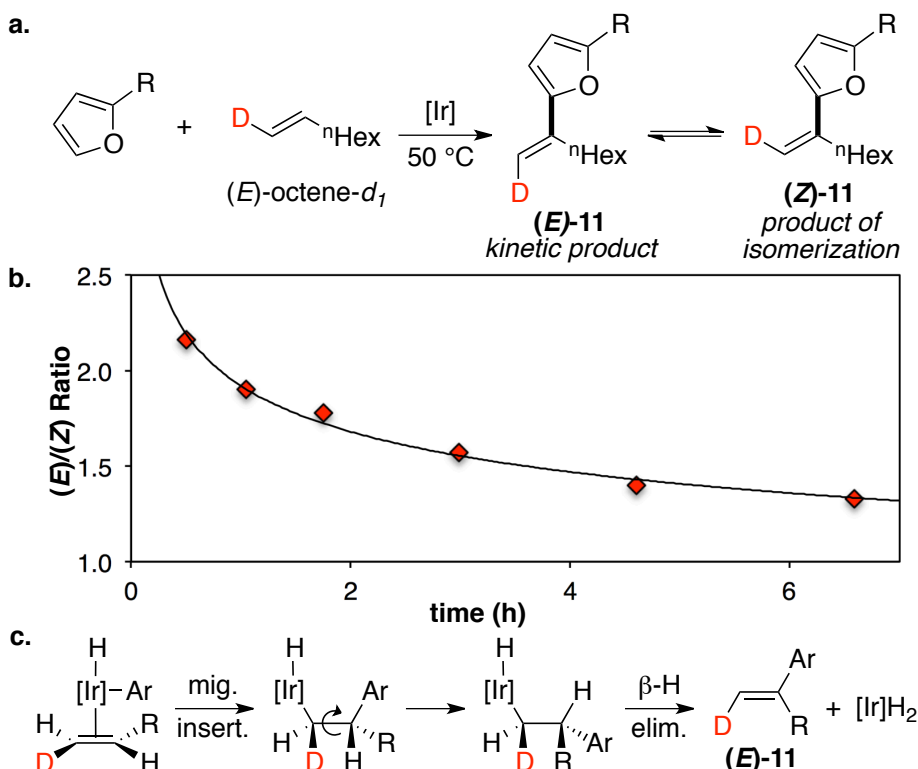
Figure 6.5. (a) Ir-catalyzed olefination of 2-pentylfuran with (*E*)-octene-d_1. (b) Ratio of (*E*)-**11** to (*Z*)-**11** vs. time. (c) Proposed mechanism for the stereospecific formation of (*E*)-**11**.

To gain insight into the mechanism of C–C bond formation, the geometry of the vinylfuran products from reactions with geometrically defined alkenes was determined. The Ir-catalyzed reaction was performed with 2-pentyfuran and (*E*)-octene-d_1 (Figure 6.5a). When the reaction was monitored at low conversions, (*E*)-**11** was observed as the major vinyl-indole isomer (Figure 6.5b). These results suggest that (*E*)-**11** is the product of the Ir-catalyzed reaction, while the *Z* isomer is formed by isomerization of the *E* isomer. The formation of (*E*)-**11** as the kinetic product is consistent with a mechanism in-

volving migratory insertion of (*E*)-octene-d_1 into an Ir–C bond, followed by stereospecific β-H elimination (Figure 6.5c).

Kinetic experiments by the method of initial rates (to 15% conversion) on the reaction of 2-pentylfuran with 1-octene provided insight on the identity of the turnover-limiting step (TLS). The reaction was found to be first order in catalyst and furan, but the rate of the reaction was independent of the concentration of 1-octene. A comparison of the initial rates for the olefination of 2-pentylfuran and 2-pentyl-5-deuteriofuran in separate vessels revealed a small KIE of 1.4. This small KIE suggests CH bond cleavage could be reversible. These kinetic data, and data on the identity of the resting state (**21**) suggest that the TLS of the catalytic reaction occurs after cleavage of the CH bond of furan from an olefin-bound intermediate.

In parallel with these experimental mechanistic studies, we conducted computational studies by density functional theory (DFT) on the mechanism of the catalytic reaction (see the experimental section for details). These data provided insight into the stability of intermediates and rates of the elementary steps of the cycle, including migratory insertions of olefins into Ir–C bonds. They also helped explain the relative rates for reductive eliminations vs. β-H eliminations and formation of allyl complex **22** vs. catalytic turnover.
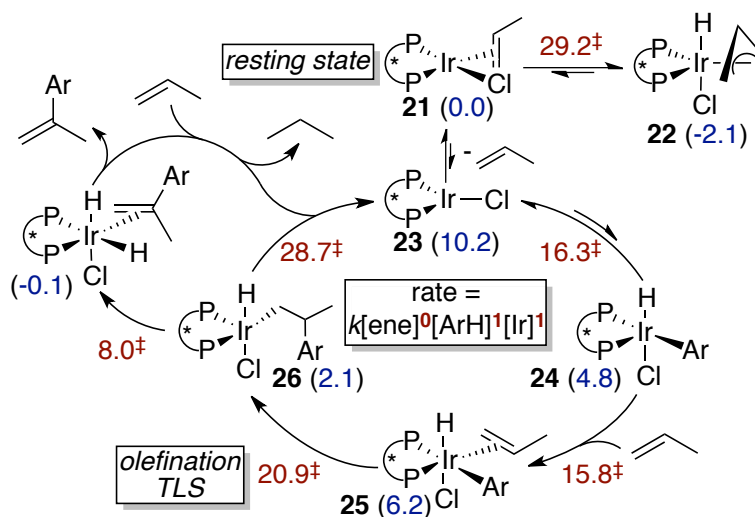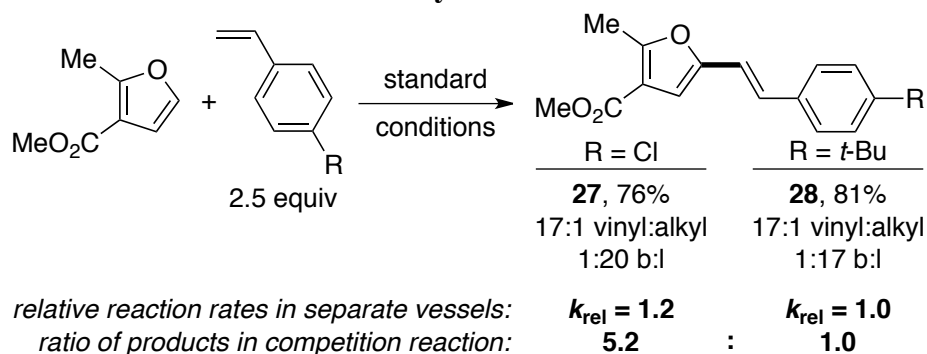

Figure 6.6. Proposed catalytic cycle with computed energies of transition states (red) and intermediates (blue) in kcal/mol.

A proposed catalytic cycle that is consistent with the experimental and computational data is illustrated in Figure 6.6. The small KIE indicates that CH activation is reversible and likely occurs to the 3-coordinate complex **23** following dissociation of olefin from the resting state **21** to form furyliridium hydride complex **24**. The barrier for CH activation directly from **21** to form **25** was computed to be 39.4 kcal/mol and is unlikely to occur. Coordination of propene to furyliridium hydride complex **24** would generate **25** prior to turnover-limiting insertion of the alkene. β-H elimination would then occur from the resulting alkyliridium intermediate **26** to release vinylfuran products more rapidly than reductive elimination to form a C–H bond in an alkyfuran would occur. Ligand exchange of the vinylfuran with the hydrogen acceptor and subsequent hydrogenation would regenerate the active Ir(I) intermediate.

Scheme 6.2. Furan Olefination with Vinylarenes

	R = Cl	R = t-Bu
	27, 76%	**28**, 81%
	17:1 vinyl:alkyl	17:1 vinyl:alkyl
	1:20 b:l	1:17 b:l

relative reaction rates in separate vessels:	$k_{rel} = 1.2$		$k_{rel} = 1.0$
ratio of products in competition reaction:	**5.2**	**:**	**1.0**

Reactions of vinylarenes were studied to gain insight into the influence of the electronic nature of the alkene on the olefination reaction. Reactions of styrenes, under the conditions outlined in Scheme 6.2, formed linear vinylfurans in good yields with exclusive (E)-olefin geometry. Formation of linear products is consistent with β-H elimination from a more stable benzyliridium intermediate, rather a terminal alkyliridium intermediate.

The initial rates of olefination with electron rich and electron deficient vinylarenes were measured in separate vessels and found to be similar (Scheme 1, bottom); both rates were faster than those for reactions of 1-octene. Next, a competition experiment was performed in which equimolar amounts of 4-chloro- and 4-*tert*-butylstyrene were charged in the same reaction vessel. At 15% conversion, a 5.2:1 ratio of products favoring reaction with 4-chlorostyrene was observed. The difference between the independent relative rates of olefination and the ratio of products in a competition suggests that the olefin reaction with vinylarenes is under Curtain-Hammett control, and coordination of the styrene to iridium is irreversible. Thus, coordination of the alkene is the product-determining step. This scenario of turnover-limiting alkene coordination is likely unique to reactions of activated alkenes, which have faster rates of olefin insertion than reactions of unactivated alkenes. DFT calculations support reversible coordination of the unactivated alkene propene.

The computed barriers and energies of intermediates are consistent with the mechanism described in Figure 6.6. At 298 K, the barriers for catalyst decomposition to the most stable species **22** (29.2 kcal/mol) and reductive elimination to release alkylfuran products (28.7 kcal/mol) are much higher than the highest barrier in the olefination process (20.9 kcal/mol). Consequently, vinylfuran is formed selectively in the process catalyzed by **21**.

6.3 Conclusions and Future Directions

In conclusion, we have reported a rare example of the oxidative olefination of furans with unactivated alkenes to form branched vinylfurans in high yields and selectivities. Mechanistic studies, including the observation of faster rates of reaction at lower temperatures, led to the development of new ligands that form complexes capable of catalyzing olefination of a wide range of furans under mild conditions. Efforts to extend the scope of this process to arenes are ongoing.

6.4 Experimental

General Remarks

Unless noted otherwise, all manipulations were performed in an argon-filled glove-box. Glassware was dried at 130 °C for at least 4 hours before use. Pentane, Et_2O, THF, benzene and toluene were collected from a solvent purification system containing a 0.33 m column of activated alumina under nitrogen. Benzene-d_6 was degassed and subjected to 4 Å molecular sieves for at least 4 hours prior to use. All furan reagents purchased from commercial suppliers were distilled and subsequently stored in the glove box. Commercially available bisphosphine ligands were purchased from Strem Chemical Co. and used as received. $[Ir(coe)_2Cl]_2$ was prepared following a published procedure.[46]

^1H NMR spectra were obtained at 500 MHz or 600 MHz with a 45° pulse and a 15 s delay time, and chemical shifts were recorded relative to protiated solvents ($CHCl_3$ in $CDCl_3$: δ7.27 ppm; $C_6H_nD_{6-n}$ in C_6D_6: δ7.15 ppm). ^{13}C NMR spectra were obtained at 126 MHz or 151 MHz on a 500 MHz or 600 MHz instrument, respectively. ^{31}P NMR spectra were obtained at 202.2 MHz on a 500 MHz instrument, and chemical shifts were reported in parts per million downfield of 85% H_3PO_4. ^{19}F NMR spectra were referenced to an external standard of $CFCl_3$. Proof of purity is demonstrated by elemental analysis and by copies of NMR spectra.

GC analysis was performed on an Agilent 7890 GC equipped with an HP-5 column (25 m x 0.20 mm x 0.33 μm film) and an FID detector. Quantitative analysis by ^1H NMR spectroscopy was performed by adding mesitylene as an internal standard to the reaction mixture upon completion of the reaction. Quantitative GC analysis was performed by adding dodecane as an internal standard to the reaction mixture upon completion of the reaction. Response factors for the products relative to the internal standard were measured for kinetic studies and reaction development. GC-MS data were obtained on an Agilent 6890-N GC system containing an Alltech EC-1 capillary column and an Agilent 5973 mass selective detector.
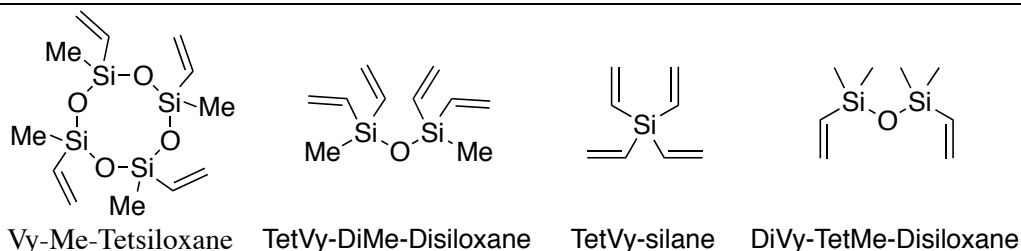
Vy-Me-Tetsiloxane   TetVy-DiMe-Disiloxane   TetVy-silane   DiVy-TetMe-Disiloxane

Figure 6.7. List of hydrogen acceptors.

Table 6.3. Effect of added hydrogen acceptors at 140 °C[a]

Entry	1-octene equiv	H₂ Acceptor (equiv)	% conv	% 1	% 1-H₂	Ratio 1/1-H₂
1	3	none	79	52	23	2.3
2	3	Vy-Me-Tetsiloxane (1)	84	60	14	4.3
3	3	DiVy-TetMe-Disiloxane (1)	86	62	14	4.4
4	3	DiVy-Me-Disiloxane (1)	92	59	17	3.6
5	3	TetVy-silane (1)	53	35	7	5.3
6	3	Vy-Me-Tetsiloxane (2)	94	65	15	4.3
7	3	DiVy-TetMe-Disiloxane (2)	89	62	13	5.0
8	3	DiVy-Me-Disiloxane (2)	87	60	14	4.2
9	3	TetVy-silane (2)	37	20	3	6.3
10	6	none	77	59	16	3.6
11	6	Vy-Me-Tetsiloxane (1)	91	72	15	4.8
12	6	DiVy-TetMe-Disiloxane (1)	92	74	15	4.8
13	6	DiVy-Me-Disiloxane (1)	71	54	9	5.9
14	6	TetVy-silane (1)	57	44	7	6.5
15	6	Vy-Me-Tetsiloxane (2)	94	73	14	5.1
16	6	DiVy-TetMe-Disiloxane (2)	93	72	13	5.4
17	6	DiVy-Me-Disiloxane (2)	92	45	12	3.6
18	6	TetVy-silane (2)	30	21	3	7.1

[a]% conversions of the starting material and product ratios were determined by quantitative GC with dodecane as an internal standard.
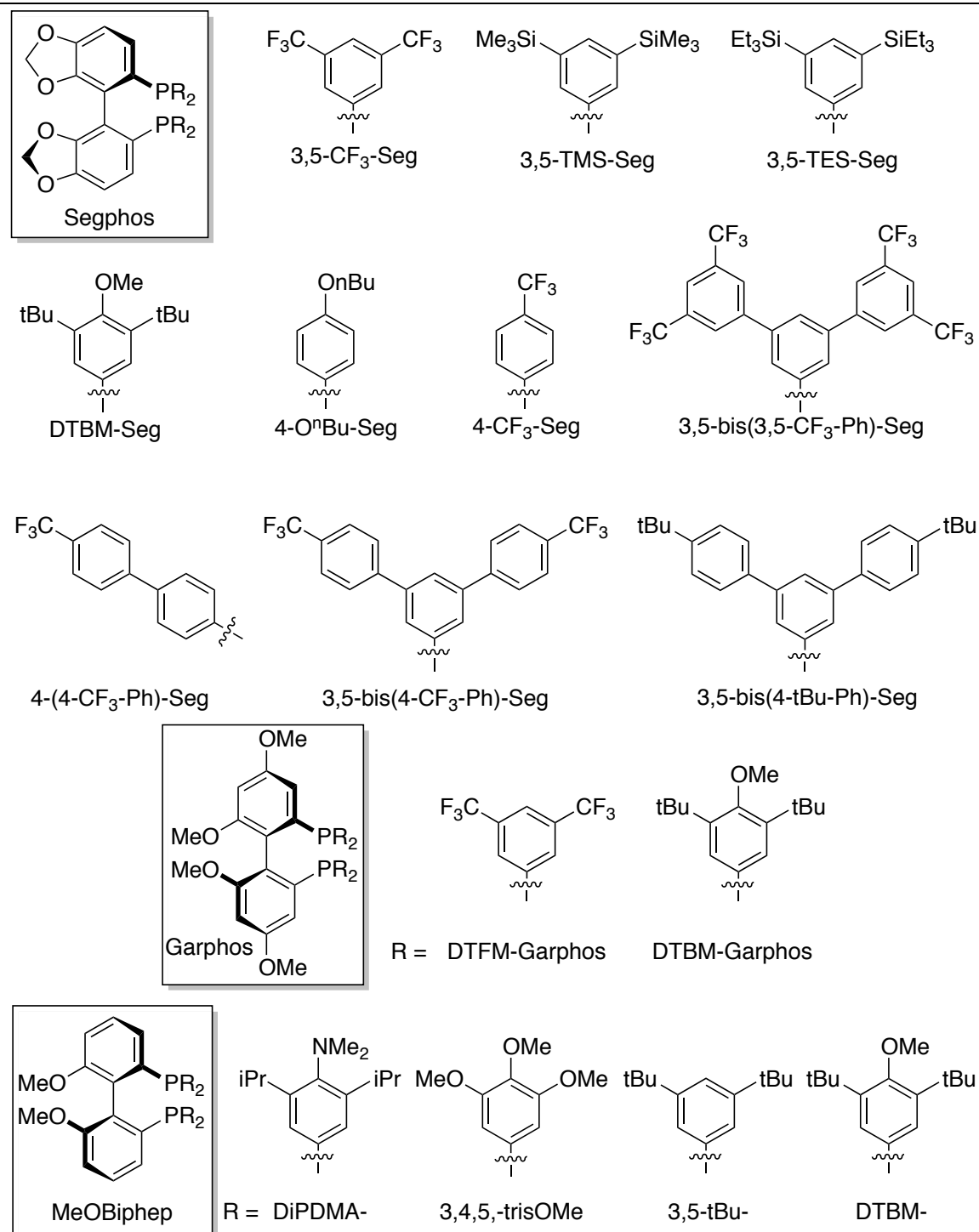
222

Table 6.4. Furan olefination at variable temperatures after 1 hour reaction time[a]

Entry	Ir Precursor	Temp (°C)	% conv	% 1	% 1-H$_2$	Ratio 1/1-H$_2$	% 1-octene remaining
1	[Ir(cod)Cl]$_2$	140	25	22	2	11.0	27
2	[Ir(cod)Cl]$_2$	120	24	22	2	11.0	30
3	[Ir(cod)Cl]$_2$	100	22	19	2	9.5	32
4	[Ir(cod)Cl]$_2$	80	30	27	3	12.3	60
5	[Ir(cod)Cl]$_2$	50	35	30	2	14.0	82
6	[Ir(coe)$_2$Cl]$_2$	50	42	38	3	14.0	80

[a]% conversions of the starting material and product ratios were determined by quantitative GC with dodecane as an internal standard.

Table 6.5. Effect of temperature and additives on reaction % conversion and selectivity.[a]

conditions	45 °C	50 °C	55 °C	60 °C	65 °C
no variation	86 (7:1)	85 (7:1)	83 (6:1)	85 (7:1)	72 (6:1)
2.5 additional equiv 1-octene	77 (15:1)	79 (15:1)	75 (14:1)	77 (13:1)	58 (16:1)
2.5 equiv octane	78 (9:1)	78 (8:1)	78 (7:1)	88 (6:1)	63 (9:1)
1.5 equiv tBu-ethylene	84 (12:1)	67 (11:1)	84 (11:1)	83 (7:1)	72 (11:1)
1.0 equiv EtOAc	82 (8:1)	24 (13:1)	13 (11:1)	73 (15:1)	60 (11:1)
0.75 equiv divinyl-methyl-disiloxane	36 (16:1)	24 (18:1)	38 (15:1)	33 (16:1)	67 (13:1)

[a]First value is % conversion. Values in parentheses represent observed ratio of **1:1-H$_2$**. % Conversions of the starting material and product ratios were determined by quantitative GC with dodecane as an internal standard.

F$_3$C   CF$_3$

Me$_3$Si   SiMe$_3$

Et$_3$Si   SiEt$_3$

Segphos

3,5-CF$_3$-Seg

3,5-TMS-Seg

3,5-TES-Seg

DTBM-Seg

4-O^{n}Bu-Seg

4-CF$_3$-Seg

3,5-bis(3,5-CF$_3$-Ph)-Seg

4-(4-CF$_3$-Ph)-Seg

3,5-bis(4-CF$_3$-Ph)-Seg

3,5-bis(4-tBu-Ph)-Seg

Garphos

R = DTFM-Garphos   DTBM-Garphos

MeOBiphep

R = DiPDMA-   3,4,5,-trisOMe   3,5-tBu-   DTBM-

Figure 6.8. List of compounds tested as ligands for iridium under catalytic conditions for the olefination of furans.

Table 6.6. Olefination of a poorly reactive substrate catalyzed by complexes of various bisphosphine ligands.[a]
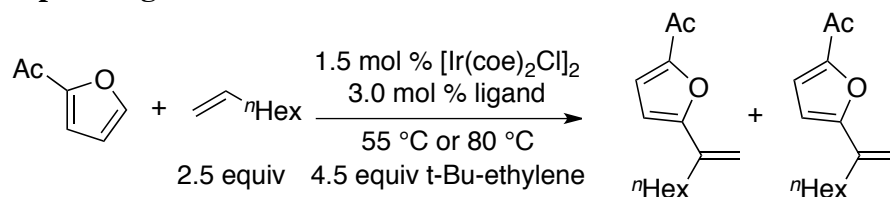
Entry	Ligand	Temp (°C)	% conv	% 1	% 1-H$_2$	Ratio 1/1-H$_2$
1	dcpm	55	7	0	0	33
2	dcpm	80	10	0	0	43
3	DTMB-Seg	55	36	25	9	3
4	DTMB-Seg	80	29	20	6	3
5	3,5-TMS-Seg	55	63	50	12	4
6	3,5-TMS-Seg	80	53	42	9	5
7	4-CF$_3$-Seg	50	18	16	2	8
8	4-OBu-Seg	50	8	2	0	11
9	3,5-CF$_3$-Seg	55	4	2	0	14
10	3,5-CF$_3$-Seg	80	8	5	0	23
11	4-(4-CF$_3$-Ph)-Seg	55	3	0	0	54
12	4-(4-CF$_3$-Ph)-Seg	80	6	3	0	13
13	3,5-(4-CF$_3$-Ph)-Seg	55	8	5	0	22
14	3,5-(4-CF$_3$-Ph)-Seg	80	8	5	0	19
15	3,5-(4-tBu-Ph)-Seg	80	9	5	0	10
16	3,5-(3,5-CF$_3$-Ph)-Seg	55	9	2	0	24
17	3,5-(3,5-CF$_3$-Ph)-Seg	80	29	20	1	15
18	DTBM-Garphos	55	18	9	3	3
19	DTBM-Garphos	80	15	6	2	3
20	DTFM-Garphos	55	11	1	0	14
21	DTFM-Garphos	80	15	5	0	15
22	iPr-MeOBiphep	55	6	1	0	20
23	iPr-MeOBiphep	80	6	1	0	20
24	3,4,5-OMe-MeOBiphep	55	6	1	0	16
25	3,4,5-OMe-MeOBiphep	80	15	2	0	19
26	3,5-tBu-MeOBiphep	55	25	13	3	4
27	3,5-tBu-MeOBiphep	80	19	9	2	4
28	DiPDMA-MeOBiphep	55	14	5	2	3
29	DiPDMA-MeOBiphep	80	14	4	1	3
30	DTBM-MeOBiphep	55	27	15	5	3
31	DTBM-MeOBiphep	80	20	7	2	4

[a] % conversions of the starting material and product ratios were determined by quantitative GC with dodecane as an internal standard.

Synthesis of Substrates

3-Allylcyclohex-1-ene
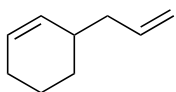
In an argon-filled dry-box, an oven dried round-bottom flask (250 ml) was charged with 3-bromocyclohexene (5.5 ml, 48 mmol, 90%), diethyl ether (60 ml), and a magnetic stirbar. The flask was capped with a septum, and removed from the dry-box. The solution was placed in an ice bath, and allyl magnesium bromide (1 M in diethyl ether (60. ml, 60. mmol) was added via cannula over 10 minutes. The solution was allowed to warm to room temperature over 30 minutes. Conversion of the starting material was determined by TLC, and the reaction was complete after stirring the solution at room temperature for 1 hour. The suspension was placed in an ice batch and quenched with brine. The mixture was filtered through celite, and the organic material was extracted with diethyl ether. The organic phase was concentrated to a residue and further purified by flash chromatography with pentane as eluent. Elution of the product was monitored by TLC with a permanganate stain. The solvent was removed by rotary evaporation to yield the title compound as a clear liquid (5.8 g, 98% yield). Spectral data matched those of previous reports.[47]

^{1}H NMR (400 MHz, CDCl$_3$): δ 5.82 (ddt, J = 17.0, 10.0, 7.0 Hz, 1H), 5.74-5.65 (m, 1H), 5.60 (d, J = 10.2 Hz, 1H), 5.04 (d, J = 11.0 Hz, 1H), 5.01 (d, J = 1.6 Hz, 1H), 2.22-2.12 (m, 1H), 2.12-2.02 (m, 2H), 1.98 (d, J = 2.6 Hz, 2H), 1.84-1.66 (m, 2H), 1.60-1.47 (m, 1H), 1.32-1.20 (m, 1H).

^{13}C NMR (101 MHz, CDCl$_3$): δ 137.2, 131.4, 127.2, 115.7, 40.6, 35.0, 28.8, 25.3, 21.4.

2-(Methoxymethyl)furan
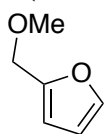
In an argon-filled dry-box, an oven dried round-bottom flask (250 ml) was charged with sodium hydride (60% by weight, 2.5 g, 63 mmol), DMF (50 ml), and a magnetic stirbar. The flask was capped with a septum and removed from the dry-box. Furfural alcohol (2.2 ml, 25 mmol) was added via syringe through the septum to the flask while vigorously stirring over 5 minutes. After stirring the suspension for an additional 20 minutes, iodomethane (3.8 ml, 63 mmol) was added to the reaction mixture via syringe. After stirring the reaction mixture for 2 hours at room temperature, the reaction was quenched with a solution of NaOH (2 M, 25 ml), and the organic material was extracted with diethyl ether (25 ml x 3). The organic solution was washed with a saturated solution of sodium bisulfite, washed with brine, and dried over magnesium sulfate. The crude material was purified by flash chromatography with 15% diethyl ether in pentane as eluent. The title compound was isolated as a clear liquid and stored in the freezer under argon (910 mg, 32% yield). Spectral data matched those of previous reports.[48]

^{1}H NMR (400 MHz, C$_6$D$_6$): δ 7.16 (s, 1H), 6.13 (d, J = 4.3 Hz, 2H), 4.23 (s, 2H), 3.14 (s, 3H).

Triethyl(furan-2-ylmethoxy)silane
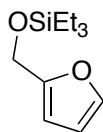
In an argon-filled dry-box, a screw-capped vial (20 ml) was charged furfural (1.7 ml, 20. mmol), [Ru(p-cymene)Cl$_2$]$_2$ (12 mg, 0.20 mmol), and a magnetic stirbar. While stirring, triethylsilane (3.8 ml, 24 mmol) was added to the solution. The vial was sealed with a Teflon-lined cap and placed in a 50 °C heating block. After 12 h, the volatile materials were removed by rotary evaporation, and the crude material was purified by flash chromatography with 2% EtOAc in hexanes as eluent. The title compound was isolated as a clear liquid and stored in the freezer under argon (1.5 g, 35% yield). Spectral data matched those of previous reports.[49]

^{1}H NMR (500 MHz, CDCl$_3$): δ 7.40 (d, *J* = 1.0 Hz, 1H), 6.34 (dd, *J* = 3.0, 1.9 Hz, 1H), 6.26 (d, *J* = 3.1 Hz, 1H), 4.65 (s, 2H), 0.98 (t, *J* = 8.0 Hz, 9H), 0.65 (q, *J* = 8.0 Hz, 6H).

2-(Furan-2-yl)-1,3-dioxolane
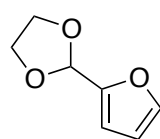
A round-bottom flask (250 ml) was charged with furfural (13.2 g, 138 mmol), ethylene glycol (9.94 g, 158 mmol), p-toluenesulfonic acid (53 mg, 0.28 mmol), toluene (35 ml) and a magnetic stirbar. A Dean-Stark distillation trap was connected to the flask, and the solution was brought to reflux (125 °C). After 12 h, the reaction was complete as determined by TLC. The title compound was isolated after distillation (400 mTorr, 60 °C) as a clear liquid (13.2 g, 68% yield). Spectral data matched those of previous reports.[50]

^{1}H NMR (500 MHz, CDCl$_3$): δ 7.64-7.39 (m, 1H), 6.47 (d, *J* = 3.2 Hz, 1H), 6.44-6.33 (m, 1H), 5.94 (s, 1H), 4.15 (dd, *J* = 8.8, 5.0 Hz, 2H), 4.11-4.00 (m, 2H).

General Procedure A: Ir-catalyzed olefination of furans with -olefins.
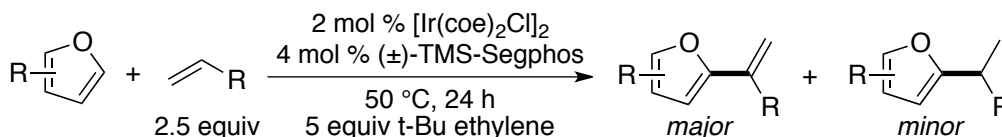
In an argon-filled dry-box, a screw-capped vial (4.0 ml) was charged with [Ir(coe)$_2$Cl]$_2$ (5.3 mg, 0.0060 mmol), (±)-TMS-Segphos (14.3 mg, 0.0120 mmol), *tert*-butylethylene (190 μl, 1.5 mmol), and a magnetic stirbar. The vial was sealed with a Teflon-lined cap and allowed to stir at room temperature. After 15 minutes, a red homogeneous solution had formed. The furan (0.30 mmol) and alkene (0.75 mmol) were added to the vial via syringe. The vial was sealed, removed from the dry-box, and placed in a 50 °C heating block. After 24 h, the vial was allowed to cool to room temperature, and the solvent was removed by rotary evaporation. An aqueous solution of H$_2$O$_2$ (1.5 ml, 2%) was added to the residue and the mixture was stirred vigorously for 20 minutes to oxidize residual metal complexes. The organic materials were extracted with ethyl acetate. The organic solution was concentrated, and the residue was purified by flash chromatography on a column (height = 20. cm, diameter = 3.0 cm) of Silacycle Siala-P60 silica gel (30 g). The conditions for chromatography and other data that are specific to each compound are given below.
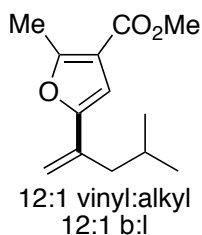
Methyl 2-methyl-5-(oct-1-en-2-yl)furan-3-carboxylate
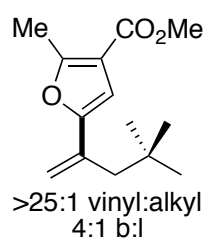
Me CO$_2$Me

n-Pent

15:1 vinyl:alkyl
>25:1 b:l

Following the general procedure **A** described above, methyl 2-methylfuran-3-carboxylate (38 μl, 0.30 mmol) was allowed to react with 1-octene (110 μl, 0.75 mmol, 2.5 equiv) in the presence of *tert*-butyl ethylene (190 μl, 1.5 mmol, 5.0 equiv) for 24 h at 50 °C. The crude material was purified by flash chromatography with 1.5% ethyl acetate in hexanes as eluent. The fractions were monitored by thin layer chromatography with a UV lamp. Fractions containing the desired product (R_f = 0.25, 5% EtOAc in hexanes) were collected, and the solvent was removed by rotary evaporation. Residual solvent impurities were removed under high vacuum (50 mTorr, 1 h) to yield a mixture of the title compound and the alkyl furan in a 15:1 ratio (as determined by ^{1}H NMR) as a clear oil (74 mg, 99% yield).

^{1}H NMR (600 MHz, C$_6$D$_6$): δ 6.64 (s, 1H), 5.63 (s, 1H), 4.90 (s, J = 0.8 Hz, 1H), 3.44 (s, 3H), 2.36 (s, 3H), 2.20-2.12 (m, 2H), 1.47-1.40 (m, 2H), 1.23-1.17 (m, J = 4H, 1.14 (ddd, J = 15.7, 6.7, 3.2 Hz, 2H), 0.83 (t, J = 7.2 Hz, 3H).

^{13}C NMR (151 MHz, C$_6$D$_6$): δ 163.6, 158.5, 152.6, 136.9, 114.9, 109.3, 106.7, 50.4, 32.8, 31.6, 29.0, 28.5, 22.6, 13.8, 13.2.

GC-MS: *m/z* 250 (15%, [M]$^+$), 180 (100%, [M-C$_5$H$_{10}$]$^+$).

Anal. Calcd for C$_{15}$H$_{22}$O$_3$: C 71.97%, H 8.86%; Found: C 72.20%, H 9.14%.

Methyl 2-methyl-5-(4-methylpent-1-en-2-yl)furan-3-carboxylate
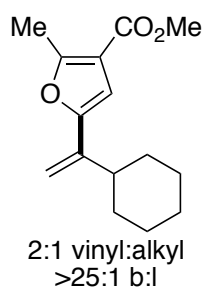
Me CO$_2$Me

12:1 vinyl:alkyl
12:1 b:l

Following the general procedure **A** described above, methyl 2-methylfuran-3-carboxylate (38 μl, 0.30 mmol) was allowed to react with 4-methyl pent-1-ene (92 μl, 0.75 mmol, 2.5 equiv) in the presence of *tert*-butyl ethylene (190 μl, 1.5 mmol, 5.0 equiv) for 24 h at 50 °C. The crude material was purified by flash chromatography with 1.5% ethyl acetate in hexanes as eluent. The fractions were monitored by thin layer chromatography with a UV lamp. Fractions containing the desired product (R_f = 0.25, 5% EtOAc in hexanes) were collected, and the solvent was removed by rotary evaporation. Residual solvent impurities were removed under high vacuum (50 mTorr, 1 h) to yield a mixture of the title compound, the linear vinyl furan isomer, and alkyl furan in a 15:1:1 ratio (as determined by ^{1}H NMR) as a clear oil (64 mg, 97% yield).

^{1}H NMR (600 MHz, C$_6$D$_6$): δ 6.62 (s, 1H), 5.63 (d, J = 1.2 Hz, 1H), 4.84 (s, 1H), 3.44 (d, J = 2.9 Hz, 3H), 2.35 (s, 3H), 2.03 (d, J = 7.3 Hz, 2H), 1.75 (dp, J = 13.6, 6.8 Hz, 1H), 0.79 (d, J = 6.6 Hz, 6H).

^{13}C NMR (151 MHz, C$_6$D$_6$): δ 163.6, 158.5, 152.7, 135.8, 114.9, 110.6, 106.9, 50.4, 42.5, 27.2, 22.2, 13.2.

GC-MS: *m/z* 222 (20%, [M]$^+$), 180 (100%, [M-C$_3$H$_6$]$^+$).

Anal. Calcd for C$_{13}$H$_{18}$O$_3$: C 70.24%, H 8.16%; Found: C 69.92%, H 8.34%.
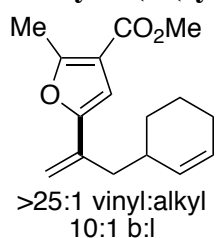
Methyl 5-(4,4-dimethylpent-1-en-2-yl)-2-methylfuran-3-carboxylate

Following the general procedure **A** described above, methyl 2-methylfuran-3-carboxylate (38 μl, 0.30 mmol) was allowed to react with 4,4-dimethyl pent-1-ene (110 μl, 0.75 mmol, 2.5 equiv) in the presence of *tert*-butyl ethylene (190 μl, 1.5 mmol, 5.0 equiv) for 24 h at 50 °C. The crude material was purified by flash chromatography with 1.5% ethyl acetate in hexanes as eluent. The fractions were monitored by thin layer chromatography with a UV lamp. Fractions containing the desired product (R_f = 0.25, 5% EtOAc in hexanes) were collected, and the solvent was removed by rotary evaporation. Residual solvent impurities were removed under high vacuum (50 mTorr, 1 h) to yield a mixture of the title compound and the linear vinyl furan isomer in a 4:1 ratio (as determined by ^{1}H NMR) as a clear oil (57 mg, 77% yield).

>25:1 vinyl:alkyl
4:1 b:l

^{1}**H NMR** (600 MHz, C$_6$D$_6$): δ 6.65 (s, 1H), 5.70 (s, 1H), 4.81 (s, 1H), 3.43 (s, 3H), 2.35 (s, 3H), 2.11 (s, 2H), 0.82 (s, 9H).

^{13}**C NMR** (151 MHz, C$_6$D$_6$): δ 163.6, 158.3, 153.7, 134.5, 114.9, 113.1, 107.3, 50.4, 45.8, 31.1, 29.5, 13.2.

GC-MS: *m*/*z* 236 (30%, [M]$^+$), 179 (100%, [M-C$_4$H$_9$]$^+$).

Anal. Calcd for C$_{14}$H$_{20}$O$_3$: C 71.16%, H 8.53%; Found: C 71.46%, H 8.79%.

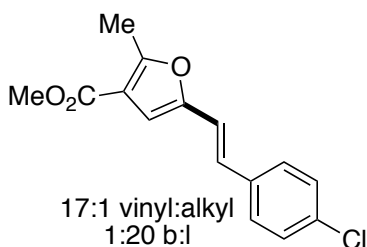## Methyl 5-(1-cyclohexylvinyl)-2-methylfuran-3-carboxylate

Following the general procedure **A** described above, methyl 2-methylfuran-3-carboxylate (38 μl, 0.30 mmol) was allowed to react with vinyl cyclohexane (100 μl, 0.75 mmol, 2.5 equiv) in the presence of *tert*-butyl ethylene (190 μl, 1.5 mmol, 5.0 equiv) for 24 h at 50 °C. The crude material was purified by flash chromatography with 1.5% ethyl acetate in hexanes as eluent. The fractions were monitored by thin layer chromatography with a UV lamp. Fractions containing the desired product (R_f = 0.25, 5% EtOAc in hexanes) were collected, and the solvent was removed by rotary evaporation. Residual solvent impurities were removed under high vacuum (50 mTorr, 1 h) to yield a mixture of the title compound and the alkyl furan in a 2:1 ratio (determined by ^{1}H NMR) as a clear oil (65 mg, 88% yield). Elemental analysis on the isolated material was not performed because the material contained a 2:1 mixture of the vinylfuran and alkylfuran products.

2:1 vinyl:alkyl
>25:1 b:l

^{1}**H NMR** (600 MHz, CDCl$_3$): δ 6.52 (s, 1H), 5.50 (s, 1H), 4.97 (s, 1H), 3.81 (s, 3H), 2.57 (s, 3H), 2.25 (t, *J* = 11.6 Hz, 1H), 1.86 (d, *J* = 12.5 Hz, 2H), 1.80 (d, *J* = 13.0 Hz, 2H), 1.77-1.67 (m, 2H), 1.34 (dd, *J* = 25.7, 12.8 Hz, 2H), 1.25 (dt, *J* = 13.6, 11.3 Hz, 2H).

^{13}**C NMR** (151 MHz, C$_6$D$_6$): δ 163.6, 158.6, 152.8, 135.2, 114.9, 110.6, 106.9, 50.4, 41.2, 36.7, 33.2, 26.1, 13.2.

GC-MS: *m*/*z* 248 (40%, [M]$^+$), 180 (100%, [M-C$_5$H$_9$]$^+$).

Methyl 5-(3-(cyclohex-2-en-1-yl)prop-1-en-2-yl)-2-methylfuran-3-carboxylate
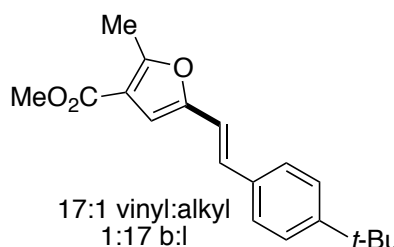
Me CO$_2$Me

O

>25:1 vinyl:alkyl
10:1 b:l

Following the general procedure **A** described above, methyl 2-methylfuran-3-carboxylate (38 μl, 0.30 mmol) was allowed to react with 3-allylcyclohex-1-ene (110 μl, 0.75 mmol, 2.5 equiv) in the presence of *tert*-butyl ethylene (190 μl, 1.5 mmol, 5.0 equiv) for 24 h at 50 °C. The crude material was purified by flash chromatography with 1.5% ethyl acetate in hexanes as eluent. The fractions were monitored by thin layer chromatography with a UV lamp. Fractions containing the desired product (R_f = 0.25, 5% EtOAc in hexanes) were collected, and the solvent was removed by rotary evaporation. Residual solvent impurities were removed under high vacuum (50 mTorr, 1 h) to yield a mixture of the title compound and the linear vinyl furan in a 10:1 ratio (determined by ^{1}H NMR) as a clear oil (60. mg, 77% yield).

^{1}H NMR (600 MHz, C$_6$D$_6$): δ 6.65 (s, 1H), 5.67 (s, 1H), 5.65-5.59 (m, 2H), 4.88 (s, 1H), 3.42 (s, 3H), 2.35 (s, 3H), 2.24 (dd, J = 13.9, 7.1 Hz, 1H), 2.15 (dd, J = 13.8, 8.0 Hz, 1H), 1.85-1.79 (m, 2H), 1.67-1.60 (m, 1H), 1.56-1.49 (m, 1H), 1.34 (dddd, J = 13.9, 11.0, 8.3, 2.8 Hz, 1H), 1.14 (ddd, J = 13.2, 9.8, 2.7 Hz, 1H), 0.29-0.19 (m, 1H).

^{13}C NMR (151 MHz, C$_6$D$_6$): δ 163.6, 158.6, 152.5, 140.1, 135.0, 127.1, 114.9, 111.0, 107.0, 50.4, 39.8, 34.1, 29.0, 25.2, 21.2, 13.2.

GC-MS: *m/z* 260 (25%, [M]$^+$), 180 (100%, [M-C$_6$H$_8$]$^+$).

Anal. Calcd for C$_{16}$H$_{20}$O$_3$: C 73.82%, H 7.74%; Found: C 74.08%, H 7.96%.

(*E*)-Methyl 5-(4-chlorostyryl)-2-methylfuran-3-carboxylate

Me

O

MeO$_2$C

17:1 vinyl:alkyl
1:20 b:l

Cl

Following the general procedure **A** described above, methyl 2-methylfuran-3-carboxylate (38 μl, 0.30 mmol) was allowed to react with 4-chlorostyrene (90. μl, 0.75 mmol, 2.5 equiv) in the presence of *tert*-butyl ethylene (190 μl, 1.5 mmol, 5.0 equiv) for 14 h at 50 °C. The crude material was purified by flash chromatography with 1.5% ethyl acetate in hexanes as eluent. The fractions were monitored by thin layer chromatography with a UV lamp. Fractions containing the desired product (R_f = 0.25, 5% EtOAc in hexanes) were collected, and the solvent was removed by rotary evaporation. Residual solvent impurities were removed under high vacuum (50 mTorr, 1 h) to yield a mixture of the title compound and the linear alkyl furan in a 17:1 ratio (determined by ^{1}H NMR) as a white solid (63 mg, 76% yield).

^{1}H NMR (600 MHz, C$_6$D$_6$): δ 7.02 (d, J = 8.4 Hz, 2H), 6.85-6.80 (m, 3H), 6.58 (s, 1H), 6.39 (d, J = 16.3 Hz, 1H), 3.45 (s, 3H), 2.40 (s, 3H).

^{13}C NMR (151 MHz, C$_6$D$_6$): δ 163.4, 158.9, 150.9, 135.1, 133.2, 128.7, 127.9, 126.1, 116.2, 115.5, 109.4, 50.6, 13.3.

GC-MS: *m/z* 276 (100%, [M]$^+$), 202 (40%, [M-C$_3$H$_3$Cl]$^+$).

Anal. Calcd for C$_{15}$H$_{13}$ClO$_3$: C 65.11%, H 4.74%; Found: C 65.31%, H 5.13%.

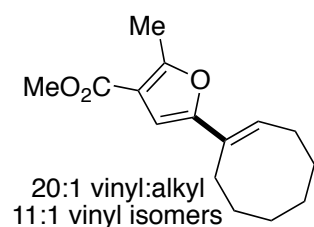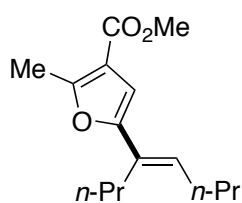## (*E*)-Methyl 5-(4-(*tert*-butyl)styryl)-2-methylfuran-3-carboxylate

Following the general procedure **A** described above, methyl 2-methylfuran-3-carboxylate (38 μl, 0.30 mmol) was allowed to react with 4-*tert*-butyl styrene (140 μl, 0.75 mmol, 2.5 equiv) in the presence of *tert*-butyl ethylene (190 μl, 1.5 mmol, 5.0 equiv) for 14 h at 50 °C. The crude material was purified by flash chromatography with 1.5% ethyl acetate in hexanes as eluent. The fractions were monitored by thin layer chromatography with a UV lamp. Fractions containing the desired product (R_f = 0.25, 5% EtOAc in hexanes) were collected, and the solvent was removed by rotary evaporation. Residual solvent impurities were removed under high vacuum (50 mTorr, 1 h) to yield a mixture of the title compound, the linear alkyl furan, and the branched vinyl furan isomer in a 17:1:1 ratio (determined by ^{1}H NMR) as a white solid (72 mg, 81% yield).

^{1}H NMR (600 MHz, C$_6$D$_6$): δ 7.25 (d, *J* = 8.4 Hz, 2H), 7.20 (d, *J* = 8.4 Hz, 2H), 7.12 (d, *J* = 14.2 Hz, 1H), 6.67 (d, *J* = 16.2 Hz, 1H), 6.57 (s, 1H), 3.46 (s, 3H), 2.42 (s, 3H), 1.19 (s, 9H).

^{13}C NMR (151 MHz, C$_6$D$_6$): δ 163.5, 158.6, 151.4, 150.6, 134.1, 128.0, 126.3, 125.5, 115.3, 115.0, 108.6, 50.5, 34.2, 30.9, 13.3.

GC-MS: *m/z* 298 (100%, [M]$^+$), 283 (95%, [M-CH$_3$]$^+$).

Anal. Calcd for C$_{19}$H$_{22}$O$_3$: C 76.48%, H 7.43%; Found: C 76.33%, H 7.51%.

(*E*)-Methyl 5-(cyclooct-1-en-1-yl)-2-methylfuran-3-carboxylate

Following the general procedure **A** described above, methyl 2-methylfuran-3-carboxylate (38 μl, 0.30 mmol) was allowed to react with *cis*-cyclooctene (100 μl, 0.75 mmol, 2.5 equiv) in the presence of *tert*-butyl ethylene (190 μl, 1.5 mmol, 5.0 equiv) for 24 h at 50 °C. The crude material was purified by flash chromatography with 1.5% ethyl acetate in hexanes as eluent. The fractions were monitored by thin layer chromatography with a UV lamp. Fractions containing the desired product (R_f = 0.25, 5% EtOAc in hexanes) were collected, and the solvent was removed by rotary evaporation. Residual solvent impurities were removed under high vacuum (50 mTorr, 1 h) to yield a mixture of the title compound, the allyl furan isomer, and cyclooctyl furan in a 20:2:1 ratio (determined by ^{1}H NMR) as a clear oil (71 mg, 95% yield).

^{1}H NMR (600 MHz, C$_6$D$_6$): δ 6.55 (s, 1H), 6.33 (t, *J* = 8.5 Hz, 1H), 3.45 (s, 3H), 2.39 (s, 3H), 2.31-2.24 (m, 2H), 2.11-2.03 (m, 2H), 1.44 (br s, 2H), 1.39 (br s, 2H), 1.36-1.29 (m, 4H).

^{13}C NMR (151 MHz, C$_6$D$_6$): δ 163.8, 157.9, 153.2, 129.8, 125.2, 114.9, 105.0, 50.4, 30.0, 28.9, 26.6, 26.4, 25.9, 25.7, 13.2.

GC-MS: *m/z* 248 (30%, [M]$^+$), 220 (100%, [M-C$_2$H$_4$]$^+$).

Anal. Calcd for C$_{15}$H$_{20}$O$_3$: C 72.55%, H 8.12%; Found: C 72.29%, H 8.34%.

## (*E*)-Methyl 2-methyl-5-(oct-4-en-4-yl)furan-3-carboxylate

Following the general procedure **A** described above, methyl 2-methylfuran-3-carboxylate (38 μl, 0.30 mmol) was allowed to react with 4-octyne (170 μl, 1.2 mmol, 4.0 equiv) in the presence of octane (100 μl), rather than *tert*-butyl ethylene, for 24 h at 100 °C. The crude material was purified by flash chromatography with 1.5% ethyl acetate in hexanes as eluent. The fractions were monitored by thin layer chromatography with a UV lamp. Fractions containing the desired product (R_f = 0.25, 5% EtOAc in hexanes) were collected, and the solvent was removed by rotary evaporation. Residual solvent impurities were removed under high vacuum (50 mTorr, 1 h) to yield the title compound as a clear oil (49 mg, 65% yield). The olefin geometry of the title compound was unambiguously determined by NOE correlations of select resonances in the ^{1}H NMR spectrum. See copies of spectral data.

^{1}**H NMR** (600 MHz, C$_6$D$_6$): δ 6.59 (s, 1H), 6.16 (t, *J* = 7.5 Hz, 1H), 3.45 (s, 3H), 2.40 (s, 3H), 2.23-2.16 (m, 2H), 2.02 (q, *J* = 7.4 Hz, 2H), 1.47-1.41 (m, 2H), 1.36-1.29 (m, 2H), 0.83 (t, *J* = 6.1 Hz, 3H), 0.81 (t, *J* = 6.1 Hz, 3H).

^{13}**C NMR** (151 MHz, C$_6$D$_6$): δ 163.8, 157.8, 153.6, 128.9, 126.3, 114.8, 105.0, 50.4, 29.8, 29.7, 22.8, 22.5, 13.8, 13.7, 13.2.

GC-MS: *m/z* 250 (95%, [M]$^+$), 221 (100%, [M-C$_2$H$_5$]$^+$), 189 (90%).

HR-MS (EI): exact mass calcd for C$_{15}$H$_{22}$O$_3$: *m/z* 250.1569 ([M]$^+$); Found, 150.1565 ([M]$^+$).

2-Methyl-5-(oct-1-en-2-yl)furan
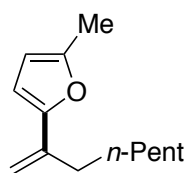
Following the general procedure **A** described above, 2-methyl furan (27 μl, 0.30 mmol) was allowed to react with 1-octene (110 μl, 0.75 mmol, 2.5 equiv) in the presence of *tert*-butyl ethylene (190 μl, 1.5 mmol, 5.0 equiv) for 24 h at 50 °C. The crude material was purified by flash chromatography with hexanes as eluent. The fractions were monitored by thin layer chromatography with a UV lamp. Fractions containing the desired product (R_f = 0.8, hexanes) were collected, and the solvent was removed by rotary evaporation to yield the title compound as a clear oil (51 mg, 88% yield).

^{1}**H NMR** (600 MHz, C$_6$D$_6$): δ 6.10 (d, *J* = 2.0 Hz, 1H), 5.77 (s, 1H), 5.72 (s, 1H), 4.92 (s, 1H), 2.28 (t, *J* = 7.7 Hz, 2H), 1.97 (s, 3H), 1.57-1.47 (m, 2H), 1.28-1.14 (m, 6H), 0.84 (t, *J* = 7.0 Hz, 3H).

^{13}**C NMR** (151 MHz, C$_6$D$_6$): δ 153.4, 151.5, 137.8, 107.6, 107.1, 107.0, 33.2, 31.7, 29.1, 28.8, 22.6, 13.9, 13.1.

GC-MS: *m/z* 192 (45%, [M]$^+$), 135 (100%, [M-C$_4$H$_9$]$^+$).

HR-MS (EI): exact mass calcd for C$_{13}$H$_{20}$O: *m/z* 192.1510 ([M]$^+$); Found, 192.1514 ([M]$^+$).

## Triethyl((5-(oct-1-en-2-yl)furan-2-yl)methoxy)silane
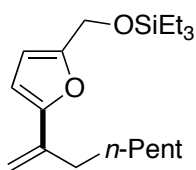
Following the general procedure **A** described above, triethyl(furan-2-ylmethoxy)silane (63 mg, 0.30 mmol) was allowed to react with with 1-octene (110 μl, 0.75 mmol, 2.5 equiv) in the presence of *tert*-butyl ethylene (190 μl, 1.5 mmol, 5.0 equiv) for 24 h at 50 °C. The crude material was purified by flash chromatography with 1% ethyl acetate in hexanes as eluent. The fractions were monitored by thin layer chromatography with a UV lamp. Fractions containing the desired product (R_f = 0.25, 5% EtOAc in hexanes) were collected, and the solvent was removed by rotary evaporation. Residual solvent impurities were removed under high vacuum (50 mTorr, 12 h) to yield the title compound as a clear oil (61 mg, 63% yield).

¹H NMR (600 MHz, C_6D_6): δ 6.08 (s, 2H), 5.73 (d, J = 1.4 Hz, 1H), 4.93 (d, J = 1.2 Hz, 1H), 4.48 (s, 2H), 2.28-2.20 (m, 2H), 1.48 (dt, J = 15.3, 7.6 Hz, 2H), 1.26-1.19 (m, 4H), 1.17 (ddd, J = 12.4, 7.1, 3.8 Hz, 2H), 0.95 (t, J = 8.0 Hz, 9H), 0.84 (t, J = 7.1 Hz, 3H), 0.57 (q, J = 7.9 Hz, 6H).

¹³C NMR (151 MHz, C_6D_6): δ 154.4, 153.9, 137.7, 108.7, 108.7, 106.6, 57.7, 33.1, 31.7, 29.1, 28.7, 22.6, 13.9, 6.6, 4.5.

GC-MS: *m/z* 322 (20%, [M]⁺), 223 (90%), 121 (100%).

Anal. Calcd for $C_{19}H_{34}O_2Si$: C 70.75%, H 10.62%; Found: C 70.57%, H 10.24%.

2-(Oct-1-en-2-yl)-5-pentylfuran
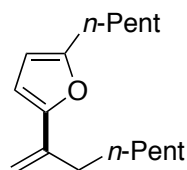
Following the general procedure **A** described above, 2-pentyl furan (47 μl, 0.30 mmol) was allowed to react with 1-octene (110 μl, 0.75 mmol, 2.5 equiv) in the presence of *tert*-butyl ethylene (190 μl, 1.5 mmol, 5.0 equiv) for 24 h at 50 °C. The crude material was purified by flash chromatography with hexanes as eluent. Fractions containing the desired product (R_f = 0.8, hexanes) were collected, and the solvent was removed by rotary evaporation. Residual solvent impurities were removed under high vacuum (50 mTorr, 3 h) to yield the title compound as a clear oil (67 mg, 90% yield).

¹H NMR (600 MHz, C_6D_6): δ 6.15 (d, J = 3.0 Hz, 1H), 5.87 (d, J = 2.9 Hz, 1H), 5.74 (s, 1H), 4.93 (s, 1H), 2.45 (t, J = 7.6 Hz, 2H), 2.29 (t, J = 7.7 Hz, 2H), 1.57-1.47 (m, 4H), 1.28-1.14 (m, 10H), 0.84 (t, J = 7.0 Hz, 3H), 0.78 (t, J = 6.4 Hz, 3H).

¹³C NMR (151 MHz, C_6D_6): δ 156.0, 153.3, 137.9, 107.6, 106.8, 106.3, 33.2, 31.7, 31.2, 29.1, 28.8, 28.0, 27.7, 22.6, 22.3, 13.9, 13.7.

GC-MS: *m/z* 248 (40%, [M]⁺), 191 (100%).

HR-MS (EI): exact mass calcd for $C_{17}H_{28}O$: *m/z* 248.2140 ([M]⁺); Found, 248.2135 ([M]⁺).

2-(Methoxymethyl)-5-(oct-1-en-2-yl)furan
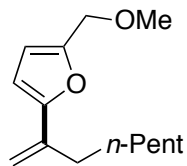
Following the general procedure **A** described above, 2-methoxymethyl furan (34 mg, 0.30 mmol) was allowed to react with 1-octene (110 μl, 0.75 mmol, 2.5 equiv) in the presence of *tert*-butyl ethylene (190 μl, 1.5 mmol, 5.0 equiv) for 24 h at 50 °C. The crude material was purified by flash chromatography with 1.5% ethyl acetate in hexanes as eluent. Fractions containing the desired product (R_f = 0.3, 5% EtOAc in hexanes)

were collected, and the solvent was removed by rotary evaporation. Residual solvent impurities were removed under high vacuum (50 mTorr, 1 h) to yield the title compound as a clear oil (48 mg, 72% yield).

¹H NMR (600 MHz, C_6D_6): δ 6.08 (d, J = 3.2 Hz, 1H), 6.06 (d, J = 3.1 Hz, 1H), 5.74 (s, 1H), 4.92 (s, 1H), 4.13 (s, 2H), 3.05 (s, 3H), 2.24 (t, J = 7.7 Hz, 2H), 1.51-1.42 (m, 2H), 1.21 (dd, J = 14.2, 7.0 Hz, 4H), 1.1801.11 (m, 2H), 0.84 (t, J = 7.1 Hz, 3H).

¹³C NMR (151 MHz, C_6D_6): δ 154.9, 151.6, 137.6, 110.4, 109.1, 106.6, 66.1, 57.0, 33.1, 31.6, 29.0, 28.7, 22.6, 13.9.

GC-MS: m/z 222 (15%, $[M]^+$), 152 (60%), 121 (100%).

Anal. Calcd for $C_{14}H_{22}O_2$: C 75.63%, H 9.97%; Found: C 75.24%, H 10.17%.

1-(5-(Oct-1-en-2-yl)furan-2-yl)ethanone
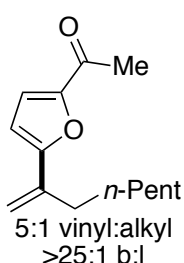
Following the general procedure **A** described above, 2-acetyl furan (30 μl, 0.30 mmol) was allowed to react with 1-octene (110 μl, 0.75 mmol, 2.5 equiv) in the presence of *tert*-butyl ethylene (95 μl, 0.75 mmol, 2.5 equiv) for 24 h at 50 °C. The crude material was purified by flash chromatography with 1.5% ethyl acetate in hexanes as eluent. The fractions were monitored by thin layer chromatography with a UV lamp. Fractions containing the desired product (R_f = 0.35, 5% EtOAc in hexanes) were collected, and the solvent was removed by rotary evaporation. Residual solvent impurities were removed under high vacuum (50 mTorr, 1 h) to yield a mixture of the title compound and the alkyl furan in a 5:1 ratio (determined by ¹H NMR) as a clear oil (40 mg, 61% yield).

¹H NMR (600 MHz, C_6D_6): δ 6.78 (d, J = 3.5 Hz, 1H), 5.93 (d, J = 3.6 Hz, 1H), 5.70 (s, 1H), 4.94 (s, 1H), 2.14 (t, J = 7.7 Hz, 2H), 2.03 (s, 3H), 1.42-1.35 (m, 2H), 1.24-1.16 (m, 6H), 0.85 (t, J = 7.2 Hz, 3H).

¹³C NMR (151 MHz, C_6D_6): δ 184.9, 157.3, 152.0, 137.2, 117.3, 112.7, 108.0, 32.7, 31.6, 28.9, 28.4, 25.2, 22.6, 13.9.

GC-MS: m/z 220 (10%, $[M]^+$), 150 (100%), 135 (80%).

Anal. Calcd for $C_{14}H_{20}O_2$: C 76.33%, H 9.15%; Found: C 76.11%, H 9.50%.

2-(5-(Oct-1-en-2-yl)furan-2-yl)-1,3-dioxolane
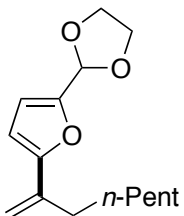
Following the general procedure **A** described above, 2-(furan-2-yl)-1,3-dioxolane (42 mg, 0.30 mmol) was allowed to react with 1-octene (110 μl, 0.75 mmol, 2.5 equiv) in the presence of *tert*-butyl ethylene (190 μl, 1.5 mmol, 5.0 equiv) for 24 h at 50 °C. The crude material was purified by flash chromatography, without treatment of the material with a solution of H_2O_2, using 1% ethyl acetate in hexanes as eluent. The fractions were monitored by thin layer chromatography with a UV lamp. Fractions containing the desired product (R_f = 0.25, 5% EtOAc in hexanes) were collected, and the solvent was removed by rotary evaporation. Residual solvent impurities were removed under high vacuum (50 mTorr, 2 h) to yield the title compound as a clear oil (38 mg, 51% yield).

¹H NMR (600 MHz, C_6D_6): δ 6.29 (d, J = 3.3 Hz, 1H), 6.03 (d, J = 3.2 Hz, 1H), 5.90 (s, 1H), 5.71 (s, 1H), 4.91 (s, 1H), 3.60 (dd, J = 8.5, 5.2 Hz, 2H), 3.39 (dd, J = 7.4, 6.3 Hz,
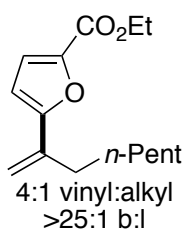
2H), 2.20 (t, J = 7.7 Hz, 2H), 1.48-1.40 (m, 2H), 1.25-1.12 (m, 6H), 0.84 (t, J = 7.1 Hz, 3H).

^{13}**C NMR** (151 MHz, C$_6$D$_6$): δ 155.2, 151.4, 137.5, 109.6, 109.5, 106.3, 97.9, 64.5, 33.0, 31.6, 29.0, 28.6, 22.6, 13.9.

GC-MS: m/z 250 (30%, [M]$^+$), 180 (100%).

Anal. Calcd for C$_{15}$H$_{22}$O$_3$: C 71.97%, H 8.86%; Found: C 71.85%, H 9.21%.

Ethyl 5-(oct-1-en-2-yl)furan-2-carboxylate

Following the general procedure **A** described above, 2-ethyl furoate (42 mg, 0.30 mmol) was allowed to react with 1-octene (110 μl, 0.75 mmol, 2.5 equiv) in the presence of *tert*-butyl ethylene (95 μl, 0.75 mmol, 2.5 equiv) for 24 h at 50 °C. The crude material was purified by flash chromatography with 1.5% ethyl acetate in hexanes as eluent. The fractions were monitored by thin layer chromatography with a UV lamp. Fractions containing the desired product (R_f = 0.25, 5% EtOAc in hexanes) were collected, and the solvent was removed by rotary evaporation. Residual solvent impurities were removed under high vacuum (50 mTorr, 1 h) to yield a mixture of the title compound and the alkyl furan in a 4:1 ratio (determined by ^{1}H NMR) as a clear oil (47 mg, 63% yield).

^{1}**H NMR** (600 MHz, C$_6$D$_6$): δ 7.01 (d, J = 3.5 Hz, 1H), 5.94 (d, J = 3.5 Hz, 1H), 5.79 (s, 1H), 4.91 (s, 1H), 4.06 (q, J = 7.0 Hz, 2H), 2.14 (t, J = 7.7 Hz, 2H), 1.36 (dt, J = 15.2, 7.5 Hz, 2H), 1.22-1.13 (m, 6H), 0.96 (t, J = 7.1 Hz, 3H), 0.84 (t, J = 7.2 Hz, 3H).

^{13}**C NMR** (151 MHz, C$_6$D$_6$): δ 165.0, 157.8, 144.1, 137.0, 118.8, 112.6, 107.5, 60.2, 35.4, 32.7, 31.5, 28.9, 28.3, 22.6, 13.9, 13.9.

GC-MS: m/z 250 (10%, [M]$^+$), 180 (100%).

Anal. Calcd for C$_{15}$H$_{22}$O$_3$: C 71.97%, H 8.86%; Found: C 71.71%, H 9.20%.

Ethyl 5-(oct-1-en-2-yl)furan-3-carboxylate
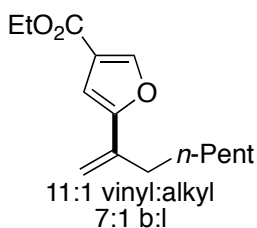
Following the general procedure **A** described above, 3-ethyl furoate (42 μl, 0.30 mmol) was allowed to react with 1-octene (110 μl, 0.75 mmol, 2.5 equiv) in the presence of *tert*-butyl ethylene (95 μl, 0.75 mmol, 2.5 equiv) for 24 h at 50 °C. The crude material was purified by flash chromatography with 1.5% ethyl acetate in hexanes as eluent. The fractions were monitored by thin layer chromatography with a UV lamp. Fractions containing the desired product (R_f = 0.25, 5% EtOAc in hexanes) were collected, and the solvent was removed by rotary evaporation. Residual solvent impurities were removed under high vacuum (50 mTorr, 1 h) to yield a mixture of the title compound, the alkyl furan, and the linear vinyl furan in an 11:1:1.5 ratio (determined by ^{1}H NMR) as a clear oil (49 mg, 65% yield).

^{1}**H NMR** (600 MHz, C$_6$D$_6$): δ 7.68 (s, 1H), 6.73 (s, 1H), 5.62 (s, 1H), 4.90 (s, 1H), 4.04 (q, J = 7.0 Hz, 2H), 2.15-2.06 (m, 2H), 1.37 (dt, J = 15.3, 7.5 Hz, 2H), 1.19 (dd, J = 14.2, 7.1 Hz, 2H), 1.15-1.08 (m, 4H), 0.96 (t, J = 7.2 Hz, 3H), 0.83 (t, J = 7.2 Hz, 3H).

^{13}**C NMR** (151 MHz, C$_6$D$_6$): δ 162.3, 155.9, 146.4, 137.0, 121.1, 110.5, 105.7, 59.9, 35.4, 32.8, 31.5, 28.9, 28.3, 22.6, 13.9.
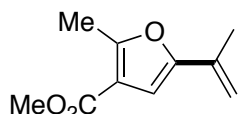
GC-MS: m/z 250 (10%, [M]$^+$), 180 (100%).

Anal. Calcd for $C_{15}H_{22}O_3$: C 71.97%, H 8.86%; Found: C 71.68%, H 8.63%.

General Procedure B: Ir-catalyzed olefination of furans with propylene
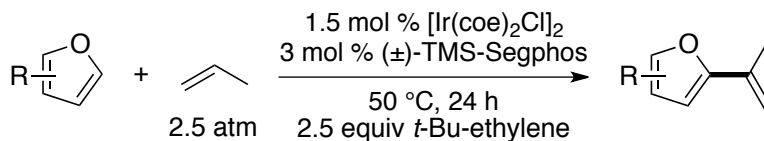
In an argon-filled dry-box, an oven-dried, round-bottom Schlenk flask (14 ml volume) [Ir(coe)₂Cl]₂ (4.0 mg, 0.0045 mmol), (±)-TMS-Segphos (10.7 mg, 0.00900 mmol), *tert*-butyl ethylene (100 μl, 0.7 mmol), the corresponding furan (0.30 mmol), and a magnetic stirbar. The flask was sealed with a Kontes valve, removed from the dry-box, and allowed to stir at room temperature. After 15 minutes, a red homogeneous solution had formed. The flask was charged with propylene gas (1.5 mmol) according to the following procedure. A manifold bulb adapter (62 ml) was attached to the Schlenk flask, the solution was frozen in liquid nitrogen, and the flask was placed under vacuum. The flask was sealed under vacuum, and a manifold bulb adapter (62 ml) was charged with the alkene gas (450 Torr at 23 °C). The gas in the adapter was condensed into the Schlenk flask at 77 K, and the flask was resealed. After allowing the flask to warm to room temperature, the flask was placed in a 50 °C oil bath. After 24 h, the solution was allowed to cool to room temperature, and the solvent was removed under vacuum. An aqueous solution of H_2O_2 (1.5 ml, 2%) was added to the residue, and the mixture was stirred vigorously for 20 minutes to oxidize residual metal complexes. The organic materials were extracted with ethyl acetate. The organic solution was concentrated, and the residue was purified by flash chromatography on a column (height = 20. cm, diameter = 3.0 cm) of Silacycle Siala-P60 silica gel (30 g). The conditions for chromatography, and other data that are specific to each compound, are given below.

## Methyl 2-methyl-5-(prop-1-en-2-yl)furan-3-carboxylate

Following the general procedure **B** described above, methyl 2-methylfuran-3-carboxylate (38 μl, 0.30 mmol) was allowed to react with propene in the presence of *tert*-butyl ethylene (100 μl, 0.75 mmol, 2.5 equiv) for 24 h at 50 °C. A 98% yield of the title compound was measured by ^{1}H NMR spectroscopy with mesitylene as an internal standard. The crude material was purified by flash chromatography with 1.5% ethyl acetate in hexanes as eluent. The fractions were monitored by thin layer chromatography with a UV lamp. Fractions containing the desired product (R_f = 0.25, 5% EtOAc in hexanes) were collected, and the solvent was removed by rotary evaporation. Residual solvent impurities were removed under high vacuum (100 mTorr, 10 min) to yield a mixture of the title compound and the isopropyl furan in a 20:1 ratio (determined by ^{1}H NMR) as a clear oil (51 mg, 94% yield).

^{1}H NMR (600 MHz, C_6D_6): δ 6.53 (s, 1H), 5.54 (s, 1H), 4.81 (s, 1H), 3.44 (s, 3H), 2.34 (s, 3H), 1.71 (s, 3H).

^{13}C NMR (151 MHz, C_6D_6): δ 163.6, 158.6, 152.8, 132.0, 114.9, 109.9, 107.0, 50.4, 18.6, 13.1.

**GC-MS**: m/z 180 (100%, [M]⁺), 165 (95%, [M-CH₃]⁺).

Anal. Calcd for $C_{10}H_{12}O_3$: C 66.65%, H 6.71%; Found: C 66.70%, H 6.87%.

4-methyl-2-(prop-1-en-2-yl)furan
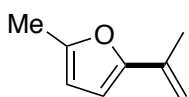
Following the general procedure **B** described above, 2-methyl furan (27 μl, 0.30 mmol) was allowed to react with propene in the presence of *tert*-butyl ethylene (100 μl, 0.75 mmol, 2.5 equiv) for 24 h at 50 °C. An 87% yield of the title compound was measured by ^{1}H NMR spectroscopy with mesitylene as an internal standard. The material was passed through a plug of silica with hexanes as eluent. The title compound was isolated with hexane impurities due to its volatility. Spectral data matched those of previous reports.[51]

^{1}H NMR (600 MHz, C$_6$D$_6$): δ 6.01 (d, *J* = 3.1 Hz, 1H), 5.76-5.72 (m, 1H), 5.66 (s, 1H), 4.84 (s, 1H), 1.95 (s, 3H), 1.82 (s, 3H).

GC-MS: *m/z* 122 (100%, [M]$^+$), 107 (40%).

2-(5-(Prop-1-en-2-yl)furan-2-yl)-1,3-dioxolane
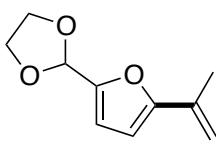
Following the general procedure **B** described above, 2-(furan-2-yl)-1,3-dioxolane (42 mg, 0.30 mmol) was allowed to react with propene in the presence of *tert*-butyl ethylene (100 μl, 0.75 mmol, 2.5 equiv) for 24 h at 50 °C. A 55% yield of the title compound was measured by ^{1}H NMR spectroscopy with mesitylene as an internal standard. The crude material was purified by flash chromatography without treatment of the material with a solution of H$_2$O$_2$. Fractions containing the desired product (R_f = 0.20, 5% EtOAc in hexanes) were collected, and the solvent was removed by rotary evaporation. Residual solvent impurities were removed under high vacuum (100 mTorr, 20 min) to yield a mixture of the title compound and the isopropyl furan in a 22:1 ratio (determined by ^{1}H NMR) as a clear oil (25 mg, 47% yield).

22:1 vinyl:alkyl
>25:1 b:l

^{1}H NMR (600 MHz, C$_6$D$_6$): δ 6.26 (d, *J* = 3.3 Hz, 1H), 5.93 (d, *J* = 3.3 Hz, 1H), 5.88 (s, 1H), 5.64 (s, 1H), 4.87-4.77 (m, 1H), 3.59 (td, *J* = 6.2, 4.1 Hz, 2H), 3.39 (td, *J* = 6.2, 4.1 Hz, 2H), 1.74 (s, 3H).

^{13}C NMR (151 MHz, C$_6$D$_6$): δ 155.3, 151.5, 132.6, 110.3, 109.5, 106.6, 97.9, 64.5, 18.8.

**GC-MS**: *m/z* 180 (70%, [M]$^+$), 135 (60%), 121 (100%).

HR-MS (EI): exact mass calcd for C$_{10}$H$_{12}$O$_3$: *m/z* 180.0786 ([M]$^+$); Found, 180.0782 ([M]$^+$).

General Procedure C: Ir-catalyzed CH bond addition of furans to ethylene.
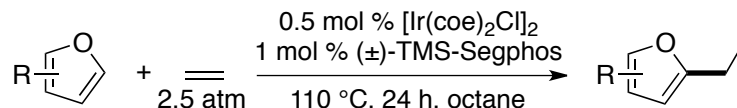
In an argon-filled dry-box, an oven-dried, round-bottom Schlenk flask (14 ml volume) [Ir(coe)$_2$Cl]$_2$ (1.3 mg, 0.0015 mmol), (±)-TMS-Segphos (3.6 mg, 0.0030 mmol), octane (100 μl), the corresponding furan (0.30 mmol), and a magnetic stirbar. The flask was sealed with a Kontes valve, removed from the dry-box, and allowed to stir at room temperature. After 15 minutes, a red homogeneous solution had formed. The flask was charged with ethylene gas (1.5 mmol) according to the following procedure. A manifold bulb adapter (62 ml) was attached to the Schlenk flask, the solution was frozen in liquid nitrogen, and the flask was placed under vacuum. The flask was sealed under vacuum, and a manifold bulb adapter (62 ml) was charged with the alkene gas (450 Torr at 23 °C).

The gas in the adapter was condensed into the Schlenk flask at 77 K, and the flask was resealed. After allowing the flask to warm to room temperature, the flask was placed in a 50 °C oil bath. After 24 h, the solution was allowed to cool to room temperature, and the solvent was removed under vacuum. An aqueous solution of H_2O_2 (1.5 ml, 2%) was added to the residue, and the mixture was stirred vigorously for 20 minutes to oxidize residual metal complexes. The organic materials were extracted with ethyl acetate. The organic solution was concentrated, and the residue was purified by flash chromatography on a column (height = 20. cm, diameter = 3.0 cm) of Silacycle Siala-P60 silica gel (30 g). The conditions for chromatography, and other data that are specific to each compound, are given below.

Methyl 5-ethyl-2-methylfuran-3-carboxylate
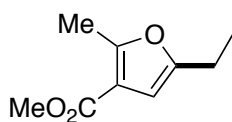
Following the general procedure **C** described above, 2-methylfuran-3-carboxylate (38 μl, 0.30 mmol) was allowed to react with ethylene in the presence of octane (100 μl) for 24 h at 110 °C. A 98% yield of the title compound was measured by ^{1}H NMR spectroscopy with mesitylene as an internal standard. The crude material was purified by flash chromatography with 1% ethyl acetate in hexanes as eluent. Fractions containing the desired product (R_f = 0.35, 5% EtOAc in hexanes) were collected, and the solvent was removed by rotary evaporation. Residual solvent impurities were removed under high vacuum (100 mTorr, 20 min) to yield the title compound as a clear oil (41 mg, 81% yield).
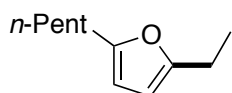
^{1}H NMR (600 MHz, C_6D_6): δ 6.29 (s, 1H), 3.45 (s, 3H), 2.40 (s, 3H), 2.26 (q, J = 7.5 Hz, 2H), 0.92 (t, J = 7.5 Hz, 3H).

^{13}C NMR (151 MHz, C_6D_6): δ 163.9, 157.3, 155.4, 113.9, 104.9, 50.3, 20.8, 13.1, 11.6.

GC-MS: m/z 168 (55%, [M]$^+$), 153 (100%), 121 (50%).

HR-MS (EI): exact mass calcd for $C_9H_{12}O_3$: m/z 168.0786 ([M]$^+$); Found, 168.0787 ([M]$^+$).

2-Ethyl-5-pentylfuran

Following the general procedure **C** described above, 2-pentyl furan (47 μl, 0.30 mmol) was allowed to react with ethylene in the presence of octane (100 μl) for 24 h at 110 °C. A 91% yield of the title compound was measured by ^{1}H NMR spectroscopy with mesitylene as an internal standard. The crude material was purified by flash chromatography with hexanes as eluent. Fractions containing the desired product (R_f = 0.8, hexanes) were collected, and the solvent was removed by rotary evaporation. Residual solvent impurities were removed under high vacuum (100 mTorr, 20 min) to yield the title compound as a clear oil (37 mg, 75% yield).

^{1}H NMR (600 MHz, C_6D_6): δ 5.85 (d, J = 2.9 Hz, 1H), 5.83 (d, J = 2.9 Hz, 1H), 2.50 (t, J = 7.7 Hz, 2H), 2.48-2.45 (m, 2H), 1.56 (dq, J = 14.9, 7.4 Hz, 2H), 1.21-1.15 (m, 4H), 1.06 (t, J = 7.5 Hz, 3H), 0.79 (t, J = 9.5, 4.6 Hz, 3H).

^{13}C NMR (151 MHz, C_6D_6): δ 155.6, 154.4, 105.1, 104.4, 31.3, 28.1, 27.9, 22.4, 21.4, 13.8, 12.1.

GC-MS: m/z 166 (25%, [M]$^+$), 109 (100%).

HR-MS (EI): exact mass calcd for $C_{11}H_{18}O$: m/z 166.1358 ([M]$^+$); Found, 166.1355 ([M]$^+$).

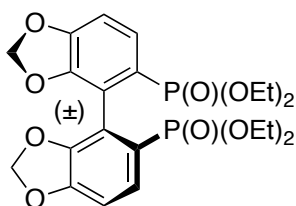### Diethyl benzo-1,3-dioxol-5-ylphosphonate
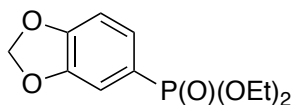
In an argon-filled dry-box, an oven dried round-bottom flask (200 ml) was charged with magnesium turnings (1.8 g, 75 mmol), THF (10 ml), a crystal of iodine, and a magnetic stirbar. The flask was sealed with a septum and placed in an ice bath. A solution of 5-bromobenzo-1,3-dioxole (10. g, 50 mmol) in THF (15 ml) was added via syringe to the flask over 20 minutes. The flask was allowed to warm to room temperature over the course of 1 h and stirred at room temperature for an additional 2 h. A separate flask was charged with diethyl chlorophosphate (9.7 ml, 65 mmol), a magnetic stirbar, and THF (20 ml) under argon. The solution was placed in an ice bath, and the Grignard solution was added via syringe to the flask containing the diethyl chlorophosphate over 20 minutes. Once all of the Grignard solution was added, the flask was removed from the ice bath and allowed to stir at room temperature for 4 hours. The reaction was quenched with a solution of HCl (2 M, 20 ml), and the organic material was extracted with EtOAc. The organic solution was washed with brine and dried over magnesium sulfate. The solvent was removed by rotary evaporation, and the residue was crudely purified by flash chromatography with hexanes as eluent to remove arene side products. The column was then flushed with EtOAc and to collect the title compound as a brown solution. The solution was distilled (80 mTorr, 100 °C) to yield the title compound as a clear liquid (8.14 g, 63% yield).[52]

^{1}H NMR (400 MHz, CDCl$_3$): δ 7.38 (ddd, J = 14.0, 7.9, 1.4 Hz, 1H), 7.20 (dd, J = 12.9, 1.3 Hz, 1H), 6.89 (dd, J = 7.9, 3.6 Hz, 1H), 6.03 (s, 2H), 4.19-3.99 (m, 4H), 1.32 (t, J = 7.1 Hz, 6H).

^{31}P NMR (162 MHz, CDCl$_3$): δ 17.4.

(±)-Tetraethyl [4,4'-bibenzo[*d*][1,3]dioxole]-5,5'-diylbis(phosphonate)

In an argon-filled dry-box, an oven dried round-bottom flask (500 ml) was charged with diethyl benzo-1,3-dioxol-5-yl phosphonate (5.00 g, 19.4 mmol), THF (12 ml), and a magnetic stirbar. The flask was sealed with a septum and placed in a bath at -78 °C. A freshly prepared solution of LDA in THF (0.95 M, 22.4 ml, 21.3 mmol) was added to the flask via syringe over 10 minutes. Lithiation of the arene was noted by the rapid formation of an orange solution. Separately, a solution of FeCl$_3$ in THF was prepared (4.4 g, 27 mmol in 20 ml THF. *Caution: dissolution of FeCl$_3$ is in THF exothermic*) in a dry-box. The solution was added via syringe to the aryl lithium species at -78 °C. The solution turned a purple color and was allowed to warm to room temperature overnight. The solvent was removed by rotary evaporation, and the residue was dissolved in CH$_2$Cl$_2$ (40 ml). To this solution was added an aqueous solution of NaOH (2M, 40 ml). The mixture was stirred at room temperature for 30 minutes after which point solid formed. The solids were removed by filtration through celite, and the organic material was extracted with CH$_2$Cl$_2$. The organic material was washed with brine and dried over magnesium sulfate. The solvent was removed by rotary evaporation, which formed an

off-pink solid. The solid was washed with cold (0 °C) diethyl ether to yield the title compound as a white solid (3.15 g, 63% yield).

^{1}H NMR (500 MHz, CDCl$_3$): δ 7.55 (dd, J = 14.8, 8.1 Hz, 2H), 6.87 (dd, J = 8.0, 2.9 Hz, 2H), 5.98 (s, 2H), 5.96 (s, 2H), 4.05-3.70 (m, 8H), 1.17 (t, J = 7.1 Hz, 6H), 1.11 (t, J = 7.1 Hz, 6H).

^{31}P NMR (243 MHz, CDCl$_3$): δ 17.5.

Anal. Calcd for C$_{22}$H$_{28}$O$_{10}$P$_2$: C 51.47%, H 5.49%; Found: C 51.35%, H 5.62%.

(±)-[4,4'-Bibenzo[*d*][1,3]dioxole]-5,5'-diyldiphosphonic dichloride
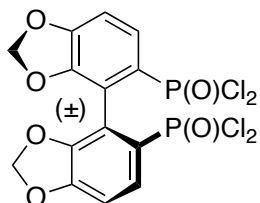
In an argon-filled dry-box, an oven dried round-bottom flask (50 ml) was charged with (±)-tetraethyl 4,4'-bibenzo-1,3-dioxole-5,5'-diylbis phosphonate (8.40 g, 16.3 mmol) and a magnetic stirbar. A reflux condenser was attached to the flask. Thionyl chloride was added to the flask via syringe (16.3 ml, 130. mmol), followed by dropwise addition of DMF (1.6 ml, 21 mmol). The solution was allowed to reflux (92 °C) for 13 hours. Upon completion, the flask was allowed to cool to room temperature, and the solvents were distilled away under high vacuum to yield a brown solid. The flask was taken into the dry-box, and the solid was washed with dry ether (10 ml x 3) to yield the title compound as a pale solid (7.15 g, 92% yield).

^{1}H NMR (400 MHz, CDCl$_3$): δ 7.71 (dd, J = 21.2, 8.3 Hz, 2H), 7.03 (dd, J = 8.3, 4.2 Hz, 2H), 6.13 (s, 2H), 6.08 (s, 2H).

^{31}P NMR (162 MHz, CDCl$_3$): δ 32.5.
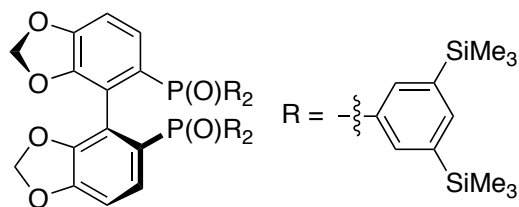
3,5-Bis(trimethylsilyl) bromobenzene
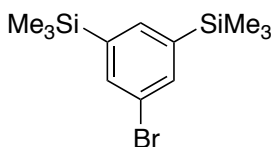
In an argon-filled dry-box, an oven dried round-bottom flask (1 L) was charged with 1,3,5-tribromobenzene (17.5 g, 55.5 mmol), diethyl ether (250 ml), and a magnetic stirbar. The flask was sealed with a septum and placed in a -40 °C bath. ^{n}BuLi (1.6 M, 36.8 ml, 58.8 mmol) was added to the white suspensions via syringe over 10 minutes, and the mixture was stirred for an additional 30 minutes. The reaction mixture was cooled to -78 °C, and TMSCl (8.0 ml, 63 mmol) was added via syringe. The reaction was removed from the cold bath and stirred for an additional 1 hour at room temperature, which caused a white precipitate to form. The procedure above was repeated, but with changes to the equivalents of nBuLi (1.6 M, 41 ml, 66 mmol) and TMSCl (9.7 ml, 78 mmol) added. The reaction was quenched with a saturated solution of NaHCO$_3$, extracted with diethyl ether, washed with brine, and dried over MgSO$_4$. Volatile products were removed under vacuum at room temperature (300 mTorr). Distillation of the residual material (75 °C, 100 mTorr) provided a clear liquid, which was a mixture of the title compound and tris(trimethylsilyl) benzene in a 6:1 ratio (14.1 g, 84% by weight, ca. 71% yield). Spectral data match those of previous reports.[53]

^{1}H NMR (600 MHz, CDCl$_3$): δ 7.60 (s, 2H), 7.54 (s, 1H), 0.29 (s, 18H).

Representative Example D: Synthesis of Aryl-Segphos Oxides

(±)-3,5-bis-TMS-Segphos(O)

In an argon-filled dry-box, an oven dried round-bottom flask (25 ml) was charged with magnesium turnings (290 mg, 12 mmol), an iodine crystal, THF (2 ml), and a magnetic stirbar. A reflux condenser was attached to the flask, and the top was sealed with a septum. 3,5-Bis(trimethylsilyl) bromobenzene (5.6 g, 10. mmol) was added dropwise to the reaction mixture via syringe at room temperature. Once all of the aryl bromide was added, the mixture was brought to reflux (73 °C). After 4 hours, the reaction was allowed to cool to room temperature, and a solution of (±)-[4,4'-bibenzo[d][1,3]dioxole]-5,5'-diyldiphosphonic dichloride (476 mg, 1.00 mmol, in 5 ml THF) was added dropwise to the reaction over 20 minutes. The reaction mixture was stirred for an additional 10 hours at room temperature. The reaction was quenched with saturated NH$_4$Cl, and the organic material was extracted with EtOAc. The organic solution was washed with brine and dried over MgSO$_4$. The solvent was removed by rotary evaporation, and the crude material was purified by flash chromatography with 15% EtOAc in hexanes as eluent. The title compound was isolated as a pale solid (765 mg, 63% yield).

^{1}H NMR (600 MHz, CDCl$_3$): δ 7.98 (d, J = 11.5 Hz, 4H), 7.76 (d, J = 11.3 Hz, 4H), 7.71 (s, 4H), 6.77 (dd, J = 13.9, 8.1 Hz, 2H), 6.66 (d, J = 8.0 Hz, 2H), 5.64 (s, 2H), 5.00 (s, 2H), 0.22 (s, 35H), 0.18 (s, 36H).
^{31}P NMR (243 MHz, CDCl$_3$): δ 28.4.

Representative Example E: Reduction of Aryl-Segphos Oxides

(±)-3,5-bis-TMS-Segphos
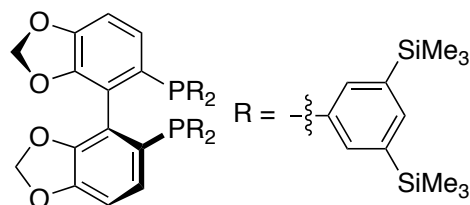
A screw-capped vial (20 ml) was charged with (±)-3,5-TMS-Segphos(O) (760 mg, 0.62 mmol) and a magnetic stirbar. Mesitylene (1.0 ml) and Et$_3$N (260 μl, 1.9 mmol) were added to the vial. The vial was placed in an ice bath under a stream of nitrogen. Trichlorosilane was added dropwise to the solution. Once the evolution of gas ceased, the vial was sealed with a Teflon-lined cap and placed in a 120 °C heating block. After 13 h, the vial was removed from the heating block and placed in an ice bath. Under a stream of nitrogen and vigorous stirring, an aqueous solution of NaOH (25%, 2 ml) was added to the vial dropwise. The vial was sealed and placed in an 80 °C heating block. After 1 hour, a biphasic mixture had formed. The organic material was extracted with EtOAc. The organic solution was washed with a 2 M solution of HCl, brine, and dried over MgSO$_4$. The crude material was purified by flash chromatography with 2% EtOAc in hexanes as eluent to yield the title compound as a white solid, which was stored under nitrogen (670 mg, 91% yield).

¹H NMR (600 MHz, CDCl₃): δ 7.79 (s, 8H), 7.65 (s, 4H), 6.93 (d, J = 7.9 Hz, 2H), 6.86 (d, J = 7.6 Hz, 2H), 5.86 (s, 2H), 5.10 (s, 2H), 0.41 (s, 36H), 0.38 (s, 36H).

³¹P NMR (243 MHz, CDCl₃): δ -12.5.

Anal. Calcd for $C_{62}H_{92}O_4P_2Si_8$: C 62.68%, H 7.81%; Found: C 62.37%, H 7.47%.

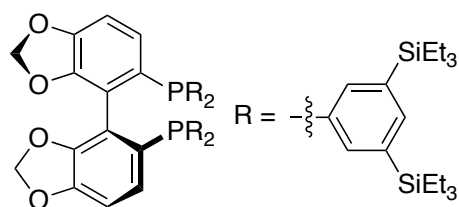## (±)-3,5-bis-TES-Segphos(O)
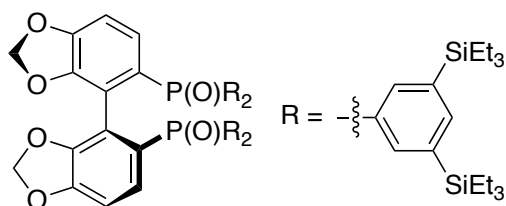
Following the procedure from representative example **D** described above, 3,5-bis(triethylsilyl) bromobenzene (4.7 g, 60% by weight, 10. mmol) was allowed to react with magnesium turnings (288 mg, 12 mmol) and (±)-[4,4'-bibenzo-1,3-dioxole]-5,5' diyldiphosphonic dichloride (476 mg, 1.00 mmol). The crude material was purified with 5% EtOAc in hexanes as eluent to yield the title compound as a tan solid (376 mg, 24% yield).

¹H NMR (500 MHz, CDCl₃): δ 7.84 (s, 2H), 7.81 (s, 2H), 7.74 (s, 2H), 7.71 (s, 4H), 7.68 (s, 2H), 6.70 (dd, J = 13.3, 8.1 Hz, 2H), 6.66 (dd, J = 8.0, 2.1 Hz, 2H), 5.58 (d, J = 1.4 Hz, 2H), 4.77 (d, J = 1.3 Hz, 2H), 0.92 (t, J = 7.8 Hz, 36H), 0.86 (t, J = 7.8 Hz, 36H), 0.75 (q, J = 14.8, 6.9 Hz, 24H), 0.71 (q, J = 7.8, 5.3 Hz, 24H).

**³¹P NMR** (162 MHz, CDCl₃): δ 29.4.

(±)-3,5-bis-TES -Segphos

Following the procedure from representative example **E** described above, (±)-3,5-TES-Segphos(O) (355 mg, 0.230 mmol) was allowed to reaction with trichlorosilane (0.52 ml, 5.0 mmol) and Et₃N (0.70 ml, 5.0 mmol) in mesitylene (1.0 ml). The crude reaction mixture was purified by flash chromatography with 3% EtOAc in hexanes as eluent. The title compound was isolated as a white solid (329 mg, 93% yield).

¹H NMR (600 MHz, CDCl₃): δ 7.53 (s, 2H), 7.46 (s, 2H), 7.37 (d, J = 2.8 Hz, 8H), 6.65 (d, J = 8.0 Hz, 2H), 6.52 (d, J = 7.9 Hz, 2H), 5.56 (s, 2H), 4.55 (s, 2H), 0.88 (t, J = 7.8 Hz, 36H), 0.83 (t, J = 7.9 Hz, 36H), 0.69 (dd, J = 15.9, 8.0 Hz, 24H), 0.66-0.61 (m, 24H).

³¹P NMR (243 MHz, CDCl₃): δ -12.5.

HR-MS (ESI): exact mass calcd for $C_{86}H_{141}O_4P_2Si_8$: m/z 1523.8454 ([M+H]⁺); Found, 1523.8460 ([M+H]⁺).

1-Bromo-4-butoxybenzene
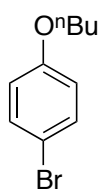
Under atmospheric conditions, a round-bottom flask (500 ml) was charged with 4-bromophenol (6.9 g, 40. mmol), K₂CO₃ (27.6 g, 200. mmol), acetone (300 ml), and a magnetic stirbar. The suspension was stirred at room temperature and iodobutane (6.0 ml, 52 mmol) was added dropwise over 5 minutes. A reflux condenser was attached to the flask, and the solution was allowed to reflux at 72 °C. Complete conversion of the starting material to product was observed after 16 hours. The solution was filtered through celite, and the solvent was removed by

rotary evaporation. The crude residue was passed through a plug of silica gel with hexanes as eluent to yield the title compound as a clear liquid (8.5 g, 93% yield). Spectral data match those of previous reports.[54]

^{1}H NMR (500 MHz, CDCl$_3$): δ 7.38 (d, J = 8.9 Hz, 2H), 6.79 (d, J = 8.9 Hz, 2H), 3.94 (t, J = 6.5 Hz, 2H), 1.91-1.68 (m, 2H), 1.64-1.44 (m, 2H), 0.99 (t, J = 7.4 Hz, 3H).
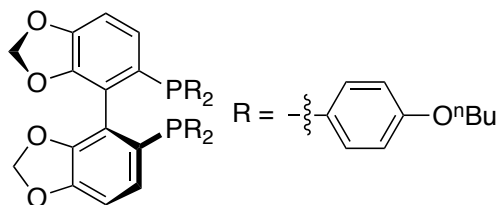
(±)-4-O^{n}Bu-Segphos(O)
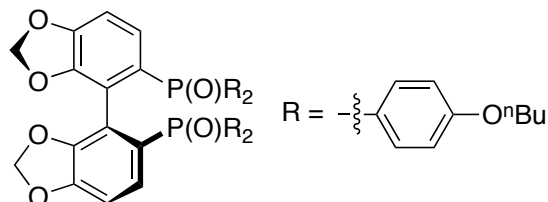
Following the procedure from representative example **D** described above, 4-n-butoxy bromobenzene (1.4 g, 6.0 mmol) was allowed to react with magnesium turnings (158 mg, 6.5 mmol) and (±)-[4,4'-bibenzo-1,3-dioxole]-5,5' diyldiphosphonic dichloride (230 mg, 0.50 mmol). The crude material was purified with 10% methanol in CH$_2$Cl$_2$ as eluent to yield the title compound as a tan solid (440 mg, 94% yield).

^{1}H NMR (500 MHz, CDCl$_3$): δ 7.70-7.52 (m, 4H), 7.51-7.37 (m, 4H), 6.90 (d, J = 7.5 Hz, 4H), 6.81 (dd, J = 13.9, 8.1 Hz, 2H), 6.72 (d, J = 7.6 Hz, 4H), 6.64 (d, J = 7.6 Hz, 2H), 5.76 (s, 2H), 5.43 (s, 2H), 3.97 (t, J = 6.3 Hz, 4H), 3.89 (d, J = 4.0 Hz, 4H), 1.74 (ddd, J = 21.1, 14.3, 6.8 Hz, 8H), 1.47 (tq, J = 14.6, 7.3 Hz, 8H), 1.01-0.93 (m, 12H).
^{31}P NMR (243 MHz, CDCl$_3$): δ 28.5.

(±)-4-O^{n}Bu-Segphos

Following the procedure from representative example **E** described above, (±)-4-O^{n}Bu-Segphos(O) (440 mg, 0.48 mmol) was allowed to reaction with trichlorosilane (0.56 ml, 5.8 mmol) and Et$_3$N (0.81 ml, 5.8 mmol) in mesitylene (1.5 ml). The crude reaction mixture was purified by flash chromatography with 5% EtOAc in hexanes as eluent. The title compound was isolated as a white solid and stored under nitrogen (237 mg, 55% yield).

^{1}H NMR (600 MHz, CDCl$_3$): δ 7.18-7.12 (m, 4H), 7.12-7.07 (m, 4H), 6.80 (s, 4H), 6.79 (s, 4H), 6.73 (s, 1H), 6.71 (s, 1H), 6.60-6.56 (m, 2H), 5.74 (d, J = 1.5 Hz, 2H), 5.16 (d, J = 1.5 Hz, 2H), 3.93 (qd, J = 6.6, 1.8 Hz, 8H), 1.79-1.70 (m, 8H), 1.52-1.43 (m, 8H), 1.00-0.93 (m, 12H).
^{31}P NMR (162 MHz, CDCl$_3$): δ -16.2.
Anal. Calcd for C$_{54}$H$_{60}$O8P$_2$: C 72.14%, H 6.73%; Found: C 72.32%, H 6.71%.

(±)-4-CF$_3$-Segphos(O)
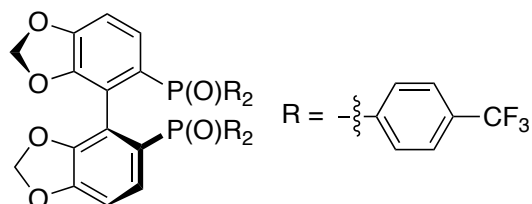
Following the procedure from representative example **D** described above, 4-trifluormethyl bromobenzene (2.25 g, 10.0 mmol) was allowed to react with magnesium turnings (288 mg, 12 mmol) at 0 °C for 3 hours. To this solution was added (±)-[4,4'-bibenzo-1,3-
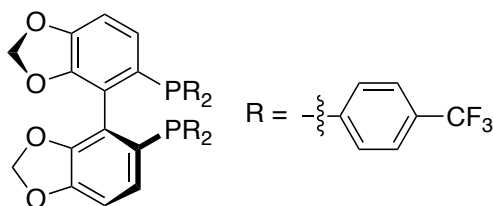
dioxole]-5,5' diyldiphosphonic dichloride (230 mg, 0.50 mmol). The crude material was purified with 40% EtOAc in hexanes as eluent to yield the title compound as a tan solid (405 mg, 89% yield).

¹H NMR (600 MHz, CDCl₃): δ 7.83-7.76 (m, 4H), 7.72 (dd, *J* = 9.6 Hz, 8H), 7.61 (d, *J* = 7.1 Hz, 4H), 6.77-6.74 (m, 2H), 6.71 (dd, *J* = 14.2, 8.1 Hz, 2H), 5.78 (s, 2H), 5.32 (s, 2H).

³¹P NMR (243 MHz, CDCl₃): δ 27.4.

¹⁹F NMR (565 MHz, CDCl₃): δ -64.1, -64.3.

(±)-4-CF₃-Segphos

Following the procedure from representative example **E** described above, (±)-4-CF₃-Segphos(O) (270 mg, 0.29 mmol) was allowed to reaction with trichlorosilane (0.31 ml, 3.0 mmol) and Et₃N (0.42 ml, 3.0 mmol) in mesitylene (2.0 ml) for 36 h. The crude reaction mixture was purified by flash chromatography with 5% EtOAc in hexanes as eluent. The title compound was isolated as a white solid (185 mg, 73% yield).

¹H NMR (600 MHz, CDCl₃): δ 7.59 (d, *J* = 7.9 Hz, 4H), 7.52 (d, *J* = 7.9 Hz, 4H), 7.40 (s, 4H), 7.26 (d, *J* = 3.1 Hz, 4H), 6.84 (d, *J* = 8.0 Hz, 2H), 6.61 (d, *J* = 7.8 Hz, 2H), 5.85 (s, 2H), 5.38 (s, 2H).

³¹P NMR (243 MHz, CDCl₃): δ -8.1.

**¹⁹F NMR** (565 MHz, CDCl₃): δ -63.8, -63.9.

(±)-3,5-bis-CF₃-Segphos(O)
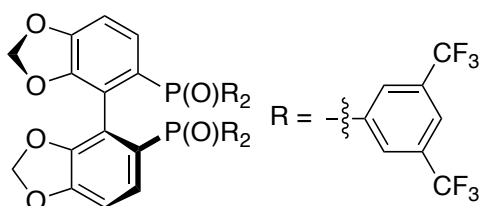
Following the procedure from representative example **D** described above, 3,5-bis(trifluormethyl) bromobenzene (2.2 ml, 12.8 mmol) was allowed to react with isopropylmagnesium chloride (6.0 ml, 2 M solution in THF, 12 mmol) at 0 °C for 1 hour. To this solution was added (±)-[4,4'-bibenzo-1,3-dioxole]-5,5' diyldiphosphonic dichloride (700. mg, 1.50 mmol). The crude material was purified by flash chromatography with 15% EtOAc in hexanes as eluent to yield the title compound as a tan solid (1.04 g, 67% yield).

¹H NMR (500 MHz, CDCl₃): δ 8.30 (d, *J* = 11.5 Hz, 4H), 8.21 (d, *J* = 11.7 Hz, 4H), 8.05 (s, 2H), 8.01 (s, 2H), 6.88 (dd, *J* = 14.8, 8.1 Hz, 2H), 6.78 (dd, *J* = 8.1, 2.1 Hz, 2H), 5.85 (s, 2H), 5.56 (s, 2H).

³¹P NMR (162 MHz, THF₂): δ 22.0.

¹⁹F NMR (376 MHz, THF): δ -63.9, -64.0.

(±)-3,5-bis-CF$_3$-Segphos
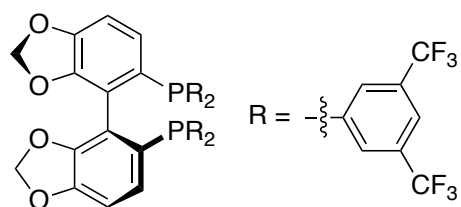
Following the procedure from representative example **E** described above, (±)-3,5-bisCF$_3$-Segphos(O) (1.0 g, 0.84 mmol) was allowed to reaction with trichlorosilane (2.1 ml, 20. mmol) and Et$_3$N (2.8 ml, 20. mmol) in mesitylene (2.0 ml) in a round-bottom (25 ml) flask with a reflux condenser for 48 h at 150 °C. The crude reaction mixture was purified by flash chromatography with 3% EtOAc in hexanes as eluent. The title compound was isolated as a white solid (408 mg, 42% yield).
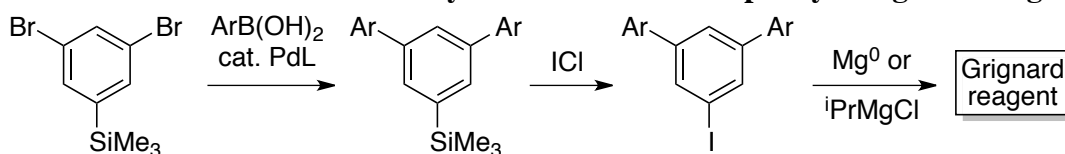
^{1}H NMR (600 MHz, CDCl$_3$): δ 7.88 (s, 2H), 7.79 (s, 2H), 7.67 (s, 4H), 7.57 (s, 4H), 6.91 (d, J = 8.0 Hz, 2H), 6.58 (d, J = 7.9 Hz, 2H), 5.97 (s, 2H), 5.67 (s, 2H).

^{31}P NMR (243 MHz, CDCl$_3$): δ -11.9.

^{19}F NMR (565 MHz, CDCl$_3$): δ -64.0, -64.2.

HR-MS (ESI): exact mass calcd for C$_{46}$H$_{21}$F$_{24}$O$_4$P$_2$: m/z 1155.0553 ([M+H]$^+$); Found, 1155.0526 ([M+H]$^+$).

Anal. Calcd for C$_{46}$H$_{20}$F$_{24}$O$_4$P$_2$: C 47.85%, H 1.75%; Found: C 47.90%, H 1.50%.

Scheme 6.3. General route for the synthesis of bi- and terphenyl Grignard reagents.

3,5-Dibromo-trimethylsilyl benzene
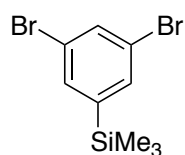
In an argon-filled dry-box, an oven dried round-bottom flask (1 L) was charged with 1,3,5-tribromobenzene (17.5 g, 55.5 mmol), diethyl ether (250 ml), and a magnetic stirbar. The flask was sealed with a septum and placed in a -78 °C bath. ^{n}BuLi (1.6 M, 36.6 ml, 58.5 mmol) was added to the white suspensions via syringe over 10 minutes, and the mixture was stirred for an additional 30 minutes. The reaction mixture was cooled to -78 °C, and TMSCl (7.7 ml, 61 mmol) was added via syringe. The reaction was removed from the cold bath and stirred for an additional 1 hour at room temperature, which caused a white precipitate to form. The reaction was quenched with a saturated solution of NaHCO$_3$, extracted with diethyl ether, washed with brine, and dried over MgSO$_4$. Volatile compounds were removed by rotary evaporation, and the title compound was distilled under reduced pressure (75 mTorr) at 100 °C. The title compound was isolated as a clear liquid that became a waxy solid after 1 hour (14.8 g, 85% yield). Spectral data match those of previous reports.[55]

^{1}H NMR (600 MHz, CDCl$_3$): δ 7.64 (s, 1H), 7.52 (s, 2H), 0.27 (s, 9H).

^{13}C NMR (151 MHz, CDCl$_3$): δ 146.0, 134.4, 134.1, 123.2, -1.4.
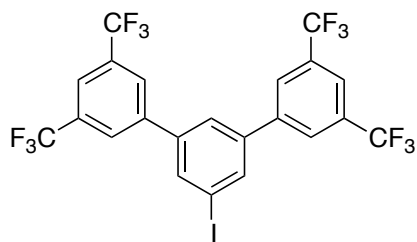
MS: m/z 308 (15%, [M]$^+$), 293 (100%).

3,5-Bis-(3,5-bis-CF$_3$-phenyl)trimethylsilyl benzene
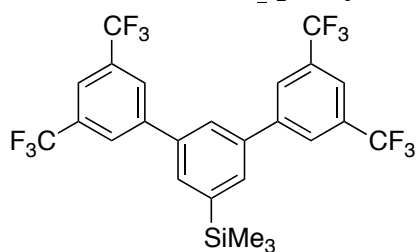
Under atmospheric conditions, a round-bottom flask (250 ml) was charged with 3,5-dibromo-trimethylsilyl benzene (2.7 g, 8.8 mmol), 3,5-bisCF$_3$-phenylboronic acid (6.2 g, 24 mmol), Pd(PPh$_3$)$_4$ (202 mg, 0.176 mmol), and toluene (24 ml). A reflux condenser was attached to the flask, and the reaction mixture was placed under a nitrogen atmosphere by evacuating the flask and refilling with nitrogen gas (x3). A degassed aqueous solution of Na$_2$CO$_3$ (1 M, 20. ml, 20. mmol) was added to the flask, and the mixture was brought to reflux. After 12 h, the organic products were extracted with EtOAc. The organic solution was washed with brine and dried over MgSO$_4$. The solvent was removed by rotary evaporation, and the crude material was purified by flash chromatography with hexanes as eluent. The title compound was isolated as a white solid (4.65 g, 92% yield).

^{1}H NMR (600 MHz, CDCl$_3$): δ 8.03 (s, 4H), 7.92 (s, 2H), 7.74 (d, J = 1.6 Hz, 2H), 7.70 (s, 1H), 0.40 (s, 9H).

^{19}F NMR (376 MHz, CDCl$_3$): δ -62.7.

3,5-Bis-(3,5-bis-CF$_3$-phenyl)-iodobenzene

Under atmospheric conditions, a round-bottom flask (100 ml) was charged with 3,5-bis(3,5-CF$_3$-phenyl)trimethylsilyl benzene (4.7 g, 8.1 mmol), CH$_2$Cl$_2$ (48 ml), and a magnetic stirbar. The solution was placed in an ice bath. A separate round-bottom flask (50 ml) was charged with ICl (2.76 g, 17.1 mmol) and CH$_2$Cl$_2$ (25 ml). The solution of ICl was added dropwise to the solution of the trimethylsilyl arene over 10 minutes. After addition, the flask was allowed to warm to room temperature and stir for an additional 10 h. The solution was quenched with a saturated solution of Na$_2$S$_2$O$_5$, and the organic material was extracted with diethyl ether. The organic solution was dried over MgSO$_4$ and concentrated by rotary evaporation. The crude material was passed through a plug of silica gel with hexanes as solvent to yield the title compound as a white solid (4.81 g, 94% yield).

^{1}H NMR (600 MHz, C$_6$D$_6$): δ 7.74 (s, 2H), 7.45 (s, 4H), 7.43 (d, J = 1.2 Hz, 2H), 6.80 (s, 1H).

^{19}F NMR (376 MHz, CDCl$_3$): δ -62.0.

(±)-3,5-Bis-(3,5-bis-CF₃-phenyl)-Segphos
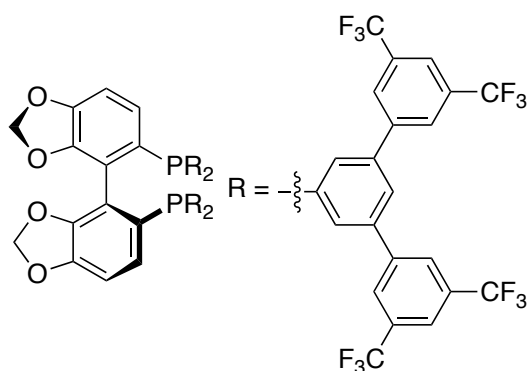
Following the procedure from representative example **D** described above, 3,5-Bis-(3,5-bis-CF₃-phenyl)-iodobenzene (3.15 g, 5.02 mmol) was allowed to react with isopropylmagnesium chloride (2.5 ml, 2 M solution in THF, 5.0 mmol) at 0 °C for 1 hour. To this solution was added (±)-[4,4'-bibenzo-1,3-dioxole]-5,5' diyldiphosphonic dichloride (310 mg, 0.65 mmol). The crude material was washed over silica gel with 5% EtOAc in hexanes to remove arene byproducts, followed by 50% EtOAc in hexanes to collect the phosphine oxide as a crude material. This material was subjected to reducing conditions without further purification by following the procedure from representative example **E** described above. The material was allowed to react with trichlorosilane (0.58 ml, 5.8 mmol) and Bu₃N (1.4 ml, 5.8 mmol) in mesitylene (1.0 ml) for 48 h at 140 °C. The crude reaction mixture was purified by flash chromatography with 2% EtOAc in hexanes as eluent. The title compound was isolated as a white solid (650 mg, 43% yield).

¹H NMR (600 MHz, CDCl₃): δ 7.96 (s, 8H), 7.91 (s, 4H), 7.81 (s, 4H), 7.80 (s, 8H), 7.78 (dd, J = 1.7 Hz, 2H), 7.69-7.65 (m, 4H), 7.63 (dd, J = 1.7 Hz, 2H), 7.55-7.53 (m, 4H), 6.90 (d, J = 8.0 Hz, 2H), 6.82-6.79 (m, 2H), 5.95 (d, J = 1.1 Hz, 2H), 5.72 (d, J = 1.1 Hz, 2H).

³¹P NMR (243 MHz, CDCl₃): δ -11.6.

¹⁹F NMR (565 MHz, CDCl₃): δ -64.0, -64.1.

HR-MS (ESI): exact mass calcd for C₁₀₂H₄₅F₄₈O₄P₂: *m/z* 2307.2113 ([M+H]⁺); Found, 2307.2021 ([M+H]⁺).

Anal. Calcd for C₁₀₁H₄₄F₄₈O₄P₂: C 53.10%, H 1.92%; Found: C 53.51%, H 1.75%.

3,5-Bis-(4-ᵗBu-phenyl)trimethylsilyl benzene
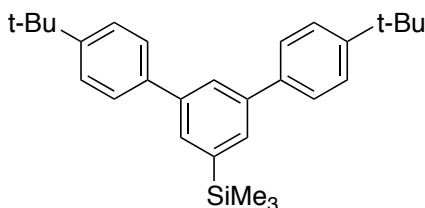
The title compound was prepared in analogy to 3,5-bis-(3,5-bis-CF₃-phenyl)-trimethylsilyl benzene described above. The reaction was conducted with 3,5-dibromo-trimethylsilyl benzene (2.5 g, 8.0 mmol), 4-*tert*-butyl-phenyl boronic acid (4.3 g, 24 mmol), Pd(PPh₃)₄ (202 mg, 0.176 mmol), aqueous Na₂CO₃ (20. ml, 1.0 M, 20. mmol) and toluene (24 ml). The crude material was purified by flash chromatography with hexanes as eluent to yield the title compound as a white solid (1.4 g, 42% yield).

¹H NMR (600 MHz, CDCl₃): δ 7.77 (s, 1H), 7.69 (d, J = 1.5 Hz, 2H), 7.59 (d, J = 8.3 Hz, 4H), 7.50 (d, J = 8.3 Hz, 4H), 1.39 (s, 18H), 0.35 (s, 9H).

3,5-bis-(4-^{t}Bu-phenyl)-iodobenzene
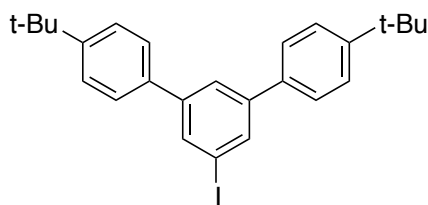
The title compound was prepared in analogy to 3,5-bis-(3,5-bis-CF$_3$-phenyl)-iodobenzene described above. The reaction was conducted with 3,5-bis-(4-^{t}Bu-phenyl)trimethylsilyl-benzene (1.4 g, 3.4 mmol) and ICl (1.2 g, 7.1 mmol). The title compound was isolated as a white solid after purification by flash chromatography with hexanes as eluent (1.33 g, 84% yield).

^{1}H NMR (600 MHz, CDCl$_3$): δ 7.92 (d, J = 1.6 Hz, 2H), 7.77 (t, J = 1.6 Hz, 1H), 7.57 (d, J = 8.4 Hz, 4H), 7.52 (d, J = 8.5 Hz, 4H), 1.41 (s, 18H).

MS: m/z 468 (5%, [M]$^+$), 336 (50%, [M-tBu-phenyl]$^+$), 321 (100%, [M-C$_{11}$H$_{16}$]$^+$).

(±)-3,5-Bis-(4-^{t}Bu-phenyl)-Segphos

Following the procedure from representative example **D** described above, 3,5-bis-(4-^{t}Bu-phenyl)-iodobenzene (1.5 g, 3.2 mmol) was allowed to react with isopropylmagnesium chloride (1.6 ml, 2 M solution in THF, 3.2 mmol) at room temperature for 1 hour. To this solution was added (±)-[4,4'-bibenzo-1,3-dioxole]-5,5' diyldiphosphonic dichloride (55 mg, 0.20 mmol). The crude material was washed over silica gel with 5% EtOAc in hexanes to remove arene byproducts, followed by 50% EtOAc in hexanes to collect the phosphine oxide as a crude material. This material was subjected to reducing conditions without further purification by following the procedure from representative example **E** described above. The material was allowed to react with trichlorosilane (0.23 ml, 2.3 mmol) and Bu$_3$N (0.53 ml, 2.3 mmol) in mesitylene (0.3 ml) at 120 °C for 18 h. The crude reaction mixture was purified by flash chromatography with 2% EtOAc in hexanes as eluent. The title compound was isolated as a white solid (147 mg, 44% yield).

^{1}H NMR (600 MHz, CDCl$_3$): δ 7.78 (t, J = 1.6 Hz, 2H), 7.72 (t, J = 1.6 Hz, 2H), 7.69-7.65 (m, 4H), 7.64-7.61 (m, 4H), 7.54 (d, J = 8.5 Hz, 8H), 7.47-7.43 (m, 18H), 7.33 (d, J = 8.5 Hz, 8H), 5.78 (d, J = 1.3 Hz, 2H), 5.21 (d, J = 1.3 Hz, 2H), 1.37 (s, 36H), 1.29 (s, 36H).

^{31}P NMR (243 MHz, CDCl$_3$): δ -11.9.

Anal. Calcd for C$_{118}$H$_{124}$O$_4$P$_2$: C 84.96%, H 7.49%; Found: C 84.58%, H 7.65%.
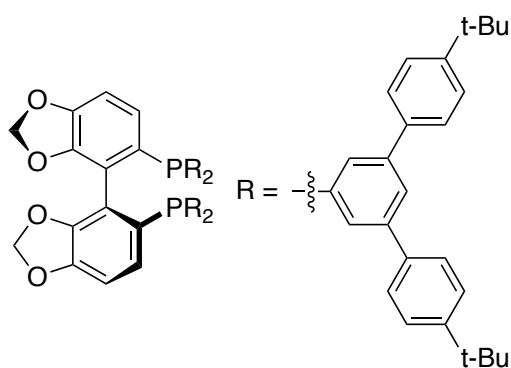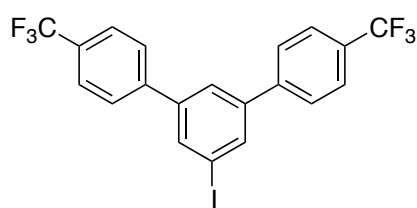

3,5-Bis-(4-CF$_3$-phenyl)-iodobenzene

The title compound was prepared in analogy to 3,5-bis-(3,5-bis-CF$_3$-phenyl)-iodobenzene described above. The reaction was conducted with 3,5-bis-(4-CF$_3$-phenyl)trimethylsilyl-benzene (3.55 g, 8.10 mmol) and ICl (2.69 g, 16.6 mmol). The title compound was isolated as a white solid after purification

248

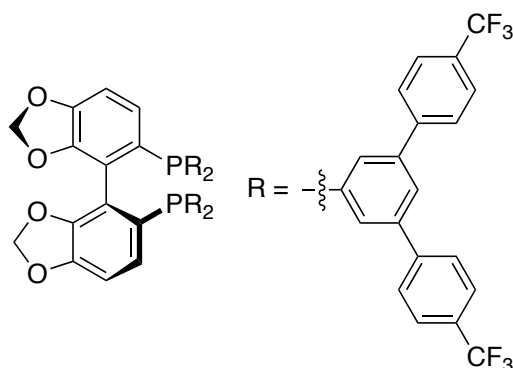by flash chromatography with 0.5% EtOAc in hexanes as eluent (2.0 g, 50% yield).

^{1}H NMR (600 MHz, CDCl$_3$): δ 7.96 (d, J = 1.3 Hz, 2H), 7.73 (d, J = 8.1 Hz, 5H), 7.70 (d, J = 8.3 Hz, 4H).

^{13}C NMR (151 MHz, CDCl$_3$): δ 142.7, 142.5, 135.8, 130.2 (q, J = 32.5 Hz), 127.5, 125.9 (q, J = 3.7 Hz), 125.7, 124.1 (q, J = 272.1 Hz), 95.4.

^{19}F NMR (565 MHz, CDCl$_3$): δ -63.4.

MS: m/z 492 (100%, [M]$^+$), 296 (60%).

(±)-3,5-Bis-(4-CF$_3$-phenyl)-Segphos

Following the procedure from representative example **D** described above 3,5-bis-(4-CF$_3$-phenyl)-iodobenzene (740 mg, 1.5 mmol) was allowed to react with isopropylmagnesium chloride (0.70 ml, 2 M solution in THF, 1.4 mmol) at room temperature for 1 hour. To this solution was added (±)-[4,4'-bibenzo-1,3-dioxole]-5,5' diyldiphosphonic dichloride (95 mg, 0.20 mmol). The crude material was washed over silica gel with 5% EtOAc in hexanes to remove arene byproducts, followed by 50% EtOAc in hexanes to collect the phosphine oxide as a crude material. This material was subjected to reducing conditions without further purification by following the procedure from representative example **E** described above. The material was allowed to react with trichlorosilane (0.50 ml, 5.0 mmol) and Bu$_3$N (1.2 ml, 5.0 mmol) in mesitylene (0.5 ml) at 140 °C for 18 h. The crude reaction mixture was purified by flash chromatography with 5% EtOAc in hexanes as eluent. The title compound was isolated as a white solid (170 mg, 48% yield).

^{1}H NMR (600 MHz, CDCl$_3$): δ 7.76 (t, J = 1.7 Hz, 2H), 7.69 (d, J = 8.3 Hz, 8H), 7.63 (d, J = 8.2 Hz, 8H), 7.60-7.57 (m, 6H), 7.51 (t, J = 5.2 Hz, 8H), 7.50-7.48 (m, 4H), 7.44 (d, J = 8.2 Hz, 8H), 6.88 (s, 4H), 5.93 (d, J = 1.3 Hz, 2H), 5.61 (d, J = 1.3 Hz, 2H).

^{31}P NMR (243 MHz, CDCl$_3$): δ -12.6.

^{19}F NMR (565 MHz, CDCl$_3$): δ -63.5, -63.6.

Anal. Calcd for C$_{94}$H$_{52}$F$_{24}$O$_4$P$_2$: C 64.03%, H 2.97%; Found: C 64.16%, H 2.72%.

4-(4-Trifluoromethylphenyl)-bromobenzene
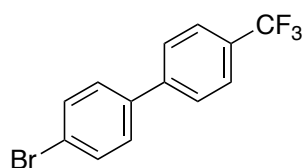
The title compound was prepared in analogy to 3,5-bis-(3,5-bis-CF$_3$-phenyl)-trimethylsilyl benzene described above. The reaction was conducted with 1,4-dibromobenzene (9.4 g, 40. mmol), 4-CF$_3$-phenyl boronic acid (1.9 g, 10. mmol), Pd(PPh$_3$)$_4$ (251 mg, 0.22 mmol), aqueous Na$_2$CO$_3$ (20. ml, 1.0 M, 20. mmol) and toluene (24 ml). The crude material was purified by flash chromatography with hexanes as eluent to yield the title compound as a white solid (2.76 g, 92% yield).

¹H NMR (600 MHz, CDCl₃): δ 7.71-7.69 (m, 2H), 7.66 (d, J = 8.2 Hz, 2H), 7.60 (d, J = 8.5 Hz, 2H), 7.46 (d, J = 8.5 Hz, 2H).

¹⁹F NMR (565 MHz, CDCl₃): δ -63.4.

MS: *m/z* 300/302 (100%, [M]⁺), 201 (50%).

(±)-4-(4-Trifluoromethylphenyl)-Segphos
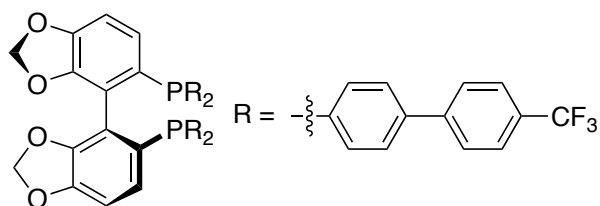
Following the procedure from representative example **D** described above 4-(4-trifluoromethylphenyl)-bromobenzene (0.80 g, 3.0 mmol) was allowed to react with magnesium turnings (70. mg, 3.3 mmol) at 0 °C for 2 hour. To this solution was added (±)-[4,4'-bibenzo-1,3-dioxole]-5,5' diyldiphosphonic dichloride (240 mg, 0.50 mmol). The crude material was washed over silica gel with 5% EtOAc in hexanes to remove arene byproducts, followed by 67% EtOAc in hexanes to collect the phosphine oxide as a crude material. This material was subjected to reducing conditions without further purification by following the procedure from representative example **E** described above. The material was allowed to react with trichlorosilane (0.31 ml, 3.0 mmol) and Bu₃N (0.72 ml, 3.0 mmol) in mesitylene (0.3 ml) at 135 °C for 27 h. The crude reaction mixture was purified by flash chromatography with 10% EtOAc in hexanes as eluent. The title compound was isolated as a white solid (155 mg, 26% yield).
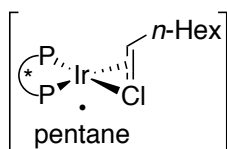
¹H NMR (600 MHz, CDCl₃): δ 7.71 (br s, 8H), 7.61 (d, J = 8.3 Hz, 4H), 7.58 (d, J = 7.9 Hz, 4H), 7.53 (d, J = 8.3 Hz, 4H), 7.44 (dd, J = 8.1, 3.7 Hz, 8H), 7.30-7.26 (m, 4H), 6.86 (d, J = 8.0 Hz, 2H), 6.80-6.75 (m, 2H), 5.87 (d, J = 1.4 Hz, 2H), 5.46 (d, J = 1.4 Hz, 2H).

³¹P NMR (243 MHz, CDCl₃): δ -14.6.

¹⁹F NMR (565 MHz, CDCl₃): δ -63.4, -63.5.

Anal. Calcd for C₆₆H₄₀F₁₂O₄P₂: C 66.79%, H 3.40%; Found: C 66.89%, H 3.60%.

[(S)-DTBM-Segphos]IrCl(1-octene)•pentane, (21)

In an argon-filled dry-box, a screw-capped vial (20 ml) was charged with (S)-DTBM-Segphos (295 mg, 0.250 mmol), [Ir(COE)₂Cl]₂ (111 mg, 0.125 mmol), 1-octane (6.0 ml), and pentane (7.5 ml). The vial was sealed with a Teflon-lined cap and shaken by hand to dissolve all of the solids. The resulting dark red solution was allowed to sit undisturbed at room temperature for 24 h. During this time, the title complex precipitated as a red crystalline material. The solid was filtered through a glass frit and washed with cold (-15 °C) pentane. Residual solvents were removed under vacuum to yield the title compound as a red powder (352 mg, 88% yield). Spectral data matched those of previous reports.[43]

**¹H NMR** (500 MHz, C₆D₆): δ 9.74-7.28 (m, 8H), 7.07-6.94 (m, 1H), 6.92-6.79 (m, 1H), 6.24 (d, J = 7.6 Hz, 1H), 6.13 (d, J = 7.7 Hz, 1H), 5.42 (s, 1H), 5.39 (dd, J = 9.1, 5.0 Hz, 1H), 5.12 (s, 1H), 5.00 (s, 1H), 4.94 (s, 1H), 4.47 (br s, 1H), 3.83 (br d, J = 8.0 Hz, 1H), 3.49 (s, 6H), 3.32 (s, 3H), 3.26 (s, 3H), 2.90 (br s, 1H), 2.62 (br s, 1H), 2.07 (br s, 1H),

1.94 (dd, J = 12.8, 6.1 Hz, 1H), 1.64-1.35 (m, 72H), 1.31-1.19 (m, 15H), 0.90-0.77 (m, 6H).

^{31}P NMR (202 MHz, C_6D_6): δ 24.2 (d, J = 29.8 Hz), 13.4 (d, J = 28.7 Hz).

Anal. Calcd for $C_{87}H_{128}ClIrO_8P_2$: C 65.65%, H 8.11%; Found: C 65.46 %, H 8.32%.

Kinetic studies on the Ir-catalyzed olefination of 2-pentylfuran: variable [2-pentylfuran]
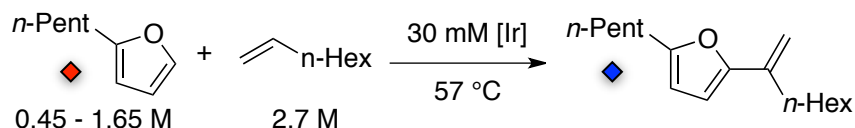
0.45 - 1.65 M   2.7 M

In a nitrogen-filled glove box, a screw-capped vial (4.0 ml) was charged with [Ir(coe)$_2$Cl]$_2$ (6.7 mg, 0.0075 mmol) and (S)-DTBM-Segphos (17.7 mg, 0.0150 mmol). The solids were dissolved in 1-octene (0.20 ml). To this dark red solution was added the appropriate volume of 2-pentylfuran, mesitylene (20. μl, 0.14 mmol) as an internal standard, and C_6D_6 (0.10 ml). The appropriate amount of octane (50 – 170 μl) was added as a volume-makeup solvent (0.55 total reaction volume). The solution was transferred to an NMR tube, capped, removed from the dry-box, and placed in an ice bath. Initial reaction rates were determined at 57 °C by monitoring the attenuation of the C5 proton resonance of 2-pentylfuran as a function of time.

Figure 6.9. (a) Data plots of consumption of 2-pentylfuran as a function of time. (b) Comparison of the initial rate of furan olefination as a function of the concentration of 2-pentylfuran.

Kinetic studies on the Ir-catalyzed olefination of 2-pentylfuran: variable [1-octene]
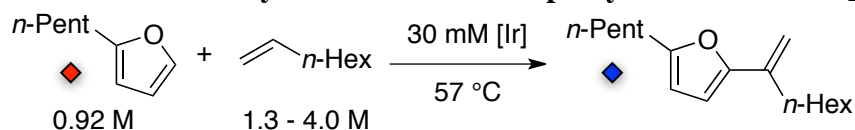
In a nitrogen-filled glove box, a screw-capped vial (4.0 ml) was charged with [Ir(coe)$_2$Cl]$_2$ (6.7 mg, 0.0075 mmol) and (S)-DTBM-Segphos (17.7 mg, 0.0150 mmol). The solids were dissolved in the appropriate amount of 1-octene (0.10 – 0.30 ml). To this dark red solution was added 2-pentylfuran (75 μl, 0.50 mmol), mesitylene (20. μl, 0.14 mmol) as an internal standard, and C$_6$D$_6$ (0.10 ml). The appropriate amount of octane (25 – 225 μl) was added to create a total volume of 0.55 ml. The solution was transferred to a NMR tube, capped, removed from the dry-box, and placed in an ice bath. Initial reaction rates were determined at 57 °C by monitoring the attenuation of the C5 proton resonance of 2-pentylfuran as a function of time.

Figure 6.10. (a) Data plots of consumption of 2-pentylfuran as a function of time. (b) Comparison of the initial rate of furan olefination as a function of olefin concentration.

Kinetic studies on the Ir-catalyzed olefination of 2-pentylfuran: variable [Ir]
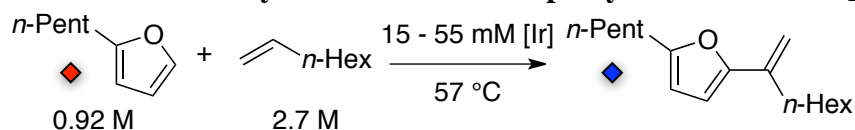
n-Pent $\diamond$ O + $\diagup$ n-Hex $\xrightarrow[57\ °C]{15 - 55\ \text{mM [Ir]}}$ n-Pent $\diamond$ O $\diagup$ n-Hex

0.92 M   2.7 M

In a nitrogen-filled glove box, a screw-capped vial (4.0 ml) was charged with the appropriate amount of [Ir(coe)$_2$Cl]$_2$ and corresponding amount of (S)-DTBM-Segphos. The solids were dissolved in 1-octene (0.200 ml, 1.48 mmol). To this dark red solution was added 2-pentylfuran (75 μl, 0.50 mmol), and mesitylene (20. μl, 0.14 mmol) as an internal standard, C$_6$D$_6$ (0.10 ml). Octane (125 μl) was added to create a final volume of 0.55 ml. The solution was transferred to a NMR tube, capped, removed from the dry-box, and placed in an ice bath. Initial reaction rates were determined at 57 °C by monitoring the attenuation of the C5 proton resonance of 2-pentylfuran as a function of time.

a.

[Ir] = 15 mM
y = -3.67E-05x + 8.72E-01
R² = 9.73E-01

[Ir] = 30 mM
y = -6.82E-05x + 8.42E-01
R² = 9.96E-01

[Ir] = 50 mM
y = -1.13E-04x + 7.71E-01
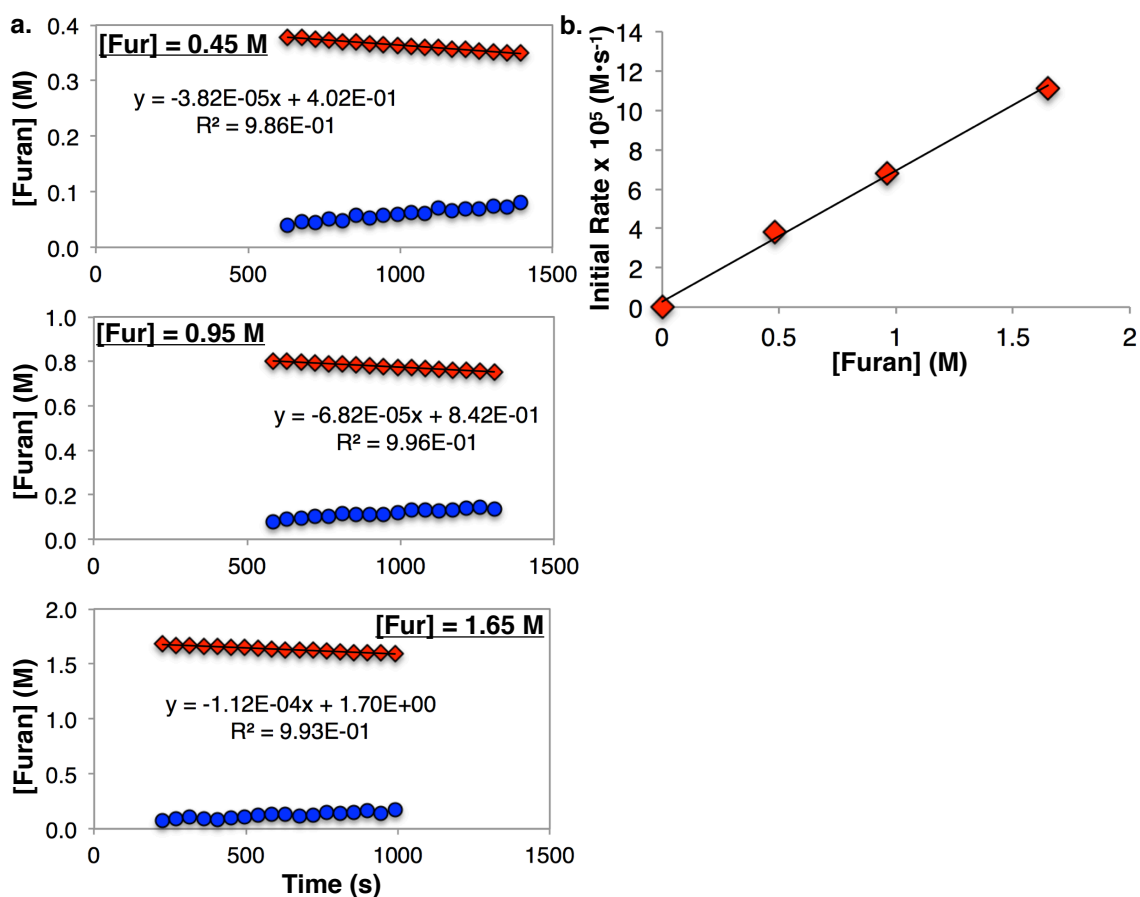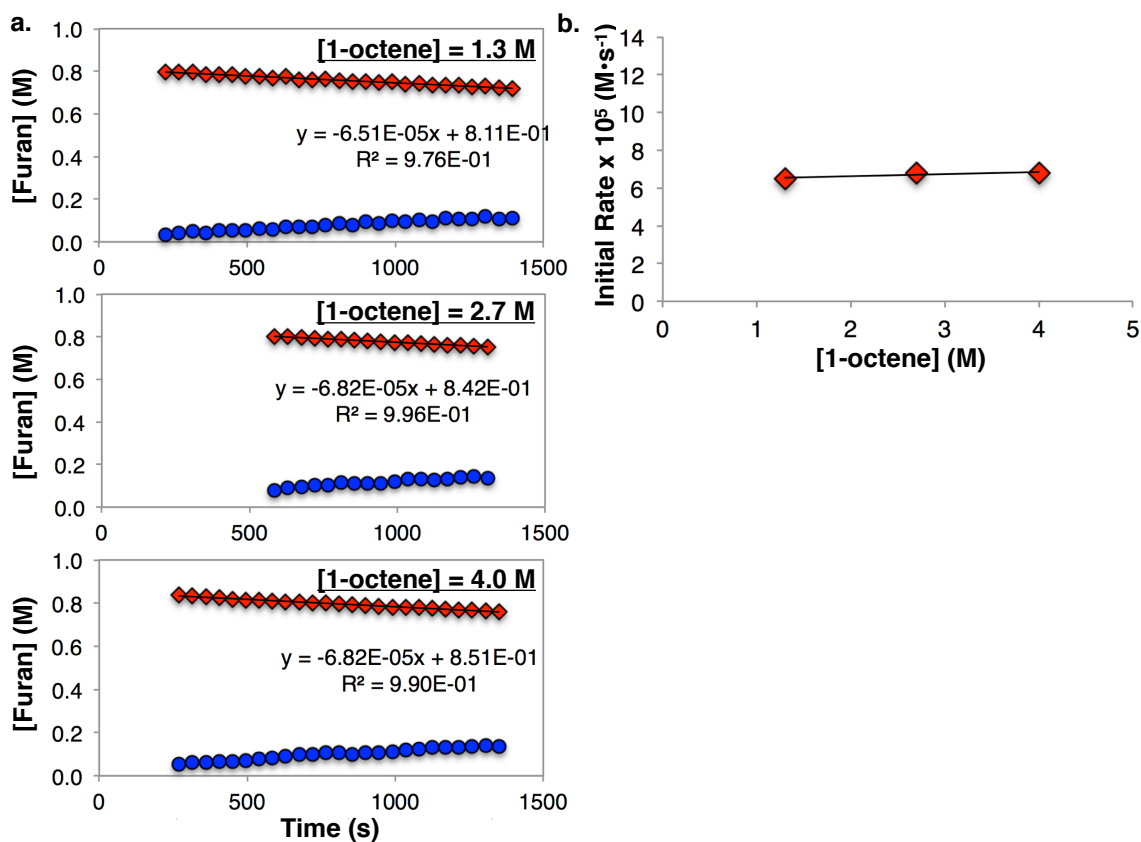R² = 9.94E-01

b.
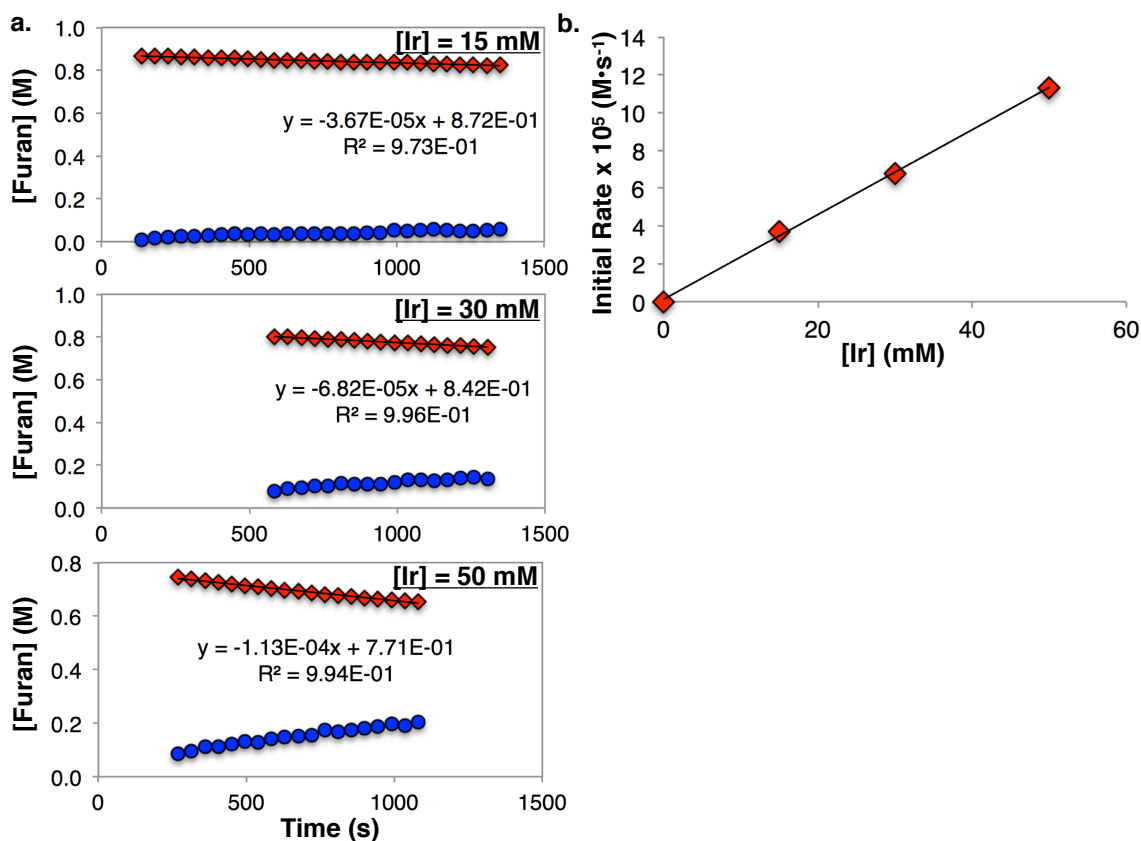
Figure 6.11. (a) Data plots of consumption of 2-pentylfuran as a function of time. (b) Comparison of the initial rate of furan olefination as a function of iridium concentration.

253

Kinetic studies on the Ir-catalyzed olefination of 2-pentylfuran: kinetic isotope effect

n-Pent $\diagdown$ O (D) $+$ $\diagup$ n-Hex $\xrightarrow[57\,°C]{20\ mM\ [Ir]}$ $k_H = 5.4 \pm 0.2\ M{\cdot}s^{-1}$
$k_D = 3.8 \pm 0.1\ M{\cdot}s^{-1}$
KIE = 1.4 ± 0.1

0.84 M   2.7 M
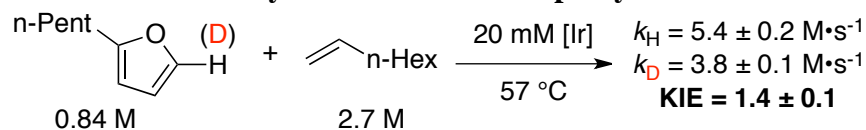
The rate of olefination of 2-pentyl-5-deuterofuran was compared to the rate of olefination of 2-pentylfuran in separate reaction vessels. The measurements were conducted by procedures analogous to those described above for the determination of the kinetic orders in reactants and catalyst.

y = -3.78E-05x + 8.33E-01
R² = 9.89E-01

y = -5.41E-05x + 8.52E-01
R² = 9.88E-01
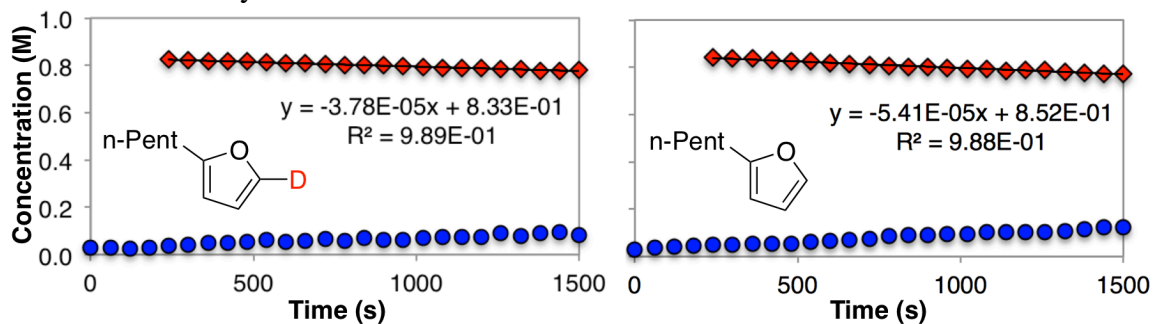
Figure 6.12. Plots of the rate of olefination of 5-deutero- and 5-proteo-2-pentylfuran.

Eyring analysis: activation parameters for the formation of Ir(allyl)H (22)

$\Delta H^{\ddagger} = 22.5 \pm 0.8$ kcal/mol

$\Delta S^{\ddagger} = -8 \pm 2$ eu
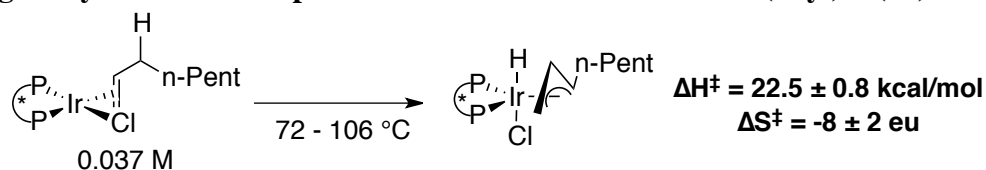
In a nitrogen-filled glove box, a screw-capped vial (4.0 ml) was charged with complex **21** (196 mg, 0.124 mmol) and triphenylphosphine oxide (28 mg, 0.10 mmol) as an internal standard. The solid was dissolved to form a dark red solution after addition of 1-octene (3.45 ml) and mesitylene (1.45 ml). A portion of the solution (0.50 ml) was transferred to an NMR tube, capped, removed from the dry-box, and placed in an ice bath. Formation of the Ir(allyl)(H) species was monitored by ^{31}P NMR spectroscopy at temperatures ranging from 72-106 °C.
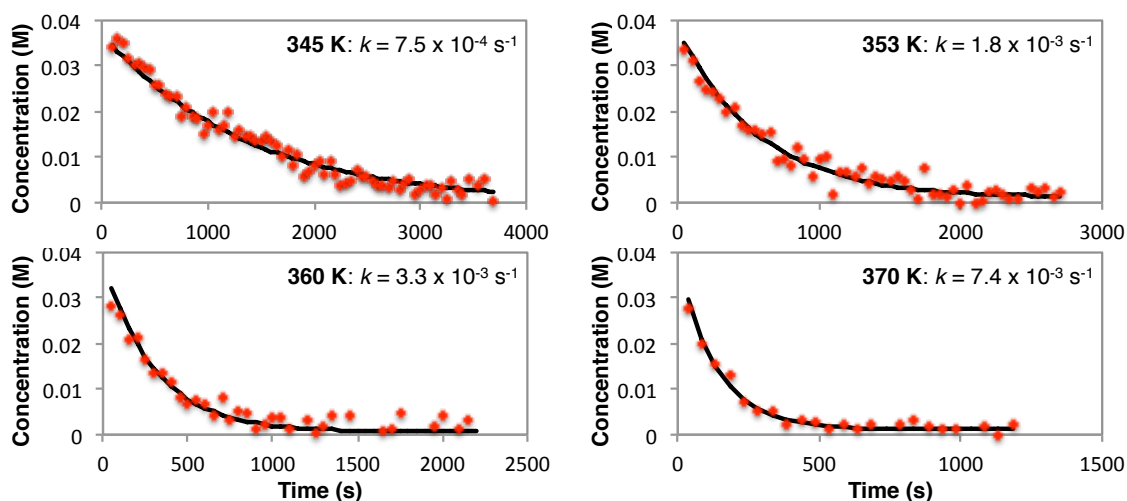
Figure 6.13. Rate data for formation of the Ir(allyl)(H) complex at variable temperatures. Plots were fit to a first order decays.

Eyring analysis: activation parameters for the Ir-catalyzed olefination of 2-pentylfuran

$\Delta H^{\ddagger} = 8.2 \pm 0.4$ kcal/mol
$\Delta S^{\ddagger} = -45 \pm 2$ eu
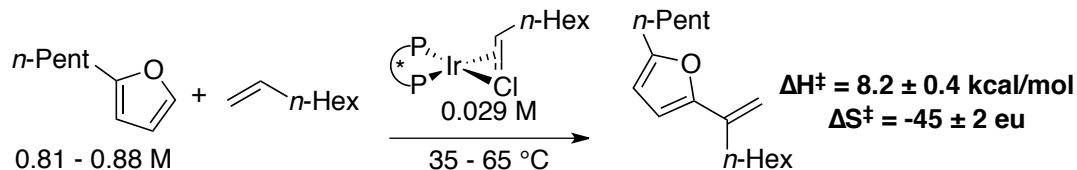
In a nitrogen-filled glove box, screw-capped vial (4.0 ml) was charged complex **21** (120 mg, 0.075 mmol). The solid were dissolved in 1-octene (0.88 ml, 5.6 mmol), mesitylene (100. μl, 0.719 mmol), and octane (0.75 ml). To this dark red solution was added 2-pentylfuran (390 μl, 2.5 mmol) and C_6D_6 (0.58 ml). The solution was distributed equally into NMR tubes (0.50 ml volume). The NMR tubes were capped, removed from the dry-box, and placed in an ice bath. Initial reaction rates were determined at temperatures ranging 35-65 °C by monitoring the attenuation of the C5 proton resonance of 2-pentylfuran as a function of time. Rate constants ($M^{-1} \cdot s^{-1}$) were calculated by dividing the observed rate (M/s) by the concentration of iridium and the concentration of 2-pentylfuran in solution, as summarized in Figure S10.
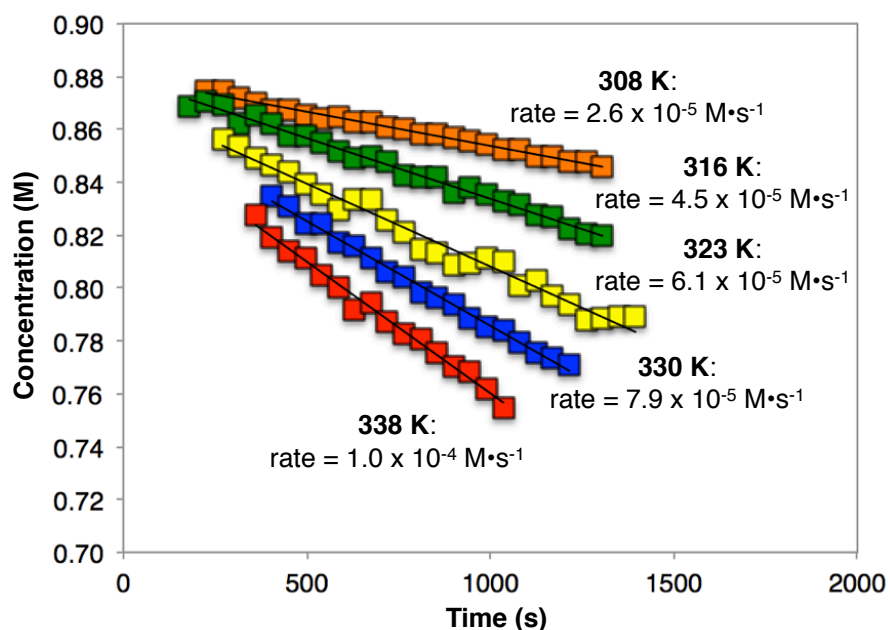
Figure 6.14. Initial rates for the Ir-catalyzed olefination 2-pentylfuran at variable temperatures.

$$\text{rate} = k[\text{Ir}]^1[\text{furan}]^1[\text{alkene}]^0$$

$$k = \frac{\text{rate}}{[\text{Ir}]^1[\text{furan}]^1} \; ; [\text{Ir}] = 0.029 \text{ M}; [\text{furan}] = 0.81\text{-}0.88 \text{ M}$$

Figure 6.15. Calculation of rate constants (1/(M•s)) from observed rates (M/s)
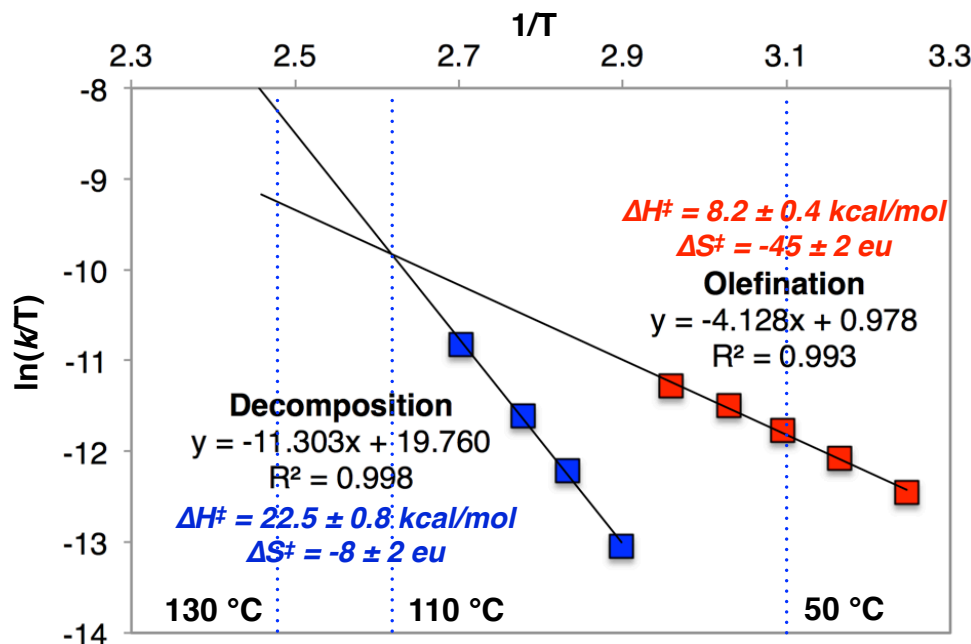
Figure 6.16. Overlaid plots of Eyring analyses of catalyst decomposition by allylic C-H bond activation (blue) and of Ir-catalyzed olefination of 2-pentylfuran (red).

Computational Details

All DFT calculations were performed with the Gaussian 09 software package. Geometry optimization of all the minima and transition states involved was carried out at the M06 level of theory at 298 K. The LANL2DZ basis set and ECP was used for the iridium atom, and the 6-31g(d,p) basis set was used for other atoms. Five d-type orbitals were used as basis sets in all elements of the calculations. Vibrational frequencies were computed at the same level for each structure to determine if it is an energy minimum or a transition state and to evaluate its zero-point vibrational energy (ZPVE). Single-point energies were calculated with the M06 functionals with the lanl2tz(f) basis set and ECP for iridium and the 6-311++g** basis set for all other atoms. Solvation in mesitylene was modeled with the IEFPCM by a self-consistent reaction field (SCRF) using the CPCM model in which a universal force field model (UFF) was used to define the atomic radii. In this paper, all energies discussed are Gibbs free energies in mesitylene ($\Delta G_{\text{mes 298 K}}$ and $\Delta G_{\text{mes 298 K}}$) unless specified; the entropy contributions were estimated by using the gas phase entropy values. The Gibbs free energy ($\Delta G_{\text{gas 298 K}}$) and the enthalpies ($\Delta H_{\text{gas 298 K}}$) in the gas phase are also given for reference.

Computational Results

Computational analysis was conducted on the Segphos-ligated analogues of catalytic intermediates, rather than the DTBM-Segphos ligated complexes. All eight possible diastereomeric transition states that result from olefin or furyl rotation were found for propene insertion into the Ir–C bond of the furyl complex. Gibbs free energies are related to the energy of the experimentally identified Ir(olefin) resting state complex.
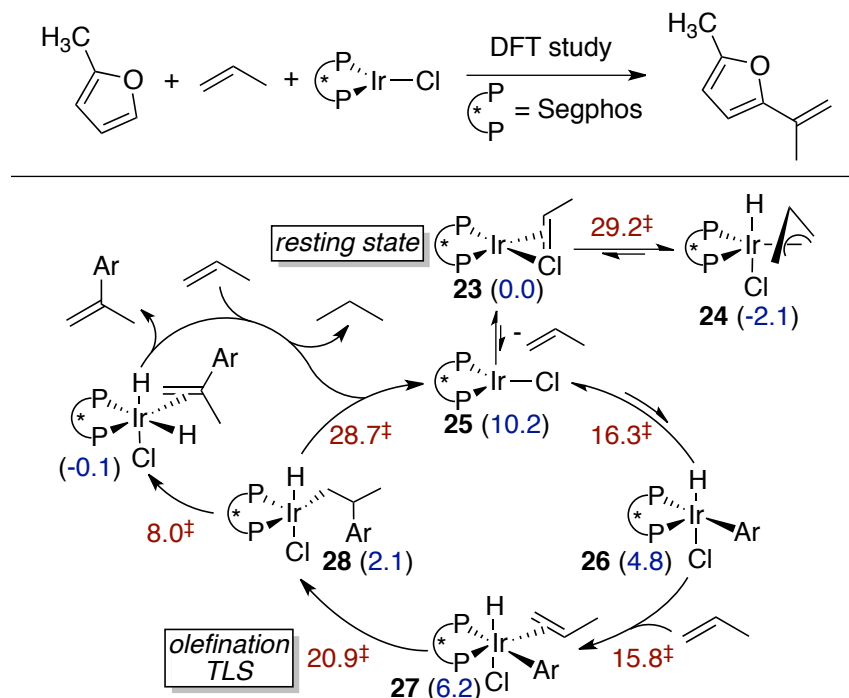
Figure 6.17. Proposed catalytic cycle with computed energies of intermediates (blue) and transition states (red) for the olefination of 2-methylfuran with propene.

Table 6.7. Relative energies of computed possible ground states.[a]

Components	G_{gas}	H_{gas}	G_{corr}	H_{corr}	$Solv_{Mes}$	ΔG_{mes}	ΔH_{mes}
COD	-311.6272	-311.5869	0.1476	0.1879	-311.8506	---	---
Me-Furan	-269.0881	-269.0527	0.0685	0.1039	-269.2264	---	---
Propene	-117.7495	-117.7194	0.0543	0.0843	-117.8353	---	---
Vinyl-CF$_3$	-415.4215	-415.3872	0.0289	0.0632	-415.5744	---	---
Resting States	G_{gas}	H_{gas}	G_{corr}	H_{corr}	$Solv_{Mes}$	ΔG_{mes}	ΔH_{mes}
LIr(propene)Cl	-3710.0760	-3709.8793	0.7846	0.9813	-3711.5554	**0.0**	**0.0**
LIr(vinyl-CF$_3$)Cl	-4125.5060	-4125.2743	0.8137	1.0453	-4127.1382	**-5.2**	**-4.8**
LIr(COD)Cl	-3710.0931	-3709.9036	0.7918	0.9812	-3711.5775	**-9.4**	**-13.9**
LIrCl	-3710.0598	-3709.8405	0.7596	0.9789	-3711.5177	**8.0**	**22.1**

[a]Values for H and G are in Hartree. Values for ΔH and ΔG are in kcal/mol.

Table 6.9. Relative energies decomposition to Ir(allyl)(H) complex.[a]

Decomposition	G_{gas}	H_{gas}	G_{corr}	H_{corr}	$Solv_{Mes}$	ΔG_{mes}	ΔH_{mes}
LIr(allyl)H_GS	-3710.0763	-3709.8838	0.7862	0.9787	-3711.5603	**-2.1**	**-4.7**
LIr(allyl)H_TS‡	-3710.0243	-3709.8300	0.7813	0.9757	-3711.5056	**29.2**	**27.7**

[a]Values for H and G are in Hartree. Values for ΔH and ΔG are in kcal/mol.

Table 6.10. Relative energies for CH activation of 2-methylfuran.[a]

C–H Activation	G_{gas}	H_{gas}	G_{corr}	H_{corr}	$Solv_{Mes}$	ΔG	ΔH
LIr(Me-Fur)_GS	-3710.0690	-3709.8762	0.7877	0.9806	-3711.5508	**4.8**	**2.4**
LIr(H)(Me-Fur)_TS2‡	-3710.0458	-3709.8496	0.7788	0.9750	-3711.5237	**16.3**	**15.9**
LIr(H)(Me-Fur)Olefin_TS‡	-3710.0149	-3709.8423	0.8064	0.9790	-3711.5144	**39.4**	**24.3**
CH_Act_Prod_GS1	-3710.0548	-3709.8606	0.7836	0.9778	-3711.5407	**8.6**	**7.1**
CH_Act_Prod_GS2	-3710.0470	-3709.8527	0.7838	0.9781	-3711.5322	**14.0**	**12.6**

[a]Values for H and G are in Hartree. Values for ΔH and ΔG are in kcal/mol.

Table 6.11. Relative energies for barriers to olefin coordination and insertion.[a]

Olefin Binding	G_{gas}	H_{gas}	G_{corr}	H_{corr}	$Solv_{Mes}$	ΔG_{mes}	(++)ΔH_{mes}
Binding_1_TS‡	-3710.0532	-3709.8808	0.8068	0.9791	-3711.5522	**15.8**	**0.6**
Binding_3_TS‡	-3710.0408	-3709.8690	0.8081	0.9798	-3711.5476	**19.6**	**4.0**
MI_Me_GS1	-3710.0654	-3709.8911	0.8057	0.9800	-3711.5665	**6.2**	**-7.8**
MI_Me_GS2	-3710.0624	-3709.8913	0.8111	0.9821	-3711.5673	**9.1**	**-7.0**
MI_Me_GS3	-3710.0608	-3709.8888	0.8094	0.9814	-3711.5655	**9.2**	**-6.3**
MI_Me_GS4	-3710.0614	-3709.8885	0.8076	0.9805	-3711.5651	**8.3**	**-6.6**
MI_Me_GS5	-3710.0633	-3709.8913	0.8087	0.9807	-3711.5674	**7.6**	**-7.9**
Mig. Insertion	G_{gas}	H_{gas}	G_{corr}	H_{corr}	$Solv_{Mes}$	ΔG_{mes}	ΔH_{mes}
MI_Me_1_TS‡	-3710.0390	-3709.8694	0.8098	0.9794	-3711.5412	**24.7**	**7.7**
MI_Me_2_TS‡	-3710.0431	-3709.8730	0.8093	0.9793	-3711.5431	**23.2**	**6.5**
MI_Me_3_TS‡	-3710.0414	-3709.8726	0.8110	0.9798	-3711.5428	**24.5**	**7.0**
MI_Me_4_TS‡	-3710.0375	-3709.8662	0.8077	0.9790	-3711.5379	**25.4**	**9.5**
MI_Me_5_TS‡	-3710.0451	-3709.8725	0.8062	0.9787	-3711.5424	**21.6**	**6.5**
MI_Me_6_TS‡	-3710.0460	-3709.8744	0.8077	0.9794	-3711.5452	**20.9**	**5.2**
MI_Me_7_TS‡	-3710.0385	-3709.8689	0.8101	0.9798	-3711.5404	**25.4**	**8.4**
MI_Me_8_TS‡	-3710.0403	-3709.8699	0.8094	0.9797	-3711.5415	**24.2**	**7.7**

[a]Values for H and G are in Hartree. Values for ΔH and ΔG are in kcal/mol.

Table 6.12. Relative energies for barriers to CH reductive elimination or β-hydrdide elimination.ᵃ

Alkyl Intermediate	G_{gas}	H_{gas}	G_{corr}	H_{corr}	$Solv_{Mes}$	ΔG_{mes}	ΔH_{mes}
(alkyl)Ir(H)	-3710.0777	-3709.9062	0.8105	0.9819	-3711.5778	**2.1**	**-13.7**
Beta-H-Elim	G_{gas}	H_{gas}	G_{corr}	H_{corr}	$Solv_{Mes}$	ΔG_{mes}	ΔH_{mes}
H-Elim_Me_1_TS‡	-3710.0640	-3709.8918	0.8054	0.9776	-3711.5635	**8.0**	**-7.4**
H-Elim_Me_1_GS1	-3710.0766	-3709.9019	0.8039	0.9786	-3711.5749	**-0.1**	**-13.9**
Red. Elim.	G_{gas}	H_{gas}	G_{corr}	H_{corr}	$Solv_{Mes}$	ΔG_{mes}	ΔH_{mes}
RE_Me_1_TS‡	-3710.0338	-3709.8639	0.8101	0.9800	-3711.5351	**28.7**	**11.9**
RE_Me_1_GS	-3710.0780	-3709.9069	0.8133	0.9844	-3711.5783	**3.6**	**-12.5**

ᵃValues for H and G are in Hartree. Values for ΔH and ΔG are in kcal/mol.

Table 6.13. Barrier to CH reductive elimination to release propane.ᵃ

Hydrogenation	G_{gas}	H_{gas}	G_{corr}	H_{corr}	$Solv_{Mes}$	ΔG_{mes}	ΔH_{mes}
Ir(propyl)H_GS	-3130.5301	-3130.4083	0.5882	0.7100	-3131.6679	**0.0**	**0.0**
Ir(propyl)H_TS	-3130.5191	-3130.3963	0.5856	0.7085	-3131.6569	**5.3**	**5.9**

ᵃValues for H and G are in Hartree. Values for ΔH and ΔG are in kcal/mol.
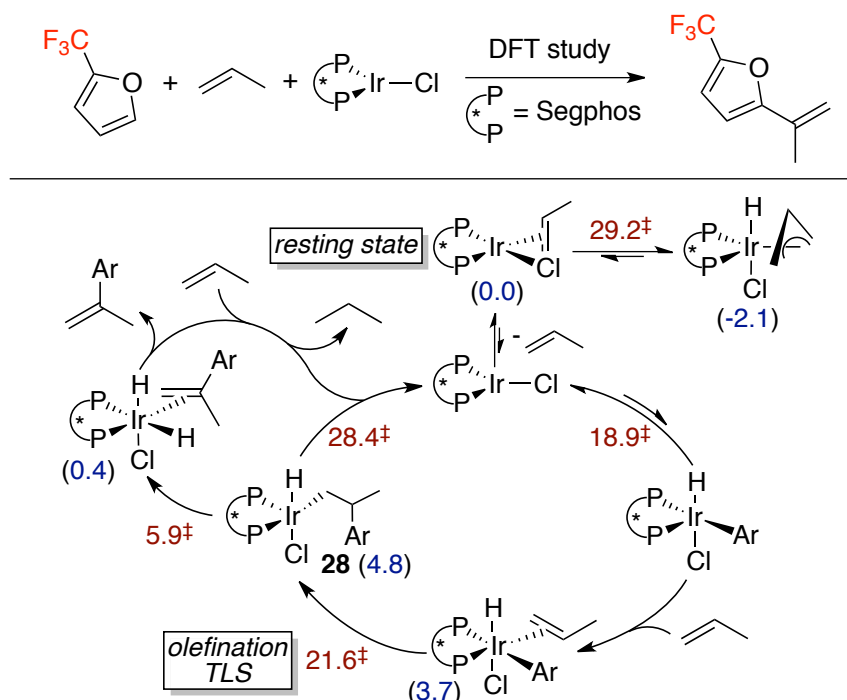

Figure 6.18. Proposed catalytic cycle with computed energies of intermediates (blue) and transition states (red) for the olefination of 2-trifluoromethylfuran with propene.

260

Table 6.14. Relative energies of barriers to CH activation and olefin insertion into the Ir–furyl bond.[a]

C–H Activation	G_{gas}	H_{gas}	G_{corr}	H_{corr}	$Solv_{Mes}$	ΔG_{mes}	ΔH_{mes}
Ir(CF3-Fur)_GS	-4007.7395	-4007.5417	0.7623	0.9600	-4009.2851	**4.2**	**1.7**
Ir(H)(CF3-Fur)_TS_1	-4007.7088	-4007.5075	0.7542	0.9555	-4009.2536	**18.9**	**18.7**
Ir(H)(CF3-Fur)_TS_2	-4007.7071	-4007.5073	0.7559	0.9557	-4009.2534	**20.2**	**19.0**
Mig. Insertion	G_{gas}	H_{gas}	G_{corr}	H_{corr}	$Solv_{Mes}$	ΔG_{mes}	ΔH_{mes}
MI_CF3_GS	-4007.7378	-4007.5610	0.7847	0.9615	-4009.3085	**3.7**	**-12.0**
MI_CF3_2_TS	-4007.7124	-4007.5388	0.7860	0.9596	-4009.2780	**23.6**	**6.0**
MI_CF3_3_TS	-4007.7121	-4007.5383	0.7856	0.9593	-4009.2768	**24.1**	**6.5**
MI_CF3_5_TS	-4007.7124	-4007.5390	0.7864	0.9598	-4009.2799	**22.6**	**4.9**
MI_CF3_6_TS	-4007.7139	-4007.5407	0.7871	0.9603	-4009.2823	**21.6**	**3.7**

[a]Values for H and G are in Hartree. Values for ΔH and ΔG are in kcal/mol.

Table 6.15. Relative energies for barriers to CH reductive elimination or $\boldsymbol{\beta}$-hydrdide elimination.[a]

Ir-Alkyl	G_{gas}	H_{gas}	G_{corr}	H_{corr}	$Solv_{Mes}$	ΔG_{mes}	ΔH_{mes}
Alkyl_CF3_1_INT	-4007.7432	-4007.5687	0.7879	0.9624	-4009.3098	**4.8**	**-12.3**
Beta-H-Elim	G_{gas}	H_{gas}	G_{corr}	H_{corr}	$Solv_{Mes}$	ΔG_{mes}	ΔH_{mes}
H-Elim_CF3_1_TS	-4007.7350	-4007.5562	0.7781	0.9569	-4009.2983	**5.9**	**-8.5**
H-Elim_CF3_GS1	-4007.7450	-4007.5678	0.7826	0.9597	-4009.3116	**0.4**	**-15.1**
H-Elim_CF3_GS2	-4007.7343	-4007.5577	0.7827	0.9593	-4009.3012	**7.0**	**-8.8**
Red. Elim.	G_{gas}	H_{gas}	G_{corr}	H_{corr}	$Solv_{Mes}$	ΔG_{mes}	ΔH_{mes}
RE_CF3_1_TS	-4007.7040	-4007.5299	0.7864	0.9605	-4009.2707	**28.4**	**11.1**
RE_CF3_GS	-4007.7443	-4007.5689	0.7890	0.9645	-4009.3106	**5.0**	**-11.4**

[a]Values for H and G are in Hartree. Values for ΔH and ΔG are in kcal/mol.

6.5 References

(1)   Le Bras, J.; Muzart, J. *Chem. Rev.*, **2011**, *111*, 1170.
(2)   Jia, C.; Kitamura, T.; Fujiwara, Y. *Acc. Chem. Res.*, **2001**, *34*, 633.
(3)   Chen, X.; Engle, K. M.; Wang, D.-H.; Yu, J.-Q. *Angew. Chem. Int. Ed.*, **2009**, *48*, 5094.
(4)   Fujiwara, Y.; Moritani, I.; Matsuda, M.; Teranishi, S. *Tetrahedron Lett.*, **1968**, *9*, 633.
(5)   Moritanl, I.; Fujiwara, Y. *Tetrahedron Lett.*, **1967**, *8*, 1119.
(6)   Fujiwara, Y.; Maruyama, O.; Yoshidomi, M.; Taniguchi, H. *J. Org. Chem.*, **1981**, *46*, 851.
(7)   Tang, R.-Y.; Li, G.; Yu, J.-Q. *Nature*, **2014**, *507*, 215.
(8)   Parthasarathy, K.; Bolm, C. *Chem. Eur. J.*, **2014**, n/a.
(9)   Ma, W.; Ackermann, L. *Chemistry*, **2013**, *19*, 13925.
(10)   Huang, X.; Huang, J.; Du, C.; Zhang, X.; Song, F.; You, J. *Angew. Chem. Int. Ed.*, **2013**, *52*, 12970.
(11)   Ackermann, L.; Wang, L.; Wolfram, R.; Lygin, A. V. *Org. Lett.*, **2012**, *14*, 728.
(12)   Wang, D.-H.; Engle, K. M.; Shi, B.-F.; Yu, J.-Q. *Science*, **2010**, *327*, 315.
(13)   Kozhushkov, S. I.; Ackermann, L. *Chem. Sci.*, **2013**, *4*, 886.
(14)   Dai, H.-X.; Li, G.; Zhang, X.-G.; Stepan, A. F.; Yu, J.-Q. *J. Am. Chem. Soc.*, **2013**, *135*, 7567.
(15)   Li, G.; Leow, D.; Wan, L.; Yu, J.-Q. *Angew. Chem. Int. Ed.*, **2013**, *52*, 1245.
(16)   Baxter, R. D.; Sale, D.; Engle, K. M.; Yu, J.-Q.; Blackmond, D. G. *J. Am. Chem. Soc.*, **2012**, *134*, 4600.
(17)   Li, J.; Kornhaa; Ackermann, L. *Chem. Commun.*, **2012**, *48*, 11343.
(18)   Leow, D.; Li, G.; Mei, T.-S.; Yu, J.-Q. *Nature*, **2012**, *486*, 518.
(19)   Yang, Y.-F.; Cheng, G.-J.; Liu, P.; Leow, D.; Sun, T.-Y.; Chen, P.; Zhang, X.; Yu, J.-Q.; Wu, Y.-D.; Houk, K. N. *J. Am. Chem. Soc.*, **2013**, *136*, 344.
(20)   Kubota, A.; Emmert, M. H.; Sanford, M. S. *Org. Lett.*, **2012**, *14*, 1760.
(21)   Rossi, R.; Bellina, F.; Lessi, M. *Synthesis*, **2010**, *2010*, 4131.
(22)   Li, P.; Gu, J.-W.; Ying, Y.; He, Y.-M.; Zhang, H.-f.; Zhao, G.; Zhu, S.-Z. *Tetrahedron*, **2010**, *66*, 8387.
(23)   Ye, M.; Gao, G.-L.; Yu, J.-Q. *J. Am. Chem. Soc.*, **2011**, *133*, 6964.
(24)   Zhang, Y.; Li, Z.; Liu, Z.-Q. *Org. Lett.*, **2011**, *14*, 226.
(25)   Aouf, C.; Thiery, E.; Le Bras, J.; Muzart, J. *Org. Lett.*, **2009**, *11*, 4096.
(26)   Zhao, J.; Huang, L.; Cheng, K.; Zhang, Y. *Tetrahedron Lett.*, **2009**, *50*, 2758.
(27)   Liu, W.; Yu, X.; Kuang, C. *Org. Lett.*, **2014**, *16*, 1798.
(28)   Boultadakis-Arapinis, M.; Hopkinson, M. N.; Glorius, F. *Org. Lett.*, **2014**, *16*, 1630.
(29)   Pawar, G. G.; Singh, G.; Tiwari, V. K.; Kapur, M. *Adv. Synth. Catal.*, **2013**, *355*, 2185.
(30)   Grimster, N. P.; Gauntlett, C.; Godfrey, C. R. A.; Gaunt, M. J. *Angew. Chem. Int. Ed.*, **2005**, *44*, 3125.
(31)   Boele, M. D. K.; van Strijdonck, G. P. F.; de Vries, A. H. M.; Kamer, P. C. J.; de Vries, J. G.; van Leeuwen, P. W. N. M. *J. Am. Chem. Soc.*, **2002**, *124*, 1586.

(32)   Beck, E. M.; Grimster, N. P.; Hatley, R.; Gaunt, M. J. *J. Am. Chem. Soc.*, **2006**, *128*, 2528.

(33)   Yokota, T.; Tani, M.; Sakaguchi, S.; Ishii, Y. *J. Am. Chem. Soc.*, **2003**, *125*, 1476.

(34)   Jia, C.; Lu, W.; Kitamura, T.; Fujiwara, Y. *Org. Lett.*, **1999**, *1*, 2097.

(35)   Tani, M.; Sakaguchi, S.; Ishii, Y. *J. Org. Chem.*, **2004**, *69*, 1221.

(36)   Mochida, S.; Hirano, K.; Satoh, T.; Miura, M. *J. Org. Chem.*, **2011**, *76*, 3024.

(37)   Gigant, N.; Bäckvall, J.-E. *Org. Lett.*, **2014**, *16*, 1664.

(38)   Kwon, K.-H.; Lee, D. W.; Yi, C. S. *Organometallics*, **2010**, *29*, 5748.

(39)   Gandini, A.; Belgacem, M. N. In *Monomers, Polymers and Composites from Renewable Resources*; Belgacem, M. N., Gandini, A., Eds.; Elsevier: Amsterdam, 2008, p 115.

(40)   Arekion, J.; Delmas, M.; Gaset, A. *Biomass*, **1983**, *3*, 59.

(41)   Gandini, A.; Belgacem, M. N. *Progress in Polymer Science*, **1997**, *22*, 1203.

(42)   Gandini, A. In *Biopolymers – New Materials for Sustainable Films and Coatings*; John Wiley & Sons, Ltd: 2011, p 179.

(43)   Sevov, C. S.; Hartwig, J. F. *J. Am. Chem. Soc.*, **2013**, *135*, 2116.

(44)   Sevov, C. S.; Hartwig, J. F. *J. Am. Chem. Soc.*, **2013**, *135*, 9303.

(45)   Anslyn, E. V.; Dougherty, D. A.; University Science: 2006, p 896.

(46)   Herde, J. L.; Lambert, J. C.; Senoff, C. V.; Cushing, M. A. In *Inorganic Syntheses*; John Wiley & Sons, Inc.: 2007, p 18.

(47)   Meyer, V. J.; Niggemann, M. *Eur. J. Org. Chem.*, **2011**, *2011*, 3671.

(48)   Greeves, N.; Torode, J. S. *Synthesis*, **1993**, *1993*, 1109.

(49)   Chatterjee, B.; Gunanathan, C. *Chem. Commun.*, **2014**, *50*, 888.

(50)   Barbasiewicz, M.; Makosza, M. *Org. Lett.*, **2006**, *8*, 3745.

(51)   Weyerstahl, P.; Brendel, J. *Liebigs Annalen der Chemie*, **1988**, *1988*, 1015.

(52)   Ma, M.-L.; Peng, Z.-H.; Chen, L.; Guo, Y.; Chen, H.; Li, X.-J. *Chin. J. Chem.*, **2006**, *24*, 1391.

(53)   Bo, Z.; Schluter, A. D. *Chem. Commun.*, **2003**, 2354.

(54)   An, P.; Shi, Z.-F.; Dou, W.; Cao, X.-P.; Zhang, H.-L. *Org. Lett.*, **2010**, *12*, 4364.

(55)   Klotz, E. J. F.; Claridge, T. D. W.; Anderson, H. L. *J. Am. Chem. Soc.*, **2006**, *128*, 15374.